L-vehicles Emissions and Noise mitigation Solutions

D3.5 RW driving patterns to assess LV noise and emissions

This project has received funding from the European Union's Horizon Europe research and innovation programme under grant agreement No 101056777

Deliverable No.	D3.5	
Deliverable title	RW driving patterns to assess LV noise and emissions	
Deliverable type	Report	
Dissemination level	PU - Public	
Deliverable leader	IDIADA	
Contractual due date	31.05.2025	
Actual submission date	01.08.2025	
Version	1.0	
Written by	A. Garbí, B. Garcia (IDIADA), C. Schliephake, S. Shariatinia, M. Winter (ika, RWTH Aachen University), I. Riemersma, P. van Mensch, J. Aschersleben, Dittrich, M.G. (TNO), H. Steven (EMISIA/HSDAC)	11.07.2025
Reviewed by	Hervé Denayer (KU Leuven), Francesco Sini (DUCATI)	18.07.2025
Approved by	All partners	01.08.2025

Revisions table

Version	Date	Change
1.0	01.08.2025	First submission to EC

This project has received funding from the European Union's Horizon Europe research and innovation programme under grant agreement No 101056777

Table of Contents

This project has received funding from the European Union's Horizon Europe research and innovation programme under grant agreement No 101056777

This project has received funding from the European Union's Horizon Europe research and innovation programme under grant agreement No 101056777

This project has received funding from the European Union's Horizon Europe research and innovation programme under grant agreement No 101056777

Executive summary

The LENS project deliverable D3.5 presents comprehensive evidence-based findings on driving patterns for emissions and noise assessment of L-category vehicles, derived from an extensive measurement campaign totaling 112 vehicle measurements. Of these, 90 measurements focused on real-world (RW) procedure evaluations, with 22 vehicles additionally tested under both real-world and current type-approval conditions to enable comparative analysis. The analysis characterizes noise and pollutant emissions performance for a variety of real-world operating conditions, including high accelerations, speed variations, high-speed operation, and cold engine starts—conditions frequently not included in current type-approval procedures. Both regulated and non-regulated pollutants were systematically analyzed across the comprehensive 112-vehicle dataset. Vehicles tested are meant to reflect current European L-category fleet composition, including Euro class distribution, mileage diversity, prevalent brands/models, tampered vehicles, etc.

The comprehensive methodology, encompassing 112 vehicles across multiple sub-categories, represents a significant advancement in understanding real-world vehicle performance, offering critical data for future regulatory frameworks and vehicle design strategies.

Real-world driving patterns represent vehicle the actual operation of vehicles in everyday traffic conditions, fundamentally diverging from the controlled laboratory environments of test tracks or chassis dynamometers. These real-world driving patterns encapsulate a complex array of interactions, including variable speed dynamics with accelerations, braking events, and periods of constant speed, as well as intricate traffic interactions involving stop-and-go behavior, intersection navigation, and diverse maneuvers. The driving scenarios encountered range from congestion to free-flowing traffic situations.
Furthermore, extensive documentation was conducted on the environmental influences impacting real-world driving, such as road surface quality, gradients, and topographical features of the landscape. Alongside these environmental factors, nuanced driver behavior parameters were also meticulously recorded, including driving aggressiveness, efficiency patterns, and operational variations across urban, rural, and motorway settings.

In summary, real-world driving patterns represent the complex, multifaceted nature of vehicle operation in everyday traffic, in contrast to the controlled conditions of laboratory testing environments. Evaluation of real-world driving patterns considers three fundamental pillars. The first pillar examines the frequency and prevalence of specific driving events as they are observed in actual everyday usage conditions. The second pillar evaluates the environmental impact magnitude associated with the identified real-world driving patterns, such as emissions and energy consumption. The third pillar assesses the practical implementation potential for incorporating these real-world driving scenarios into standard testing procedures. By strategically evaluating real-world operation across these three pillars, the framework enables a comprehensive understanding of the complex interactions and environmental influences at play during everyday vehicle usage.

This project has received funding from the European Union's Horizon Europe research and innovation programme under grant agreement No 101056777

The comprehensive testing program involved a carefully selection of the current vehicle fleet representing the complete L-category spectrum, with 90 vehicles undergoing on-road tailpipe emissions and 22 vehicles tested under both real-world and current type-approval conditions.

The noise assessment methodology, initially developing the RW procedure through 14 vehicles instrumented with on-board sensors, which captured on-road measurements with GPS loggers and microphones. These 14 on-road measurements formed the basis for deriving the real-world test track procedures, enabling a synchronized analysis of vehicle dynamics and sound pressure levels during actual traffic operation. It was found that several driving patterns produce noise levels significantly higher than current type-approval limits. Based on the identified noise-relevant driving conditions, dedicated driving cycles were developed and executed on an acoustic test track to systematically evaluate their impact on vehicle noise emissions.

The Rotranomo model was also applied to measured RDE driving cycles, to evaluate high noise emissions from real on-road usage and the comparison of the impact of both aggressive and normal driving behavior.

Driving dynamics analysis provided deep insights into vehicle performance, comparing v*a and relative positive acceleration (RPA) between type-approval procedures and real-world usage. The study comprehensively examined power-to-mass ratio distributions across different light vehicle sub-categories and compared these metrics against passenger car performance.

The analysis of high emission events has been conducted through a multifaceted approach. This includes directly incorporating the high emission events identified in the LENS report D6.1, as well as detecting additional high emission events by processing the entirety of data contained within the LENS database. Heatmap visualizations were also generated, depicting the instantaneous data against various established key performance indicators (KPIs) such as acceleration, v*a, engine speed, and others. The principal pollutants considered in this analysis are carbon monoxide (CO), hydrocarbons (HC), and nitrogen oxides (NOx). Specific data clustering techniques were employed to assess the behavioral characteristics of different L-vehicle sub-categories, engine configurations, and transmission technologies.
The analysis of high emission events focused on evaluating the impact of cold starts, accelerations, and the transitions from accelerations or constant speed to decelerations. A more detailed analysis was also conducted on specific representative L3e-A2 and L3-A3 vehicle models.

Emissions monitoring focused on tailpipe emissions characterization across diverse operating conditions and validation of current emission limits against actual usage patterns. Researchers developed representative driving cycles to better capture real-world driving behavior and enable laboratory reproducibility. High-emission event analysis concentrated on critical scenarios including cold start conditions, accelerations, and transitions between acceleration and deceleration.

This project has received funding from the European Union's Horizon Europe research and innovation programme under grant agreement No 101056777

List of Abbreviations

AMT	Automated Manual Transmission
ASEP	Additional Sound Emission Provisions
BCPM	Black Carbon Particle Mass
CVS	Fourier Transform Infrared Spectroscopy Constant Volume Sampling System
CVT	Continuously Variable Transmission
ECE	Economic Commission for Europe
FTIR	Fourier Transform Infrared Spectroscopy
GA	Grant Agreement
ICE	Internal Combustion Engine
KPI	Key Point Indicator
LAF	A-weighted sound level with Fast time weighting
LDV	Light Duty Vehicles
LV	L-category vehicle
MC	Motorcycle
MEMS	Micro Electro Mechanical Systems
mFTIR	mini Fourier Transform Infrared Spectroscopy
MT	Manual Transmission
NEDC	New European Driving Cycle
NO	Nitric Oxide
NOx	Nitrogen Oxides
PC	Passenger cars
PEMS	Portable Emissions Measurement System
RDC	Real Driving Cycle
RDE	Real Driving Emissions
PHEM	Passenger Car and Heavy Duty Emission Model
PTFM	Pitot Flow Meter
ReTEMS	Real Time Emissions Measurement System
RPA	Relative positive acceleration
RW	Real World
RWC	Real World Cycle
SEMS	Smart Emissions Measurement System
SPL	Sound Pressure Level
TA	Type Approval
WLTP	Worldwide Harmonized Light Vehicle Test Procedure
WMTC	World Harmonized Motorcycle Test Cycle

This project has received funding from the European Union's Horizon Europe research and innovation programme under grant agreement No 101056777

List of figures

This project has received funding from the European Union's Horizon Europe research and innovation programme under grant agreement No 101056777

This project has received funding from the European Union's Horizon Europe research and innovation programme under grant agreement No 101056777

This project has received funding from the European Union's Horizon Europe research and innovation programme under grant agreement No 101056777

This project has received funding from the European Union's Horizon Europe research and innovation programme under grant agreement No 101056777

This project has received funding from the European Union's Horizon Europe research and innovation programme under grant agreement No 101056777

This project has received funding from the European Union's Horizon Europe research and innovation programme under grant agreement No 101056777

This project has received funding from the European Union's Horizon Europe research and innovation programme under grant agreement No 101056777

This project has received funding from the European Union's Horizon Europe research and innovation programme under grant agreement No 101056777

This project has received funding from the European Union's Horizon Europe research and innovation programme under grant agreement No 101056777

This project has received funding from the European Union's Horizon Europe research and innovation programme under grant agreement No 101056777

This project has received funding from the European Union's Horizon Europe research and innovation programme under grant agreement No 101056777

List of tables

This project has received funding from the European Union's Horizon Europe research and innovation programme under grant agreement No 101056777

1. Introduction

The primary aim of this deliverable is to provide comprehensive methodological recommendations for the assessment of driving patterns in relation to emissions and acoustic characterization, grounded in empirical measurements and rigorous analytical surveys.

The study focuses on a *comprehensive characterization* of pollutant emissions and noise performance for L-category vehicles (LVs), encompassing a broad spectrum of real-world operational conditions, specifically including pronounced acceleration profiles, dynamic velocity variations, high-speed operating regimes, and cold engine start conditions.

The research incorporates a detailed analysis of fine particulate matter (PN) and non-regulated pollutant emissions across multiple evaluation environments, including laboratory settings, test track configurations, and real-world (RW) driving scenarios. The ultimate objective is to gain in-depth insights into acoustic and pollutant emission levels, as well as to identify operational events triggering high emission rates. The investigation is substantiated by an extensive dataset derived from comprehensive testing of over 150 vehicles, representing all major L-vehicle subcategories. This approach ensures a robust and representative research framework, providing a comprehensive understanding of vehicle emissions and acoustic performance under diverse operational conditions. As represented in Figure 1-1, regarding exhaust emissions in this case, an evaluation of current Type Approval (TA) test procedure is going to be developed, as well as a specific assessment of driving dynamics. The purpose of this analysis is to improve current test procedure throughout developing more representative test cycles which better cover real-world driving patterns.

Real-world driving patterns are records or characterizations of how vehicles are actually driven in everyday situations, as opposed to ideal or controlled laboratory conditions. These patterns include as key characteristics:

- Speed variability: Accelerations, braking events, constant speed periods
- Intersection behavior: Stops, starts, turns
- Traffic influence: Congestion, saturated traffic, heavy traffic, free-flowing conditions
- Environmental factors: Weather, road conditions, road gradient, topography
- Driver behavior: Aggressiveness, efficiency, anticipation, trip duration and influence of cold start, share of driving operation (urban, rural, motorway) among others.

This project has received funding from the European Union's Horizon Europe research and innovation programme under grant agreement No 101056777

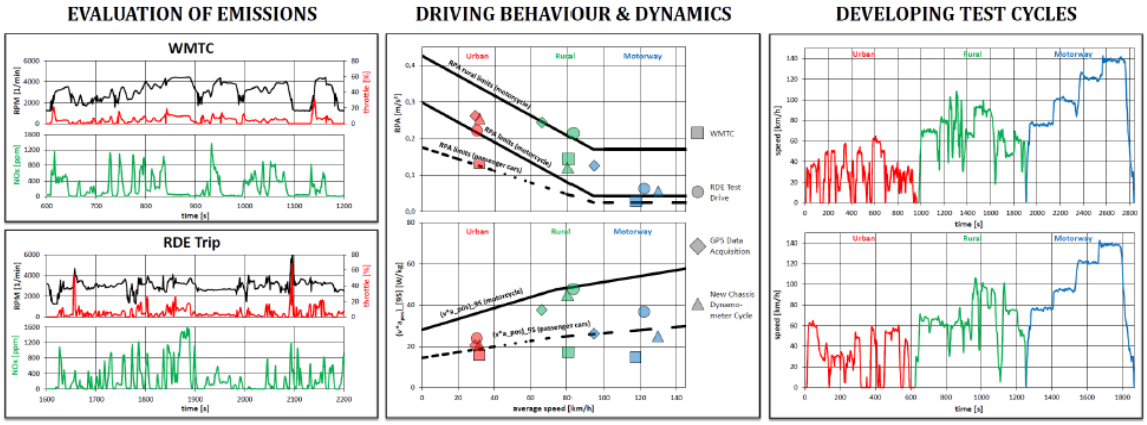

Figure 1-1: Real driving Test Cycles developed for LVs using driving behavior and dynamics (RDE trips and WMTC).

The real-world operation events identified to be of relevance for assessing emission should consider the three following pillars: occurrence, severity and feasibility.

In terms of noise, a total of 14 L-category vehicles were instrumented and measured in actual road traffic using GPS loggers and microphones mounted directly on the vehicles. This setup enabled a synchronized analysis of vehicle dynamics and corresponding sound pressure levels. In this report, two of these vehicles are selected as representative examples for in-depth evaluation. To complement the measurement data, a survey and a controlled sound monitoring study were conducted to assess which driving behaviors are perceived as particularly noisy. Additional findings from other work packages within the project are also considered to ensure a comprehensive understanding of noise-relevant behavior. The patterns identified through this combined approach were then formalized and reproduced on certified acoustic test tracks. This transfer from public roads to controlled testing environments is essential, as motorcycle noise type approval is performed under such standardized conditions. The acoustic analysis in this report therefore focuses primarily on the A-weighted sound pressure level, which is the regulatory reference metric. For the selected driving patterns, the temporal progression of the noise emissions is also examined across different vehicle categories to provide further insights into spectral and dynamic characteristics of the emitted noise.

In terms of real-world tailpipe emissions, vehicles are tested with emissions equipment specified and the defined procedure described in deliverable D3.1 of the project. This equipment comprises:

- AIP PEMS: used to determine the gaseous emission components CO, CO2, NOx (NO + NO2) and the particle number concentration PN. Includes also ambient temperature and relative humidity sensors, a GPS module and a CAN interface for reading out ECU data.
- HORIBA SEMS: Smart Emissions Measurement System (SEMS) able to measure NOx emissions. Tested in laboratory with a deviation below 10% to a direct raw analyzer. Includes a Pitot Flow Meter (PTFM) that determines the exhaust gas mass flow.
- EMISIA ReTEMS: prototype SEMS named ReTEMS (Real Time Emissions Measurement System) is device capable of measuring the CO, CO2, NO and Black Carbon Particle Mass (BCPM) concentration of exhaust gases (the BC sensor provided by Maurus Oy).
- IFPEN REAL-e SEMS: able to measure CO2, HC, CO, O2, NOx, NO, NO2, NH3 and PN. Includes OBD connection for GPS data and read out ECU data. Exhaust flow should be modelled.

This project has received funding from the European Union's Horizon Europe research and innovation programme under grant agreement No 101056777

- CZU FTIR: compact FTIR for on-road testing developed by CZU. able to measure CO2, CO, CH4, HCHO, CH3CHO, N2O, NH3, NO, NO2 and NOx.

Regarding chassis dyno measurements of pollutant emissions, procedure and equipment are defined in Deliverable D4.1. Standard measurement devices and requirements procedures as defined in the homologation legislation Regulation (EU) No. 134/2014 and No. 168/2013 are considered. Measurement equipment includes:

- Constant Volume Sampler (CVS): CVS systems are used for the collection and dilution of the exhaust gases, as well as for the determination of the exhaust gas mass flow. These systems have been rigorously compared during the Round Robin procedure to ensure repeatability and reproducibility of the measurements across laboratories. Components measured are CO, CO_2, HC and NOx.
- Additionally, other devices like Fourier Transform Infrared Spectroscopy (FTIR), Particulate Matter (PM) and Particle Number (PN) systems may be used. Therefore, Particulate mass and/or number, and non-regulated pollutants are measured.

2. Methodology and testing procedure

According to Grant Agreement Nº 101056777, HORIZON-CL5-2021-D5-01, the characterization of on-road noise and tailpipe emissions takes a very important role for developing greener and quieter LVs. In order to have enough data for being able to assess RW driving behavior of LVs, 112 total vehicles have been tested for noise, and then 112 vehicles for emissions. In some cases same vehicles has been tested for both noise and pollutants, but not necessarily. Out of the total number of 112 vehicles, 90 of them have been tested only on-road, regarding tailpipe emissions, or on the test track following the established RW driving patterns respectively. The 22 remaining vehicles have been tested both following the RW driving patterns for noise, and on-road for tailpipe emissions, and also according to the current Type Approval (TA) procedure respectively, to deliver comparison data between RW operation and TA measurements.

TA measures from current EU regulations are very poor in covering RW driving behavior, so a RW noise procedure has been developed to better analyze noise emissions from LVs. In order to develop this new measurement procedure, on-road data from 14 vehicles has been considered, so all events identified in this dataset have been analyzed and then, driving patterns causing high emissions were integrated in the new measurement procedure. The 14 tested vehicles include models from the categories L1e (1 vehicle), L3e-A1 (2 vehicles), L3e-A2 (2 vehicles), L3e-A3 (6 vehicles), L3e-AxE (1 vehicle), L5e (1 vehicle), L6e (1 vehicle), and L7e (1 vehicle). As such, all L-vehicle subcategories are represented with the exception of L2e. Unfortunately, due to the very low market penetration of L2e vehicles in national fleets – 0% in Germany, for example – no suitable test vehicles could be sourced. However, given the small contribution of this vehicle class, its exclusion does not impact the representativeness of the overall results. These preliminary on-road noise measurements are developed in paragraph 2.1, and in Appendix A: On-board noise measurements.

An overview of all 112 vehicles measured following the new noise RW procedure is represented in Figure 2-1, where vehicles are classified by sub-category. Each segment of the pie chart is labeled in two lines: the first line denotes the corresponding vehicle class based on the definitions set out in the LENS grant

This project has received funding from the European Union's Horizon Europe research and innovation programme under grant agreement No 101056777

agreement, while the second line specifies the respective percentage share of the total number of measured vehicles. Regarding noise measurements, the Euro standards do not correspond to the most representative classification of the vehicles, as there are different regulations for different types of vehicles. As mentioned in D4.5, the regulations for noise TA are the following:

- UN Regulation No. 9 [2] – Applicable to tricycles
- UN Regulation No. 41 [3]– Applicable to motorcycles
- UN Regulation No. 63 [4]– Applicable to mopeds

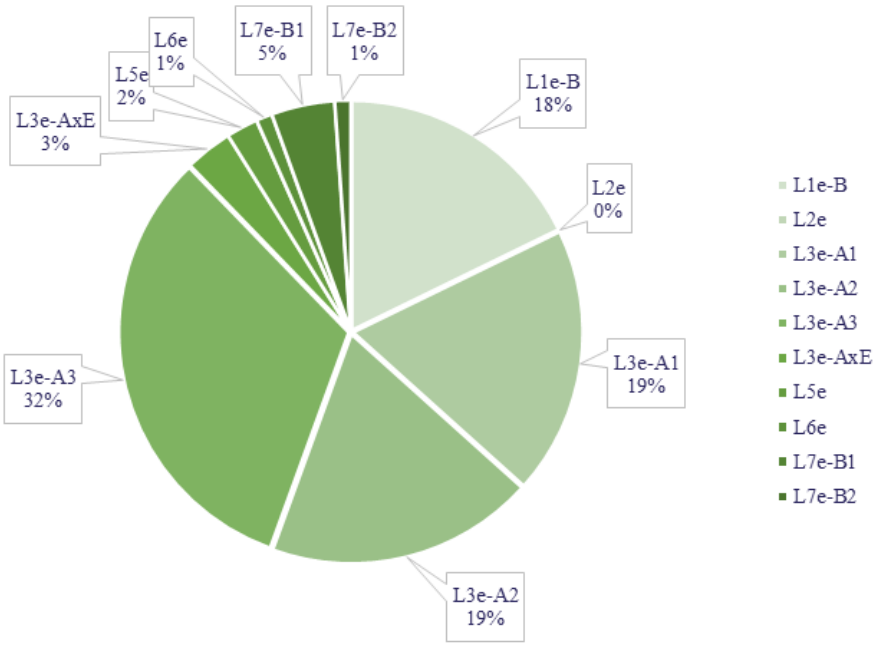

Figure 2-1: Overview of noise RW measured vehicles.

All vehicles have been carefully selected to accurately reflect the composition of the current LVs fleet in Europe. This means that the share of the Euro Classes, mileage, brands and models is highly diversified, including best-selling models, which tend to be more prevalent, and also known tampered vehicles, to assess their performance. It is important to mention that a large number of the latest Euro 5 vehicles is considered, because we wanted to obtain a reliable picture for the latest technology vehicles and check potential deficiencies of the regulation. The distribution of the LVs over different EU standards for each sub-category is shown in Figure 2-2. No on-road testing of L3e-AxE regarding tailpipe pollutant emissions has been conducted due to difficulties in mounting the equipment.

Specific on-road routes have been carefully developed to better cover several real-world driving patterns which are not included in current regulatory driving cycles. Additionally, specific Real Driving Cycles (RDC) have been developed, which have already been introduced in LENS Deliverable D4.1. Their objective is to replicate real-world driving conditions as closely as possible. Different RDC cycles have been developed for

This project has received funding from the European Union's Horizon Europe research and innovation programme under grant agreement No 101056777

the following L-vehicles sub-categories L1e-B, L3e-A1, L3e-A2 and L3e-A3. For each L3e-Ax subcategory, "low" and "high" versions are available depending on vehicle's capabilities. These "low" variants have their maximum speed clipped to the maximum speed that the vehicle can develop. There are some specific cases in which the chassis dyno cannot reach such a high speed, so then the RDC speed is clipped too. Both on-road and RDC characteristics are presented in detail later in this document.

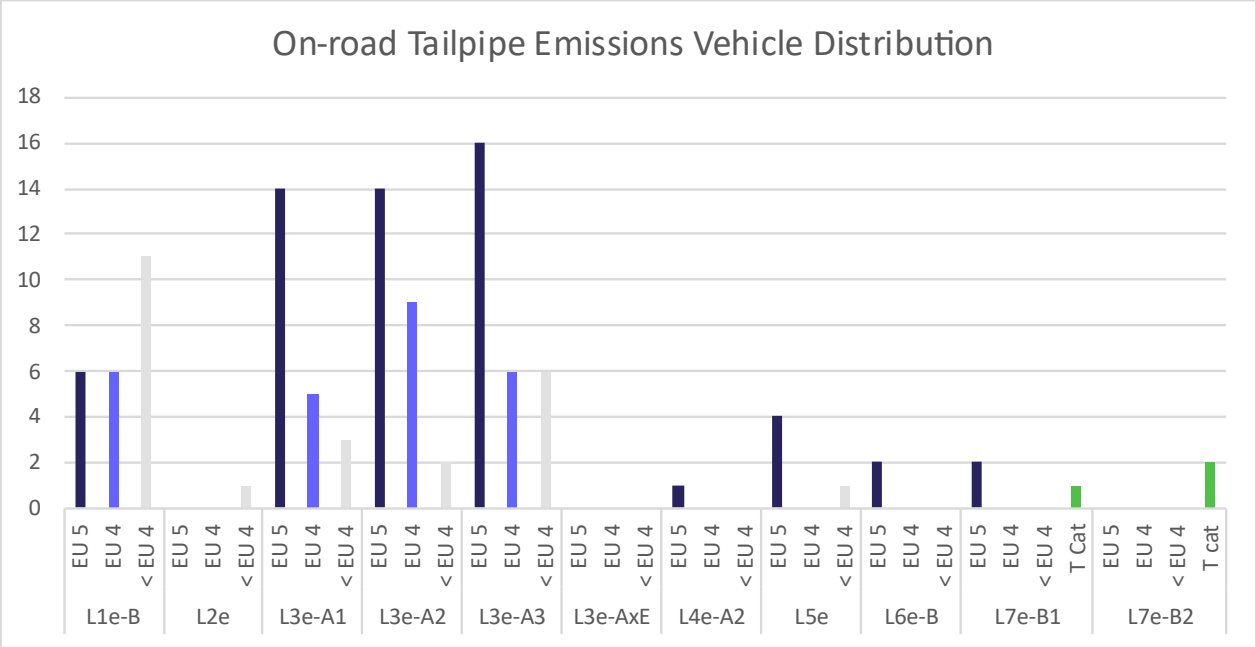

Figure 2-2: Vehicles subjected to On-road tailpipe emissions. Distribution of EU Standard.

2.1 On-road noise measurements

L-category vehicles such as motorcycles and scooters are significant contributors to road traffic noise and are often perceived as more disturbing than other vehicle types [1; 2] . One of the main reasons for this is their specific driving behavior in real traffic, where certain L-category vehicles operate across wide ranges of engine and vehicle speeds [3]. This highlights the shortcomings of current type approval procedures in accurately capturing real-world noise emissions. Over the years, regulations have been revised to better address these issues. For example, UN Regulation No. 41 introduced the Additional Sound Emission Provisions (ASEP) in its 04 series of amendments to improve the representativity of noise testing for L3 vehicles [4]. This was further extended in the 05 series with the Real Driving ASEP (RD-ASEP), which added more operating conditions and a broader testing range to better reflect actual driving situations [5]. Nonetheless, further studies are needed to fully understand which driving behaviors are most noise-intensive and to identify remaining gaps in the updated approval procedures.

Previous research has investigated the noise impact of various driving conditions and vehicle parameters for L-category vehicles. In the IMAGINE project, for example, such vehicles were fitted with on-board sensors and were driven in real traffic to gather relevant data [6]. These measurements were analyzed to identify key factors influencing noise emissions. Additionally, a study by the German Environment Agency compared test results from UN Regulation No. 41 (04 series) with predefined worst-case scenarios—driving

This project has received funding from the European Union's Horizon Europe research and innovation programme under grant agreement No 101056777

conditions likely to be perceived as particularly disruptive [7]. The LENS project has built on these findings, providing further recommendations on noise-critical driving maneuvers for L-category vehicles, based on extensive roadside measurement campaigns carried out in different locations [8; 9].

Some characteristic examples of the on-board measurements performed are included in Appendix A: On-board noise measurements. These show several plots of sound level, speed and acceleration during a run for several vehicles on different routes. The strong dynamics of vehicle speed and noise are clearly visible. Also, several spectrograms are shown for selected vehicles and selected parts of runs, which help identify loud events and their frequency spectrum. The basic engine frequency and its harmonics are clearly visible, which are indicative of engine speed. In general, on-board measurements can be used to identify particularly loud driving conditions as they can occur on the road. Then, if required, these can be selected for more reproducible measurements on a test track.

2.2 RW noise emissions measurements on test track

Based on the investigations from chapter 2.1, a set of representative noisy driving conditions was defined and documented in Table 2-2 from Deliverable D6.1 [8]. These conditions are grounded both in empirical measurement data and in underlying physical principles. Table 2-1 provides an overview of the nine distinct conditions identified. Each is associated with a specific vehicle operation mode and assigned a short identifier, which is consistently used across Deliverables D6.1 and D4.5 [14].

Table 2-1 Recommended driving conditions from LENS-Deliverable D6.1 [8]

No.	Condition	Vehicle operation	Short name	Already in TA?
(1)	Cold start	Engine start	'coldstart'	✕
(2)	rpm burst	Stationary, short activation and release of accelerator	'rpmburst'	✕
(3)	Acceleration from standstill	Acceleration, late gear change	'rpmlongacc'	✕
(4)	Max rpm pass by (esp. Mopeds, scooters, sport MCs)	Constant speed with max rpm	'rpmconthi'	✕
(5)	Transition from constant speed/	Deceleration	'rpmdropoff'	✕

This project has received funding from the European Union's Horizon Europe research and innovation programme under grant agreement No 101056777

	acceleration to deceleration phase			
(6)	"Max" acceleration from standstill	Acceleration	'rpmshortacc'	✗
(7)	Acceleration from 50 km/h to 100 km/h	Acceleration may be varied	'rpmidspeedacc'	R41 ✓ R9 & R 63 ✗
(8)	rpm fluctuation	Variable speed	'rpmfluct'	✗
(9)	Backfire	Multiple gear changing or manual operation	'bang'	R41 ✓ R9 & R 63 ✗

Many of the defined noise-relevant conditions are linked to particular driving behaviors (e.g. acceleration, gear shifts), vehicle dynamics, or specific components. As they typically involve higher engine power outputs, these conditions are also considered relevant in the context of pollutant emissions. However, for integration into regulatory vehicle testing frameworks, these noise-critical scenarios require further specification regarding measurable parameters and boundary conditions to ensure reproducibility and comparability. Lastly, Table 2-1 shows the comparison with the current type approvals for L-class vehicles [4; 15; 16]. This clearly states that the maneuvers defined in D6.1 are mainly not included in the current TA testing.

2.2.1 Measurement Setup

The measurement setup and equipment used for the test track are based on the specifications outlined in relevant regulations and standards [4; 15–17]. Figure 2-3 illustrates the standardized microphone and equipment positioning relative to the vehicle path.

This project has received funding from the European Union's Horizon Europe research and innovation programme under grant agreement No 101056777

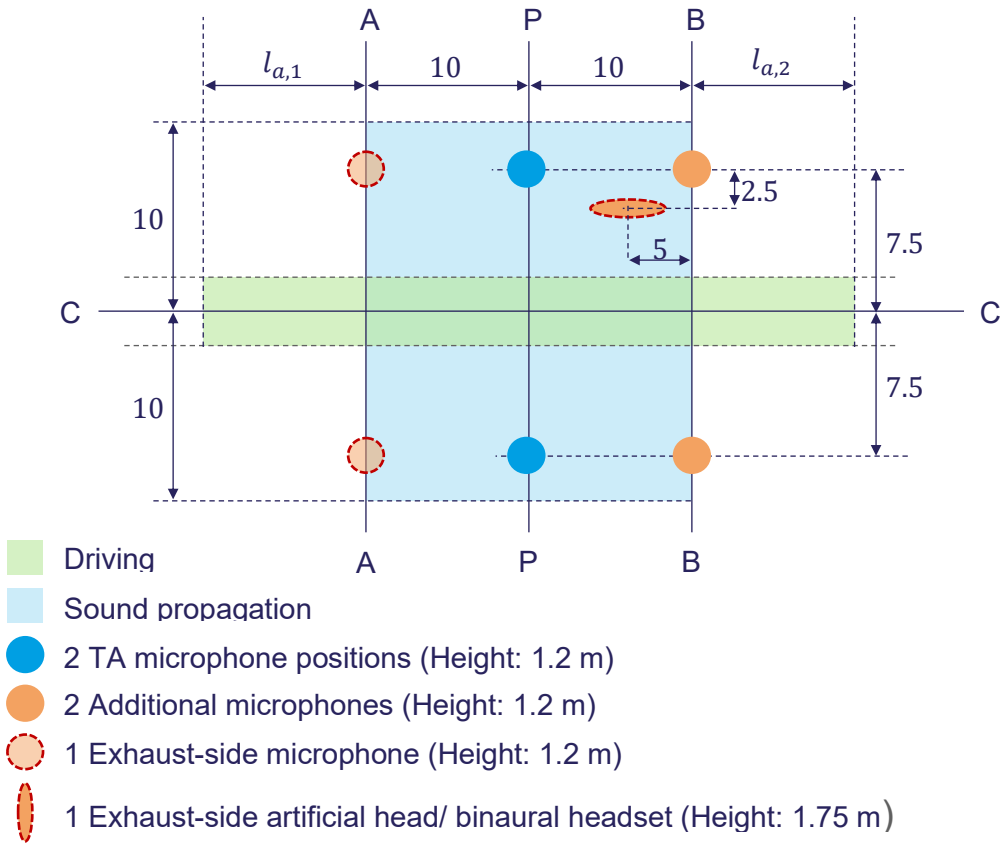

Figure 2-3: Measurement setup for the adapted test track testing.

The measurement area is defined by several key reference lines which can also be found in [17]:

- Line AA': marks the entrance to the measurement zone, placed perpendicular to the vehicle's direction of travel
- Line BB': marks the exit of this zone, also oriented perpendicular to the driving direction.
- Line CC': corresponds to the centerline of the vehicle's driving path. For public road measurements, this line aligns with the center of the relevant traffic lane (typically the right lane in countries with right-hand traffic)
- Line PP': defines the standard position of the primary roadside microphone: it is placed 7.5 meters laterally from the centerline (CC') and at a height of 1.2 meters

For real-world driving noise measurements following real-word driving procedure, only one microphone—positioned at PP' on the exhaust side of the vehicle—is mandatory. However, an enhanced measurement configuration is recommended for more comprehensive data collection and is described here in this extended setup:

- A second roadside microphone is placed at the non-exhaust side at the same PP' location and height, in line with type approval procedures defined in UN Regulations Nos. 9, 41, and 63 [4; 15; 16]
- Two additional microphones are positioned on the exit side of the measurement area (along BB'), as shown in Figure 2-3.

This project has received funding from the European Union's Horizon Europe research and innovation programme under grant agreement No 101056777

- Between PP' and BB', a binaural headset or artificial head is placed, offset 2.5 meters towards the vehicle path (closer to line CC') and located on the exhaust side. This allows for the capture of psychoacoustic parameters and a more accurate representation of human perception of vehicle noise.
- One further microphone is positioned at line AA' on the exhaust side, capturing sound at the entrance of the vehicle into the measurement zone.

The focus on the exhaust side is justified by its known contribution as a dominant noise source in L-category vehicles. A data acquisition system with a sampling frequency of at least 16384 Hz is required.
In addition to the roadside setup, each vehicle is equipped with on-board instrumentation, including at least one on-board microphone, and a vehicle speed sensor. This can be implemented via GPS tracking or by tapping into the CAN bus signal of the vehicle, ensuring synchronized data collection of vehicle dynamics and noise emissions.

2.2.2 New procedure to characterize high noise conditions for LVs – RW driving patterns

This comprehensive setup allows for a detailed and standardized evaluation of vehicle sound emissions under both controlled test track conditions and real-world driving scenarios.
In total, three different test campaigns are defined:

1. Preliminary stationary measurements
2. Preliminary transfer function measurements
3. Real-world driving patterns

Campaign 1 and 2 measurement procedure is required to be performed for each individual vehicle prior to dynamic testing, this is, Campaign 3. Its primary purpose is to establish a relationship between the recorded acoustic data and the engine speed under controlled, stationary conditions. However, if the engine speed can be accurately recorded during the real-world driving campaign (Campaign 3), this stationary test may be omitted.

During Campaign 1, the vehicle is positioned so that its lateral axis is aligned with line PP' as defined in Figure 2-3. Two stationary noise measurements are then conducted. In each measurement, the throttle is held at a constant position for approximately 10 seconds to maintain a stable engine speed. Typically, two distinct engine speeds are selected (e.g., 2000 min^{-1} and 5000 min^{-1}), although the specific values depend on the individual vehicle characteristics. Engine speed is read manually from the tachometer and documented accordingly. Minor deviations of up to ±10% from the target RPM are considered acceptable due to measurement tolerances. These data points are critical for correlating engine RPM with emitted sound levels, especially for later processing and data validation. Although, engine speed is not always available to be measured.

Campaign 2 goal is to determine a transfer function between the roadside microphone and the on-board microphone. It is specific to the vehicle and the microphone position on the vehicle and at the trackside. Additionally, vehicles have different noise sources in different locations. Some of the noise sources are affected by distance to the microphone, shielding effects, directivity, etc. Regarding speed, doppler effect

This project has received funding from the European Union's Horizon Europe research and innovation programme under grant agreement No 101056777

should be also be considered. This function allows for later estimations of the on-board sound levels in real-world scenarios (Campaign 3) without requiring additional on-board equipment.
For this purpose, two controlled pass-by runs are executed at constant speeds between lines AA' and BB'. Each run is performed at a different constant vehicle speed, typically at 30 km/h and 50 km/h. These measurements provide the acoustic correlation between the external and internal (on-board) noise measurements. Once validated, this transfer function enables post-processing estimations of interior noise or engine-compartment noise, measured from rear side of the vehicle, for Campaign 3, thus simplifying instrumentation requirements and reducing complexity during field testing. Ideally both road-side and on-board measured have been developed.

Campaign 3 focuses on the execution of real-world driving maneuvers to capture dynamic noise emission behavior under realistic operating conditions. If Campaigns 1 and 2 have been completed successfully, Campaign 3 can be conducted without on-board instrumentation, using only roadside microphones. However, for highest accuracy and validation of the transfer function, it is still recommended to apply the full measurement setup, including on-board microphones and speed sensors. A total of 14 standardized driving maneuvers are executed, as outlined in Table 2-2 and Table 2-3, where maneuvers from Table 2-1 are integrated.

Table 2-2: Overview of real-world driving patterns for LVs with manual transmissions (MT)

No.	Pattern	Description
1-MT	Cold start / engine start	Stationary engine start
2-MT	Throttle control	Shortly activating and releasing throttle control, stationary
3-MT	Aggressive acc. from standstill	Aggressive acceleration from standstill, first gear
4-MT	Moderate acc. from standstill	Moderate acceleration from standstill, first gear
5-MT	Gear shift, first to second, from standstill	Short acceleration in first gear from standstill, shift into second gear, aggressive acceleration
6-MT	Aggressive acc. from const. speed, first gear	Aggressive acceleration from constant speed (< 10 km/h), first gear
7-MT	Gear shift, first to second, const. speed	Short acceleration in first gear from constant speed (< 10 km/h), shift into second gear, aggressive acceleration

This project has received funding from the European Union's Horizon Europe research and innovation programme under grant agreement No 101056777

8-MT	Full/ max. throttle acc., different gears	Full throttle acceleration from constant speed, different gears (e.g. gear 2, 3, 4 if feasible)
9-MT	Gear shift *i* to *i* + 1, from const. speed	Short acceleration in gear *i* from constant speed, shift into gear *i* + 1, aggressive acceleration
10-MT	Constant speed, gear *i*, high/max. engine speed	Constant speed in gear *i* with high/max. engine speed
11-MT	Gear shift, *i* to *i* - 1, from const. speed	Constant speed in gear *i* and downshift to gear *i* - 1, aggressive acceleration
12-MT	Gear shift, *i* to *i* - 2, from const. speed	Constant speed in gear *i* and downshift to gear *i* - 2, aggressive acceleration
13-MT	Intermittent throttle control, gear *i*	Constant speed in gear *i*, intermittent throttle control, fluctuating engine speed
14-MT	Deceleration, gear *i*	Constant speed in gear *i*, releasing throttle control, deceleration

The actual number of applicable maneuvers varies depending on the vehicle class and the transmission technology as some maneuvers from Table 2-2 are proposed to be driven in every gear possible. For example, vehicles of class L1e-B equipped with continuously variable transmissions (CVTs) do not feature discrete gear shifts. Therefore, maneuvers related to gear changes (e.g., maneuvers 5-MT, 7-MT, 9-MT, and 11-MT from Table 2-2) are either omitted or adjusted to speed-based variants. These modifications are detailed in Table 2-3 and are also applicable to all other CVT-equipped vehicles in the L-category.

Cold starts (maneuver 1-MT in Table 2-2 and maneuver 1-CVT in Table 2-3) are a relevant condition for acoustic testing, as they reflect a typical situation at the beginning of a vehicle trip. The engine operates with increased idling speed and less efficient combustion, which can result in higher mechanical and exhaust noise. This condition is important not only because it is acoustically prominent, but also because it occurs frequently in everyday vehicle use, especially in urban areas.

Maneuver 2-MT in Table 2-2 and 2-CVT in Table 2-3 simulate throttle control in neutral, where the engine speed is increased manually and held constant for a few seconds. This allows the acoustic response of the powertrain and exhaust system to be observed without the influence of vehicle movement. This test is useful to separate mechanical noise components and determine baseline noise behavior over engine speed. It serves as an important reference for the interpretation of dynamic driving noise.

This project has received funding from the European Union's Horizon Europe research and innovation programme under grant agreement No 101056777

Aggressive acceleration from standstill (Table 2-2, maneuver 3-MT and Table 2-3, maneuver 3-CVT) represents a situation where the rider accelerates rapidly from a full stop, such as when entering traffic or leaving an intersection. These events are acoustically significant due to high engine loads and rapid throttle changes, often resulting in pronounced exhaust and mechanical noise. This maneuver is also commonly encountered in urban and sub-urban traffic.

Moderate acceleration from standstill (Table 2-2, maneuver 4-MT /Table 2-3, maneuver 4-CVT) complements maneuver 3 by simulating a more typical start-up behavior under lower load. It provides contrast to the aggressive version and captures conditions that might be less acoustically extreme but more representative of average driving. Both maneuvers help to evaluate how engine behavior under different throttle demands affects noise levels.

Maneuver 6-MT from Table 2-2 (aggressive acceleration from low speed in first gear) and 5-CVT from Table 2-3 (aggressive acceleration from approx. 10 km/h) are acoustically relevant due to the high engine load, engine speed increase, and possible gear shift events. This situation often occurs when merging into traffic or overtaking from low speeds. For CVT vehicles, where no gear shifts occur, engine speed still rises significantly, producing strong acoustic output.
Maneuver 8-MT in Table 2-2 and its CVT in Table 2-3 equivalents (6-CVT and 7-CVT) simulate full-throttle acceleration from constant speeds of approximately 20 km/h and 50 km/h. These maneuvers are designed to replicate overtaking or fast merging scenarios. They are critical in acoustic studies due to the sustained high load and associated high sound pressure levels. Especially at higher speeds, aerodynamic and rolling noise components may also contribute.

Deceleration maneuvers (Table 2-2 maneuver 11-MT; Table 2-3 maneuvers 9-CVT and 10-CVT) represent a key aspect of real-world driving, particularly in urban traffic when approaching traffic lights or reducing speed in traffic flow. These events can lead to characteristic engine braking sounds, increased vibration noise, or exhaust backpressure effects. Although typically quieter than acceleration, they still provide relevant acoustic data due to their frequent occurrence.

Lastly, constant speed driving with intermittent throttle input (Table 2-2, maneuver 13-MT; Table 2-3, maneuvers 12-CVT and 13-CVT) replicates cruising behavior with slight speed and load variations, as seen in traffic-following situations. This maneuver is essential to capture noise variability due to engine and drivetrain behavior under partial load, which may lead to resonance or modulation effects in the noise signal. It also helps evaluate the vehicle's acoustic signature during steady-state operation, which may be important for long-term noise exposure assessments.

Table 2-3: Overview of real-world driving patterns for CVTs

No.	Pattern	Description
1-CVT	Cold start / engine start	Stationary engine start

This project has received funding from the European Union's Horizon Europe research and innovation programme under grant agreement No 101056777

2-CVT	Throttle control	Shortly activating and releasing throttle control, stationary
3-CVT	Aggressive acc. from standstill	Aggressive acceleration from standstill,
4-CVT	Moderate acc. from standstill	Moderate acceleration from standstill
5-CVT	Aggressive acc. from const. speed	Aggressive acceleration from constant speed (< 10 km/h)
6-CVT	Aggressive acc. from const. speed	Aggressive acceleration from constant speed (approx. 20 km/h)
7-CVT	Aggressive acc. from const. speed	Aggressive acceleration from constant speed (approx. 50 km/h)
8-CVT	Constant speed, high/ engine speed	Constant speed with high engine speed
9-CVT	Deceleration	Deceleration from 50 km/h
10-CVT	Deceleration	Deceleration from 30 km/h
11-CVT	Constant speed	Constant speed driving at 50 km/h
12-CVT	Low const. speed, rpm fluctuation, variable speed, accelerator intermittent	Shortly activating and releasing throttle control at low speeds
13-CVT	High const. speed, rpm fluctuation, variable speed, accelerator intermittent	Shortly activating and releasing throttle control at high speeds

This campaign provides the most comprehensive data on the acoustic behavior of L-category vehicles in conditions that closely resemble everyday use, contributing essential input for TA revisions and noise policy evaluation. All maneuvers are highly vehicle dependent and were only tested if feasible.

This project has received funding from the European Union's Horizon Europe research and innovation programme under grant agreement No 101056777

2.3 On-road and RDC exhaust emissions measurements

According to what was recommended in D6.1 (Table 4-2) each lab designed its own route, trying to cover the maximum engine operating points, including events not present in type approval operation conditions and therefore prone to generating high emissions. These routes have been developed to replicate the scenarios of the real-life usage of L- vehicles. All routes are meant to equally include urban, rural and motorway road types. They were computed taking into consideration the vehicle characteristics of each sub-category, this means engine size, power, usage, intended use, etc. Therefore, the distance covered depends on the vehicle sub-category. For mopeds, the total distance is typically around 20 km, for L3e-Ax subcategories (both A1, A2 and A3) and L5e- A and B, the total distance is around 40 km and finally, for L6e and L7e, the total distance is between 30 km. Driving dynamics have also been considered. Routes are designed to follow, typically, urban, rural and motorway shares as it is currently done on passenger cars, this means 33% respectively, discretized by speed according to Regulation (UE) 2017/1151.

To better examine the performance of LVs, in addition to the standard TA measurements on the chassis dyno, nearly all vehicles selected have also been subjected to RDC cycles. In addition to the standard on-road measurements, more complex routes have been conducted in which vehicles have been subjected to more aggressive or demanding dynamic conditions, this means, higher accelerations, late gear change, higher speeds, stop and go driving, etc. In sections 4.2 and 4.3, an analysis of how these more aggressive driving patterns affect pollutant emissions can be found.

The combination of both types of test cycles outside the current regulation (EU) 134/2014 has been designed with the main purpose of better covering the real-driving conditions, both in the chassis dyno, and on-road testing. In Figure 2-4 and Figure 2-5, different standard routes defined for LENS activities are shown. Additionally, in Appendix B: RDE Routes and Appendix C: RDC Cycles, all routes from RDE measurements and RDC cycles from L1eB and L3e-A1, A2 and A3, L5e, L6e and L7e are represented.

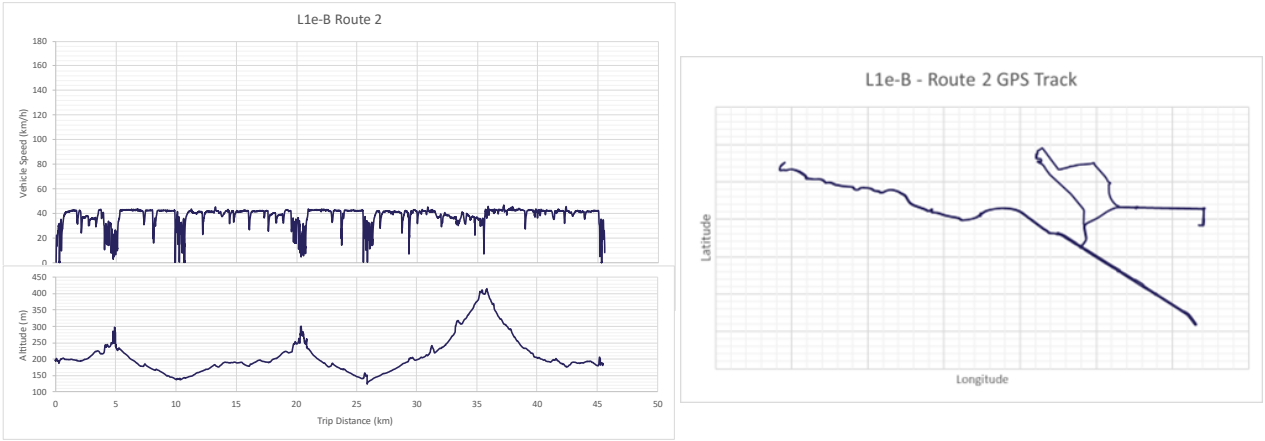

Figure 2-4: L1e-B route driving characteristics.

This project has received funding from the European Union's Horizon Europe research and innovation programme under grant agreement No 101056777

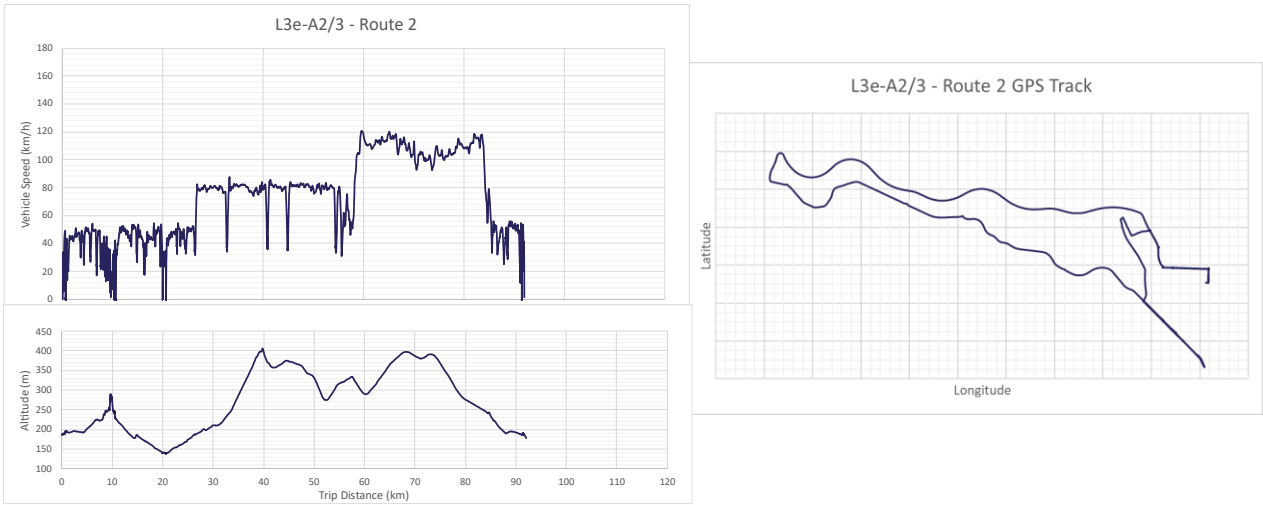

Figure 2-5: L3e-A2/A3 route driving characteristics.

This project has received funding from the European Union's Horizon Europe research and innovation programme under grant agreement No 101056777

3. RW Operation events to assess noise emissions

3.1 Introduction

Within the LENS project, a range of measurement campaigns was conducted to capture noise emissions from L-category vehicles under realistic and controlled conditions. These included on-road measurements performed in real traffic using on-board sensor technology [10] exemplary introduced in Chapter 2.1, as well as dedicated measurements on certified acoustic test tracks equipped with stationary microphone arrays. The primary objectives of these measurement activities were twofold: firstly, to identify driving maneuvers that are particularly critical in terms of noise emissions; and secondly, to support the evaluation and potential revision of existing vehicle TA procedures. These efforts aim to ensure that regulatory testing better reflects real-world driving scenarios and their associated noise emissions. As noise measurements in real traffic are difficult to obtain due to, e.g., background noise and the TA testing for noise is done on acoustic test tracks – meaning the emissions are evaluated there – the RW driving patterns were conducted on the acoustic test track.

Additionally, on-road data from L3e-A2 and L3e-A3 RDE measurements have been processed with Rotranomo, and therefore noise emissions simulations have been produced. Some high emission events documented in Table 2-2 from Deliverable D6.1 have been considered and deeply analyzed in Section 3.4.

3.2 On-road measurements to develop RW driving patterns to assess noise emissions

Within the LENS project, an on-board sensor system for capturing noise data in real traffic conditions was developed [10]. This sensor unit is equipped with a microphone and a GPS module. The primary function of the system is the simultaneous recording of sound pressure levels and vehicle location data. This enables the correlation of vehicle movement with noise emissions, allowing the identification of acoustically relevant driving scenarios. The system is designed to be portable and adaptable to various L-category vehicles [11]. At its core, a microcontroller serves as the control unit, featuring serial peripheral interfaces. The Micro-Electro-Mechanical Systems (MEMS) microphone converts sound pressure into electrical signals, while the GPS module records the location data. Both noise and position data are stored on a micro-SD card. For user-friendly operation, the device includes only a single switch to start and stop data recording. Due to the low power consumption of its components, the system is particularly well suited for battery-powered operation.

The sensor system was distributed to several project partners for testing and integration on different L-category vehicles. The objective is to use the recorded data to develop a methodology capable of detecting acoustically significant driving situations. As a first step, the optimal mounting position of the sensor on the vehicle was evaluated. To this end, the sensor was installed in various positions on multiple vehicles, and equivalent measurements were performed [12]. The measurement microphones showed similar temporal patterns, indicating that the identification of acoustically relevant driving scenarios is not significantly

This project has received funding from the European Union's Horizon Europe research and innovation programme under grant agreement No 101056777

affected by microphone position. Based on the results, the recommended mounting location for the system was selected to be centrally at the rear of the vehicle. On-road measurements test procedure has been already introduced in both this section, and section 2.1. In this chapter results from this specific campaign are analyzed both by driving patterns, and by engine operation points.

3.2.1 Results by driving patterns

In the following, the data evaluation of on-road measurements is discussed using two representative examples of L-category vehicles, both equipped with manual transmissions (MT) [13]. One vehicle is from the L3e-A1 class (shown in Figure 3-1) and the other is an L5e three-wheel motorcycle, with the results visible in Figure 3-2. It is important to note that the results from these two examples are not directly comparable to each other, due to differences in acoustic near-field measurement conditions. For each vehicle, the events with the highest A-weighted sound pressure levels (LAF) exceeding the 90th percentile were identified and analyzed individually. In the corresponding level-versus-time plots (see Figure 3-1 and Figure 3-2) the 90th percentile threshold is marked to highlight the relevant noise events.

Each identified condition in the dataset is assigned a number to represent the corresponding driving scenario. Driving conditions associated with elevated noise levels above the 90th percentile include short acceleration phases during driving (Figure 3-1, No. 1), acceleration from near standstill (Figure 3-1, No. 2 and No. 3), and steady-state driving (Figure 3-1, No. 5), as illustrated in Figure 3-1. Specifically, scenario No. 1 represents a short acceleration event, while No. 2 refers to acceleration from a near standstill. Scenario No. 3 involves acceleration from a standstill including gear shifts. No. 4 corresponds to acceleration during driving, also with gear shifts, and No. 5 denotes a phase of nearly constant driving. These events often involve dynamic engine behavior such as throttle application, gear changes, and typically end with deceleration phases due to throttle release and decreasing engine speed.

This project has received funding from the European Union's Horizon Europe research and innovation programme under grant agreement No 101056777

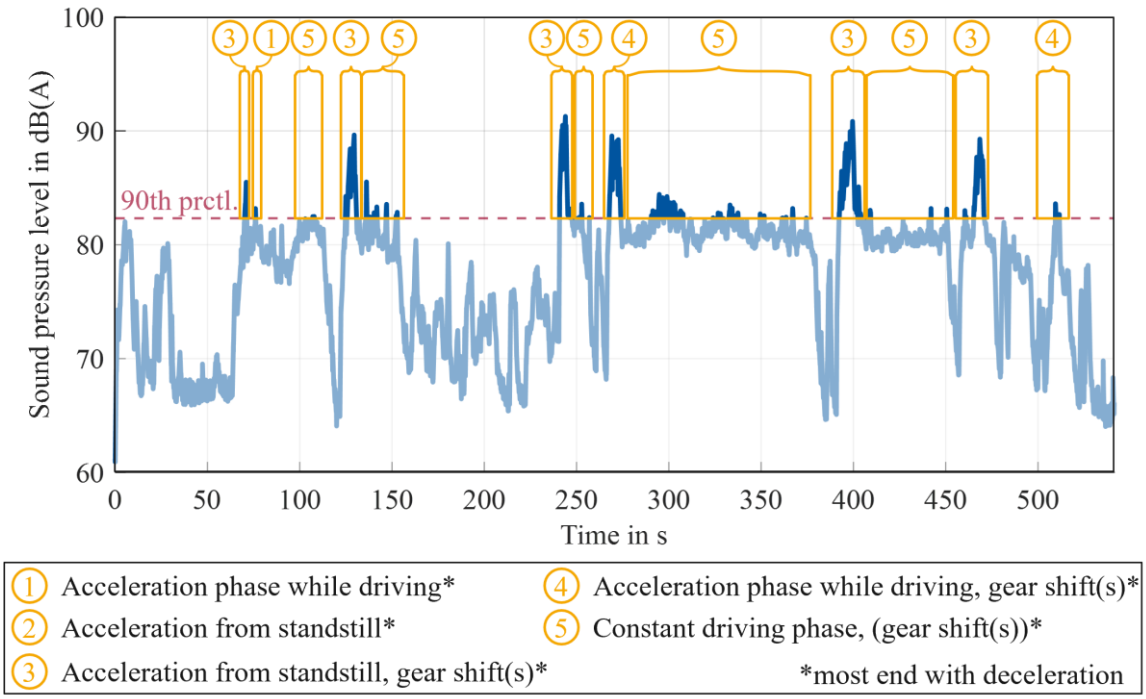

Figure 3-1: Level vs. Time on-road measurements of an L3e-A1 vehicle [13].

Regarding the frequency of these scenarios within the evaluated data sample: scenario No. 1 occurred once, No. 2 did not appear in the observed time segment, No. 3 occurred five times, No. 4 occurred twice, and No. 5—representing the longest durations—appeared five times. It should be noted that only events exceeding the 90th percentile threshold of the A-weighted sound pressure level are shown in this analysis. As a result, some typical driving maneuvers are not visible in this excerpt.

Following the previous analysis, Figure 3-2 presents the results for a second vehicle, representing the L5e category. As before, each identified condition is assigned a number indicating the corresponding driving scenario. Driving conditions associated with high noise levels above the 90th percentile include short acceleration phases during driving (Figure 3-2, No. 1), acceleration from near standstill (Figure 3-2, No. 2 and No. 3), and dynamic acceleration while already in motion involving gear shifts (Figure 3-2, No. 4). In this dataset, steady-state driving (Figure 3-2, No. 5) does not appear above the 90th percentile threshold and is therefore not visualized in Figure 3-2.

This project has received funding from the European Union's Horizon Europe research and innovation programme under grant agreement No 101056777

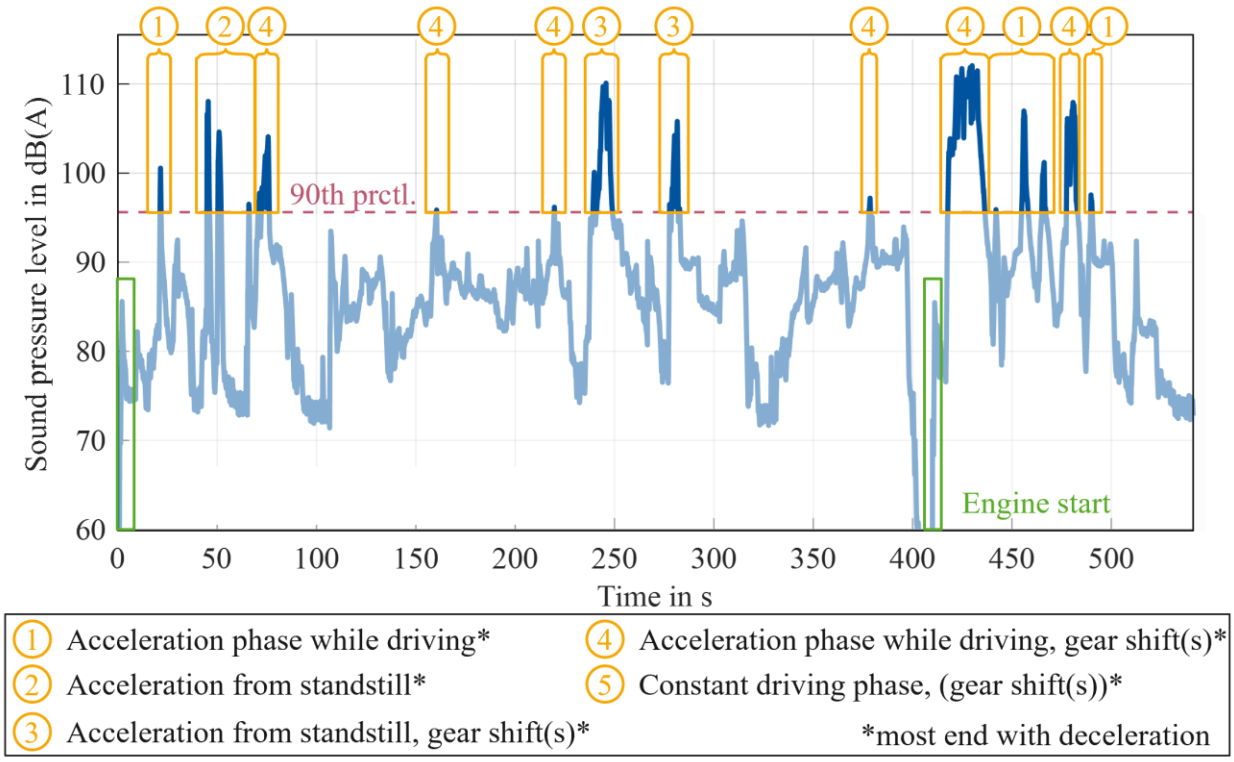

Figure 3-2: Level vs. Time on-road measurements of an L5e vehicle [13].

More specifically, scenario No. 1 (short acceleration phase) occurred twice, No. 2 (acceleration from near standstill) occurred once, and No. 3 (acceleration from near standstill including gear shifts) was observed twice. The most frequent pattern, No. 4 (acceleration during driving with gear shifts), was recorded six times. In contrast, scenario No. 5 (nearly constant driving phase) did not exceed the 90th percentile in this excerpt and is not represented in Figure 3-2. This absence of steady-state driving (No. 5) in the 90th percentile range is plausible for an L5e-category vehicle. Due to their design, weight, and typical powertrain characteristics, L5e vehicles often emit significantly higher sound pressure levels during dynamic operations such as acceleration, particularly when combined with gear shifts. In contrast, during phases of constant driving especially at moderate speeds – the engine load and associated acoustic output tend to be substantially lower. As a result, such conditions are less likely to produce sound levels high enough to surpass the 90th percentile threshold. This underlines the importance of focusing on transient driving events when assessing real-world noise emissions in this vehicle category. Noise increases with engine speed and engine load. A 90th percentile analysis will always provide a comparable picture. Driving situations with high dynamics or excessive engine speeds will always stand out. However, the level will shift.

3.2.2 Results by engine and vehicle speed

Figure 3-3 and Figure 3-4Figure 3-4 provide a detailed visual analysis of the sound pressure levels (SPL) measured during real-world driving conditions, presented for the two vehicle types previously discussed. In both figures, the left-hand plots display the SPL in dB(A) as a function of engine speed and vehicle speed, visualized using a color scale. The right-hand plots present the engine speed over the vehicle speed, again color-coded by the corresponding SPL in dB(A). These plots offer insights into how various operating

This project has received funding from the European Union's Horizon Europe research and innovation programme under grant agreement No 101056777

conditions—such as throttle application, gear selection, and speed—affect noise emissions, with a focus on their alignment with existing regulatory frameworks.

The left-hand plot in Figure 3-3 shows that high throttle application—approaching full throttle—typically results in elevated sound pressure levels, with values reaching approximately 90 dB(A). This trend highlights that substantial acoustic output is linked to engine load and throttle demand. A generally linear relationship is observed between engine speed and SPL, suggesting that noise emissions increase proportionally with rising engine speed. This finding supports previous observations reported in [6], underlining the consistency of this behavior across similar L-category vehicles.

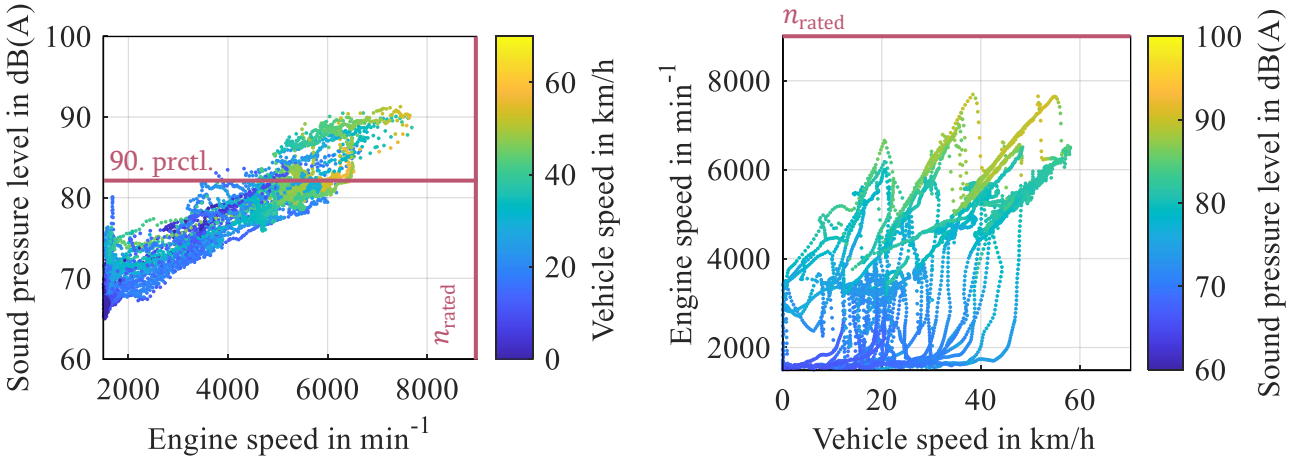

Figure 3-3: Relationship between SPL and engine speed and engine speed and vehicle speed for an L3e-A1 vehicle [13].

The right-hand plot of Figure 3-3 reveals further detail by illustrating SPL across combinations of vehicle speed and engine speed within specific gear ranges. The data suggest that certain gear selections—especially in combination with moderate vehicle speeds—are associated with peak SPL values. The relationship is not strictly linear, indicating the influence of additional factors such as gear shifts, transient throttle input, and engine load. An important regulatory consideration arises when these measurements are compared with the provisions of UN Regulation No. 41, which applies to L3 vehicles with a PMR greater than 50. According to this regulation, the RD-ASEP require that the engine speed at the moment the rear of the vehicle passes the designated line BB' of the test area (nBB') must not exceed 80% of the rated engine speed. For this specific vehicle, with a rated engine speed of 9000 min^{-1}, the upper limit for the RD-ASEP control range is thus 7200 min^{-1}. The right-hand side of Figure 3-3demonstrates that, under certain real-world urban driving conditions, some engine speed data points exceed this 80% threshold—despite occurring at moderate vehicle speeds. This observation raises the question of whether the current RD-ASEP boundary conditions accurately reflect real-world driving behavior. In practice, it may be necessary to reassess the RD-ASEP upper control limit for engine speed to ensure that all relevant and noise-critical scenarios are adequately covered by the regulation. Repeatable testing at very high speeds must be ensured.

Turning to Figure 3-4, which presents data for the second vehicle category, additional noise-critical driving behaviors are observed. The left-hand plot indicates that throttle inputs exceeding 80% are consistently associated with very high sound pressure levels reaching up to 110 dB(A). These values significantly exceed

This project has received funding from the European Union's Horizon Europe research and innovation programme under grant agreement No 101056777

those observed for the L3e-A1 vehicle and reflect the higher acoustic output potential of this vehicle category under load.

The right-hand plot shows a more nuanced view of how SPL varies across combinations of vehicle speed and engine speed. Notably, it becomes evident that the rated engine speed is exceeded under real-world driving conditions in multiple gears, especially within the vehicle speed range of approximately 50 km/h to 115 km/h, although specific driving behavior is dependent on the driver and driving conditions. This is particularly relevant in the context of UN Regulation No. 9, which governs noise emissions for vehicles with manual transmission. The regulation stipulates that the rated engine speed must not be exceeded when the vehicle passes line BB' in the test scenario. If this occurs, a higher gear should be selected to bring engine speeds within regulatory limits. However, the plots in Figure 3-4 show that this requirement is not consistently met in real-world conditions. Instead, the data demonstrates that high engine speeds are sustained even in lower gears and across a wide range of vehicle speeds, contributing to intense noise emissions. These findings underscore the limitations of the current regulatory approach when applied to unconstrained, real-world driving.

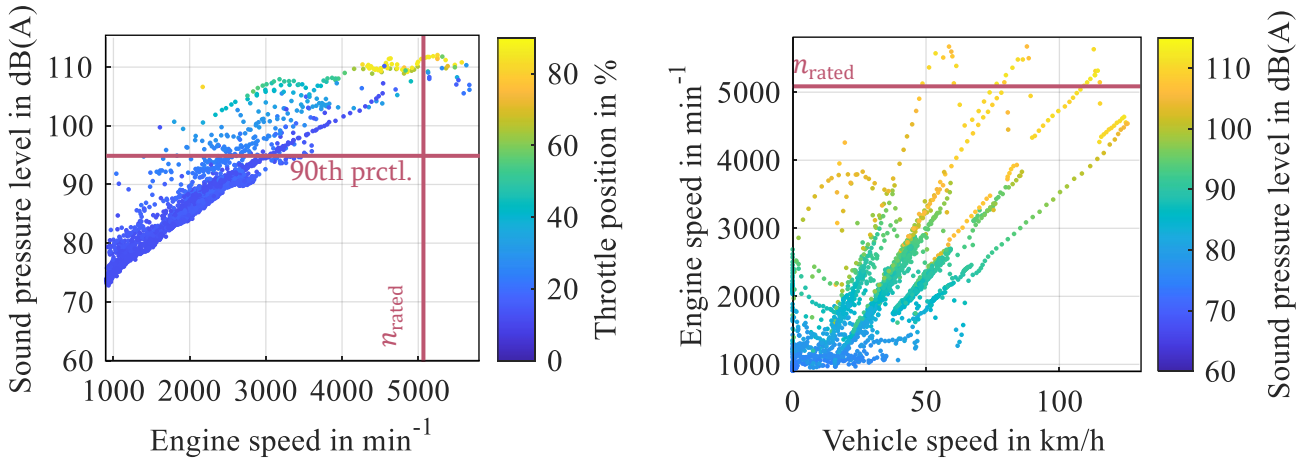

Figure 3-4: Relationship between SPL and engine speed and engine speed and vehicle speed for an L5e vehicle [13].

In addition, UN Regulation No. 9 defines an ASEP procedure for vehicles in the L4 and L5 categories with a PMR greater than 50—a condition which applies to the vehicle under study. According to the regulation, the ASEP control range for vehicle speed lies between 20 km/h and 80 km/h. However, as illustrated in the right-hand plot of Figure 3-4, high SPL values are also recorded outside this control range, particularly below 20 km/h and above 80 km/h. These elevated noise levels outside the regulatory control window suggest that the existing ASEP framework does not fully capture all noise-critical driving conditions for this vehicle type. This mismatch between regulation and empirical observation highlights the need to potentially expand the ASEP control range or revise its boundaries.

Additionally to this objective evaluation of different vehicles, a subjective approach is also done. Here, a listening experiment based on the measurement data shown above as well as an online survey conducted with people driving motor bikes was done. The subjective approach includes a time intensive listening and evaluation process by acoustic experts to manually evaluate the acoustic data for noise-intensive sound level classification. For each driving condition perceived as loud, the start time, the duration and the

This project has received funding from the European Union's Horizon Europe research and innovation programme under grant agreement No 101056777

corresponding noise-intensive driving condition are noted. This provides insight into the frequency of occurrence of various noise intensive driving conditions [13].

3.2.3 Subjective evaluation

Real-world driving patterns can generate high noise emissions in conditions not currently covered by the regulation, such as low-speed but high-throttle scenarios or high-speed driving in lower gears. A more comprehensive regulatory framework could ensure that noise emissions are adequately managed across the full spectrum of real-world driving conditions. Based on those measurements and surveys, critical driving patterns are analyzed in the following, with Figure 3-5 shown the results from the listening study. The characteristic driving conditions were taken from Deliverable D6.1 [8] and were supplemented with an additional driving condition, downshifting (number 10), that was also perceived as acoustically critical.

Additionally, some of the driving conditions were slightly adapted for evaluation purposes—for example, certain conditions were originally defined for first or second gear only. A driving condition refers to a time-defined segment of acoustic measurement data associated with potentially critical noise emissions. In the evaluation, the blue line represents the occurrence of each driving condition as a percentage of the total number of detected conditions, while the green line reflects the duration of each condition relative to the total recorded duration.

According to the blue line in Figure 3-5, driving conditions nr 1, 2, 5, and 9 each occur in less than 5% of the total events, indicating they are relatively rare in the data. Conditions nr 3, 4, 7, 8, and 10 appear more frequently, ranging between 5% and approximately 15%. Driving condition 6—characterized by a short but intense acceleration—has the highest occurrence rate. Looking at the green line, conditions nr 1, 2, 5, 9, and 10 each account for less than 5% of the total duration, whereas conditions nr 3, 4, 7, and 8 each contribute around 10% to 25%. Again, condition 6 stands out with the longest cumulative duration.

This analysis shows that every defined driving condition occurs at least once and could be subjectively perceived as loud or disturbing. Therefore, all identified driving conditions should be considered when developing representative real-world driving patterns. In the end, it is important to note that these findings may differ for in use vehicles including tampered or aged ones.

This project has received funding from the European Union's Horizon Europe research and innovation programme under grant agreement No 101056777

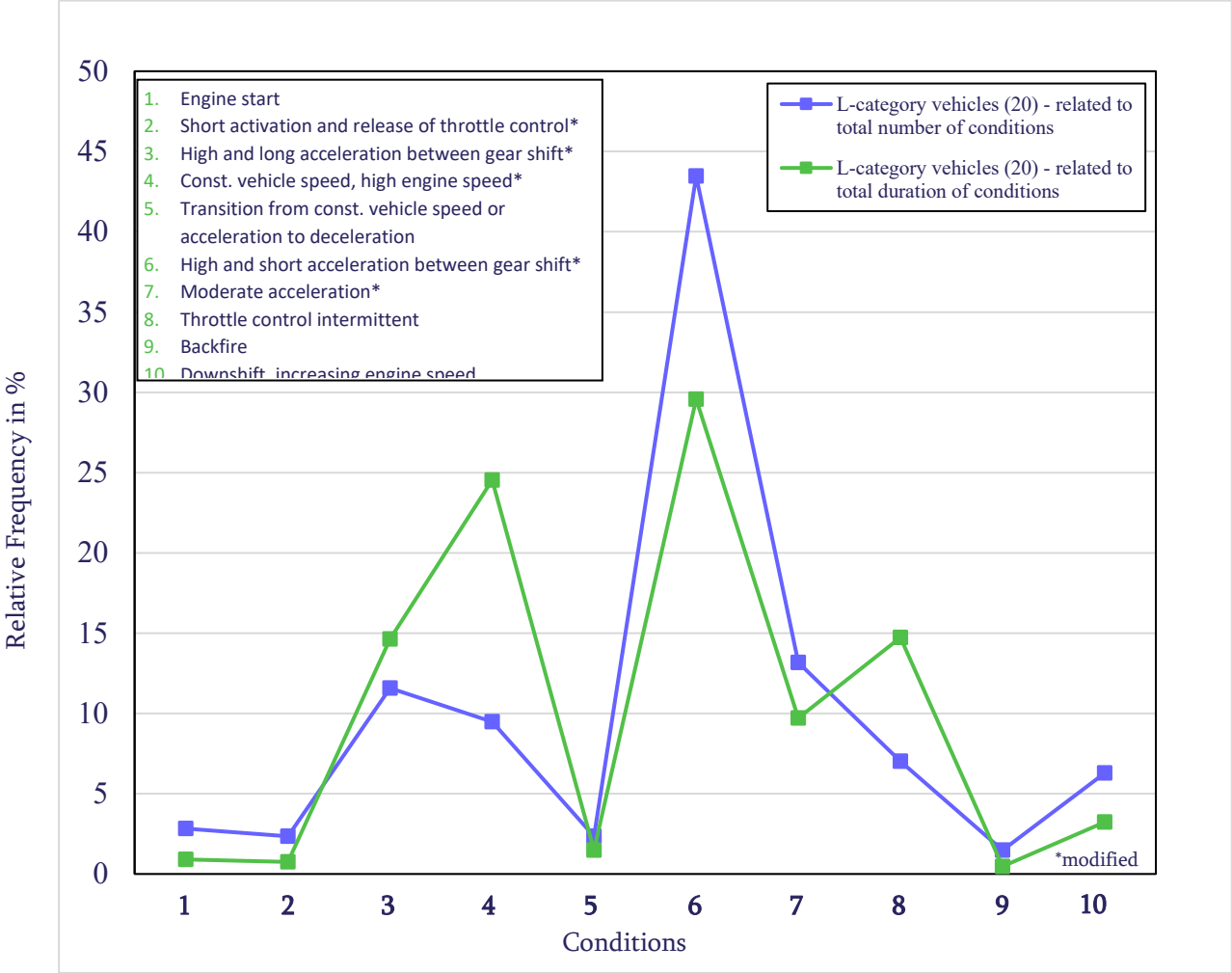

Figure 3-5: Results of the subjective listening evaluation for each driving condition [13].

Additionally, some of the driving conditions were slightly adapted for evaluation purposes—for example, certain conditions were originally defined for first or second gear only. A driving condition refers to a time-defined segment of acoustic measurement data associated with potentially critical noise emissions. In the evaluation, the blue line represents the occurrence of each driving condition as a percentage of the total number of detected conditions, while the green line reflects the duration of each condition relative to the total recorded duration.

According to the blue line in Figure 3-5, driving conditions nr 1, 2, 5, and 9 each occur in less than 5% of the total events, indicating they are relatively rare in the data. Conditions nr 3, 4, 7, 8, and 10 appear more frequently, ranging between 5% and approximately 15%. Driving condition 6—characterized by a short but intense acceleration—has the highest occurrence rate. Looking at the green line, conditions nr 1, 2, 5, 9, and 10 each account for less than 5% of the total duration, whereas conditions nr 3, 4, 7, and 8 each contribute around 10% to 25%. Again, condition 6 stands out with the longest cumulative duration.

This analysis shows that every defined driving condition occurs at least once and could be subjectively perceived as loud or disturbing. Therefore, all identified driving conditions should be considered when

This project has received funding from the European Union's Horizon Europe research and innovation programme under grant agreement No 101056777

developing representative real-world driving patterns. In the end, it is important to note that these findings may differ for in use vehicles including tampered or aged ones.

3.3 Assessment of the real-world driving patterns causing noise emissions

Based on the identified noise-relevant driving conditions, dedicated driving cycles were developed and executed on an acoustic test track to systematically evaluate their impact on vehicle noise emissions. These cycles were designed to replicate real-world maneuvers under controlled and repeatable conditions, enabling consistent comparison between vehicles and scenarios [13].

The following section first describes the measurement setup used during the test track sessions. This includes the positioning and specifications of the stationary microphones, data acquisition systems, vehicle instrumentation, and environmental parameters such as weather and surface conditions. Particular attention was paid to comply with the relevant international standards to ensure the validity and comparability of the results. Subsequently, the derived driving cycles are introduced. Each cycle was constructed to incorporate one or more of the previously defined critical noise conditions, such as acceleration from standstill, gear-shifting under load, or constant high-speed driving. The cycles vary in duration, speed profile, and gear usage, reflecting the diversity of driving behaviors observed in real traffic. These test track cycles form the basis for the subsequent evaluation of vehicle sound performance and the exploration of potential enhancements to current TA procedures.

3.3.1 Results of the analysis

The RW measurements were carried out by the project partners IDIADA, TUG, and RWTH Aachen University. In Section 2.2, Figure 2-1, the composition of the measured L-category vehicles is illustrated using a pie chart. This visual representation provides a clear overview of the distribution of vehicle classes within the scope of the measurement campaigns conducted in the LENS project.

The comprehensive measurement methodology described in the preceding sections, including on-board sensors, an artificial head for binaural recordings, and a multi-campaign test strategy, was designed to generate a rich dataset for various analyses within the LENS project. For the specific scope of this deliverable D3.5, the main analytical focus lies on roadside pass-by measurements, particularly the A-weighted maximum sound pressure level. This metric was prioritized as it is directly comparable to current Type Approval procedures and provides a practical basis for assessing real-world driving patterns in relation to existing regulatory limits. As such, the following sections primarily present and discuss results obtained from stationary roadside microphones recorded during driving events conducted on the test track.
While the full measurement setup also included on-board acoustic recordings and artificial head data for subsequent psychoacoustic and source-related analyses, these more complex evaluations are outside the scope of this report and will be covered in separate deliverables. The complete methodology is nonetheless presented in this report to ensure transparency and traceability of the measurement framework.

The data show that the largest portion of measured vehicles falls under the L3e category, which includes conventional two-wheeled motorcycles. Among these, vehicles classified as L3e-A3 – typically high-performance motorcycles without limitations on power or weight – represent the largest subgroup,

This project has received funding from the European Union's Horizon Europe research and innovation programme under grant agreement No 101056777

accounting for 32% of the total sample. L3e-A1 motorcycles, which are limited to 125 cm³ and 11 kW, amounts to 19% of the sample, while L3e-A2 vehicles, typically medium-powered motorcycles (up to 35 kW), represent also 19%. Another subgroup within L3e, the L3e-AxE class (mainly off-road motorcycles and enduros), is included with a share of 3%. Vehicles of the L1e category, which mainly include light two-wheelers such as mopeds and e-scooters with a maximum speed of 45 km/h, account for 18% of the samples. In contrast, no vehicles of the L2e class (three-wheeled mopeds) were included in the measurement campaign. This is primarily due to the very limited availability of such vehicles in the market and in real-world traffic. Given their low prevalence, the lack of L2e vehicles is not expected to significantly affect the overall conclusions regarding noise emissions of L-category vehicles. Beyond the core categories, a smaller share of the sample consists of other vehicle types. L5e vehicles (three-wheeled motorcycles, including tilting three-wheel scooters) and L6e vehicles (light quadricycles, often comparable to small city cars with limited performance) representing 2% and 1% of the measured fleet respectively. Vehicles from the L7e category – which includes heavy quadricycles with higher performance and weight capacity – are divided into L7e-B1 and L7e-B2 classes. L7e-B1 vehicles (generally passenger-type quadricycles) account for 5%, and L7e-B2 vehicles (typically cargo-type quadricycles) account for 1% of the measured sample.

Overall, the distribution of measured vehicles reflects the diversity of L-category vehicles currently in circulation, with a clear focus on those classes most relevant to noise emissions in everyday traffic, particularly the dominant L3e categories. Of all 112 vehicles subjected to RW noise measurements, only 2 vehicles were tampered, both L3e-A2 MT that originally were L3e-A3, now limited in power. Both tampering methods were aftermarket muffler with their corresponding db-killer.

Some selected results for all measurements can be found in the following figures which are sorted by the table order of Table 2-2 and Table 2-3, namely showing the results for vehicles with Manual Transmission (MT) first, followed by vehicles with Continuously Variable Transmission (CVT). Therefore, Figure 3-6, Figure 3-7 , and Figure 3-8 show the first three driving patterns for manual transmissions and Figure 3-9, Figure 3-10 and Figure 3-11 show the same three patterns for the CVT-vehicles These three first driving patterns are grouped due to their high degree of reproducibility and its capacity for being performed on almost all vehicles. This also results in Figure 3-6 and Figure 3-9 showing the results for driving pattern 1 (cold start), Figure 3-7 and Figure 3-10 showing the second driving pattern, namely the throttle control and lastly, and Figure 3-8 and Figure 3-11Figure 3-11 visualize the results of driving pattern 3, the acceleration from standstill. All other results from the different driving patterns can be found in Appendix D: Sound level distributions per vehicle class and driving condition. Visible is always the maximum sound pressure level (SPL), A-weighed, and with fast time weighting, measured on the PP' line distributed over the different vehicle classes as a violin plot. For each analyzed driving pattern, two individual measurements were generally conducted per vehicle; each data point shown in the plots represents the maximum of these two runs. The width of the violin is a normalized representation of the data distribution, it always reaches its maximum at the peak of the distribution. Therefore, the absolute width has no direct meaning; instead, it shows the relative density of the measured SPL values. This visualization helps to quickly see whether the SPL values for a given motorcycle category are concentrated around a specific level or more evenly spread across a wider range. Since the width is scaled, it's not a direct count of data points, but it does indicate how values are distributed relative to each other. When combined with a scatter plot of individual

This project has received funding from the European Union's Horizon Europe research and innovation programme under grant agreement No 101056777

measurements, the violin plot also makes it easier to spot outliers. More detailed analysis is presented in Deliverable D4.5 *Suggested revisions to TA procedure*.

Figure 3-6 shows the cold start for the manual transmissions, which only includes L3e vehicles, as the remaining vehicles where not MT. As this pattern is not highly dependent on the transmission, it shall be analyzed in close alignment with Figure 3-9. Both graphs show values from 50 dB(A) ranging to 80 dB(A) as a maximum. Most vehicles show a maximum SPL between 60 and 70 dB(A). Especially in Figure 3-6, the change in sub-categories from A1 through A2 to A3 an increase in the maximum SPL is visible. As the change to higher classes correlates to higher engine power, the conclusion can be drawn that higher engine power leads to louder engine starts. Although there is a considerable overlap in the sound pressure level distributions between the L3e subcategories, a general trend is observable: the medians and overall distributions tend to shift upwards with increasing engine power. This suggests that higher engine power tends to result in louder engine starts. However, due to the substantial variance within each class, this correlation should be interpreted with caution. Additional factors such as exhaust configuration, engine tuning, and cold start control strategies may also contribute significantly to the observed noise levels.

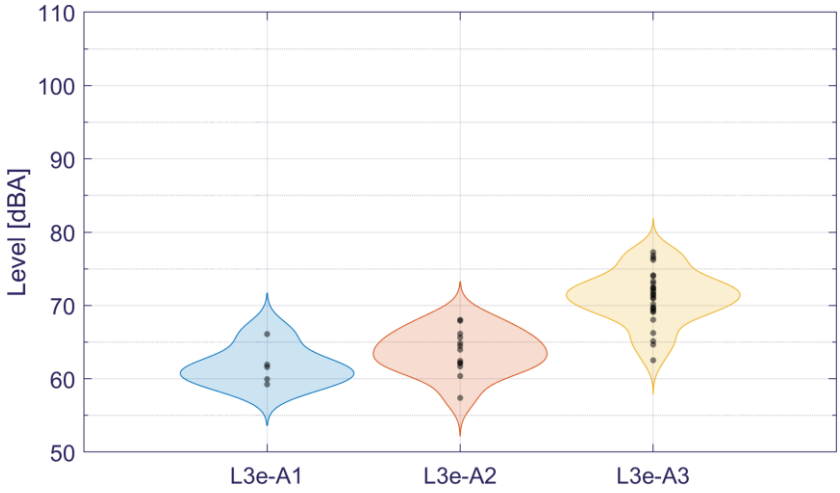

Figure 3-6: Level vs. Class on-road measurements for Driving Pattern 1-M: Cold start.

Figure 3-7 shows the second driving pattern which is the throttle control. This is also defined as a noisy pattern in D6.1. As this is also a procedure done in neutral, Figure 3-7 can again be analyzed together with Figure 3-9. It is worth mentioning that the darker the dot, the greater the overlap between measurements as opacity increases.

This project has received funding from the European Union's Horizon Europe research and innovation programme under grant agreement No 101056777

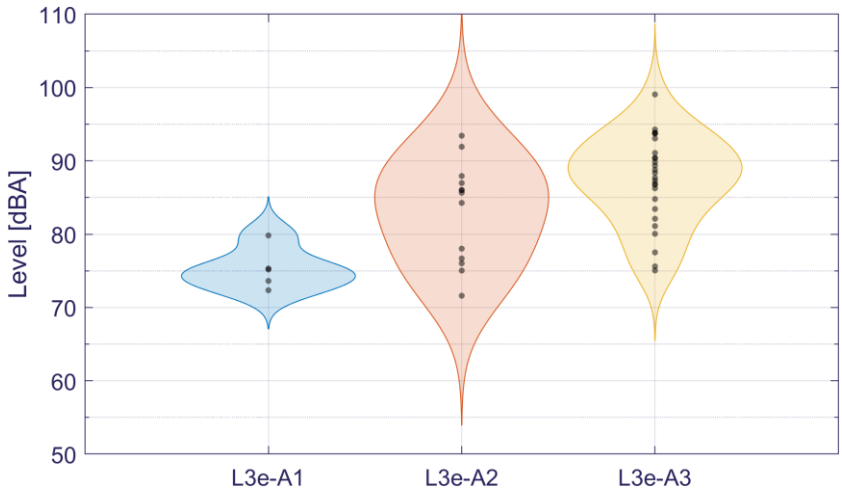

Figure 3-7: Level vs. Class on-road measurements for Driving Pattern 2-MT: Throttle control.

For Figure 3-7, values between 70 and 100 dB(A) can be seen, whereas Figure 3-9 shows values between 60 and 87 dB(A) leading to rather high values and showing rather a high range between lowest and highest values, where 60 dB(A) is not an exceptionally loud condition. This pattern is specifically interesting, as this is a maneuver which is known to be done while standing at a traffic light or a crossing. Those high values and therefore quite noisy maneuvers which occur in urban areas can be considered as quite disruptive. In correlation to Figure 3-6, Figure 3-7 shows the same trend over the different subcategories: Higher engine power leads to higher values and therefore louder phenomena. The third results explained here are derived from the third driving pattern which a heavy acceleration from standstill. Here, the motorcycle is placed on AA' in standstill and a wide open throttle acceleration is driven until the vehicle reaches BB'. The results for the manual transmission are shown in Figure 3-8. The results are even higher than the one for the second driving pattern just analyzed in Figure 3-7. The results vary between 77 dB(A) from an L3e-A2 to over 105 dB(A) for an L3e-A3 vehicle. The trend which is also analyzed in the last two patterns is visible here: The subcategory for the highest engine powers (L3e-A3) reach the highest values, whereas the subcategory for the lower engine powers (L3e-A1) has the lowest deviation (visible through the outline of the violin plot).

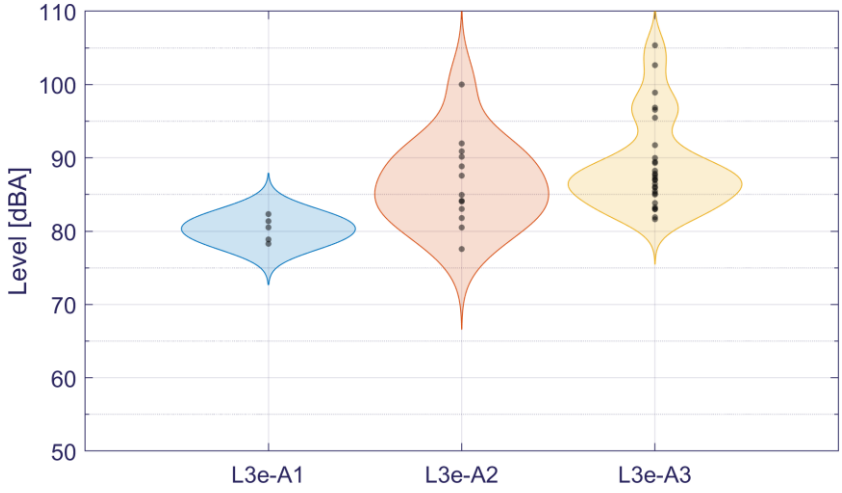

Figure 3-8: Level vs. Class on-road measurements for Driving Pattern 3-MT: Aggressive acceleration from standstill.

This project has received funding from the European Union's Horizon Europe research and innovation programme under grant agreement No 101056777

For the CVT-vehicles, Figure 3-9 shows the driving pattern 1, the engine start. Here, all medians are rather close together between 60 and 70 dB(A), especially compared to the Figure 3-6. As the database is smaller for L5e, L6e, and L7e, the statistical analysis shall be looked at cautiously. However, it is quite interesting to note the two distributions for the two L7e subcategories as well as slightly for the L5e vehicles.

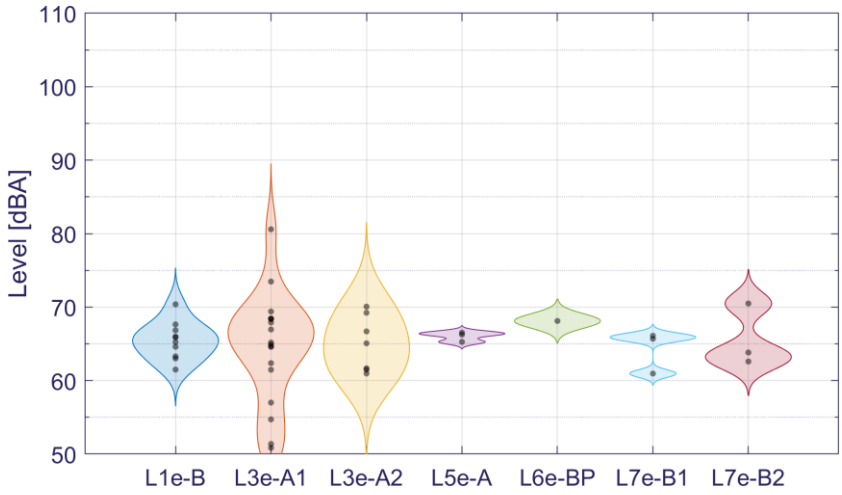

Figure 3-9 Level vs. Class on-road measurements for Driving Pattern 1-CVT: Cold start.

The throttle control for CVT-vehicles is shown in Figure 3-10. Comparing those values for throttle control to the engine start from the previous analysis, the increase in the overall level is shown. The violins in Figure 3-10 show generally higher values than the ones in Figure 3-9. This is surely reasonable due to the increase in the engine speed per maneuver definition.

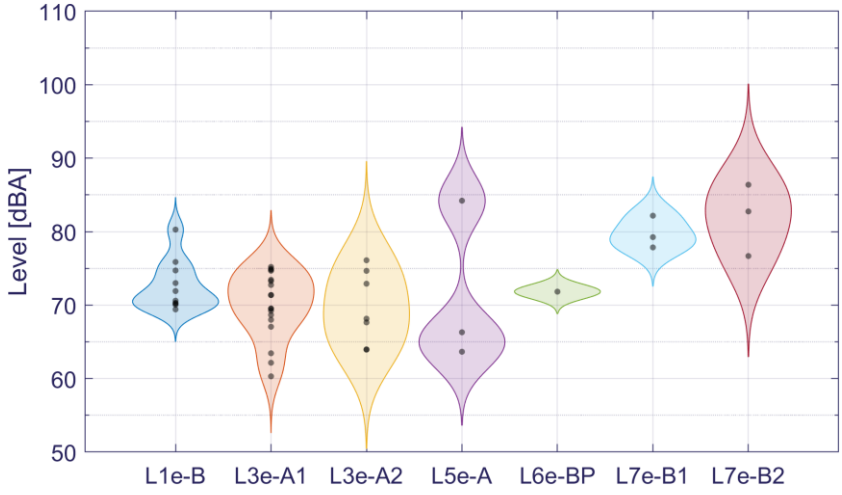

Figure 3-10 Level vs. Class on-road measurements for Driving Pattern 2-CVT: Throttle control.

For the L7e categories, small deviation of the measurements is shown. Here, the L5e vehicles show a more prominent shape. Again, due to the smaller data basis for those vehicle categories, the statistical analysis shall be looked at with caution.

This project has received funding from the European Union's Horizon Europe research and innovation programme under grant agreement No 101056777

For the last driving pattern analyzed in detail, Figure 3-11 shows the high acceleration from standstill for CVT vehicles. Here, no gear change is possible and therefore an engine speed ramp up correlating to the vehicle speed is assumed. For the subcategories L1e, L3e-A1 and L3e-A2 an increasing level over those three categories due to the higher engine power is shown which was also visible in the previous analysis of the manual transmissions. The L5e shows high dispersion, with two nearest values of over 10 dB(A) and one value near 85 dB(A) whereas the L7e-B1 only covers a range of a few dB(A).

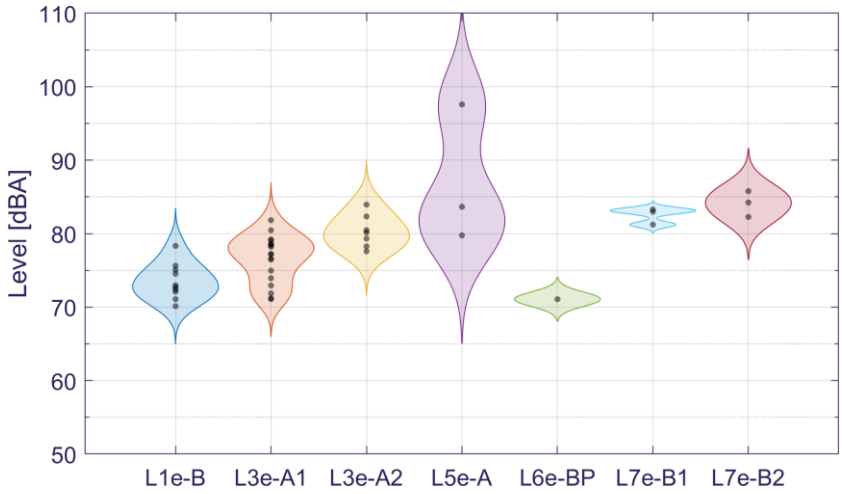

Figure 3-11: Level vs. Class on-road measurements for Driving Pattern 3-CVT: Aggressive acceleration from standstill.

Additionally, for two vehicles being representative for their respective sub-category, some patterns shall be looked at slightly more detail. For this more detailed analysis, sampling frequency of 48 kHz, with Hanning window of 2048 and a 50% overlap has been considered. The selected vehicles are, an L3e-A1 vehicle and an L3e-A3 due to their high relevance in current fleets. This L3e-A1 motorcycle also has a measured L_{urban} value of 71 dB(A) obtained according to current type approval procedure [18]. This provides a reference for the typical overall noise level expected under standardized legislative testing conditions. In Figure 3-12, Figure 3-13 and Figure 3-14 the results from three different driving patterns are shown for this L3e-A1 vehicle. Figure 3-12 shows the engine start which is driving pattern 1. The maximum sound pressure level recorded was 61.59 dB(A) on the exhaust side of the vehicle, where microphone was positioned in line PP'. This peak occurs during the ignition phase, manifesting as a short 100 ms burst with strong spectral content between 1 kHz and 8 kHz. After ignition, the signal stabilizes to a steady idle level.
The spectrogram reveals dominant tonal components during the ignition, which quickly diminish as the engine enters a steady idle state.

Compared to the broader database shown in the violin plot in Figure 3-6, this maximum level lies in the densely populated region of the distribution for this class and driving condition, indicating that the measurement is representative of typical engine start behavior for L3e-A1 motorcycles.

This project has received funding from the European Union's Horizon Europe research and innovation programme under grant agreement No 101056777

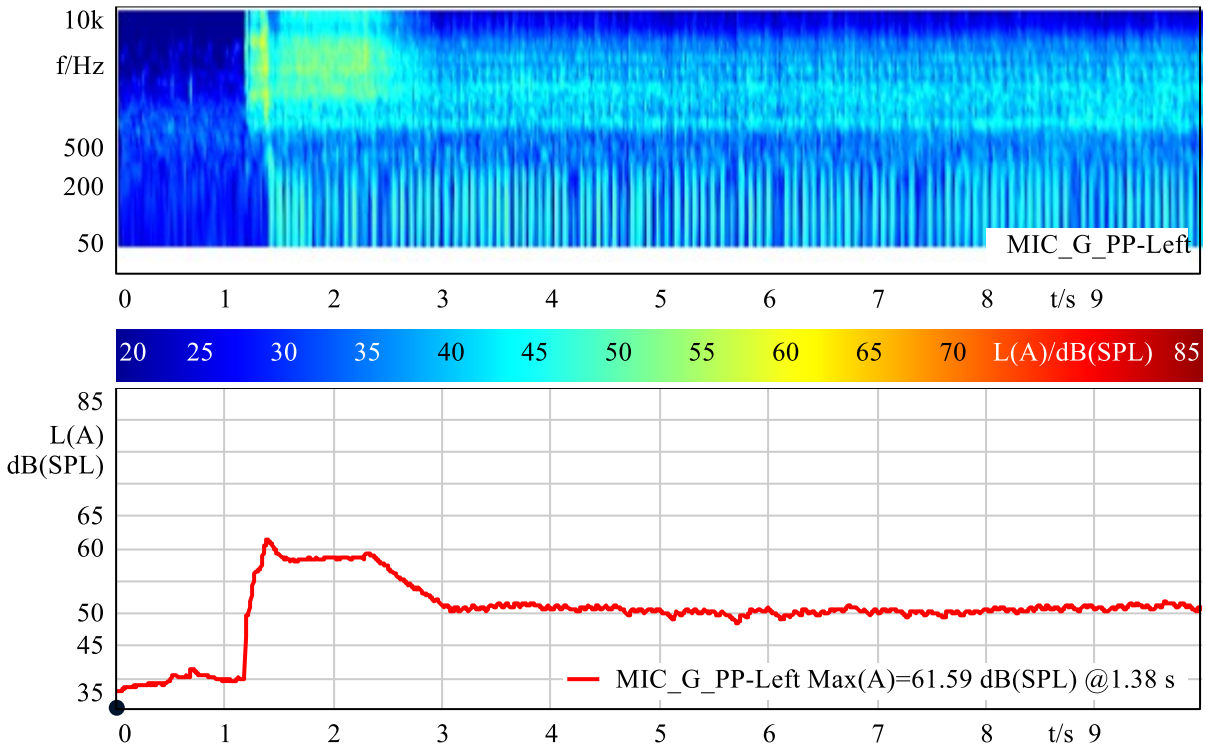

Figure 3-12: Spectrogram and SPL over time of an L3e-A1 during engine start (driving pattern 1) from microphone positioned in PP' at a 48 kHz sampling frequency.

Figure 3-13 shows the driving pattern 3 for the L3e-A1 vehicle which is heavy acceleration from standstill in the first gear. A maximum of 81.36 dB(A) was registered by the right microphone, which is coherent with the exhaust position. The event begins with stationary idling, followed by full-throttle acceleration through the pass-by microphone zone. The spectrogram shows a broad dB(A) and an increase in noise level with significant energy up to 8 kHz, especially between 6 and 8 seconds. In contrast to engine start, the spectrogram reveals a strong contribution from tire–road interaction noise, along with tonal engine components. The rising and falling tonal bands reflect the variation in engine RPM. This sound level falls within the most frequent range of the distribution in the violin plot for this class and driving condition, confirming that the measurement is characteristic of L3e-A1 motorcycles during strong acceleration from standstill. It is worth noting that this driving condition can be compared to the L_{wot} measurement defined in current type approval procedures, where the vehicle accelerates at wide open throttle. Explanations regarding the type approval procedures can be found in [14]. For this motorcycle, the L_{wot} value reported under those conditions is 73.1 dB(A) [18]. The difference of approximately 8 dB between the L_{wot} value and the levels observed here is expected, as the initial conditions vary. Consequently, it is reasonable that this situation produces higher noise levels than those typically measured in standardized L_{wot} tests. This discrepancy is important to note as this driving pattern is very common in real traffic scenarios, such as at traffic lights or urban intersections, where pedestrians are often exposed to such noise levels.

This project has received funding from the European Union's Horizon Europe research and innovation programme under grant agreement No 101056777

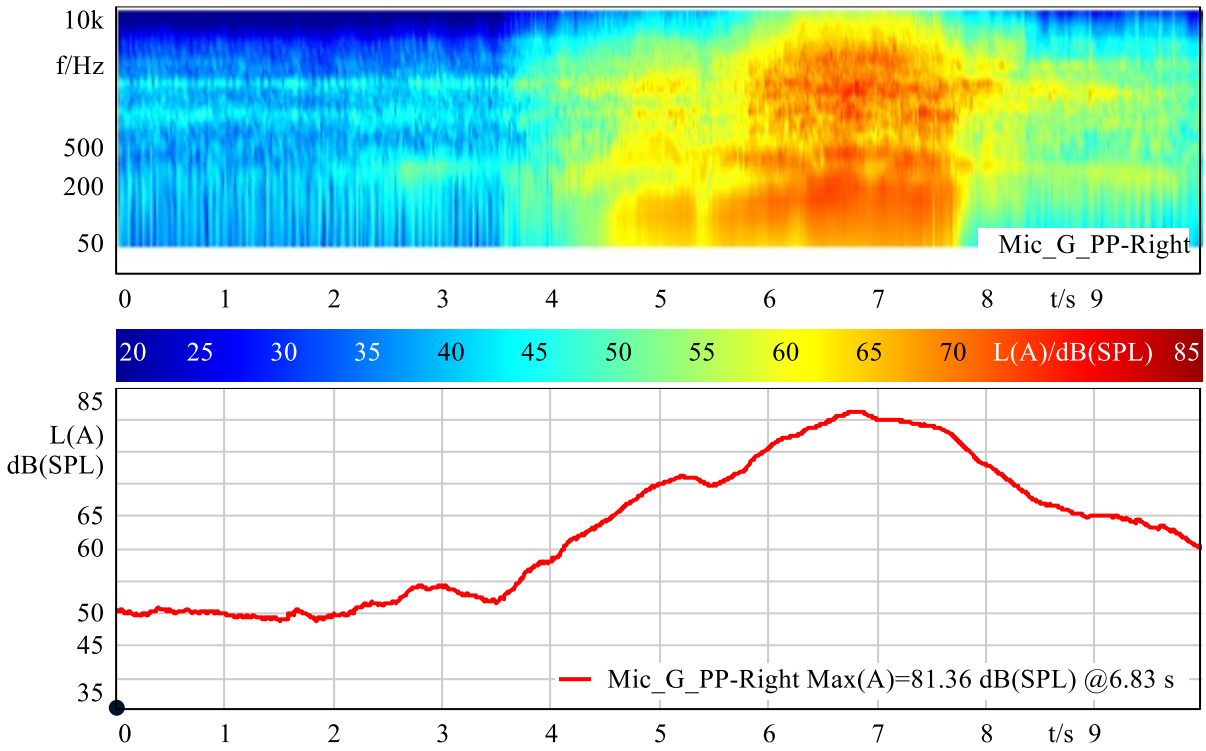

Figure 3-13: Spectrogram and SPL over time of an L3e-A1 during heavy acceleration from standstill (driving pattern 3) from microphone positioned in PP'.

The last measurement shown for the L3e-A1 vehicle is a stationary rpm measurement conducted at 3000 min^{-1} shown in Figure 3-14. The maximum sound pressure level was 59.85 dB(A), recorded by the right microphone, consistent with the exhaust side. The sound pressure level remains stable within ±1 dB, indicating high repeatability and good control of engine RPM during the condition. The spectrogram displays a strong stationary tonal component around 2 kHz, with minimal frequency modulation, this could be related to a structural resonance excited by combustion pulses, or possibly a dominant exhaust-related acoustic mode. The limited frequency resolution in the low-frequency range may have also contributed to the weak visibility of lower orders in the spectrogram. This level is located within the high-density region of the violin plot, meaning the measurement is representative of standard behavior for this class under stationary condition at 3000 min^{-1}.

This project has received funding from the European Union's Horizon Europe research and innovation programme under grant agreement No 101056777

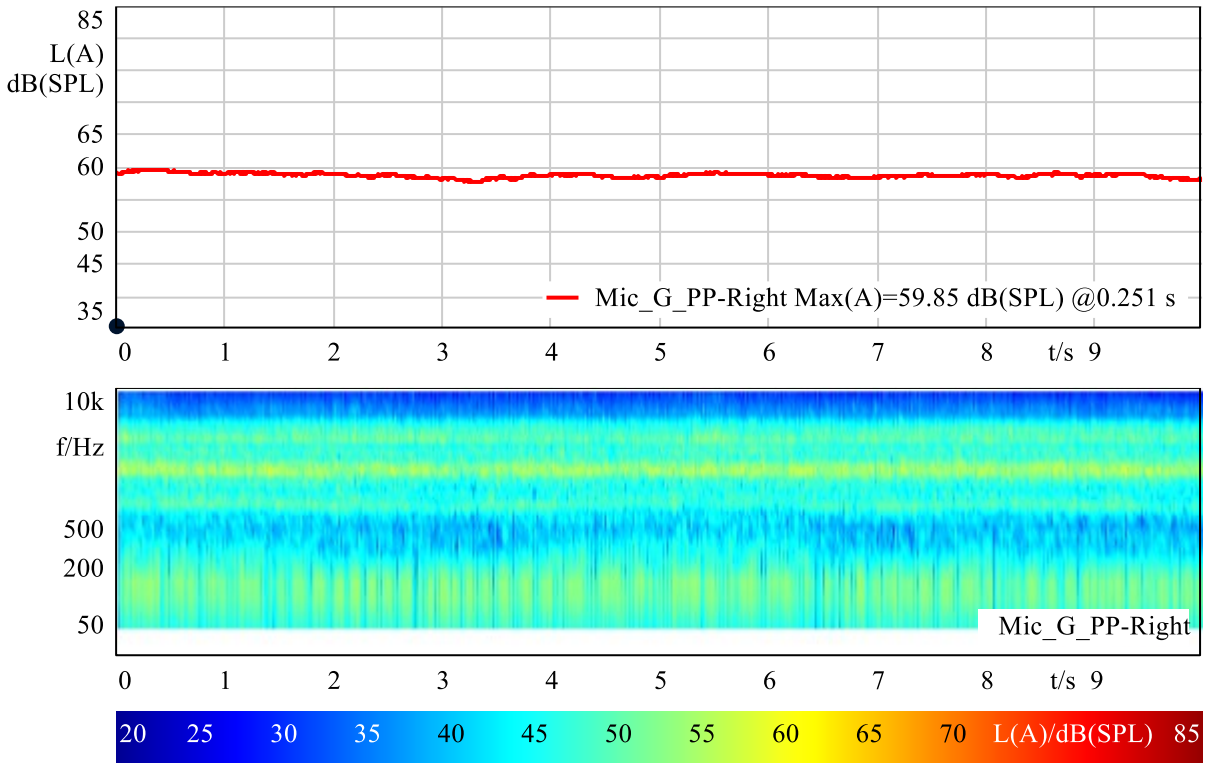

Figure 3-14: Spectrogram and SPL over time of an L3e-A1 at stationary rpm from microphone positioned in PP'.

Lastly, one L3e-A3 vehicle shall be analyzed according to the previously done analysis. This motorcycle also features a Type Approval measurement, with a reported value L_{urban} of 75 dB(A), offering a useful baseline for interpreting the sound levels observed under the various driving conditions presented here. Figure 3-15 shows the driving pattern 1, engine start, for a this L3e-A3 vehicle. The highest level was 73.01 dB(A), measured by the right microphone, which matches the actual position of the exhaust. The ignition peak occurs at 3.6 seconds, about one second after starter motor engagement, with dominant frequency components from 50 to 500 Hz and 1 to 6 kHz. The sound pressure level stabilizes at around 65 dB(A), which is only 8 dB below the ignition peak — less abrupt than the 12 dB difference observed in the L3e-A1 vehicle. This higher and more continuous or relatively steady SPL idle noise is characteristic of motorcycles in this power category, with some exceptions in which idle is relatively low. The measured peak falls within the most populated range of the distribution for class L3e-A3 in this driving condition, confirming the measurement as typical of engine start events for this class.

This project has received funding from the European Union's Horizon Europe research and innovation programme under grant agreement No 101056777

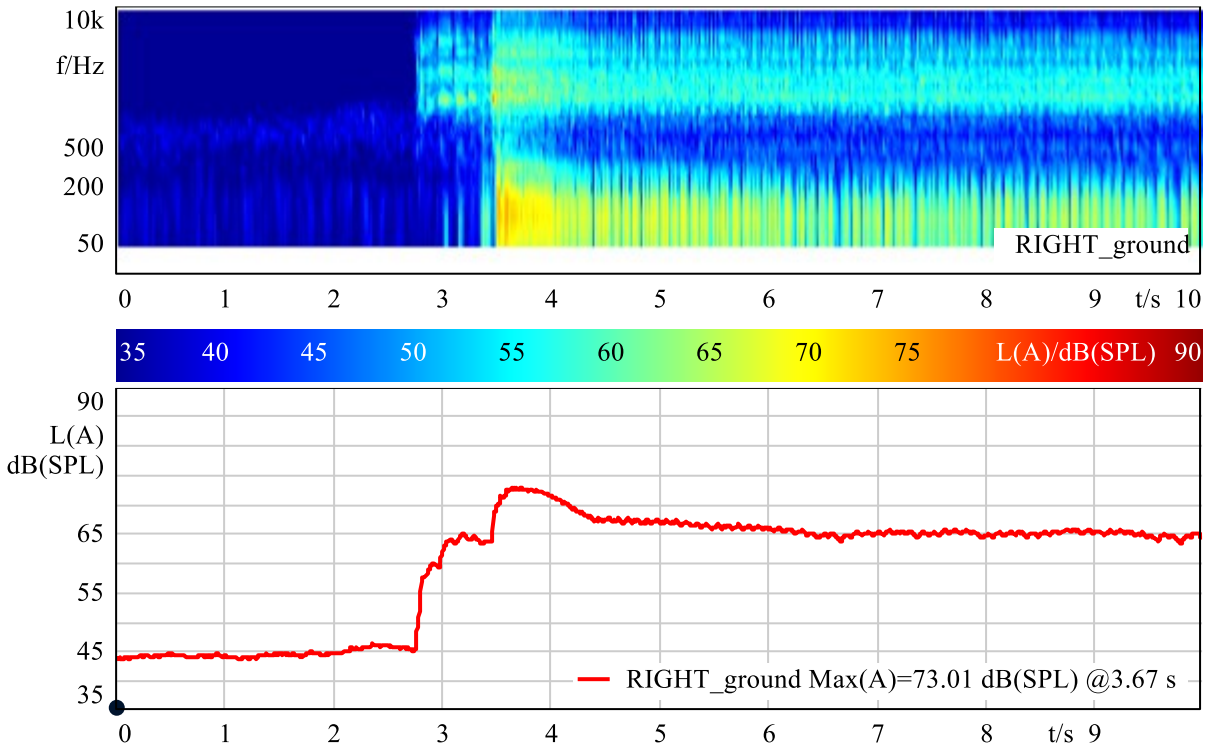

Figure 3-15: Spectrogram and SPL over time of an L3e-A3 during engine start (driving pattern 1).

Figure 3-16 shows the third driving condition. A maximum of 87.65 dB(A) was recorded on the left microphone, which is not consistent with the known exhaust location on the right. However, the difference in maximum levels between the two microphones is less than 1 dB, which may be attributed to minor asymmetries or environmental effects. The sequence begins with idle, followed by strong acceleration through the pass-by zone. The spectrogram shows intense low-frequency components between 50 and 200 Hz, along with broad energy up to 8 kHz. A sudden drop in level around 5.2 seconds reflects an abrupt throttle release. This level is within the main cluster of values observed in the violin plot for L3e-A3 motorcycles under this driving pattern, making it typical despite the minor channel discrepancy. In this case, the L_{wot} value obtained under type approval conditions is 79.5 dB(A), which differs by approximately 8 dB from the maximum level observed in this driving pattern. This difference is consistent and expected, considering that the standardized L_{wot} test starts in moving conditions, unlike the current condition which starts from idle. Additionally, for this motorcycle, the L_{ASEP} (2nd gear) value is also available [18]. This procedure involves crossing the AA-line at 20 km/h and accelerating at full throttle, making it more comparable to the present condition. The reported L_{ASEP} (2nd gear) value is 86.6 dB(A), which differs by only about 1 dB from the maximum value measured in this test.

Lastly, Figure 3-17 shows the stationary rpm measurement. The maximum sound pressure level was 70.73 dB(A), captured by the right microphone, consistent with the exhaust side. Level variation remains within ±1 dB, confirming repeatability of the measurement. The spectrogram reveals broad frequency content with clear tonal components around 2 kHz (which could be again originated from structural resonances, excited under stationary conditions, while not directly linked to the engine firing frequency), resembling the pattern observed in the L3e-A1 previously analyzed.

This project has received funding from the European Union's Horizon Europe research and innovation programme under grant agreement No 101056777

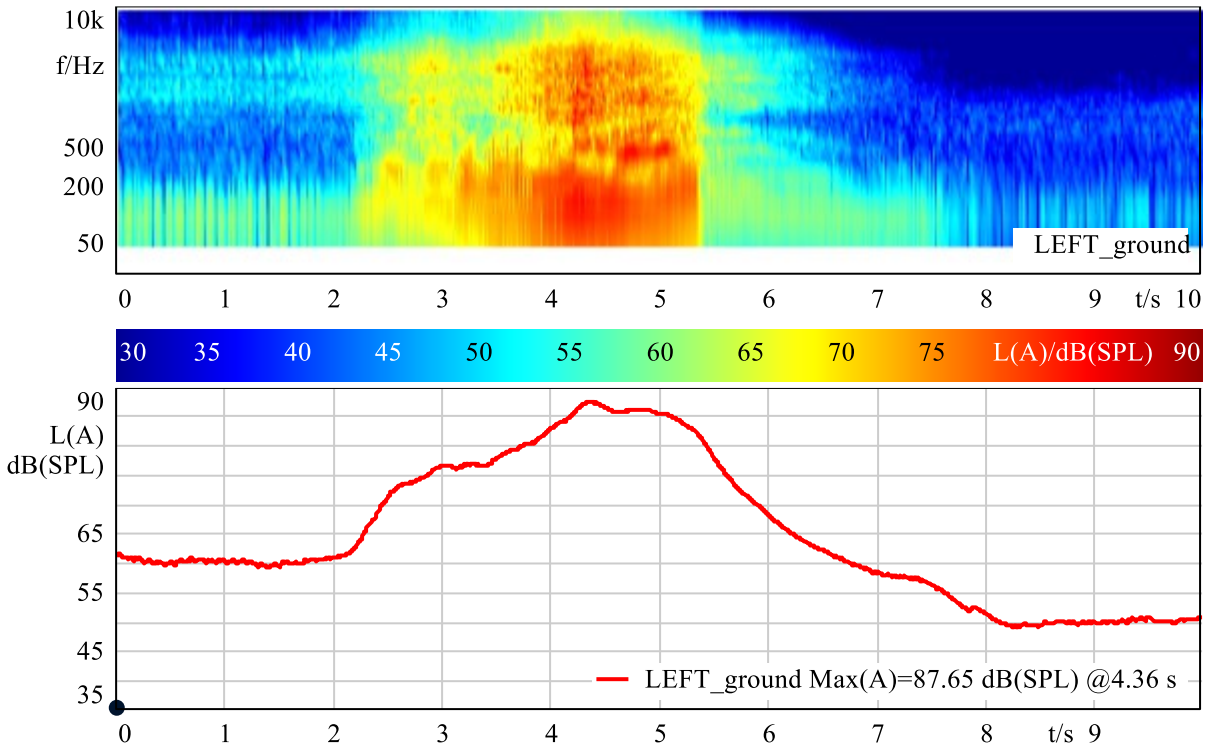

Figure 3-16: Spectrogram and SPL over time of an L3e-A3 during heavy acceleration from standstill (driving pattern 3).

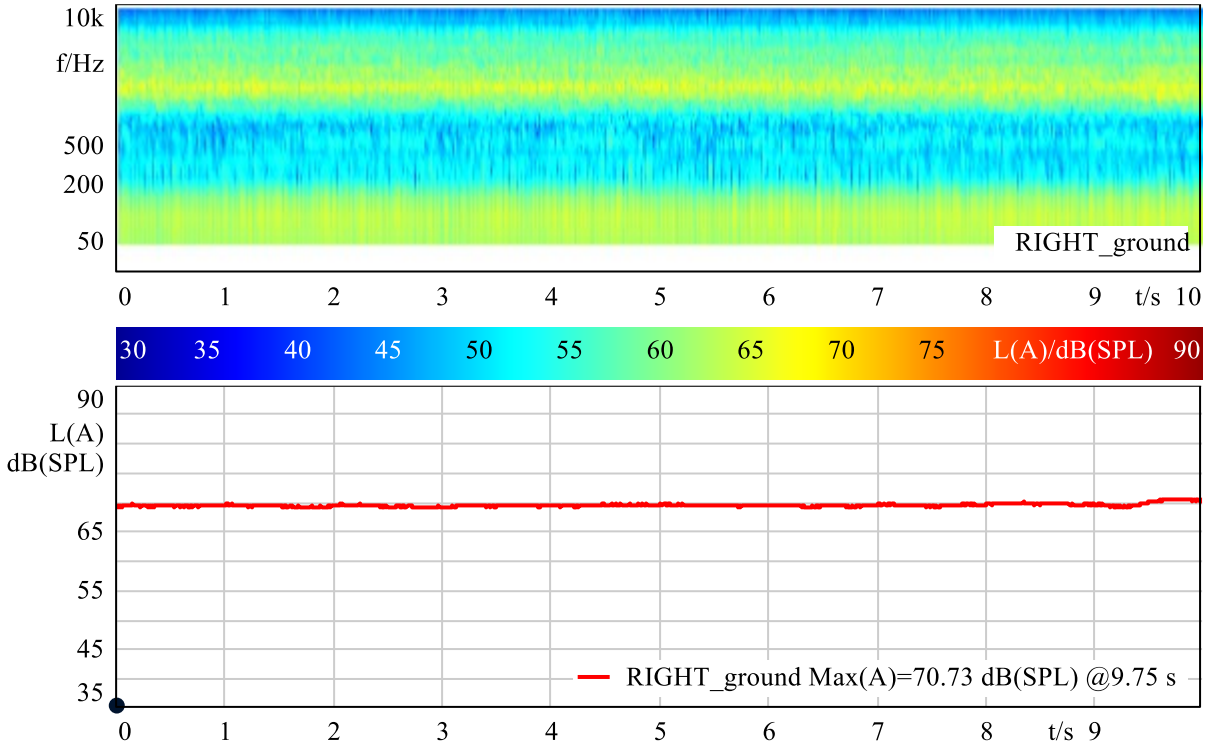

Figure 3-17: Spectrogram and SPL over time of an L3e-A3 at stationary rpm.

This project has received funding from the European Union's Horizon Europe research and innovation programme under grant agreement No 101056777

However, the overall level in Figure 3-17 is roughly 10 dB higher, in line with the general increase in engine output and power for class L3e-A3. This measurement falls within the central concentration of values in the violin plot, confirming it as typical for this class and condition.

When comparing the noise levels measured in the present analysis with those reported under type approval procedures, a relevant observation emerges. The L_{urban} values—71 dB(A) for the L3e-aA1 and 75 dB(A) for the L3e-A3—are notably lower than the levels measured in the alternative driving conditions analyzed here. For instance, the Heavy Acceleration from Standstill resulted in maximum levels of 81 dB(A) and 87.5 dB(A) respectively, exceeding the TA values by more than 10 dB in both cases.

It becomes evident that the L_{urban} value alone does not necessarily reflect the actual noise exposure experienced by pedestrians and residents in real-life traffic situations. Since it is derived from a specific and limited set of conditions, it may fail to capture the peak levels produced during more dynamic or aggressive driving patterns. As a result, relying solely on this indicator can lead to an underestimation of the true acoustic impact of motorcycles in urban settings.

Some examples of the sound characteristics of individual driving conditions measured on test tracks are shown in Appendix E: Sound characteristics of critical driving conditions measured on test tracks. These show frequency content and time dependency of some selected driving conditions. Most of these produce high enough sound levels to merit including in a type test and show similarities with roadside measurements in normal traffic included in LENS deliverable report D6.1. Indeed, the analysis confirms that several real-world driving conditions, many of which are not covered by current Type Approval (TA) procedures, produce significant noise levels. An overview of the key conditions identified as acoustically critical includes aggressive acceleration from standstill, rapid engine revving (rpm bursts) while stationary, and constant speed driving at high engine RPMs. The test track measurements demonstrate that these maneuvers, particularly aggressive accelerations, can generate peak sound levels exceeding a vehicle's overall TA limit value by more than 10 dB. Given their frequent occurrence in real-world traffic and their substantial acoustic impact, the findings strongly suggest that incorporating such dynamic driving patterns into future TA test procedures would lead to a more representative assessment of motorcycle noise emissions.

3.4 Assessment of the real-world driving patterns causing noise emissions from RDE modelled data

In this chapter the RDE cycles derived within the project for the assessment of exhaust emissions and described in detail in chapters 4.2 to 4.5 of this report were used to estimate the noise emissions using the Rotranomo model in order to assess driving conditions with high noise emissions. The noise emissions modelling was based on measured engine speeds whenever possible but for some cases in addition based on engine speeds that were calculated with the transmission module of the model for different gearshift behavior (low revs, average and high revs) in order to assess the gearshift behavior of the measured engine speeds.

This project has received funding from the European Union's Horizon Europe research and innovation programme under grant agreement No 101056777

3.4.1 Approach for the analysis: Rotranomo noise level modelling

The noise modelling is based on linear functions of the noise emission at no or negative engine load and at full engine load versus normalized engine speed as shown in Figure 3-18. Partial load conditions are interpolated between both curves depending on the load factor. The engine speed normalization is done in a way that idling speed is 0 and rated engine speed is 100%.

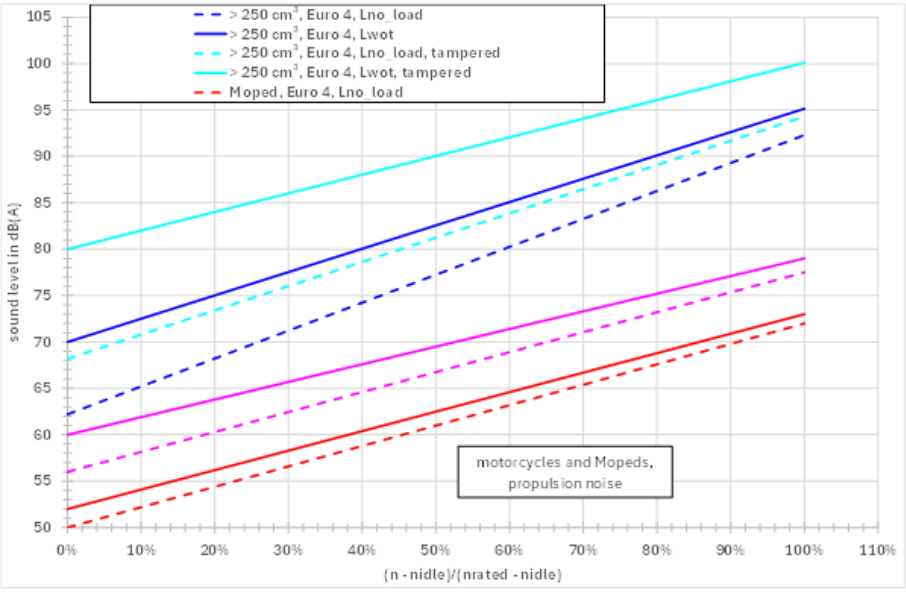

Figure 3-18: LAF Noise level at a 7.5m distance vs normalized engine speed used in the Rotranomo model.

3.4.2 Real-world driving emission events analysis

3.4.2.1 RPM burst

The first noise relevant condition in is nr 2, rpm burst. RPM bursts were performed for one of the RDE vehicles at the beginning of the trip during the first idling phase. The measured normalized engine speed values are shown in Figure 3-19 together with noise emissions that were modelled with the Rotranomo model. Nine bursts can be seen; 6 of them not exceeding 75 dB(A), 1 was close to 80 dB(A) and 2 exceeded 80 dB(A). 75 dB(A) is exceeded for normalized engine speeds above 40%, 80 dB(A) is exceeded when the normalized engine speed exceeds 60% of the span between rated speed and idling speed. 80 dB(A) is quite frequently used as a threshold for the detection of loud noise emission events.

This project has received funding from the European Union's Horizon Europe research and innovation programme under grant agreement No 101056777

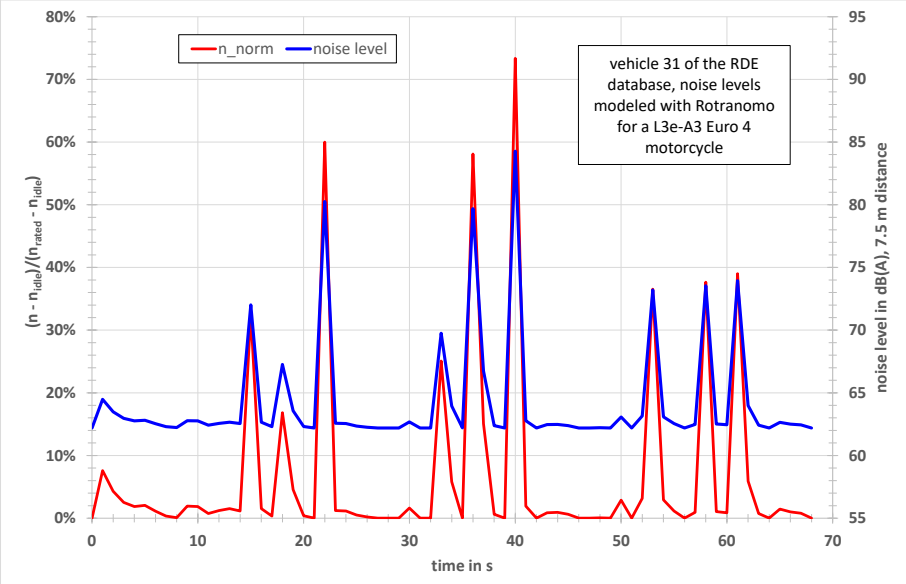

Figure 3-19: Example of RPM bursts, engine speeds measured, noise levels modelled.

3.4.2.2 Acceleration from standstill

Points 3 and 6 in the table are related to accelerations from standstill which quite often occur at crossings or intersections with traffic lights. But leaving roundabouts at low speeds and accelerations at transitions from urban to rural areas (point 7) should also be considered here.

In order to assess such conditions the time series of the complete cycle for RDE vehicle 31 is shown in Figure 3-20 to Figure 3-23. In those Figures, "*vg*" means smoothed vehicle speed, "*n_norm*" means normalized engine speed and "*Lt*" means the sound pressure level at 7.5 m distance. Once again, the engine speeds were measured and the noise levels modeled with Rotranomo for a distance of 7.5 m. The rpm bursts at the beginning of the cycle can also be detected.

This project has received funding from the European Union's Horizon Europe research and innovation programme under grant agreement No 101056777

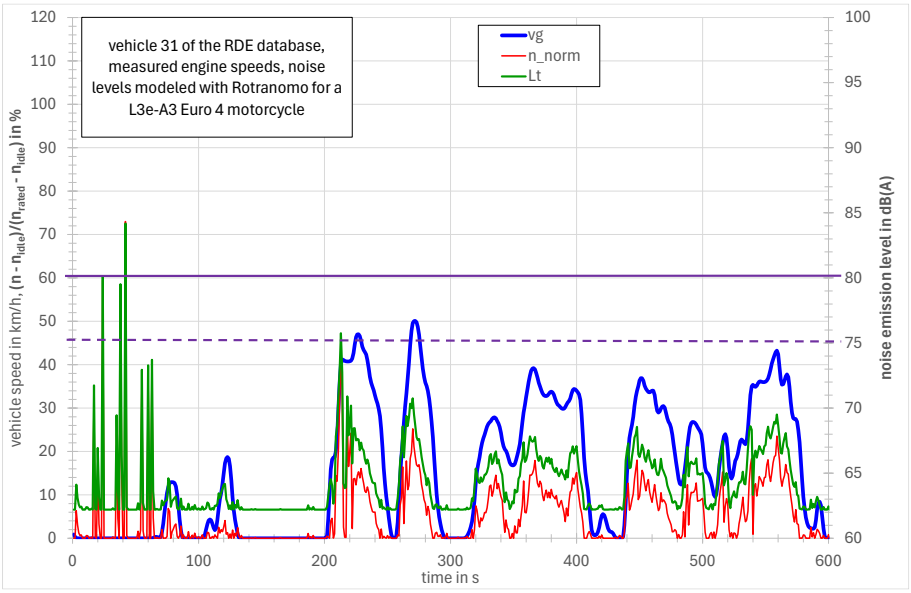

Figure 3-20: Vehicle speed, normalized engine speed and noise level vs time (seconds 0 to 600).

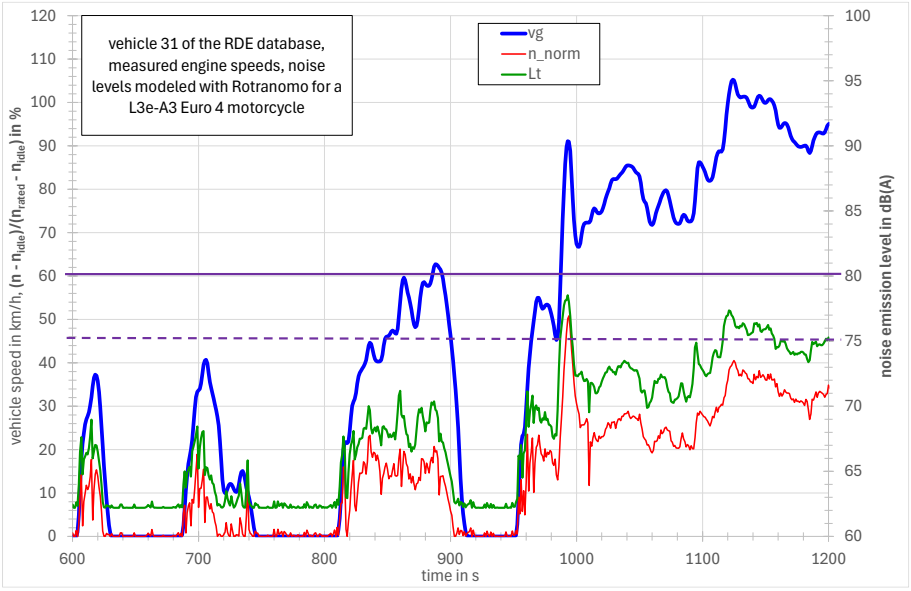

Figure 3-21: Vehicle speed, normalized engine speed and noise level vs time (seconds 600 to 1200).

This project has received funding from the European Union's Horizon Europe research and innovation programme under grant agreement No 101056777

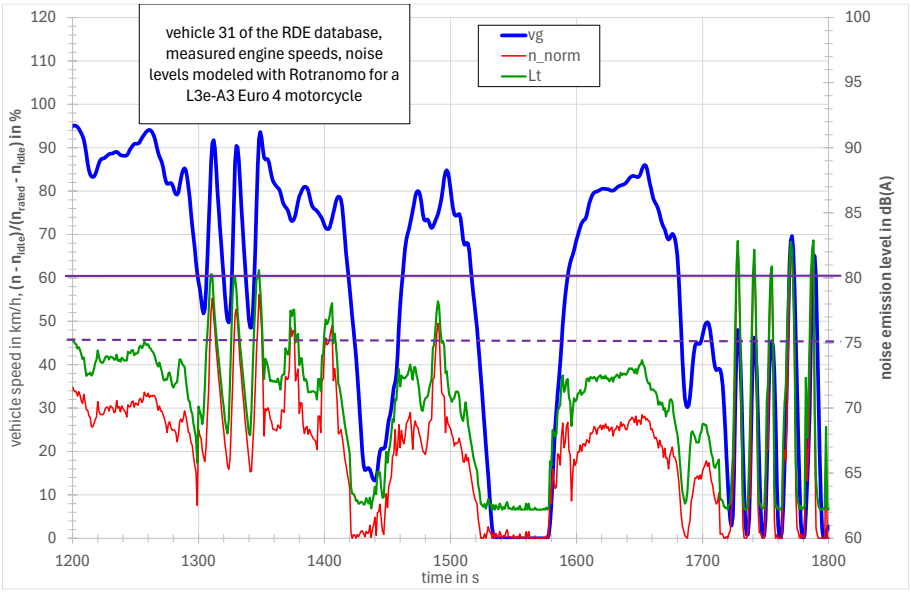

Figure 3-22: Vehicle speed, normalized engine speed and noise level vs time (seconds 1200 to 1800).

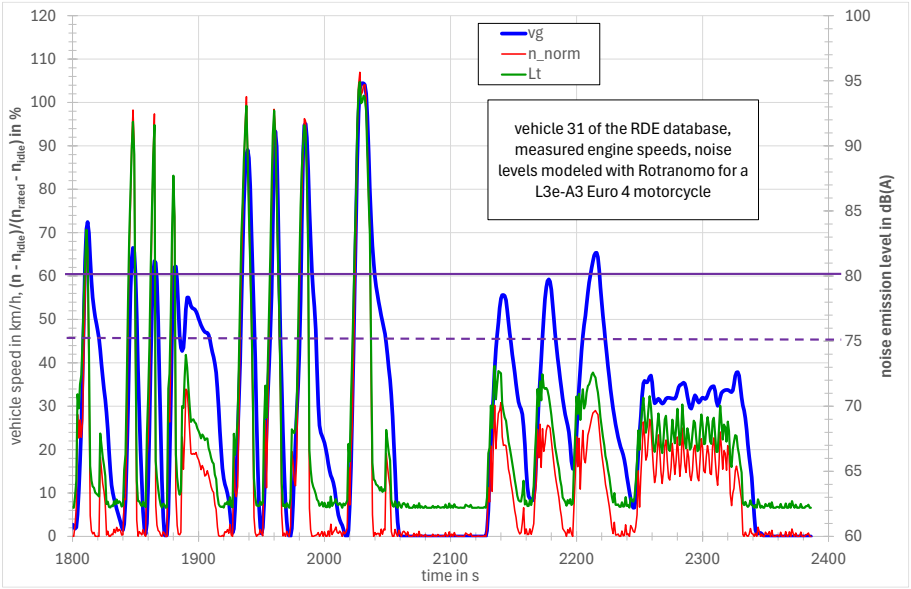

Figure 3-23: Vehicle speed, normalized engine speed and noise level vs time (seconds 1800 to 2400).

Besides these rpm bursts, the noise level in the urban part (till second 950 does not exceed 75 dB(A) except for one high acceleration event shortly after second 200 where 76 dB(A) is reached.

In the rural part (seconds 950 to 1700) 75 dB(A) is exceeded more often due to the higher vehicle speeds demanding higher engine speeds but 80 dB(A) is only reached 3 times (between seconds 1300 to 1350).

High noise emissions above 80 dB(A) are only reached in the special cycle part (between seconds 1700 and 2100) where accelerations from standstill to target speeds of 50 km/h, 70 km/h and 100 km/h with full load were performed on a closed road without other traffic.

This project has received funding from the European Union's Horizon Europe research and innovation programme under grant agreement No 101056777

3.4.2.3 Acceleration and driving behavior

More impressive examples of high acceleration events are shown in Figure 3-24 and Figure 3-25 where 1200 seconds of the RDE cycle trace of vehicle 6 is shown. The noise emission is modelled based on measured engine speed.

Please note that the color code is different compared to the previous figures and that positive acceleration is shown in addition.

Between seconds 1170 and 2116, a total of 12 acceleration events with peak noise levels between 86 dB(A) to 98 dB(A) are shown all related to high engine speed peaks (71% to 113% normalized engine speed) and high acceleration values (between 2 m/s² to 3.44 m/s²). The first 6 events occurred in a time period of less than 5 minutes.

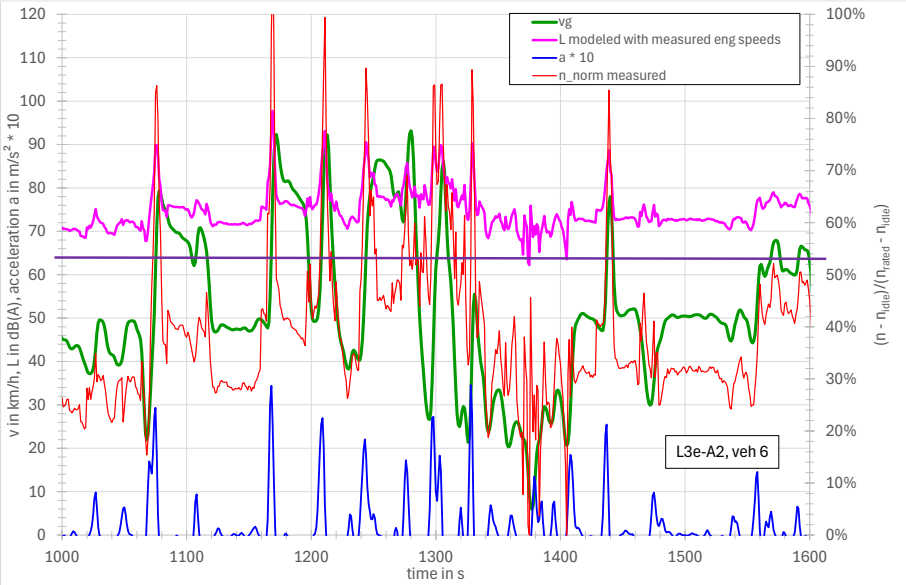

Figure 3-24 : 600 seconds of the RDE cycle trace of vehicle 6 (seconds 1000 to 1600).

This project has received funding from the European Union's Horizon Europe research and innovation programme under grant agreement No 101056777

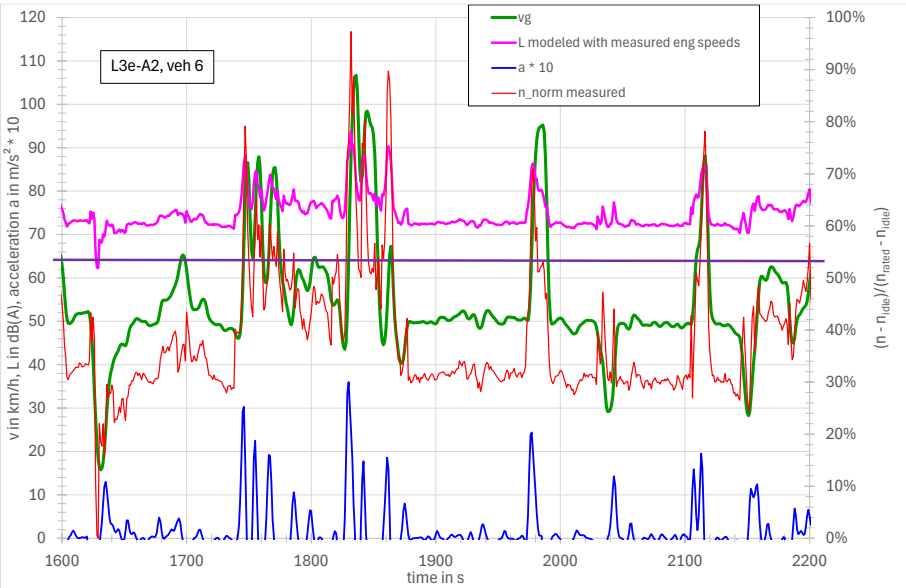

Figure 3-25 : 600 seconds of the RDE cycle trace of vehicle 6 (seconds 1600 to 2200).

From the results in Figure 3-24 and Figure 3-25, it can be concluded that high acceleration events do not only occur at the transition from urban to rural but also within urban streets, most likely in combination with the exceedance of the speed limit of 50 km/h.

The importance of the influence of different driving behavior on noise emissions is discussed in more detail in the following section 3.4.2.4.

3.4.2.4 Comparison of normal and aggressive cycles for the same route

Vehicle speed cycles were provided by TU Graz, derived with a 900 cm³ sports-tourer bike driven on the same route in two different driving styles: average and aggressive (see Figure 3-26).

The cycles were analyzed and inconsistencies in the stop phases (see Figure 3-26, extremely long stop phases for the average cycle, 2 of them longer than 200s) were eliminated.

It is obvious that aggressive driving behavior means higher accelerations and higher vehicle speeds in addition to higher engine speeds compared to average driving behavior. The indicated speed limits are quite frequently exceeded for aggressive driving behavior.

This project has received funding from the European Union's Horizon Europe research and innovation programme under grant agreement No 101056777

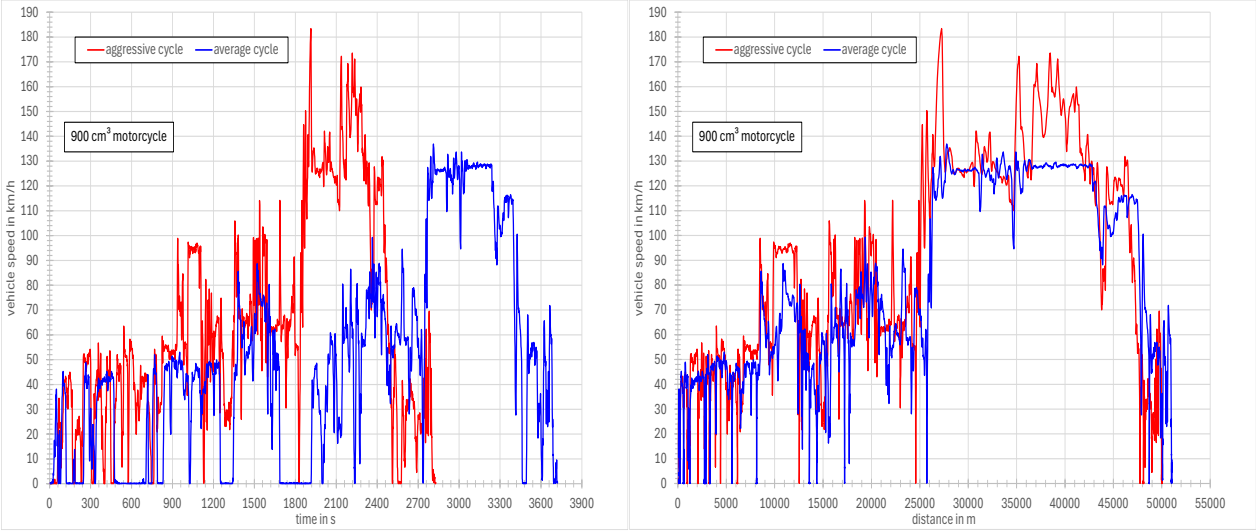

Figure 3-26 : Vehicle speed cycles vs distance driven on the same route in two different driving styles: average and aggressive.

The time series of the cycle with average driving behavior is shown in Figure F-1 to Figure F-4, in Appendix F: Rotranomo RDE Processed data for noise emissions modelling. The first 500s were driven on urban streets with speed limit of 50 km/h. The normalized engine speeds in this cycle part vary around an average of 20% leading to noise emissions not exceeding 75 dB(A).

The time period from second 500 to second 1680 is dedicated to rural operation with vehicle speeds up to 100 km/h and significantly higher vehicle and engine speed fluctuations than in the urban part. The vehicle accelerations in the rural part are significantly higher than in the urban part (maximum values 3.85 m/s² vs 2.02 m/s², average positive values 0.62 m/s² vs 0.41 m/s²). This leads to significantly higher normalized engine speed and noise emission values (maximum values 71% vs 37% and 85.4 dB(A) vs 74.6 dB(A), average values 24% vs 18% and 70.7 dB(A) vs 68.2 dB(A)). But the number of cycle sections where the threshold of 80 dB(A) is exceeded is still very limited (4 events in total).

The situation for the motorway part (seconds 1681 to 2400) is different. The acceleration values are not higher than in the rural part, but the normalized engine speed values and the noise emission values are higher due to the higher vehicle speeds demanding higher engine power (maximum values 77% and 87.6 dB(A) vs 74.6 dB(A), average values 53% and 80.0 dB(A)). So, the average noise emission value is exactly at the threshold.

It should be mentioned that the average noise emission values are arithmetic averages and not energy equivalent averages.

The time series of the cycle with aggressive driving behavior is shown in Figure F-5 to Figure F-8 in Appendix F: Rotranomo RDE Processed data for noise emissions modelling.

The first 530s were driven on urban streets with speed limit of 50 km/h. But the speed limit is exceeded several times although the average vehicle speed is not higher than for the average cycle. But the vehicle

This project has received funding from the European Union's Horizon Europe research and innovation programme under grant agreement No 101056777

acceleration values are significantly higher than for the urban part of the average cycle (maximum 4 m/s² vs 2 m/s², average positive values 0.55 m/s² vs 0.41 m/s²). The normalized engine speeds in this cycle part vary around an average of 22% leading to noise emissions exceeding 75 dB(A) four times and 80 dB(A) once.

The time period from second 531 to second 1421 is dedicated to rural operation with vehicle speeds up to 114km/h and significantly higher vehicle and engine speed fluctuations than in the urban part. The vehicle accelerations in the rural part are significantly higher than in the urban part and of course higher than in the rural part of the average cycle (maximum values 6.3 m/s² vs 3.85 m/s² for rural part of the average cycle, average positive values 0.85 m/s² vs 0.62 m/s²). This leads to significantly higher normalized engine speed and noise sound pressure levels (maximum values 85% vs 71% and 88.7 dB(A) vs 85.4 dB(A), average values 35% vs 24% and 74.0 dB(A) vs 70.7 dB(A)). And the number of cycle sections where the threshold of 80 dB(A) is exceeded is significantly higher (20 events compared to 4 events in the average cycle).

The situation for the motorway part (seconds 1422 to 2400) is as follows. The vehicle maximum vehicle speed is 180 km/h compared to 137 km/h for the average cycle. The acceleration values are higher than for the average cycle (maximum values 5.1 m/s² vs 3.3 m/s², average positive values 0.76 m/s² vs 0.53 m/s²). The differences between both cycles for the motorway part for the normalized engine speed values and the noise emission values are 110% vs 77% and 96.6 dB(A) vs 87.6 dB(A) for the maximum values and 62% vs 53% and 82.6 dB(A) vs 80.0 dB(A) for the average values. So, the average noise emission value for the aggressive cycle is 2.6 dB(A) above the threshold.

In order to present the discussed differences between the two cycles in more depth time based frequency distributions for the parameters vehicle speed, acceleration, normalized engine speed and noise emission were calculated and compared per road category.

Figure 3-27 shows the vehicle speed distributions. For the urban part the differences are small and even for the aggressive cycle the speed limit of 50 km/h is almost respected. For the rural part the vehicle speed distribution of the aggressive cycle is shifted towards higher values over the whole speed range compared to the average cycle. In the speed range up to 70 km/h the differences are between 7 and 10 km/h, above this value the differences increase up to 18 km/h. But, interestingly enough, the speed limit of 100 km/h is respected for both cycles.

For the motorway part the speed limit of 130 km/h is almost strictly respected in case of the average cycle while it is extremely exceeded (by up to 50 km/h) in case of the aggressive cycle. Below the speed limit both frequency distributions are much smaller.

Figure 3-28 shows the acceleration frequency distributions of the two cycles per road category. It is obvious that the aggressive cycle has higher accelerations and decelerations than the average cycle for all road categories. And it should be mentioned that the acceleration distribution for the rural part of the average cycle is almost identical to the curve for the motorway part of the aggressive cycle. This supports the finding that the highest accelerations are practiced on rural roads.

This project has received funding from the European Union's Horizon Europe research and innovation programme under grant agreement No 101056777

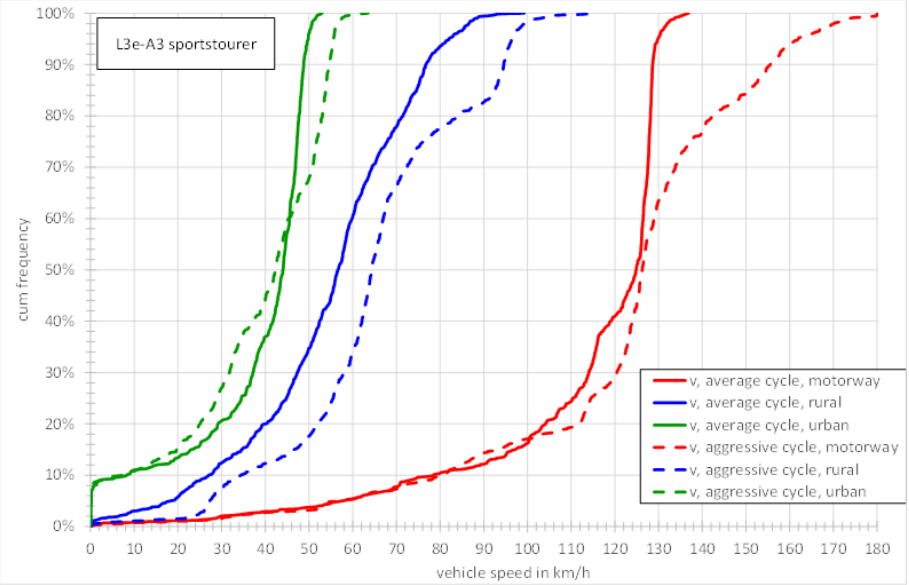

Figure 3-27: Vehicle speed distributions for the 3 parts of the average and aggressive cycles.

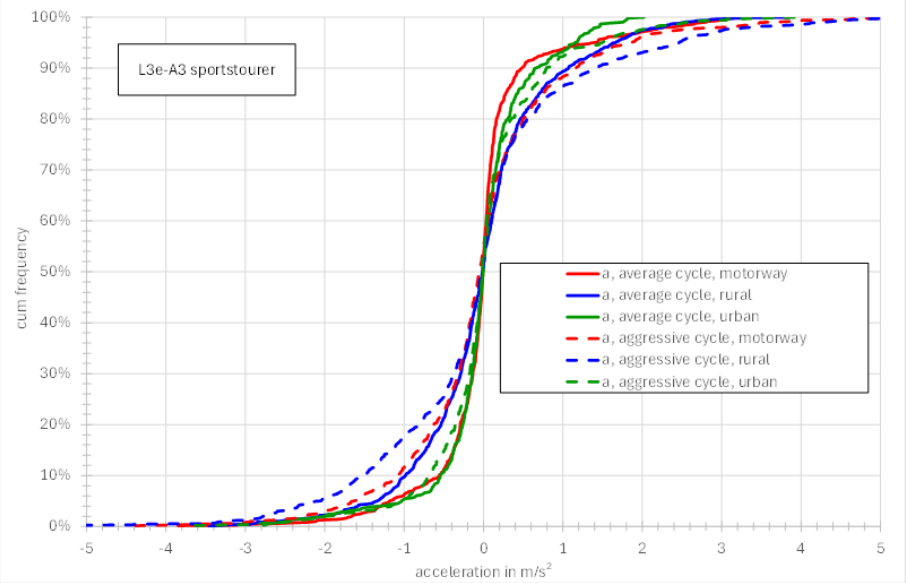

Figure 3-28: Vehicle speed distributions for the 3 parts of the average and aggressive cycles.

Figure 3-29 shows the frequency distributions of normalized engine speed values for both cycles and each road category. A comparison with the vehicle speed distributions (see Figure 3-27Figure 3-27) and the key parameters (see Table 2-2) leads to the conclusion that for the urban part the differences in engine speeds are more influenced by differences in gearshift behavior than in vehicle speed while the situation is just the other way round for the motorway part not least because on the motorway the vehicle is mostly driven in the highest gear also for the aggressive cycle. For the rural part the influences of gearshift behavior and vehicle speed are almost equal.

This project has received funding from the European Union's Horizon Europe research and innovation programme under grant agreement No 101056777

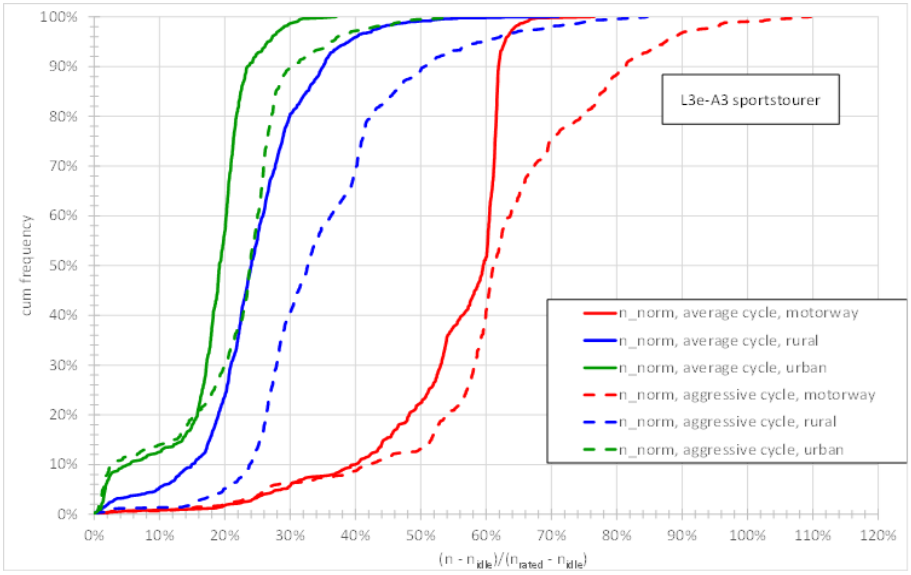

Figure 3-29: Normalized engine speed distributions for the 3 parts of the average and aggressive cycles.

Figure 3-30 shows the frequency distributions of the noise emission values modelled with Rotranomo based on the measured engine speeds and the individual technical data of the vehicle under consideration. Thresholds of 75 dB(A) and 80 dB(A) are marked by vertical lines. In the urban part the threshold of 75 dB(A) is not even reached by the average cycle, while it is exceeded by the aggressive cycle but less than 3 % of the time. And the threshold of 80 dB(A) is reached by this cycle but only once.

And even the average cycle for the rural part exceeds 75 dB(A) for only 7.3% of the time and 80 dB(A) is exceeded by this cycle for less than 0.5% of the time. And also, the aggressive cycle exceeds 80 dB(A) only for 7% of the time.

Totally different is the situation for the motorway parts. Here 80 dB(A) is exceeded for 70.7% of the time in case of the average cycle and 80.2% of the time in case of the aggressive cycle. For vehicle speeds between 80 km/h and 120 km/h this exceedance occurs in combination with high acceleration values, above 120 km/h 80 dB(A) is exceeded for any case. And this is independent of the cycle.

This project has received funding from the European Union's Horizon Europe research and innovation programme under grant agreement No 101056777

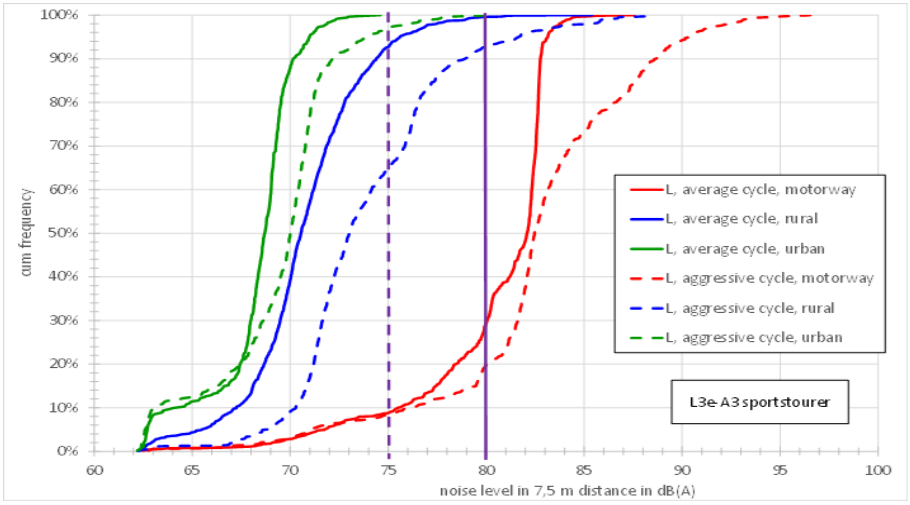

Figure 3-30: Noise level distributions for the 3 parts of the average and aggressive cycles.

Figure 3-31 shows the normalised engine speeds vs vehicle speed (gear use) for both cycles for the urban part. The main differences in terms of cycle time share are related to gears 3rd, 4th and 5th. Gear 5th is not used for the aggressive cycle, gears 3rd and 4th are used up to higher engine speeds for the aggressive cycle which is in principle also the case for gears 1st and 2nd but less frequently. It needs to be mentioned that the maximum vehicle speed for the aggressive cycle is reached in 3rd gear and that the normalized engine speed for the average cycle is limited to less than 40% and does only exceed 50% in case of the aggressive cycle in 2nd Gear by up to 5%.

Figure 3-32 shows the equivalent figure as Figure 3-31 but for the rural part. For the average cycle a threshold of 60% normalised engine speed is only exceeded for less than 0.2% of the cycle time while the corresponding threshold for the aggressive cycle is 80%, reached in 2nd and 3rd gear. And it needs to be mentioned that the maximum speeds reached in 3rd, 4th and 5th gear are higher than in 6th gear. That leads to the conclusion that the maximum vehicle speeds are reached during overtaking maneuvers, which was also the case in the urban part.

Figure 3-33 shows the normalised engine speeds vs vehicle speed (gear use) for both cycles for the motorway part. For the aggressive cycle the highest engine speed values are reached in gears 2nd, 3rd and 4th, most probably during high acceleration phases. This behavior is much less pronounced for the average cycle. And the maximum speed of the average cycle is exceeded by the aggressive cycle predominantly in 6th gear but to a low extend also in 4th gear, once again most probably during an overtaking maneuver.

This project has received funding from the European Union's Horizon Europe research and innovation programme under grant agreement No 101056777

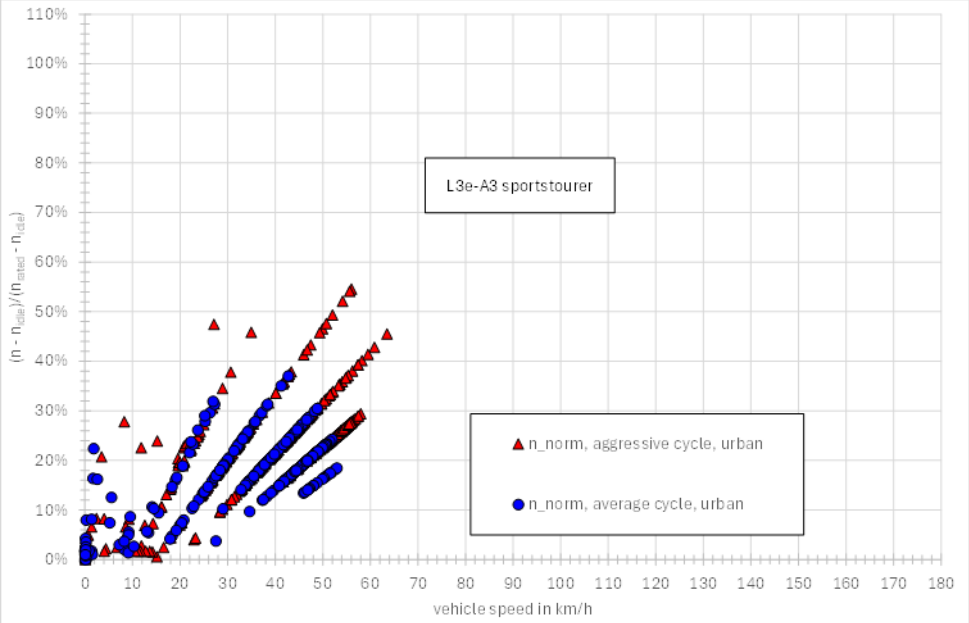

Figure 3-31: Gear use for the urban parts of the average and aggressive cycle.

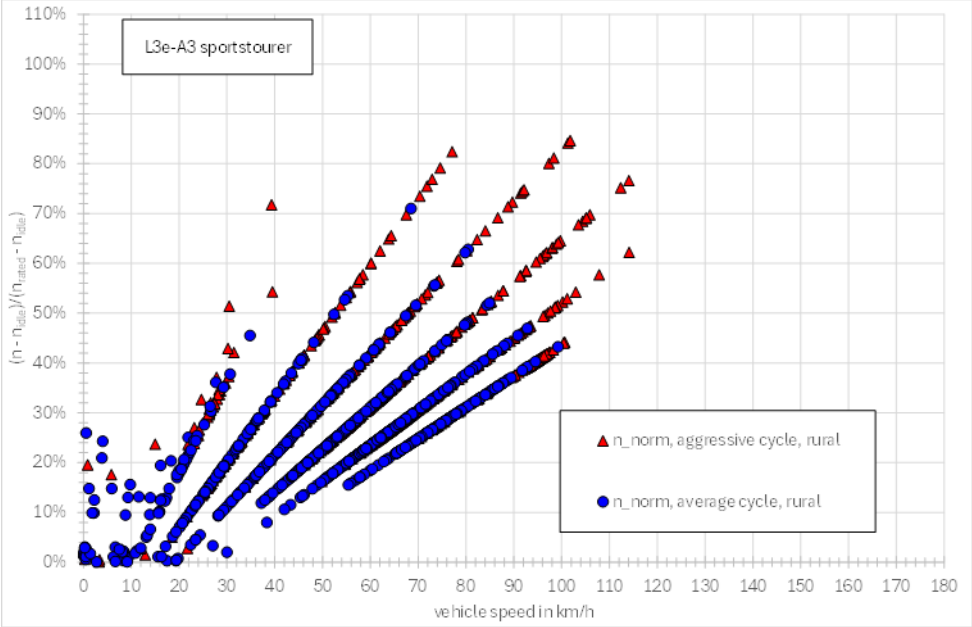

Figure 3-32: Gear use for the rural parts of the average and aggressive cycle.

This project has received funding from the European Union's Horizon Europe research and innovation programme under grant agreement No 101056777

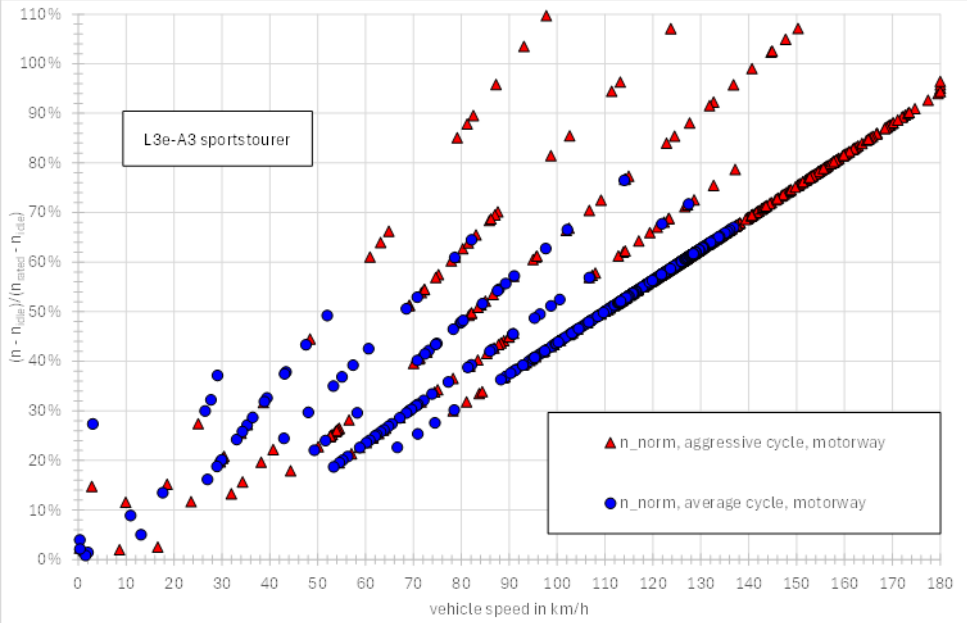

Figure 3-33: Gear use for the motorway parts of the average and aggressive cycle.

A comparison with modelled engine speeds for average and high rev gearshift behavior using the Rotranomo model (see Figure 3-34,and Figure 3-35Figure 3-35) resulted in much higher engine speeds for the aggressive cycle compared to the measured engine speeds, especially for the rural part.

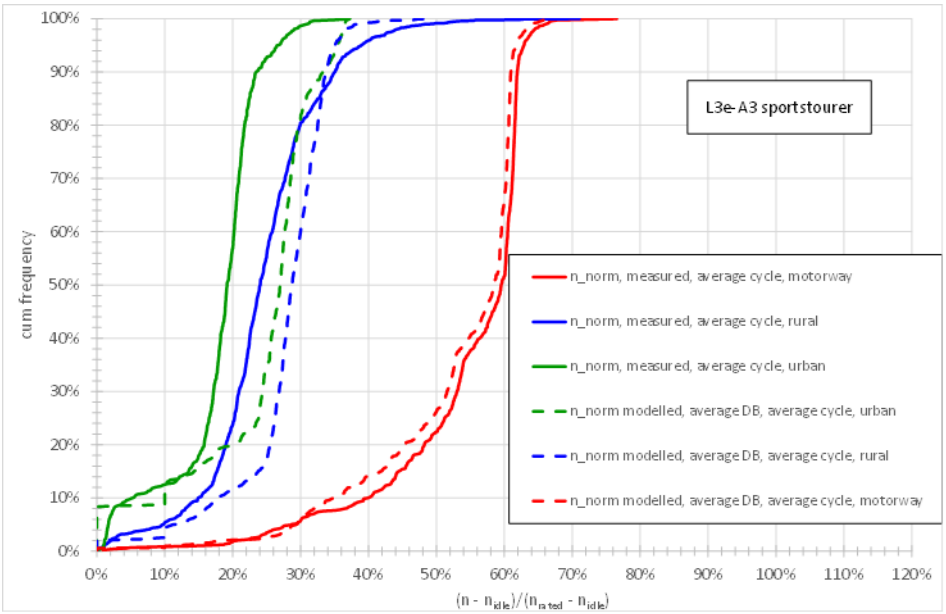

Figure 3-34: Comparison of normalized engine speed distributions, measured speeds vs modelled speeds, average cycle.

This project has received funding from the European Union's Horizon Europe research and innovation programme under grant agreement No 101056777

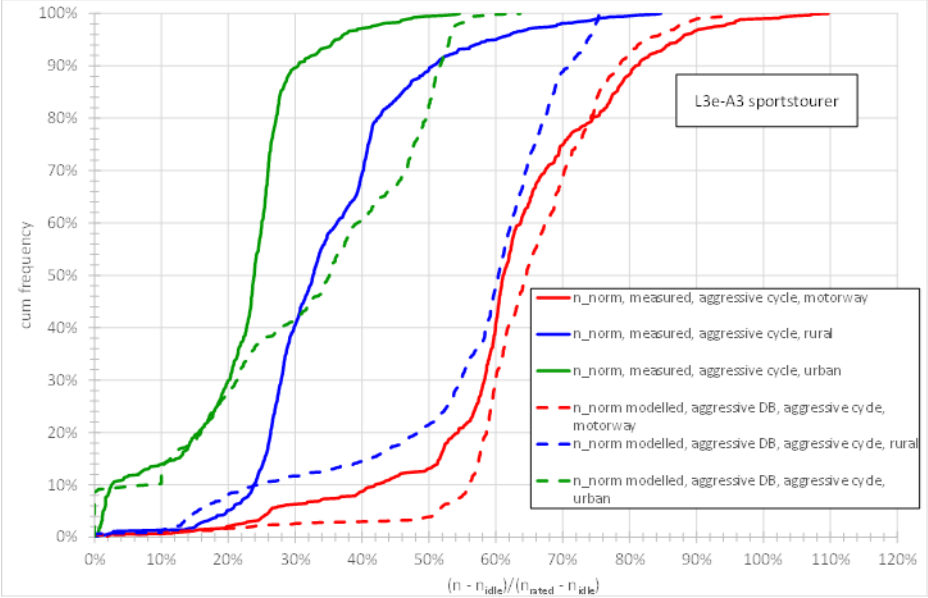

Figure 3-35: Comparison of normalized engine speed distributions, measured speeds vs modelled speeds, aggressive cycle.

3.4.3 Results of the analysis

In general, the noise results show the same trend as the normalized engine speed values:

Conclusion: the driving condition "*acceleration from standstill*" or "*accelerations from low speeds*" cause only high noise emissions if:

- Vehicle speed exceeds 60 km/h for average gearshift behavior or 40 km/h for high rev gearshift behavior or/and
- Vehicle is tampered with noise increasing measures

More important for high noise emission events are acceleration phases starting at speeds between 20 km/h and 60 km/h and leading to a speed increase of 30 km/h or higher. Such events can frequently be observed at the transition from urban to rural streets.

With respect to driving behavior, one has to differentiate between differences in vehicle speed and acceleration behavior on one hand, and gearshift behavior on the other hand. Both influences are not strongly correlated especially for vehicles with high power to mass ratio as it is the case for most of the L3e-A2/A3 vehicles. The findings and conclusions in this presentation are related to big motorcycles and can be different for smaller, low powered motorcycles.

This project has received funding from the European Union's Horizon Europe research and innovation programme under grant agreement No 101056777

4. RW operation events to assess pollutant emissions

4.1 Introduction

Real-world data and RDC data from the testing program have been used to provide recommendations for the real-world operation events that have to be considered to assess pollutant emissions. The real-world operation events identified to be of relevance to assessing emissions should consider the three following pillars: occurrence, severity and feasibility. The real-world diving patterns to assess the emissions in order to understand the impact of the LVs in air pollution should find a balance and trade-off between these 3 pillars.

Several activities have been performed with the focus of understanding the real-world driving patterns more representative of LVs. RDE trip requirements from the different routes in LENS have been discussed and compared with current RDE regulations and the differences per LV subcategory are highlighted. An intensive analysis is done for the driving dynamics and the impact on different urban, rural and motorway share definition and the subsequent impact on the overall emissions. Furthermore, representative cycles have been calculated from all the data gathered that will serve as basis for computing the emissions factor with the Passenger Car and Heavy-Duty Emission Model (PHEM) model in WP6 analyses. Additionally, more detailed analyses of some relevant L-category vehicles have been developed, in order to identify how real-word driving conditions have an impact on emissions, for several sub-categories and technology variants, as well as emissions heatmaps analysis of most relevant LV subcategories, and particularities of manual transmissions (MT) and CVT for each of them.

To enable efficient analysis of the large amount of measurement data and to automatize the development of the parametrization of the emission models developed in LENS, all emission test data is also imported into the LENS database (LENS_DB). Further details about LENS db can be found in Deliverable D1.4.

The driving patterns that cause high emissions are analyzed in two different ways: (1) identify from LENS db the driving patterns that are hypothesized to cause high emissions (from Table 4-2, D6.1) and evaluate the impact and (2) identify from LENS db the high emission events and identify the driving patterns or any other reasons that cause it.

The data from the LENS db was filtered to include only vehicles following the Euro 5 emissions class, as these findings are considered the most relevant for a more accurate assessment of high-emission events that will need to be addressed in upcoming regulations.

This project has received funding from the European Union's Horizon Europe research and innovation programme under grant agreement No 101056777

4.2 Assessment of real-world driving operation characteristics and exhaust emissions impact

As was introduced in section 2.3, RDE trip characteristics developed for LVs depend on their specific use and subcategory. LVs cover a wide range of vehicle characteristics and huge variability in their modes of use. It covers vehicles designed exclusively for urban mobility with maximum speeds of less than 45 km/h and that can be used without full driving license, it also covers all-terrain on-road vehicles for rural areas and medium and high-performance motorcycles for road trips, long trips or for recess. Urban mobility predominates in the usage of LVs in European regions; it also includes enthusiasts (touring and sports) profile drivers that are mainly for occasional use. It is also important to highlight that in Southern Europe L-vehicles are more commonly in use than in Northem Europe and used through the year due to ambient conditions.

In summary, we can consider the following bullet points for the LVs diversity of use particularities:

- Mopeds and Scooter: primarily urban usage, rare rural use at limited speed
- Three- and four-wheelers for transportation in urban and rural areas (or even off-road)
- Touring bikes and cruisers: primarily use for leisure driving on rural roads or motorways
- High-performance sports bikes: mostly leisure driving
- Naked bikes: very versatile and diverse in engine capacity are driven from urban to highway, and leisure driving

The RDE routes for LVs have been, then, developed depending on the subcategory characteristics in terms of maximum speed and usage. In section 4.2.1 main characteristics of the performed routes are included. For L1e, L2e and L6e vehicles with maximum designed vehicle speed of 45 km/h an urban route has been developed, in 3 different locations, more detailed information about on-road routes can be found on Appendix B: RDE Routes. For the rest of LVs subcategories, a route containing urban, rural and motorway driving operation in a balanced way has been developed, in 5 different locations and containing also a dedicated aggressive driving part to evaluate high emission events.

Driving operation scenarios of urban, rural and motorway behavior have been discretized as baseline consideration like the RDE regulation((UE) 2017/1151), in accordance with Table 4-1. For the analysis, other speed discretization criteria for phases definitions have been considered in order to assess how this could have an impact on both emissions and driving dynamics.

Table 4-1: Speed classes according to PC (EU) no 2017/1151

Speed Class	Speed Range (km/h)
Urban	0 to <= 60
Rural	60 to 90
Motorway	> 90

This project has received funding from the European Union's Horizon Europe research and innovation programme under grant agreement No 101056777

Additionally, this same exercise has been developed by road type, considering actual road legal speed limits as a reference for discretizing the phases. Following this procedure, more dynamic events, this means, strong accelerations, high speed driving, etc., are then classified on their respective phase, and not following speed phase discretization criteria, which means that driving at speeds above the limit does not lead to misclassification of phases. This driving behavior is very frequent on leisure driving and with sports bikes.

4.2.1 RDE trip characteristics of LENS routes

The following tables contain a summary of the trip characteristics of the RDE routes that have been performed within the LENS project. Main requirements consider average speed and share for each driving operation (urban, rural, motorway and total). For motorway operation also a specific Key Performance Indicator (KPI) is included, which is the share of speed higher than 120 km/h. The purpose of this KPI is to assess the occurrence of this type of events, which is quite high in RW. It has also been analyzed how much impact these high-speed events could have on emissions. Furthermore, the overall average temperature for each route has also been included. These routes speed profile, altimetry and GPS data are available in Appendix B: RDE Routes. The summary of the trip characteristics of the routes for each of most representative LV sub-categories (L1e-B, L3e-A1 and L3e-A2/A3) are shown below on Table 4-2, Table 4-3 and Table 4-4. Each route corresponds with one of the participating labs. Each route ID refers to the same laboratory on all tables.

Regarding L1e-B, trip distances are typically quite short, as not many different RW driving events have to be developed, and maximum speed is limited. This is represented by the 100% values of urban phase, with exception of one route, in which one vehicle has reached a maximum speed over 60 km/h for a very short period of time.

Table 4-2: Trip characteristics L1e-B routes

L1e-B	N Vehicles	Distance Covered (km)	Average Altitude (m)	Urban		Rural		Total		
				Avg Speed (km/h)	Distance Share	Avg Speed (km/h)	Distance Share	Avg Temp (ºC)	Distance (km)	Avg Speed (km/h)
Total	**11**	**306.8**	**259.5**	**26.1**	**100.0%**	**66.8**	**0.03%**	**25.2**	**27.9**	**26.1**
Route 1	3	17.6	491.5	16.2	99.5%	66.8	0.5%	28.6	5.9	16.3
Route 2	6	273.4	205.7	34.2	100.0%	0.0	0.0%	23.1	45.6	34.2
Route 3	2	15.7	72.8	16.9	100.0%	0.0	0.0%	No data	7.9	16.9

For L3e category vehicles, some laboratories have developed the same route for A1, A2 and A3, with the peculiarity that, the maximum speed is reduced on L3e-A1: depending on the vehicle, it nearly hits 110 km/h, or cannot go higher than 90 km/h. This is noticed when revising that the motorway phase minimum speed of 90km/h is reached only on one route, and the maximum speed has not been over 120 km/h. There are no differences between L3e-A2 and A3 routes. That is why their trip characteristics are compiled in one single table. Both subcategories have enough power to follow the same routes. Some L5e vehicles have followed the same L3e routes.

This project has received funding from the European Union's Horizon Europe research and innovation programme under grant agreement No 101056777

Table 4-3: Trip characteristics L3e-A1 routes

L3e-A1	N Vehicles	Distance Covered (km)	Average Altitude (m)	Urban		Rural		Motorway			Total		
				Avg Speed (km/h)	Distance Share	Avg Speed (km/h)	Distance Share	Avg Speed (km/h)	Distance Share	Share over 120 km/h	Avg Temp (ºC)	Distance (km)	Avg Speed (km/h)
Total	**21**	**1079.1**	**246.5**	**28.0**	**48.3%**	**71.4**	**38.5%**	**96.6**	**13.2%**	**0.0%**	**22.4**	**33.7**	**38.9**
Route 1	4	144.4	410.6	29.2	52.4%	75.1	18.1%	100.7	29.5%	0.0%	23.7	36.1	43.1
Route 2	4	185.0	246.1	34.2	41.4%	74.2	39.7%	96.5	18.9%	0.0%	21.1	46.3	51.6
Route 3	4	69.8	77.1	24.1	47.4%	73.0	52.2%	91.0	0.4%	0.0%	No data	23.3	37.2
Route 4	4	429.5	126.6	33.1	46.0%	70.7	44.9%	97.2	9.1%	0.0%	No data	85.9	47.3
Route 5	5	250.4	260.1	25.4	55.2%	69.0	34.7%	95.2	10.1%	0.0%	No data	15.6	32.3

Table 4-4: Trip characteristics L3e-A2/3 routes

L3e-A2/A3	N Vehicles	Distance Covered (km)	Average Altitude (m)	Urban		Rural		Motorway			Total		
				Avg Speed (km/h)	Distance Share	Avg Speed (km/h)	Distance Share	Avg Speed (km/h)	Distance Share	Share over 120 km/h	Avg Temp (ºC)	Distance (km)	Avg Speed (km/h)
Total	**50**	**3004.3**	**251.5**	**27.6**	**41.6%**	**71.1**	**27.4%**	**111.8**	**31.0%**	**18.8%**	**24.6**	**28.9**	**43.7**
Route 1	12	602.1	425.5	32.1	40.0%	72.2	17.8%	118.9	42.2%	24.6%	26.6	50.2	54.1
Route 2	12	642.9	242.5	34.5	38.2%	75.9	33.5%	109.9	28.3%	3.2%	23.0	45.9	55.2
Route 3	7	236.9	67.7	22.8	44.3%	72.7	36.3%	98.6	19.4%	2.2%	No data	26.3	37.5
Route 4	8	906.6	116.3	31.0	38.7%	70.3	28.8%	110.0	32.5%	12.1%	No data	82.4	51.3
Route 5	11	615.9	276.1	25.1	49.8%	69.1	24.9%	115.8	25.3%	27.0%	No data	10.6	38.2

The missing sub-categories do not follow such a standardized route, due to the reduced total number of vehicles measured because of difficulties for getting them and the low occurrence on the current vehicle fleet. Singular routes have been considered for those specific vehicles and are included in Appendix B: RDE Routes.

4.2.2 RDE & lab emissions results per phase

Computing emissions by phases is another way of understanding the behavior of vehicles that allows us to understand how vehicles perform along the route for each one of the phases and its specific driving conditions. For this analysis, several phases discretization have been selected, taking the one mentioned in Table 4-1 as a reference. When discretizing route phases by road type, only on-road measurements have been considered. The pollutants analyzed are CO, HC, NOx and PN (both PN23 and PN10 when available), as presented in D3.1, and they have been weighed by the distance covered on each phase. They have been represented both against average speed and $v*a_{,pos(perc95)}$.

Figure 4-1 shows the total emissions of CO per phase vs the average vehicle speed for that phase. Although L3e-A1 vehicles have low-capacity engines, emissions on rural and motorway phases are higher than the

This project has received funding from the European Union's Horizon Europe research and innovation programme under grant agreement No 101056777

rest of the subcategories, even when average speed is lower. The vehicles run at maximum power and speed when they are driven over 90 km/h. For L3e-A3, average speed values are higher for on-road measurements (dispersed values, TA measurements are represented by the ones that follow a column of values at the same mean vehicle speed), and CO emissions are slightly higher too.

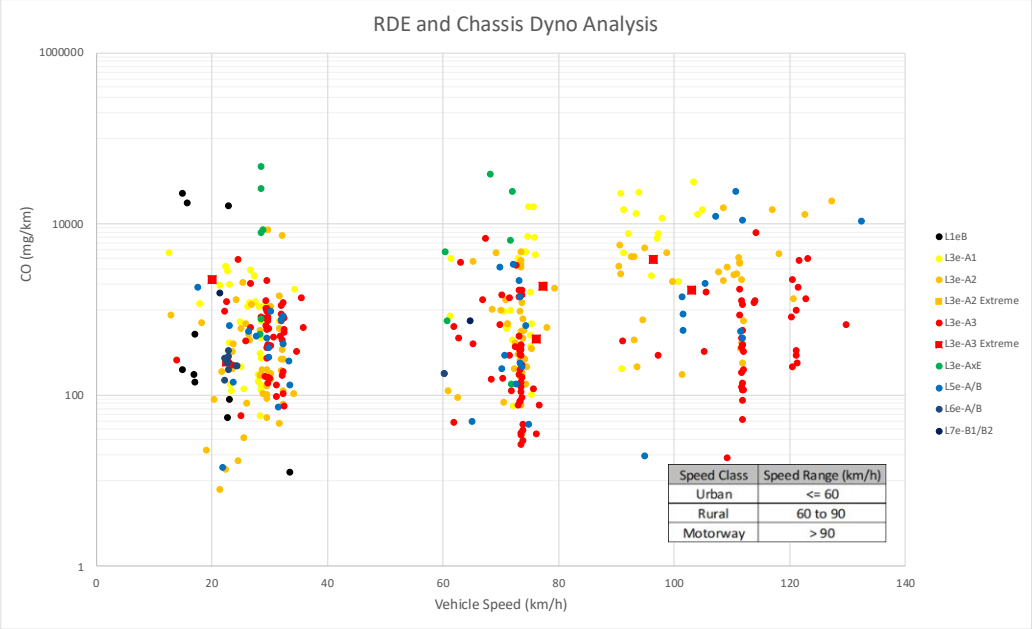

Figure 4-1: CO emissions vs mean speed per subcategory. Phases discretization according to regulation (UE) 2017/1151.

When representing CO emissions vs $v*a_{,pos}$, Figure 4-2, emissions slightly increase for greater values of $v*a_{,pos}$. The most problematic sub-categories regarding CO emissions are represented by 2-stroke mopeds (L1e-B), L3e-A1, A2, L3e-AxE and L5e-A/B. The vast majority of those vehicles are positioned over 1000mg/km. Some L3e-A3 vehicles are also positions above this value, but the overall values remain under it.

This project has received funding from the European Union's Horizon Europe research and innovation programme under grant agreement No 101056777

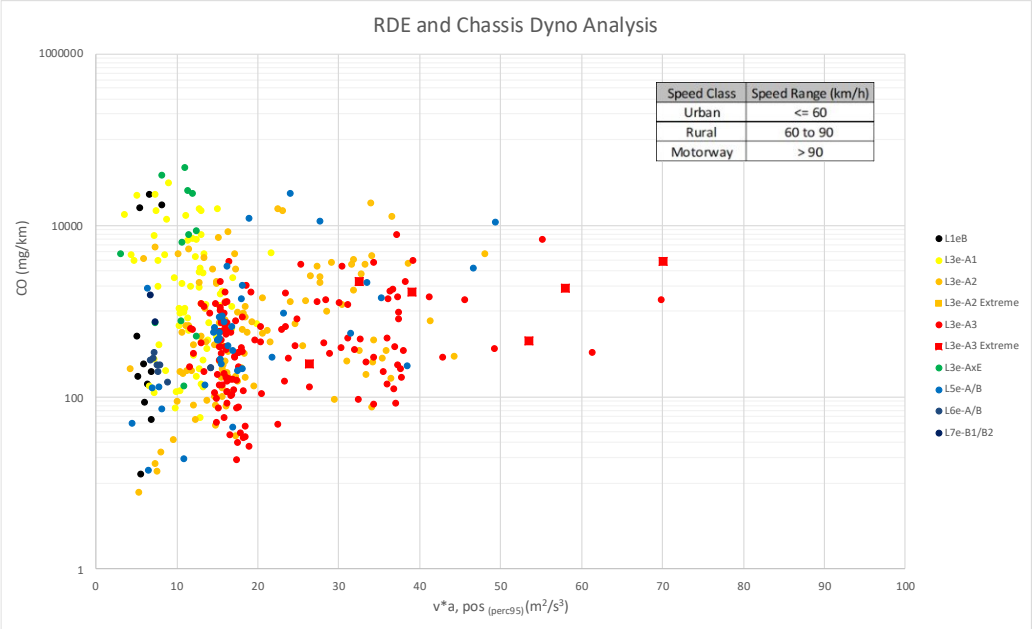

Figure 4-2: CO emissions vs v*a,pos per subcategory. Phases discretization according to regulation (UE) 2017/1151.

Regarding HC emissions, in Figure 4-3, it can be shown that there is no big differences between subcategories, except for mopeds (L1e-B) and L3e-AxE, which show relatively high emissions in comparison with the other LVs.

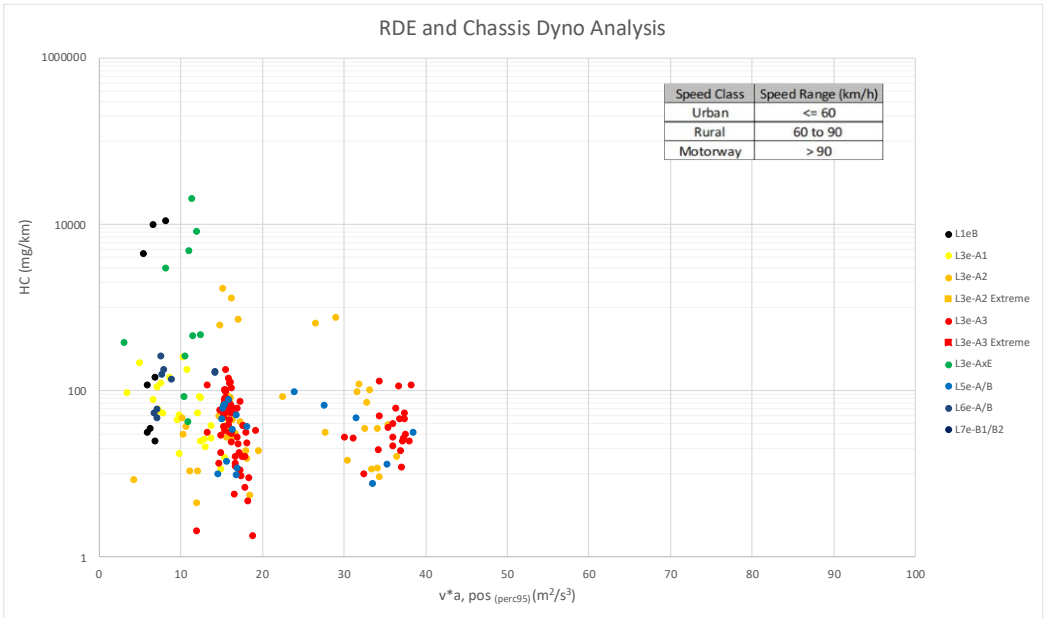

Figure 4-3: HC emissions vs v*a,pos per subcategory. Phases discretization according to regulation (UE) 2017/1151.

Regarding NOx emissions, in Figure 4-4, the predominance of L6e-A/B can be shown, mainly powered by diesel Internal Combustion Engine (ICE), and L3e-A1 and A2 sub-categories. Some L3e-A3 vehicles reach emissions values over 100 mg/km.

This project has received funding from the European Union's Horizon Europe research and innovation programme under grant agreement No 101056777

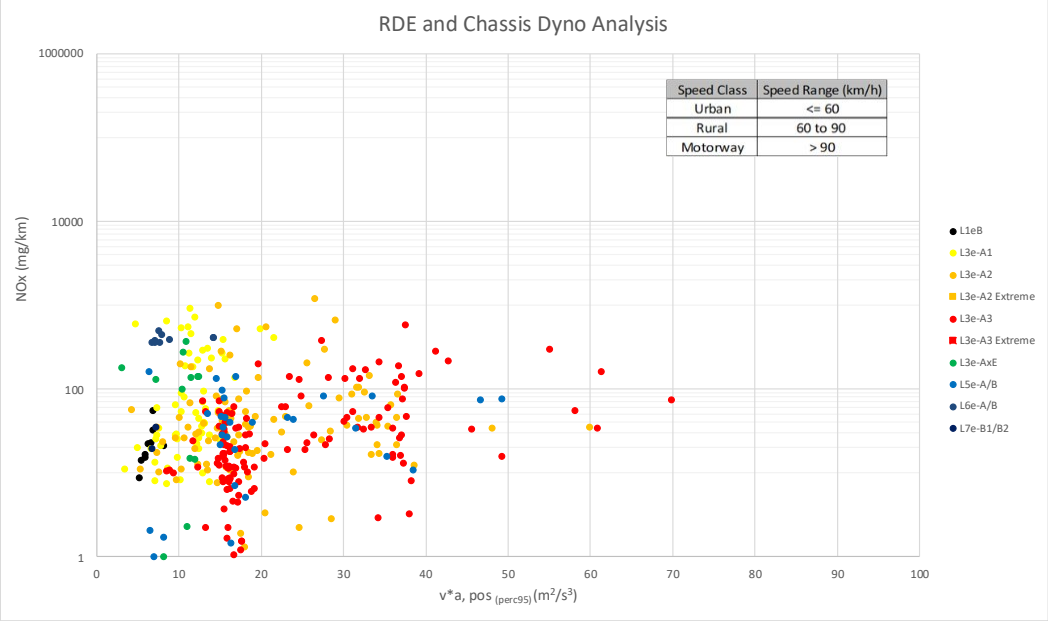

Figure 4-4: NOx emissions vs v*a,pos per subcategory. Phases discretization according to regulation (UE) 2017/1151.

4.2.2.1 Speed segmentation phases discretization impact on emissions

Different variations have been also considered to assess how different speed classes could have an impact on emissions. These variations are included in Table 4-5, Table 4-6 and

Table 4-7, and the findings are commented upon them.

Table 4-5: Speed classes variation where motorway speed classes are limited to 120 km/h

Speed Class	Speed Range (km/h)
Urban	0 to <= 60
Rural	60 to 90
Motorway	> 90 and <=120

Table 4-6: Speed classes variation where motorway speed class is set to >100 km/h

Speed Class	Speed Range (km/h)
Urban	0 to <= 60
Rural	60 to 100
Motorway	> 100

This project has received funding from the European Union's Horizon Europe research and innovation programme under grant agreement No 101056777

Table 4-7: Speed classes variation where urban and motorway speed classes are set to <50 and >100 km/h respectively

Speed Class	Speed Range (km/h)
Urban	0 to <= 50
Rural	50 to 100
Motorway	> 100

0-60-90-120 phases discretization emissions results

When neglecting all points of operation with speed values over 120 km/h, no important impact on total emissions has been identified. The only change identified was the lower mean speed because of the cut based on maximum speed. This finding reflects that driving above 120km/h, which on a standard route could represent near 25% of the motorway phase, does not have an important impact on the total nor motorway phase emissions. Small reduction on CO and NOx emissions. HC values show minor changes. Figure G-9 to Figure G-16 are included in Appendix G: Impact of Phases discretization on emissions. Those figures include all plots of CO, HC, NOx and PN emissions values against $v*a_{,pos}$ (m^2/s^3) and against mean vehicle speed (km/h) for each phase (urban, rural and motorway).

0-60-100 phases discretization emissions results

As in the previous analysis no important impact to emissions have been noticed. Both rural and motorway values are displaced to the right side of the graphs, as both mean speed values are higher in both phases, but there are no important changes on phase emissions. Regarding L3e-A1 on motorway phase, values are now mostly on rural phases because of their reduced maximum speed, sometimes lower than 100km/h. Total emissions of the rural phase do not show any clear evidence of an increase. Figure G-17 to Figure G-24 are included in Appendix G: Impact of Phases discretization on emissions.

0-50-100 phases discretization emissions results

Generally, no important impact on emissions has been noticed either for this phase discretization, except for L3e-A1. On this sub-category some vehicles rural phase is now positioned at 50 km/h average speed, and as the rural phase I now extends up to 100km/h, PN emissions have slightly increased on that phase. Regarding all vehicle sub-categories, rural phase has been affected only on the way that average speed is now lower. In that case, some previously urban values are now on the rural phase for those low-powered vehicles. The main change for this phase discretization is the displacement of the dots across the x axis when representing the emissions against mean vehicle speed for each phase, and not in terms of emissions. Figure G-25 to Figure G-32 are included in Appendix G: Impact of Phases discretization on emissions.

4.2.2.2 Road type phases discretization impact on emissions

In the RDE regulation the discretization of driving phases is done by vehicle speed. Urban, rural and motorway phases are defined according to vehicle speed. While driving on-road, urban operation (vehicle

This project has received funding from the European Union's Horizon Europe research and innovation programme under grant agreement No 101056777

speed <60 km/h) may occur on both rural or motorway phases, rural operation (vehicle speed over 60 km/h and under 90 km/h) may also occur on motorways or even on urban roads when the speed limit is exceeded. In the study of defining the correct urban, rural and motorway phase discretization for L-category vehicles the way these phases are discretized might have a high influence of the final emissions and driving dynamics calculated with both approaches.

Figure 4-5 shows an example of the RW behavior of a typical LV user, and how this route segmentation processes the data. When driving in rural areas, vehicle speed can be equal to an urban phase, and there can also be some stops and thus accelerations from standstill. In this specific case, the motorway speed limit was 90 km/h, so all these events will be typically considered on rural phase if we only take into consideration the actual vehicle speed and no road type information is available to classify those segments correctly as motorway ones. Additionally, some stop-and-go driving can be found on motorway areas, as well as strong accelerations on road junctions. If not discretizing phases by road type, all these events are wrongly analyzed. It is a philosophical question whether traffic jams and stop-and-go driving occurring on motorway roads should be considered as urban or motorway driving. This report does not provide recommendations on that, just has the purpose of enlightening the issue and its impact. Furthermore, some harsh accelerations in urban areas exceeding 60 km/h are counting on urban and rural operation simultaneously meaning that the emissions generated in this acceleration is split wrongly in the two phases.

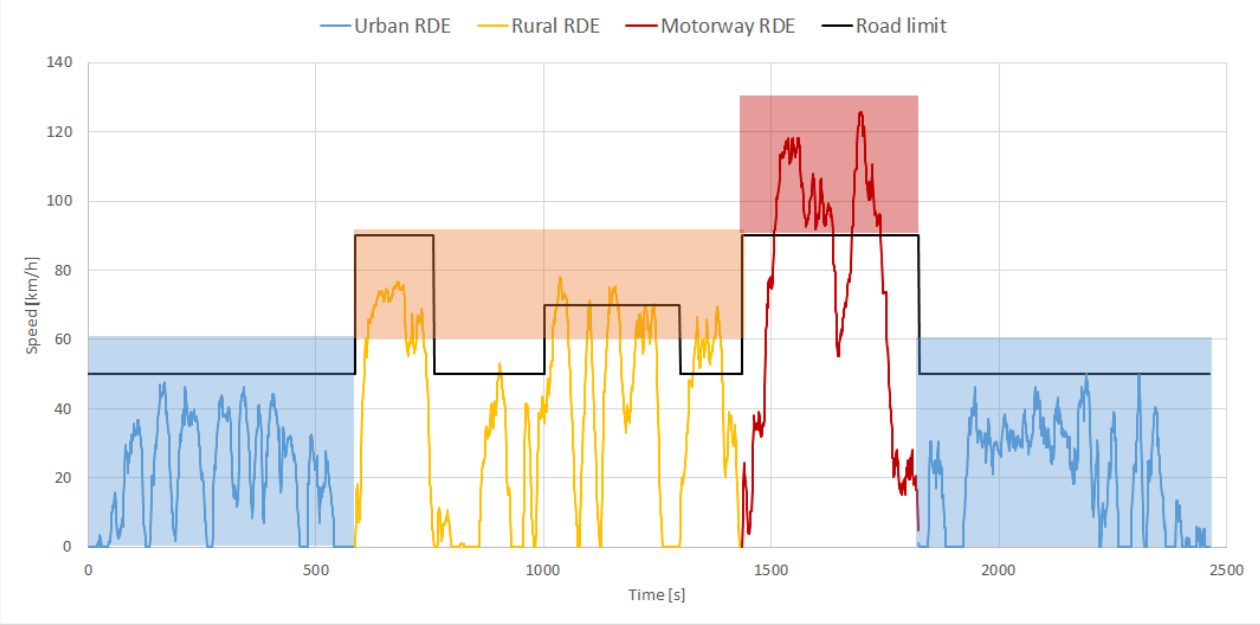

Figure 4-5: Road-type route phases segmentation.

Only on-road measurements from the most representative sub-categories (L1e-B, L3e-A1, L3e-A2 and L3e-A3) have been considered. These were the only subcategories with a more standardized route that can be compared between them. In this case, only NOx and HC are available because of the low number of measurements with data from the other pollutants considered in LENS db. Only the graph against $v*a_{,pos}$ has been analyzed because of the dispersion of the mean speed values on each phase for this phase's characterization. Even though, no important changes have been noticed regarding the emissions values. Figure G-33 to Figure G-36 are included in Appendix G: Impact of Phases discretization on emissions.

This project has received funding from the European Union's Horizon Europe research and innovation programme under grant agreement No 101056777

4.2.3 RDC & TA emissions results per phase

A more detailed analysis has been developed regarding CO, HC, NOx and PN emissions. The emissions have been computed by urban, rural and motorway phases, following the speed segmentation from Table 4-1, this is, 0-60-90 km/h.

Data filtering

To ensure quality of the data used in this analysis, and to be able to establish a 1:1 comparison of the behavior of specific vehicles under different operation conditions, a set of filter criteria was applied.

- **Vehicle sub-category**: most relevant LV subcategories L1e-B, L3e-A1, L3e-A2 and L3e-A3
- **Test cycle**: only those vehicles that have been tested both RDC and TA World Harmonized Motorcycle Test Cycle (WMTC)
- **Emissions signal**: as only laboratory measurements have been considered, Constant Volume Sampler (CVS) signal for each pollutant have been considered

RDE measurements have not been considered on this analysis, as the number of vehicles that have been subjected to TA and on-road measurements was reduced at the time that this analysis has been developed. Additionally, for those few vehicles mainly information on NOx emissions was available.

When filtering the data throughout all these conditions, we can assess the impact that a more representative of RW driving patterns test cycle has on emissions. Further analysis with latest on-road measurements from LENS db should be developed to better assess how these RW driving conditions affect emissions also on RDE measurements and not only on RDC.

L1e-B

Regarding L1e-B sub-category, a second disaggregation of data has been done by the engine technology, 2-stroke or 4-stroke, in order to highlight difference in emissions that engine characteristics might have. The results are shown Figure 4-6 and Figure 4-7.

Regarding 4-stroke vehicles, not many samples are available, and results do not differ a lot between RDC and WMTC. It is interesting that CO and PN emissions are higher on TA measurement. A reason for that might be the Cold Start impact on TA cycle lasting 1195 sec and the RDC cycle lasting 1650 sec, which is near 40% longer in terms of time duration.

This project has received funding from the European Union's Horizon Europe research and innovation programme under grant agreement No 101056777

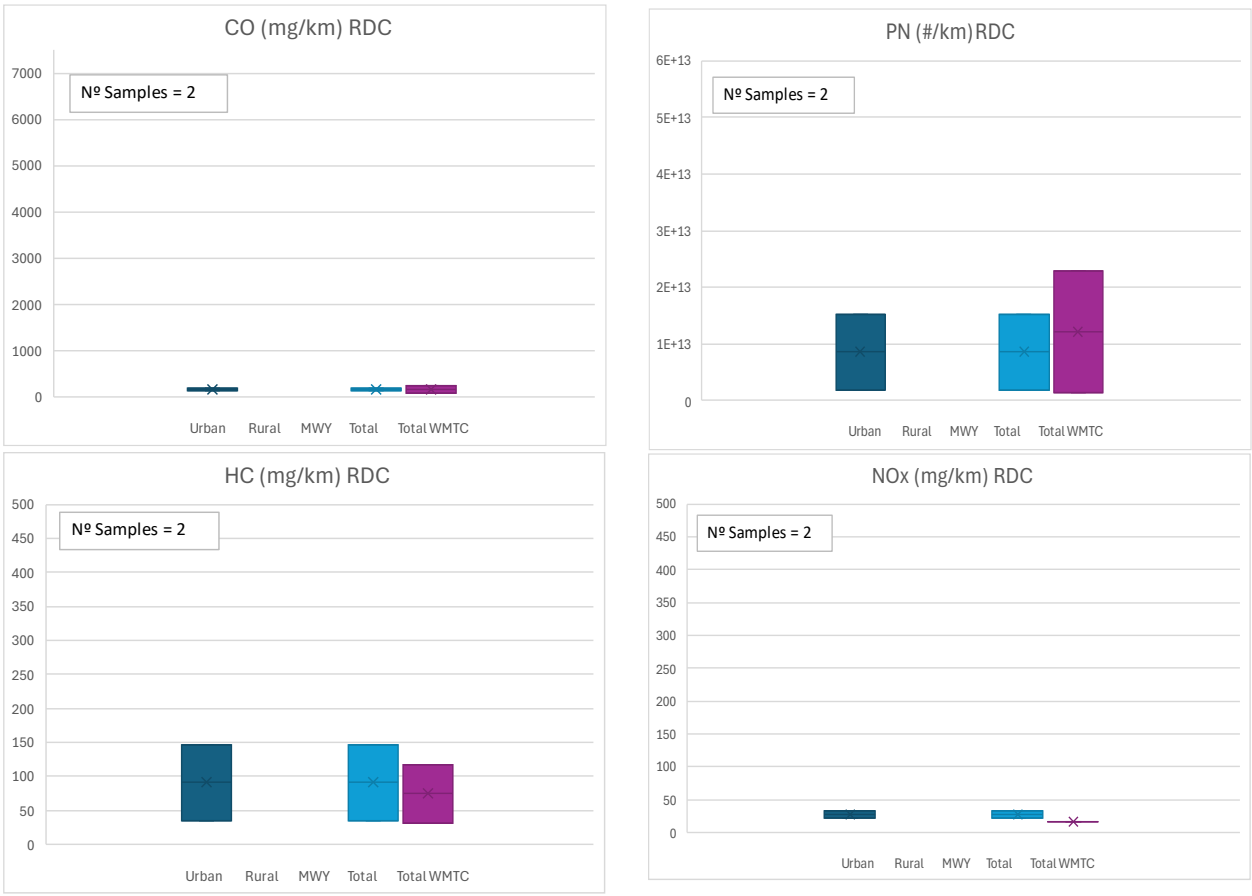

Figure 4-6: Emissions analysis per phase of L1e-B 4-stroke Euro 5.

Regarding 2-stroke vehicles, only one sample has been considered, so no relevant conclusions can be derived. In this case, TA WMTC values are always lower than RDC ones. Particularly for HC, the RDC value is +100% of WMTC one.

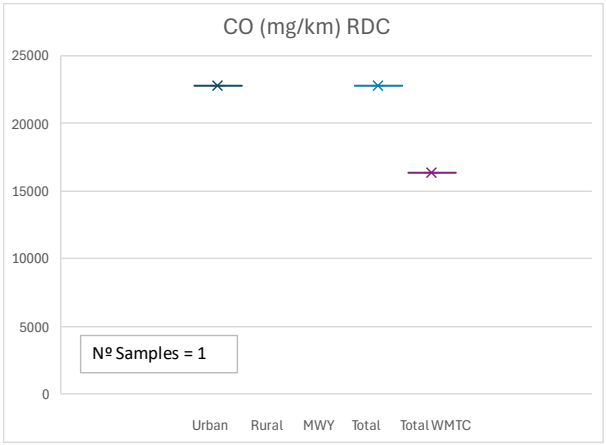

This project has received funding from the European Union's Horizon Europe research and innovation programme under grant agreement No 101056777

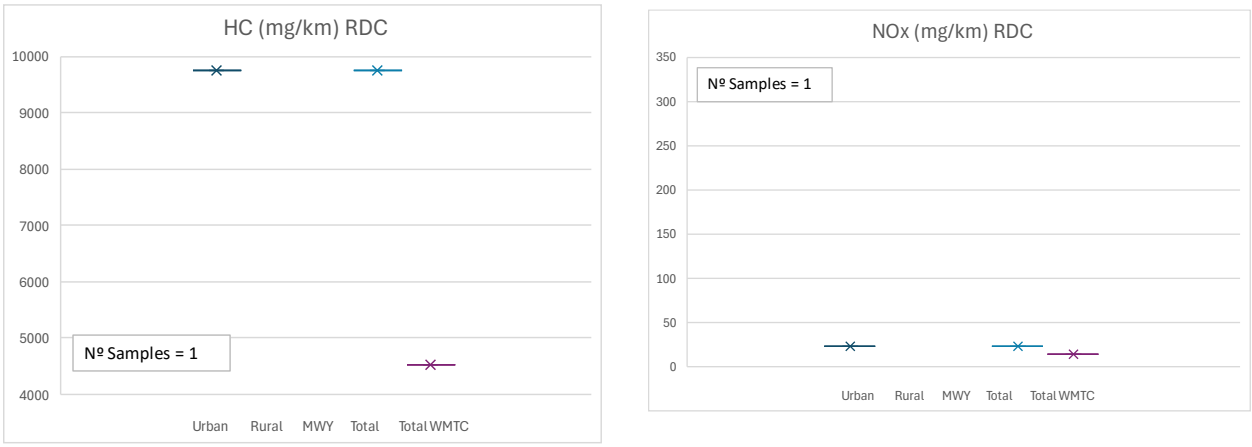

Figure 4-7: Emissions analysis per phase of L1e-B 2-stroke Euro 5.

When comparing both technologies, completely different pictures are represented. Regarding 2-Stroke engines, HC and CO emissions are +130x times higher, and NOx emissions only 0.5x times higher than 4-stroke engines.

L3e-A1

On L3e-A1 is important to mention that those L3e-A1 vehicles considered on this analysis have been tested in WMTC Class 1 according to the current regulation (EU) 134/2014, following the criteria presented in Figure 4-17. This means that they are tested like L1e-B, and no data from rural nor motorway phases are available. Regarding RDC , data for each one of the phases is available as they are ideally driven up to 120 km/h, when possible. Results here are much more revealing than on L1e-B. All phases have completely different emissions patterns. All pollutants have higher emissions on RDC, except HC. Regarding how the emissions distribute for the different phases, CO, HC and PN follow similar patterns, where the motorway phase is the most critical one. Regarding CO emissions, they are completely out of control, reaching an average value of 12,698 mg/km on the motorway phase, when WMTC total average unweighted value is 694 mg/km, +20x times higher and a total value of 3,766.6 mg/km for RDC, near +4x times higher. Regarding NOx emissions, the motorway phase is the one where emissions are lower. Fuel enrichment could be the reason for this finding, as temperatures remain low. For those pollutants where the motorway phase is the most critical, CO is the most affected one, with a value of +2.3 times higher than the total RDC one.

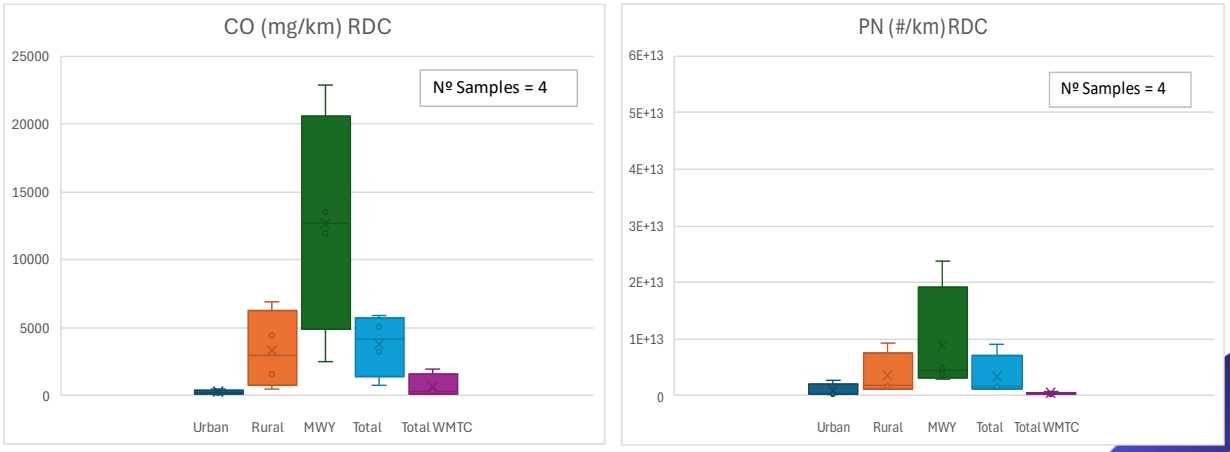

This project has received funding from the European Union's Horizon Europe research and innovation programme under grant agreement No 101056777

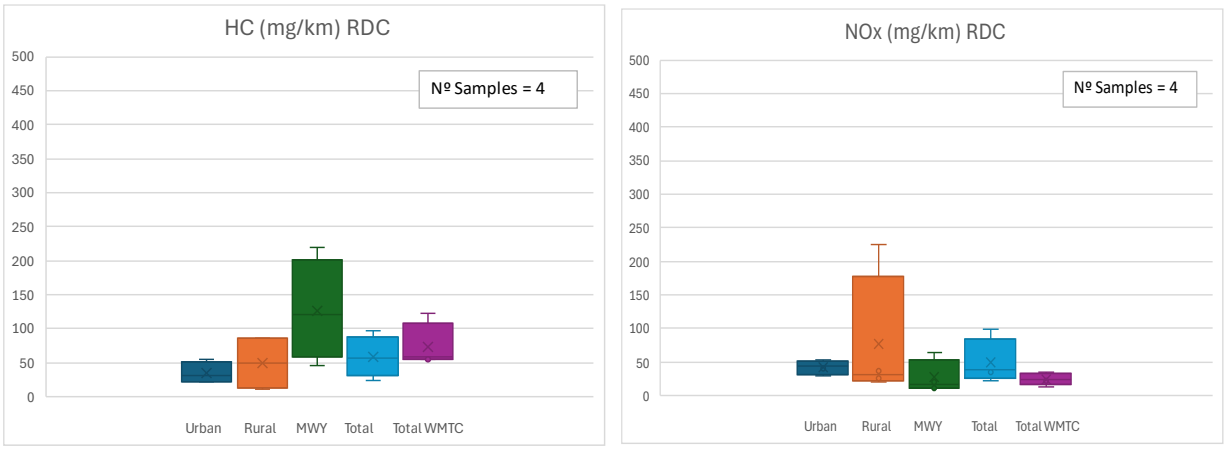

Figure 4-8: Emissions analysis per phase of L3e-A1 Euro 5.

L3e-A2

Regarding L3e-A2, data from all phases is available now for both RDC and WMTC. All pollutant emissions, but especially HC, are mostly influenced by one single vehicle. If this vehicle is not considered, new average HC emissions are reduced by 6.7x times on urban phase, 7.8x times on rural phase, 2x times for motorway phase, and therefore this results on lower values by 4.6x times on the overall emissions when referring to RDC. On this way, HC emissions pattern is not so influenced by vehicle speed as CO emissions are, reaching motorway HC emissions +1.6x times the overall average value of TA measurements. PN and CO emissions are very sensitive to vehicle speed as they are importantly triggered on motorway phase, representing a higher extent of the overall average emissions, this is, +3.3x times on PN emissions, +2.5x times on CO. NOx is also influenced by the same outlier vehicle from HC, reaching overall average emissions of 699.7 mg/km on this outlier, when overall average NOx emissions without counting it remains at 54.2 mg/km, +13x times lower. Without considering this outlier, NOx emissions seem also to be triggered on motorway phase, representing nearly +2x times higher value than the overall average emissions.

The vehicle shown as outlier has some specific characteristics that differ from the other vehicles. It refers to a sports bike with high engine capacity (650cc). On WMTC measurement the same situation of higher emissions have been identified.

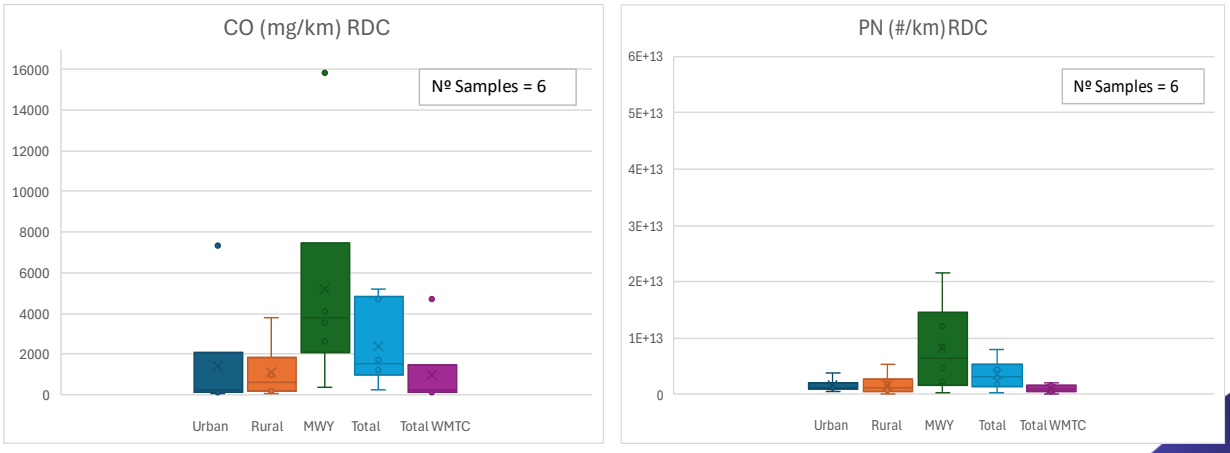

This project has received funding from the European Union's Horizon Europe research and innovation programme under grant agreement No 101056777

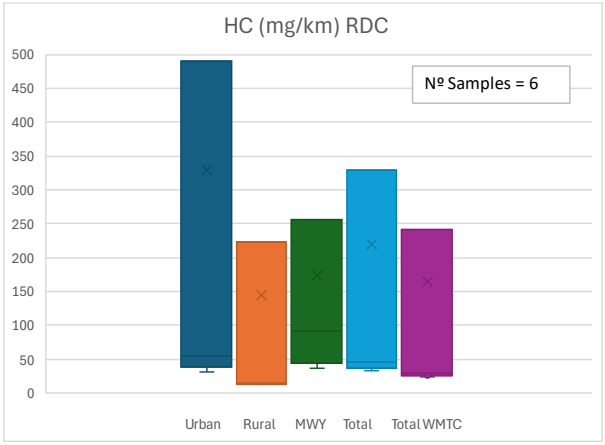

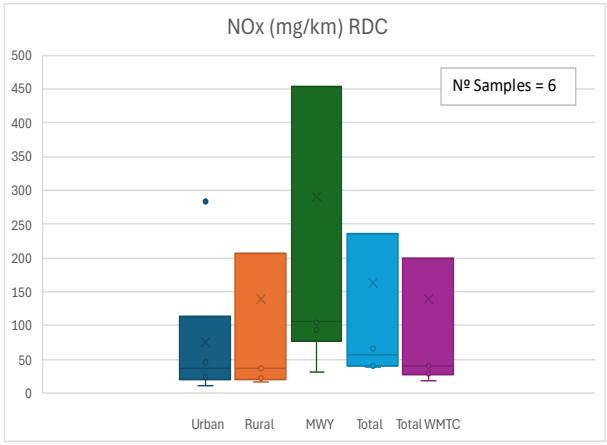

Figure 4-9: Emissions analysis per phase of L3e-A2 Euro 5.

L3e-A3

Regarding L3e-A3, data from all phases is available now for both RDC and WMTC. No outliers are present in this sub-category; all data is much more condensed and presents lower emissions than L3e-A2. L3e-A3 are all high powered so then this is not a limiting factor and there is no necessity of operating them at 100% throttle. On following section, detailed analysis of some specific vehicles shows that L3e-A3 vehicle is only driven up to 75% of its max power rated engine speed. Additionally, L3e-A2 comprises both MT and CVT, whereas L3e-A3 are only composed of MT or Automated Manual Transmissions (AMT) vehicles, and RW driving patterns differ for each kind of transmissions technology. Even without considering L3e-A2 outlier measurement, all pollutant emissions are lower for the A3 sub-category. HC emissions are quite affected by cold start, as the urban phase present slightly higher emissions. Regarding CO, no trends can be noticed regarding the emissions per phase. On the other hand, for NOx and PN, the emissions get triggered on the motorway phase. Regarding PN emissions, this is caused by a high emitter vehicle which reaches a value of 5.7 E+13. The vehicle that is causing high increase on average NOx emissions reaches 581.3 mg/km whereas the average value without it remains at 64.5 mg/km for motorway phase, this is 9 times higher emissions.

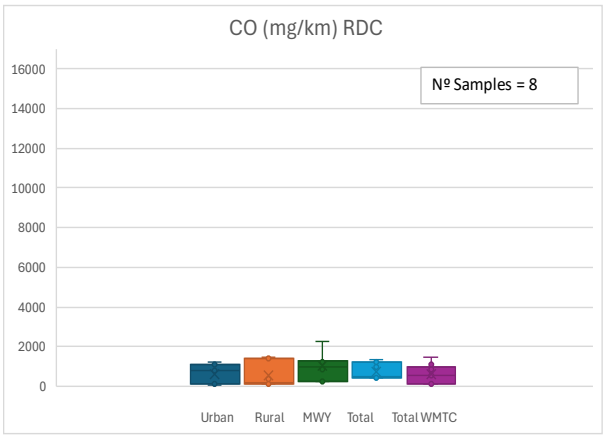

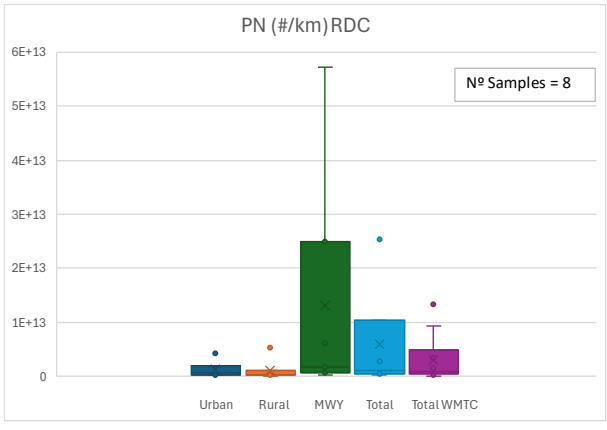

This project has received funding from the European Union's Horizon Europe research and innovation programme under grant agreement No 101056777

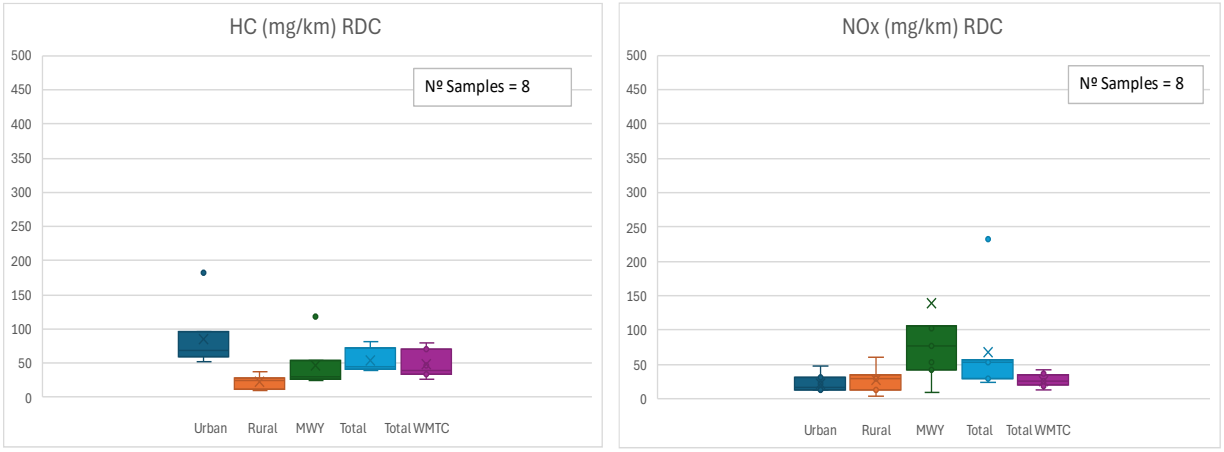

Figure 4-10: Emissions analysis per phase of L3e-A3 Euro 5.

4.3 Assessment of real-world driving dynamics

The driving dynamics of L-Category vehicles cover a wide range of driving scenarios, which goes beyond what passenger cars (PC) are intended to. The low mass and high power that they have are reflected in the following analysis of all WMTC, RDC and RDE measurements developed under the LENS project.

In the following sections a study of the behavior of the driving dynamics of LVs is done. It includes a comparison with PC, with type approval tests, RDC and RW driving operation, and the effect of different driving operation (urban, rural and motorway phases) speed segmentations and the classification by road type instead of vehicle speed, as it was also studied in the previous chapter regarding the impact on emissions.

4.3.1 PMR distribution

The power-to-mass ratio represents a critical performance metric for L-category vehicles, encompassing motorcycles, mopeds, and tricycles. This parameter is fundamental in defining the vehicle's dynamic capabilities, energy efficiency, and overall mechanical performance.

On the Figure 4-11, the overall distribution of the power-to-mass ratio for the different sub-categories is shown. Additionally, typical PC values are represented. For this representation, vehicles homologated as T-Category are excluded as they do not have the same vehicle' mass requirements. Excluding L3e-A3 vehicles, the vast majority is condensed under the average value of 0.2 kW/kg. The green shadowed area represents the average values of PMR for passenger cars. L3e-A3 vehicles are highly powered, with PMR values which are nearly to hit 0.8 kW/kg, nearly +4X times the maximum typical value for passenger cars. An average family car is near 0.07kW/kg, and a hyper car up to 0.25 kW/kg.

These vehicle characteristics reflect that the driving scenarios to which they are subjected present not so many similarities with passenger cars.

This project has received funding from the European Union's Horizon Europe research and innovation programme under grant agreement No 101056777

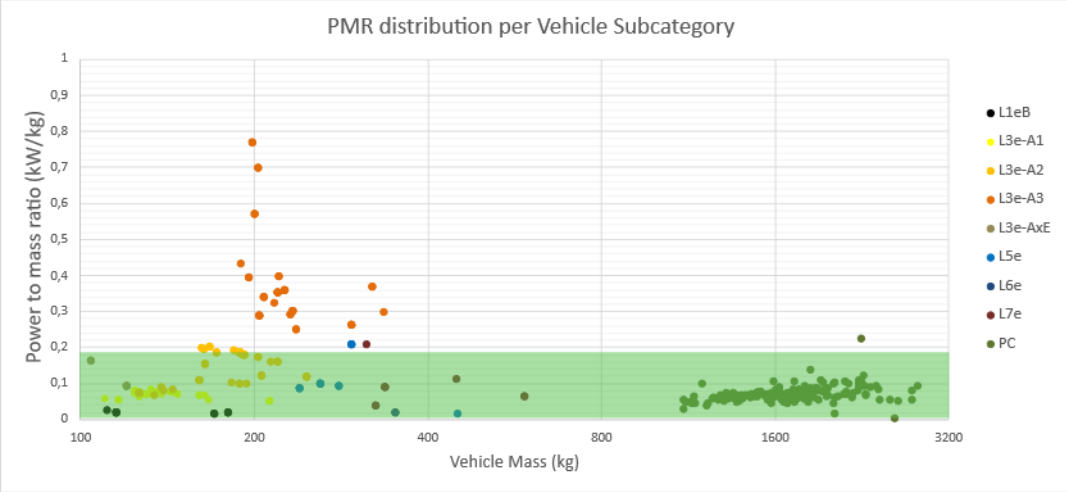

Figure 4-11: Power to mass ratio distribution of the vehicles measured in LENS db per subcategory. Additionally, more than a total of 100 Passenger Cars from GreenNCAP PMR values are represented.

4.3.2 Analysis of v*a pos (95th perc)

As it was introduced in the previous Section 4.3.1, the performance of L-Category vehicles is much higher than typical PCs. On this way higher values of $v*a_{,pos}$ could be expected on a real-driving situations. In Figure 4-12, $v*a_{,pos(perc95)}$ values from +100 PC are represented. Data from PC is obtained from Green NCAP Database.

On a standard RDE, for complying with regulations, values should be positioned under the dashed line. This limits how dynamic the speed profile of the measurement is. It is important to mention that these trip requirements from "*Standard RDE*" are according to the Regulation (UE) 2017/1151, same situation with the speed classes, which are present on Table 4-1. Extra official measurements, named as "*Extreme RDE*" represent values obtained on more demanding on-road test cycle, in which higher accelerations are mandatory. This extra-official RDE cycle is not regulated under (UE) 2017/1151, it is shown as an example of how dynamic a PC can be under more aggressive driving conditions.

Regardless of the test performed, the same phase discretization has been assumed for all of them, with the aim of maintaining comparability between all test cycles. This means that no WMTC predefined phases have been considered in this analysis.

This project has received funding from the European Union's Horizon Europe research and innovation programme under grant agreement No 101056777

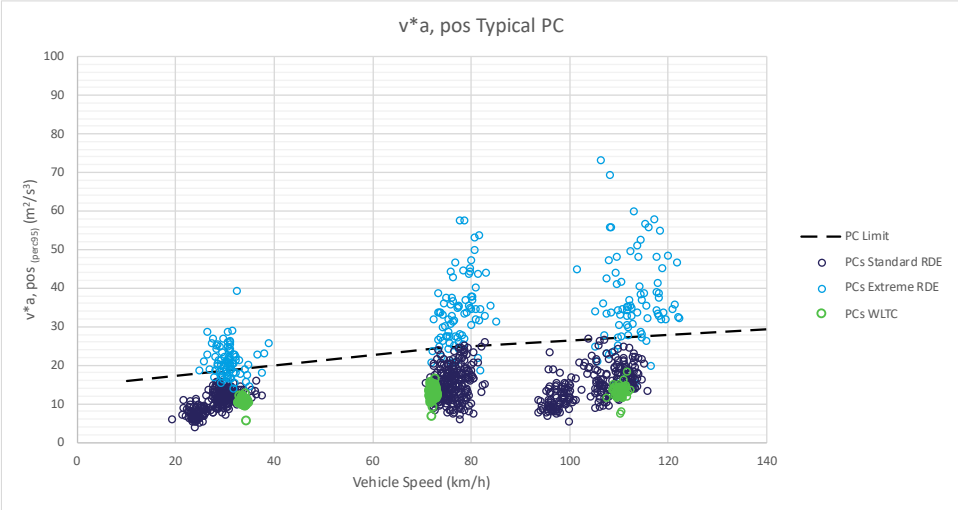

Figure 4-12: v*a, pos values from +100 typical PCs from Green NCAP.

Analysis of the driving dynamics from LENS db has been also conducted. For this activity, all KPIs have been calculated from the raw signal of the vehicle speed (dyno speed for TA measurements, and GPS vehicle speed for RDE). No filter has been applied to the speed signal. The KPIs that have been considered for this analysis are the $v^*a_{,pos(perc95)}$ and the RPA. For computing a, pos, the condition of ai > 0.1 m/s^2 was applied.

In Figure 4-13, $v^*a_{,pos(perc95)}$ values computed for all vehicles on the LENS db are represented. These values are composed of all LV sub-categories and both normal and aggressive driving conditions. Only three "extreme RDE" measurements are available. In terms of mean vehicle speed, not necessarily higher mean vehicle speed corresponds with higher values of $v^*a_{,pos(perc95)}$. As in most cases, speed limits had to be respected, no high values of mean vehicle speed are represented on the motorway phase, nor high accelerations. This explains why the rural phase seems to be more dynamic.

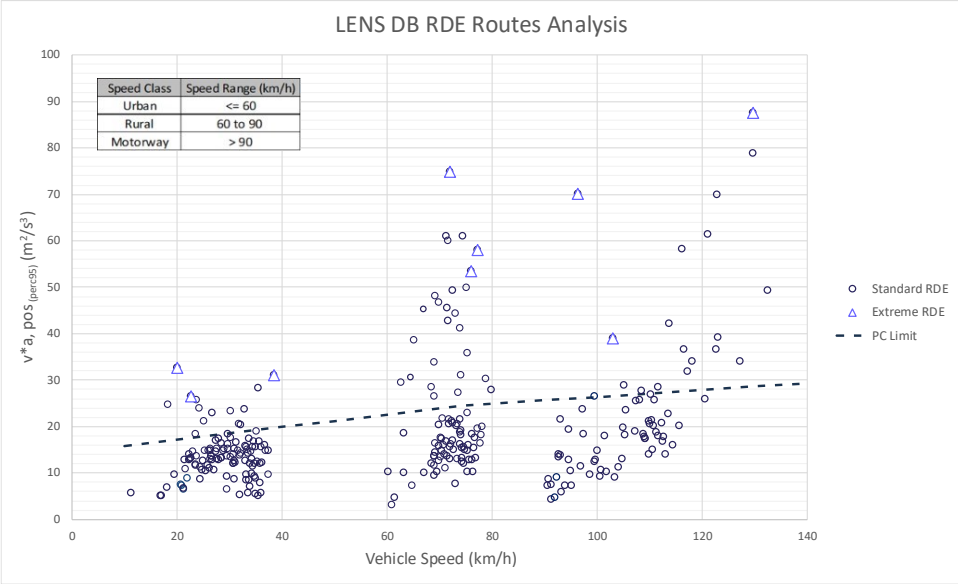

Figure 4-13: v*a, pos values from +100 LVs from LENS db corresponded with normal and aggressive usage.

This project has received funding from the European Union's Horizon Europe research and innovation programme under grant agreement No 101056777

Conclusion is that LVs and PCs are not comparable in terms of on-road driving dynamics. Therefore, driving dynamics that are in a different range of values and depend on vehicle characteristics need further development for LVs requirements. The evidence of how different driving dynamics from LVs and PCs are, is shown in Figure 4-14.

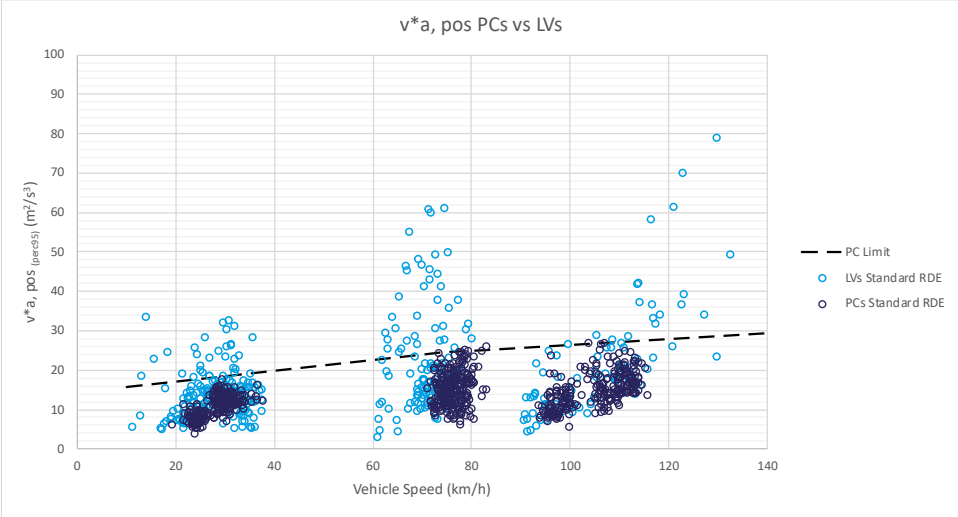

Figure 4-14: v*a,pos values comparison of PCs and LVs on standard RDE conditions.

When comparing the driving dynamics from homologation cycles of PCs and LVs, trip requirements are quite aligned. This makes evident that WMTC is not representative enough of the RW driving patterns of LVs. In Figure 4-15 all WMTC variants of all vehicles subjected to LENS measurements, and from Worldwide Harmonized Light Vehicle Test Procedure (WLTP) measurements from Green NCAP.

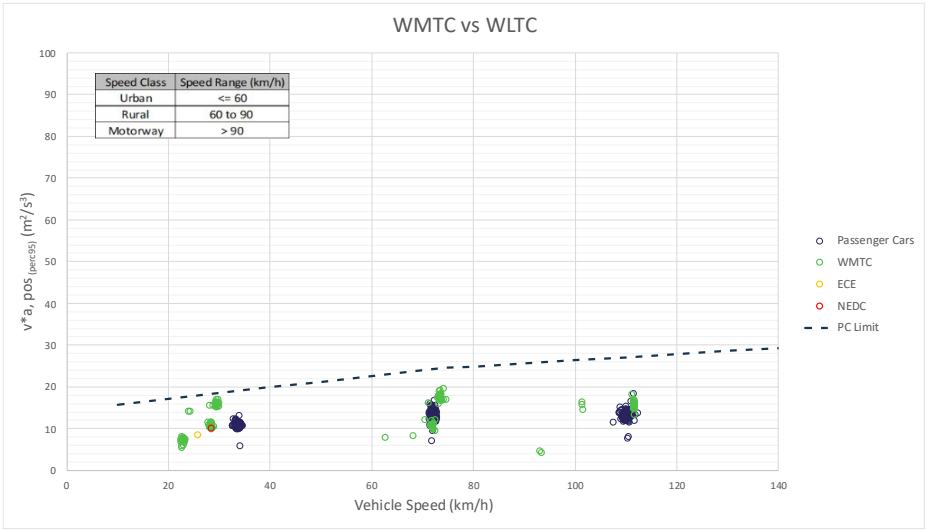

Figure 4-15: WMTC vs WLTC driving dynamics comparison. Theoretic WLTC speed profile considered.

Driving dynamics of the measurements executed on the chassis dyno are represented on Figure 4-16. In LENS measurements, New European Driving Cycle (NEDC) and Economic Commission for Europe (ECE) test cycles refer only to L1e-B vehicles. RDCs measurement yield more dynamic values than WMTC, which

This project has received funding from the European Union's Horizon Europe research and innovation programme under grant agreement No 101056777

remains under PC limits in all phases, whereas RDC values are mostly above it. RDC values located with mean speed value under 100 km/h on the right side (mean speed values under 90 km/h, motorway phase), corresponds with L3e-A1 RDC measurements. This sub-category, normally, does not have the capability of reaching maximum speeds above 110 km/h, therefore the acceleration on at high speeds are almost negligible and there is a slight dispersion since in some vehicles higher speed traces of the cycle were not reached because of top speed limitations. In addition, different WMTC Classes defined in Figure 4-17, are presented as different point clouds.

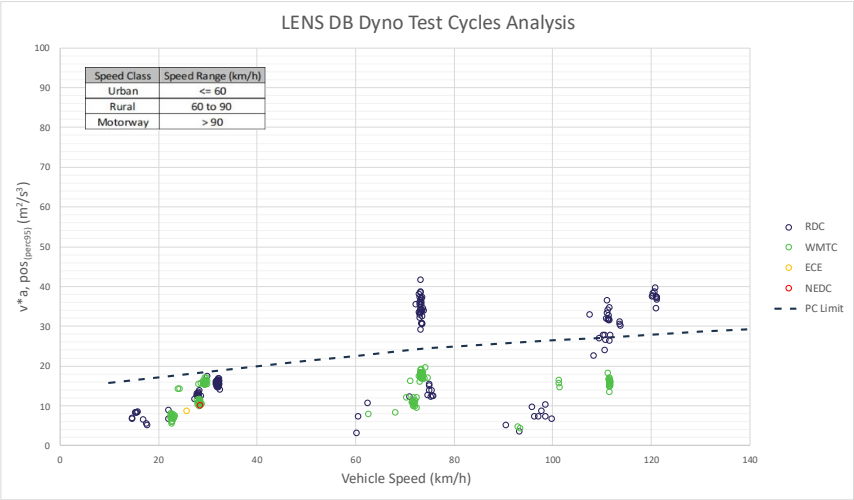

Figure 4-16: v*a, pos values from +100 LVs from LENS db corresponded with chassis dyno measurements for different test cycles.

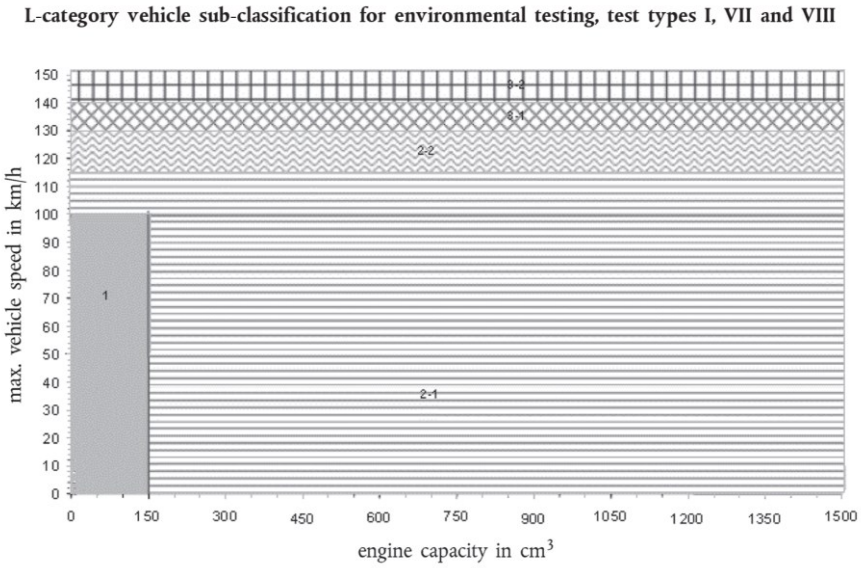

Figure 4-17: WMTC Classes for environmental testing. From regulation (EU) 134/2014.

Regarding RDC measurements on both L3e-A2 and L3e-A3 sub-categories, some dispersion is shown too. The explanation of this is that, not all dynos have the same characteristics and maximum designed speed, therefore they cannot follow the test cycle when speed reaches dyno limitation. For those dynos limited

This project has received funding from the European Union's Horizon Europe research and innovation programme under grant agreement No 101056777

on speed, the maximum speed is not the same, each dyno has its own limitation, and it is different from the others.
Small dispersion of the rural phase is because some L3e-AxE and a real L7e-B2 have been tested. Both vehicles are low-powered and thus not able to follow RDC speed traces.

A first comparison between on-road and chassis dyno measurements could be established when representing all measurements on a unique plot, as shown in Figure 4-18. As we have already mentioned, only few "extreme" on-road measurements have been developed. Even though on-road $v*a_{,pos(perc95)}$ values are importantly higher than actual RDC or WMTC. This means that normal driving is usually much more demanding than WMTC, and higher also than RDC on high-powered vehicles. For those whose power is more limited, both WMTC, RDC and on-road measurements are quite close, so engine operating points are better covered. More detailed analysis will be developed in the next section, where evidence is the high density of on-road $v*a_{,pos}$ values close to WMTC and RDC ones, are mostly corresponded with those low-powered sub-categories (L1e-B and L3e-A1).

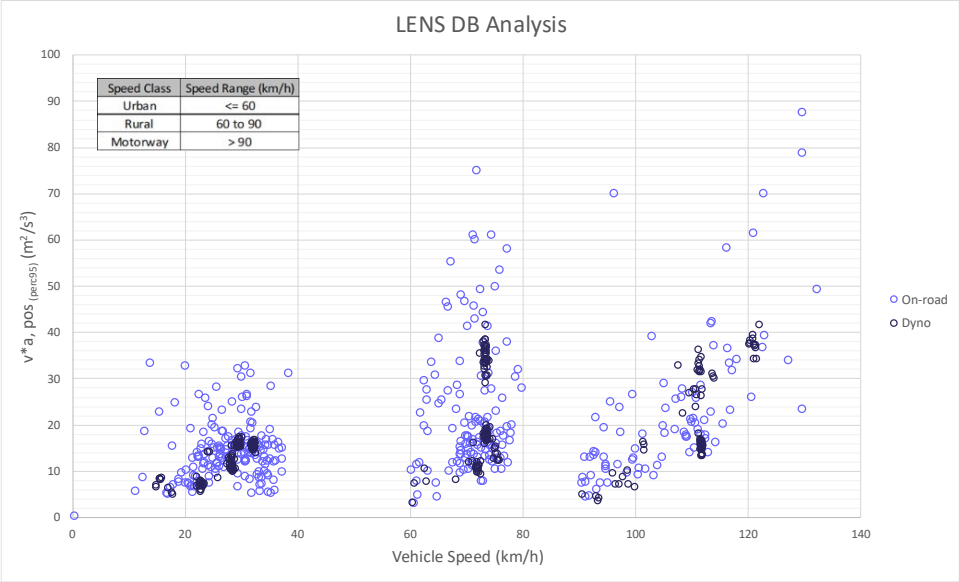

Figure 4-18: v*a, pos values from +150 LVs from LENS db corresponded with on-road and chassis dyno measurements.

4.3.2.1 Detailed analysis of representative LV sub-categories

Specific analysis has been developed independently for each L-category vehicle sub-categories. All measurements have been included in this analysis (RDE, RDC, WMTC, NEDC, etc). The wide PMR that all these vehicles cover leads to the necessity of a specific analysis. Low-powered mopped could not be compared with high-powered motorcycles. In Figure 4-19, this could be proved. As it was already mentioned, low powered vehicles or sub-categories do not have an important dispersion between the different types of measurements in terms of driving dynamics. Their respective $v*a_{,pos}$ values are clustered in a small area. This is not the case, especially for L3e-A2 and L3e-A3.

This project has received funding from the European Union's Horizon Europe research and innovation programme under grant agreement No 101056777

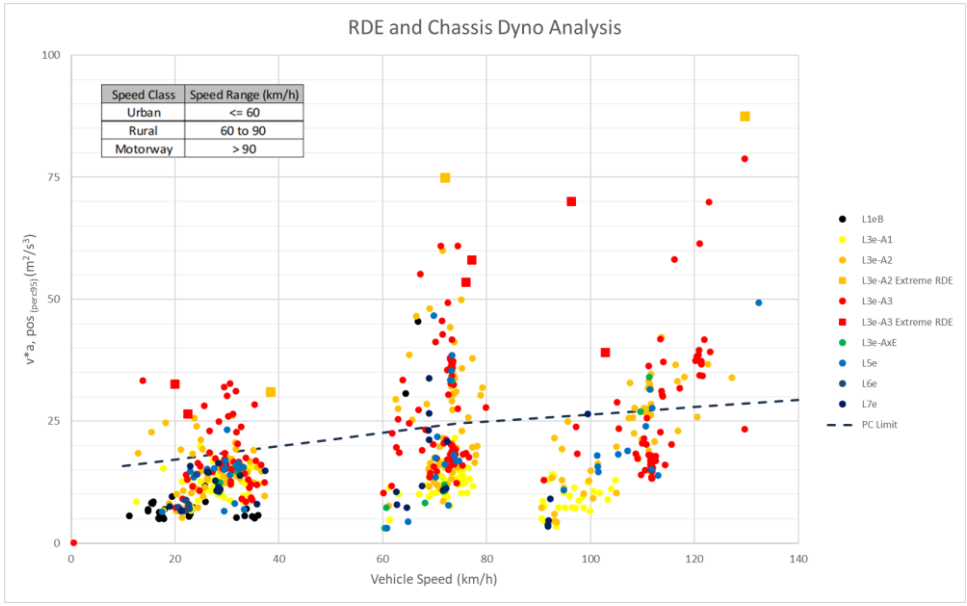

Figure 4-19: v*a,pos from both chassis dyno and on-road LENS db measurements colored by vehicle sub-category.

L3e-A1

In the previous sections, it has already been discussed that in the sub-categories of low-power vehicles, there is no significant difference in the dynamic conditions for the different types of tests carried out. In Figure 4-20, this finding is reflected. There is no important vertical dispersion, only mean speed values for each phase showing dispersion. This is normal since on-road measurements have been developed on public roads, so speed should be adapted to each road type and traffic situation, and therefore no fixed mean vehicle speed could be reached. Additionally, L3e-A1 vehicles do not have enough power to perform strong accelerations as A2/A3 are.

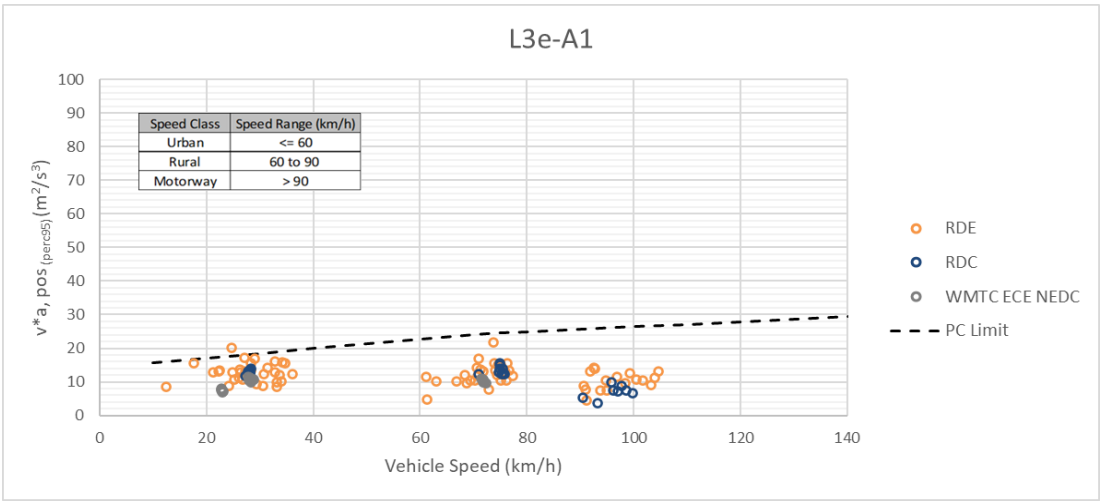

Figure 4-20: L3e-A1 v*a,pos values for each type of LENS db measurement.

This project has received funding from the European Union's Horizon Europe research and innovation programme under grant agreement No 101056777

L3e-A2

In Figure 4-21 v*$a_{,pos}$ from all L3e-A2 measurements is represented. It is important to mention that these measurements have been developed without breaking local traffic regulations. More than 50% of the measurements represent v*$a_{,pos}$ values much higher than WMTC ones. RDC coverage is more representative, especially in the motorway phase, where there were not so many possibilities of reproducing high accelerations. This is not the case for the rural phase since acceleration from 60 km/h presents a bigger occurrence on normal driving conditions. Regarding "Extreme RDE" measurements, significant differences are noticed. This vehicle sub-category is powered enough to be driven in an extremely aggressive manner. This specific measurement has been conducted in a controlled environment.

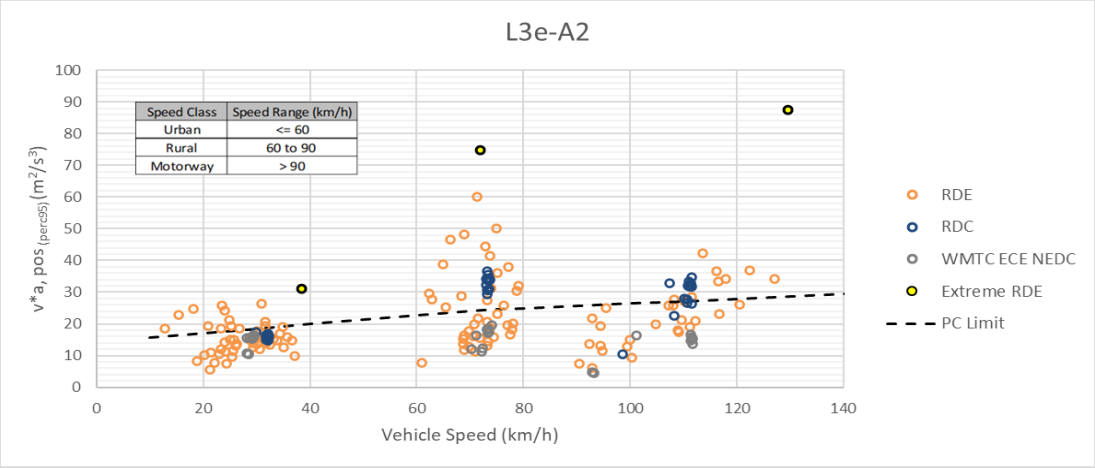

Figure 4-21: L3e-A2 v*a,pos values for each type of LENS db measurement. One "Extreme RDE" measurement too.

L3e-A3

In Figure 4-22 v*$a_{,pos}$ from all L3e-A3 measurements is represented. For this sub-category, where engine power is not limited to 35 kW, the driving dynamics results do not differ much from A2 sub-category. As it was mentioned, 35 kW is enough power for aggressive driving. Beyond this power limitation, what limit driving aggressiveness are the traffic regulations, and drivers' abilities. Every day use does not differ so much from what can be shown on the v*$a_{,pos}$ graph. On this case, "Extreme RDE" measurements do not come from same laboratory as on A2 sub-category; therefore, results are not comparable at all. Even though, in the rural phase, both measurements present high values of v*$a_{,pos}$.

When comparing with both WMTC and RDC, as with A2 vehicles, almost 50% of the measurements are located so close to WMTC. It should be mentioned that, unlike A2, higher values of v*a,pos have been obtained, thus WMTC and RDC are not representative at all. Regarding the rural and motorway phase, RDC works well, as it is positioned near on average of all RDE results.

This project has received funding from the European Union's Horizon Europe research and innovation programme under grant agreement No 101056777

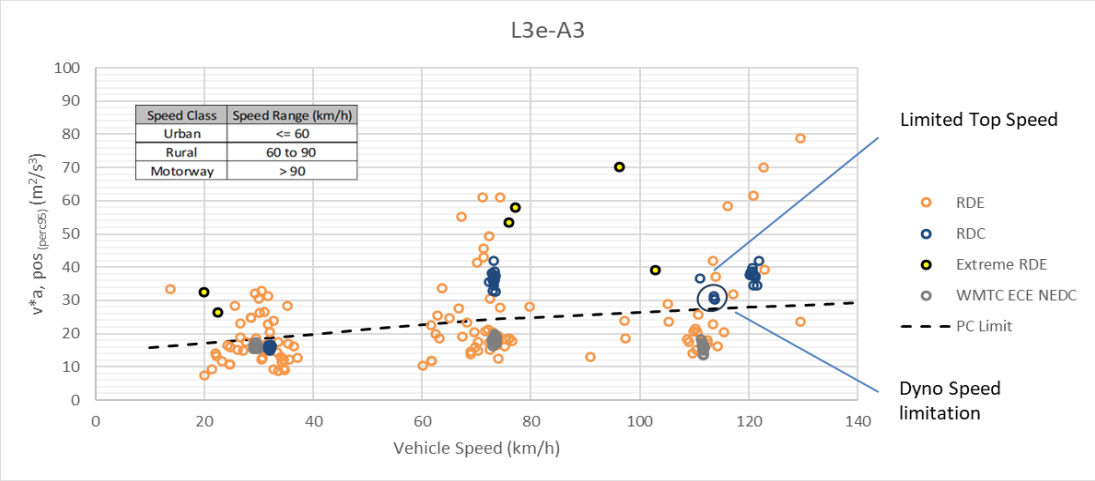

Figure 4-22: L3e-A4 v*a,pos values for each type of LENS db measurement. One "Extreme RDE" measurement too.

In Appendix H: v*a_{pos} analysis, figures of all L-Vehicle's subcategories are available.

4.3.2.2 Speed segmentation phases discretization impact on driving dynamics

Different discretization of phases has also been proposed. The first approach of the analysis has been developed according to Regulation (EU) no 2017/1151, where the speed classes are defined as represented on previous section on Table 4-1. Different variations have been also considered to assess how different speed classes could have an impact on the driving dynamics. These variations are included on Table 4-5, Table 4-6 and

Table 4-7. The proposed alternatives have not resulted in significant differences; however, results are shown in Appendix I: Impact of Phases discretization on driving dynamics.

4.3.2.3 Road type phases discretization impact on driving dynamics

An analysis of the impact has been done with representative routes performed. Figure 4-23 shows the results of the analysis performed which is also contained in Appendix I: Impact of Phases discretization on driving dynamics so a comparison between all previous phases discretization method could be figured out. Once again, no relevant modifications on driving dynamics have been noticed.

This project has received funding from the European Union's Horizon Europe research and innovation programme under grant agreement No 101056777

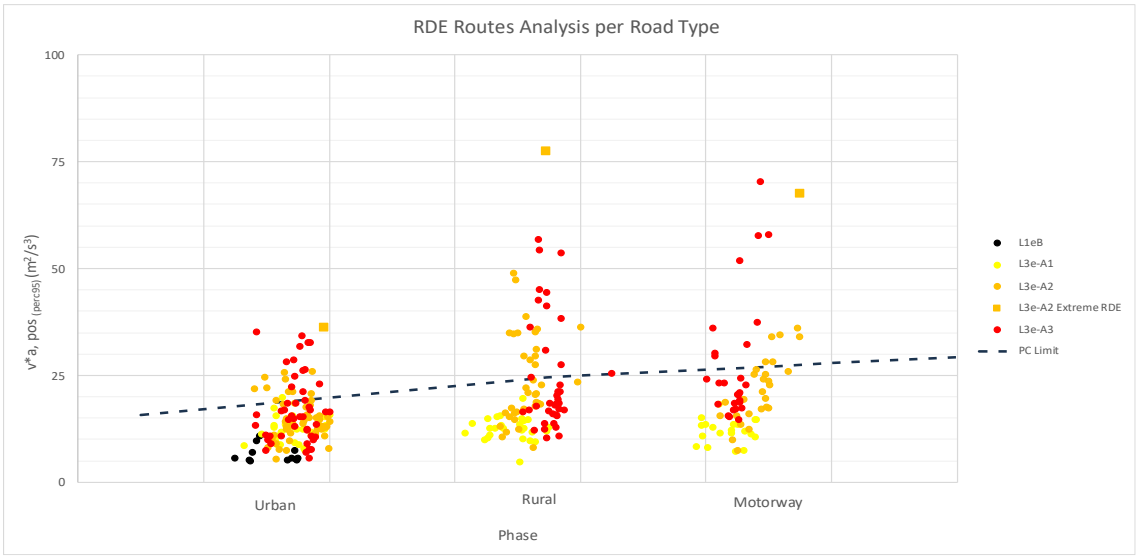

Figure 4-23: vehicle dynamics v*a pos perc 95 (m^2/s^3) against vehicle mean speed (km/h) for urban, rural and motorway. when discretizing phases per road type.

4.3.3 Analysis of RPA

In this section, relative positive acceleration (RPA) is analyzed. Starting with PCs comparison between the different types of measurements, in Figure 4-24 is represented the RPA values from WLTC and both standard an extreme RDE. Points are much more clustered than on $v*a_{,pos}$, with WLTC positioned above standard RDE in most cases.

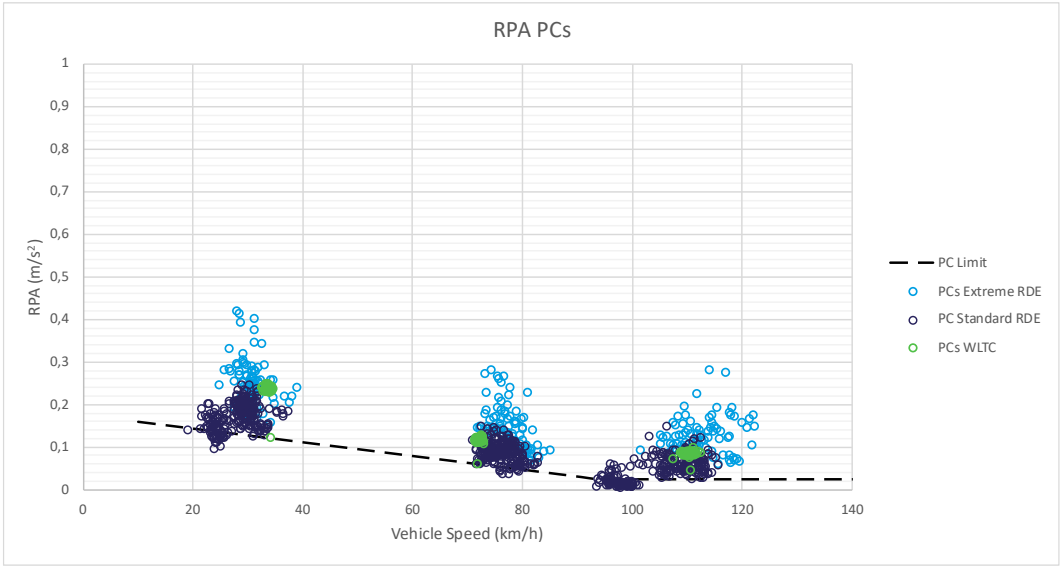

Figure 4-24: passenger cars RPA values for different on-road and lab measurements from GreenNCAP db.

The behavior of RPA is in consonance with $v*a_{,pos}$ trends for LVs where ranges of values are higher than for PC standard RDE, and higher than extreme RDE too. Figure 4-25 provide RPA values of PC in Green NCAP db and for LENS db, distinguished by color. RPA values of standard RDE measurements are considerably higher on LVs, especially on both urban and rural phases.

This project has received funding from the European Union's Horizon Europe research and innovation programme under grant agreement No 101056777

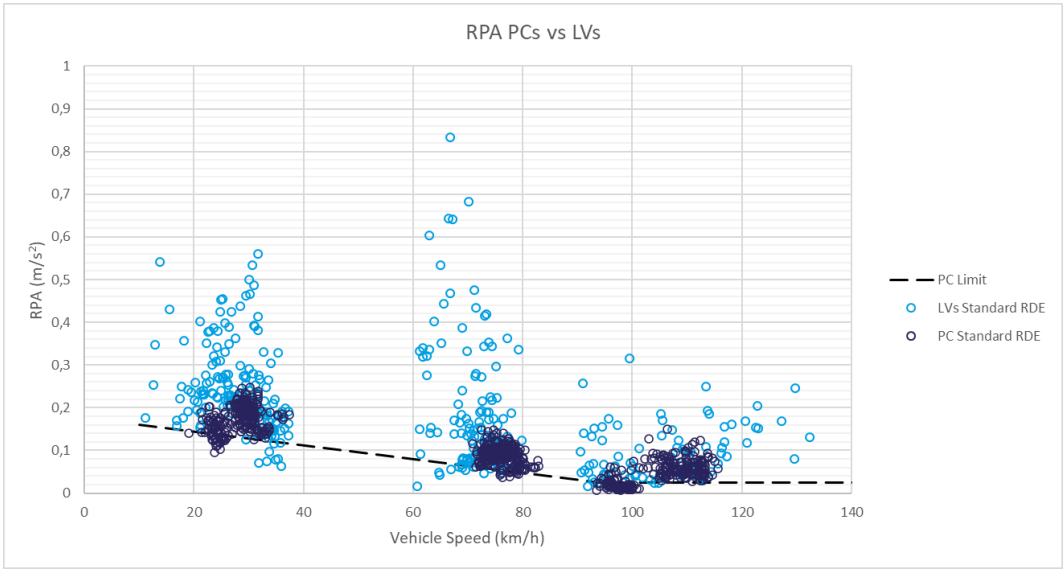

Figure 4-25: Comparison of RPA values of PC and LV of LENS db on-road measurements for standard RDE.

When comparing on-road with chassis dyno measurements from LENS db, an important difference can be noticed. On-road measurements are represented by considerably higher RPA values. Evidence is also that WMTC values are much more clustered than on $v*a_{,pos}$, as RPA considers all values from the measurement on each phase, and not one single value from percentile 95 of the entire series, this can be shown in Figure 4-26.

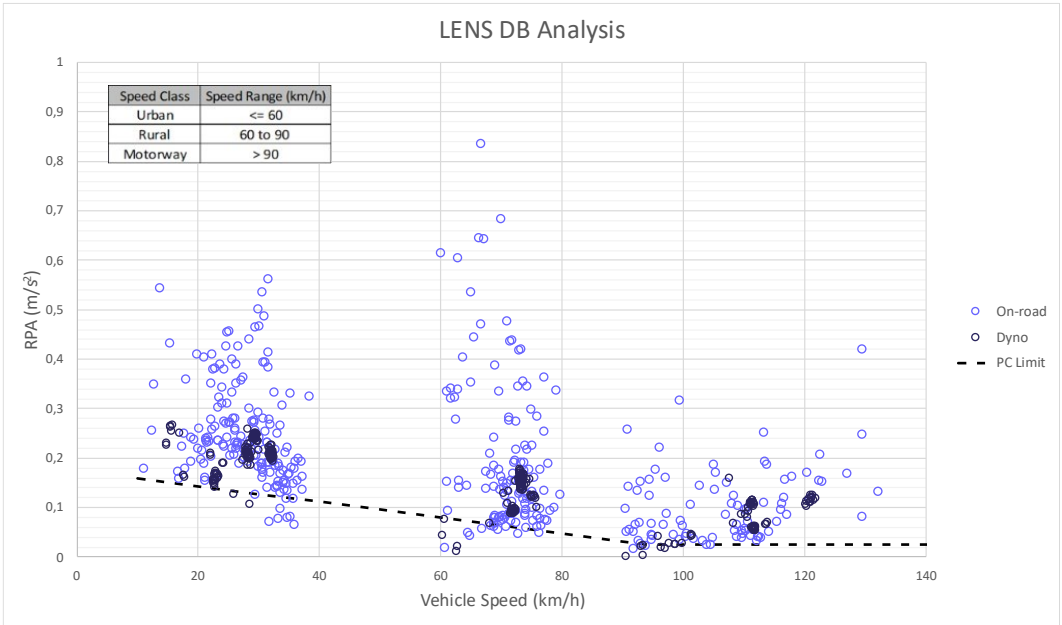

Figure 4-26: Comparison between RPA values from on-road and lab measurements on LENS db.

Regarding the "*aggressive*" routes performed, no big differences have been noticed in Figure 4-27, only one measurement is evaluated as the most dynamic one for the motorway phase. The remaining measurements show no significant differences.

This project has received funding from the European Union's Horizon Europe research and innovation programme under grant agreement No 101056777

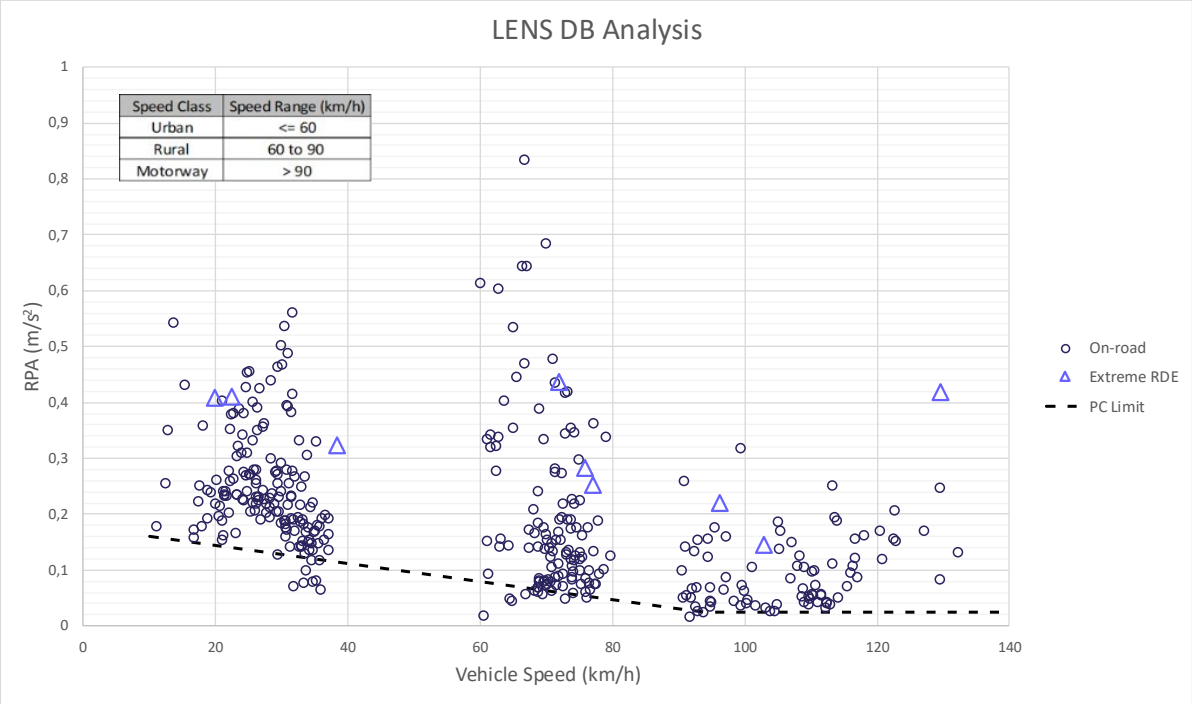

Figure 4-27: Comparison between RPA values from extreme and standard on-road measurements on LENS db.

An example of the trends for L3e-A3 is shown below in Figure 4-28 and Figure 4-29 where it can be seen that RPA of on-road tests cover a wider range of accelerations than the RDC and TA dyno test. Evidence that chassis dyno measurements are more clustered for RPA that for v*a$_{,pos}$ is now represented and comparable between both figures. The inversely proportional relationship of dispersion with increasing speed has also been identified when analyzing the graphs. As we progress through the phases from lower to higher speed, the RPA values become more similar to those of chassis dyno measurements.

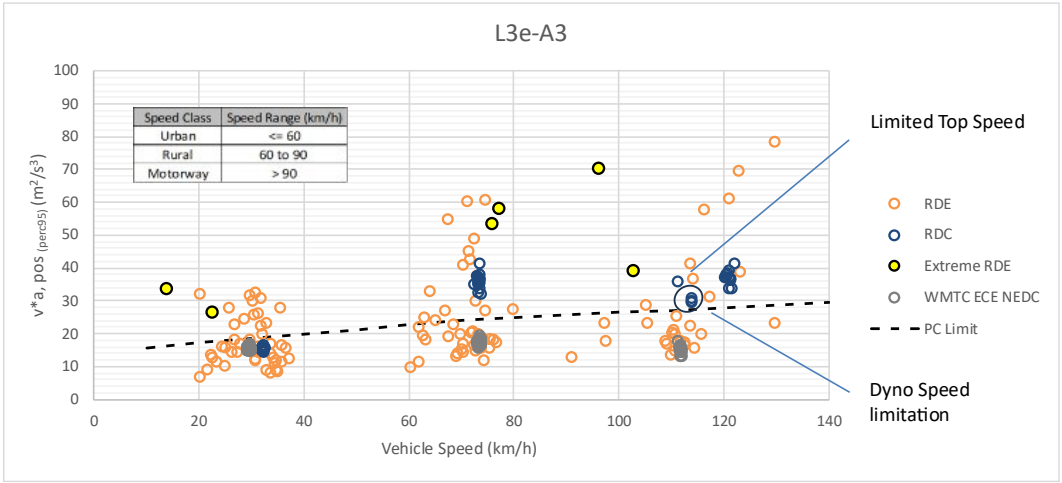

Figure 4-28: v*a,pos from L3e-A3 LENS db measurements.

This project has received funding from the European Union's Horizon Europe research and innovation programme under grant agreement No 101056777

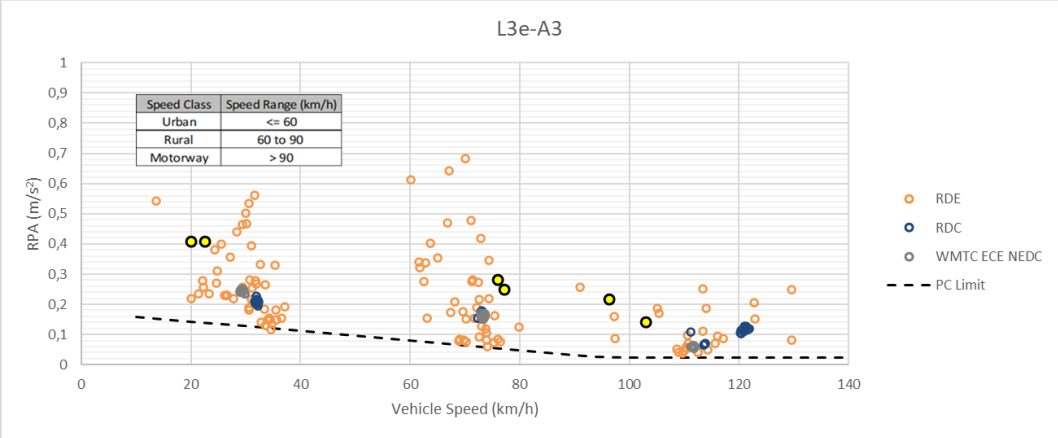

Figure 4-29: RPA from L3e-A3 LENS db measurements.

4.4 Representative real-world driving cycles from LENS data

The development of representative real world driving cycles from the samples studied was performed in order to calculate emission factors with the PHEM model for Euro 5 vehicles for urban, rural and motorway operation and to differentiate between emissions from engine map areas that are covered by the corresponding TA cycle WMTC and areas of the engine map outside these areas. A comparison of these emissions and an analysis of the underlying causes should lead to proposals for amendments of the TA procedure with the aim of achieving a closer link between TA and real-world driving emissions.

The following data from the LENS db was delivered for analysis:

- L1e-B: 6 cycles from 6 different vehicles,
- L3e-A1: 21 cycles from 14 different vehicles,
- L3e-A2: 13 cycles from 13 different vehicles,
- L3e-A3: 14 cycles from 12 different vehicles.

The technical data are specified in Table 4-8 to Table 4-11.

4 of the vehicles delivered as L3e-A2 were put into the L3e-A1 class for the following reasons:

- Vehicle 8 clearly belongs to L3e-A1 because its engine capacity is 125 cm³
- Vehicles 11, 12 and 13 have engine capacities of 153/155 cm³ and rated power values of 9.2 to 12.4 kW which is closer to L3e-A1 than to the rest of the L3e-A2 class (278 to 900 cm³, 17.5 to 35 kW).

Table 4-8: Technical data of the L1e-B vehicles in the LENS database

	Idveh / Idcycle	Lab name	make	model	Size Class delivered	Size Class final	EU emission class	registration year	eng cap in cm³	number of cylinders	max power in kW	rated speed in min-1	idling speed in min-1	empty mass in kg	gross mass in kg	gearbox type	n gears
10	1	IDIADA	Piaggio	Primavera 50	L1e-B	L1e-B	Euro 5	2022	49	1	2.2	7500	2200	115	295	CVT	
10	2	IDIADA	Piaggio	Fly 50 4T	L1e-B	L1e-B	Euro 2	2008	50	1	2.66	8500	1800	111	295	CVT	
10	3	TUG-P7	Peugeot	Speedfight 3	L1e-B	L1e-B	Euro 3		49.9	1	3.5	7000		97		CVT	
10	4	TUG-P7	CPI	SM 50	L1e-B	L1e-B	Euro 3	2009	49	1	2.2	7000		92	270	MT	6
10	5	TUG-P7	Beeline	Memory	L1e-B	L1e-B	Euro 4	2017	49	1	1.6	6500		92	242	CVT	
10	6	EMISIA	PIAGGIO	LIBERTY IGET 50	L1e-B	L1e-B	Euro 5	2022	49	1	2.2	7750	2200	115	290	CVT	

This project has received funding from the European Union's Horizon Europe research and innovation programme under grant agreement No 101056777

Table 4-9: Technical data of the L3e-A1vehicles in the LENS database

Idveh / Idcycle	Lab name	make	model	Size Class delivered	Size Class final	EU emission class	registration year	eng cap in cm³	number of cylinders	max power in kW	rated speed in min-1	idling speed in min-1	empty mass in kg	gross mass in kg	gearbox type	n gears
1	TUG-P7	KTM	Duke 125	L3e-A1	L3e-A1	Euro 5	2022	124.7	1	11	9500	1400	212	355	MT	6
2	IDIADA	Piaggio	Vespa	L3e-A1	L3e-A1	Euro 5	2022	124	1	8.1	8000	1800	126	305	CVT	
3	TUG-P7	Online	Pista 125 R ABS	L3e-A1	L3e-A1	Euro 5	2023	125	1	11	10000		132	282	MT	6
4	IDIADA	Honda	PS 125	L3e-A1	L3e-A1	Euro 3	2011	124.6	1	10.1	9000	1500	135	317	CVT	
5	IDIADA	Honda	Forza 125	L3e-A1	L3e-A1	Euro 5	2023	125	1	10.7	8750	1700	164	346	CVT	
6	IDIADA	Honda	SH 125	L3e-A1	L3e-A1	Euro 5	2023	125	1	9.67	8250	1700	138	317	CVT	
7	TUG-P7	Yamaha	Xmax 125	L3e-A1	L3e-A1	Euro 5	2021	124.7	1	9	8000		166	351	CVT	1
8	TUG-P7	Daelim	Otello	L3e-A1	L3e-A1	Euro 3	2005	125	1	9	8500	1400	124	245	CVT	
9	EMISIA	PIAGGIO	VESPA GTS 125	L3e-A1	L3e-A1	Euro 5	2022	125	1	10.3	8750	1710	147	340	CVT	1
10	EMISIA	PIAGGIO	MEDLEY S 125	L3e-A1	L3e-A1	Euro 5	2022	125	1	11	8750	1790	144	340	CVT	1
11	TU	Zontes	ZT125	L3e-A1	L3e-A1	Euro 5	2022	125	1	10.8	9000		160	340	CVT	
12	TU	Zontes	ZT125	L3e-A1	L3e-A1	Euro 5	2022	125	1	10.8	9000		160	340	CVT	
13	TU	Maxon	Blade	L3e-A1	L3e-A1	Euro 4	2018	125	1	6.2	7500		116	300		
14	TU	Honda	PCX125	L3e-A1	L3e-A1	Euro 5	2022	125	1	9.2	8750		130	310	CVT	
15	TU	Honda	PCX125	L3e-A1	L3e-A1	Euro 5	2022	125	1	9.2	8750		130	310	CVT	
16	TU	Honda	PCX125	L3e-A1	L3e-A1	Euro 5	2022	125	1	9.2	8750		130	310	CVT	
17	TU	Yamaha	Nmax 125	L3e-A1	L3e-A1	Euro 5	2022	125	1	9	8000		131	298	CVT	
18	TU	Yamaha	Nmax 125	L3e-A1	L3e-A1	Euro 5	2022	125	1	9	8000		131	298	CVT	
19	TU	Yamaha	Nmax 125	L3e-A1	L3e-A1	Euro 5	2022	125	1	9	8000		131	298	CVT	
20	TU	Maxon	Blade	L3e-A1	L3e-A1	Euro 4	2018	125	1	6.2	7500		116	300		
21	TU	Maxon	Blade	L3e-A1	L3e-A1	Euro 4	2018	125	1	6.2	7500		116	300		

Table 4-10: Technical data of the L3e-A2vehicles in the LENS database

Idveh / Idcycle	Lab name	make	model	Size Class delivered	Size Class final	EU emission class	registration year	eng cap in cm³	number of cylinders	max power in kW	rated speed in min-1	idling speed in min-1	empty mass in kg	gross mass in kg	gearbox type	n gears
22/8	TUG-P7	Yamaha	XSR 125	L3e-A2	L3e-A1	Euro 5	2022	124.5	1	11	10000		139	330	MT	6
23/11	EMISIA	PIAGGIO	VESPA PRIMAVERA 150	L3e-A2	L3e-A1	Euro 5	2022	155	1	9.2	7750	1710	126	305	CVT	1
24/12	EMISIA	PIAGGIO	MEDLEY	L3e-A2	L3e-A1	Euro 4	2020	155	1	12.1	8750	1800	144	340	CVT	1
25/13	EMISIA	HONDA	SH150AD	L3e-A2	L3e-A1	Euro 5	2024	153	1	12.4	8500	1670	138	317	CVT	1
1	TUG-P7	Yamaha	MT07	L3e-A2	L3e-A2	Euro 5	2023	689	2	35	7750	1250	184	355	MT	6
2	IDIADA	BMW	F900XR	L3e-A2	L3e-A2	Euro 5	2022	895	2	35	6500	1250	219	438	MT	6
3	IDIADA	Piaggio	Vespa GTS 300	L3e-A2	L3e-A2	Euro 5	2022	278	1	17.5	8250	1700	160	340	CVT	
4	IDIADA	Honda	Forza 300	L3e-A2	L3e-A2	Euro 4	2019	279	1	18.49	7000	1500	182	362	CVT	
5	TUG-P7	BMW	C400X	L3e-A2	L3e-A2	Euro 5	2022	350	1	25	7500	1450	206	405	CVT	
6	TUG-P7	KTM	390 Adventure	L3e-A2	L3e-A2	Euro 5	2020	390	1	32	9000	1600	172	375	MT	6
7	TUG-P7	KTM	690 Duke	L3e-A2	L3e-A2	Euro 4	2016	693	1	32	8000	1650	162	350	MT	6
9	TUG-P7	KTM	390 Duke	L3e-A2	L3e-A2	Euro 4	2017	373	1	32	9000	1600	163	355	MT	6
10	TUG-P7	BMW	G310R	L3e-A2	L3e-A2	Euro 5	2022	313	1	25	9250		164	345	MT	6

Table 4-11: Technical data of the L3e-A3 vehicles in the LENS database

Idveh / Idcycle	Lab name	make	model	Size Class delivered	Size Class final	EU emission class	registration year	eng cap in cm³	number of cylinders	max power in kW	rated speed in min-1	idling speed in min-1	empty mass in kg	gross mass in kg	gearbox type	n gears
21	IDIADA	BMW	F850GS	L3e-A3	L3e-A3	Euro 5	2022	853	2	70	8250	1250	233	445	MT	6
22	IDIADA	DUCATI	Multistrada	L3e-A3	L3e-A3	Euro 5	2023	1158	4	125	5250		250	470	MT	6
23	IDIADA	Ducati	Monster	L3e-A3	L3e-A3	Euro 5	2023	937	2	81.8	9250	1350	189	414	MT	6
24	TUG-P7	Husqvar	901 Norden	L3e-A3	L3e-A3	Euro 5	2022	889	2	77	8000	1400	294	450	MT	6
25	TUG-P7	BMW	S 1000RR	L3e-A3	L3e-A3	Euro 5	2022	999	4	152	13750	1270	272	407	MT	6
26	IDIADA	BMW	F900XR	L3e-A3	L3e-A3	Euro 5	2022	895	2	77	8500	1250	219	438	MT	6
27	TUG-P7	KTM	790 Duke	L3e-A3	L3e-A3	Euro 4	2019	799	2	77	8500	1650	187	430	MT	6
28	TUG-P7	BMW	F900XR	L3e-A3	L3e-A3	Euro 5	2019	895		77	8500	1400	219	438	MT	6
29	TUG-P7	Husqvar	701 Enduro	L3e-A3	L3e-A3	Euro 5	2020	693	1	55	8000	1650	160	350	MT	6
30	EMISIA	CFMOTO	800MT	L3e-A3	L3e-A3	Euro 5	2023	799	2	67	9250	1500	231	413	MT	6
31	EMISIA	CFMOTO	800MT	L3e-A3	L3e-A3	Euro 5	2023	799	2	67	9250	1500	231	413	MT	6
32	EMISIA	TRIUMP	TIGER 900 Rally	L3e-A3	L3e-A3	Euro 5	2020	888	3	70	8750	1200	216	447	MT	6
33	EMISIA	BMW	R12NINE T	L3e-A3	L3e-A3	Euro 5	2022	1170	2	81	7750	1180	225	430	MT	6
34	EMISIA	BMW	R12NINE T	L3e-A3	L3e-A3	Euro 5	2022	1170	2	81	7750	1180	225	430	MT	6

This project has received funding from the European Union's Horizon Europe research and innovation programme under grant agreement No 101056777

From the vehicle speed signals the following parameters were calculated:

- $a_i = (v_{i+1} - v_i)/3.6/delta\_t$ in m/s², delta_t = 1 s, v in km/h,
- $v_i * a_i$ in m²/s³.

Implausible or faulty data was corrected, if possible, otherwise excluded from further analysis. Figure 4-30 and Figure 4-31 show examples.

Since the acceleration signal showed a high scatter in most cases the vehicle signal was smoothed by a Hanning Filter according to the requirements of the EU RDE directive and the calculation of a and v*a was repeated for the smoothed speed signal. These values built the basis for further analysis.

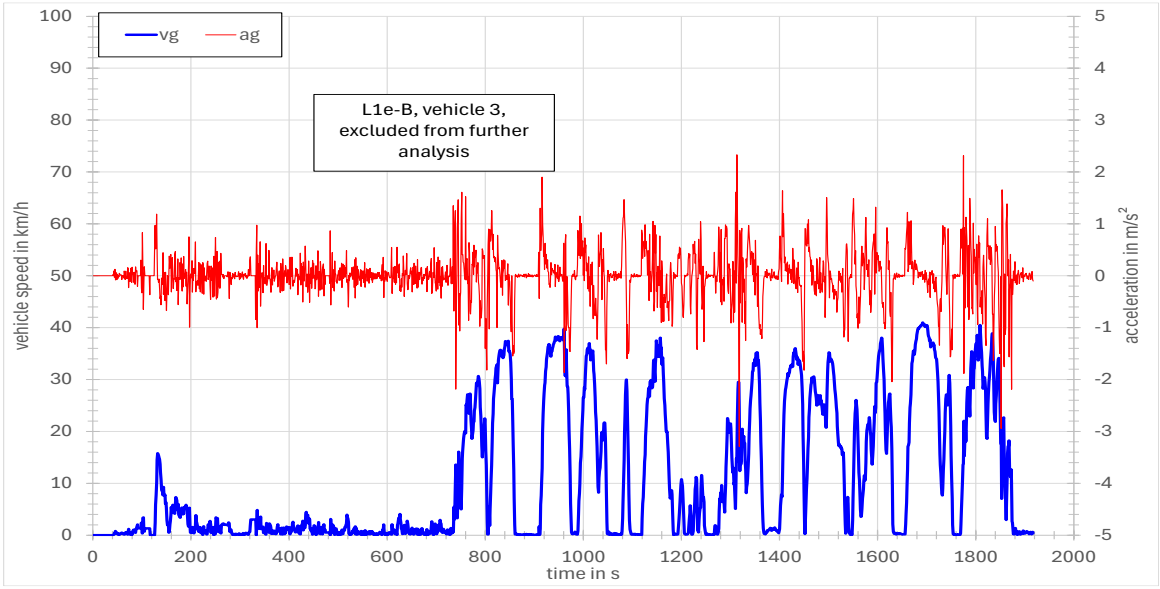

Figure 4-30: Example for faulty data that was excluded from further analysis.

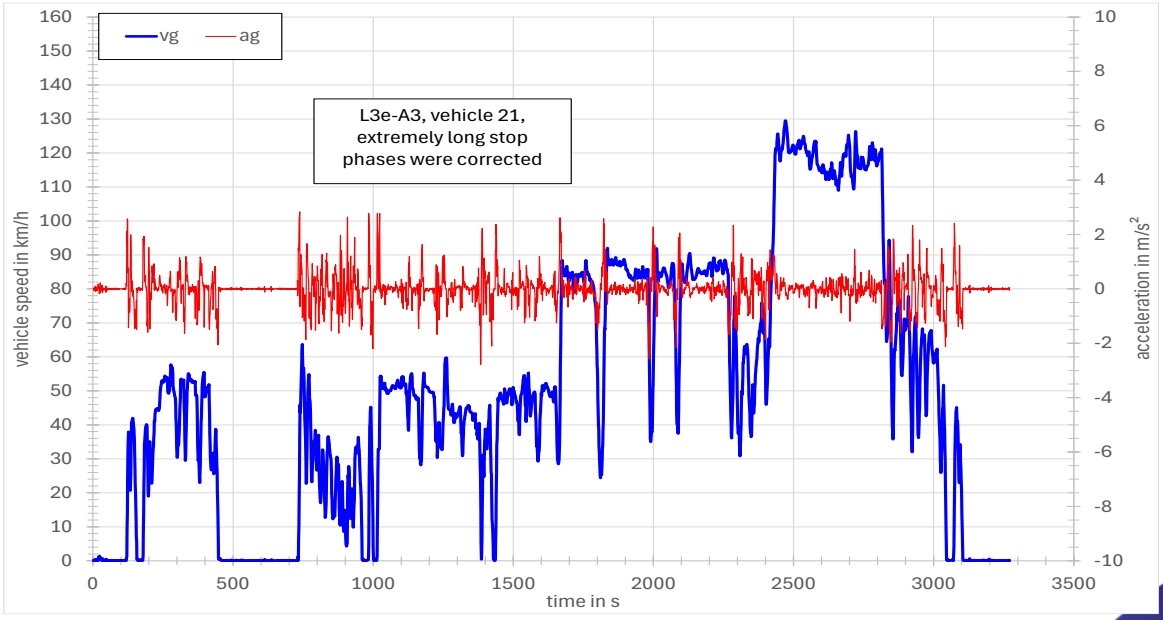

Figure 4-31: Example for faulty data that was corrected.

This project has received funding from the European Union's Horizon Europe research and innovation programme under grant agreement No 101056777

The main goal of the analysis was the development of representative cycles per vehicle sub-category to be used for the determination of emission factors for newer technologies. These emission factors will then be compared to existing ones from the established emission models.

For this reason, the parameter road category, or road type (urban, rural, motorway) was assigned to each cycle trace using figures of the speed trace instead of fixed speed thresholds. This results sometimes in exceedances of speed limits, which is more in line with in-use driving behavior than fixed speed thresholds. A further advantage of this approach is that complete short trips are assigned to a specific road category while fixed speed thresholds split short trips with high maximum speeds into parts belonging to different speed categories. A short trip is a cycle section with vehicle speeds >= 1 km/h between two consecutive stop periods.

In a second step the following key cycle parameters were calculated per road category:

- Average speed (v_ave), Maximun speed (v_max), Speed standard deviation (stddev_v)
- Positive acceleration average (a_pos_ave), average speed times positive acceleration (v*a_pos_ave), Relative positive acceleration (RPA)
- Positive acceleration average: a_pos_ave = sum(a_i, if a_i >= 0.1 m/s²)/sum(dt, if a_i >= 0.1 m/s²)
- v*a_pos_ave is calculated accordingly.
- RPA = sum(v*a_pos_ave, , if a_i >= 0.1 m/s²)/sum($dist_i$),
- sum($dist_i$) is the distance driven within the whole cycle.

The results are shown in the following tables.

Id_{road} = 1 means urban, 2 – rural, 3 – motorway and 4 is designated to a special cycle part, driven with vehicle 31 on a closed road, consisting of several starts from standstill with full throttle accelerations to top speeds of 50, 70, 90 and 100 km/h.

Table 4-12: Key cycle parameters for L1e-B and L3e-A1 vehicles and road category urban

idroad	Size Class	Idvehcat	cycle	duration	stop_dur	p_stop	distance	v_ave	v_max	stddev_v	a_min	a_max	a_pos_ave	v*a_pos_ave	RPA
				s	s		m	km/h	km/h	km/h	m/s²	m/s²	m/s²	m²/s³	m/s²
1	L1e-B	10	6	1698	489	28.8%	7933	16.8	44.5	14.04	-2.16	1.59	0.44	2.28	0.1451
1	L1e-B	10	4	1180	308	26.1%	5950	18.2	47.3	15.57	-2.22	1.37	0.42	2.26	0.1410
1	L1e-B	10	3	1917	692	36.1%	5932	11.1	40.7	13.25	-1.70	1.64	0.42	1.85	0.1372
1	L1e-B	10	5	1064	172	16.2%	5752	19.5	49.0	14.45	-2.57	1.85	0.55	3.04	0.1836
1	L3e-A1	8	4	1838	191	10.4%	16553	32.4	63.3	17.25	-2.15	1.88	0.44	3.38	0.1234
1	L3e-A1	8	2	1841	114	6.2%	16412	32.1	57.1	15.05	-1.69	2.25	0.40	2.85	0.0973
1	L3e-A1	8	22	2082	287	13.8%	16268	28.1	56.5	16.51	-2.13	2.12	0.51	3.49	0.1432
1	L3e-A1	8	5	1722	123	7.1%	15270	31.9	49.7	14.15	-2.29	1.85	0.45	2.92	0.0994
1	L3e-A1	8	6	1511	149	9.9%	13543	32.3	59.2	17.16	-2.34	2.40	0.52	3.63	0.1331
1	L3e-A1	8	7	1863	449	24.1%	13097	25.3	61.6	19.00	-2.78	2.83	0.64	4.45	0.1879
1	L3e-A1	8	21	1401	117	8.4%	11552	29.7	65.0	14.31	-2.18	1.80	0.57	4.36	0.2283
1	L3e-A1	8	1	1524	207	13.6%	10553	24.9	61.6	15.96	-3.25	2.08	0.60	3.92	0.1878
1	L3e-A1	8	11	1284	63	4.9%	9364	26.3	61.6	13.84	-2.58	2.02	0.68	5.05	0.2882
1	L3e-A1	8	15	1160	204	17.6%	7259	22.5	55.6	16.13	-2.52	2.25	0.78	5.38	0.3151
1	L3e-A1	8	25	1327	331	24.9%	7255	19.7	52.8	15.66	-2.01	2.80	0.48	2.89	0.1715
1	L3e-A1	8	23	1263	282	22.3%	7249	20.7	52.6	15.32	-1.71	1.74	0.50	3.06	0.1818
1	L3e-A1	8	24	1145	244	21.3%	6555	20.6	51.8	15.01	-1.70	2.71	0.56	3.32	0.1777
1	L3e-A1	8	14	946	200	21.1%	5858	22.3	54.6	16.16	-2.48	1.98	0.76	5.50	0.2987
1	L3e-A1	8	9	850	124	14.6%	5530	23.4	47.2	14.13	-1.34	2.10	0.46	2.95	0.1572

This project has received funding from the European Union's Horizon Europe research and innovation programme under grant agreement No 101056777

Table 4-13: Key cycle parameters for L3e-A2/A3 vehicles and road category urban

idroad	Size Class	Idvehcat	cycle	duration	stop_dur	p_stop	distance	v_ave	v_max	stddev_v	a_min	a_max	a_pos_ave	v*a_pos_ave	RPA
				s	s		m	km/h	km/h	km/h	m/s^2	m/s^2	m/s^2	m^2/s^3	m/s^2
1	L3e-A2	9.1	2	1627	58	3.6%	16573	36.7	53.9	12.99	-2.47	1.79	0.48	3.53	0.1021
1	L3e-A2	9.1	3	1683	143	8.5%	16475	35.2	59.0	14.89	-2.59	2.13	0.56	4.18	0.1184
1	L3e-A2	9.1	5	2274	630	27.7%	14832	23.5	61.6	19.19	-3.12	2.53	0.59	4.07	0.1979
1	L3e-A2	9.1	9	2136	449	21.0%	14330	24.2	64.8	18.29	-2.40	3.54	0.61	3.86	0.1837
1	L3e-A2	9.1	4	1587	170	10.7%	13676	31.0	62.7	16.81	-2.46	3.47	0.52	3.69	0.1424
1	L3e-A2	9.1	10	1962	290	14.8%	13365	24.5	59.9	16.17	-2.04	2.16	0.55	3.55	0.1783
1	L3e-A2	9.1	1	1289	256	19.9%	10635	29.7	56.5	18.42	-1.92	1.72	0.38	2.70	0.0915
1	L3e-A2	9.1	6	1274	201	15.8%	9862	27.9	67.4	18.61	-2.10	2.65	0.58	3.85	0.1260
1	L3e-A2	9.1	7	677	54	8.0%	6163	32.8	94.9	18.66	-2.61	3.72	0.79	7.08	0.2667
1	L3e-A3	9.2	22	1765	162	9.2%	16651	34.0	54.1	15.55	-2.94	2.05	0.43	3.05	0.0965
1	L3e-A3	9.2	26	1818	196	10.8%	16585	32.8	60.9	16.24	-2.21	1.80	0.44	3.00	0.0962
1	L3e-A3	9.2	23	1765	163	9.2%	16505	33.7	50.8	15.64	-2.24	2.08	0.44	3.07	0.0841
1	L3e-A3	9.2	21	1706	473	27.7%	13466	28.4	60.5	20.83	-2.34	2.59	0.61	4.87	0.1407
1	L3e-A3	9.2	29	1135	144	12.7%	11907	37.8	74.7	20.32	-3.31	3.91	0.76	7.09	0.2127
1	L3e-A3	9.2	28	1320	141	10.7%	11426	31.2	63.7	16.84	-2.02	2.55	0.58	4.00	0.1316
1	L3e-A3	9.2	27	1395	212	15.2%	11184	28.9	66.0	19.38	-3.03	3.41	0.72	5.26	0.2199
1	L3e-A3	9.2	125	1026	140	13.6%	8561	30.0	66.8	18.70	-3.06	3.28	0.74	5.19	0.1903
1	L3e-A3	9.2	25	1163	278	23.9%	8554	26.5	66.8	20.06	-3.06	3.28	0.74	5.19	0.1904
1	L3e-A3	9.2	24	1312	502	38.3%	8132	22.3	52.2	20.44	-2.75	1.77	0.53	3.46	0.1267
1	L3e-A3	9.2	32	1258	252	20.0%	7200	20.6	47.7	14.73	-2.19	2.41	0.50	2.93	0.1595
1	L3e-A3	9.2	34	1406	388	27.6%	7190	18.4	64.2	16.75	-2.00	2.64	0.58	3.47	0.1956
1	L3e-A3	9.2	33	1224	347	28.3%	6799	20.0	53.2	16.55	-1.83	2.09	0.50	3.10	0.1671
1	L3e-A3	9.2	30	1219	327	26.8%	6696	19.8	52.9	15.85	-1.96	2.16	0.54	3.22	0.1644
1	L3e-A3	9.2	31	934	352	37.7%	4291	16.5	62.7	17.54	-1.66	1.87	0.53	3.11	0.1735

Table 4-14: Key cycle parameters for L1e-B and L3e-A1vehicles and road category rural

idroad	Size Class	Idvehcat	cycle	duration	stop_dur	p_stop	distance	v_ave	v_max	stddev_v	a_min	a_max	a_pos_ave	v*a_pos_ave	RPA
				s	s		m	km/h	km/h	km/h	m/s^2	m/s^2	m/s^2	m^2/s^3	m/s^2
2	L1e-B	10	2	4667	150	3.2%	45946	35.4	55.0	11.59	-2.27	1.53	0.34	2.51	0.0685
2	L1e-B	10	1	5162	414	8.0%	45653	31.8	48.8	13.65	-2.37	1.76	0.34	2.31	0.0580
2	L1e-B	10	11	2700	165	6.1%	24097	32.1	47.6	12.50	-2.37	1.76	0.32	2.12	0.0562
2	L3e-A1	8	16	4503	975	21.7%	48879	39.1	96.7	29.73	-2.24	2.22	0.49	5.24	0.1351
2	L3e-A1	8	12	2561	591	23.1%	28065	39.5	89.9	28.32	-2.05	1.99	0.47	5.39	0.1445
2	L3e-A1	8	13	1844	311	16.9%	21615	42.2	80.2	25.26	-1.99	1.80	0.41	4.23	0.0987
2	L3e-A1	8	6	1058	0	0.0%	17942	61.0	87.5	14.34	-2.42	1.60	0.42	6.09	0.1213
2	L3e-A1	8	24	1215	127	10.5%	17259	51.1	98.7	27.30	-2.08	1.77	0.37	4.87	0.1293
2	L3e-A1	8	5	905	0	0.0%	16710	66.5	77.9	8.20	-1.96	0.97	0.30	4.82	0.0660
2	L3e-A1	8	9	1257	203	16.1%	16686	47.8	90.5	28.45	-1.84	2.51	0.49	5.64	0.1371
2	L3e-A1	8	25	1182	165	14.0%	16660	50.7	97.3	30.20	-2.29	2.55	0.43	4.90	0.1147
2	L3e-A1	8	2	824	0	0.0%	15506	67.7	86.1	14.45	-1.71	2.20	0.40	5.66	0.0803
2	L3e-A1	8	4	874	0	0.0%	15088	62.1	86.6	15.83	-1.77	1.18	0.39	5.60	0.0955
2	L3e-A1	8	1	693	39	5.6%	9395	48.8	85.7	22.91	-3.27	2.15	0.43	5.15	0.1353
2	L3e-A1	8	23	832	163	19.6%	8966	38.8	77.5	26.03	-2.12	2.46	0.59	5.76	0.1695
2	L3e-A1	8	7	443	0	0.0%	7169	58.3	90.7	20.16	-3.01	2.16	0.52	7.09	0.1939
2	L3e-A1	8	22	298	54	18.1%	3807	46.0	79.2	27.33	-3.34	1.98	0.63	7.55	0.1883

This project has received funding from the European Union's Horizon Europe research and innovation programme under grant agreement No 101056777

Table 4-15: Key cycle parameters for L3e-A2/A3 vehicles and road category rural

idroad	Size Class	Idvehcat	cycle	duration	stop_dur	p_stop	distance	v_ave	v_max	stddev_v	a_min	a_max	a_pos_ave	v*a_pos_ave	RPA
				s	s		m	km/h	km/h	km/h	m/s^2	m/s^2	m/s^2	m^2/s^3	m/s^2
2	L3e-A2	9.1	7	1248	24	1.9%	21219	61.2	158.1	23.39	-3.71	3.78	0.88	15.14	0.3261
2	L3e-A2	9.1	10	1210	4	0.3%	18345	54.6	109.0	17.90	-2.45	2.58	0.55	8.53	0.1850
2	L3e-A2	9.1	4	1026	0	0.0%	17975	63.1	91.1	19.39	-2.58	1.93	0.51	7.50	0.1481
2	L3e-A2	9.1	105	1151	5	0.4%	17903	56.0	103.0	18.48	-4.37	3.06	0.57	8.58	0.2285
2	L3e-A2	9.1	9	1129	34	3.0%	17419	55.5	113.3	20.99	-3.34	3.48	0.69	10.52	0.2554
2	L3e-A2	9.1	1	1399	223	15.9%	16933	43.6	106.4	26.96	-4.18	3.72	0.60	7.59	0.2030
2	L3e-A2	9.1	6	1119	0	0.0%	16666	53.6	106.7	16.03	-3.48	3.60	0.80	12.27	0.2341
2	L3e-A2	9.1	5	1033	5	0.5%	16262	56.7	103.0	19.33	-4.37	3.06	0.59	8.94	0.2396
2	L3e-A2	9.1	3	824	27	3.3%	15067	65.8	79.2	15.72	-2.37	1.30	0.40	6.32	0.0709
2	L3e-A2	9.1	2	670	0	0.0%	14022	75.3	87.6	9.75	-2.23	1.16	0.34	6.03	0.0654
2	L3e-A3	9.2	34	1879	159	8.5%	28754	55.1	114.8	30.09	-2.94	3.83	0.89	11.94	0.2723
2	L3e-A3	9.2	125	1364	29	2.1%	23660	62.4	99.6	20.30	-3.16	3.62	0.61	9.90	0.2176
2	L3e-A3	9.2	25	1364	29	2.1%	23644	62.4	99.6	20.29	-3.16	3.62	0.61	9.81	0.2154
2	L3e-A3	9.2	27	1567	59	3.8%	22753	52.3	146.9	25.19	-3.63	3.84	0.83	12.84	0.3289
2	L3e-A3	9.2	24	1704	301	17.7%	20692	43.7	96.2	26.52	-3.15	3.15	0.75	9.53	0.2188
2	L3e-A3	9.2	21	952	18	1.9%	18521	70.0	91.5	20.26	-2.04	2.30	0.54	8.57	0.1338
2	L3e-A3	9.2	31	1101	161	14.6%	16382	53.6	105.3	32.62	-1.82	3.20	0.62	8.53	0.1672
2	L3e-A3	9.2	23	793	0	0.0%	15523	70.5	82.2	9.66	-1.96	1.27	0.34	5.78	0.0834
2	L3e-A3	9.2	29	913	33	3.6%	15344	60.5	113.0	24.58	-3.64	3.83	0.85	13.28	0.2866
2	L3e-A3	9.2	28	998	7	0.7%	15063	54.3	97.6	16.34	-2.91	3.26	0.85	12.73	0.2129
2	L3e-A3	9.2	26	743	0	0.0%	14850	71.9	82.2	10.63	-1.94	1.11	0.39	6.50	0.0784
2	L3e-A3	9.2	22	751	0	0.0%	14654	70.2	79.1	10.88	-1.79	1.12	0.37	5.76	0.0668
2	L3e-A3	9.2	30	788	130	16.5%	9326	42.6	79.8	26.44	-2.46	2.25	0.60	6.27	0.1902
2	L3e-A3	9.2	33	639	43	6.7%	9078	51.1	76.1	22.35	-1.93	2.06	0.50	6.06	0.1548
2	L3e-A3	9.2	32	886	170	19.2%	9029	36.7	77.3	26.90	-2.13	2.42	0.57	5.36	0.1835

Table 4-16: Key cycle parameters for L3e-A1vehicles and road category motorway

idroad	Size Class	Idvehcat	cycle	duration	stop_dur	p_stop	distance	v_ave	v_max	stddev_v	a_min	a_max	a_pos_ave	v*a_pos_ave	RPA
				s	s		m	km/h	km/h	km/h	m/s^2	m/s^2	m/s^2	m^2/s^3	m/s^2
3	L3e-A1	8	4	654	0	0.0%	14944	82.3	101.7	15.78	-1.91	1.35	0.32	6.06	0.0661
3	L3e-A1	8	6	595	0	0.0%	14944	90.4	106.8	12.65	-1.35	1.62	0.31	6.46	0.0609
3	L3e-A1	8	1	672	22	3.3%	14843	79.5	114.4	26.94	-2.28	1.66	0.42	6.93	0.0939
3	L3e-A1	8	22	562	5	0.9%	14711	94.2	115.9	22.57	-1.54	1.81	0.38	7.22	0.0427
3	L3e-A1	8	7	567	3	0.5%	14548	92.4	109.9	22.45	-1.59	1.01	0.30	6.53	0.0543
3	L3e-A1	8	2	586	0	0.0%	14087	86.5	101.6	11.53	-0.98	0.83	0.23	5.09	0.0430
3	L3e-A1	8	5	518	0	0.0%	14074	97.8	110.4	8.92	-1.42	0.97	0.26	6.49	0.0369
3	L3e-A1	8	12	424	5	1.2%	10016	85.0	108.0	24.19	-1.86	1.66	0.34	5.82	0.0761
3	L3e-A1	8	23	369	1	0.3%	7802	76.1	97.6	24.68	-0.95	1.62	0.35	4.94	0.0564

This project has received funding from the European Union's Horizon Europe research and innovation programme under grant agreement No 101056777

Table 4-17: Key cycle parameters for L3e-A2/A3vehicles and road category motorway

idroad	Size Class	Idvehcat	cycle	duration	stop_dur	p_stop	distance	v_ave	v_max	stddev_v	a_min	a_max	a_pos_ave	v*a_pos_ave	RPA
				s	s		m	km/h	km/h	km/h	m/s^2	m/s^2	m/s^2	m^2/s^3	m/s^2
3	L3e-A2	9	6	840	5	0.6%	23357	100.1	146.4	33.75	-1.99	2.13	0.45	11.01	0.0872
3	L3e-A2	9	5	754	0	0.0%	23126	110.4	153.1	26.10	-2.50	2.03	0.44	12.25	0.1552
3	L3e-A2	9	105	754	0	0.0%	23126	110.4	153.1	26.10	-2.50	2.03	0.44	12.25	0.1552
3	L3e-A2	9	9	785	0	0.0%	22472	103.1	156.3	24.76	-1.56	1.95	0.38	10.48	0.1460
3	L3e-A2	9	7	663	4	0.6%	22289	121.0	185.5	32.38	-2.86	3.21	0.72	24.47	0.3008
3	L3e-A2	9	1	679	19	2.8%	22286	118.2	149.2	30.21	-5.00	1.91	0.41	12.62	0.1438
3	L3e-A2	9	10	776	2	0.3%	22272	103.3	135.0	20.32	-3.07	1.43	0.37	9.88	0.1021
3	L3e-A2	9	2	556	0	0.0%	15548	100.7	120.2	21.82	-2.49	1.40	0.48	9.96	0.0685
3	L3e-A2	9	4	551	0	0.0%	14907	97.4	127.1	23.83	-1.36	3.43	0.39	9.50	0.1435
3	L3e-A2	9	3	540	12	2.2%	14541	96.9	113.7	21.19	-1.77	3.20	0.48	8.67	0.0572
3	L3e-A3	9	29	683	6	0.9%	22547	118.8	159.9	24.98	-3.14	1.37	0.39	12.32	0.1186
3	L3e-A3	9	28	782	4	0.5%	22247	102.4	143.5	31.56	-2.10	3.06	0.54	13.72	0.0839
3	L3e-A3	9	24	679	0	0.0%	22165	117.5	136.5	18.83	-2.38	3.42	0.66	17.11	0.1104
3	L3e-A3	9	27	639	7	1.1%	21908	123.4	162.5	29.90	-2.44	3.32	0.54	17.54	0.1585
3	L3e-A3	9	25	512	0	0.0%	17727	124.6	162.1	25.16	-2.28	3.71	0.52	18.03	0.1739
3	L3e-A3	9	125	511	0	0.0%	17700	124.7	162.1	25.15	-2.28	3.71	0.51	17.82	0.1711
3	L3e-A3	9	22	525	0	0.0%	14927	102.4	115.6	18.66	-2.36	1.28	0.33	7.17	0.0509
3	L3e-A3	9	26	520	0	0.0%	14726	101.9	117.0	20.24	-2.62	1.02	0.28	6.89	0.0604
3	L3e-A3	9	21	452	0	0.0%	14077	112.1	129.4	17.32	-1.67	1.51	0.38	10.26	0.0926
3	L3e-A3	9	23	480	0	0.0%	14050	105.4	116.5	14.49	-1.51	1.02	0.30	7.74	0.0540
3	L3e-A3	9	34	389	4	1.0%	10278	95.1	119.5	24.22	-2.24	2.72	0.42	8.29	0.1081
3	L3e-A3	9	33	385	2	0.5%	8027	75.1	107.1	28.08	-1.77	1.55	0.42	8.15	0.1410
3	L3e-A3	9	32	319	0	0.0%	7603	85.8	125.8	28.49	-1.62	1.80	0.46	9.60	0.1767
3	L3e-A3	9	30	281	0	0.0%	7355	94.2	125.9	20.74	-1.33	1.34	0.40	9.70	0.1438
4	L3e-A3	9	31	351	39	11.1%	3263	33.5	104.5	27.38	-4.72	4.98	2.25	20.63	0.7209

In a 3rd step, time weighted frequency distributions of vehicle speed and accelerations were calculated per road category. The results are shown in the following figures. More detailed figures regarding this specific study are available in Appendix J: Representative real-world driving cycles from LENS data.

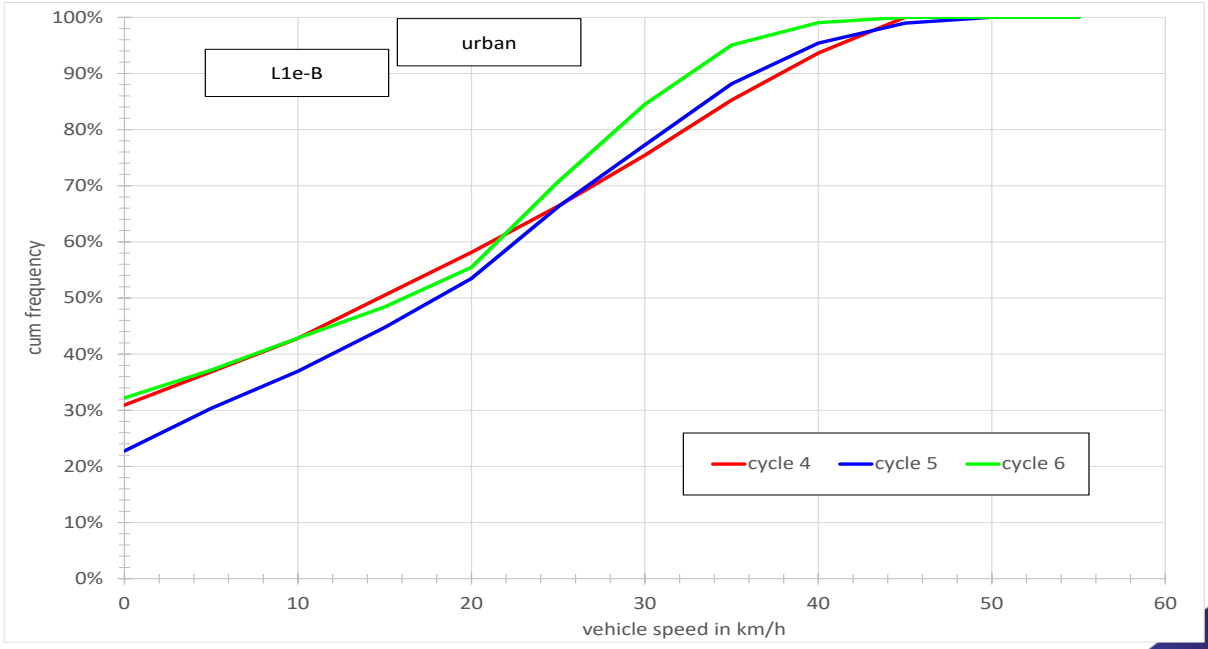

Figure 4-32: Vehicle speed distributions vtimeehicles L1e-B, urban.

This project has received funding from the European Union's Horizon Europe research and innovation programme under grant agreement No 101056777

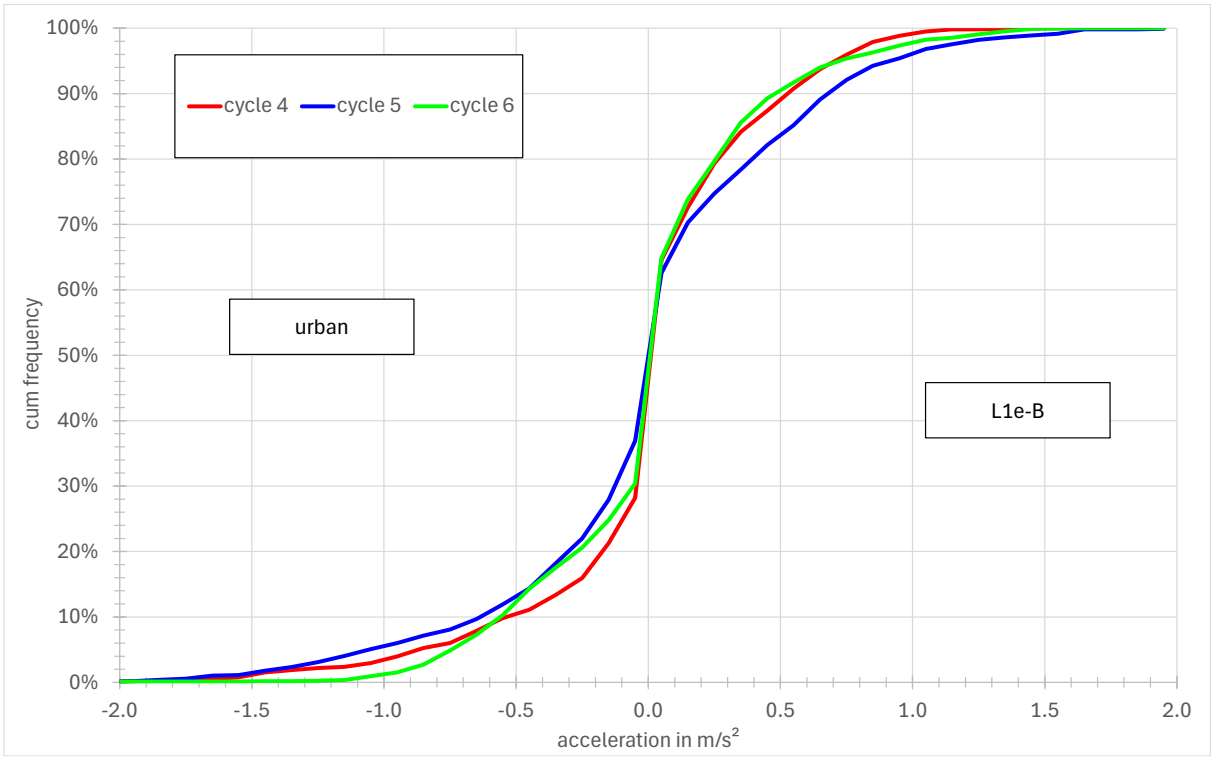

Figure 4-33: Acceleration distributions vehicles L1e-B, urban.

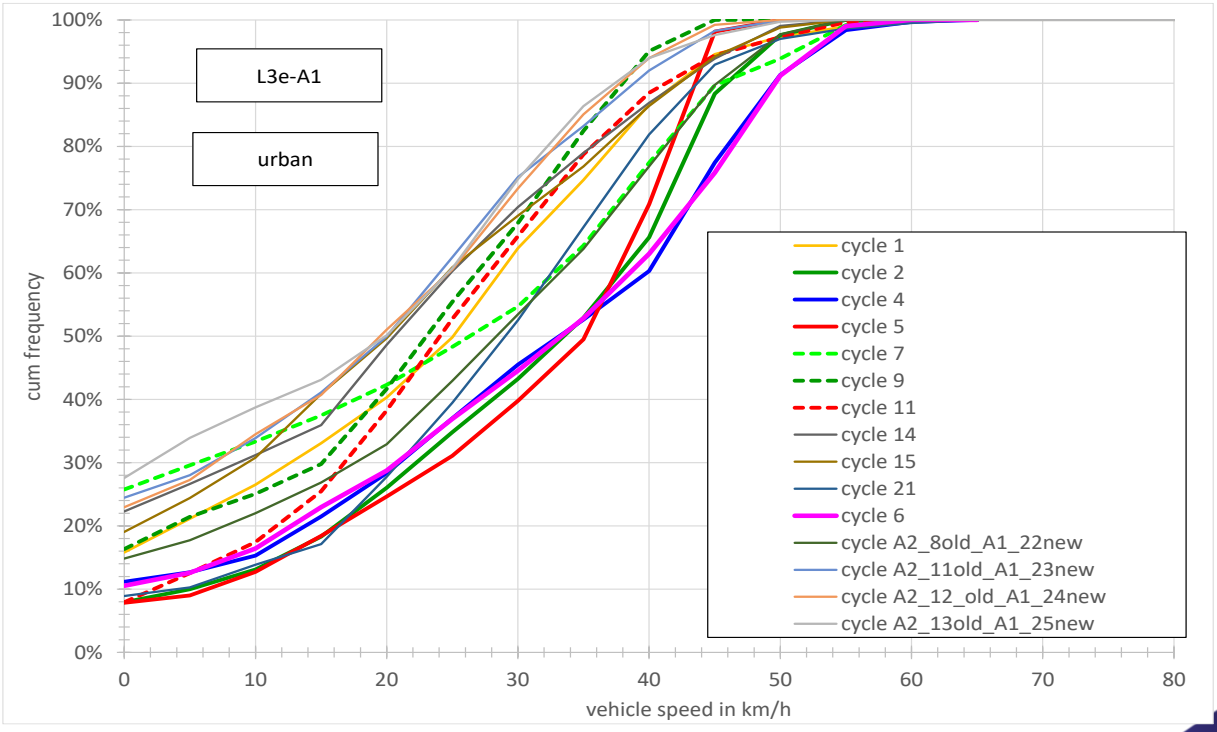

Figure 4-34: Vehicle speed distributions vehicles L3e-A1, urban.

This project has received funding from the European Union's Horizon Europe research and innovation programme under grant agreement No 101056777

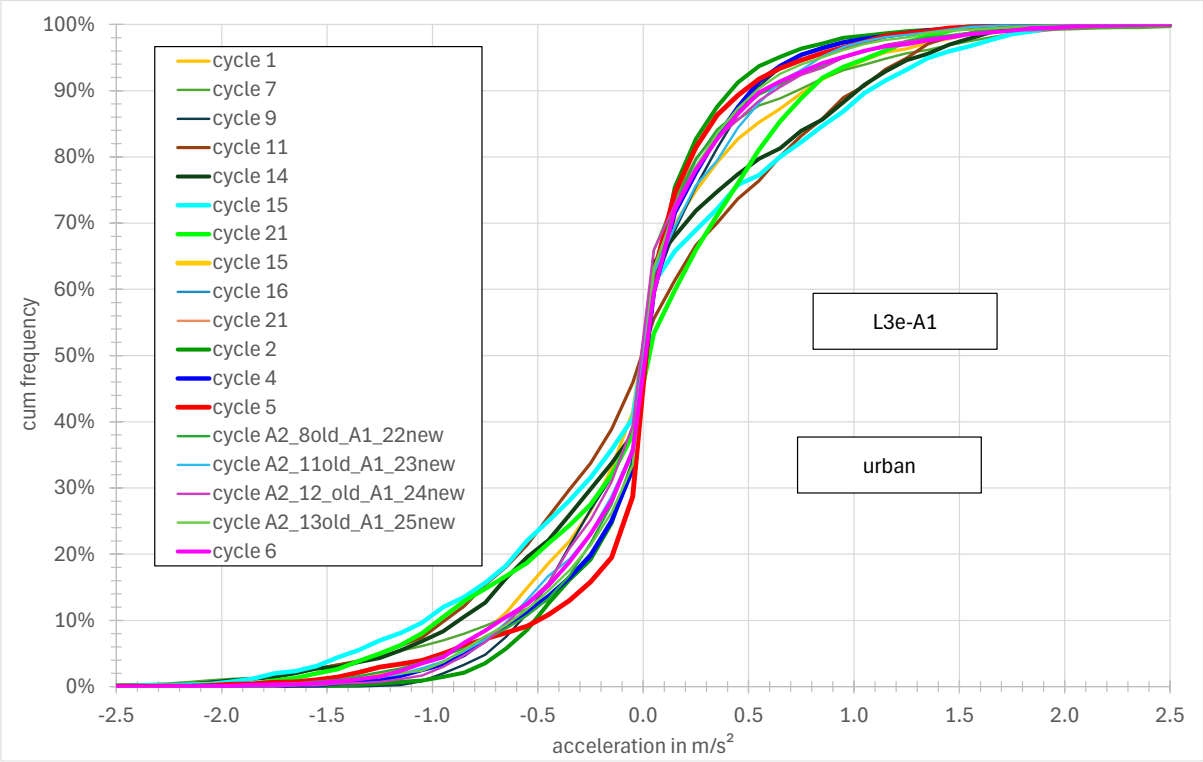

Figure 4-35: Acceleration distributions vehicles L3e-A1, urban.

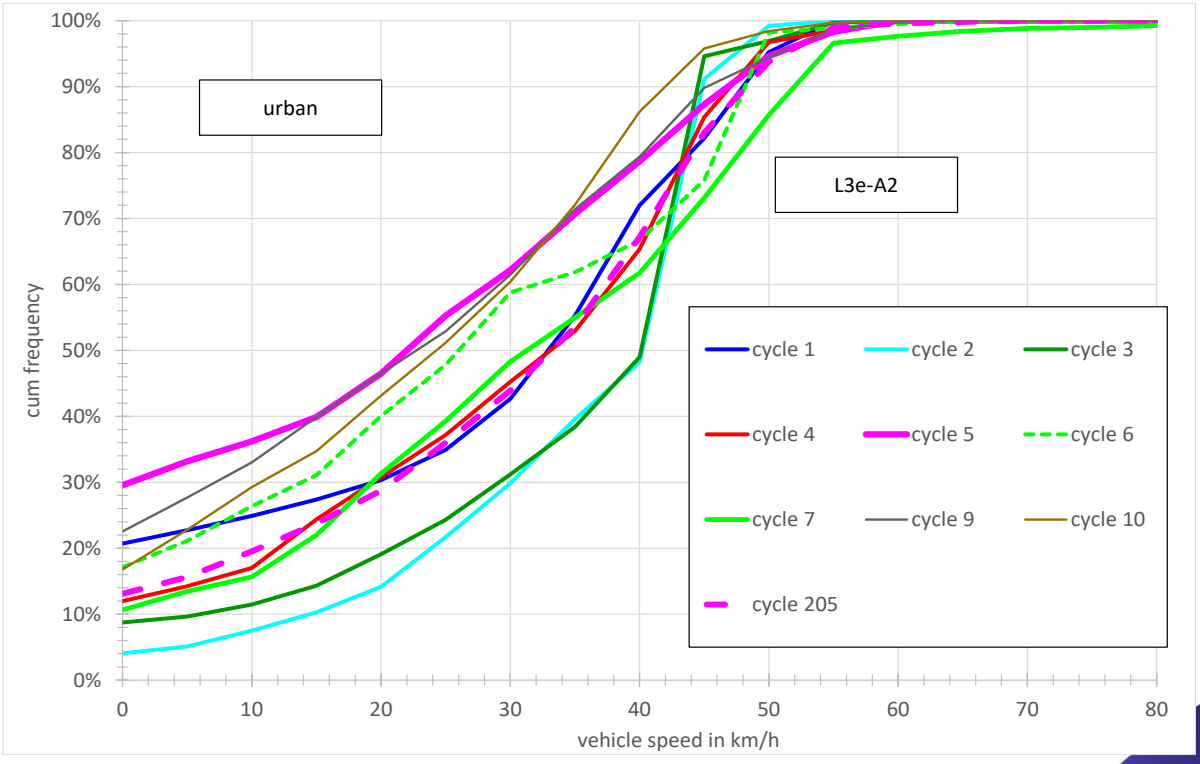

Figure 4-36: Vehicle speed distributions vehicles L3e-A2, urban.

This project has received funding from the European Union's Horizon Europe research and innovation programme under grant agreement No 101056777

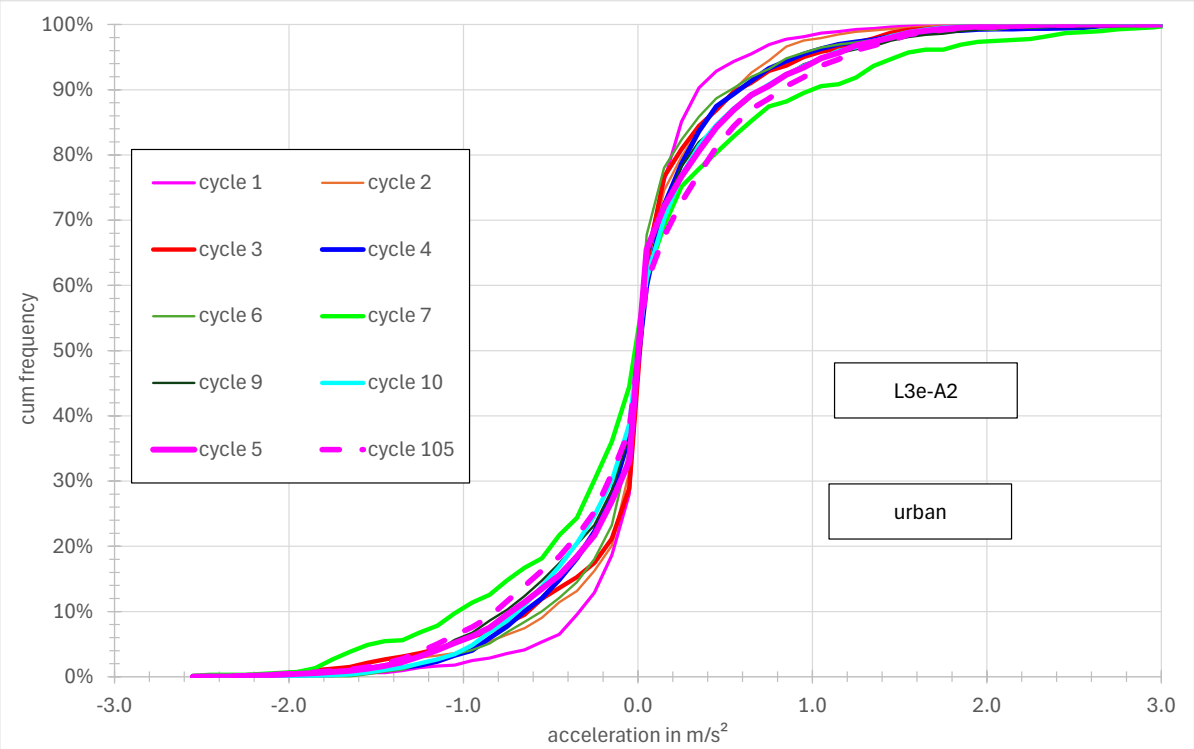

Figure 4-37: Acceleration distributions vehicles L3e-A2, urban.

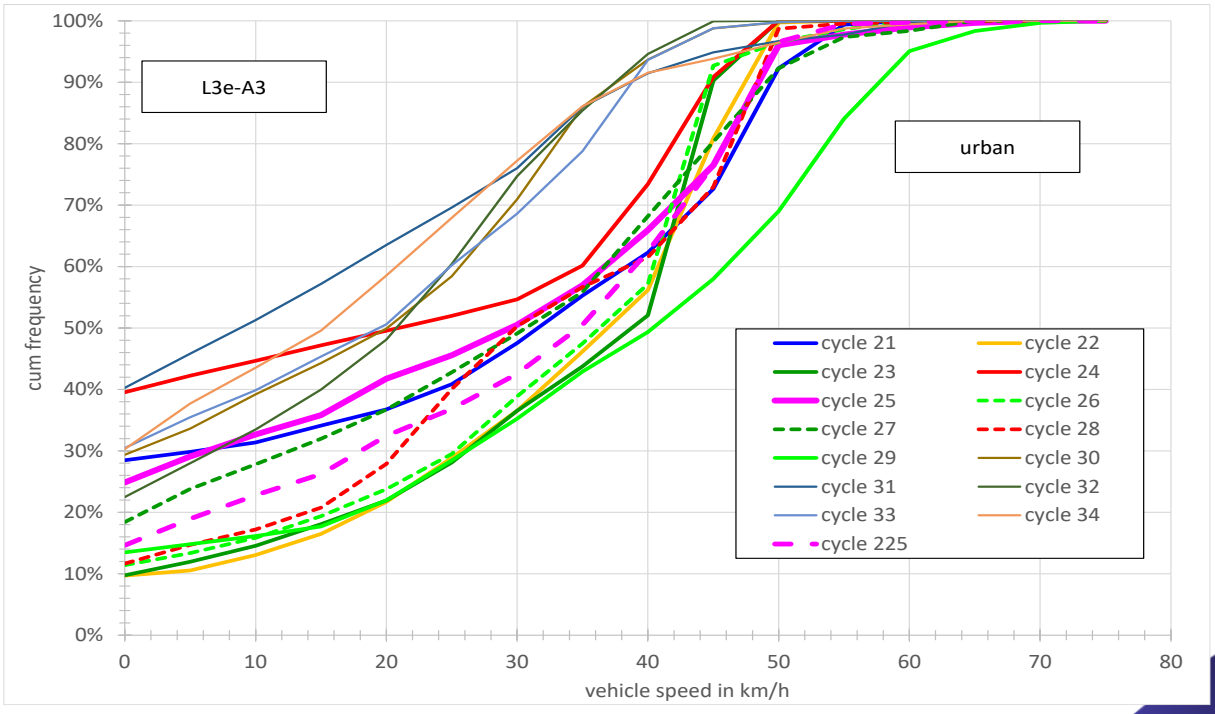

Figure 4-38: Vehicle speed distributions vehicles L3e-A3, urban.

This project has received funding from the European Union's Horizon Europe research and innovation programme under grant agreement No 101056777

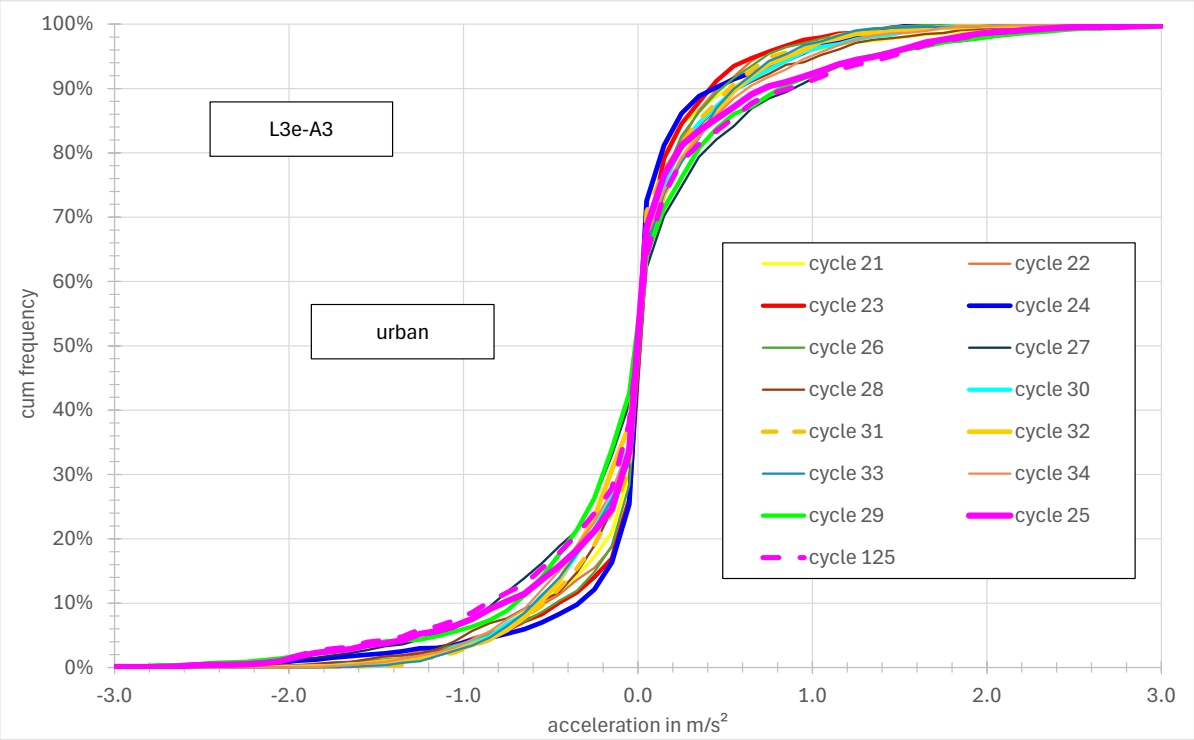

Figure 4-39: Acceleration distributions vehicles L3e-A3, urban.

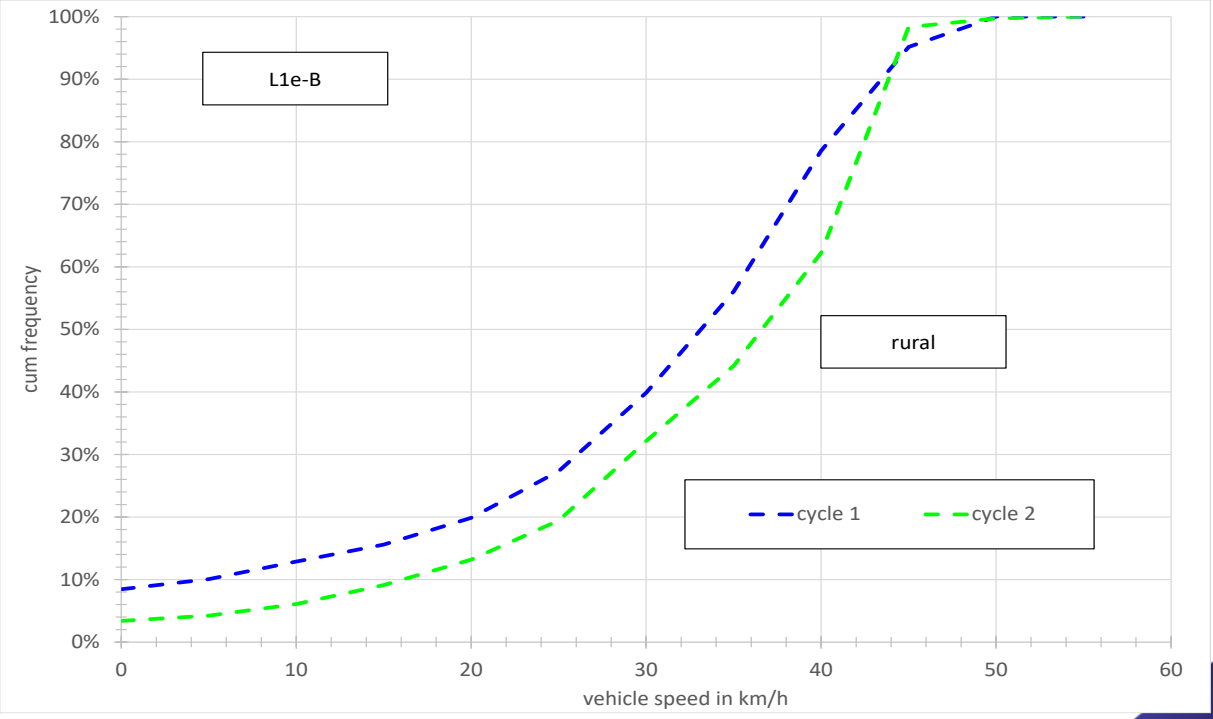

Figure 4-40: Vehicle speed distributions vehicles L1e-B, rural.

This project has received funding from the European Union's Horizon Europe research and innovation programme under grant agreement No 101056777

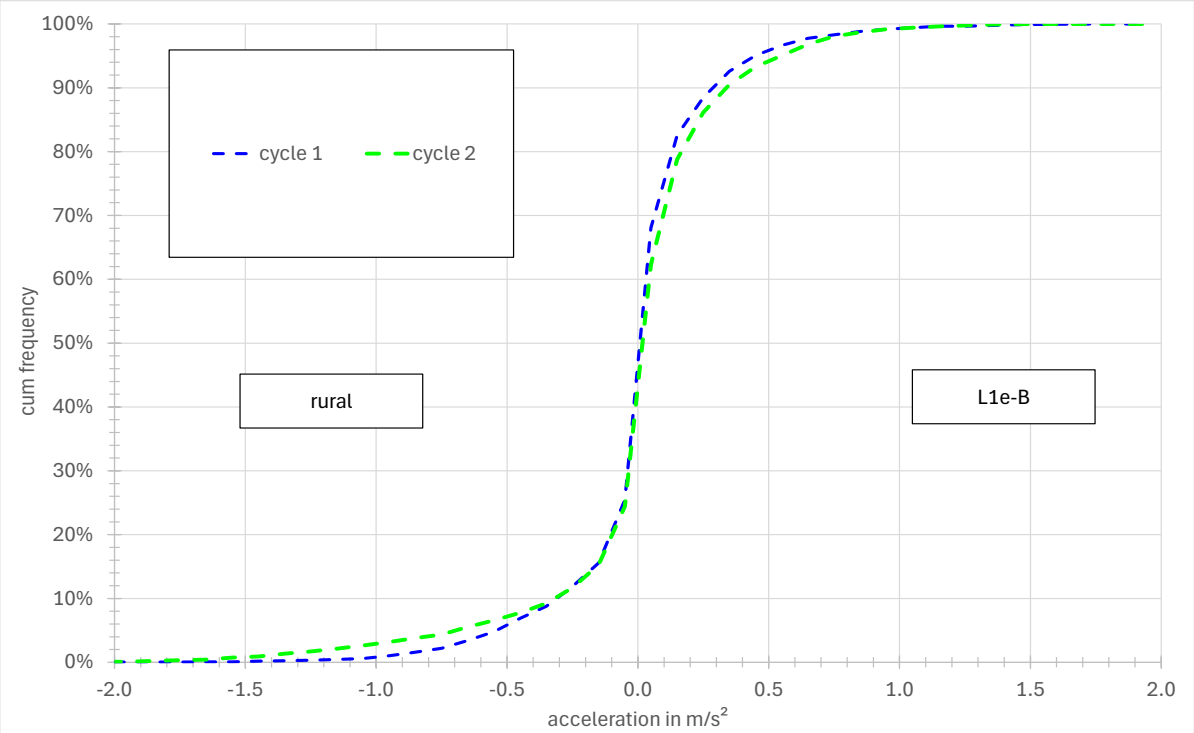

Figure 4-41: Acceleration distributions vehicles L1e-B, rural.

The final representative cycles were then derived based on the average values of the key parameters in the tables, as well as the average speed and acceleration distributions. However, extreme cycles were disregarded, e.g. those with extremely high stop percentages. The results are shown in the following figures.

This project has received funding from the European Union's Horizon Europe research and innovation programme under grant agreement No 101056777

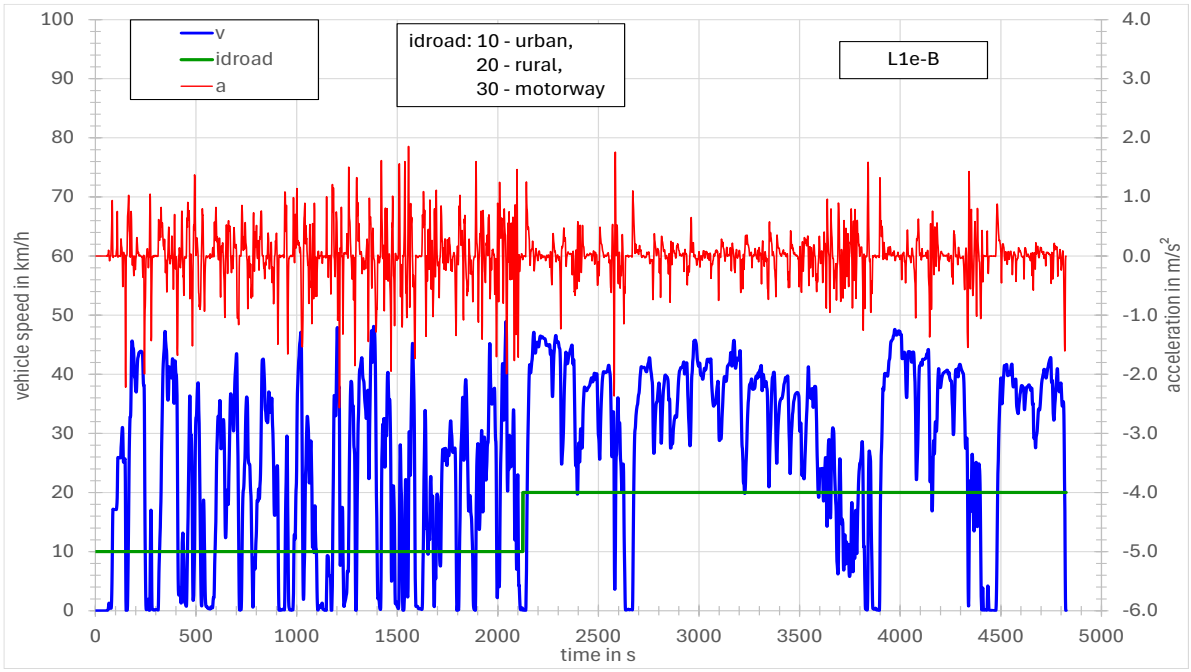

Figure 4-42: Final cycle for L1e-B vehicles.

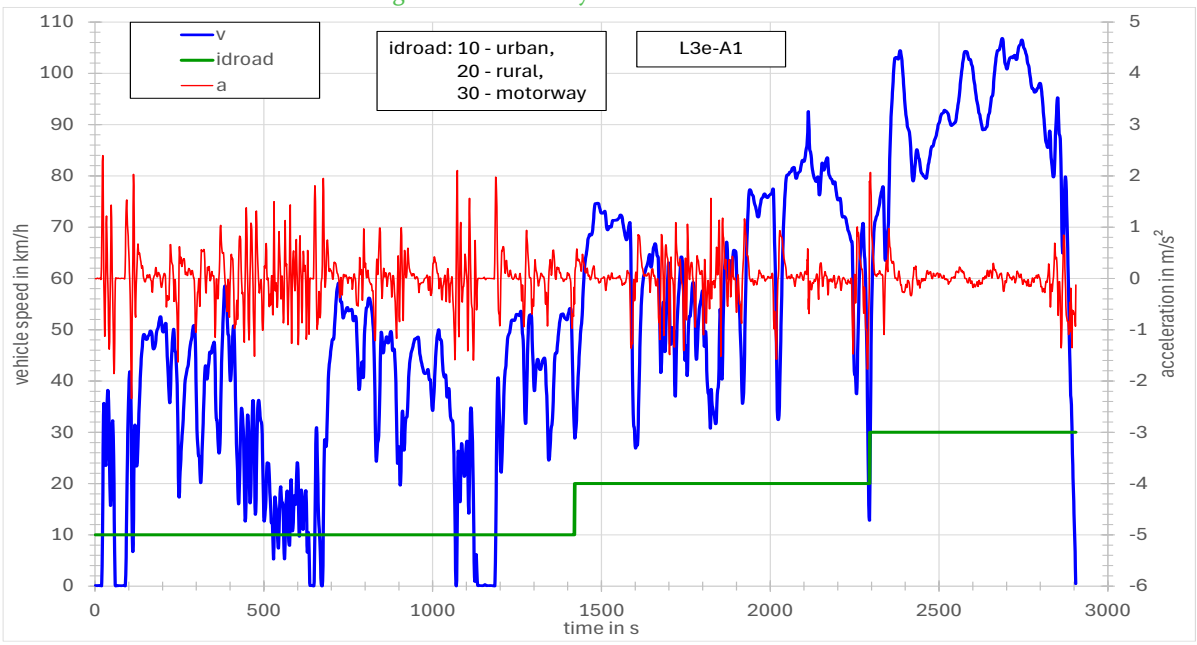

Figure 4-43: Final cycle for L3e-A1 vehicles.

This project has received funding from the European Union's Horizon Europe research and innovation programme under grant agreement No 101056777

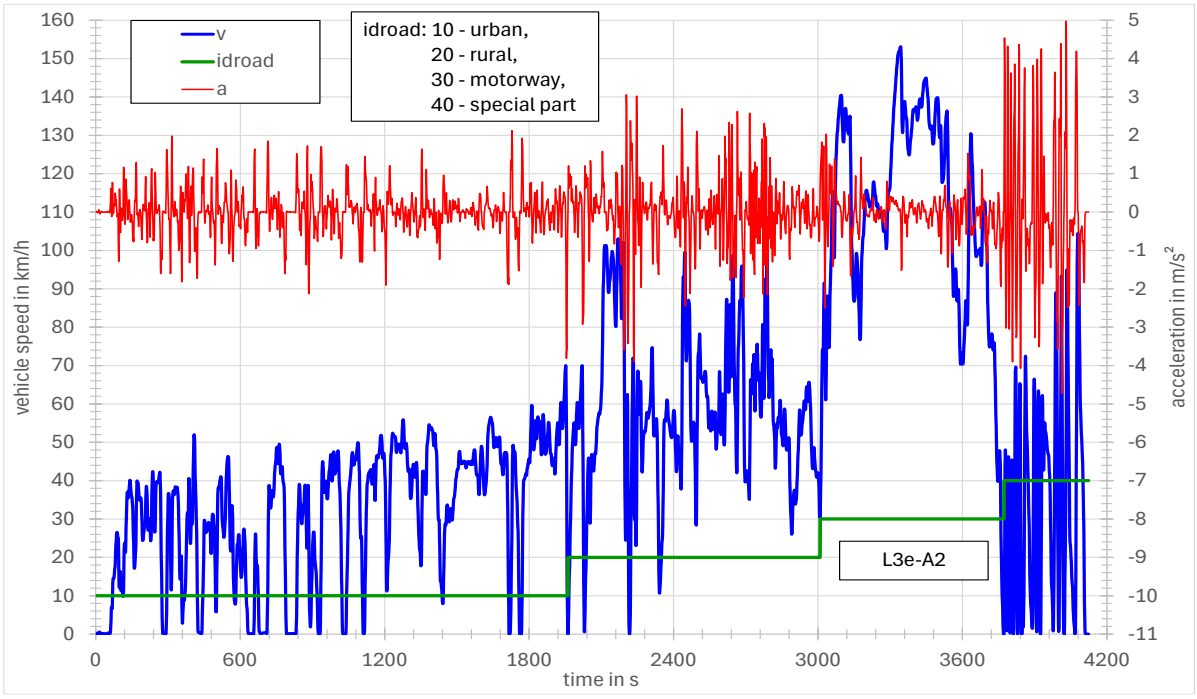

Figure 4-44: Final cycle for L3e-A2 vehicles.

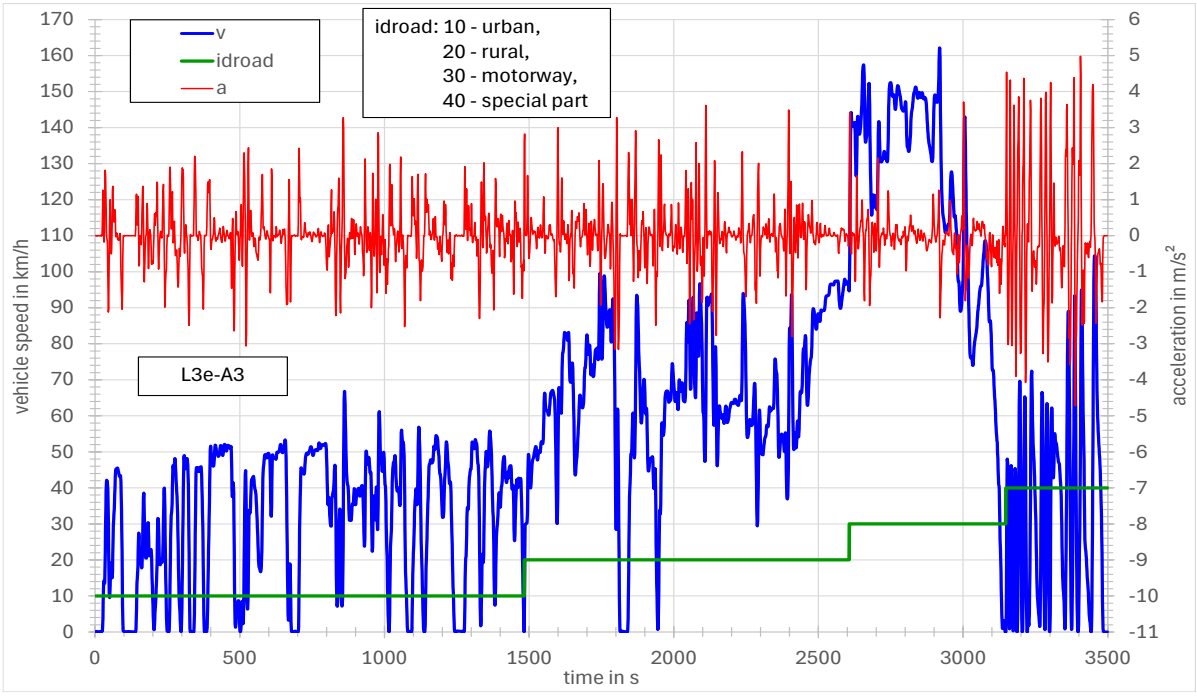

Figure 4-45: Final cycle for L3e-A3 vehicles.

This project has received funding from the European Union's Horizon Europe research and innovation programme under grant agreement No 101056777

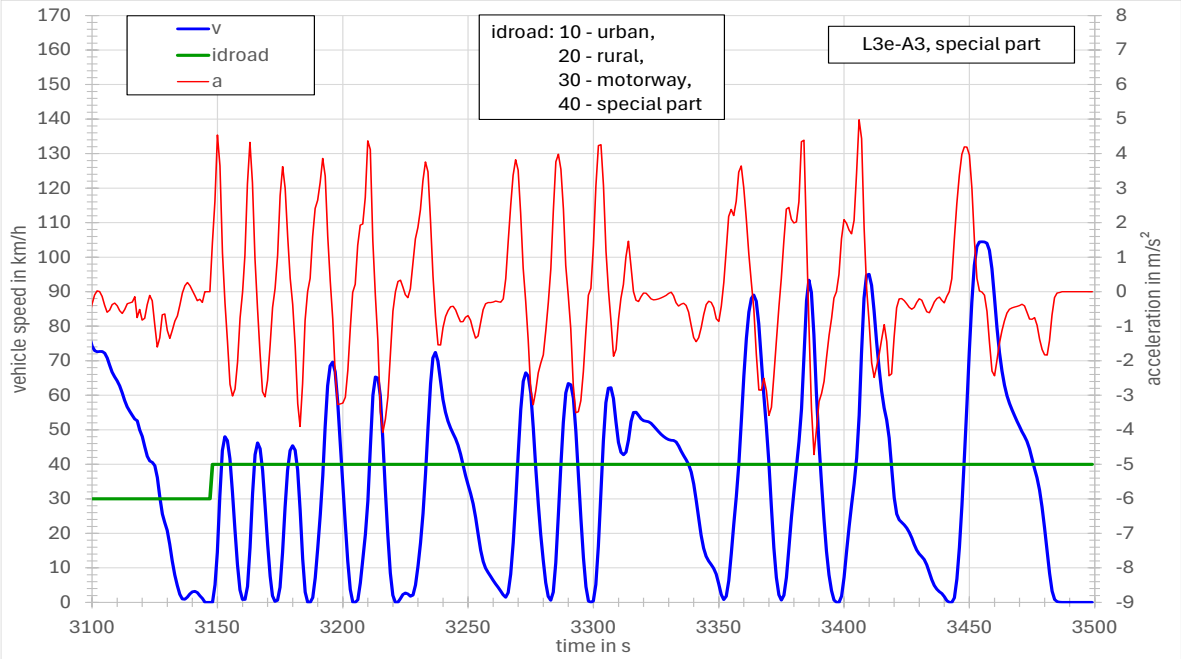

Figure 4-46: Final cycle for L3e-A2/A3 vehicles, special part.

In addition to the cycles described above, the following cycles were also delivered:

- Most aggressive cycle for L3e-A1
- Most aggressive cycle for L3e-A2/A3
- Quad cycle
- Microcar cycle

The quad cycle was measured within the LENS measurement campaign; the microcar cycle was derived from the moped cycles by modifying the accelerations and the maximum speeds.

The results are shown in the following figures. The last figure in this chapter shows a comparison of the coverage of acceleration and vehicle speed for class L3e-A3 cycles in two-dimensional v-a distributions. It can clearly be seen that the developed RDE cycles cover wide areas in the distribution compared to the TA cycle WMTC and the RDC cycle.

This project has received funding from the European Union's Horizon Europe research and innovation programme under grant agreement No 101056777

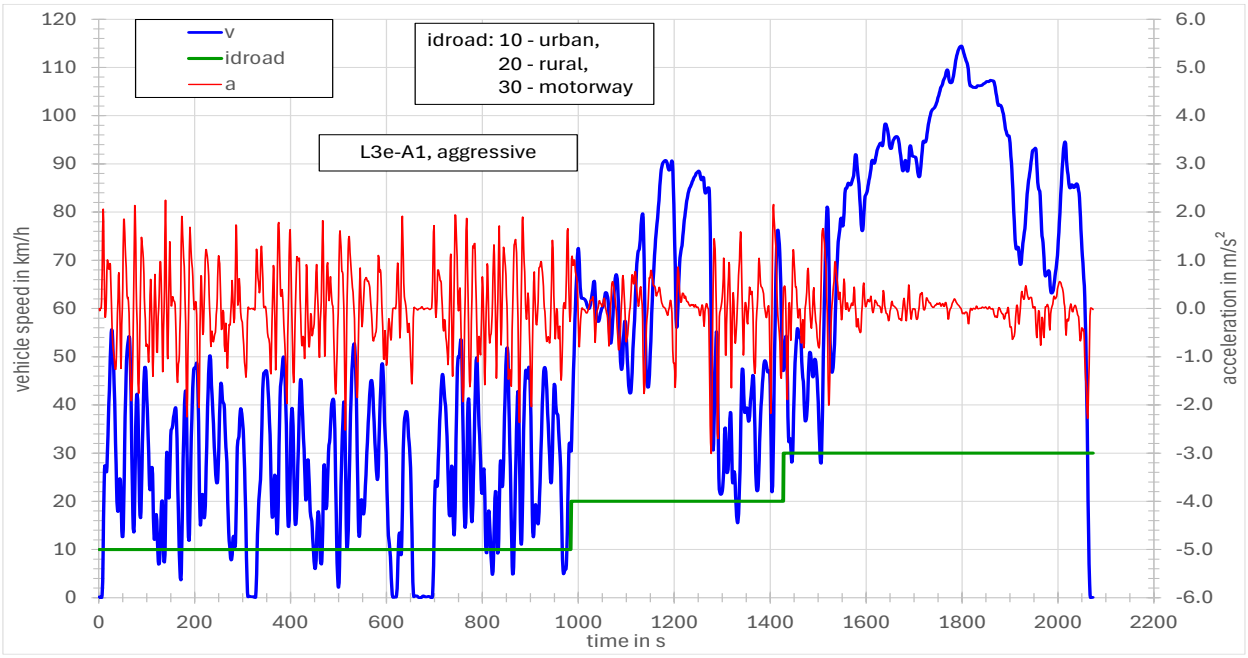

Figure 4-47: Most aggressive cycle from the LENS database, L3e-A1 vehicles.

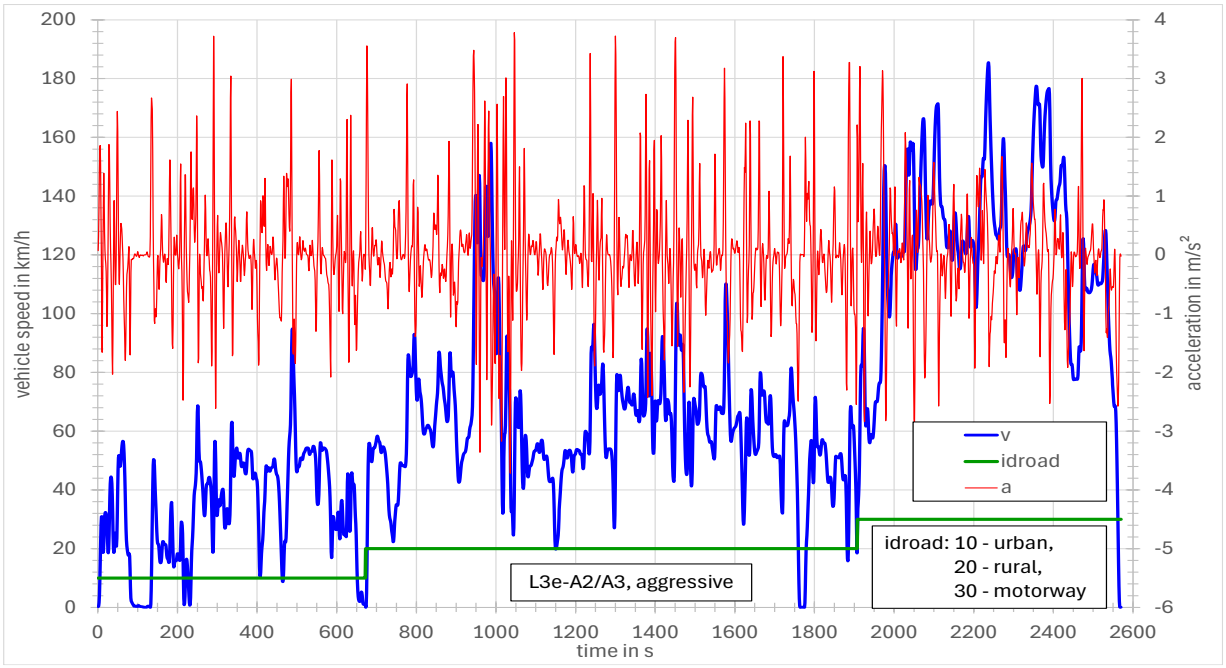

Figure 4-48: Most aggressive cycle from the LENS database, L3e-A2/A3 vehicles.

This project has received funding from the European Union's Horizon Europe research and innovation programme under grant agreement No 101056777

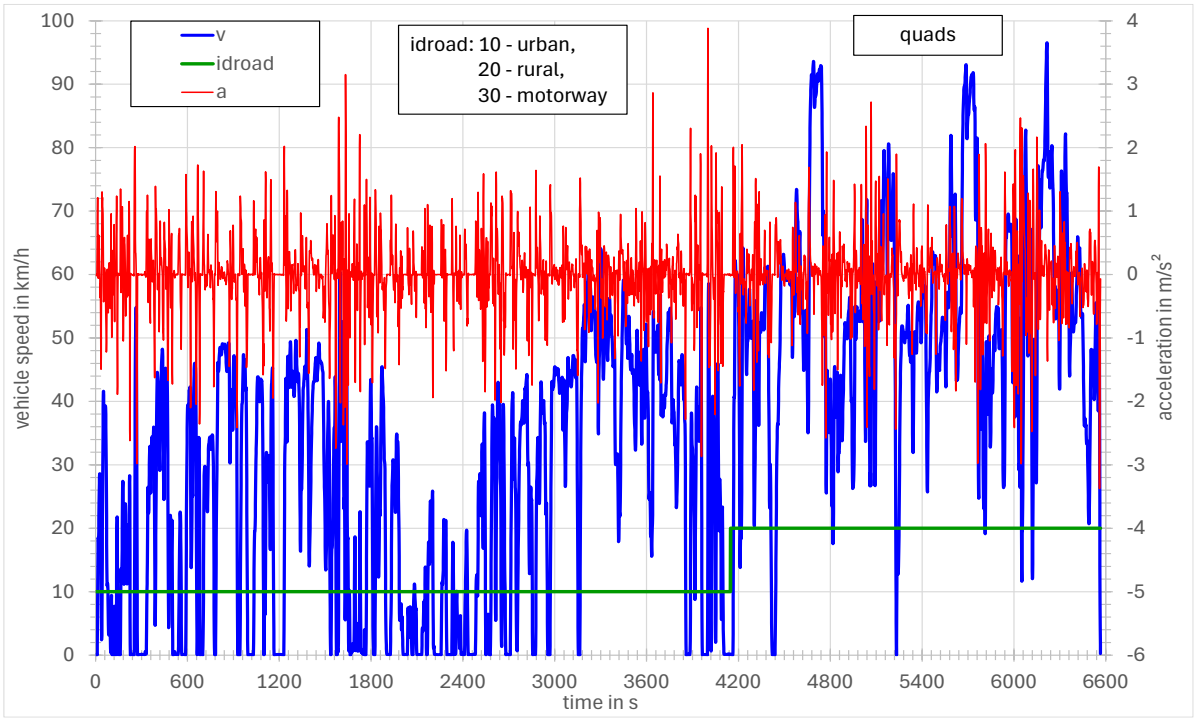

Figure 4-49: Quad cycle.

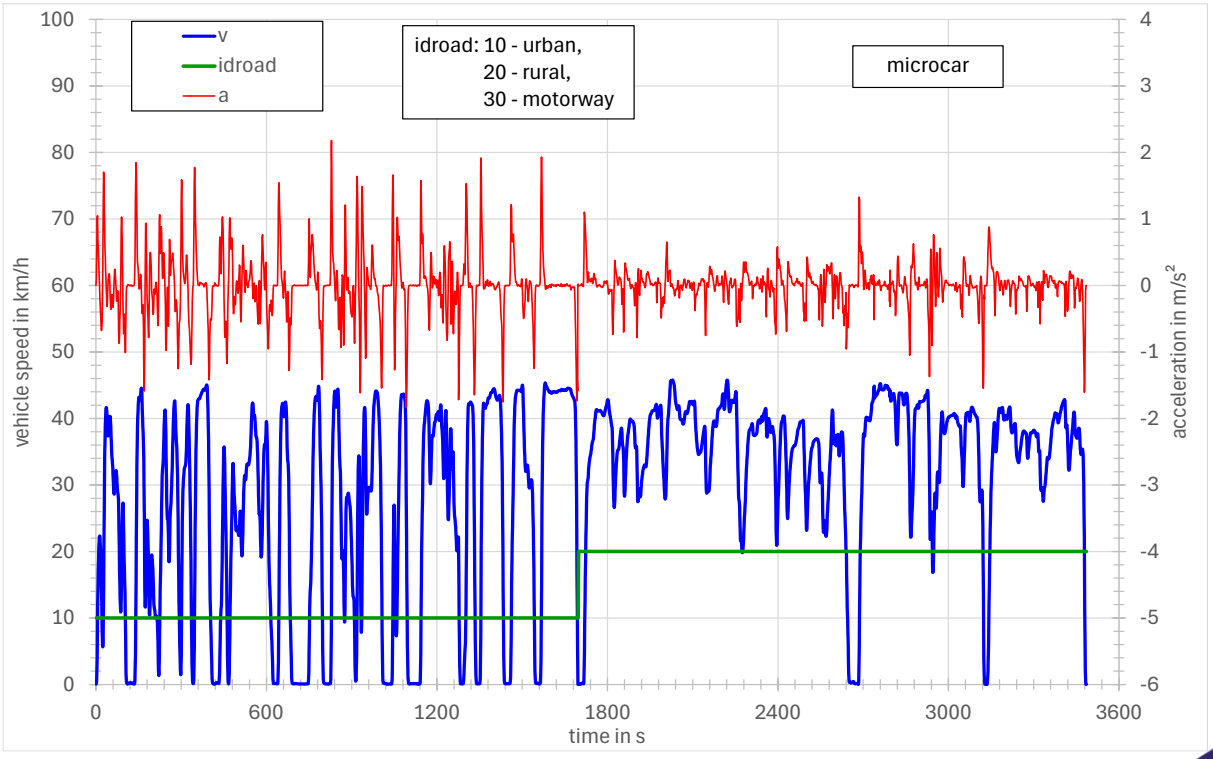

Figure 4-50: Microcar cycle.

This project has received funding from the European Union's Horizon Europe research and innovation programme under grant agreement No 101056777

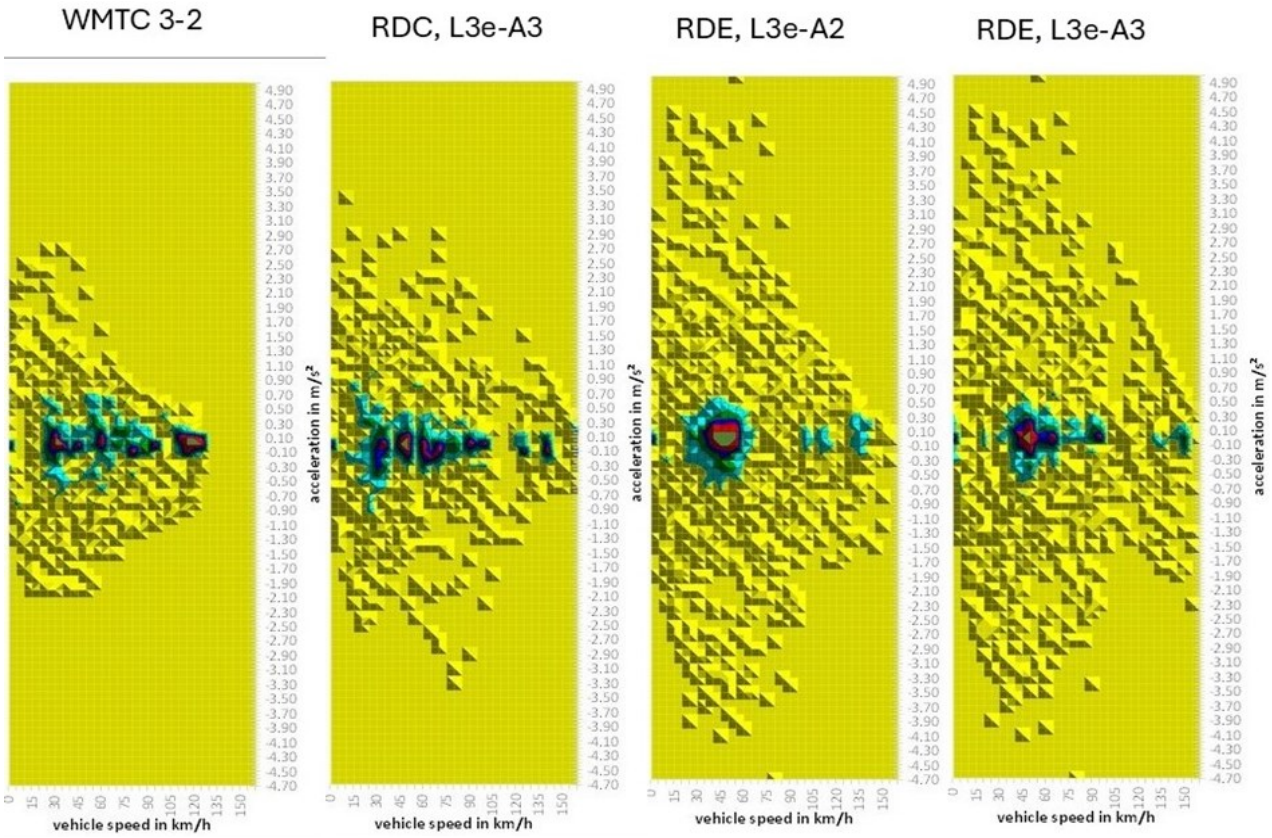

Figure 4-51: Comparison of the coverage of acceleration and vehicle speed for class L3e-A3 cycles.

4.5 Assessment of real-world driving patterns causing emissions

In Deliverable D6.1, a total of 9 driving events that were hypothesized to lead to high pollutant emissions have been identified. Many of these events, summarized in Table 4-18, were initially selected based on their known association with high noise emissions. The underlying hypothesis was that driving behaviors that generate high noise levels may also correlate with elevated pollutant emissions. However, at the time that deliverable D6.1 was published, no empirical data was available to verify this assumption.

With the availability of comprehensive measurement data in the LENS db, it is now possible to evaluate this hypothesis. The aim of this analysis is to determine the extent to which the identified high-emission events contribute to overall pollutant emissions. The findings may inform targeted recommendations for improving the current type approval procedures for motorcycles, ensuring they more accurately reflect real-world emission behavior.

To ensure a focused and practical analysis, a prioritization of the nine driving events included in Table 4-18 has been applied. Relevant events across all vehicle types and persisting for more than a few seconds are given higher priority. Consequently, events 2 (rpm burst), 4 (maximum rpm), 8 (rpm fluctuation), and 9

This project has received funding from the European Union's Horizon Europe research and innovation programme under grant agreement No 101056777

(backfire) are considered lower priority in this phase of the analysis due to their limited duration or specificity to certain vehicle types.

Table 4-18: Overview of driving events (adapted from D6.1, Table 4.2.)

Condition	Vehicle Operation	Already in Emission TA?
(1) Cold start (mainly for emissions)	Engine start	Yes
(2) Rpm burst (revving)	Stationary, short activation and release of accelerator	No
(3) Acceleration from standstill, G1, G2, loaded + unloaded	Acceleration, late gear change	Partly
(4) Max rpm: esp. mopeds, scooters, sports MCs	Constant speed with max rpm	No
(5) Transition from constant speed or acceleration phases to deceleration phases	Deceleration	Partly
(6) 'Max' acceleration from standstill, G1, G2	Acceleration	No
(7) (Heavy) acceleration at speed, from 50 to 100 km/h	Acceleration, may be varied	No
(8) Rpm fluctuation	Variable speed	No
(9) Backfire (occurrence, distance not critical)	Multiple gear changing or manual operation	No

4.5.1 Methodology

LENS filter rules

To ensure the relevance and quality of the data used in this analysis, a set of filter criteria was applied to the LENS db. These filters were selected with the aim to isolate measurements that are most suitable for evaluating high-emission events in motorcycles under real-world conditions. The following selection criteria were used:

- **Vehicle size class:** Only measurements with size class **L3e**, **L2e** and **L1eB** were included
- **EU Emissions standard:** All vehicles have been considered
- **Test cycle filter:** Only data collected under **Real Driving Emissions (RDE)** or **Real-world Cycle (RWC)** conditions were considered, as these reflect realistic on-road usage patterns.
- **Emission signal availability:** At least one of the following nitrogen oxide (NOx), carbon monoxide (CO), or hydrocarbons (HC) measurement signals had to be present in the dataset:
  - **NOx_PEMS** (Portable Emissions Measurement System)
  - **NOx_mFTIR** (mini–Fourier Transform Infrared Spectroscopy)
  - **NOx_CVS** (Constant Volume Sampling)
  - **NOx_FTIR** (Fourier Transform Infrared Spectroscopy)
  - **CO_PEMS**
  - **CO_mFTIR**
  - **CO_CVS**
  - **CO_FTIR**
  - **HC_PEMS**
  - **HC_CVS**
  - **HC_FTIR**

This project has received funding from the European Union's Horizon Europe research and innovation programme under grant agreement No 101056777

These filters ensured that the selected measurements represent real-world motorcycle operation, as they are likely to include the recommended driving events, while also providing NOx emission data. Applying these criteria resulted in a dataset of 94 measurements from the LENS db.

4.5.2 Identification of driving events

The driving events listed in Table 4-18 were identified within the measurements that passed the filter criteria described in the previous section 4.5.1. At the current stage of the analysis, the focus has been placed on the following driving conditions:

- (1) Cold start
- (3) Acceleration from standstill
- (5) Transition from acceleration or constant speed to deceleration

The analysis of the remaining driving conditions, and additional pollutants, is planned to be finished during the next period. The following subsections describe the methodology used to identify each of the selected driving events in detail.

4.5.2.1 Cold start

During the cold start period there may be higher pollutant emissions as a result of the following four reasons:

1. A low engine temperature has an influence on the fuel mixture (evaporation) in the inlet duct and in the cylinder
2. The friction is higher at cold engine temperatures which increases the internal engine load
3. It takes time for the catalyst to reach the light-off temperature, at least 20 seconds
4. The driving situations that take place during the cold start phase

From these, the catalyst light-off is the most dominant factor. To reduce the influence of the driving behavior during the cold start period the emissions in g/s are added to the analysis.

Only measurements with the parameter condition `start_condition=cold` were considered for the identification of cold start events. The cold start period was defined as the first 50 seconds of the measurement. If the total time of the measurement is less than 1000 seconds or the distance travelled during the first 50 seconds is less than 150 m, the measurement is not considered for the cold start analysis. An example of this identification method is illustrated in Figure 4-52, which shows NOx emissions (in g/s) versus measurement time.

Additionally, some measurements began recording data before the motorcycle was in motion. To ensure that only actual driving behavior was analyzed, data from the beginning of the measurement was excluded if the vehicle velocity was below 1 km/h. This step ensured that the cold start analysis focused on periods of active vehicle operation.

Once the cold start periods were identified, the average NOx, CO and HC emissions in g/s and g/km were calculated. The reason for adding emissions in the metric of g/s was to reduce the effect of driving behavior on the emissions. The distance traveled by the motorcycle was based on its velocity profile. Combined with

This project has received funding from the European Union's Horizon Europe research and innovation programme under grant agreement No 101056777

time data and pollutant emission rates (in g/s), this allowed for the computation of average emissions per kilometer. These calculations were performed for both:

1. Entire measurement trip excluding the cold start period (warm emissions)
2. Cold start period

Additionally, the excess emissions, i.e. the difference between the cold start and warm emissions have been calculated. The calculated pollutant emissions are presented in the following section.

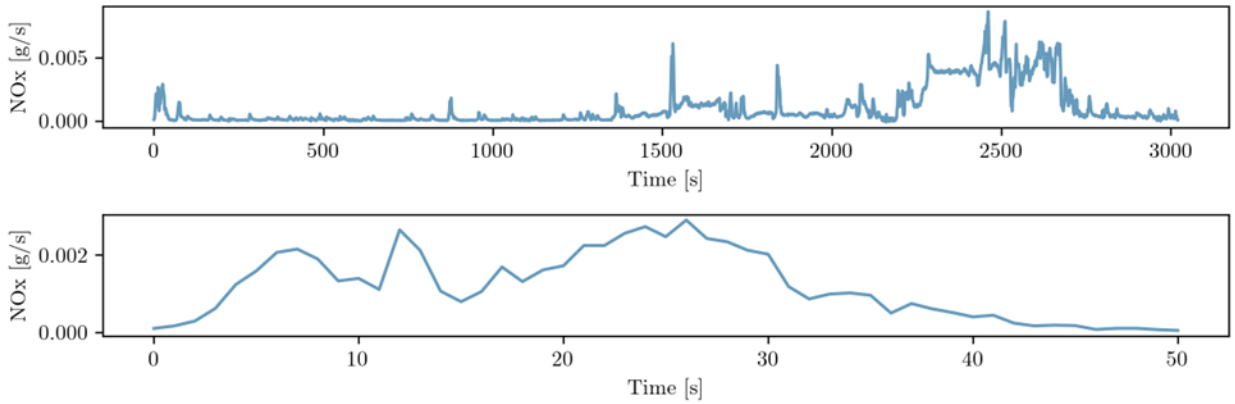

Figure 4-52: NOx emissions (g/s) over time for measurement "Vespa_300". The top panel displays the full duration of the measurement, while the bottom panel highlights the time interval identified as the cold start phase.

4.5.2.2 Acceleration from standstill

Acceleration events from standstill were identified using time-series velocity data, described by the `v` or `v_ecu` parameters in the LENS database. The velocity is smoothed using the T4253H Hanning filter to correct for faulty or implausible behaviors, such as unrealistic jumps in the speed trace. The detection process involved locating significant velocity peaks that indicate acceleration phases. For each identified peak, the algorithm traced backward in time to determine the most recent point at which the vehicle was nearly stationary, marking the beginning of the acceleration event. Nearly stationary was defined as a velocity smaller than 1 km/h.

To ensure the accuracy of the classification, events with overlapping or interfering peaks were filtered out, allowing only clean and distinct acceleration segments. The identified "*acceleration from standstill events*" are marked in orange in Figure 4-53. It clearly indicates that the algorithm extracts these events successfully.

Following a similar approach to that used for cold start events, the average NOx, CO and HC emissions were calculated for both the classified acceleration-from-standstill events and the full duration of each measurement, excluding the cold start and acceleration-from-standstill events. Furthermore, the pollutant emissions have been calculated in g/(kg CO2). This metric allows to focus more on the relative additional emissions attributed to the acceleration event, acknowledging that the fuel throughput will be much higher during accelerations. The calculated pollutant emissions are presented in Section 4.5.3.

This project has received funding from the European Union's Horizon Europe research and innovation programme under grant agreement No 101056777

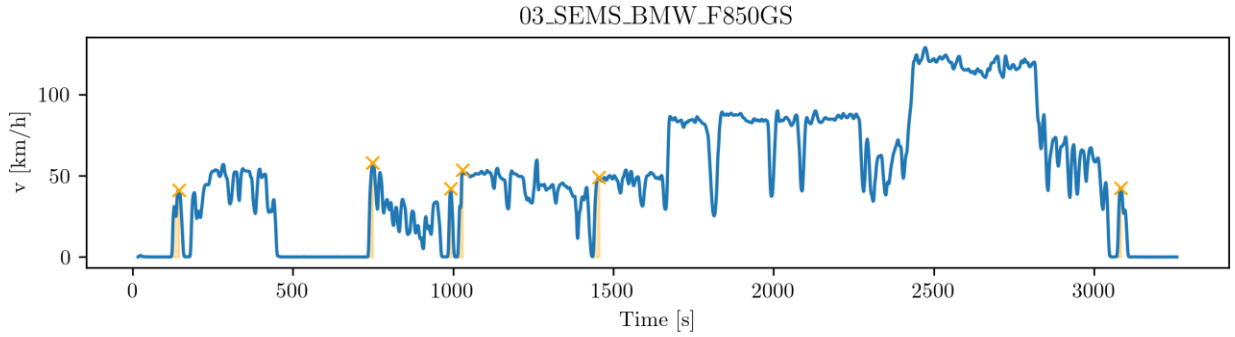

Figure 4-53: Vehicle velocity over time for measurement "*03_SEMS_BMW_F850GS*". Orange crosses mark the peak velocity of each detected "*acceleration from standstill*" event, while the orange shaded areas indicate the corresponding time intervals identified as acceleration phases.

4.5.2.3 Transition from constant speed or acceleration phases to deceleration phases

Similar to the previous section, deceleration events were identified using time-series velocity data, represented by the v parameter in the LENS db and smoothed using the T4253H Hanning filter. The velocity peaks have been identified in the exact same way as described for the "*acceleration from standstill*" events. For each identified peak, the algorithm traced forward in time to find the point at which the vehicle velocity dropped below a defined threshold, indicating a near standstill. This threshold was set to velocities smaller than 1 km/h.

To ensure the reliability of the classification, the algorithm excluded events with overlapping or interfering peaks, thereby isolating only clean and distinct deceleration segments. These "*deceleration to standstill events*" are visually marked in Figure 4-54, clearly demonstrating the algorithm's ability to extract these events accurately.

The average NOx, CO and HC emissions were calculated for each classified "*deceleration-to-standstill*" event, as well as for the entire duration of each measurement, excluding the "*cold start*" and "*deceleration-to-standstill"* events. The resulting pollutant emission values are presented in Section 4.5.3.

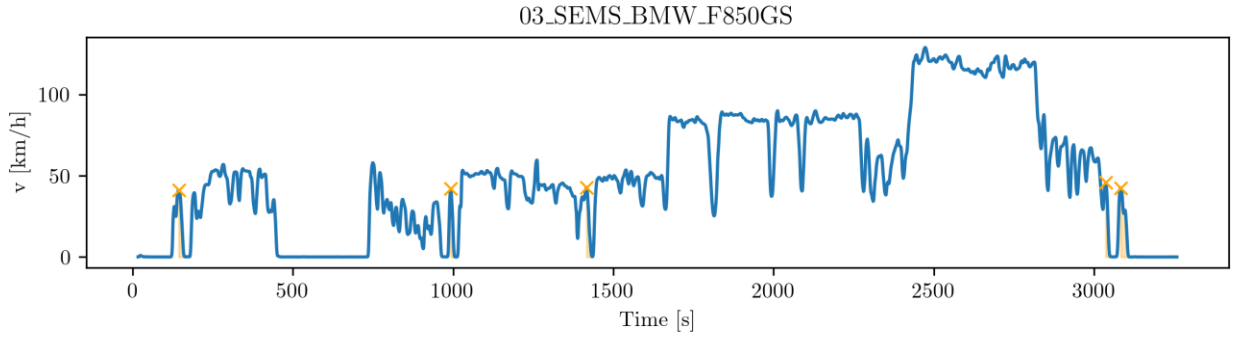

Figure 4-54**:** Vehicle velocity over time for measurement "03_SEMS_BMW_F850GS". Orange crosses mark the peak velocity of each detected "deceleration" event, while the orange shaded areas indicate the corresponding time intervals identified as deceleration phases.

This project has received funding from the European Union's Horizon Europe research and innovation programme under grant agreement No 101056777

4.5.3 Results of the analysis

In the following sections, the results of the average NOx, CO and HC emissions for each driving condition will be shown and compared to the average emissions of the total trip.

4.5.3.1 Cold start

A total of 31 (NOx), 26 (CO) and 9 (HC) cold start events were extracted from the LENS db for analysis. The corresponding average pollutant emissions (in g/km) were calculated for both the cold start periods and the warm part of each measurement.[1] These results including the excess emissions are presented in Figure 4-55, Figure 4-56 and Figure 4-57. More information about each individual measurement uniquely characterised by its measurement ID can be found in Table M-1.

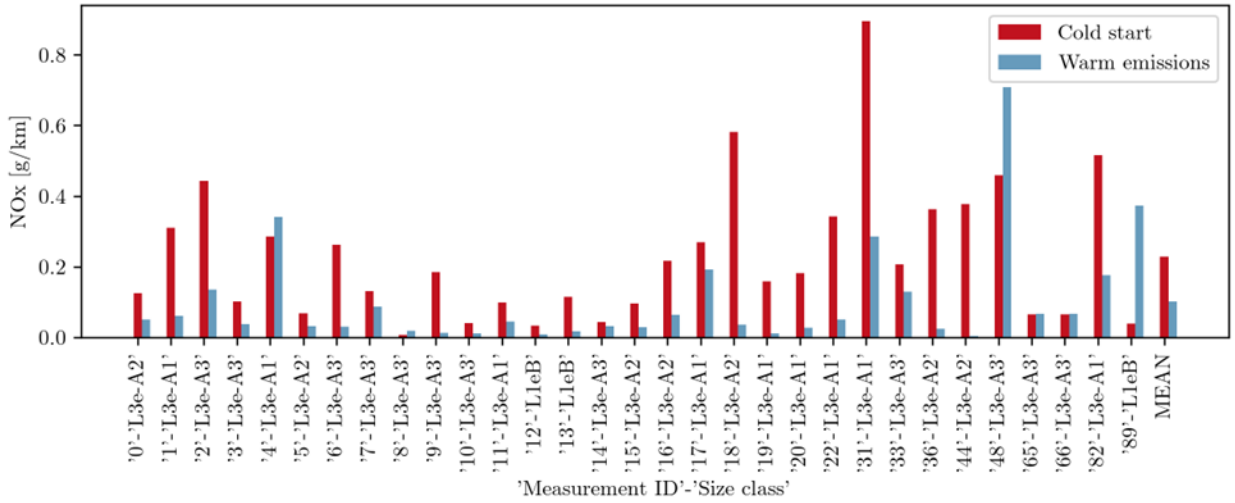

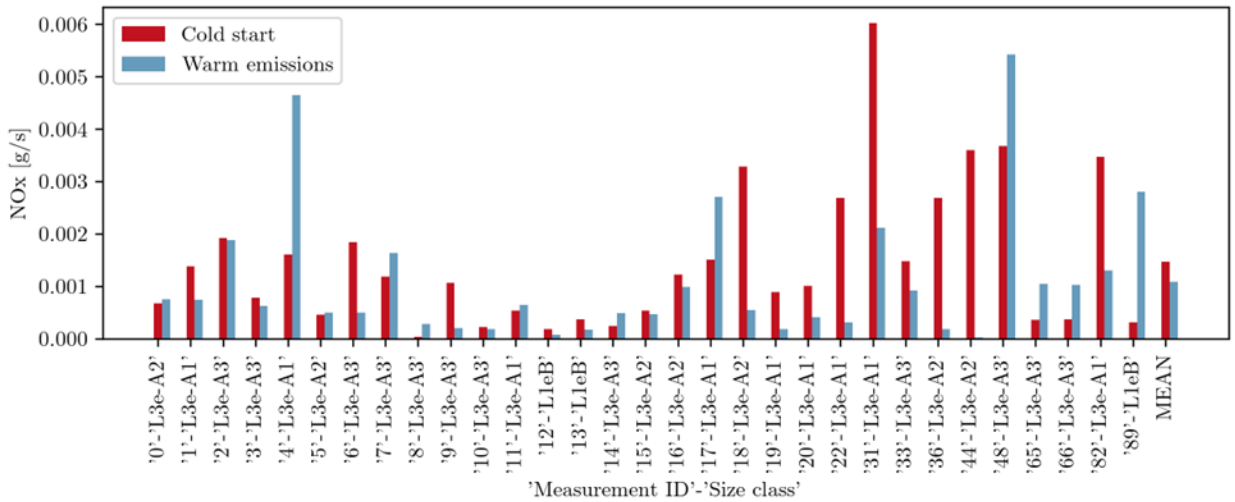

[1] The cold start period has been excluded from the total emissions to avoid that the duration of the measurement influences the ratio between cold start and warm emissions.

This project has received funding from the European Union's Horizon Europe research and innovation programme under grant agreement No 101056777

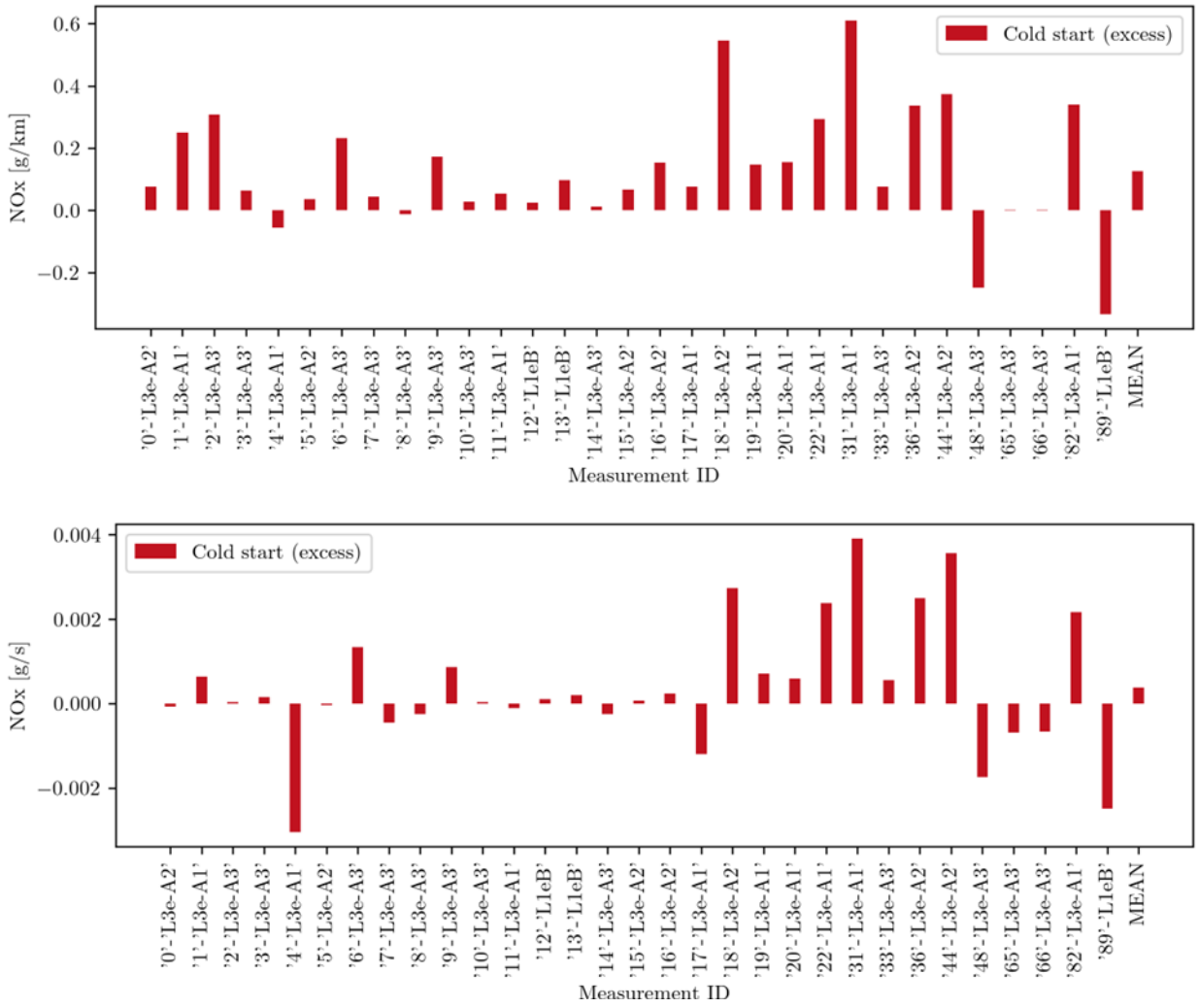

Figure 4-55: From top to bottom: NOx emissions in g/km, in g/s, excess in g/km and excess in g/s for the cold start events in comparison with the warm part of the measurements.

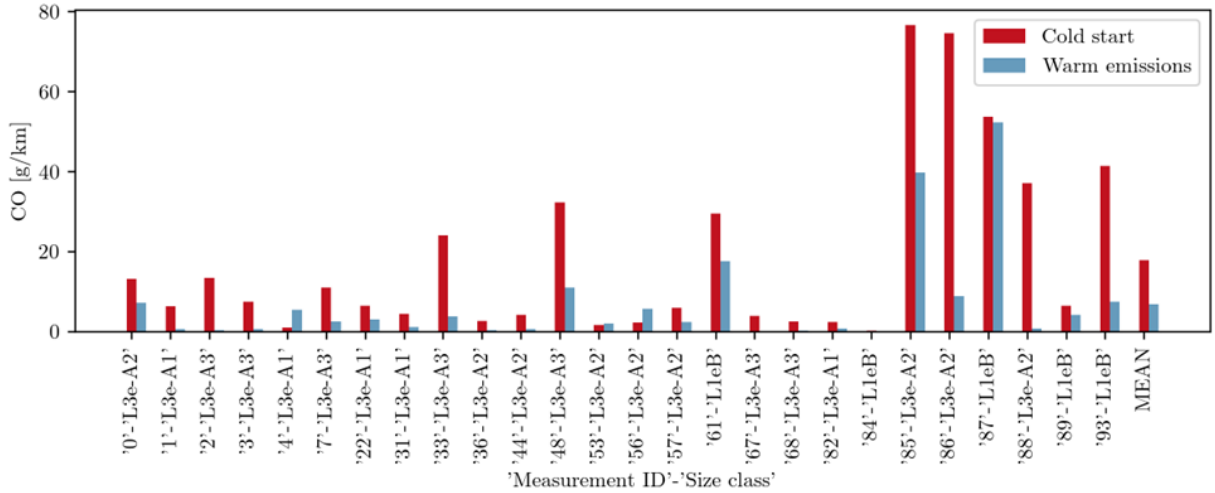

This project has received funding from the European Union's Horizon Europe research and innovation programme under grant agreement No 101056777

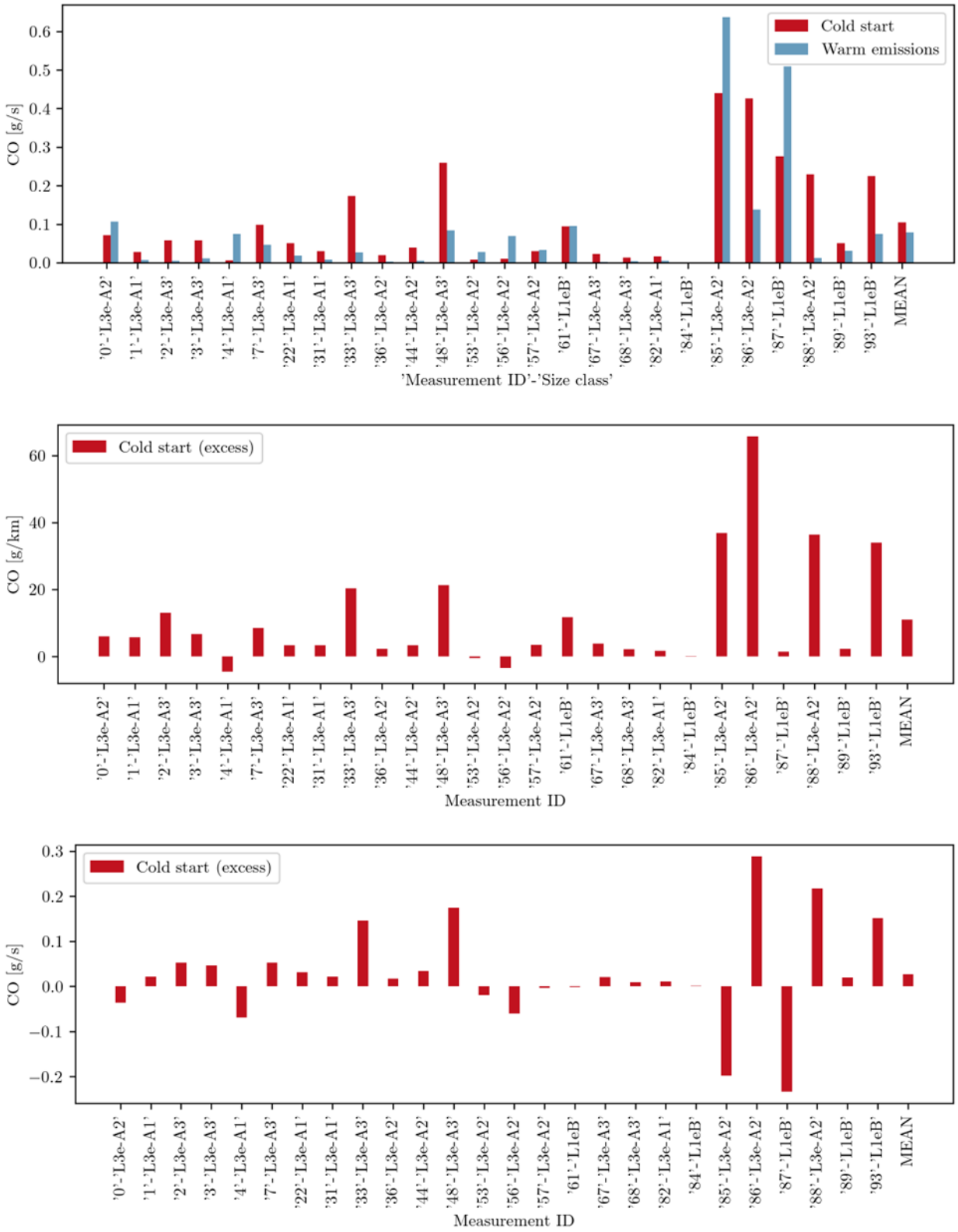

Figure 4-56: From top to bottom: CO emissions in g/km, g/s, excess in g/km and excess in g/s for the cold start events in comparison with the warm part of the measurements.

This project has received funding from the European Union's Horizon Europe research and innovation programme under grant agreement No 101056777

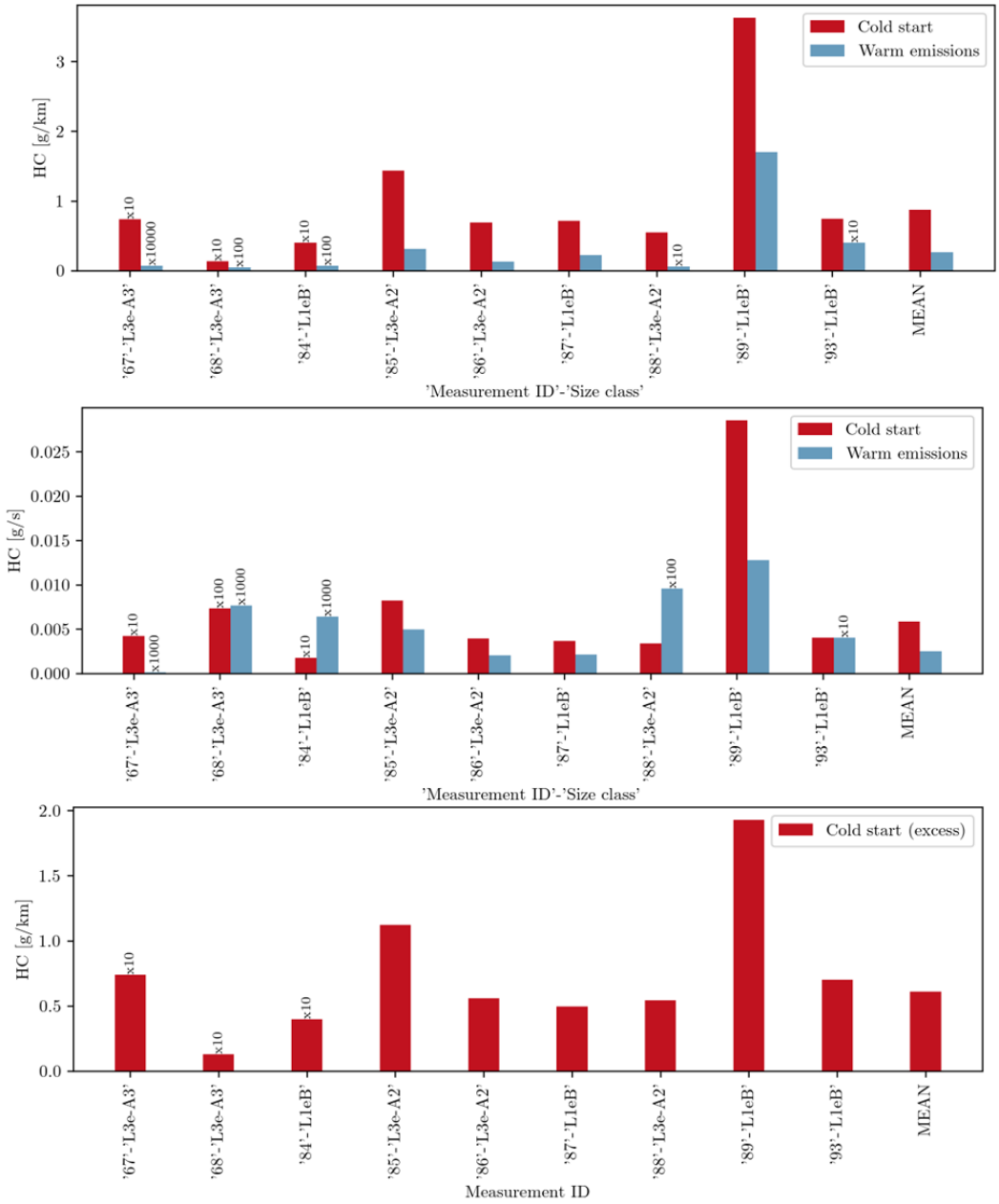

This project has received funding from the European Union's Horizon Europe research and innovation programme under grant agreement No 101056777

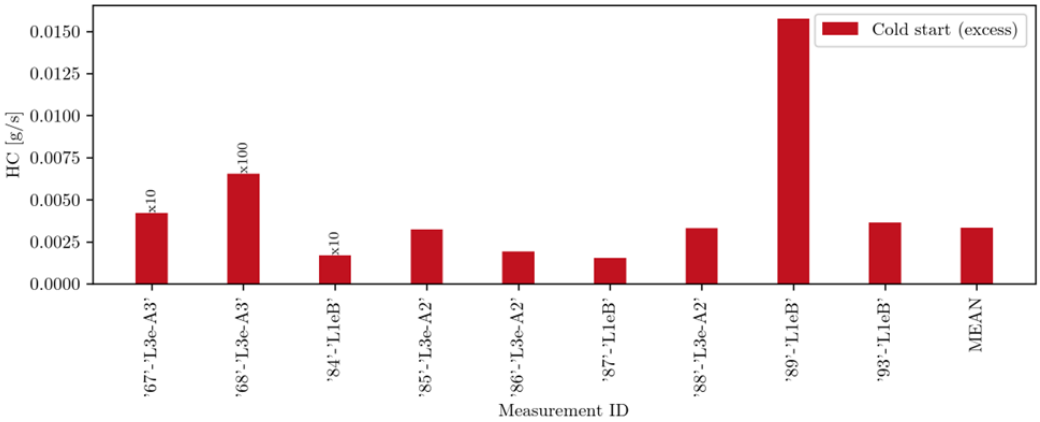

Figure 4-57: From top to bottom: HC emissions in g/km, g/s, excess in g/km and excess in g/s for the cold start events in comparison with the warm part of the measurements. Note that some values in the figure have been multiplied by a factor of 10, 100, 1000 or 10000 for visualisation purposes, i.e. their true value is 10, 100, 1000 or 10000 times lower than the value displayed in the plot.

The final bar in the plot, labelled "*MEAN*", represents the average pollutant emissions across all measurements, calculated separately for the cold start events and the warm part of the measurement. Furthermore, the ratio of cold start emissions to total emissions is calculated using two methods:

1. R_1 – First compute the average pollutant emissions separately for cold start events and for the entire measurement duration. The ratio of these two averages is then calculated.
2. R_2 – For each individual measurement, calculate the ratio of cold start emissions to total emissions. Then compute the average of these individual ratios.

These two approaches provide complementary perspectives on the contribution of cold start emissions.

Table 4-19 shows the summary of the results for the cold start events. Cold start emissions remain significantly elevated compared to total emissions, but the magnitude varies by emitter category. Overall, cold start NOx emissions are approximately 2.2 to 7.0 times higher, CO emissions are 2.6 to 9.0 times higher, and HC emissions are at least 3.3 times higher than their respective total emissions (R_2 is not presented as it is very high due to low warm emissions in one measurement). Calculated ratios tend to be higher at the level of g/km than at the level of g/s. These results highlight the disproportionate impact of cold start events.

This project has received funding from the European Union's Horizon Europe research and innovation programme under grant agreement No 101056777

Table 4-19: Summary of the results from the cold start events.

Parameter	Emissions in [mg/km]			Emissions in [g/kg CO2]		
	NOx	CO	HC	NOx	CO	HC
Mean cold start	229 ± 36 mg/km	17875 ± 4363 mg/km	876 ± 376 mg/km	1.5 ± 0.2 mg/s	105 ± 25 mg/s	5.8 ± 3.0 mg/s
Mean warm	102 ± 27 mg/km	6882 ± 2426 mg/km	268 ± 183 mg/km	1.1 ± 0.2 mg/s	78 ± 30 mg/s	2.5 ± 1.4 mg/s
R_1	2.2	2.6	3.3	1.3	1.3	2.3
R_2	7.0	9.0	-	6.0	4.3	-
Excess emissions	126 ± 35 mg/km	10993 ± 3159 mg/km	608 ± 204 mg/km	0.4 ± 0.3 mg/s	27 ± 22 mg/s	3.3 ± 1.6 mg/s

4.5.3.2 Acceleration from standstill

A total of 28 (NOx), 52 (CO) and 4 (HC) measurements with at least one acceleration event have been found in the LENS db. The corresponding NOx, CO and HC emissions in g/km and in g/kgCO2are shown in Figure 4-58, Figure 4-59 and Figure 4-60. More information about each individual measurement uniquely characterised by its measurement ID can be found in Table M-1. The final bar in the plot, labelled "*MEAN*", represents the average pollutant emissions across all measurements, calculated separately for the "*acceleration from standstill*" events and the total measurement durations.

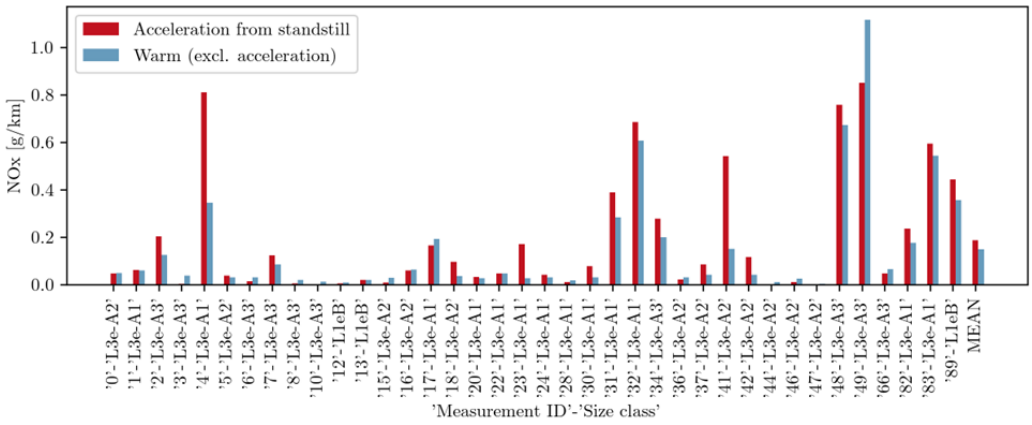

This project has received funding from the European Union's Horizon Europe research and innovation programme under grant agreement No 101056777

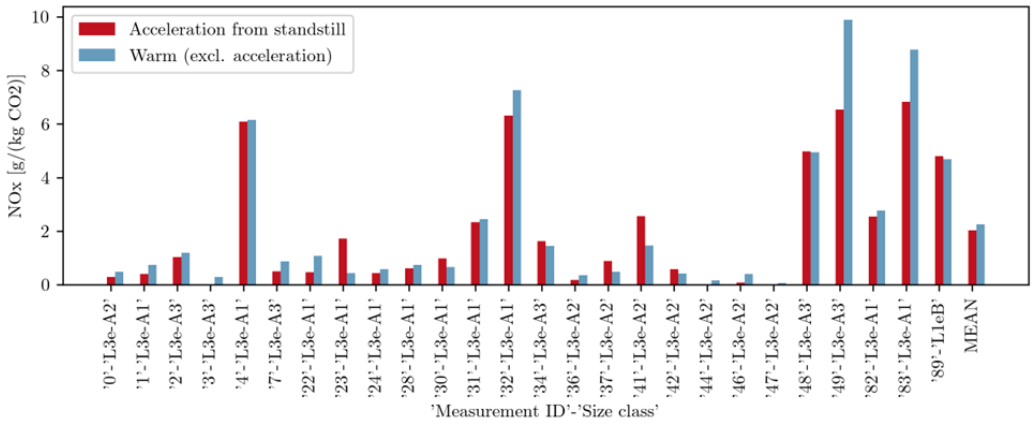

Figure 4-58: NOx emissions in g/km and g/(kg CO2) for the "Acceleration from standstill" events in comparison with the NOx emissions of the warm emissions (excluding acceleration from standstill events).

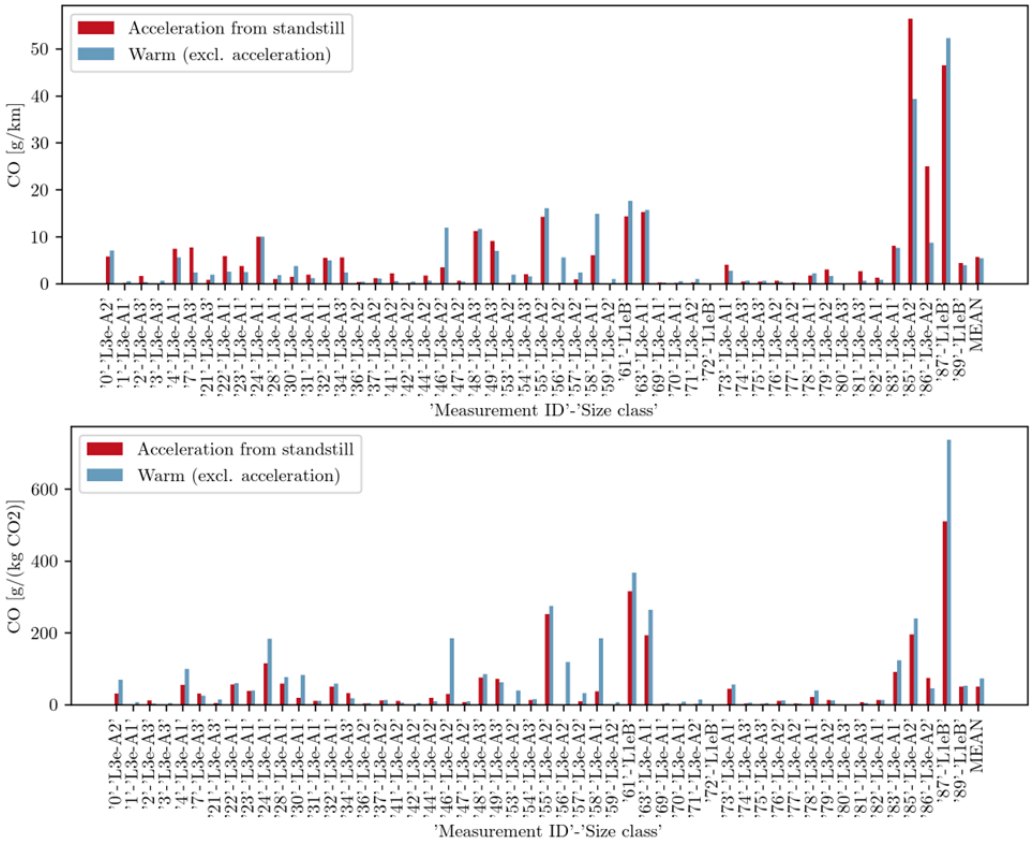

Figure 4-59: CO emissions in g/km and g/(kg CO2) for the "Acceleration from standstill" events in comparison with the CO emissions of the warm emissions (excluding acceleration from standstill events).

This project has received funding from the European Union's Horizon Europe research and innovation programme under grant agreement No 101056777

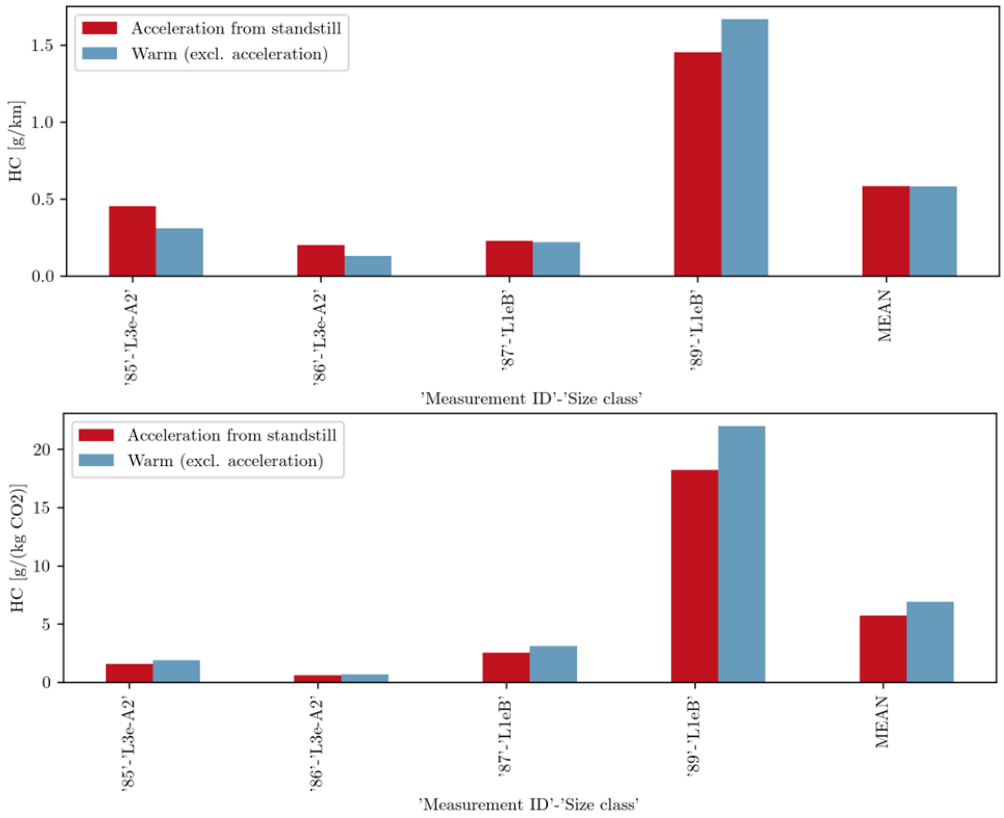

Figure 4-60: HC emissions in g/km and g/(kg CO2) for the "Acceleration from standstill" events in comparison with the HC emissions of the warm emissions (excluding acceleration from standstill events).

The summary of the "*acceleration from standstill*" events are shown in Table 4-20. The increase in emissions in mg/km during these events is relatively modest: NOx emissions are approximately 1.3 times higher, CO emissions are 1.1 to 1.2 times higher, and HC emissions are 1.0 to 1.5 times higher compared to total emissions. The NOx and HC emissions in g/(kg CO2) during the acceleration from standstill events are 0.9 times lower than the warm emissions, the CO emissions in g/(kg CO2) are lower by a factor of 0.7 to 0.8, and the HC emissions in g/(kg CO2) are a factor 0.8 times lower. These findings indicate that acceleration from a standstill leads to increased emissions when measured in g/km, but this effect is not observed when emissions are measured in g/(kg CO2).

Table 4-20: Summary of the results from the "acceleration from standstill" events.

Parameter	Emissions in [mg/km]			Emissions in [g/kg CO2]		
	NOx	CO	HC	NOx	CO	HC
Mean acceleration from standstill	187 ± 41 mg/km	5735 ± 1462 mg/km	584 ± 295 mg/km	2.0 ± 0.5 g/(kg CO2)	50 ± 13 g/(kg CO2)	5.7 ± 4.2 g/(kg CO2)
Mean warm	149 ± 38 mg/km	5443 ± 1314 mg/km	582 ± 364 mg/km	2.3 ± 0.6 g/(kg CO2)	74 ± 17 g/(kg CO2)	6.9 ± 5.1 g/(kg CO2)

This project has received funding from the European Union's Horizon Europe research and innovation programme under grant agreement No 101056777

R_1	1.3	1.1	1.0	0.9	0.7	0.8
R_2	1.3	1.2	1.5	0.9	0.8	0.8

4.5.3.3 Transition from constant speed or acceleration phases to deceleration phases

A total of 29 (NOx), 48 (CO) and 4 (HC) measurements with at least one deceleration event have been found in the LENS db. The corresponding NOx, CO and HC emissions in g/km are shown in Figure 4-61, Figure 4-62 and Figure 4-63. More information about each individual measurement uniquely characterised by its measurement ID can be found in Table M-1. Consistent with the approach used in the previous section, the final bar in the plot labelled "*MEAN*" represents the average pollutant emissions across all deceleration events.

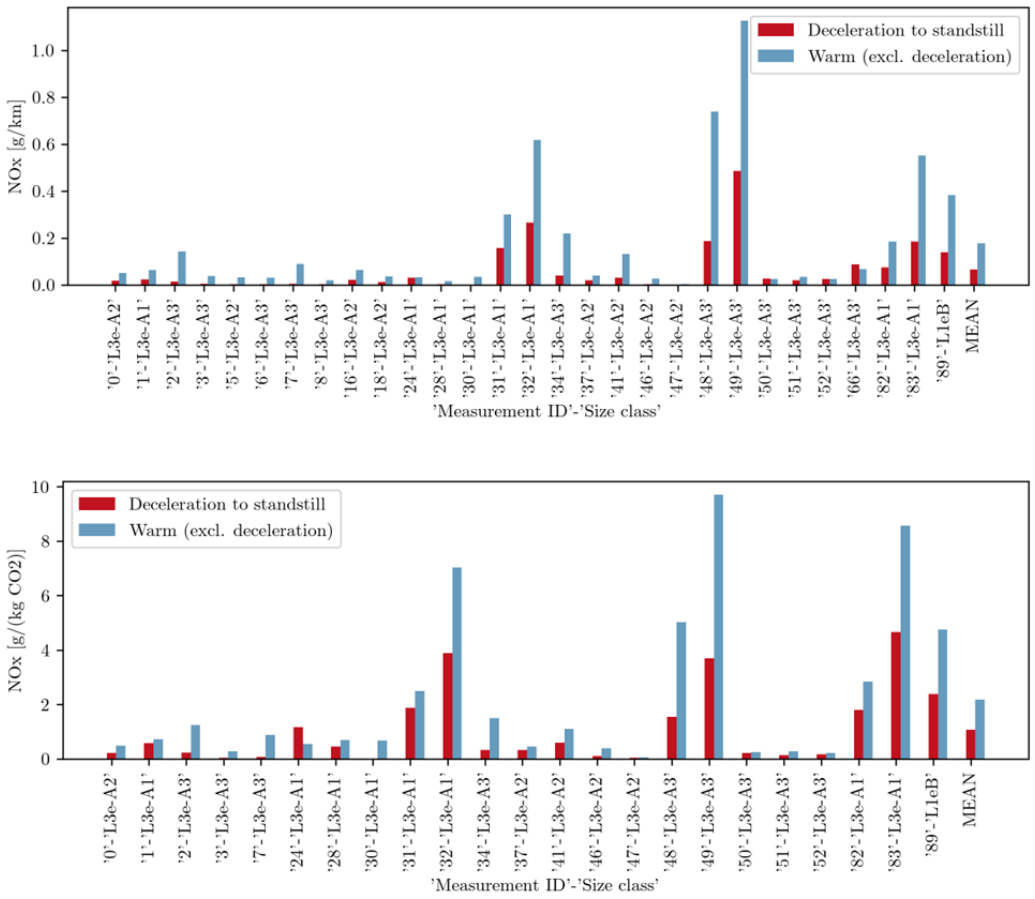

Figure 4-61: NOx emissions in g/km and g/(kg CO2) for the "deceleration to standstill" events in comparison with the NOx emissions of the warm emissions (excluding deceleration to standstill events).

This project has received funding from the European Union's Horizon Europe research and innovation programme under grant agreement No 101056777

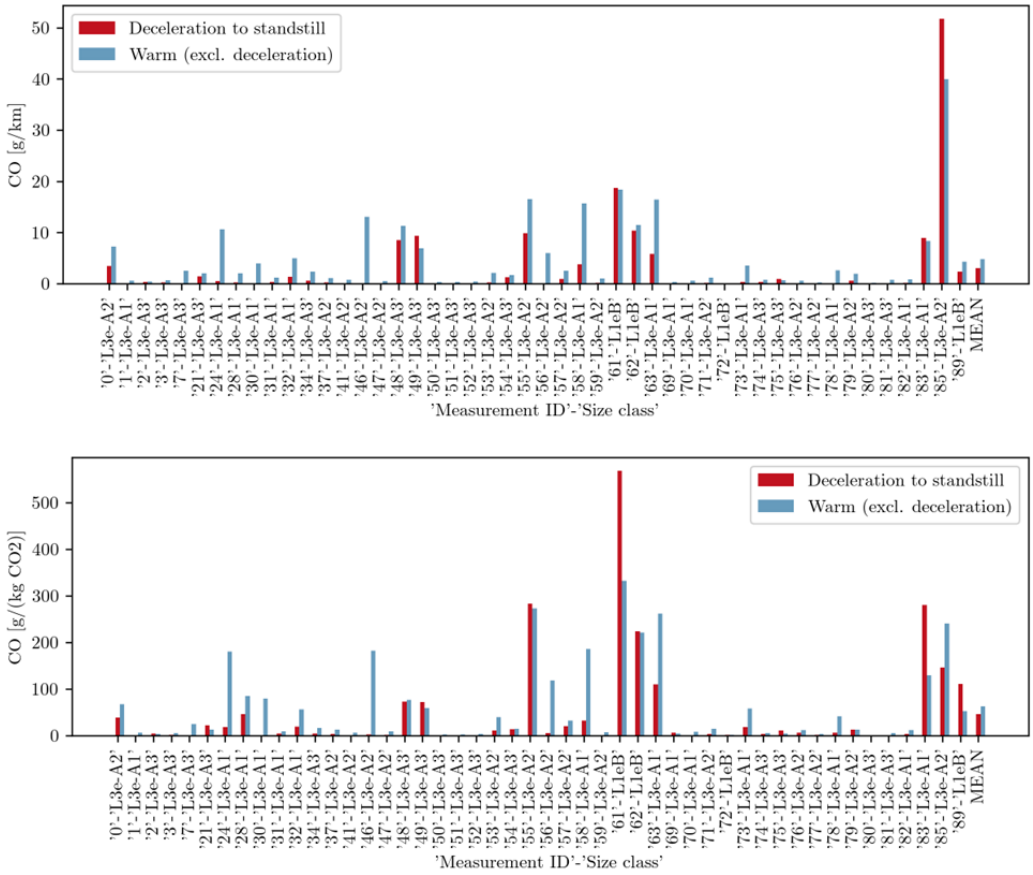

Figure 4-62: CO emissions in g/km and g/(kg CO2) for the "deceleration to standstill" events in comparison with the CO emissions of the warm emissions (excluding deceleration to standstill events).

This project has received funding from the European Union's Horizon Europe research and innovation programme under grant agreement No 101056777

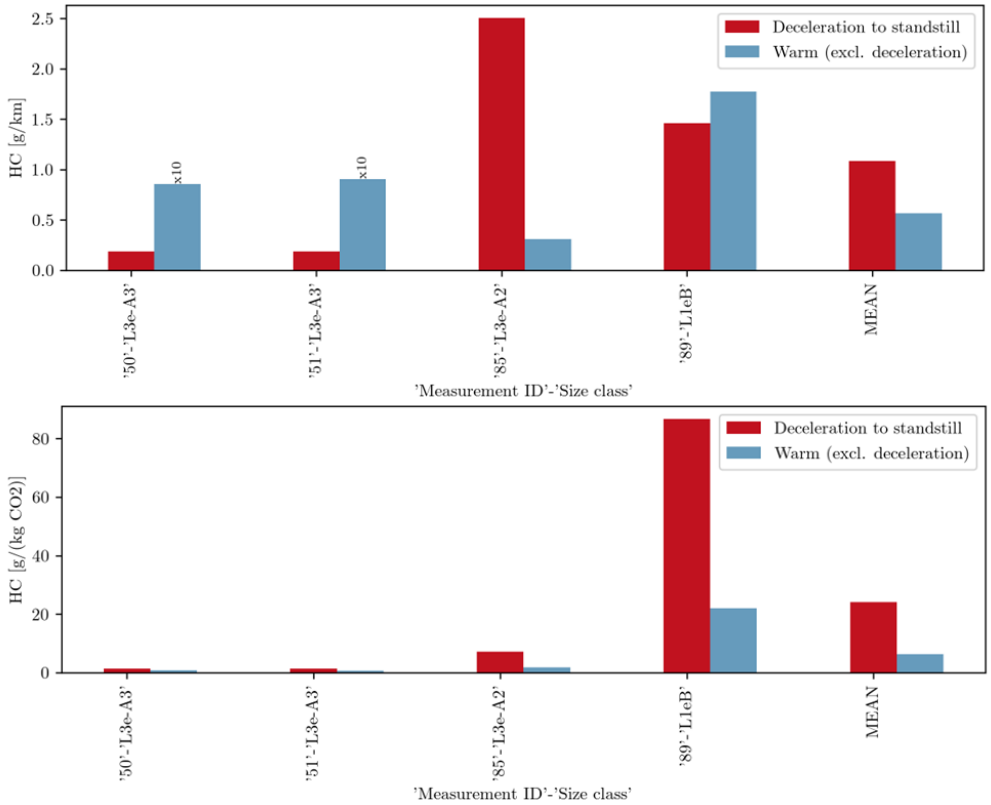

Figure 4-63: HC emissions in g/km and g/(kg CO2) for the "deceleration to standstill" events in comparison with the HC emissions of the warm emissions (excluding deceleration to standstill events). Note that some values in the figure have been multiplied by a factor of 10 for visualisation purposes, i.e. their true value is 10 times lower than the value displayed in the plot.

The summary of the "*deceleration to standstill*" events is shown in Table 4-21. NOx and CO emissions in g/km during these events are notably lower than their respective total emissions, with NOx reduced by a factor of 0.4 and CO by 0.4 to 0.6. HC emissions, however, appear 1.9 to 3.3 times higher. Similarly, the NOx and CO emissions in g/(kg CO2) are lower by a factor of 0.5 to 0.6 and 0.6 to 0.7, respectively. The HC emissions in g/(kg CO2) appear 2.8 to 3.8 times higher. It is important to note that the number of measurements for HC during deceleration events is fairly low, resulting in low statistical confidence. Therefore, the HC values should be interpreted with caution, as they may not fully represent typical emission behavior during these events.

Table 4-21: Summary of the results from the "deceleration to standstill" events.

Parameter	Emissions in [mg/km]			Emissions in [g/kg CO2]		
	NOx	CO	HC	NOx	CO	HC
Mean deceleration to standstill	66 ± 20 mg/km	3005 ± 1175 mg/km	1085 ± 561 mg/km	1.1 ± 0.3 g/(kg CO2)	46 ± 15 g/(kg CO2)	24 ± 21 g/(kg CO2)

This project has received funding from the European Union's Horizon Europe research and innovation programme under grant agreement No 101056777

Mean warm	177 ± 4 9mg/km	4830 ± 1048 mg/km	565 ± 407 mg/km	2.2 ± 0.6 g/(kg CO2)	62 ± 12 g/(kg CO2)	6.4 ± 5.2 g/(kg CO2)
R_1	0.4	0.6	1.9	0.5	0.7	3.8
R_2	0.4	0.4	3.3	0.6	0.6	2.8

4.6 Assessment of real-world driving patterns causing high emissions from LENS db

High emission events represent critical operational conditions in vehicle systems, characterized by significantly elevated levels of pollutants such as nitrogen oxides (NOx), hydrocarbons (HC), and carbon monoxide (CO). The comprehensive analysis presented in this section systematically examines raw data from the LENS db to establish a robust correlation between specific driving conditions and the generation of these high-emission events. By meticulously investigating the underlying factors that trigger heightened pollutant release, this research aims to develop targeted strategies for emission reduction and enhance the environmental efficiency of vehicular systems. The methodological approach involves a multi-parameter statistical analysis that seeks to quantify and characterize the complex interactions between driving parameters and pollutant generation, providing crucial insights.

4.6.1 Methodology

The following ways of study have been considered in order to understand specifically how high emissions correlate with real-world driving scenarios. The studies selected are:

1. Analysis from representative LVs
2. LENS db data analysis through identification of high emissions operating points
3. LENS db data analysis through identification of high emissions events

4.6.1.1 Analysis from representative LVs

With the aim of trying to find the root causes that trigger high emissions within the usage of L-Category vehicles in real-world, the decision was to compare three different bikes that share some features between them. The idea was to find similarities and differences between the events causing these high pollutant emissions.

The chosen bikes are two L3e-A2 motorbikes, but different in terms of vehicle characteristics. One 300cc equipped with CVT transmission, and a 900cc sports-tourer equipped with manual MT. This 900cc sports-tourer vehicles was originally an L3e-A3 but limited to 35 kW by changing ECUs. Through this selection of vehicles, it is possible to compare two different vehicle types under the same L3e-A2 RDC, both 300cc CVT and 900cc sports-tourer (A2 ECU); and then WMTC for the Class 3-2 for the 900cc ones with L3e-A2 and A3 ECUs.

The analysis has been developed considering instantaneous emissions in g/s or mg/s. On this way, the first thing to do was to define what was going to be considered as a "*high emission event*". If the actual European

This project has received funding from the European Union's Horizon Europe research and innovation programme under grant agreement No 101056777

regulation for LVs is considered, the emission limits are defined for the whole test in g/km, therefore a transformation into a second-by-second limit was necessary, by using the theoretical distance and time for each WMTC class cycle, knowing that emissions are weighted differently across the three phases in the WMTC, the following representation therefore exhibits a degree of uncertainty. After the calculations, to ensure a fair comparison, the decision was to use the most restrictive one (the WMTC Class 1 limited to 25 km/h) and consider a *high emission event*, every point over the following values. As no weighted values have been considered the following representation therefore exhibits a degree of uncertainty.

$$\boldsymbol{NO_x\ Cycle\ Limit}: 60\ {}^{mg}/_{km} \rightarrow \boldsymbol{NO_x\ second-by-second\ Limit}: 0.2941278\ {}^{mg}/_{s}$$
$$\boldsymbol{THC\ Cycle\ Limit}: 100\ {}^{mg}/_{km} \rightarrow \boldsymbol{THC\ second-by-second\ Limit}: 0.490213\ {}^{mg}/_{s}$$
$$\boldsymbol{CO\ Cycle\ Limit}: 1000\ {}^{mg}/_{km} \rightarrow \boldsymbol{CO\ second-by-second\ Limit}: 4.90213\ {}^{mg}/_{s}$$

The purpose of this threshold is just to establish a value from which an event is considered as a high emitter, and this threshold does not have any further objective.
The high emission events analyzed with the two bikes of the study are the following:

- Cold start (100s)[2]
- Accelerations and decelerations
- No acceleration (constant speed)
- Standstill segments
- Stable speed segments with RPM > 60 % (of max RPM)

Tables with these events were generated. Those include each contaminant and values under and over the limit mentioned previously. These are divided by:

- Occurrence (% over test time)
- Relative occurrence (% high emissions occurrence from each event)
- Average pollutant emissions (g/s)

It is important to consider that due to the comparison of RDC cycles as well as WMTC cycles, no phase-specific weighing was applied to the limits or values. Also, to separate the events during the cycle, accelerations and decelerations have been considered significant when they surpass 0.1 m/s^2, both positive and negative, and a vehicle moving is considered to have a speed of more than 1 km/h.
Once the limit is decided, the approach to the study of these *"high emitters"* is the percentage of the cycle in which they happen (total time in which these limits are exceeded with respect to the total duration of the cycle without first 100s related to cold start).
A plot of the NOx is shown in Figure 4-64 with the results of the RDC L3e-A2 CVT motorcycle in the RDC L3e-A2 test as an example of the overview of the consideration of high emitters in this study. The orange line represents the NOx that is over the limit that we established as 0.2941278 mg/s. The blue curve represents the NOx under it.

[2] Cold start was analyzed independently from the rest of events, so its high emissions are not considered there.

This project has received funding from the European Union's Horizon Europe research and innovation programme under grant agreement No 101056777

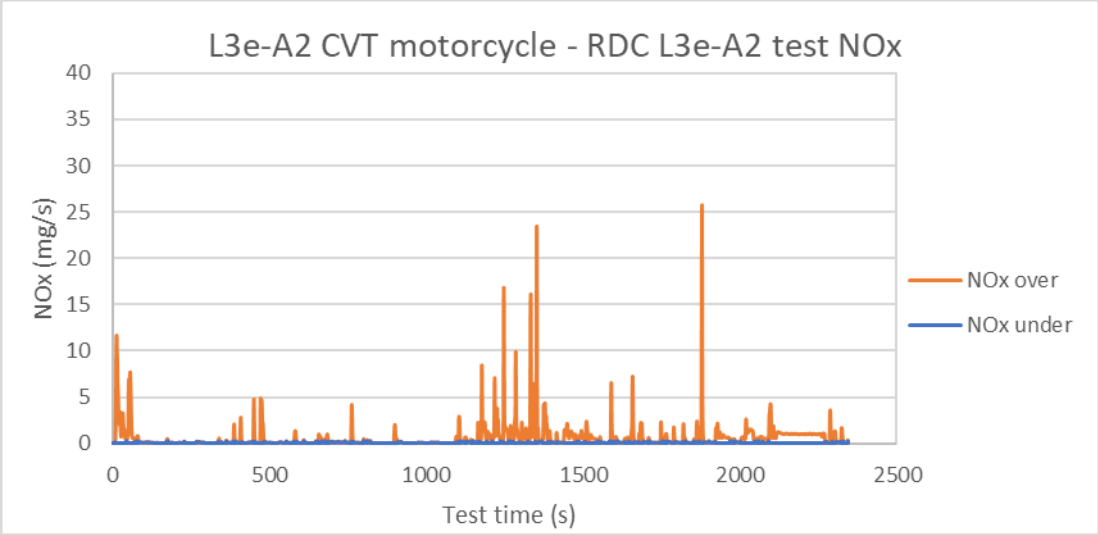

Figure 4-64: RDC L3e-A2 CVT motorcycle - NOx results in RDC L3e-A2 test.

4.6.1.2 LENS db data analysis through identification of high emissions operating points

To systematically identify and characterize high emission events, a comprehensive multivariate analysis was conducted. To ensure a more precise assessment of emissions during steady-state driving conditions, in the following section, cold start phases (first 300s in this case, as engine characteristics can differ a lot through all vehicles considered) were intentionally excluded from the dataset, thereby providing a focused analysis of the dynamic conditions associated with elevated pollutant generation. Emissions are considered in g/km, so then, only events with vehicle speed above 5km/h have been considered. Furthermore, only vehicles compliant with Euro 5 emissions standards were considered in this assessment. This filtering of data results with a total of 195 tests from the LENS db, encompassing both laboratory (RDC and WMTC) and RDE test cycles.

For each test, instantaneous data were utilized to derive and calculate the required parameters, including acceleration and v*a. Since some key operational parameters were not recorded in all the tests, the number of points can be different for each graph (ECU parameters). The investigation considered the following key operational parameters:

- Vehicle speed (km/h)
- Acceleration (m/s^2)
- v*a (m^2/s^3)
- Engine speed (rpm)
- Engine load (%)
- Throttle position (%)
- Coolant temperature (ºC)
- Air-fuel ratio (nr)

Data is classified and represented throughout heatmaps, where the z-axis corresponds to pollutant emissions (g/km) or total accumulated occurrence (nr), and both x-axis engine speed (rpm) and y-axis are taken from the KPIs introduced above. Engine speed has been normalized with engine speed at the rated max power of the engine.

This project has received funding from the European Union's Horizon Europe research and innovation programme under grant agreement No 101056777

4.6.1.3 LENS db data analysis through identification of high emissions events

After all instantaneous data analysis has been developed, a -third analysis was performed only with the instantaneous values that exceeded the limits defined previously. Throughout this analysis the purpose is to isolate the high emission events from the rest of the conditions so then each consecutive value that exceeded the limits was grouped in data segments, as can be seen in green shading in the figures below (Figure 4-65 and Figure 4-66). Each block is considered a unique event and has its own start and end time.

To characterize each block, mean, maximum, and minimum values are calculated from the instantaneous values belonging to the group of the KPIs considered, which were the following:

- Acceleration (m/s^2)
- v*a (m^2/s^3)
- RPA (m/s^2)
- Engine speed (rpm)
- Engine load (%)
- Throttle position (%)
- Air-fuel ratio (nr)
- Vehicle speed (km/h)
- Delta speed (difference between the maximum and minimum velocity in each segment)

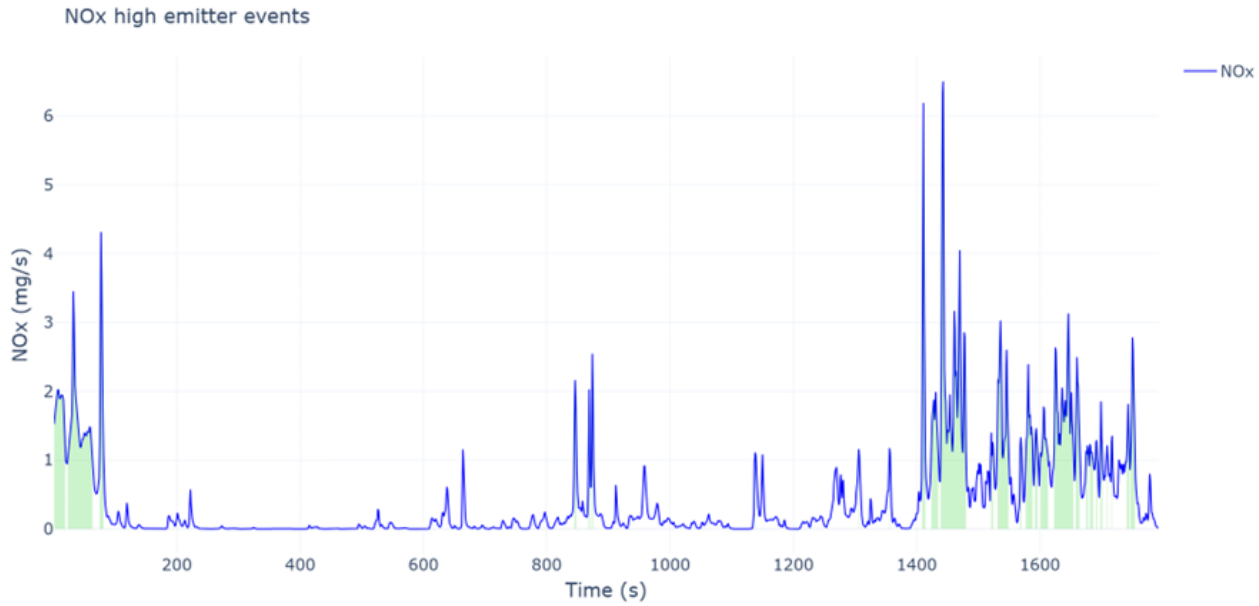

Figure 4-65: Identification of NOx high emitter events. Emissions of NOx in mg/s are represented.

This project has received funding from the European Union's Horizon Europe research and innovation programme under grant agreement No 101056777

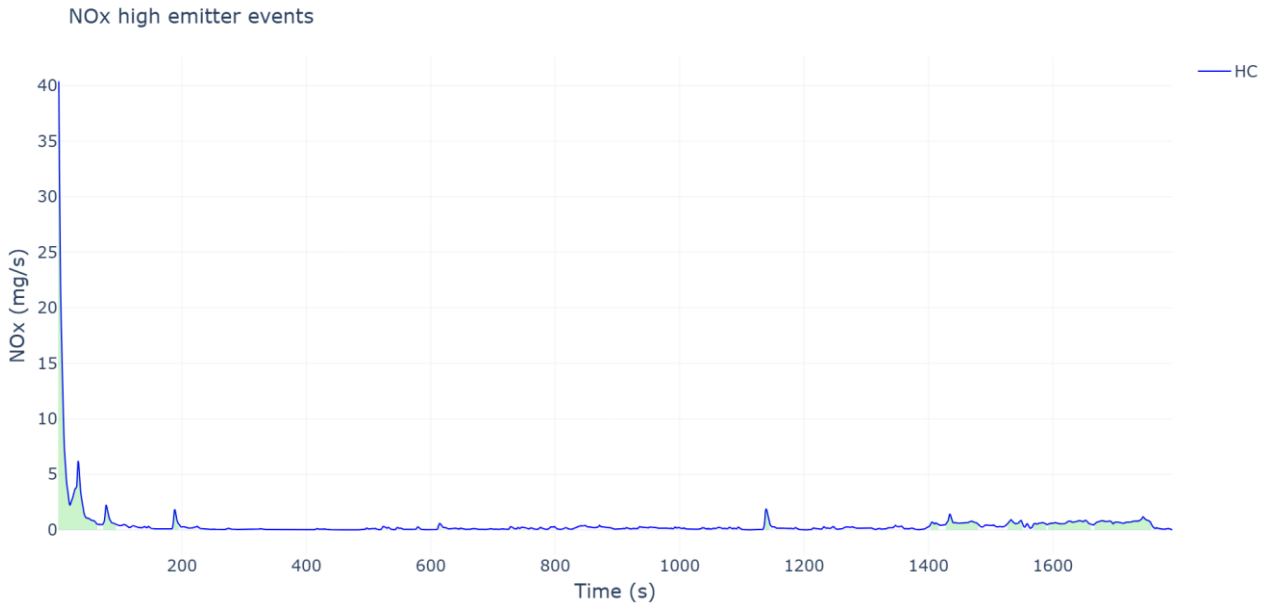

Figure 4-66: Identification of HC high emitter events. Emissions of HC in mg/s are represented. Cold start influence.

Data is classified and represented throughout bubble charts, where the z-axis corresponds to pollutant emissions, and both x-axis engine speed (rpm) and y-axis are taken from the KPIs introduced above.

4.6.2 Detailed analysis of representative vehicles

In order to develop the analysis of some representative vehicles in terms of high emissions and the occurrence of those high emissions events, three already mentioned vehicles in paragraph 4.6.1.1 have been considered. For each vehicle, the time share of operation mode in which emissions went over the established threshold have been obtained. Relative occurrences from each event is also calculated.

The sport touring L3e-A2 900cc MT 35kW EU5 vehicle has been taken as a baseline. The reason of that is because it has been tested on the cycle WMTC Class 3-2 and the RDC for L3e-A2, whereas the L3e-A2 300cc CVT 17kW EU5 has been tested on the cycle WMTC Class 2-2 and the RDC for L3e-A2. This means that both vehicles have been tested under the same RDC test cycle, therefore the results are comparable for two relatively different vehicles in terms of performance and characteristics but belonging to same L-subcategory.

As it was introduced in paragraph 4.6.1.1, the L3e-A3 is the same bike as the L3e-A2 sports tourer, but with different ECU (35kW for the A3 ECU, and 35 kW for the A2 one). Consequently, L3e-A3 version of the 900cc sports-tourer vehicle has been tested on both WMTC Class 3-2 and RDC L3e-A3 allowing 1:1 data comparison with the L3e-A2 ECU version on TA measurement with different engine management and power delivery.

In the following analysis, the most relevant tables and plots are shown. For further information, all plots' tables and heatmaps are contained in Appendix K: Tailpipe emissions analysis from representatives LV's.

This project has received funding from the European Union's Horizon Europe research and innovation programme under grant agreement No 101056777

4.6.2.1 L3e-A2 900cc MT EU5 (originally L3e-A3 with A2 ECU)

The following tables contain the occurrence and severity of emissions on the baseline vehicle. WMTC cycle represents higher share values of all pollutant emissions on the overall test than RDC. Severity of RDC high emissions events is higher, although, overall NOx and THC emissions are lower on RDC cycle, as occurrence of emissions over the established threshold is lower. CO values are higher in RDC, when operating above the established threshold, double the values from WMTC for almost all situations considered on this analysis, this means that severity is considerable higher on RDC. Regarding NOx and HC no big differences have been identified when looking at the average values of each condition.

Table 4-22: L3e-A2 Sport Touring motorcycle WMTC Class 3-2 table of occurrence (% over test time).

	WMTC Class 3-2								
	NOx			THC			CO		
	over (% time)	under (% time)	Relative over (%)	over (% time)	under (% time)	Relative over (%)	over (% time)	under (% time)	Relative over (%)
Total over threshold	33.4%	66.6%		24.9%	75.1%		15.7%	84.3%	
During cold start (100s)	2.1%	3.6%	36.6%	4.3%	1.3%	76.2%	1.8%	3.8%	32.7%
During accel (>0.1 m/s^2)	10.8%	23.0%	31.8%	7.3%	26.5%	21.5%	3.2%	30.6%	9.4%
During decel (<-0.1 m/s^2)	6.3%	23.0%	21.4%	3.2%	26.1%	10.9%	1.5%	27.8%	5.1%
No accel (-0.1< x <0.1 m/s^2) & >1 km/h	16.1%	13.5%	54.3%	11.3%	18.3%	38.3%	10.0%	19.6%	33.7%
Standstill (-0.1< x <0.1 m/s^2) & <1 km/h	0.1%	7.3%	0.8%	0.0%	7.3%	0.0%	0.0%	7.3%	0.0%
Stable speed RPM>60%	11.5%	0.0%	100.0%	11.2%	0.4%	96.9%	9.6%	1.9%	83.6%

Table 4-23: L3e-A2 Sport Touring motorcycle RDC L3e-A2 table of occurrence (% over test time)

	RDC L3e-A2								
	NOx			THC			CO		
	over (% time)	under (% time)	Relative over (%)	over (% time)	under (% time)	Relative over (%)	over (% time)	under (% time)	Relative over (%)
Total over/under threshold	24.5%	75.5%		16.0%	84.0%		10.6%	89.4%	
During cold start (100s)	1.6%	2.7%	36.6%	3.2%	1.1%	74.3%	1.7%	2.6%	38.6%
During accel (>0.1 m/s^2)	8.6%	24.5%	25.9%	5.2%	27.8%	15.8%	3.3%	29.7%	10.1%
During decel (<-0.1 m/s^2)	6.8%	30.6%	18.2%	3.7%	33.7%	9.8%	2.3%	35.1%	6.2%
No accel (-0.1< x <0.1 m/s^2) & >1 km/h	8.6%	16.8%	33.7%	4.5%	20.8%	17.9%	3.7%	21.7%	14.4%
Standstill (-0.1< x <0.1 m/s^2) & <1 km/h	0.0%	4.2%	0.0%	0.0%	4.2%	0.0%	0.0%	4.2%	0.0%
Stable speed RPM>60%	5.4%	0.5%	91.7%	4.4%	1.5%	74.2%	3.1%	2.8%	52.3%

Table 4-24: L3e-A2 Sport Touring motorcycle WMTC Class 3-2 table of averages (mg/s)

	WMTC Class 3-2					
	NOx (Total av.)	0.63	THC (Total av.)	0.69	CO (Total av.)	2.80
	Average over (mg/s)	Average under (mg/s)	Average over (mg/s)	Average under (mg/s)	Average over (mg/s)	Average under (mg/s)
Total over threshold	1.76	0.07	2.27	0.16	14.12	0.70

This project has received funding from the European Union's Horizon Europe research and innovation programme under grant agreement No 101056777

During cold start (100s)	1.35	0.13	7.49	0.31	37.42	0.72
During accel (>0.1 m/s^2)	2.47	0.09	1.08	0.20	12.23	0.92
During decel (<-0.1 m/s^2)	1.08	0.06	0.90	0.15	6.71	0.52
No accel (-0.1< x <0.1 m/s^2) & >1 km/h	1.60	0.08	1.34	0.17	11.28	0.81
No accel (-0.1< x <0.1 m/s^2) & <1 km/h	2.71	0.01	0.00	0.05	0.00	0.14
Stable speed RPM>60%	1.90	0.00	1.35	0.36	11.26	3.30

Table 4-25: L3e-A2 Sport Touring motorcycle RDC L3e-A2 table of averages (mg/s).

	RDC L3e-A2					
	NOx (Total av.)	0.59	THC (Total av.)	0.57	CO (Total av.)	3.10
	Average over (mg/s)	Average under (mg/s)	Average over (mg/s)	Average under (mg/s)	Average over (mg/s)	Average under (mg/s)
Total over/under threshold	2.18	0.07	2.74	0.16	23.57	0.68
During cold start (100s)	1.73	0.07	8.31	0.32	51.53	0.89
During accel (>0.1 m/s^2)	3.40	0.08	1.50	0.18	24.49	0.83
During decel (<-0.1 m/s^2)	1.34	0.07	1.13	0.14	12.80	0.56
No accel (-0.1< x <0.1 m/s^2) & >1 km/h	1.73	0.10	1.36	0.16	16.25	0.75
No accel (-0.1< x <0.1 m/s^2) & <1 km/h	0.00	0.01	0.00	0.08	0.00	0.15
Stable speed RPM>60%	2.37	0.23	1.36	0.31	17.44	2.47

Legend:

Table 4-26: Legend of tables of averages (mg/s)

More than 10 times over the limit	
Between 8 and 10 times over the limit	
Between 6 and 8 times over the limit	
Between 4 and 6 times over the limit	
Between 2 and 4 times over the limit	
Between the limit and 2 times over	
Under the limit	

This project has received funding from the European Union's Horizon Europe research and innovation programme under grant agreement No 101056777

CO emissions: In Figure 4-67, CO emissions against velocity and v*a are represented. Comparative examination demonstrates that elevated CO emission values are predominantly manifested in engine speed between 65-86 % and v*a ranges between 0 and 16, with a critical emission peak of 2,320 mg/km. Data indicates that emission events occurred exclusively during positive acceleration. Although negligible emissions are observed at lower RPM range. This analysis suggests that significant carbon monoxide generation is principally associated with acceleration-dominant conditions. This behavior correlates with what is shown on the tables comparing both RDC and WMTC. WMTC is not as demanding as RDC so then, CO emissions are controlled on TA cycle. Overall averaged unweighted WMTC emissions value is 174.4 mg/km. Most severe operating points goes up to 10 times this value. This value was increased on RDC by a 20%, reaching 208.1 mg/km. Overall emissions are relatively low when compared with L3e-A2 CVT vehicle, analyzed later in this section.

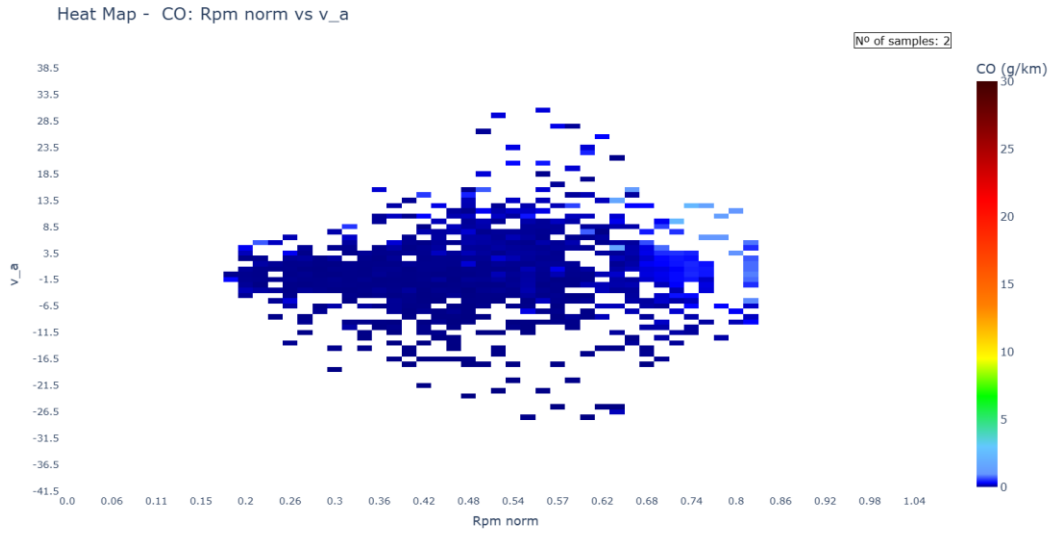

Figure 4-67: CO emissions (g/km) against engine speed (rpm) and v*a (m^2/s^3) from L3e-A2 equipped with manual transmission. RDC and RDE tests are represented.

NOx emissions: In Figure 4-68, NOx emissions are represented. As observed, high NOx emissions events are only produced during positive v*a values. Suggesting that acceleration segments and mid-high rpms are a trigger for NOx emissions. The overall view shows that NOx emissions are relatively controlled. Overall averaged unweighted WMTC emissions value is 39.4 mg/km. This value remained relatively at the same magnitude on RDC, reaching 39.6 mg/km.

This project has received funding from the European Union's Horizon Europe research and innovation programme under grant agreement No 101056777

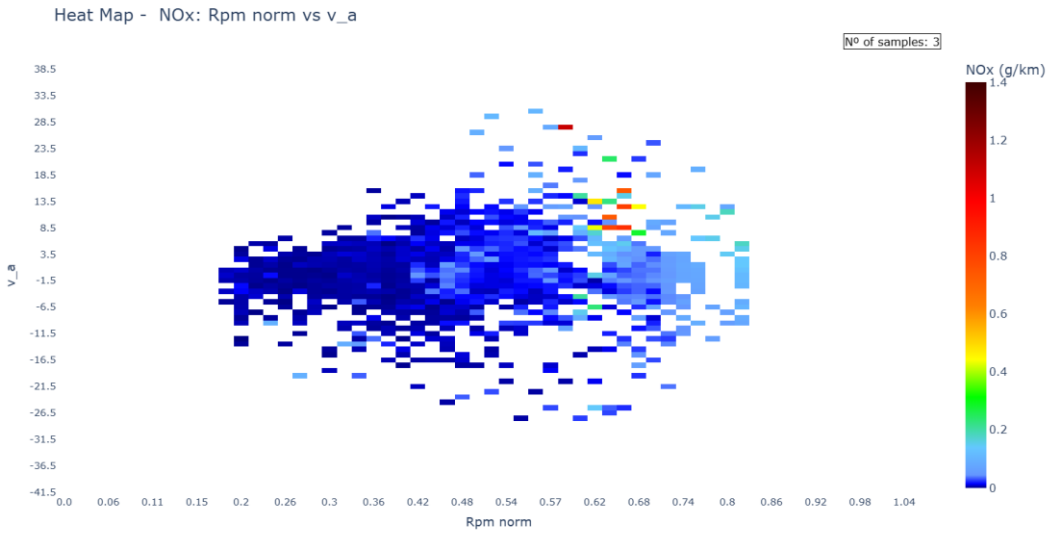

Figure 4-68: NOx emissions (g/km) against engine speed (rpm) and v*a (m^2/s^3) from L3e-A2 equipped with manual transmission. RDC and RDE tests are represented.

HC emissions: In Figure 4-69, HC emissions are represented. Analyzing these plots, higher emissions are given in a variety of circumstances. The first emerging high emissions values are shown during idle and low rpm (below 26 %), and low vehicle speed (<20 km/h). Relatively high emissions are also shown at low-mid rpm and low-mid velocity. Occurring here, the worst emissions event at 42 % rpm and 30 km/h resulting a level of 170 mg/km HC emissions. Finally, high emissions also emerge at both high vehicle speed and high rpm at 6th gear. Due to the variety of velocity and rpm events where high HC is produced, other motorcycle parameters must be evaluated to comprehensively understand those high HC emission events. Overall averaged unweighted WMTC emissions value is 42.8 mg/km. Most severe operating points go up to 2 times this value. This value decreased on RDC but not importantly, reaching 38.3 mg/km.

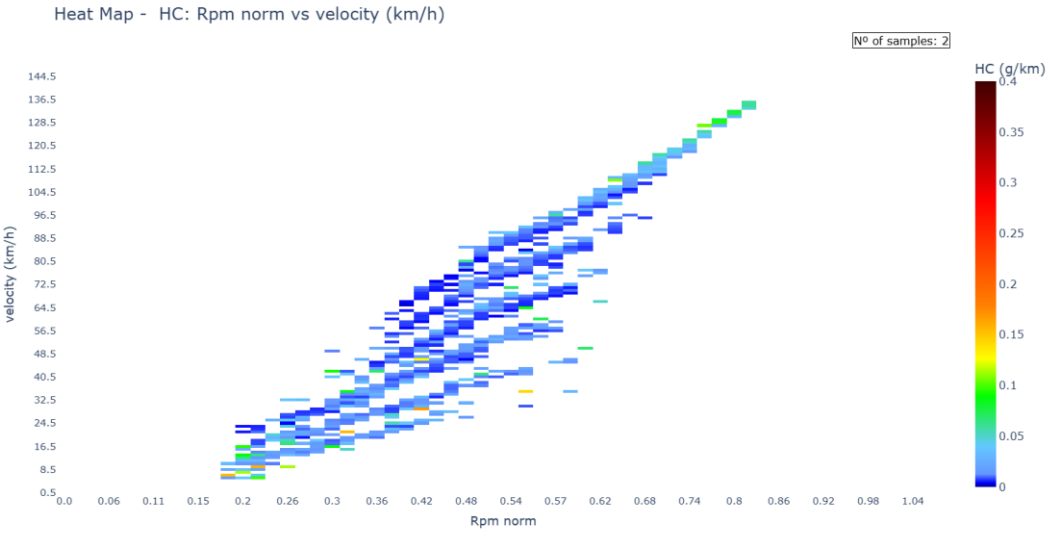

Figure 4-69: HC emissions (g/km) against engine speed (rpm) and vehicle speed (km/h) from L3e-A2 equipped with manual transmission. RDC and RDE tests are represented.

This project has received funding from the European Union's Horizon Europe research and innovation programme under grant agreement No 101056777

4.6.2.2 L3e-A2 300cc CVT EU5

A comparison between L3e-A2 sports touring bike with engine capacity of 900cc 35kW, and MT; and L3e-A2 scooter 300cc 17kW and CVT is going to be developed.

In terms of occurrence on RDC L3e-A2, CVT bike almost doubles NOx and CO share of emissions over the established limit, and the relative occurrence for all conditions considered on these pollutants when comparing it with L3e-A2 sports-tourer vehicle. In terms of severity, it is clearly shown that CO emissions are completely out of control when operating this bike under a more demanding test cycle. Total CO emissions average is almost 25 times higher than on the L3e-A2 sports-tourer vehicle. For this specific vehicle, the worst situation is the constant speed scenario in the high-speed phase of RDC L3e-A2, where the vehicle has been operating at its maximum speed with full throttle, and therefore CO emissions are triggered. Same average emissions value of 557.10 mg/s from Table 4-28 appears for both "*no acceleration*" and "*stable speed RPM > 60%*" when emissions exceed the established threshold. This is because, no acceleration events under 60% of engine RPM do not suppose a problem in terms of pollutant emissions, but when this engine speed is exceeded, emissions are triggered. This is not the case for WMTC Class 2-2 on this vehicle (see Figure K-10 and Table K-2 in Appendix K: Tailpipe emissions analysis from representatives LV's), where the overall share of high emission under both previously commented conditions are 2.4%. Instantaneous CO emissions are represented in Figure 4-70.

Regarding cold-start situation, this low-capacity engine achieves better control of emissions. Specifically, CO emissions are triggered on motorway phase, so then during first 100s (cold start) values are lower than the overall emissions average.

Table 4-27: L3e-A2 CVT motorcycle RDC L3e-A2 table of occurrence (% over test time).

	RDC L3e-A2								
	NOx			THC			CO		
	over (% time)	under (% time)	Relative occurrence (%)	over (% time)	under (% time)	Relative occurrence (%)	over (% time)	under (% time)	Relative occurrence (%)
Total over threshold	37.6%	62.4%		19.7%	80.3%		21.9%	78.1%	
During cold start (100s)	4.0%	40.7%	8.9%	0.7%	43.9%	1.6%	0.4%	44.3%	0.8%
During accel (>0.1 m/s^2)	15.3%	17.4%	46.7%	5.4%	27.3%	16.6%	6.2%	26.4%	19.1%
During decel (<-0.1 m/s^2)	5.9%	28.4%	17.2%	2.5%	31.8%	7.3%	4.7%	29.6%	13.7%
No accel (-0.1< x <0.1 m/s^2) & >1 km/h	15.1%	13.9%	52.2%	8.7%	20.2%	30.2%	9.9%	19.1%	34.0%
Standstill (-0.1< x <0.1 m/s^2) & <1 km/h	0.1%	4.0%	2.2%	0.0%	4.1%	0.0%	0.1%	3.9%	3.3%
Stable speed RPM>60%	14.1%	5.5%	72.0%	8.7%	10.9%	44.2%	9.9%	9.7%	50.3%

This project has received funding from the European Union's Horizon Europe research and innovation programme under grant agreement No 101056777

Table 4-28: L3e-A2 CVT motorcycle RDC L3e-A2 table of averages (mg/s).

	RDC L3e-A2					
	NOx (Total av.)	0.56	THC (Total av.)	0.69	CO (Total av.)	77.43
	Average over (mg/s)	Average under (mg/s)	Average over (mg/s)	Average under (mg/s)	Average over (mg/s)	Average under (mg/s)
Total over threshold	1.38	0.07	3.18	0.08	349.94	0.84
During cold start (100s)	2.72	0.09	5.28	0.29	16.76	1.59
During accel (>0.1 m/s^2)	1.80	0.08	2.24	0.09	273.48	0.82
During decel (<-0.1 m/s^2)	0.84	0.08	1.78	0.06	168.51	0.65
No accel (-0.1< x <0.1 m/s^2) & >1 km/h	0.90	0.08	3.23	0.08	557.10	1.17
No accel (-0.1< x <0.1 m/s^2) & <1 km/h	0.40	0.04	0.00	0.05	5.81	0.31
Stable speed RPM>60%	0.88	0.10	3.26	0.12	557.10	2.03

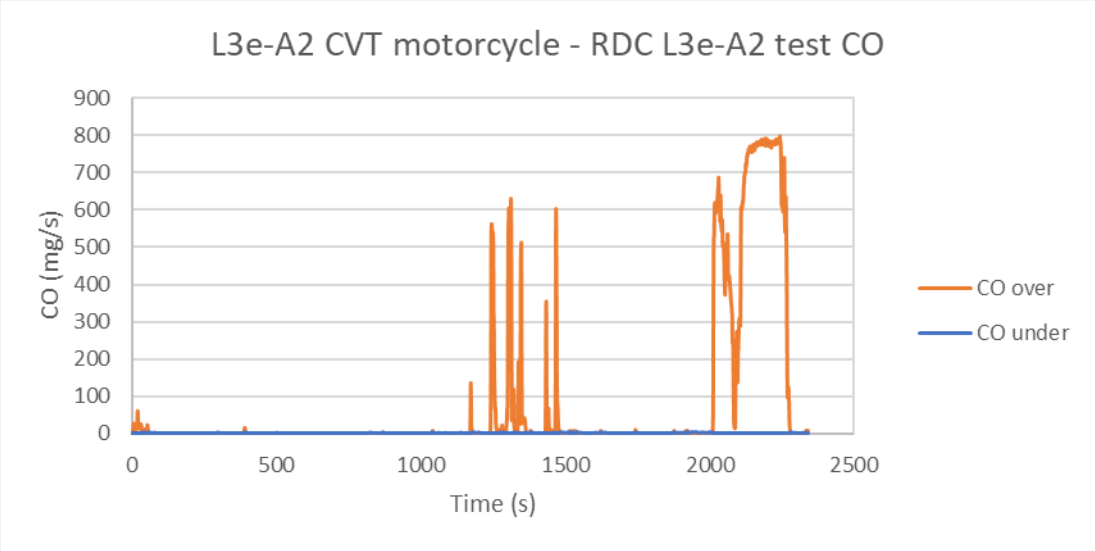

Figure 4-70: CO emissions (g(s) of RDC L3e-A2 for 300cc CVT vehicle.

CO Emissions: In Figure 4-71, CO emissions behavior against engine load and engine speed are represented. From all the pollutants considered in this analysis, CO has been the most critical one. When operating below 80% engine load and below 80% of its maximum power rated engine speed, CO emissions do not show any problem. When those values are surpassed, CO emissions emerge, reaching punctually 25,000 mg/km. Regarding overall values, RDC CO emissions reach 5221.2 mg/km, which means +35x times total averaged unweighted value of WMTC for this same vehicle and 70x times when considering only motorway phase (events above 90 km/h). Overall average unweighted WMTC Class 2-2 emissions value is 142.02 mg/km. This value is lower than sports touring vehicle on WMTC Class 3-2, but when running same RDC cycle, CO emissions on this low powered vehicle triggered due to fuel enrichment on high-speed phase. Further details can be seen in Appendix K: Tailpipe emissions analysis from representatives LV's.

This project has received funding from the European Union's Horizon Europe research and innovation programme under grant agreement No 101056777

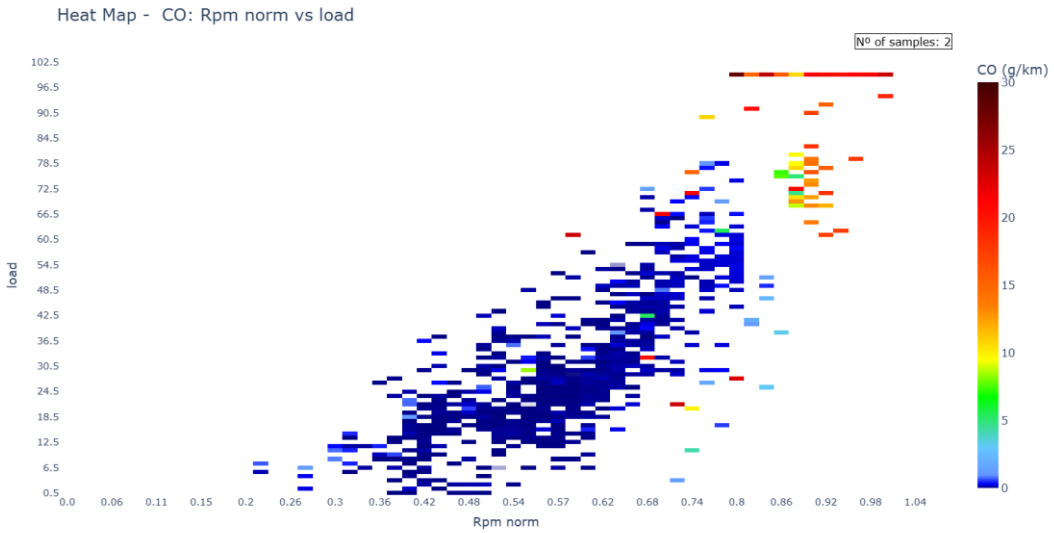

Figure 4-71: CO emissions (g/km) from L3e-A2 equipped with CVT transmission. RDC and RDE tests are represented.

NOx Emissions: NOx emissions over engine speed vs v*a are represented in Figure 4-72. Maximum values obtained reach 800 mg/km in some specific situations of high accelerations at high RPM. These events only take place in a very specific situation. During the remaining measurements' traces, emissions are adequately controlled, resulting in an overall value of ~38 mg/km on RDC, not being a problem since it corresponds to an increase of +1.3 times from WMTC total averaged unweighted value which is not critical for this kind of vehicles. Same values than L3e-A2 sports touring vehicle on RDC cycle, lower on WMTC Class 2-2 on this case. When analyzing motorway phase values, NOx emissions are lower for the RDC than on WMTC (-50 %). The high fuel enrichment could have an impact there, reducing temperatures on engine combustion chamber and thus NOx emissions.

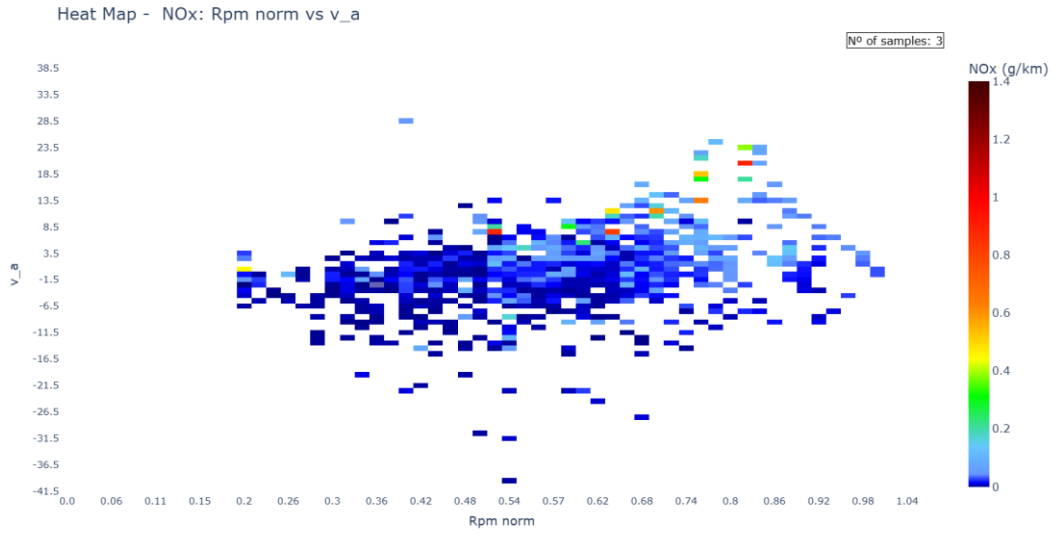

Figure 4-72: NOx emissions (g/km) from L3e-A2 equipped with CVT transmission. RDC and RDE tests are represented.

This project has received funding from the European Union's Horizon Europe research and innovation programme under grant agreement No 101056777

HC Emissions: regarding HC emissions, same behavior as with CO is represented in Figure 4-73, where HC emissions are represented against vehicle speed and normalised engine RPMs. When comparing to current legislation, HC emissions are better controlled, reaching a maximum peak value of 300 mg/km, while overall unweighted RDC emissions are 46.4 mg/km. The current regulation limit is 100 mg/km, averaged and weighted for the different test cycle phases. Considering the particular way of operation of CVT transmissions, when accelerating from constant speed, at high engine load (100% in this case), engine speed increase almost instantly, while the vehicle speed gradually increases. This scenario can be clearly shown in Figure 4-73, and there HC emissions get severe due to fuel enrichment, resulting in this case on an increase of HC emissions on RDC cycle of 2x times WLTC total averaged unweighted value. When analyzing emissions per phases, the increase on emissions of RDC are of +3.3x times on the rural phase, and near +10x times for motorway phase (according to PC (EU) no 2017/1151). When comparing with L3e-A2 MT RDC, motorway phase shows a value near +1.5x times higher on this CVT vehicle. Total averaged unweighted WMTC emissions value is 27.7 mg/km. Lower values than on sports touring vehicle on WMTC (not same cycle), but again, when operating same RDC, higher emissions on this low powered scooter equipped with CVT transmission. It could be stated that CVT vehicles are more sensitive to strong accelerations in terms of emissions.

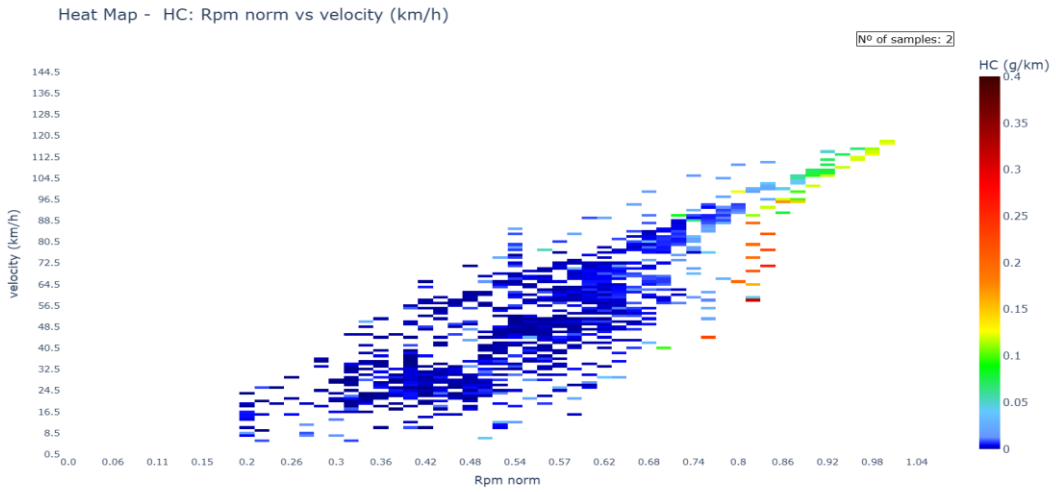

Figure 4-73: HC emissions (g/km) from L3e-A2 equipped with CVT transmission. RDC and RDE tests are represented.

4.6.2.3 L3e-A3 900cc MT EU5

A comparison between L3e-A2 sports touring bike with engine capacity of 900cc 35kW, and MT; and this same vehicle with L3e-A3 ECU is going to be developed. The RDC measurement has been selected for this comparison in terms of occurrence and severity analysis on Table 4-29 and Table 4-30. WMTC for both A2 and A3 ECU' values are quite close not showing an impact on emissions as this TA test cycle is not demanding in terms of performance for those relatively powered vehicles. Further plots and tables of this WMTC analysis can be found in Appendix K: Tailpipe emissions analysis from representatives LV's. It is important to mention that gear shift pattern was up to driver criteria, so then different patterns could be found between L3e-A2 and L3e-A3 measurements.

This project has received funding from the European Union's Horizon Europe research and innovation programme under grant agreement No 101056777

In terms of occurrence, slightly higher occurrence is presented on L3e-A3 ECU vehicle when tested on their correspondent L3e-A3 RDC cycle, especially for no acceleration, and stable speed with >60% of RPM. Relative occurrence remains the same during acceleration, but it gets increased for deceleration and constant speed scenarios.

In terms of severity, cold start issues are identified also with A3 ECU reaching almost same average value. NOx and THC emissions average when operating over the established threshold, has been slightly increased, but CO has almost doble its emissions from RDC L3e-A2 with A2 ECU. Further comments will be added when analyzing the corresponding heatmaps later on this section. As a consequence of this higher occurrence of high emissions during constant speed events, generally, or above 60% of RPM, average values for those events are especially higher in terms of CO emissions, near 3x times higher on both scenarios. NOx and THC emissions are less affected.

Table 4-29: L3e-A3 Sport Touring motorcycle RDC L3e-A3 table of occurrence (% over test time).

	RDC L3e-A3								
	NOx			THC			CO		
	over (% time)	under (% time)	Relative occurrence (%)	over (% time)	under (% time)	Relative occurrence (%)	over (% time)	under (% time)	Relative occurrence (%)
Total over/under threshold	28.4%	71.6%		18.2%	81.8%		13.4%	86.6%	
During cold start (100s)	2.2%	2.1%	51.5%	3.3%	1.0%	76.2%	1.5%	2.9%	33.7%
During accel (>0.1 m/s^2)	8.3%	24.3%	25.4%	5.2%	27.3%	15.9%	3.3%	29.2%	10.3%
During decel (<-0.1 m/s^2)	7.9%	28.8%	21.4%	3.7%	32.9%	10.2%	2.8%	33.9%	7.6%
No accel (-0.1< x <0.1 m/s^2) & >1 km/h	11.2%	15.6%	41.9%	6.6%	20.2%	24.8%	6.4%	20.4%	24.0%
Standstill (-0.1< x <0.1 m/s^2) & <1 km/h	0.0%	4.1%	0.0%	0.0%	4.1%	0.0%	0.0%	4.1%	0.0%
Stable speed RPM>60%	4.4%	0.0%	100.0%	4.4%	0.0%	100.0%	4.4%	0.0%	100.0%

Table 4-30: L3e-A3 Sport Touring motorcycle RDC L3e-A3 table of averages (mg/s).

	RDC L3e-A3					
	NOx (Total av.)	0.84	THC (Total av.)	0.71	CO (Total av.)	6.39
	Average over (mg/s)	Average under (mg/s)	Average over (mg/s)	Average under (mg/s)	Average over (mg/s)	Average under (mg/s)
Total over/under threshold	2.78	0.06	3.27	0.14	44.12	0.53
During cold start (100s)	1.67	0.09	9.09	0.31	51.31	0.64
During accel (>0.1 m/s^2)	4.03	0.07	1.99	0.16	43.13	0.67
During decel (<-0.1 m/s^2)	1.76	0.06	1.65	0.12	33.04	0.41
No accel (-0.1< x <0.1 m/s^2) & >1 km/h	2.81	0.09	2.17	0.15	47.71	0.57
No accel (-0.1< x <0.1 m/s^2) & <1 km/h	0.00	0.01	0.00	0.06	0.00	0.12
Stable speed RPM>60%	4.95	0.00	2.49	0.00	57.34	0.00

This project has received funding from the European Union's Horizon Europe research and innovation programme under grant agreement No 101056777

CO emissions: In Figure 4-74, CO emissions against rpm and v*a are represented. Comparing it with all other CO plots, this one shows higher CO emissions values than A2 ECU same vehicle, but lower than CVT one. The majority of high CO events are produced during high rpms, from 50 % to 74 %, while A2 version was driven up to 86% RPM. When comparing with L3e-A2 sports tourer vehicle measurements, CO emissions have importantly increased with A3 ECU, but distribution of those high emissions events are relatively similar for both measurements, taking place at both high engine speed and v*a. In terms of dynamics, A3 version has higher v*a values at lower % of RPMs, resulting in a more rounded uniform heatmap. Even operating at lower % of RPMs, the higher speeds of L3e-A3 RDC resulted in considerable higher emissions on this bike. Overall averaged unweighted WMTC emissions value is 133.8 mg/km while RDC is almost 4x times higher, reaching 403.4 mg/km. This reveals how sensitive is CO under a more demanding test cycle, even when engine power is high. WMTC value is lower than with A2 ECU, but the more demanding RDC cycle for A3 category has triggered CO emissions. When considering segments when vehicle speed is over 90km/h (motorway phase), A3 ECU has reached 821.7 mg/km (+4.4x times value of WMTC motorway phase), while A2 ECU value is 354.6 mg/km (+50% value of WMTC motorway phase).

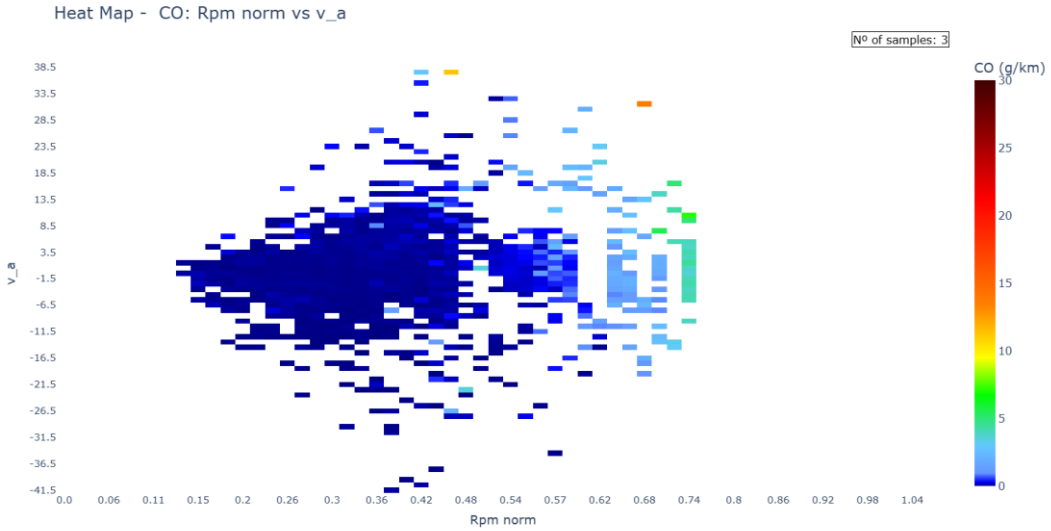

Figure 4-74: CO emissions (g/km) against engine speed (rpm) and v*a (m^2/s^3) from L3e-A3 equipped with manual transmission. RDC and RDE tests are represented.

NOx emissions: In Figure 4-75, NOx emissions against rpm and v*a are represented. Comparing it with all other NOx plots, this one shows the higher NOx emissions values. Higher NOx values are produced during mid and high rpm (between 40 % and 75%). The maximum NOx event occurs at 54 % rpm and a v*a value of 32. As observed, high NOx emissions events are produced during a variety of v*a, both positive and negative values, but always from mid rpms to above. This suggests that high NOx emission events are related to rpm or engine load, and they are essentially produced during accelerations. Emissions can remain also when maintaining engine speed at constant speed, before the engine temperature is stabilized. Overall average unweighted WMTC emissions value is 42.18 mg/km. This value was slightly increased on RDC, reaching 52.8 mg/km. Nearly the same value on WMTC from A2 version, 30% higher on RDC from A3 RDC.

This project has received funding from the European Union's Horizon Europe research and innovation programme under grant agreement No 101056777

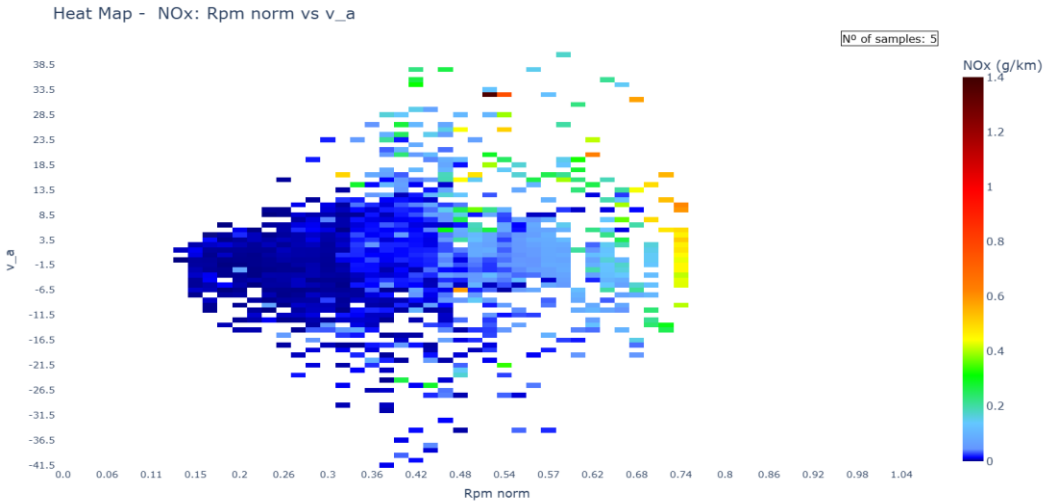

Figure 4-75: NOx emissions (g/km) against engine speed (rpm) and v*a (m^2/s^3) from L3e-A3 equipped with manual transmission. RDC and RDE tests are represented.

HC emissions: In Figure 4-76, HC emissions against engine rpm and vehicle speed are represented. In this plot, we can observe three groups of events when HC emissions are high. The first one is at low speed (<12 km/h) and low rpm (<25 %). In this group you can find the highest emitting point of 390 mg/km of HC at 15 % rpm. The final group, that follows a linear trend with rpm and velocity, has mid-high rpm (from 50% to 75 %) and high speeds above 129 km/h. This correlates with high speed and high accelerations in 6th gear, and acceleration mainly in 1st gear at low speed. Additional figures to better understand the behavior of this vehicle can be found in Appendix K: Tailpipe emissions analysis from representatives LV's. Overall average unweighted WMTC emissions value is 39.5 mg/km. This value increased on RDC but not importantly, reaching 44.8 mg/km. Slightly higher (30%) values from A2 version on RDC, and 10% lower on WMTC. When considering only the motorway phase, it shows an increment of 30% from A2 ECU RDC for this same vehicle.

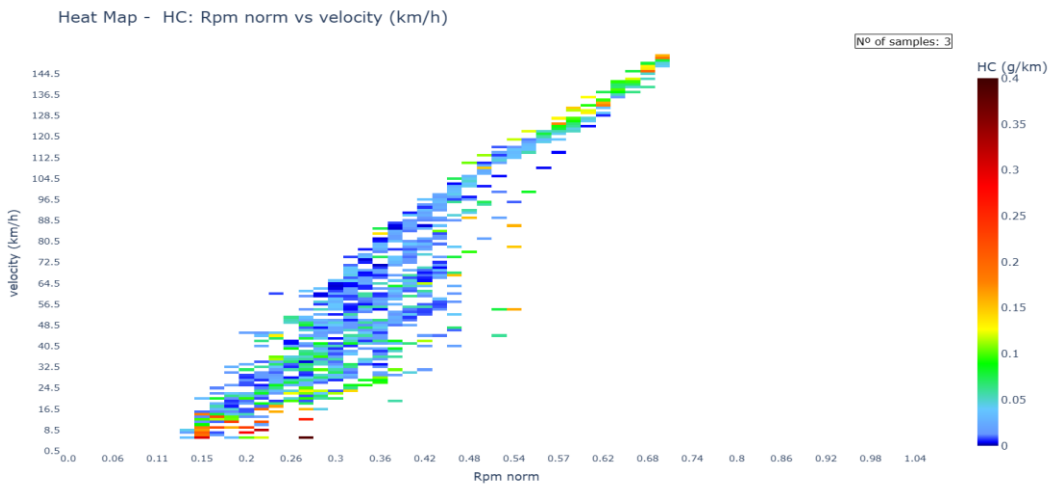

Figure 4-76: HC emissions (g/km) against engine speed (rpm) and vehicle speed (km/h) from L3e-A3 equipped with manual transmission. RDC and RDE tests are represented.

This project has received funding from the European Union's Horizon Europe research and innovation programme under grant agreement No 101056777

4.6.3 LENS db data analysis through identification of high emissions events

To provide an overview of events characterized by high emissions, the continuous periods during which NOx emissions exceed the threshold defined in paragraph 4.6.1 have been identified as unique events and represented with bubbles in Figure 4-77, where all vehicles that fulfilled filtering conditions mentioned in paragraphs 4.6.1.2 and 4.6.1.3. This approach allows us to characterize each event with its KPIs and highlight the values that trigger or significantly increase emissions.

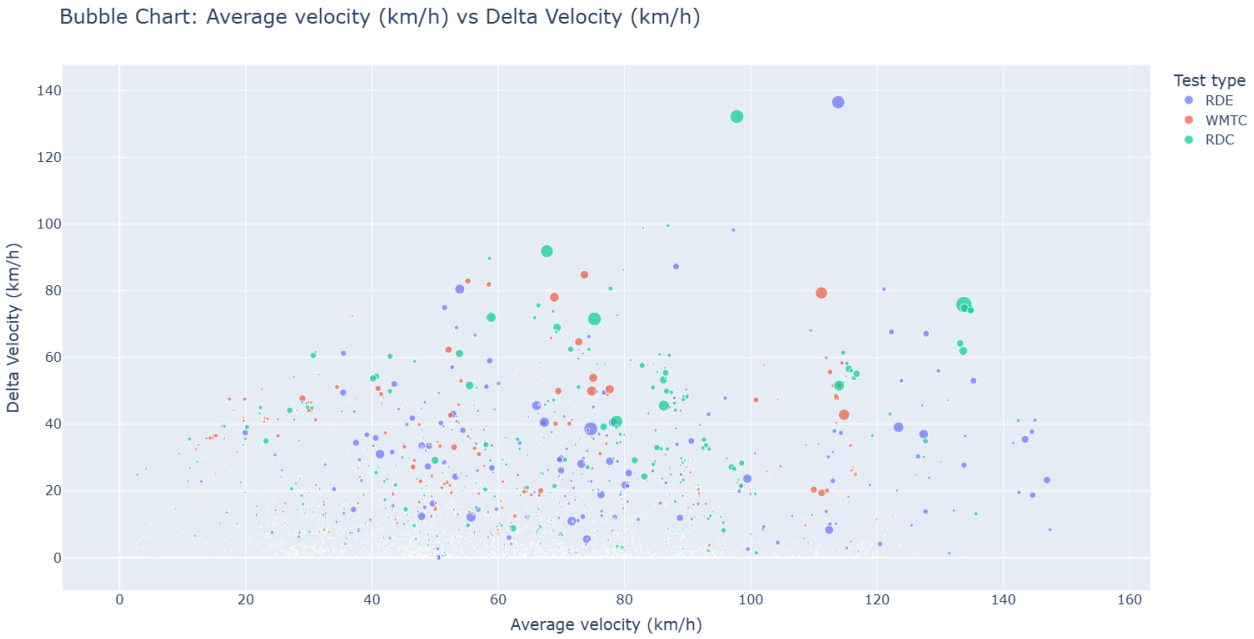

Figure 4-77: Maximum NOx emission in (mg/s) for the different vehicle speeds and delta velocities. Data obtained from high emitter events identification; each bubble corresponds to one event.

Figure 4-77 presents an analysis of NOx in relation to the delta velocities and average vehicle speed of the event. Each event is represented by a bubble in the graph, where the bubble size corresponds to the maximum NOx emissions during the specific event. The color coding distinguishes between different test protocols: RDE, WMTC, and RDC.

Upon analyzing the graph, it becomes evident that for speed variations (deltas) exceeding 40 km/h, the maximum NOx emissions demonstrate a notable increase. Furthermore, the analysis reveals that not only the speed variation but also the average velocity significantly influences emission characteristics. Specifically, for a given speed delta, a higher average velocity correlates with a higher probability of generating a significant high-emission event.

Additional plots can be seen in Appendix L: LENS db high tailpipe emissions analysis.

This project has received funding from the European Union's Horizon Europe research and innovation programme under grant agreement No 101056777

4.6.4 LENS db data analysis through identification of high emissions operating points

In the following sections, the results of the NOx, HC and CO emissions will be represented in a color scale over the engine speed (x-axis) and a third parameter (y-axis). These figures represent the results of all vehicles in LENS db, and all types of measurements, RDC, TA and RDE.

CO Emissions

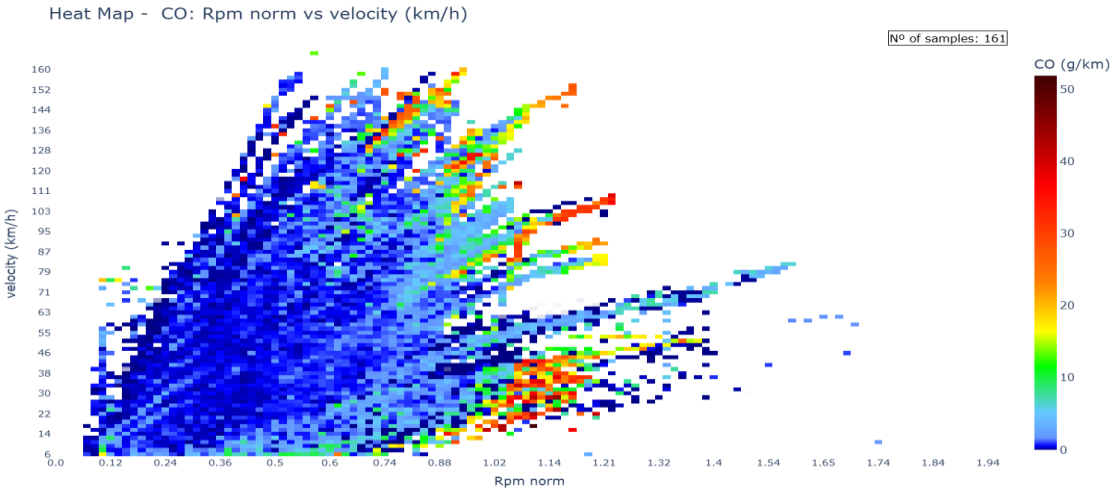

Figure 4-78: CO emission in (g/km) for the different vehicle speeds and normalized engine speeds (nr).

Figure 4-78 presents a comprehensive analysis of carbon monoxide (CO) emissions, investigating their variation in relation to vehicle speeds and engine speeds.

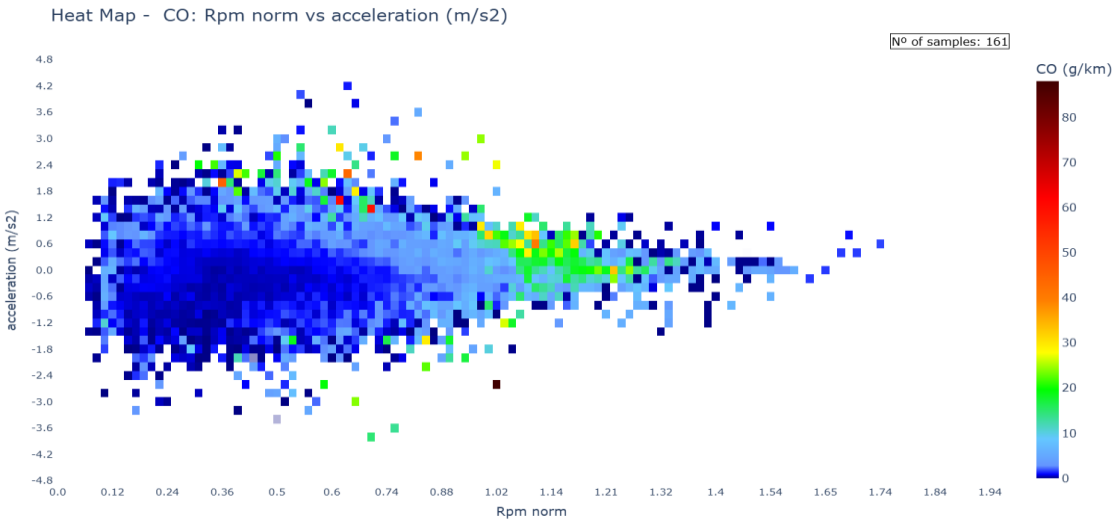

Figure 4-79: CO emission in (g/km) for the different acceleration (m/s^2) and normalized engine speeds (nr).

When looking at Figure 4-79, CO emissions reach high values when developing strong accelerations. Moreover, there is a specific cloud of points where rpm comprise 100-130%, in this specific area CO emissions are triggered.

This project has received funding from the European Union's Horizon Europe research and innovation programme under grant agreement No 101056777

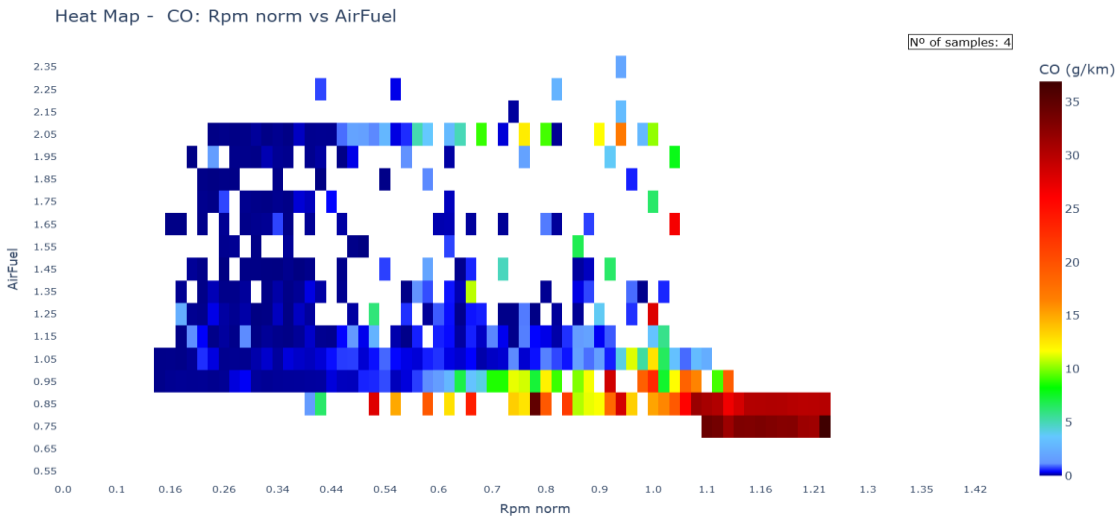

Figure 4-80: CO emission in (g/km) for the different engine speeds and Air-Fuel ratios.

Figure 4-80 presents a detailed investigation of carbon monoxide (CO) emissions, focusing on their relationship with engine speeds and air-fuel ratio. The analysis reveals a critical but evident insight: CO emissions demonstrate a significant increase when the engine operates with rich fuel mixtures.

Key Findings:

- Emissions are triggered when operating above rated max power engine speed.
- CO emissions exhibit a substantial elevation under rich mixture conditions, lambda values under 0.90, with a potentially increase of emissions by a factor of twenty.

NOx Emissions

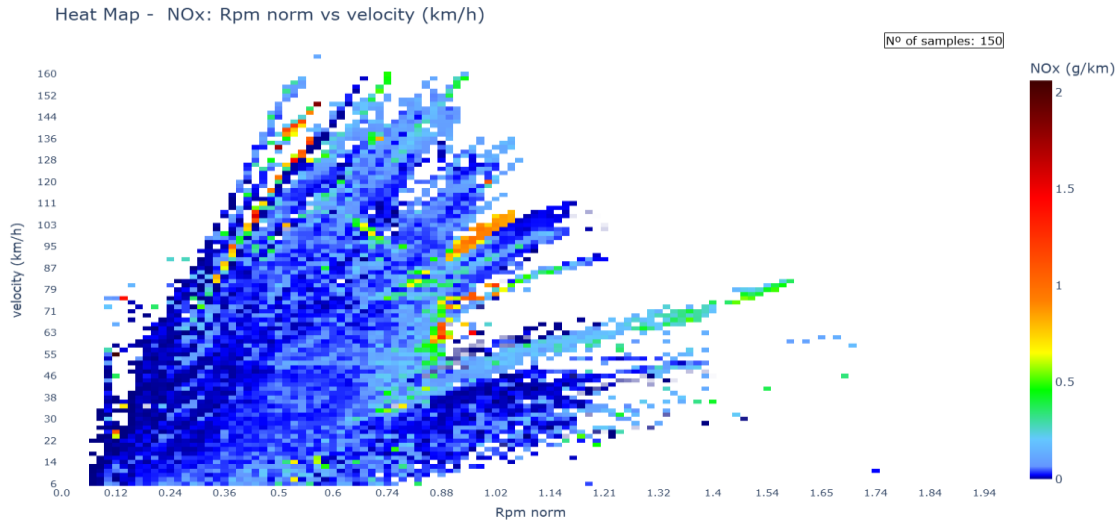

Figure 4-81:NOx emission in (g/km) for the different vehicle speeds and engine speeds.

Figure 4-81 shows NOx emissions for the different vehicle speeds and engine speeds. The color scale shows that the NOx emissions are higher for both high vehicle speeds and high engine speeds, and mostly derived

This project has received funding from the European Union's Horizon Europe research and innovation programme under grant agreement No 101056777

from high speeds, rather than engine rpm. Those vehicles that reach values of 150% rpm, correspond with L6e-B diesel vehicles. In Figure 4-81 emissions pattern could be related with the previously observed CO emission characteristics, although, Figure 4-82 shows opposite behavior when operating from 100% rpm to 130%.

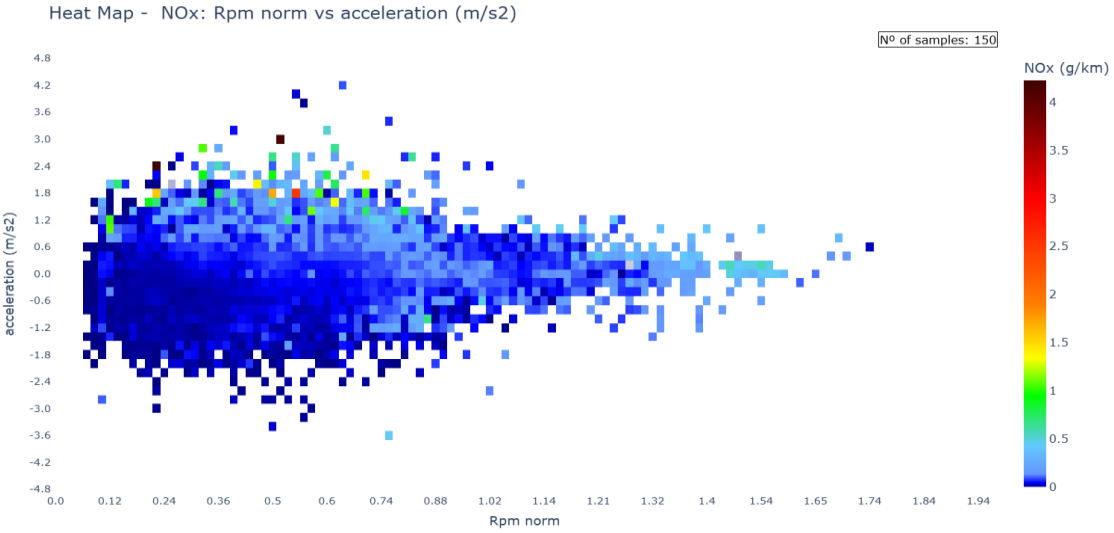

Figure 4-82: NOx emission in (g/km) for the different normalized engine speeds (nr) and acceleration.

The Figure 4-82 shows the emission of NOx for the different vehicle speeds and accelerations. The color scale shows that the NOx emissions are higher when the acceleration exceeds 1m/s^2.

HC Emissions

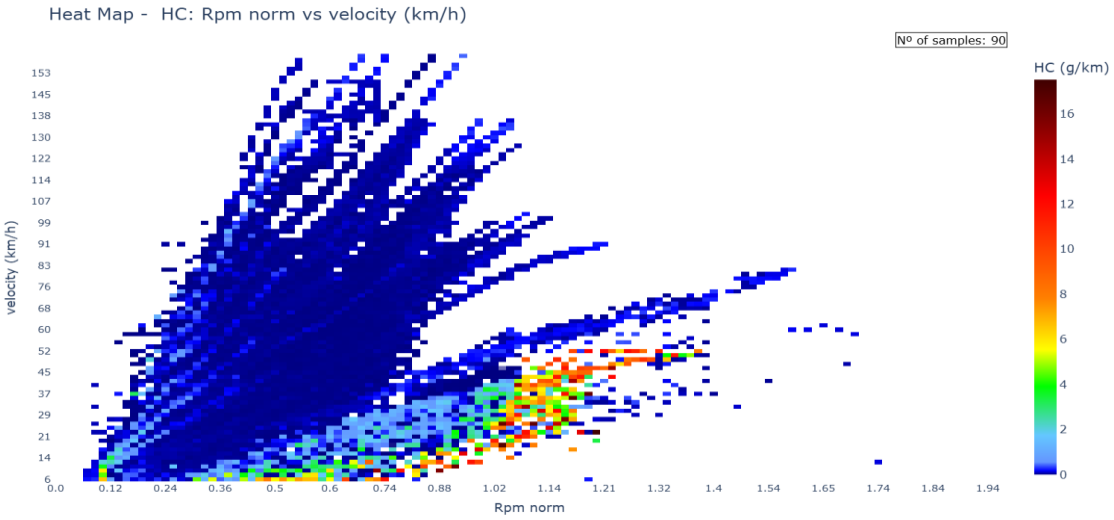

Figure 4-83: HC emission in (mg/s) for the different vehicle speeds and normalized engine speeds (nr).

Figure 4-83 presents an analysis of hydrocarbon (HC) emissions in relation to vehicle speeds and engine speeds. The graphical representation reveals that HC emissions are significantly higher for those vehicles in

This project has received funding from the European Union's Horizon Europe research and innovation programme under grant agreement No 101056777

whose maximum speed is below 50 km/h. This is related to those 2-stroke L1eB vehicles, as it would be further developed at the end of this section. Specifically, the combination of low speed and high engine revolutions generates the highest levels of hydrocarbon emissions.

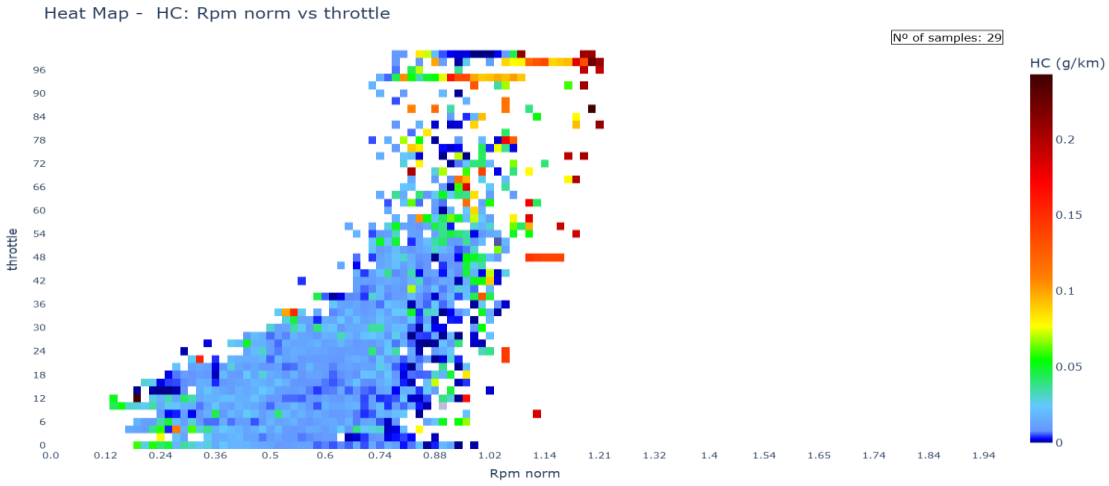

Figure 4-84 HC emission in (g/km) for the different throttle pedal and normalized engine speeds (nr).

The graphical representation illustrates the relationship between hydrocarbon (HC) emissions, engine speeds, and throttle pedal positions ranging from 0% to 100%. The analysis reveals a critical correlation between emission levels and vehicle operating parameters.

Notably, the highest HC emissions are predominantly observed when two key conditions converge:

- High engine speeds
- Substantial throttle pedal depression (approaching near-maximum positions), very usual on CVT vehicles

In the following sections we will analyze categories L1eB, L3e-A1, L3e-A2 and L3e-A3 separately, discretizing the gearbox (manual or automatic) to see if their transmission type has any influence.

L1e-B CVT Gearbox

This project has received funding from the European Union's Horizon Europe research and innovation programme under grant agreement No 101056777

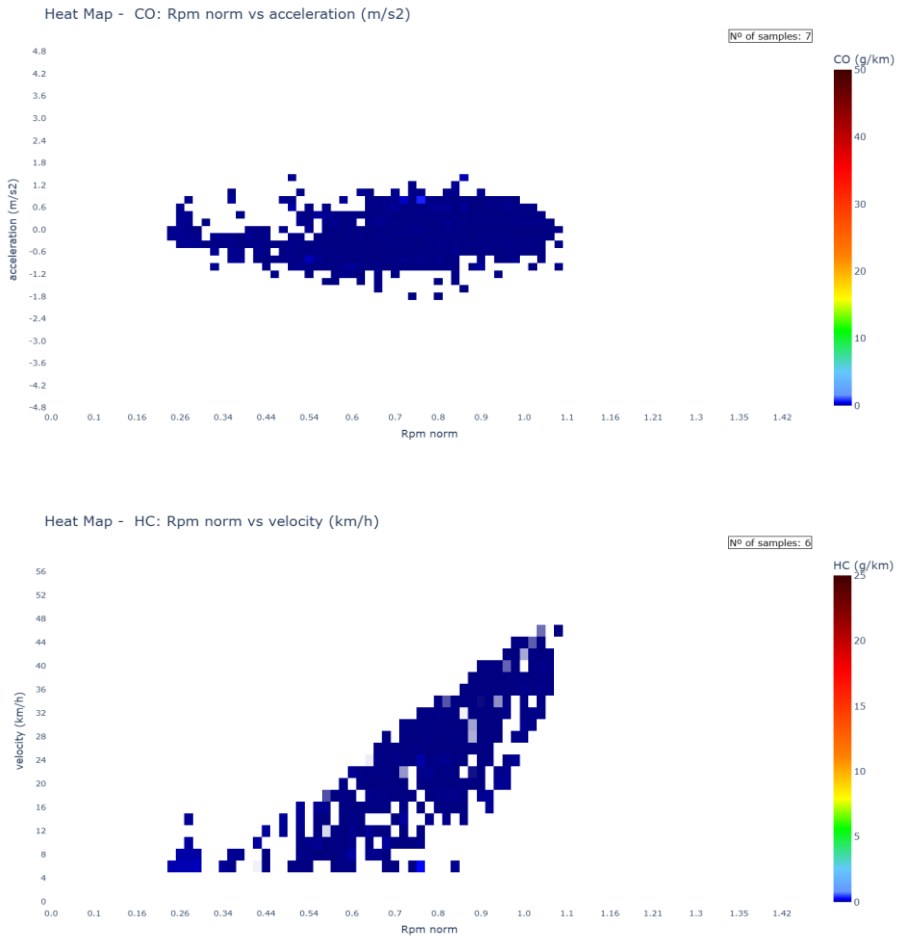

Figure 4-85 CO (top) emissions in g/km against norm rpm and acceleration (m/s²) and HC (bottom) emissions in g/km against norm rpm and vehicle speed (km/h) of L1e-B CVT 4-stroke vehicles.

This project has received funding from the European Union's Horizon Europe research and innovation programme under grant agreement No 101056777

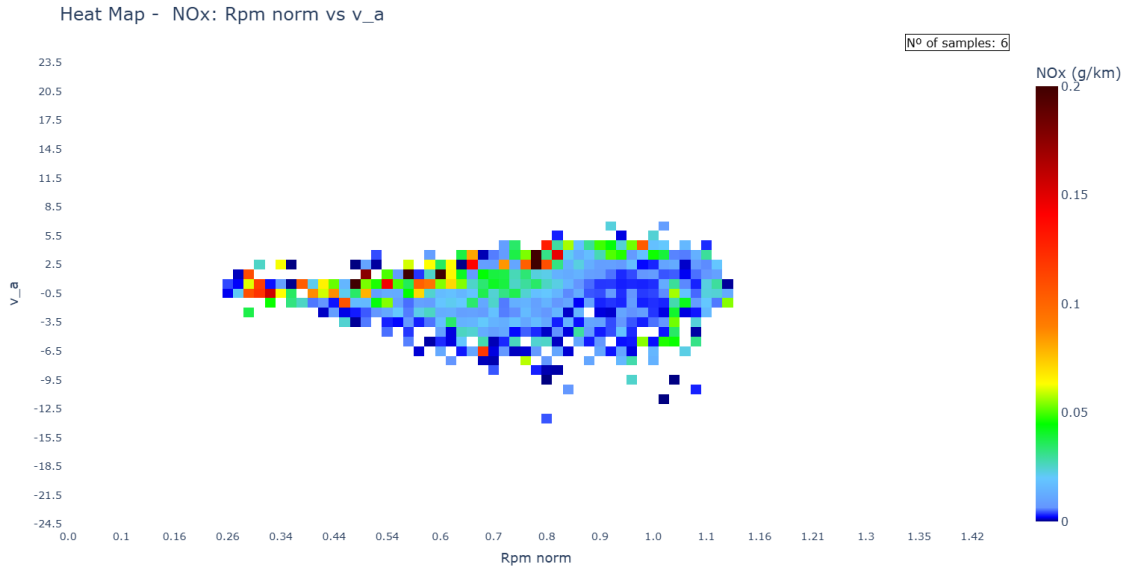

Figure 4-86: NOx emissions in g/km against norm rpm and v*a (m^2/s^3) of L1e-B CVT 4-stroke vehicles.

L1e-B Manual Gearbox

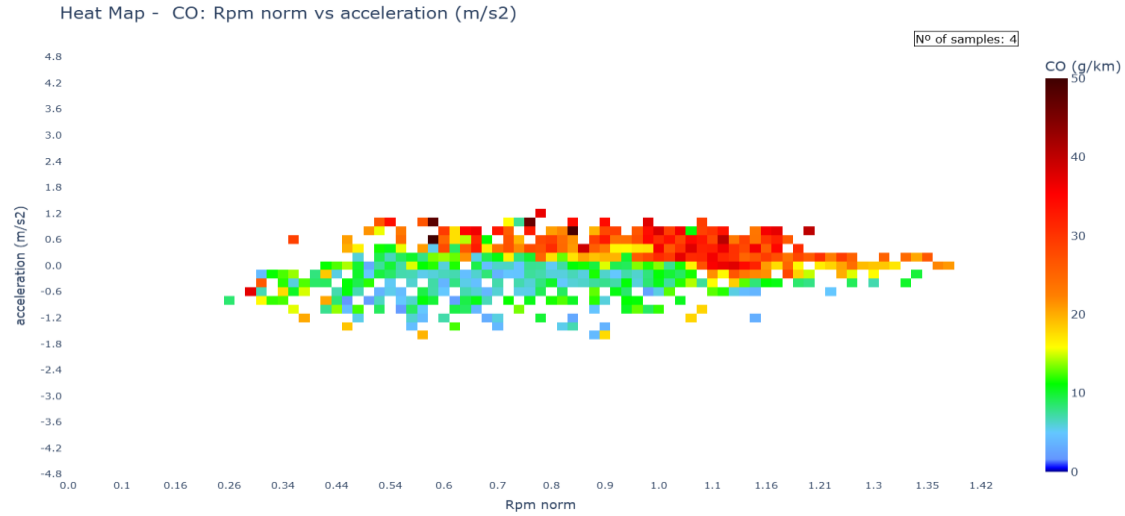

Figure 4-87: CO emissions in g/km against norm rpm and acceleration (m/s^2) of L1e-B MT 2-stroke vehicles.

This project has received funding from the European Union's Horizon Europe research and innovation programme under grant agreement No 101056777

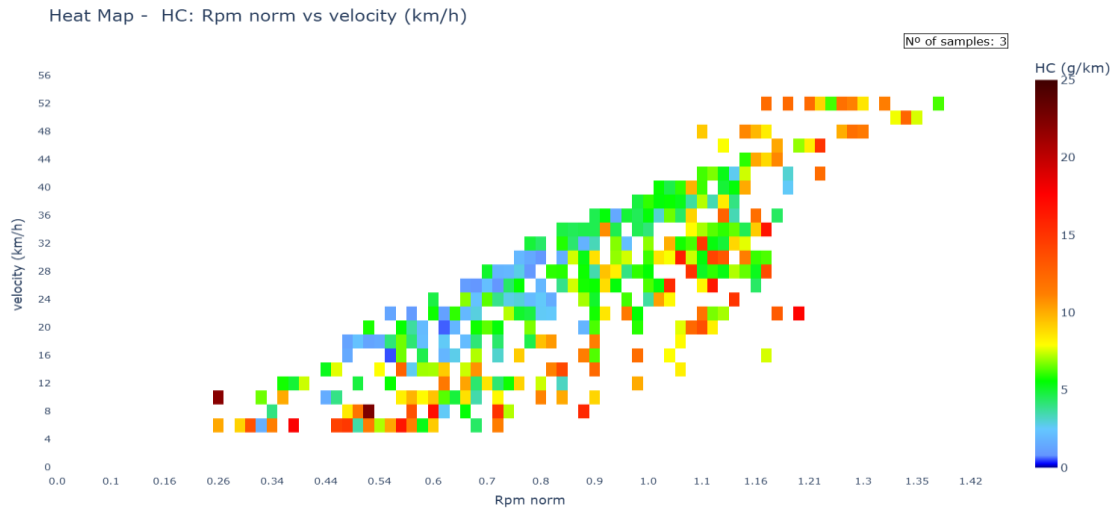

Figure 4-88: HC emissions in g/km against norm rpm and vehicle speed (km/h) of L1e-B MT 2-stroke vehicles.

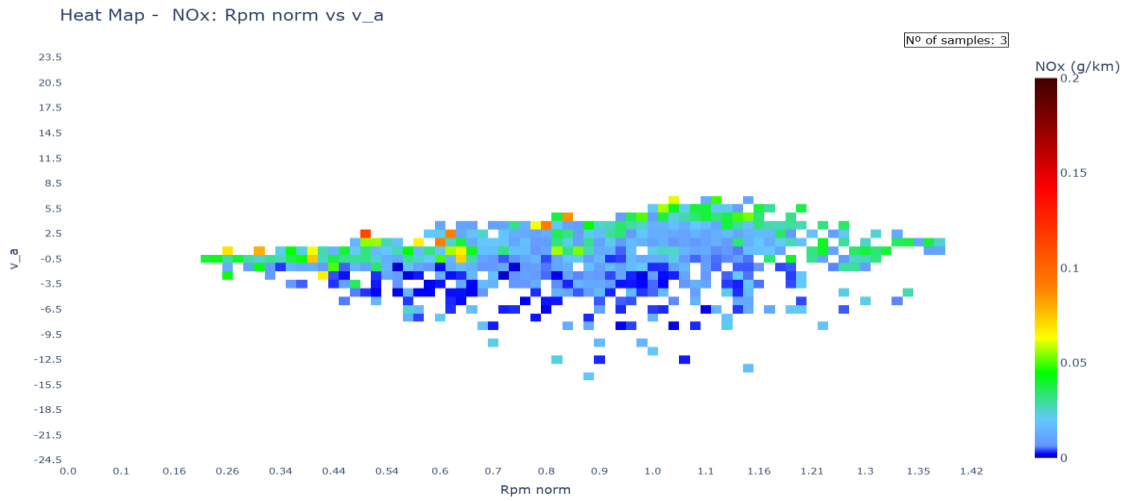

Figure 4-89: NOx emissions in g/km against norm rpm and v*a (m^2/s^3) of L1e-B MT 2-stroke vehicles.

The comparative analysis of emissions between automatic and manual transmission motorcycles reveals significant differences, particularly in CO and HC emissions. The data demonstrates that manual transmission motorcycles, predominantly featuring 2-stroke engines, exhibit substantially higher emission levels compared to automatic transmission vehicles. While CO and HC emissions are markedly elevated in manual transmission motorcycles due to the inherent combustion inefficiencies of 2-stroke engines—characterized by incomplete combustion, direct oil-fuel mixture, and less efficient exhaust gas management—these characteristics of the 2-stroke engines help to maintain the NOx emissions relatively consistent across both transmission types. This observation highlights the substantial environmental impact of engine technology, specifically demonstrating how the prevalence of 2-stroke engines in manual transmission motorcycles contributes to significantly higher pollutant output, particularly in carbon monoxide and hydrocarbon emissions.

This project has received funding from the European Union's Horizon Europe research and innovation programme under grant agreement No 101056777

L1e-B Events occurrence

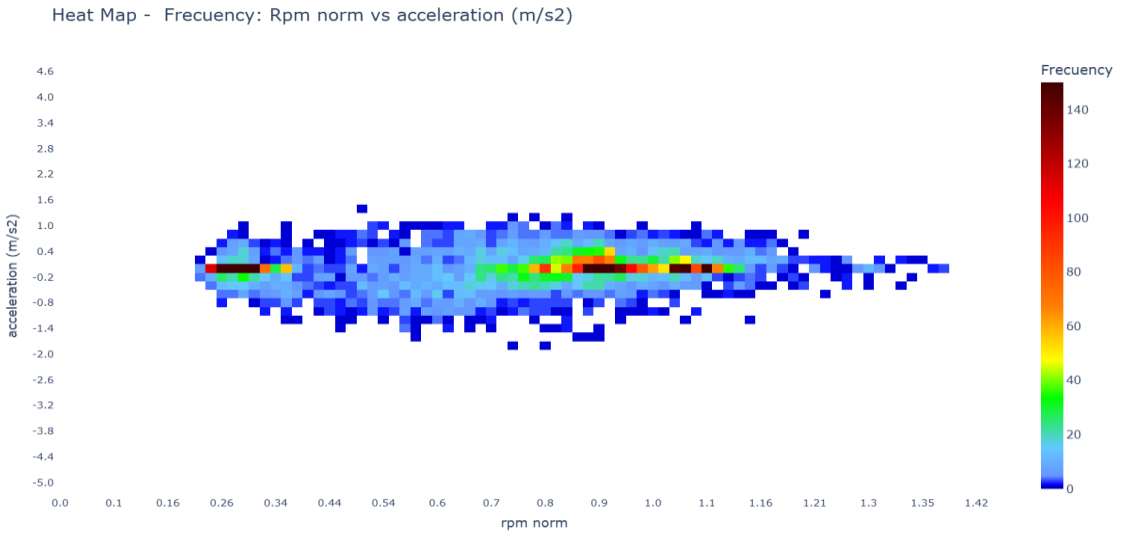

Figure 4-90: Occurrence of L1e-B events of norm rpm and acceleration (m/s²).

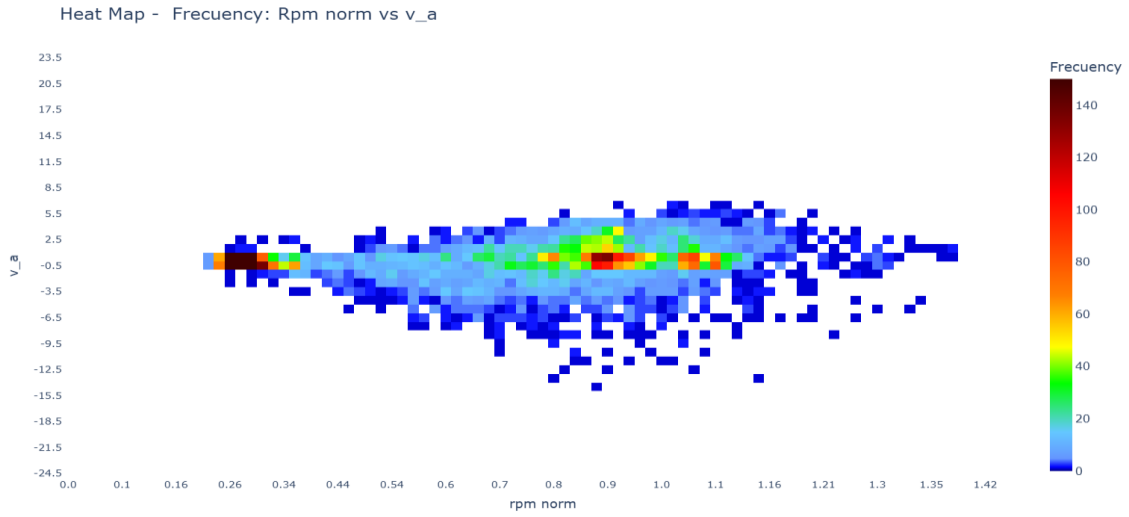

Figure 4-91: Occurrence of L1e-B events of norm rpm and v*a (m²/s³).

Based on the presented data, a comprehensive evaluation of NOx emissions reveals that low engine speed conditions, characterized by minimal acceleration and reduced vehicle velocity, emerge as a pivotal focus for emissions research. Despite being the most frequently encountered operational scenario, these low-speed conditions demonstrate a significant and persistent NOx emission profile.

In contrast, high-speed and high-acceleration scenarios, while exhibiting substantially worse emission characteristics, especially regarding CO, occur less frequently. Consequently, their overall environmental impact is relatively limited within the broader operational spectrum of the motorcycle. This nuanced understanding emphasizes the importance of concentrating research efforts on those low-speed, low-acceleration conditions that represent the majority of real-world driving experiences.

This project has received funding from the European Union's Horizon Europe research and innovation programme under grant agreement No 101056777

L3e-A1 CVT Gearbox

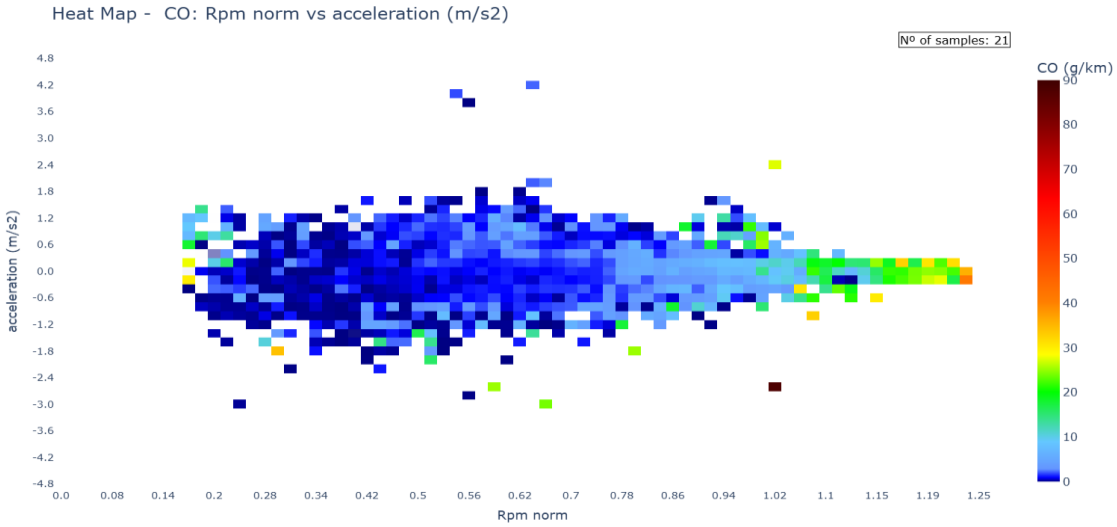

Figure 4-92: CO emissions in g/km against norm rpm and acceleration (m/s²) of L3e-A1 MT vehicles.

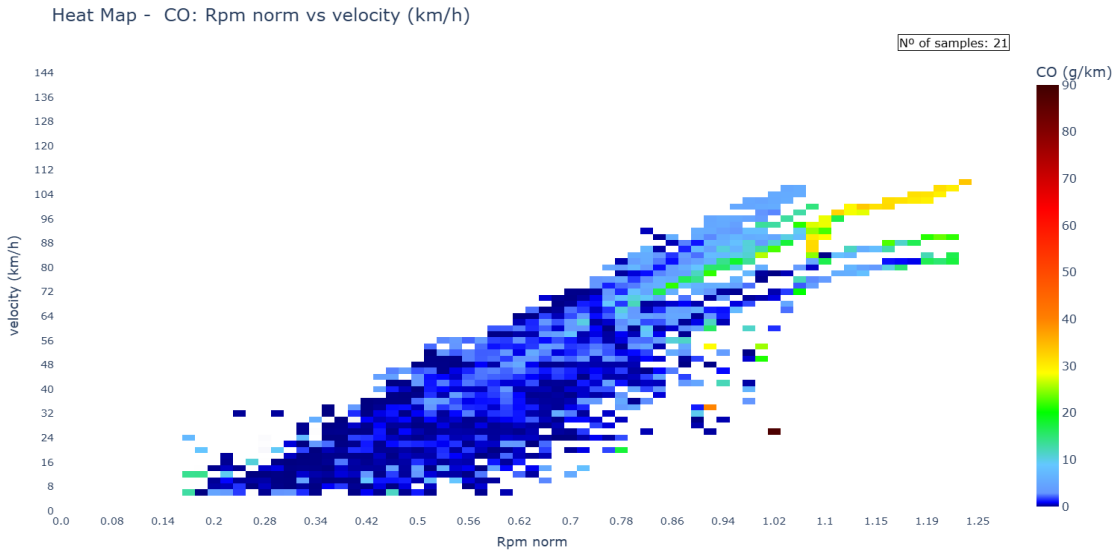

Figure 4-93: CO emissions in g/km against norm rpm and vehicle speed (km/h) of L3e-A1 CVT vehicles.

This project has received funding from the European Union's Horizon Europe research and innovation programme under grant agreement No 101056777

L3e-A1 Manual Gearbox

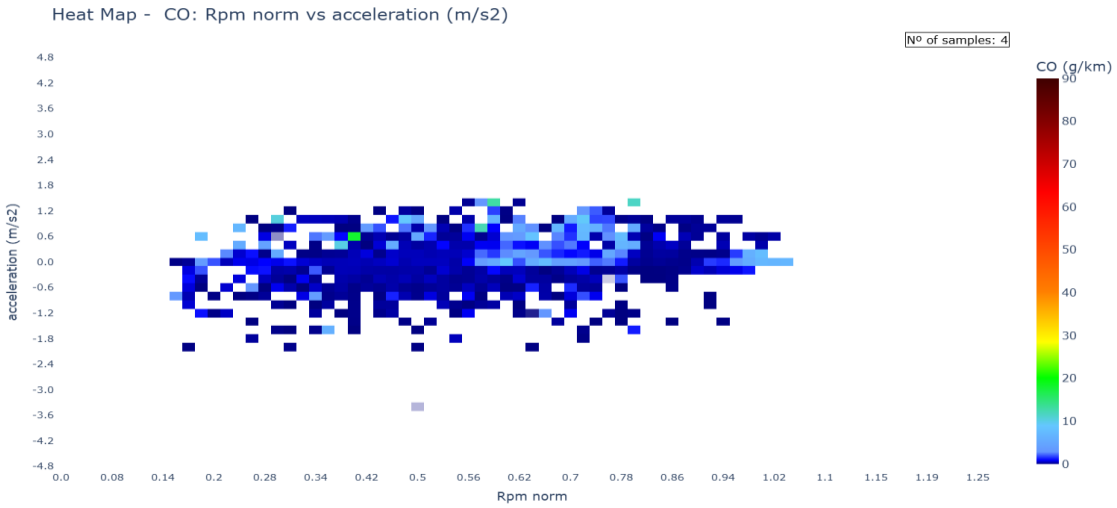

Figure 4-94: CO emissions in g/km against norm rpm and acceleration (m/s²) of L3e-A1 MT vehicles.

L3e-A1 Events occurrence

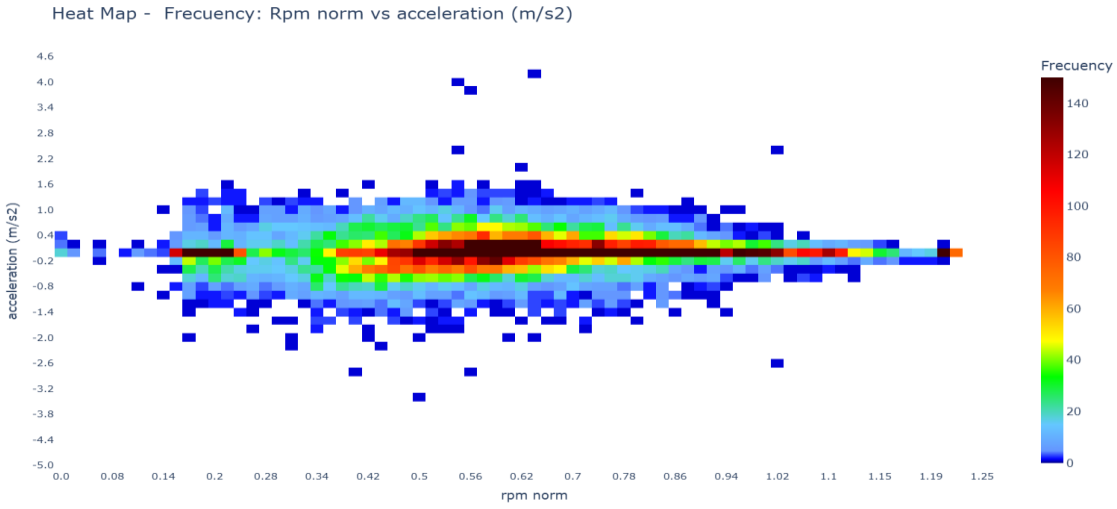

Figure 4-95: Occurrence of L3e-A1 events of norm rpm and acceleration (m/s²).

The CO emissions for both CVT and manual transmission motorcycles in the L3e-A1 category demonstrate consistent emission behavior. A notable trend emerges where emissions significantly increase when the engine speed surpasses the maximum power rated engine speed on CVT vehicles, more specifically when driving above 110% rpm.

Unlike the previous vehicle category, the L3e-A1 motorcycles exhibit a distinctive occurrence pattern, characterized by a high frequency of small acceleration events across the entire engine speed spectrum. This unique distribution pattern emphasizes the critical importance of high constant speed conditions in understanding the comprehensive emission characteristics of these vehicles.

This project has received funding from the European Union's Horizon Europe research and innovation programme under grant agreement No 101056777

L3e-A2 CVT gearbox

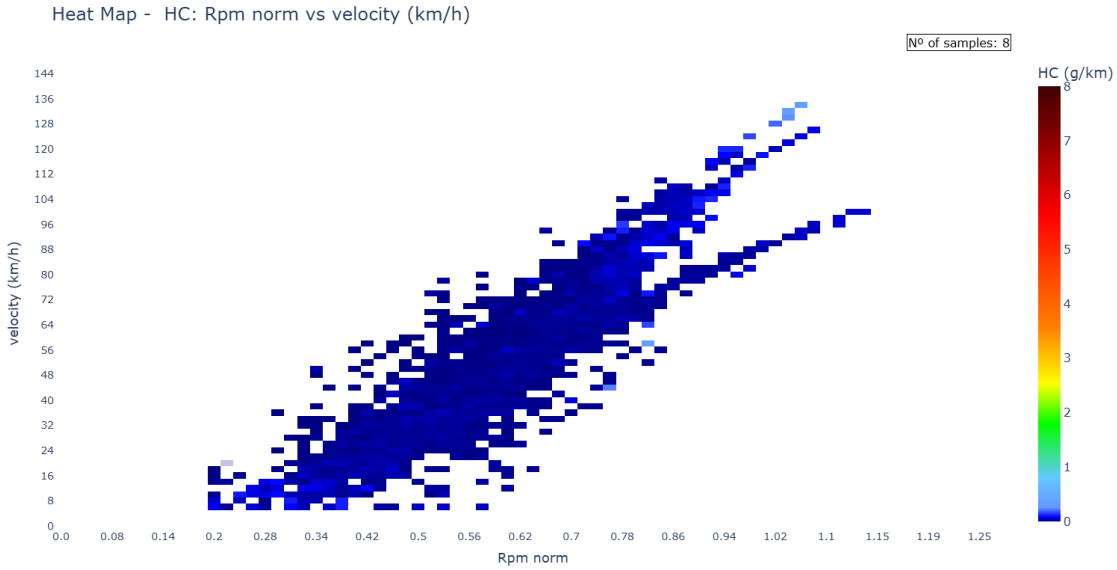

Figure 4-96: HC emissions in g/km against norm rpm and vehicle speed (km/h) of L3e-A2 CVT vehicles.

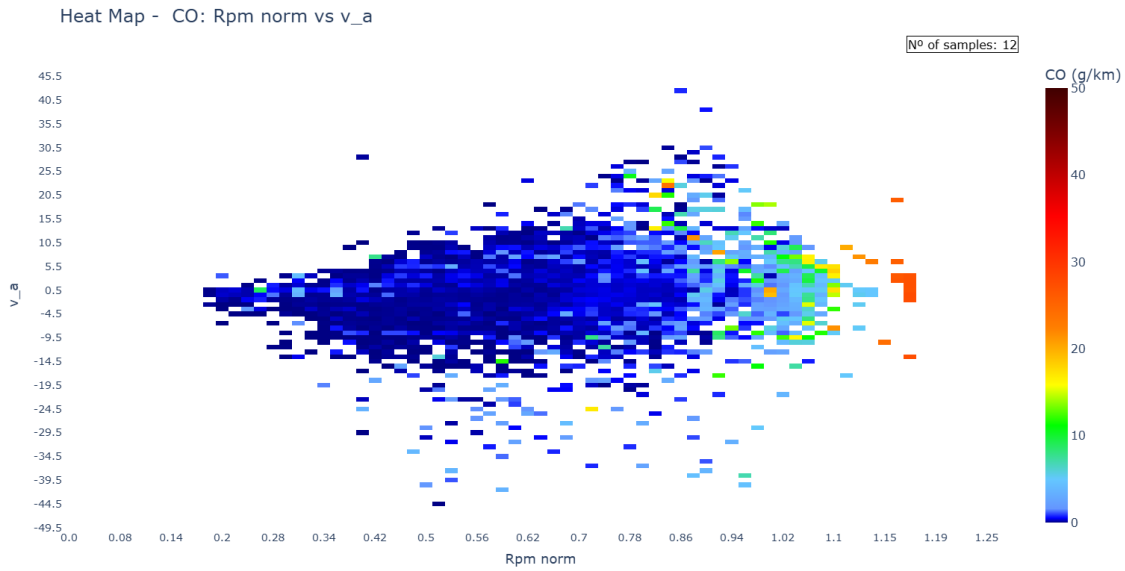

Figure 4-97: CO emissions in g/km against norm rpm and v*a (m^2/s^3) of L3e-A2 CVT vehicles.

This project has received funding from the European Union's Horizon Europe research and innovation programme under grant agreement No 101056777

L3e-A2 Manual gearbox

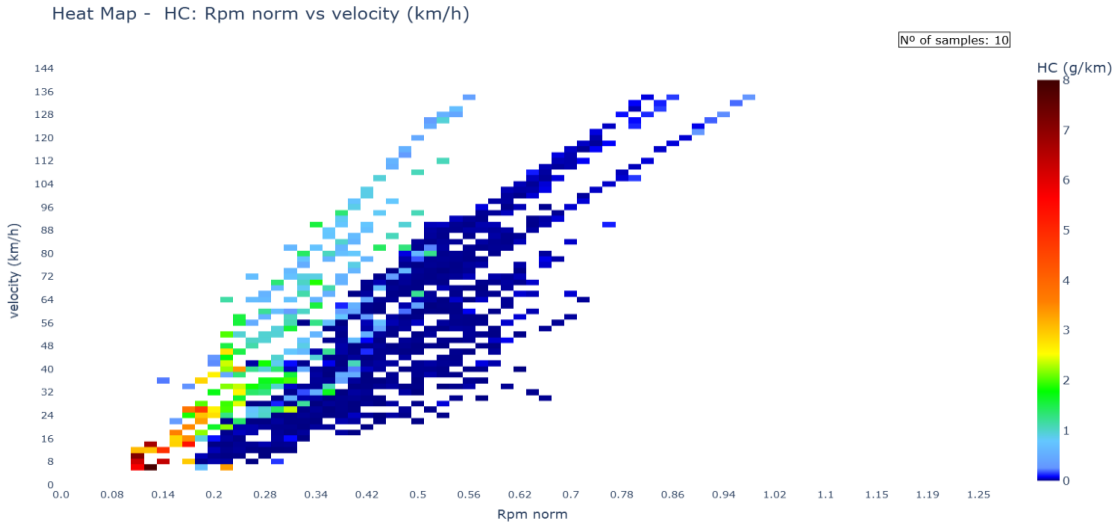

Figure 4-98: HC emissions in g/km against norm rpm and vehicle speed (km/h) of L3e-A2 MT vehicles.

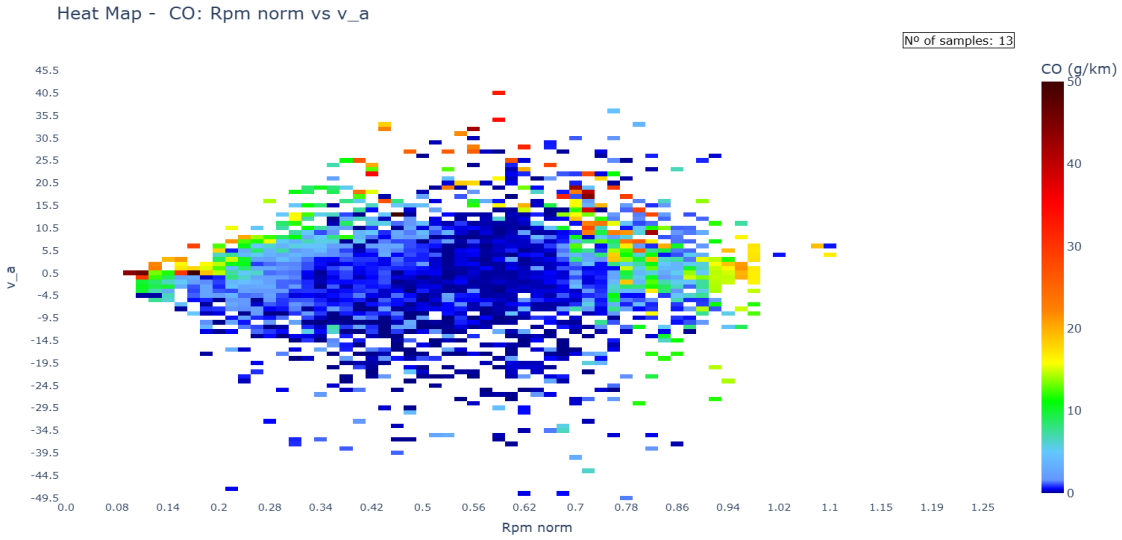

Figure 4-99: CO emissions in g/km against norm rpm and v*a (m^2/s^3) of L3e-A2 MT vehicles.

This project has received funding from the European Union's Horizon Europe research and innovation programme under grant agreement No 101056777

L3e-A2 Events occurrence

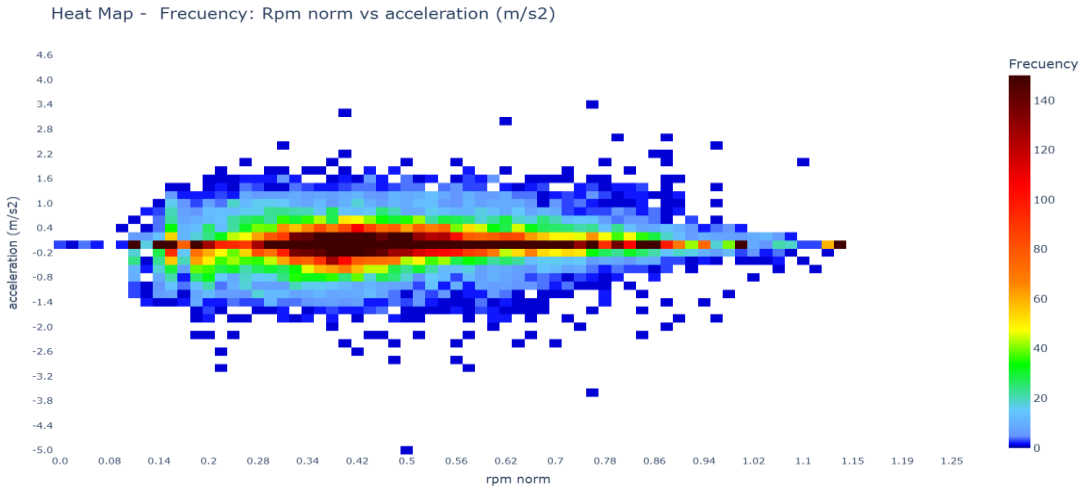

Figure 4-100: Occurrence of L3e-A2 events of norm rpm and acceleration (m/s²).

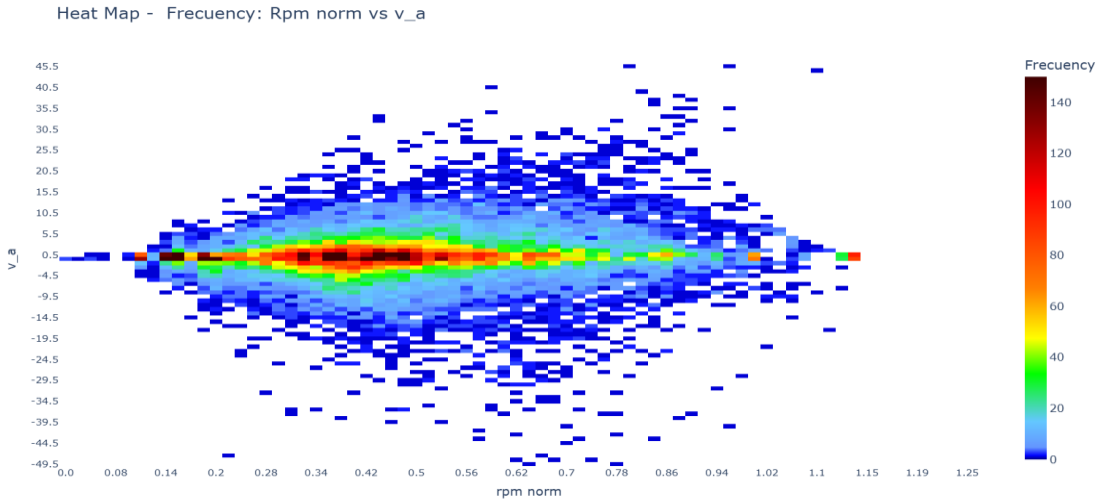

Figure 4-101: Occurrence of L3e-A2 events of norm rpm and v*a (m²/s³).

In the L3e-A2 category, the HC emissions demonstrate notably elevated levels in manual transmission vehicles, particularly pronounced in higher gears and at low engine speeds.The CO emission profile reveals a nuanced pattern across different engine speed ranges. While medium and high RPM scenarios show relatively consistent emission characteristics, MT motorcycles exhibit a unique behavior at low engine speeds. Specifically, the use of higher gears at low RPMs results in significantly increased CO emissions, highlighting the critical impact of transmission and gear selection on pollutant output. Regarding CVT vehicles, high emissions of CO are concentrated when driving above 90% rpm where emissions are triggered.

The occurrence shows a pattern similar to the L3e-A1 category where conditions of low acceleration are predominant across the entire engine speed spectrum, demonstrating again that most critical conditions of high acceleration are not representative of the driving patterns. Although, for CVT vehicles, operating at

This project has received funding from the European Union's Horizon Europe research and innovation programme under grant agreement No 101056777

115% rpm present a high occurrence and this operating point is causing also high CO emissions. As we have seen in the study of relevant vehicles, this pattern should be carefully examined.

L3e-A3

For L3e-A3, no CVT and MT gearbox type separation has been applied.

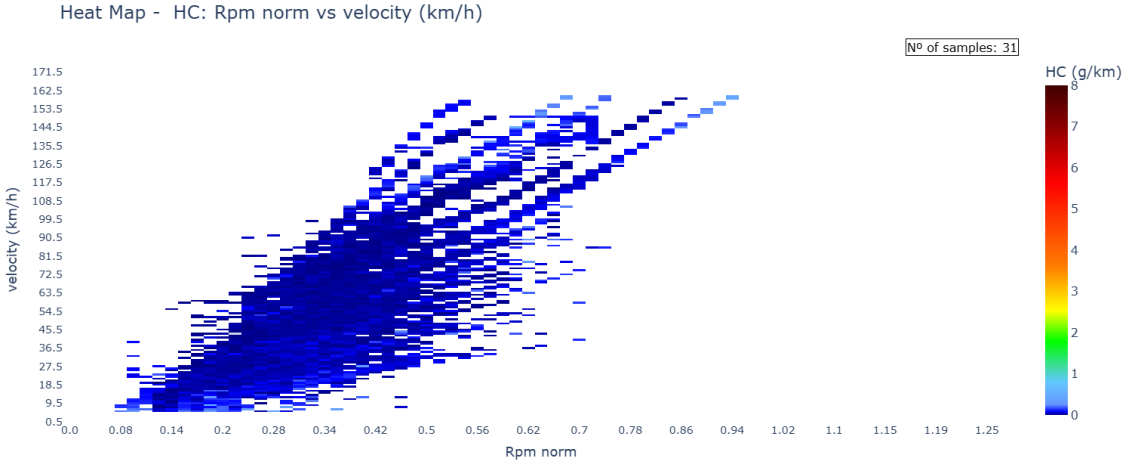

Figure 4-102: HC emissions in g/km against norm rpm and vehicle speed (km/h) of L3e-A3 vehicles.

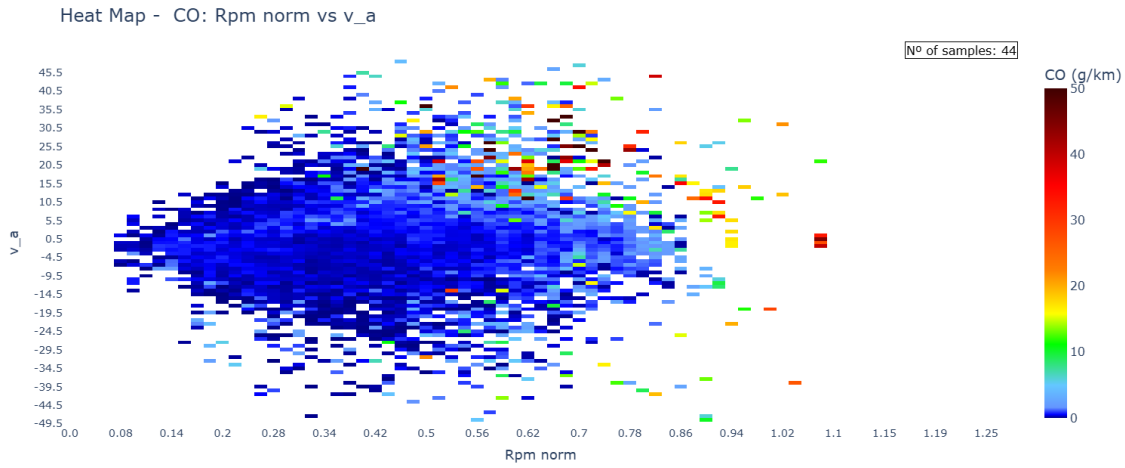

Figure 4-103: CO emissions in g/km against norm rpm and v*a (m^2/s^3) of L3e-A3 vehicles.

This project has received funding from the European Union's Horizon Europe research and innovation programme under grant agreement No 101056777

L3e-A3 Events occurrence

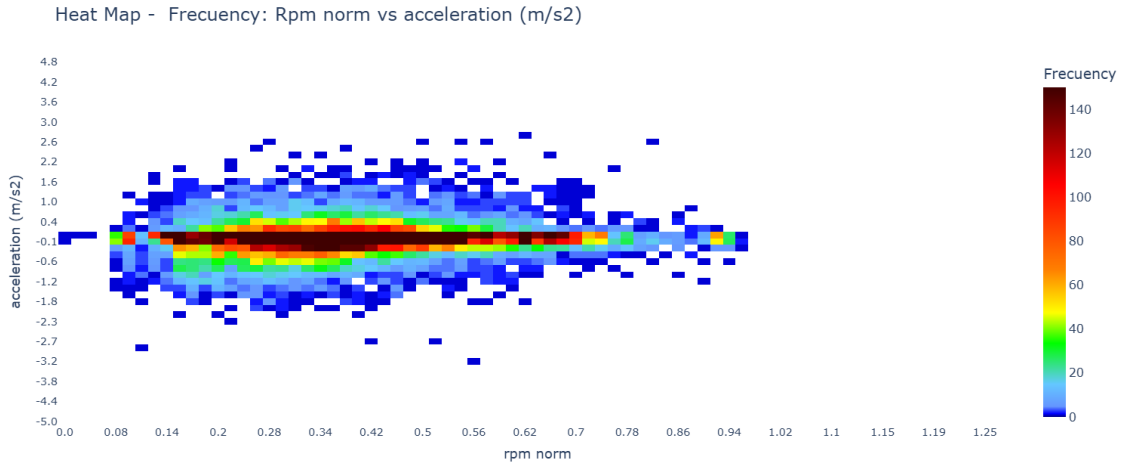

Figure 4-104: Occurrence of L3e-A3 events of norm rpm and acceleration (m/s²).

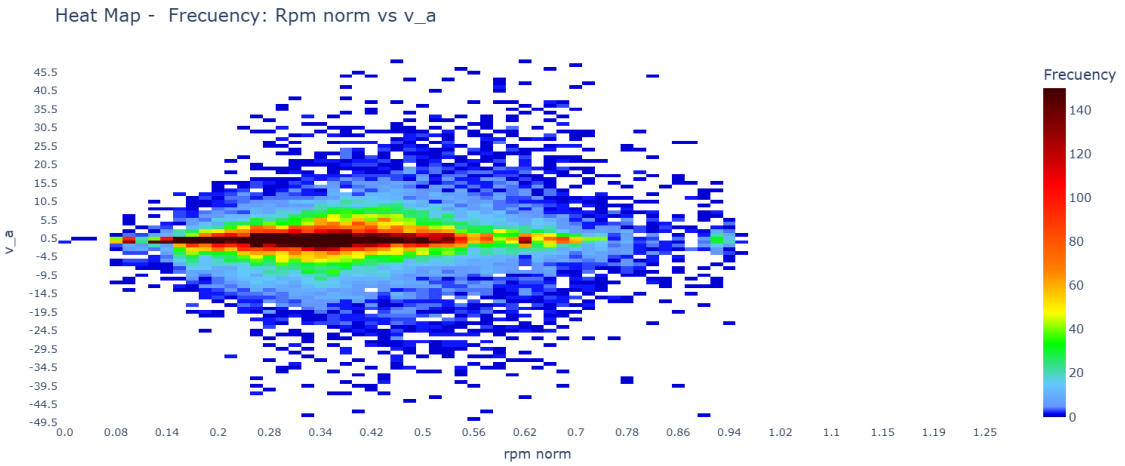

Figure 4-105: Occurrence of L3e-A3 events of norm rpm and v*a (m²/s³).

In the L3e-A3 category, the HC emissions do not show as high emissions as L3e-A2 vehicles, Figure 4-102. The CO emissions profile is not as high as it is on L3e-A2 MT vehicles when operating at high gear and low engine speed. As we can see in Figure 4-103, high CO emissions are concentrated when driving at rpms higher than 50%, and high v*a values, this means, strong accelerations. Out of these operating points, not CO high emissions are identified

The occurrence shows a pattern similar to the L3e-A2 category where conditions of low acceleration are predominant across the entire engine speed spectrum, demonstrating again that most critical conditions of high acceleration are not representative of the driving patterns, Figure 4-104. Although L3e-A3 vehicles are more frequently operated at lower rpms, under 30%, where A2 vehicles are not. In terms of $v*a_{,pos}$, in Figure 4-105 can be shown that since L3e-A3 vehicles are high powered, strong accelerations are also present at lower rpms.

This project has received funding from the European Union's Horizon Europe research and innovation programme under grant agreement No 101056777

5. Conclusions and recommendations

In this study, a series of L-vehicles have been tested for noise and for emissions in on-road, test track and laboratory conditions. The objective was to gain in-depth insights into noise and pollutant emission levels, and to identify driving conditions triggering high noise and emission rates. The aim behind this is to provide a basis for future improvements in type testing so as to better correlate with sound exposure experienced by citizens. The conclusions and recommendations are set out separately for noise in 5.1 and for emissions in 5.2.

5.1 Noise Emissions

The key findings and recommendations regarding the noise emissions of L-category vehicles are summarized here. The basis for this is an extensive measurement program conducted both in real-world traffic and under controlled conditions on test tracks. The aim was to identify real-world driving situations that lead to high noise emissions and to evaluate the current Type Approval (TA) procedures.

5.1.1 Findings and Conclusions

The analysis of the measurement data from the LENS project, which included a fleet of 112 primarily series-production Euro 5 vehicles, led to the following key insights:

- **Real-world driving patterns are significantly louder than those represented in the type approval procedure**: Many of the identified real-world driving maneuvers, especially aggressive accelerations, produce maximum sound pressure levels that significantly exceed the TA limits of the respective vehicle category. Test track measurements showed that peak levels can exceed TA values by more than 10 dB. For example, an L3e-A1 vehicle reached 81.4 dB(A) during strong acceleration, which is over 8 dB above its standardized L_{wot} test value. This indicates that current TA procedures inadequately capture the noise peaks that occur in real-world conditions.
- **Engine power, speed, and load are the main drivers of noise**: A clear trend was observed: vehicles with higher engine power (e.g., L3e-A3 compared to L3e-A1) tend to produce higher noise levels in most driving situations. Noise emissions increase consistently with rising engine speed and load, which is why accelerations with a wide-open throttle are among the loudest events.
- **Aggressive driving significantly increases noise emissions**: The analysis of RDE cycles using the Rotranomo model showed that an aggressive driving style, compared to an average one on the same route, leads to much more frequent and higher noise peaks (>80 dB(A)). Acceleration events starting at speeds between 20 km/h and 60 km/h and resulting in a speed increase of 30 km/h or more were identified as particularly critical.
- **Identification of critical driving maneuvers**: The most acoustically critical and commonly occurring driving situations include:
    - Aggressive acceleration from standstill
    - Short, strong engine revving at standstill (“*rpm burst*”)
    - Acceleration under high load at various speeds and in different gears

This project has received funding from the European Union's Horizon Europe research and innovation programme under grant agreement No 101056777

- **On-board measurements are feasible but challenging**: The project confirmed the technical feasibility of using on-board sensor systems to identify loud driving situations in real traffic. However, the analysis also revealed significant challenges, such as interference from background noise (other traffic, wind) and vehicle-internal noises (e.g., rattling components), which must be minimized or eliminated.
- **Focus on series-production vehicles**: The investigated fleet consisted mainly of standard-compliant Euro 5 vehicles to evaluate current technology. Only two manipulated vehicles were included. The results are therefore representative of compliant vehicles. It can be assumed that older or illegally modified vehicles exhibit different, likely higher, noise emissions.
- **Vehicle compliance and regulatory gap**: A key finding is that all vehicles examined complied with the limits under current TA test conditions. The significant exceedances observed occurred exclusively in the dynamically analyzed driving patterns. This highlights a gap in current regulation between compliance on the test bench and real-world emissions behavior.

5.1.2 Recommendations

Based on the findings, the following recommendations are derived for the future assessment and regulation of noise emissions from L-category vehicles:

- **Revision of type approval procedures (TA):**
  TA test procedures should be expanded to include realistic, dynamic driving patterns to better reflect actual noise emissions. Based on the findings, the inclusion of the following test scenarios is recommended:
  - A standardized test for aggressive acceleration from standstill
  - A test for “rpm bursts” (short engine revving) at standstill
  - Tests of acceleration under high load from various constant speeds (e.g., 20 km/h, 50 km/h)
- **Application of a dual measurement approach:**
  - On-board measurements are well suited for monitoring in real traffic to gather data on the frequency and nature of noise-critical events. However, due to challenges with data quality (e.g., background noise), they are not recommended for regulatory use without advanced filtering and correction methods.
  - Test track measurements should remain the standard for repeatable and comparable regulatory tests, but should incorporate the more dynamic test cycles suggested above.
- **Expansion of the scope of acoustic analysis:**
  The maximum A-weighted sound pressure level is a simple and relevant indicator of peak levels, but it may not fully capture the annoyance caused by certain noise characteristics. Further research into psychoacoustic metrics (e.g., loudness, roughness) is therefore recommended to better understand the perception of transient events such as rapid acceleration.
- **Use of noise models:**
  Validated noise models like Rotranomo should be used as a supplement to physical testing. Modeling enables efficient evaluation of a much broader range of driving maneuvers and influences than physical tests alone, and provides valuable insights for vehicle development and the impact assessment of regulations.

This project has received funding from the European Union's Horizon Europe research and innovation programme under grant agreement No 101056777

5.2 Exhaust Emissions

Complementing the extensive research into real-world noise emissions from L-category vehicles, this deliverable also provides a comprehensive investigation into tailpipe exhaust emissions performance. Drawing upon the same robust measurement program, the aim was to identify and quantify the contribution of specific real-world driving events to elevated pollutant emissions. Key findings and recommendations regarding exhaust emissions are summarized in this section.

5.2.1 Findings and Conclusions

The most representative high emission events which have been identified in this study, based on several analyses, were found to be:

- Cold Start
- Acceleration from stand-still
- Deceleration transitions
- Merging and overtaking maneuvers on highways or rural roads. These events could also be associated with sportive driving.

Those events are all common and recurring in everyday motorcycle use. "*Cold starts*" occur at the beginning of nearly every trip, especially after prolonged parking. "*Acceleration from standstill*" is frequent in urban environments, such as after red traffic lights or stop signs. Deceleration transitions are inherent to normal driving, particularly in stop-and-go traffic or during speed adjustments. Given their frequency and measurable impact on emissions, these events are not only relevant but also representative of typical real-world driving behavior.

High pollutant emissions have been also identified during deceleration events. Furthermore, it is important to note that during deceleration, mass air flow through the engine is typically very low, which can limit the formation of new emissions. As a result, the elevated emissions observed during these events are likely influenced by residual exhaust gases generated during preceding acceleration phases, or the rapid transition to fuel cut-off which floods the catalyst with oxygen while the combustion is re-engaged when the engine approaches idle speed. Additionally, this issue can be also due to synchronization issues between actual events and analyzer response, since the signals are synchronized in a general way throughout the duration of the entire trip and not in a detailed way for each of the events. This overlap introduces uncertainty in attributing emissions exclusively to deceleration, making it challenging to isolate their specific contribution without more advanced analytical methods.

CO emissions

CO emissions represent to be the most critical emissions identified in this study. Driving events that cause the highest CO emissions for this pollutant could be described as follows:

- Cold start: very severe in terms of the impact on the overall emissions. On average, cold start events resulted in approximately 15x times higher CO emissions than the average emissions over the full trip duration, when considering only WMTC unweighted value, where influence of additional high emissions events is lower.

This project has received funding from the European Union's Horizon Europe research and innovation programme under grant agreement No 101056777

- Driving at high engine load, and/or both high engine and vehicle speed: CO emissions reach relatively high values. Especially when driving above max power rated engine speed, high CO emissions are triggered.
- Running at low lambda values: fuel enrichment is also an important engine operation point that should be considered. Especially for this pollutant, severe effects have been identified. This situation is commonly reached when operating at high engine loads.

LVs sub-categories particularities:

- Very severe on 2-stroke L1e-B vehicles.
- High CO emissions are especially triggered on CVT-equipped vehicles, as these vehicles operate at 100% throttle more frequently than MT ones.
- L3e-A3 do not exhibit particularly high CO emissions.

When operating on TA conditions, no issues are present, but when operating under RW driving conditions (on-road and RDC), high emissions are triggered specially on those low powered vehicles which are commonly driven at maximum speed and/or at 100% throttle (L3e-A1 and low powered L3e-A2, especially CVT).

NOx emissions

The most frequent events, and the ones which cause high NOx emissions are fundamentally strong accelerations. Severity of NOx emissions is lower than CO, as they are not triggered on the same magnitude.

- Cold start situation: very severe in terms of the impact on the overall emissions. On average, cold start events resulted in approximately 2.2 times higher NOx emissions than the average emissions over the full trip duration, when considering only WMTC unweighted value. This confirms that cold engine operation significantly increases pollutant output, likely due to inactive after-treatment systems during engine warm-up.
- When driving at high engine load, and/or both high vehicle speed and high engine speed, NOx emissions reach relatively high values.
- Those situations of high NOx emissions when driving above max power rated engine speed have the inverse result on CO emissions (comparison between Figure 4-79 and Figure 4-82).
- Strong accelerations have been also considered an important event. Less severe than cold start in terms of total emissions, but considerably higher than average emissions, approximately 7.7 times higher than the unweighted average of WMTC.

LVs sub-categories particularities:

- Low emissions of 2-stroke L1e-B vehicles.
- L3e-A1 and L3e-A3 are shown as the most sensitive sub-categories regarding NOx emissions when comparing RDC with WMTC unweighted values. Even though, overall emissions remain under current TA limits. L3e-A2 is slightly influenced, with an increase in emissions of 1.15x times higher in RDC.

This project has received funding from the European Union's Horizon Europe research and innovation programme under grant agreement No 101056777

HC Emissions

In terms of HC, high emissions patterns are, in some cases, similar to CO ones, revealing instant values (in mg/s) 10x times lower on average than actual CO ones. Therefore, severity is lower when excluding cold start events. Driving events that cause the highest emissions include the following:

- Driving at both low vehicle and engine speed at high gears.
- High engine speed combined with substantial throttle pedal depression, this means, high engine load and therefore strong accelerations.
- Cold start: catalytic converter operating below optimal temperature. Surpassing by +10x times average values, when considering only WMTC unweighted value. HC is shown as the one with highest severity under cold start conditions.
- Rural phase: shows a decrease in emissions for all vehicle sub-categories, except L3e-AxE.

LVs sub-categories particularities:

- L3e-AxE and L1e-B show the highest HC emissions, especially 2-stroke ones.
- More frequently on low powered vehicles, very severe on 2-stroke L1e-B.
- L3e-A3 present relatively low HC emissions.
- L3e-AxE regardless of the urban and rural phases, both have a similar level of emissions.

PN Emissions

In terms of PN, no specific assessment for the driving events causing high emissions has been developed, but overall emissions by phase have been computed. Up next are shown the findings.

LVs sub-categories particularities:

- Similar patterns as CO emissions, on L3e-A1 and L3e-A2 vehicles (see Figure 4-8 and Figure 4-9)
- Increased emissions on motorway phase on L3e-A3, whereas CO emissions remain stable along all phases for this specific sub-category (see Figure 4-10)
- Most relevant LV sub-categories show relative similar behavior, where emissions are triggered on motorway phase.
- Regarding on-road measurements, L3e-A3 reflects considerable higher $v*a_{,pos}$ for the motorway phase. Even though, $v*a_{,pos}$ does not have an important influence on PN emissions on this analysis.

Driving operation emissions

Additionally, a study of how emissions are distributed among the different phases, urban, rural and motorway (according to (EU) no 2017/1151) has been considered for this summary of findings. Hereunder, most relevant findings are explained:

L3e-A1

- CO emissions on RDC are considerably high on L3e-A1 (rural and motorway phases). Emissions on motorway phase reach values of near 4x times overall emissions for RDC. Additionally, overall emissions on RDC are +5x times higher than TA unweighted values. 125cc engines are driven at maximum power to maintain a speed over 90 km/h and thus there is an increase in emissions.

This project has received funding from the European Union's Horizon Europe research and innovation programme under grant agreement No 101056777

- High HC emissions when operating on motorway phase from RDC cycle reaching values 2x times higher than overall ones. Although, the total averaged value presents an acceptable magnitude of 0.8 times the overall unweighted TA emissions.
- NOx emissions patterns are inverse to CO. RDC motorway phase are half of overall emissions for this same RDC.
- PN emissions on RDC show an increase of 2.6x times on motorway phase compared with overall values of this same cycle. Regarding overall emissions, RDC are ≈ 8x times higher on total average emissions compared with TA ones.

L3e-A2

- CO emissions in L3e-A2 vehicles are also quite influenced by RDC cycle reaching average values higher than 5000 mg/km on RDC motorway phase, which is 2x higher than overall average emissions for RDC, and +7x times higher than average emission on motorway phase for TA measurements.
- NOx emissions on RDC motorway phase reach values 1.8x times higher than overall ones for this same cycle. Overall emissions on RDC and TA do not differ importantly since they are +1.15x times higher on RDC.
- HC emissions on RDC motorway emissions are lower than overall values. Although, RDC overall emissions are +1.35x times higher than on TA.
- PN emissions on RDC motorway phases are equally affected, reaching values +2.3x times higher than the overall emissions for this same cycle. When comparing overall unweighted values of RDC and TA, there is an increase of ≈ 3x times on RDC.

L3e-A3

- NOx emissions on RDC motorway phase reach double the overall values for this same cycle. Overall emissions on RDC and TA have been also importantly affected, since average overall RDC emissions are 2.5x times higher than average overall unweighted TA values.
- L3e-A3 is shown to be even less sensible in terms of total PN emissions on RDC, but motorway phases are again equally affected with an increase of +2.25x times compared with RDC overall values. Regarding overall emissions, there is an increase of ≈ 1.7 times on total average emissions on RDC compared with TA ones.

5.2.2 Recommendations

Based on the current findings, with the analyses not yet complete, several recommendations are proposed to improve the accuracy and relevance of type-approval emission testing procedures:

1. "*Cold start*" events should be included in the testing framework in a representative way, as they are known to produce elevated emission levels during the engine warm-up phase. These events can be clearly defined either by monitoring engine coolant temperature or by applying a fixed time window after engine starts. Note that the current WMTC includes a cold start phase, and that the

This project has received funding from the European Union's Horizon Europe research and innovation programme under grant agreement No 101056777

length of the test cycle determines to what extent the cold start emissions are weighted in the overall emission measured.

2. "*Acceleration from standstill*" should be incorporated as a standard test condition. This is particularly important under both loaded and unloaded scenarios, as it reflects the frequent stop-and-go nature of urban driving, which significantly influences emission profiles. Note that the WMTC includes accelerations from standstill, but these accelerations are relatively mild.
3. In contrast, deceleration phases are less relevant in type-approval testing since they are unlikely to result in high emissions.

Together, these recommendations would enhance the representativeness of TA procedures, ensuring that regulatory testing mirrors more closely real-world driving conditions and pollutant emission behavior.

The next step will be to expand the analysis to cover the remaining high priority driving events of Table 4-18 and to extend the classification of these events to all available measurements in the LENS db to obtain more comprehensive and representative results, including other pollutants.
Further analytical approaches are essential to precisely identify and characterize high emission events and continue analyzing and identifying patterns causing high emissions.

5.3 Driving dynamics

The driving dynamics of L-category vehicles have been comprehensively analyzed to assess how well the current type-approval (TA) procedures, as well as the Real-Driving Cycles (RDCs) and on-road experimental measurements conducted within the LENS project, represent the real-world driving scenarios identified throughout this deliverable. The goal was to evaluate the extent to which the tested parameters, such as vehicle speed, acceleration, and relative positive acceleration (RPA), have captured the complex driving patterns observed under actual usage conditions. This detailed analysis provides insights to support the development of more representative testing methodologies that can accurately reflect the real-world performance and environmental impact of L-category mobility solutions.

5.3.1 Findings and Conclusions

In comparison with PC, both $v*a_{,pos}$ and RPA are considerable higher on the bigger ones. Both WMTC and WLTC cover almost the same vehicle dynamics range. Although, when comparing standard RDE measurements, no relation could be established both PC and LV, the latest are subjected to considerable higher acceleration and are driven in a much more dynamic way. This is the case especially for L3e-A2 and A3, the ones used for more sportive driving, leisure, etc, and it can be stated that 35kW is enough power to be driven in a very aggressive way. Low engine capacity vehicles, L6 and L7 do not differ too much from a PC in terms of dynamics. When analyzing RPA, we found a similar picture as on the $v*a_{,pos}$, urban phase with high dispersion from lab and PCs values, rural phase as the most dynamic, motorway phase closer to the TA procedure.

In terms of emissions, not a very clear influence can be stated. All PN, CO, HC and NOx pollutants which have been considered for this analysis, results on similar emissions per phase on all urban rural and motorway, influenced the urban phase by the cold start. When analyzing these pollutant emissions values versus $v*a_{,pos}$, it could be stated that, for those measurements with higher $v*a_{,pos}$ values, emissions are higher also due to the more dynamic conditions to which they have been subjected. Low engine and/or low

This project has received funding from the European Union's Horizon Europe research and innovation programme under grant agreement No 101056777

powered vehicles show a higher increase in emissions, as this more dynamic (and more realistic) measurement requires, in some scenarios, the maximum power from the vehicle. This is absolutely a RW driving pattern for this LVs.

Regarding the global assessment of emissions, discretizing the routes by phases does not show very clear changes in the driving dynamics, nor in the emissions. Further analysis should be carried out in this way so it can be stated if it has a real effect on emissions. Same situation regarding the discretization by road type. No further conclusion could be stated at this moment in time, when referring to the dynamics.

5.3.2 Recommendations

L-Category vehicles exhibit significantly different driving dynamics compared to passenger cars (PCs). Their power-to-mass ratios (PMRs) are notably higher, often approaching levels found in sports cars, particularly for the L3e-A2 motorcycle sub-category, and even higher when referring to L3e-A3. This stark contrast in performance capabilities suggests that the real-world driving patterns for L-category vehicles must be addressed and examined individually, with a high degree of scrutiny to accurately reflect their actual usage.

Furthermore, the current type-approval (TA) procedures for two-wheelers tend to reflect driving dynamics similar to those used for passenger cars, despite the identification that real-world scenarios involve considerably more dynamic driving behavior in L-category vehicles. This disparity between type-approval and real-world conditions is not adequately captured by the existing testing frameworks.

The analysis has revealed that the Real-Driving Cycles (RDCs) developed within the LENS project are more dynamic in nature compared to the standard WMTC test cycle. This specialized RDC, derived directly from real-world driving data collected for two-wheelers, has shown to be much more representative of the driving dynamics observed in the on-road measurements conducted throughout this study.

Collectively, these findings underscore the need for more dynamic test procedures that can adequately capture the unique driving characteristics of L-category vehicles. The real-world driving patterns identified in this deliverable should inform the development of such tailored testing methodologies, ensuring that future assessment and type-approval frameworks accurately reflect the performance and environmental impact of these specialized mobility solutions

This project has received funding from the European Union's Horizon Europe research and innovation programme under grant agreement No 101056777

6. References

[1] Paviotti, M.; Vogiatzis, K.: *On the outdoor annoyance from scooter and motorbike noise in the urban environment*, Science of the Total Environment, pages 223–230, 2012.

[2] Lechner, C.; Schnaiter, D.; Siebert, U.; Böse-O'Reilly, S.: *Effects of Motorcycle Noise on Annoyance-A Cross-Sectional Study in the Alps*, Int J Environ Res Public Health, 2020.

[3] Dittrich, M.; Papadimitriou, G.; Ntziachristos, L.; Steven, H.; Durampart, M.: *Developments in Regulations for Sound Emission of L-category vehicles*, Euronoise, Crete, 2018.

[4] UN/ECE - UN Regulation 41: *Uniform provisions concerning the approval of motor cycles with regard to noise* - Rev2, 04 series of amendments, 2012, https://unece.org.

[5] UN/ECE - UN Regulation 41: *Uniform provisions concerning the approval of motor cycles with regard to noise* - Rev2, 05 series of amendments, 2021.

[6] Peeters, B.: *Assessment Programme for Parameters of the "general" European vehicle fleet* - Deliverable 3, Public Report, Peeters, B.EU Horizon Europe project "IMAGINE", 2006.

[7] Huth, C.; Eberlei, G.; Liepert, M.: *Überprüfung der Geräuschemissionen von Motorrädern im realen Verkehr*, Huth, C.; Eberlei, G.; Liepert, M.Umweltbundesamt, 2020.

[8] Dittrich, M.; van Mensch, P.; Riemersma, I.; Paschinger, P.; Steven, H.; Karamanlis, N.; Degeilhe, P.: *Real world driving conditions and requirements for the LENS test programme* - Deliverable 6.1, Public Report, Dittrich, M.; van Mensch, P.; Riemersma, I., et al.EU Horizon Europe project "LENS", 2023.

[9] Dittrich, M.; Wessels, P.: *Noise monitoring of loud vehicles in four Dutch cities*, Inter-Noise, Nantes, 2024.

[10] Diemel, C.; Uszynski, O.: *Method and system for on-board noise measurement* - Deliverable 3.2, Demonstrator, Diemel, C.; Uszynski, O.EU Horizon Europe project "LENS", 2023.

[11] Diemel, C.; Uszynski, O.; Yordanov, V.; Städtler, L.: *Sensor System for Noise and Positioning Data Acquisition*, ATZ Worldwide, pages 30–35, 2023.

[12] Diemel, C.; Uszynski, O.; Weber, A.: *Entwicklung einer Methodik zur Ermittlung akustisch relevanter Fahrsituationen von Fahrzeugen der Klasse L*, DAGA, Hannover, 2024.

[13] Diemel, C.; Uszynski, O.; Yordanov, V.; Werner, D.; Urban, P.: *Investigation of Noise-Intensive Driving Patterns under Real Driving Conditions*, Aachen Acoustics Colloquium, Aachen, 2024.

[14] Schliephake, C.; Shariatinia, S.; Dittrich, M.: *Suggested revisions to TA procedure for noise emission* - Deliverable 4.5, Public Report, Schliephake, C.; Shariatinia, S.; Dittrich, M.EU Horizon Europe project "LENS", 2025.

[15] UN/ECE - UN Regulation 9: *Uniform provisions concerning the approval of category L2, L4 and L5 vehicles with regard to noise* - Rev2, 07 series of amendments, 2013, https://unece.org.

[16] UN/ECE - UN Regulation 63: *Uniform provisions concerning the approval of L1 category vehicles with regard to sound emission [2018/1705]* - Supplement 4 to the 02 series of amendments, 2018, http://data.europa.eu.

This project has received funding from the European Union's Horizon Europe research and innovation programme under grant agreement No 101056777

[17] International Organization for Standardization : ISO 10844: *Acoustics - Specification of test tracks for measuring noise emitted by road vehicles and their tyres*, 2014, https://dx.doi.org.

[18] Schliephake, C.; Shariatinia, S.: *Noise measurement data from standardised tests* - Deliverable 4.3, Public Data, Schliephake, C.; Shariatinia, S.EU Horizon Europe project "LENS", 2025.

This project has received funding from the European Union's Horizon Europe research and innovation programme under grant agreement No 101056777

Appendix A: On-board noise measurements

In the following figures, speed and sound level histories of selected vehicles are shown, besides sound spectrograms of selected parts of driven routes. They allow us to identify particular driving conditions, in particular the noisiest ones and those with strong dynamic behavior.

Figure A-1 and Figure A-2 below show the results of on-board measurements taken during a drive distance of around 20 km, for two different scooters with CVT transmission. The time series data was provided at 1 second intervals. The sound pressure level was measured at the back of the vehicle. This was not calibrated to adjust to 7.5 m roadside position and can therefore vary for different vehicles. The vehicle speed is derived both from the speed signal and from the ODB, the engine speed was obtained from the ODB. The acceleration is derived from the speed signal. These parameters are set out as a time series plot and as sound level vs. speed.
The general trend is that the speed dependence is clear, rising with increasing speed. However, at low speeds and standstill high levels can be observed, potentially occurring during acceleration from standstill or engine revving at start.
Figure A-3 to Figure A-5 show driving routes and sound levels, speeds and acceleration for three different motorcycles.

This project has received funding from the European Union's Horizon Europe research and innovation programme under grant agreement No 101056777

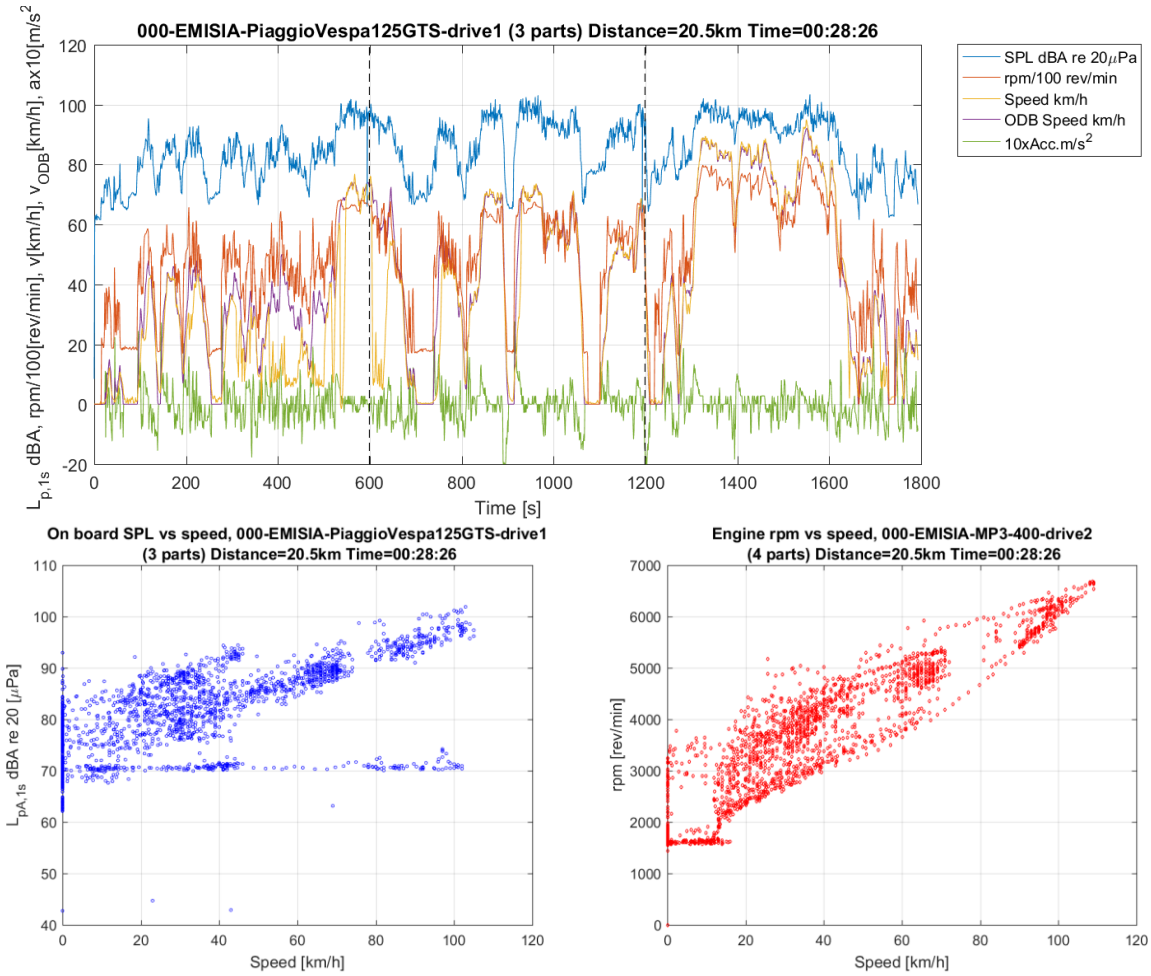

Figure A-1: On-board measurement of a real-world driving run of a 125cc scooter with CVT transmission, of 20.5 km, showing top: the on-board sound pressure level, engine speed, Speed derived from GPS and from ODB signals, and acceleration derived from the speed; middle: on-board A-weighted sound pressure level as a function of speed; bottom: engine speed vs vehicle speed.

This project has received funding from the European Union's Horizon Europe research and innovation programme under grant agreement No 101056777

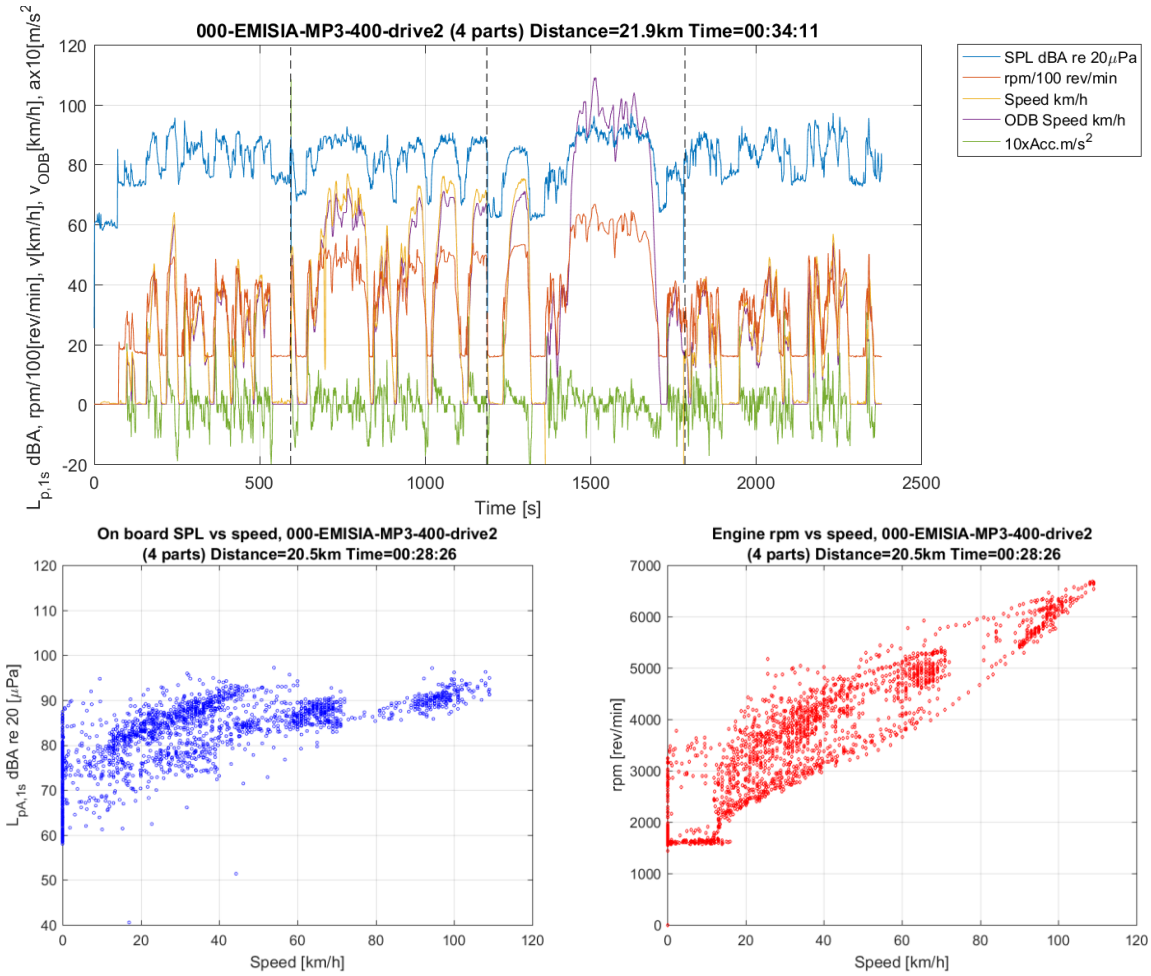

Figure A-2: On-board measurement of a real-world driving run of a 400cc 3-wheeled scooter with CVT transmission, of 21.9 km, showing top: the on-board sound pressure level, engine speed, speed derived from speed signal and from ODB signals, and acceleration derived from the speed; middle: on-board A-weighted sound pressure level as a function of speed; bottom: engine speed vs vehicle speed.

This project has received funding from the European Union's Horizon Europe research and innovation programme under grant agreement No 101056777

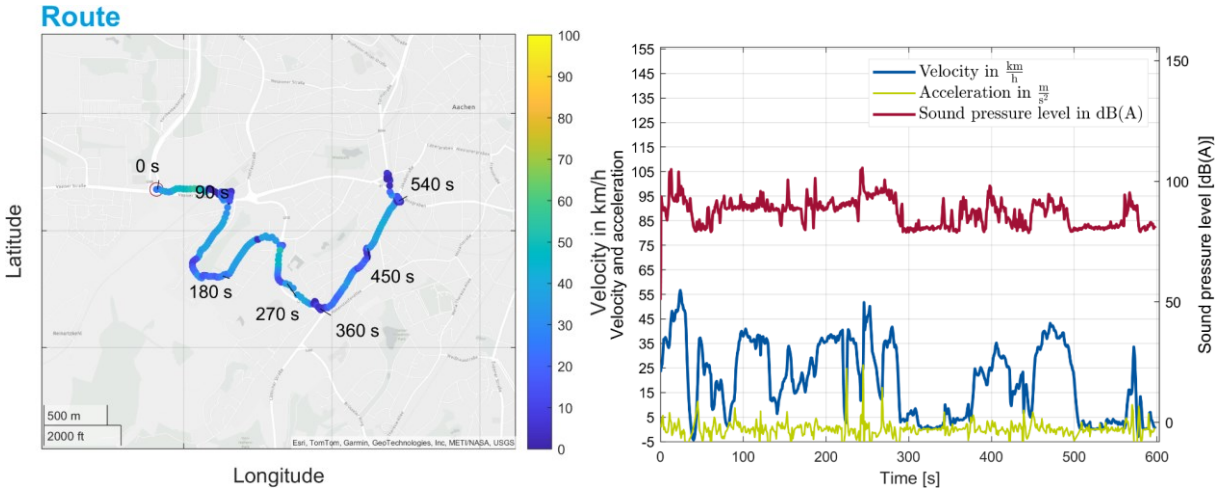

Figure A-3: On-board measurement of a real-world driving run of a 690cc motorcycle, showing top: driving route including speed indication; bottom: the on-board sound pressure level, speed derived from GPS and from ODB signals, and acceleration derived from the speed.

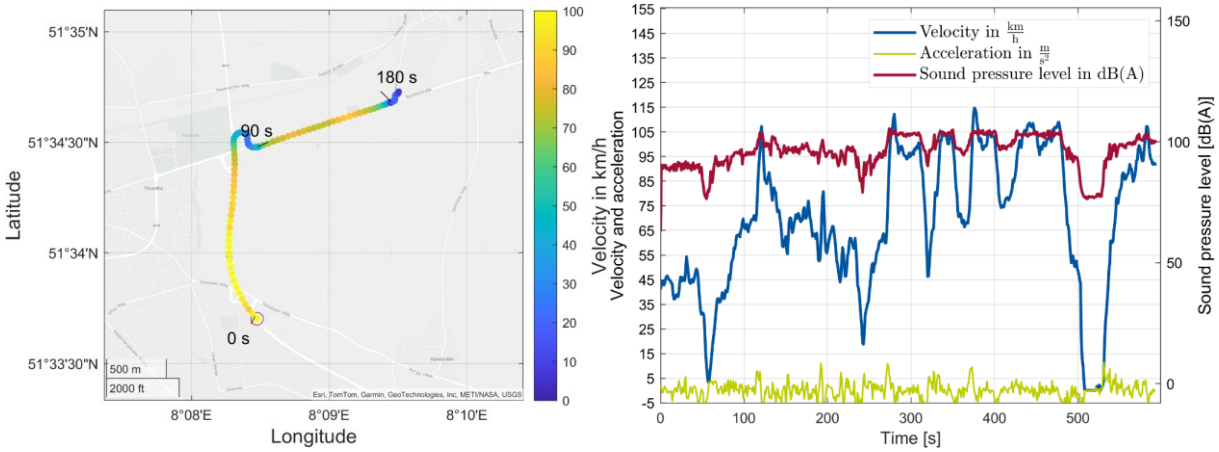

Figure A-4: a) On-board measurement of a real-world driving run of a 600cc motorcycle, showing top: driving route including speed indication; bottom: the on-board sound pressure level, speed and acceleration.

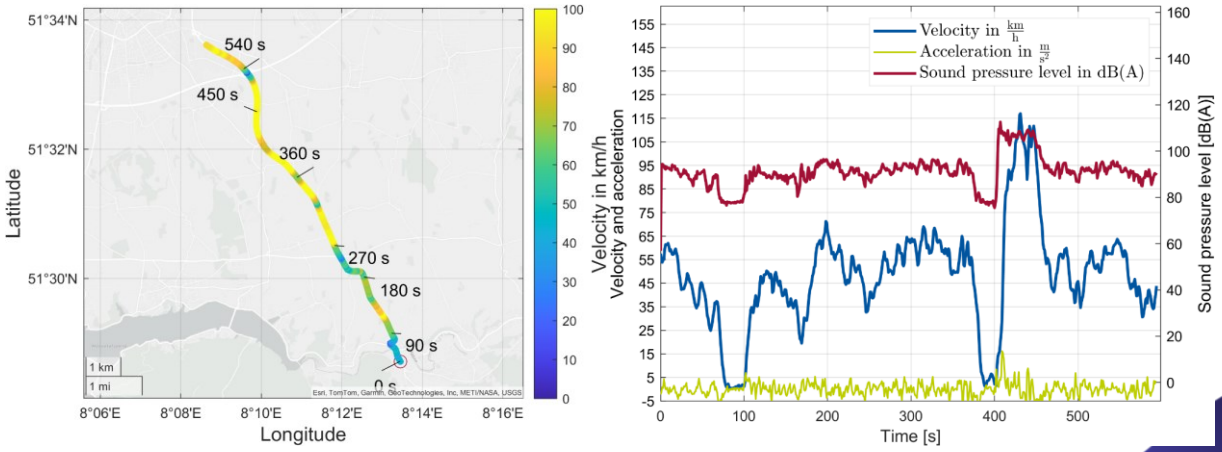

Figure A-4: b) On-board measurement of a real-world driving run of a 600cc motorcycle, showing top: driving route including speed indication; bottom: the on-board sound pressure level, speed and acceleration.

This project has received funding from the European Union's Horizon Europe research and innovation programme under grant agreement No 101056777

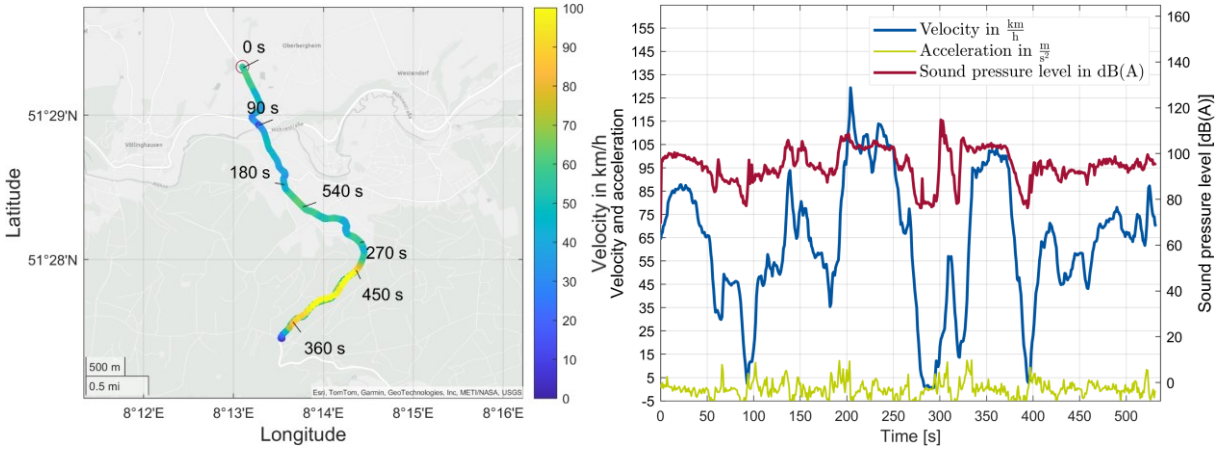

Figure A-4: c) On-board measurement of a real world driving run of a 600cc motorcycle, showing top: driving route including speed indication; bottom: the on-board sound pressure level, speed and acceleration.

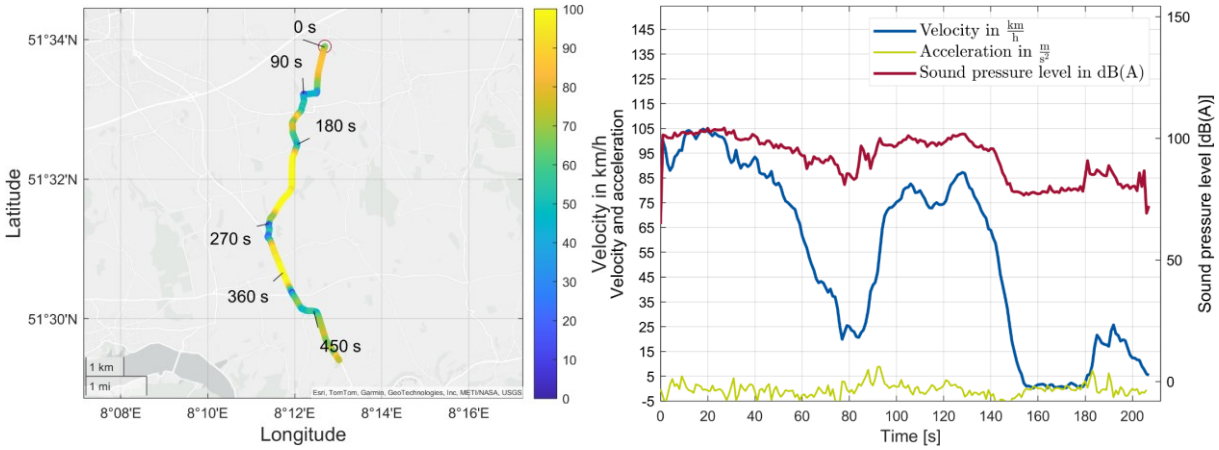

Figure A-4: d) On-board measurement of a real-world driving run of a 600cc motorcycle, showing top: driving route including speed indication; bottom: the on-board sound pressure level, speed and acceleration.

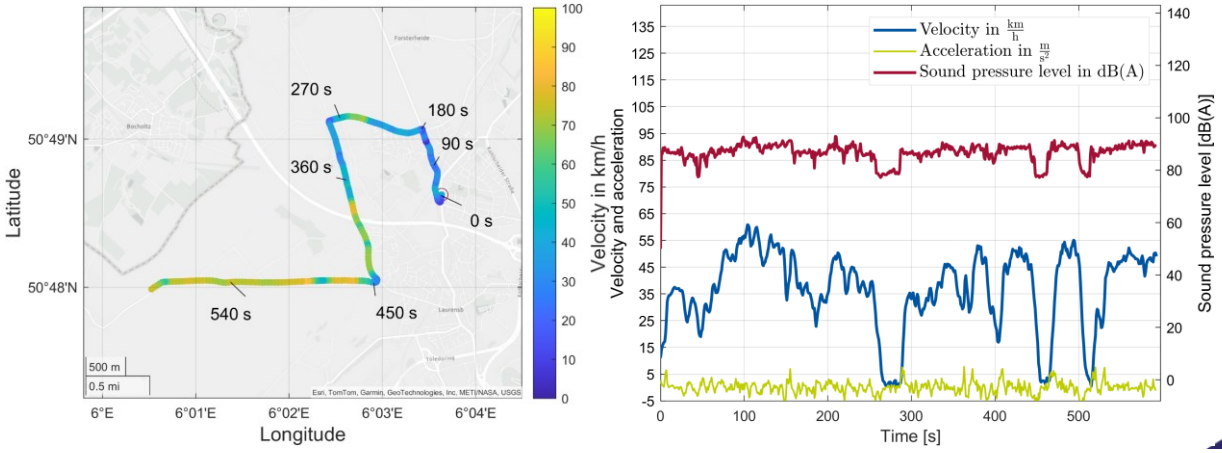

Figure A-5: a) On-board measurement of a real-world driving run of a 1200cc motorcycle, showing top: driving route including speed indication; bottom: the on-board sound pressure level, speed and acceleration.

This project has received funding from the European Union's Horizon Europe research and innovation programme under grant agreement No 101056777

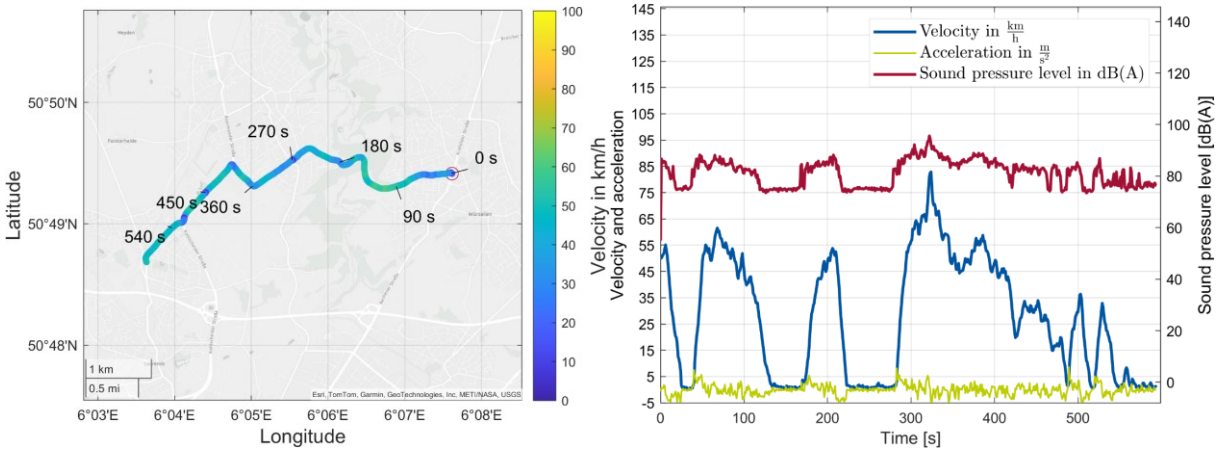

Figure A-5: b) On-board measurement of a real-world driving run of a 1200cc motorcycle, showing top: driving route including speed indication; bottom: the on-board sound pressure level, speed and acceleration.

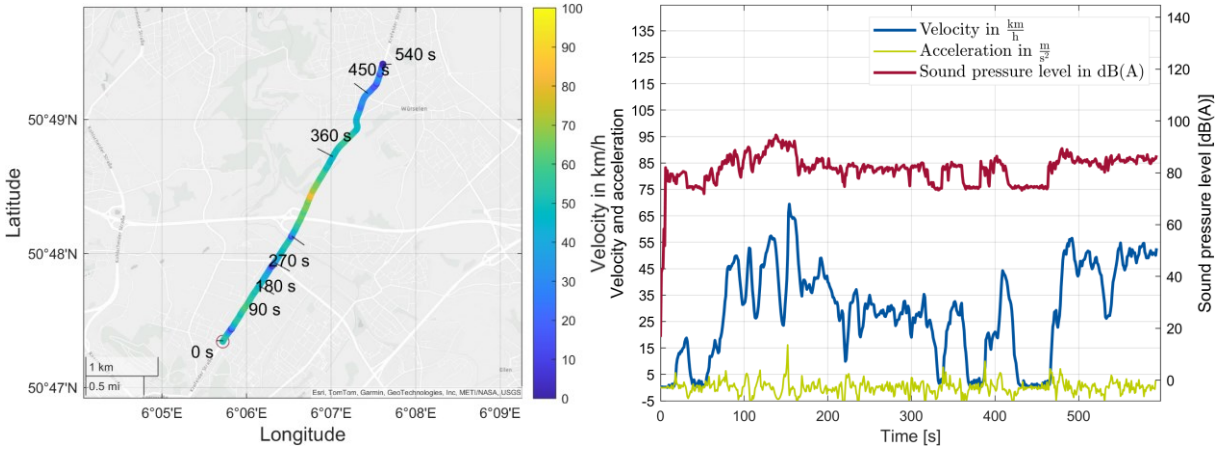

Figure A-5: c) On-board measurement of a real-world driving run of a 1200cc motorcycle, showing top: driving route including speed indication; bottom: the on-board sound pressure level, speed and acceleration.

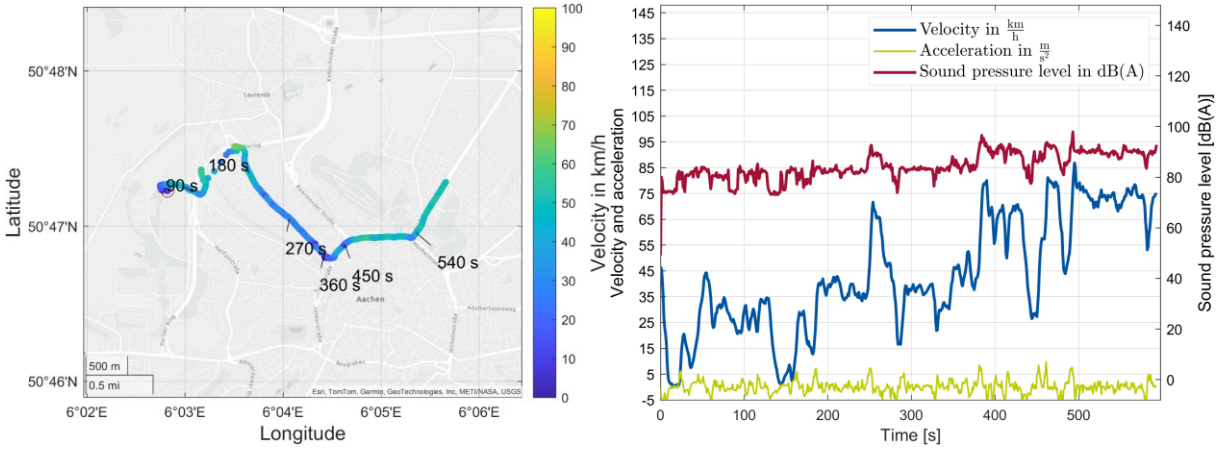

Figure A-5: d) On-board measurement of a real-world driving run of a 1200cc motorcycle, showing top: driving route including speed indication; bottom: the on-board sound pressure level, speed and acceleration.

This project has received funding from the European Union's Horizon Europe research and innovation programme under grant agreement No 101056777

Examples of spectrograms of on-board measurements

Some examples of spectrograms taken from time signals of on-board measurements are shown in Figure A-6 to A-9 below, including third octave spectrograms with time signal and level histories and narrowband spectrograms, which show engine harmonics indicative of engine speed and its changes. These allow to identify particular driving conditions, in particular the noisiest ones and those with strong dynamic behavior. The unweighted level histories differ from the A-weighted histories depending on the engine displacement and driving condition. The sound levels are not calibrated and only intended for comparison of driving conditions. A drawback of on-board measurements is the possible presence of unwanted background noises such as other traffic, driving wind noise, other mechanical noise in the proximity of the microphone. For this reason, a careful selection was made of recordings deemed most illustrative of particular driving conditions. It should also be noted that the spectrogram color scaling is chosen specifically to visualize vehicle harmonics, which for the narrowband spectrograms are best seen in the frequency range up to 1000 Hz, whereas third octave spectrograms are shown for the 32-4000 Hz third octave frequency bands. The original signals had a sample frequency of 44 kHz.

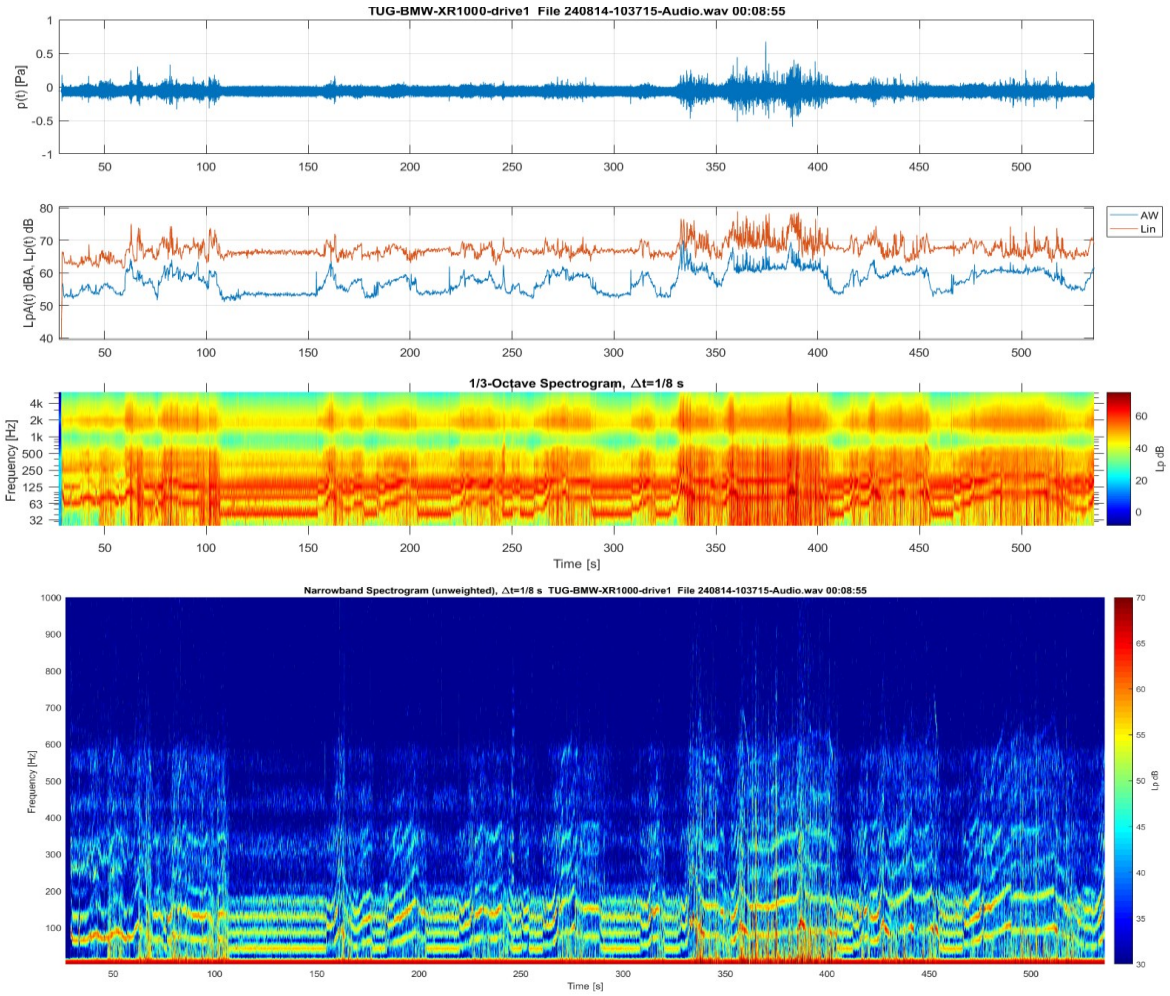

Figure A-6: On board sound measurement of a 1000 cc motorcycle, showing the sound time signal, A-weighted end unweighted level history, the third octave spectrogram and below, the narrowband spectrogram, including startup, multiple acceleration, deceleration and idling events.

This project has received funding from the European Union's Horizon Europe research and innovation programme under grant agreement No 101056777

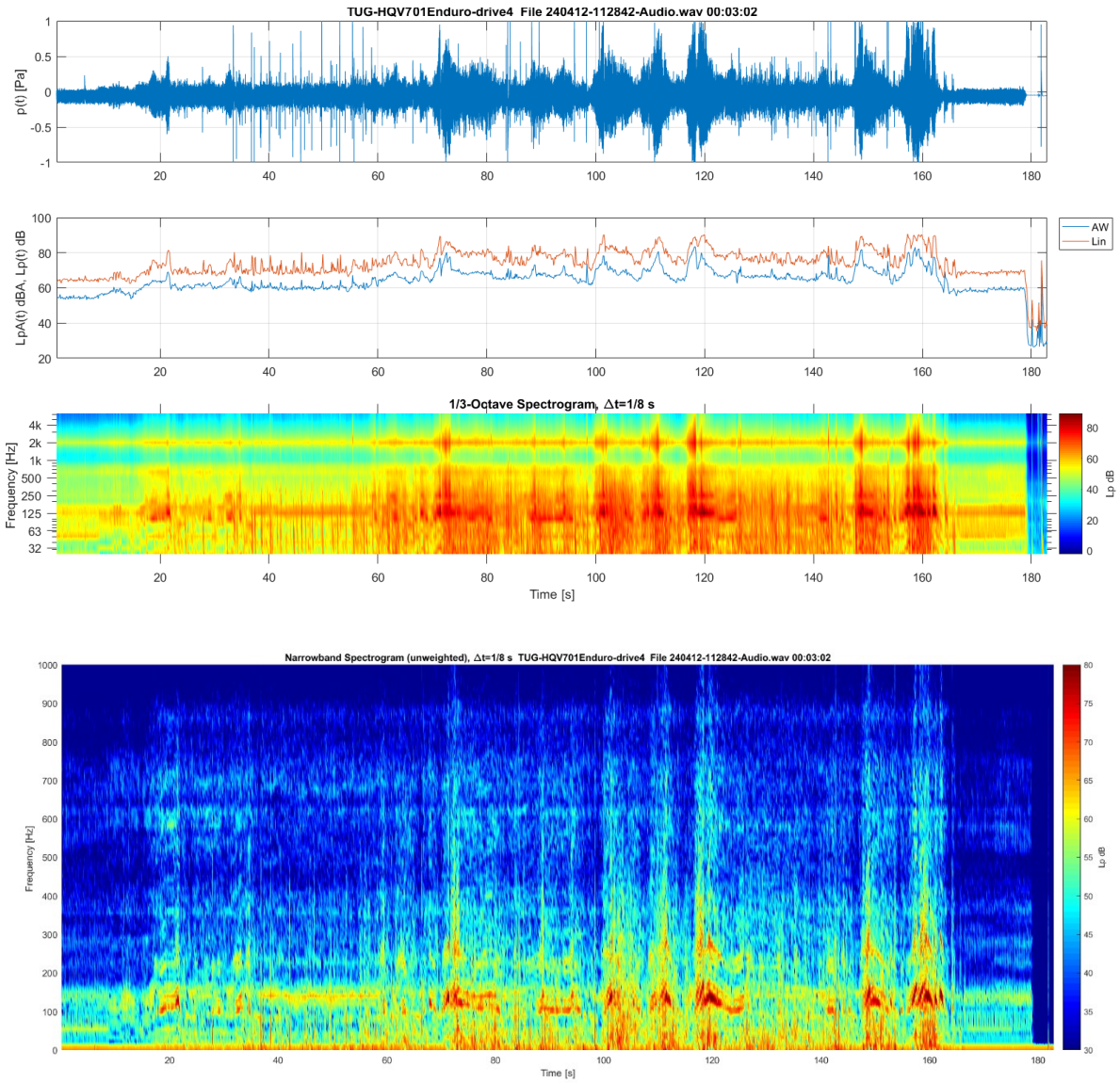

Figure A-7: On board sound measurement of a 700 cc Enduro motorcycle, showing the sound time signal, A-weighted end unweighted level history, the third octave spectrogram and below, the narrowband spectrogram, including multiple acceleration, deceleration and idling events.

This project has received funding from the European Union's Horizon Europe research and innovation programme under grant agreement No 101056777

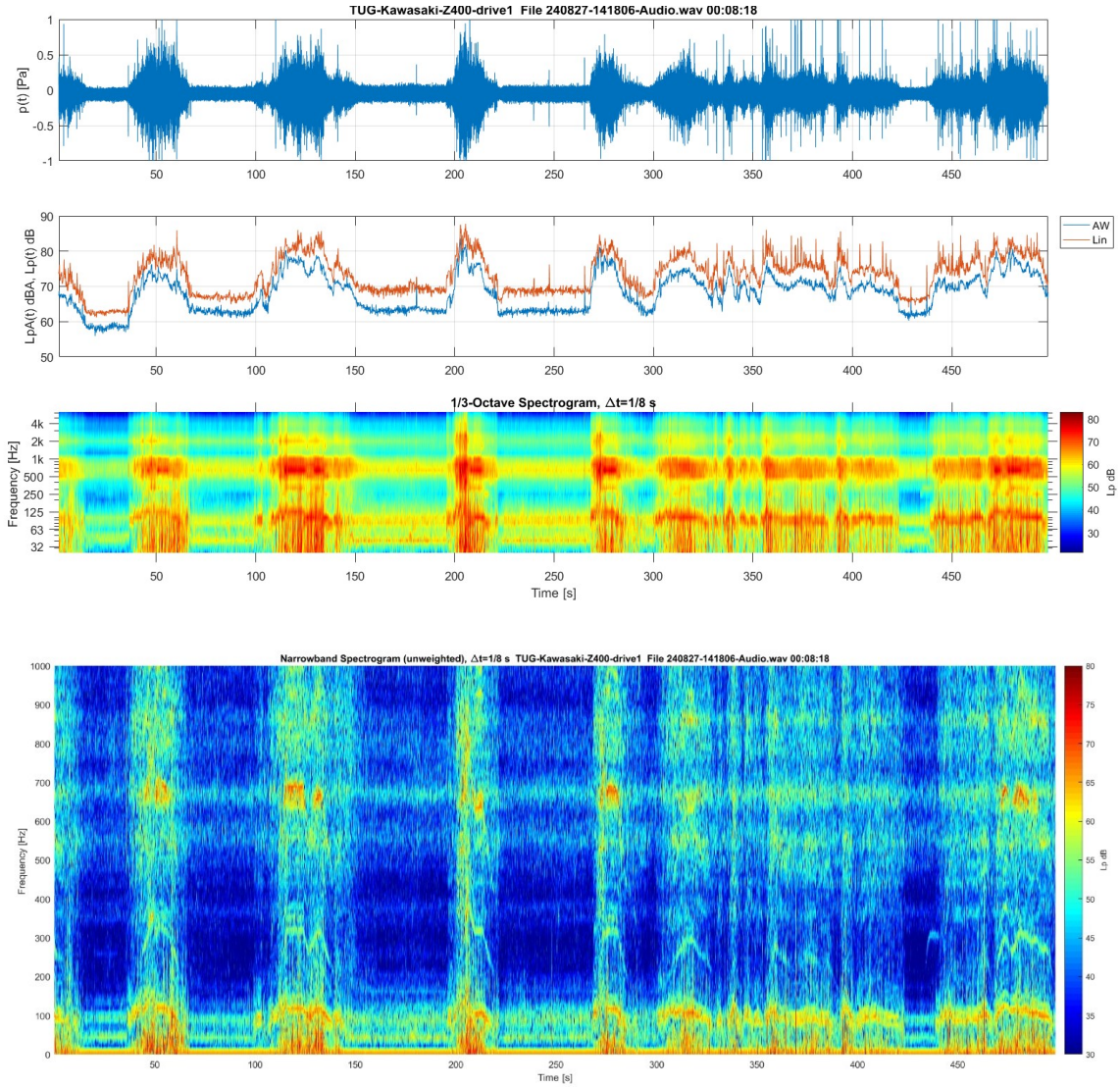

Figure A-8: On board sound measurement of a 400 cc motorcycle, showing the sound time signal, A-weighted end unweighted level history, the third octave spectrogram and below, the narrowband spectrogram, including multiple acceleration, deceleration and idling events.

This project has received funding from the European Union's Horizon Europe research and innovation programme under grant agreement No 101056777

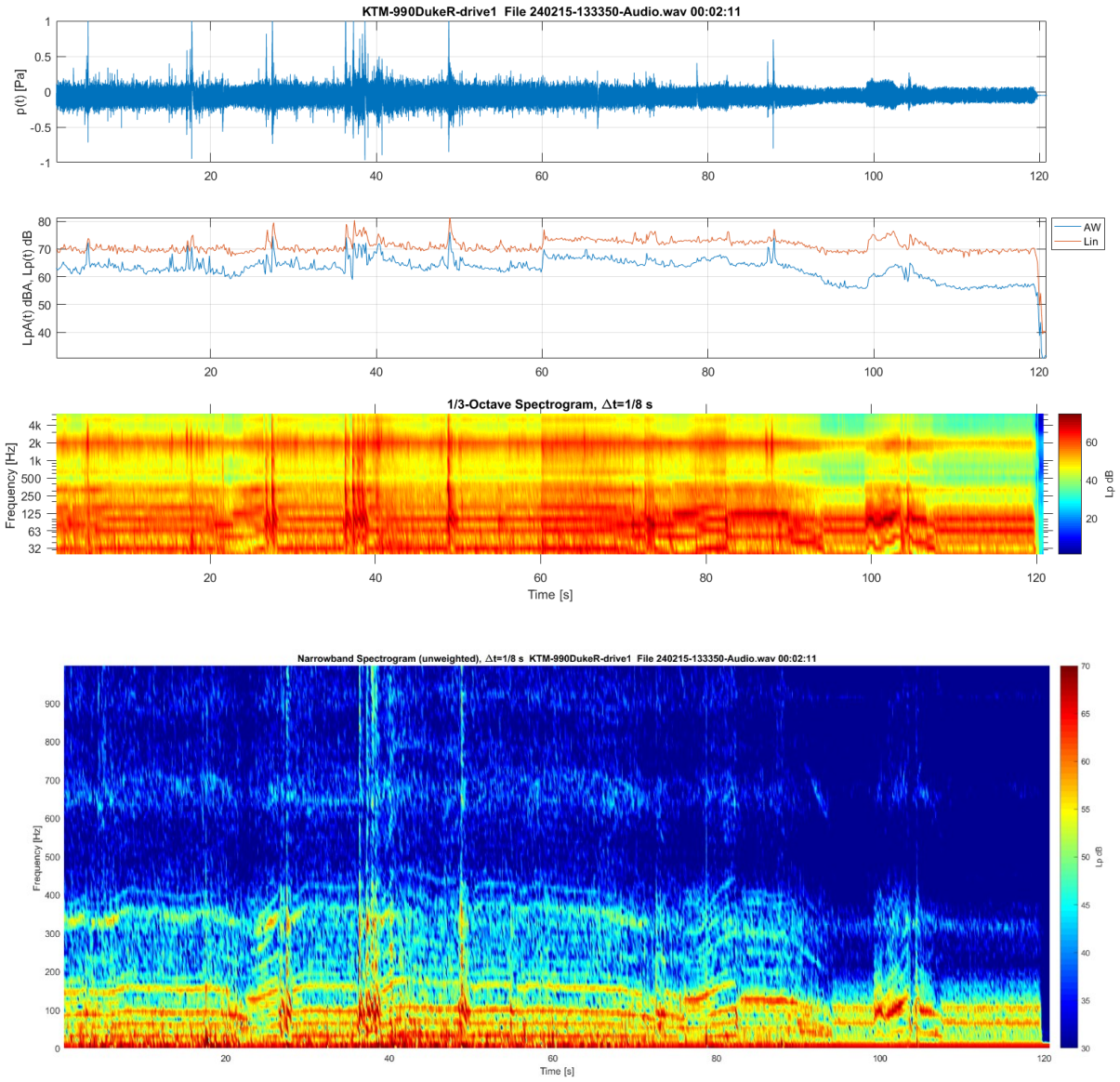

Figure A-9: On board sound measurement of a 990 cc motorcycle, showing the sound time signal, A-weighted end unweighted level history, the third octave spectrogram and below, the narrowband spectrogram, including several revving (throttle control) events, multiple acceleration, deceleration and idling events.

This project has received funding from the European Union's Horizon Europe research and innovation programme under grant agreement No 101056777

Appendix B: RDE Routes

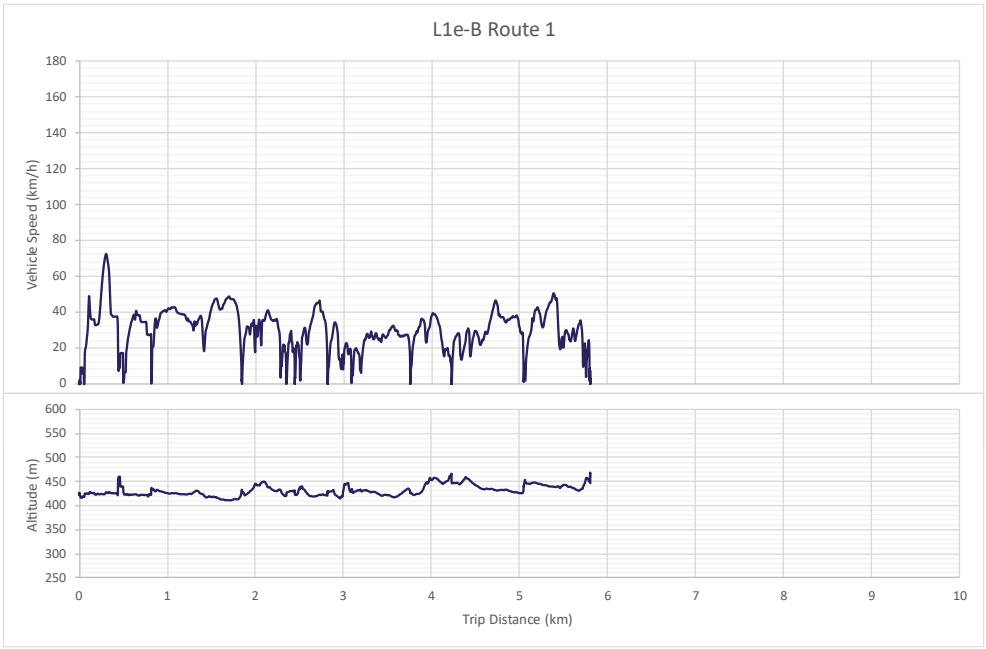

Figure B-1: L1e-B Route 1 vehicle speed (km/h) and altitude (m) traces.

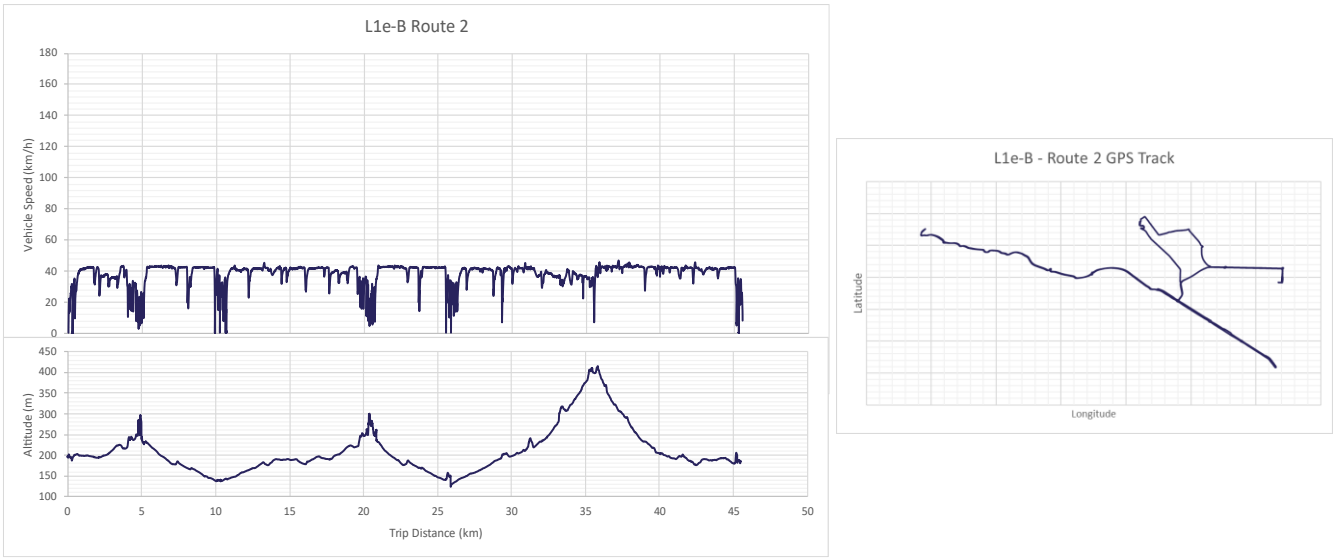

Figure B-2: L1e-B Route 2 vehicle speed (km/h) and altitude (m) traces. GPS trace.

This project has received funding from the European Union's Horizon Europe research and innovation programme under grant agreement No 101056777

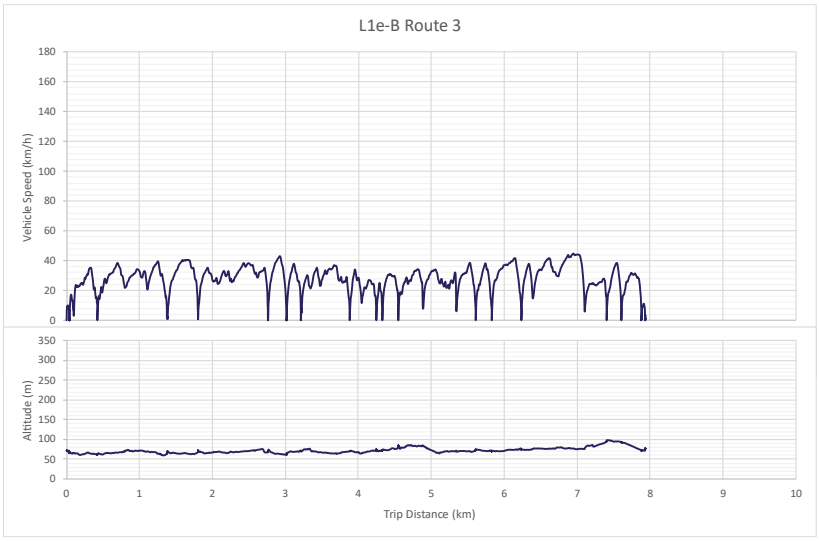

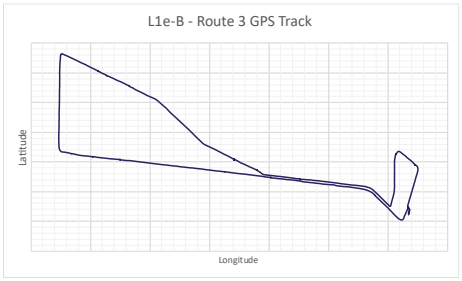

Figure B-3: L1e-B Route 3 vehicle speed (km/h) and altitude (m) traces. GPS Trace.

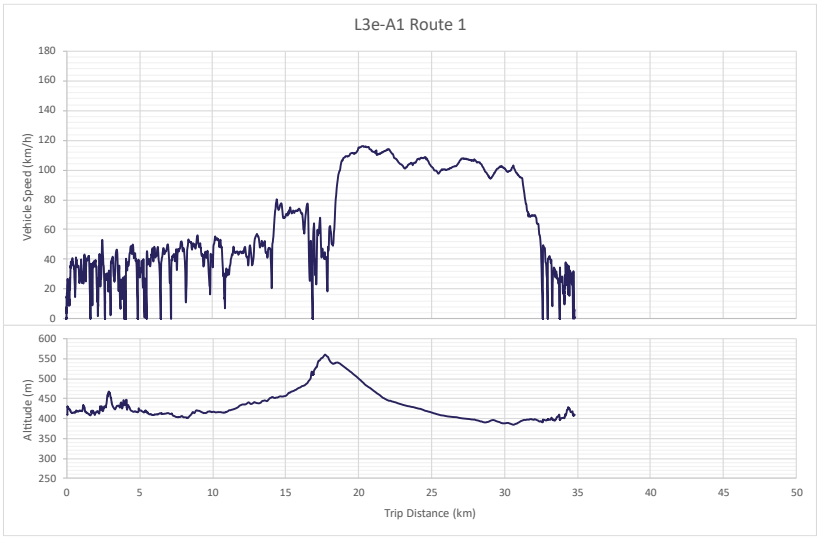

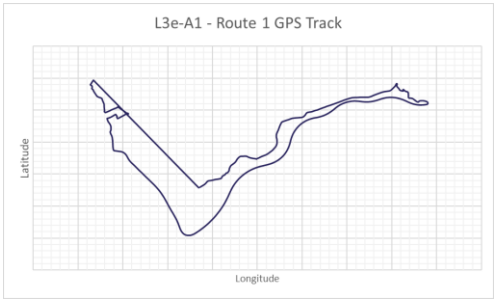

Figure B-4: L3e-A2 Route 1 vehicle speed (km/h) and altitude (m) traces. GPS Trace

This project has received funding from the European Union's Horizon Europe research and innovation programme under grant agreement No 101056777

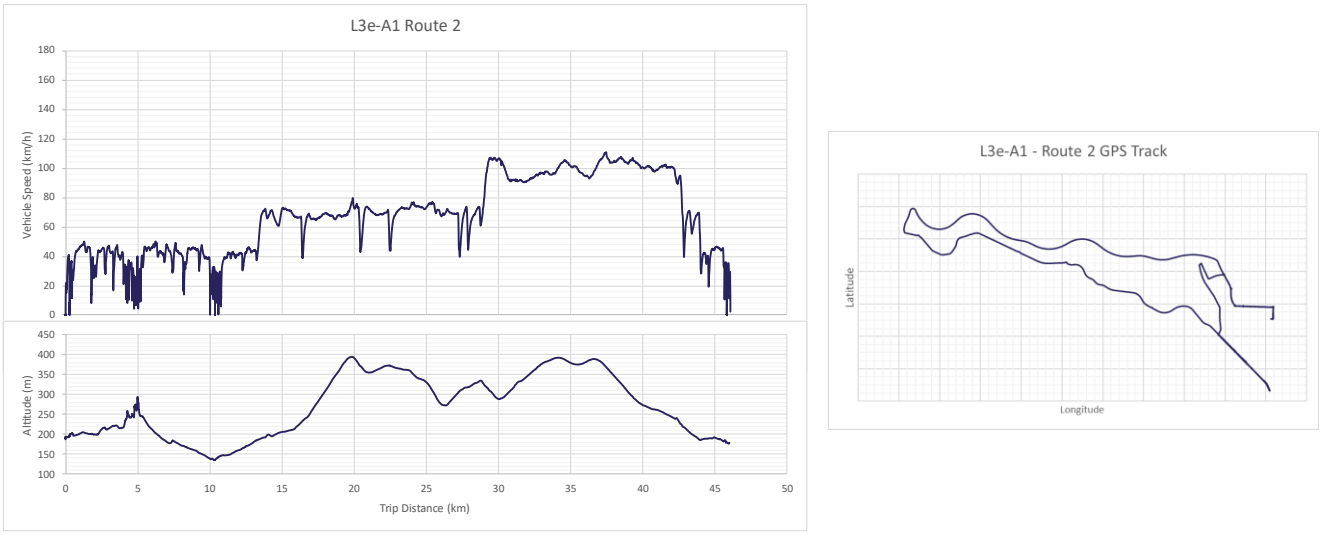

Figure B-5: L3e-A2 Route 2 vehicle speed (km/h) and altitude (m) traces. GPS Trace.

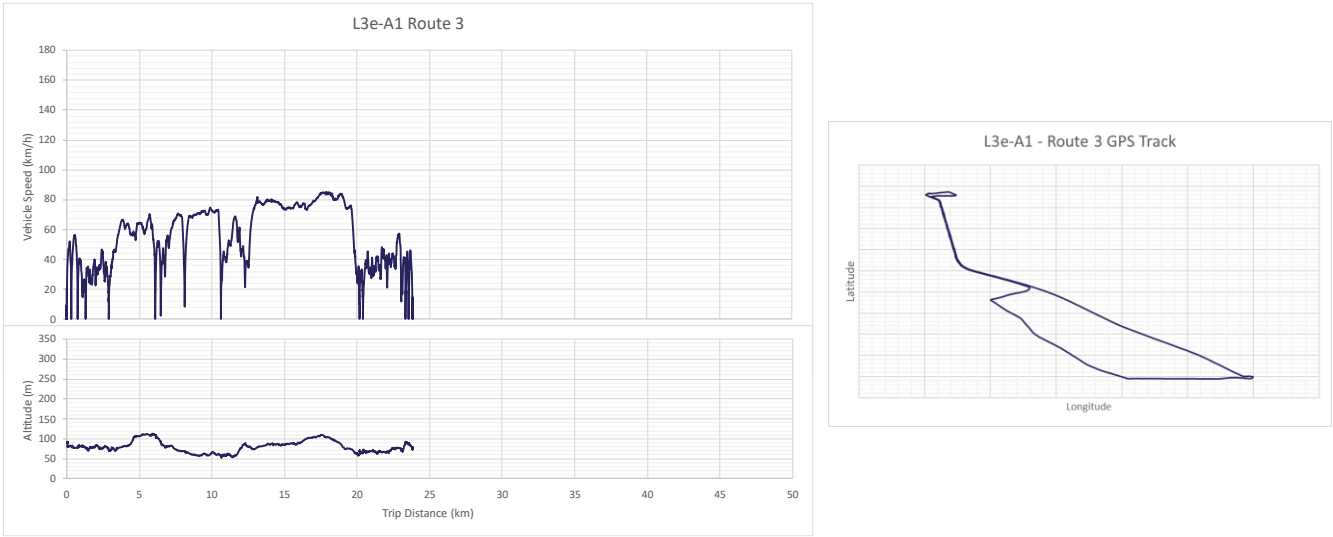

Figure B-6: L3e-A2 Route 3 vehicle speed (km/h) and altitude (m) traces. GPS Trace.

This project has received funding from the European Union's Horizon Europe research and innovation programme under grant agreement No 101056777

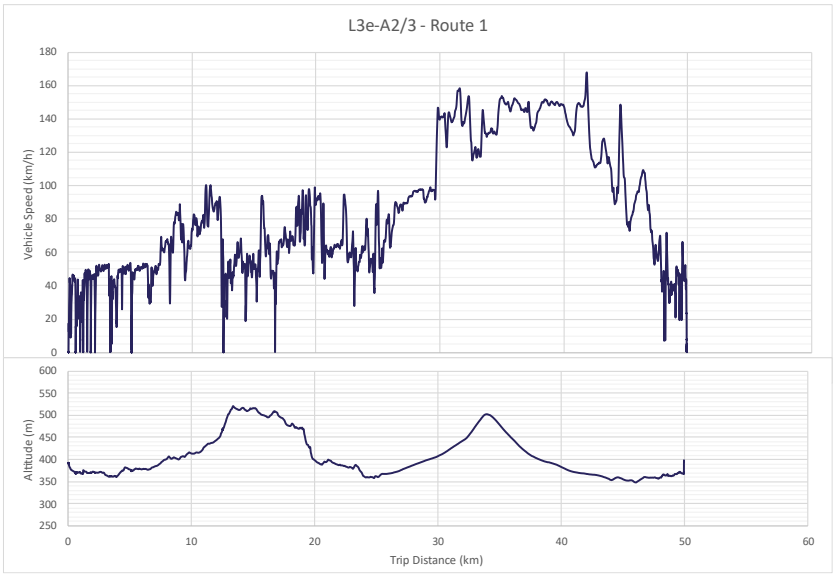

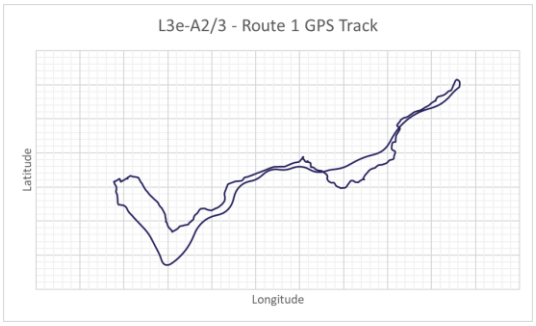

Figure B-7: L3e-A2/3 Route 1 vehicle speed (km/h) and altitude (m) traces. GPS Trace.

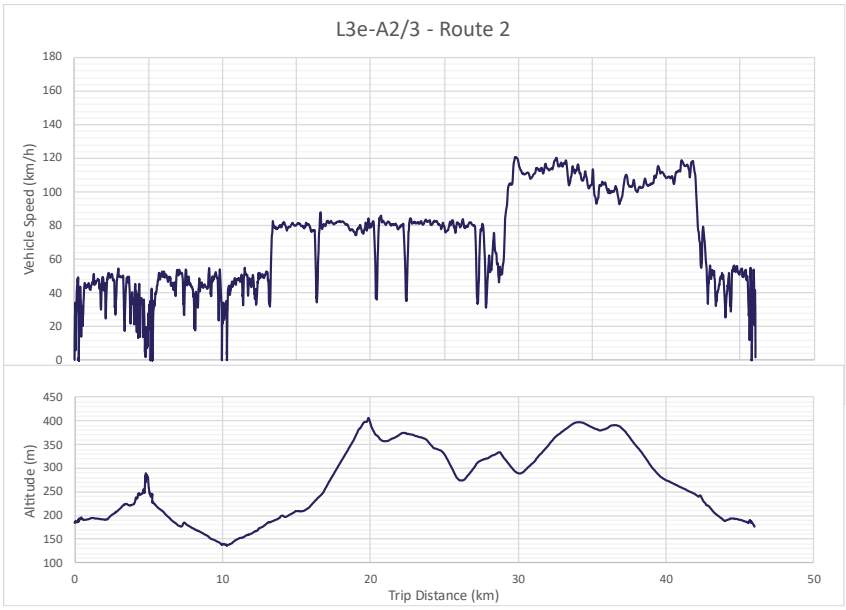

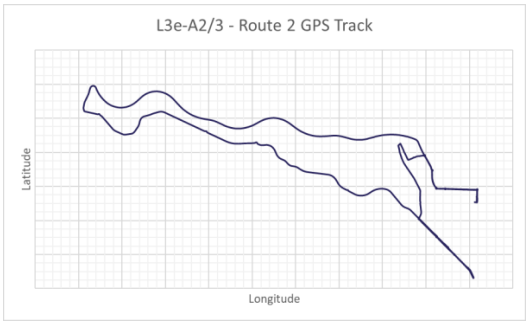

Figure B-8: L3e-A2/3 Route 2 vehicle speed (km/h) and altitude (m) traces. GPS Trace.

This project has received funding from the European Union's Horizon Europe research and innovation programme under grant agreement No 101056777

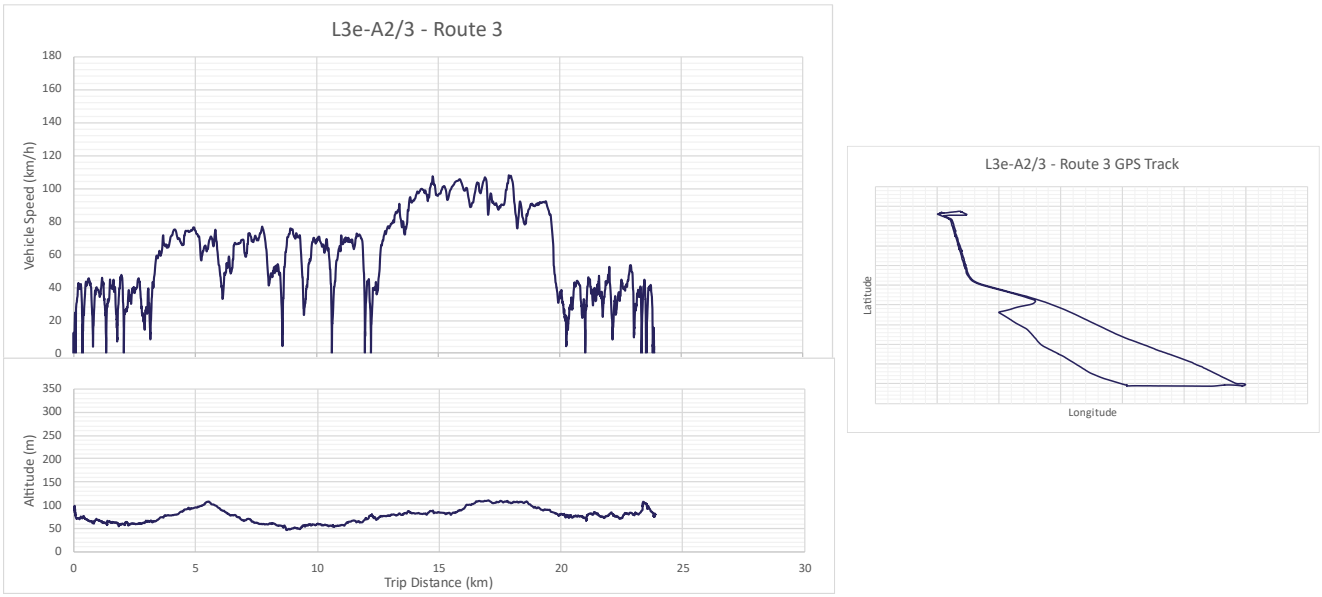

Figure B-9: L3e-A2/3 Route 3 vehicle speed (km/h) and altitude (m) traces. GPS Trace.

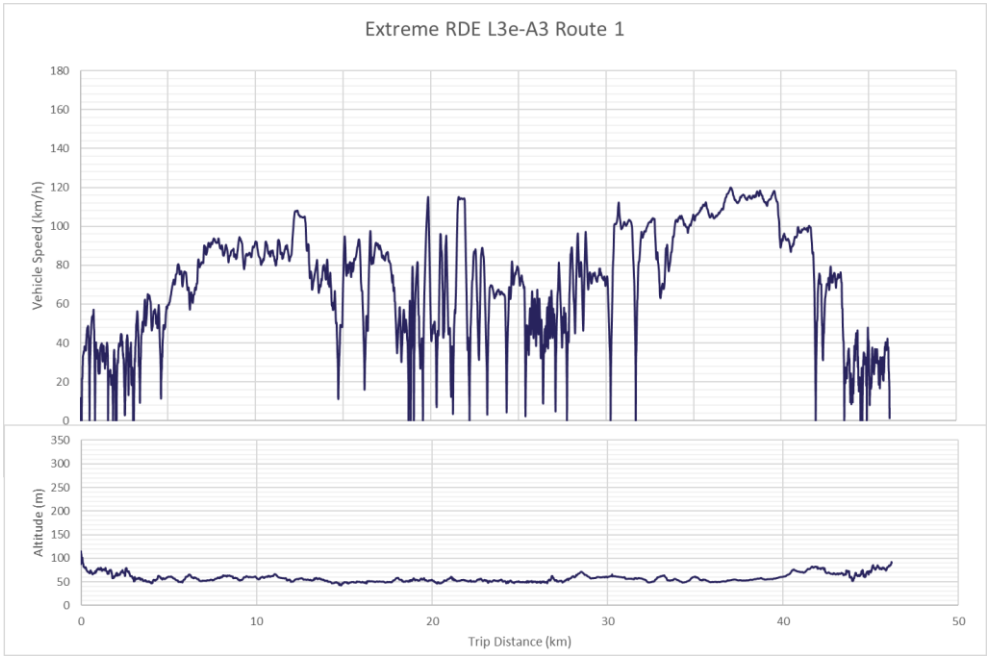

Figure B-10: L3e-A2/3 Extreme RDE Route 1 vehicle speed (km/h) and altitude (m) traces.

This project has received funding from the European Union's Horizon Europe research and innovation programme under grant agreement No 101056777

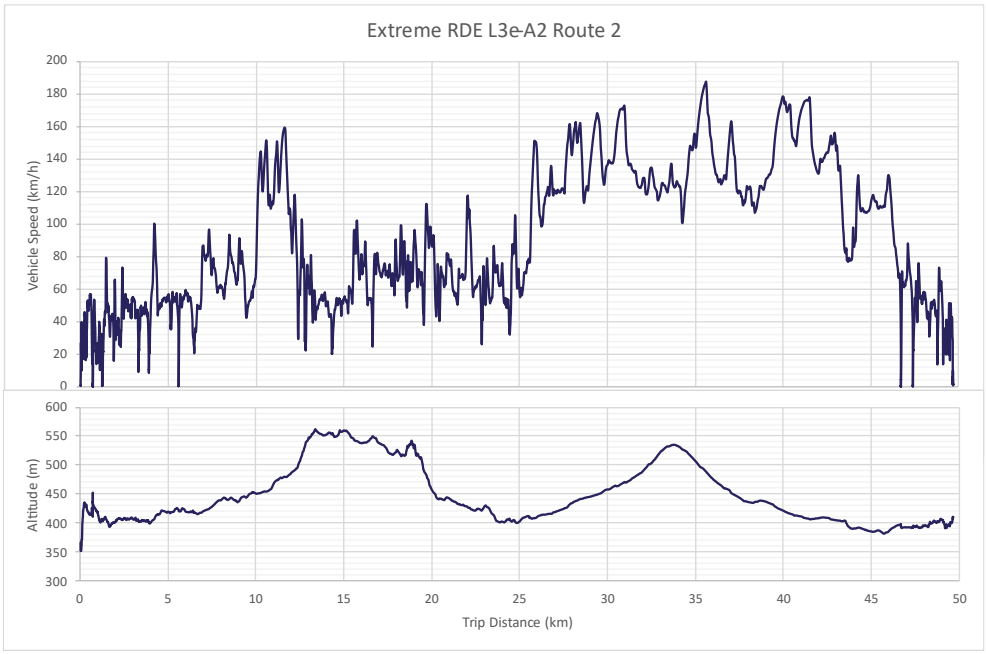

Figure B-11: L3e-A2/3 Extreme RDE Route 2 vehicle speed (km/h) and altitude (m) traces.

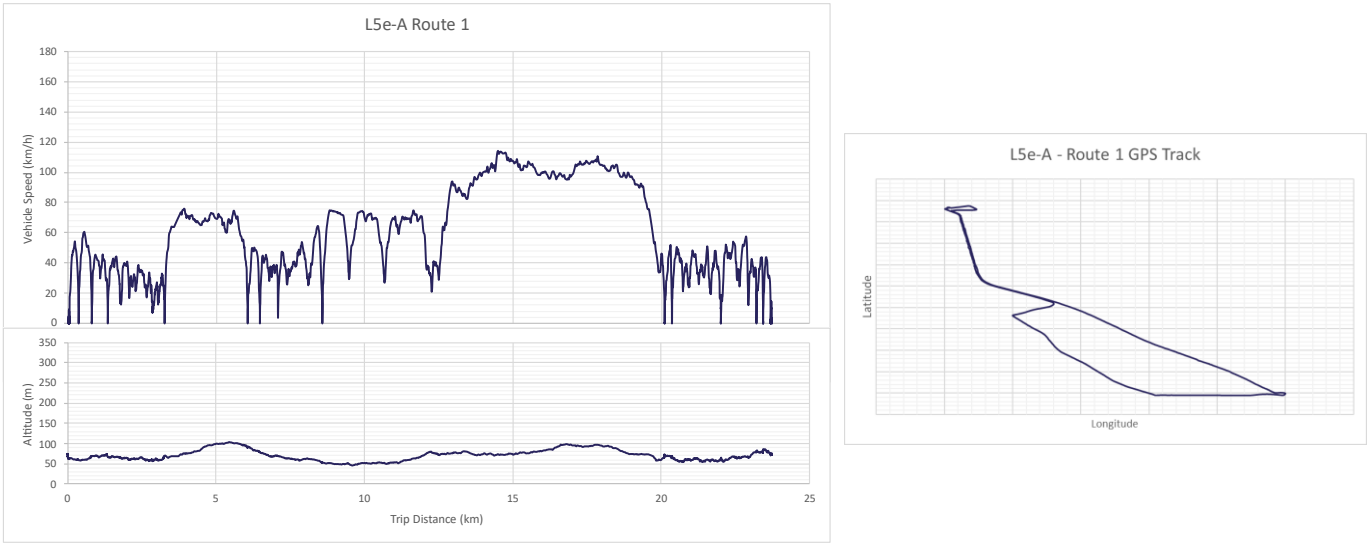

Figure B-12: L5e-A Route 1 vehicle speed (km/h) and altitude (m) traces. GPS Trace.

This project has received funding from the European Union's Horizon Europe research and innovation programme under grant agreement No 101056777

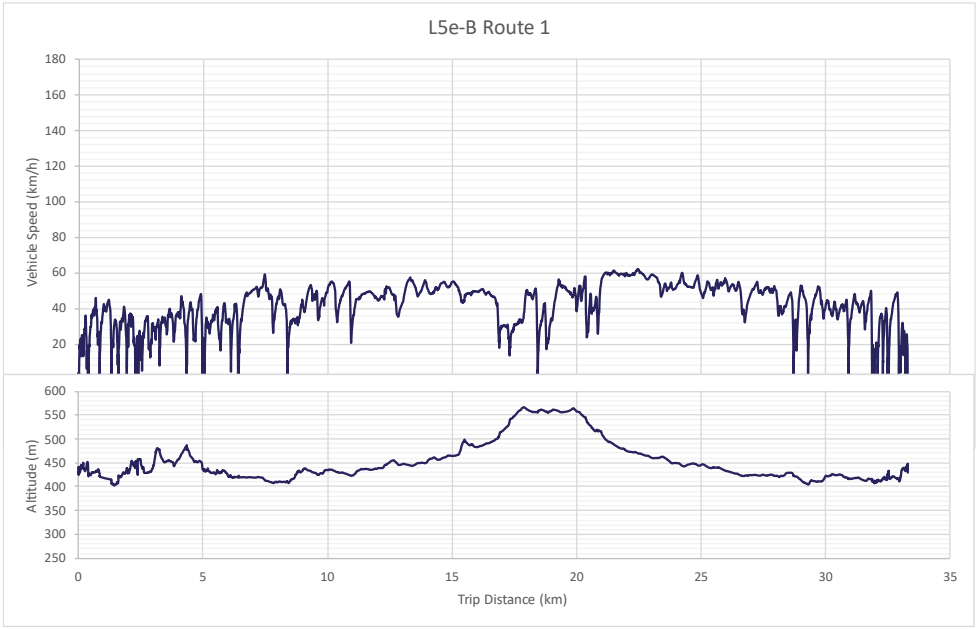

Figure B-13: L5e-B Route 1 vehicle speed (km/h) and altitude (m) traces.

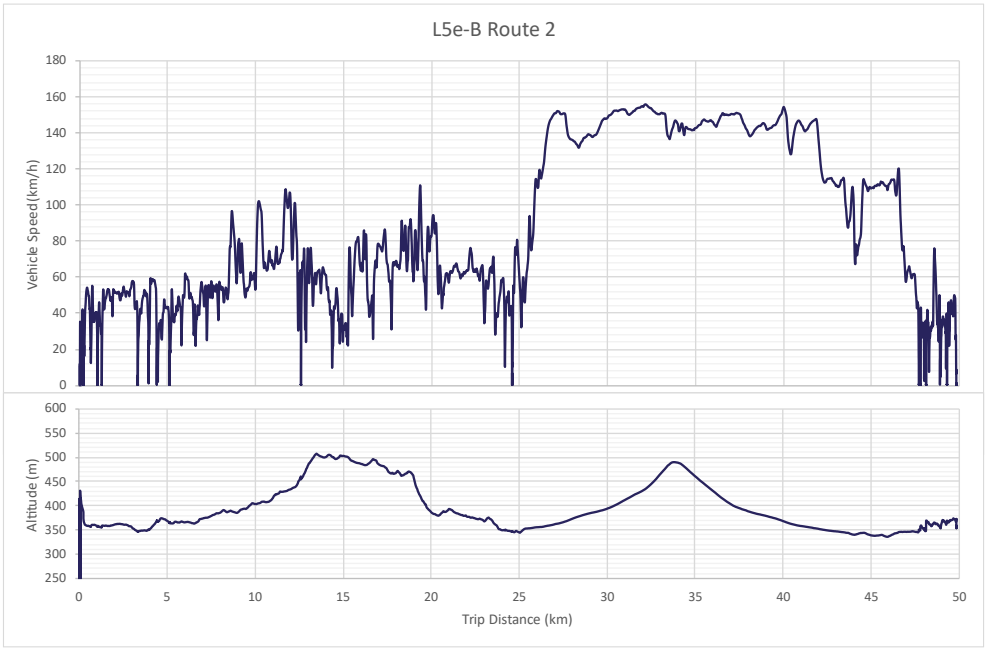

Figure B-14: L5e-B Route 2 vehicle speed (km/h) and altitude (m) traces.

This project has received funding from the European Union's Horizon Europe research and innovation programme under grant agreement No 101056777

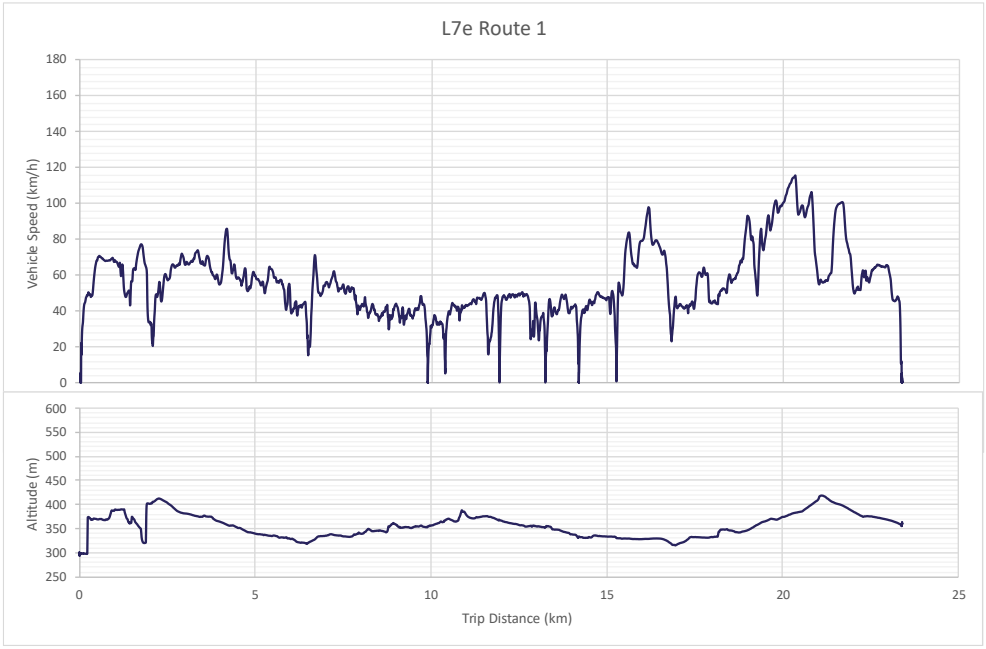

Figure B-15: L7e Route 1 vehicle speed (km/h) and altitude (m) traces.

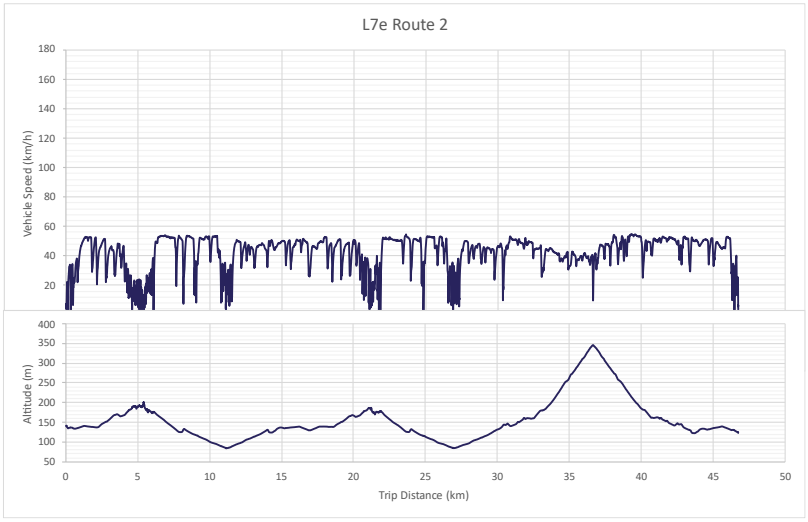

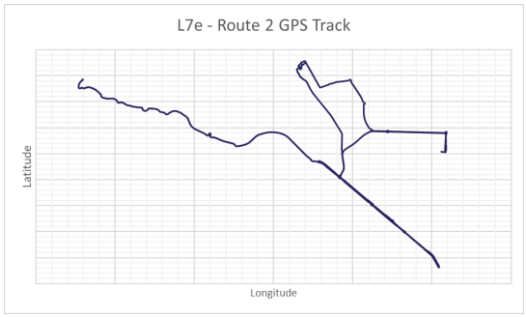

Figure B-16: L7e Route 2 vehicle speed (km/h) and altitude (m) traces. GPS Trace.

This project has received funding from the European Union's Horizon Europe research and innovation programme under grant agreement No 101056777

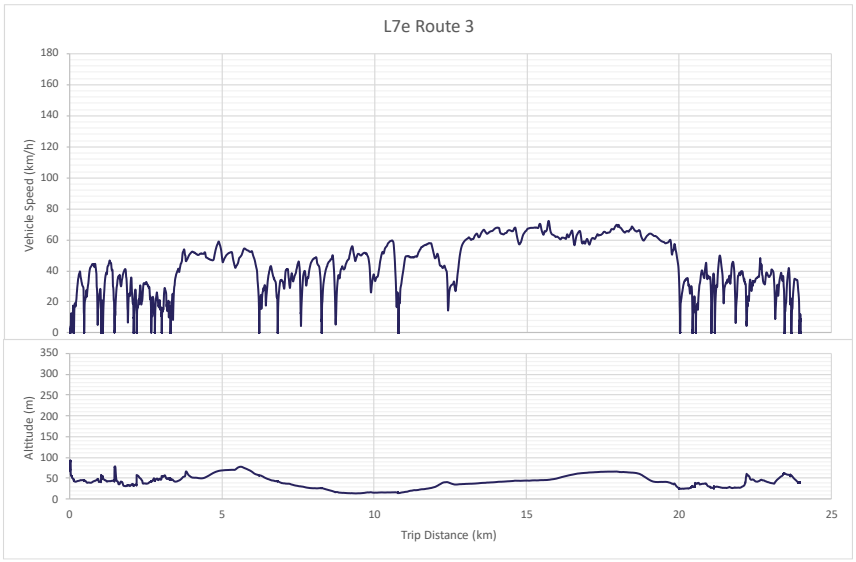

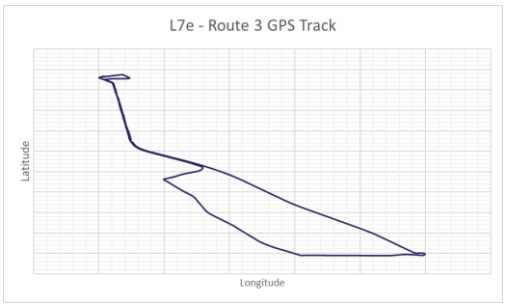

Figure B-17: L7e Route 3 vehicle speed (km/h) and altitude (m) traces. GPS Trace.

This project has received funding from the European Union's Horizon Europe research and innovation programme under grant agreement No 101056777

Appendix C: RDC Cycles

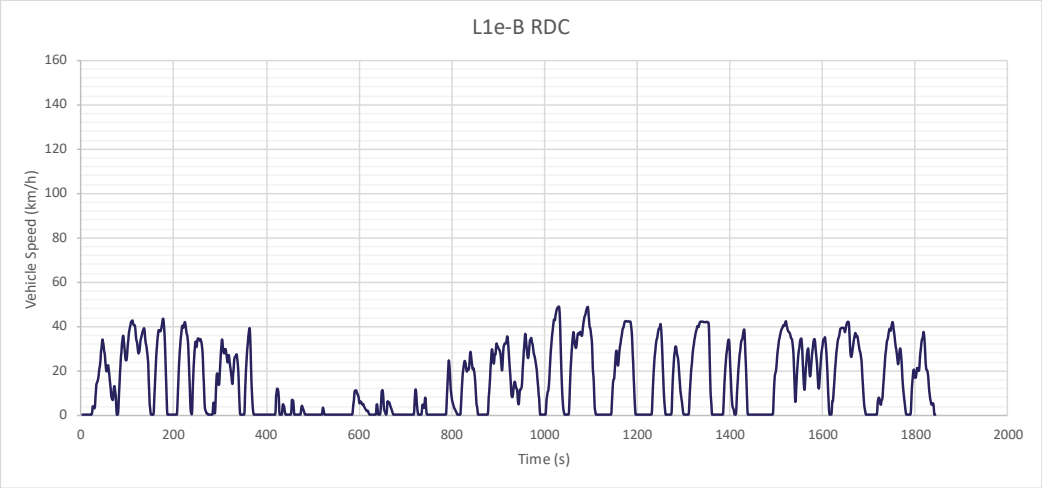

Figure C-1: L1e-B RDC chassis dyno speed trace (km/h).

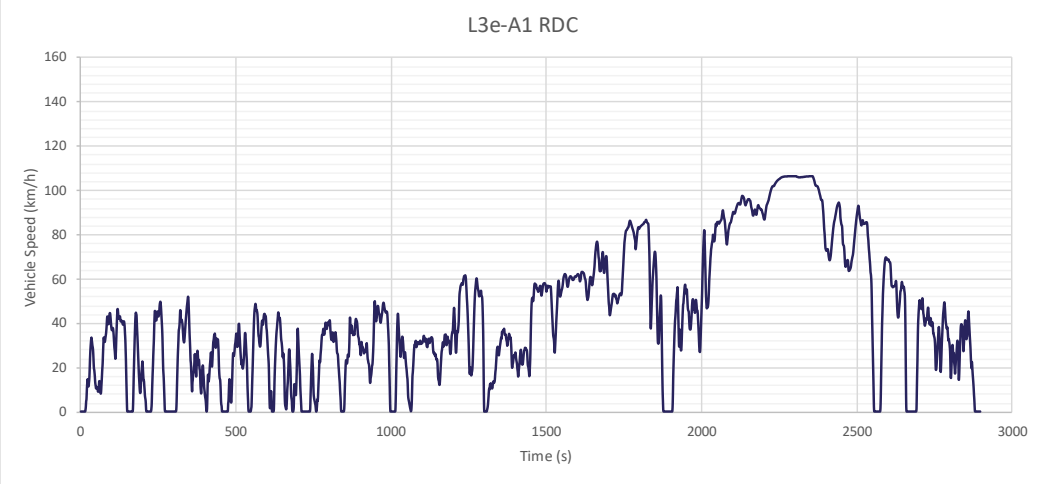

Figure C-2: L3e-A1 RDC chassis dyno speed trace (km/h).

This project has received funding from the European Union's Horizon Europe research and innovation programme under grant agreement No 101056777

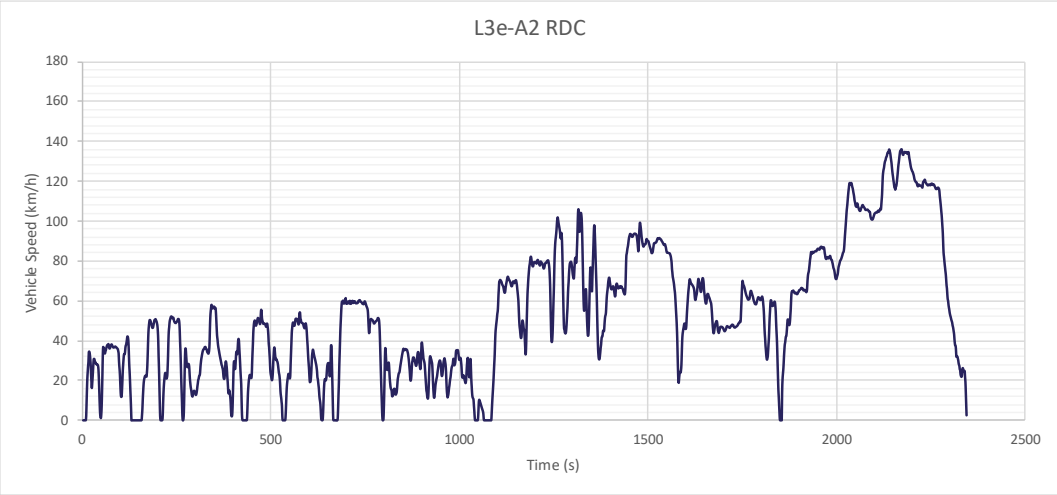

Figure C-3: L3e-A3 RDC chassis dyno speed trace (km/h).

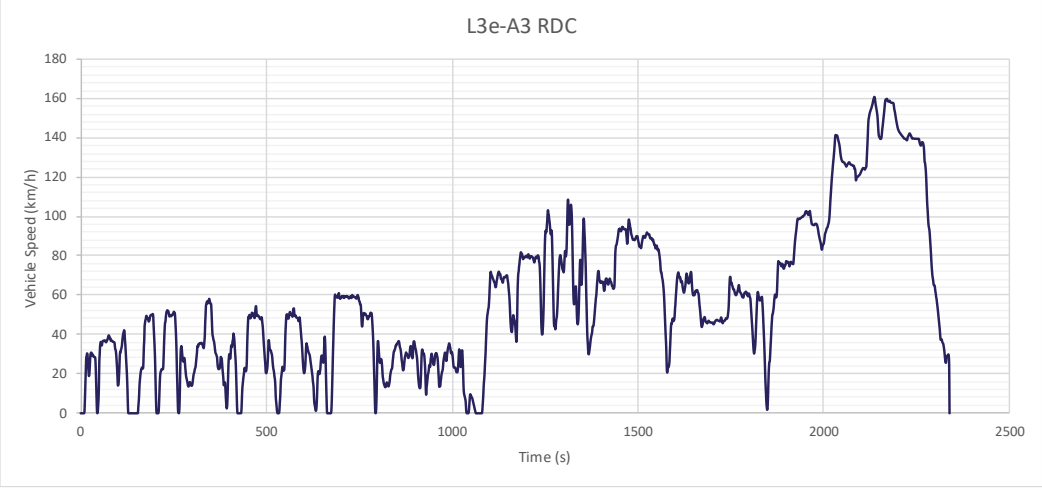

Figure C-4: L3e-A3 RDC chassis dyno speed trace (km/h).

This project has received funding from the European Union's Horizon Europe research and innovation programme under grant agreement No 101056777

Appendix D: Sound level distributions per vehicle class and driving condition

This Appendix presents a detailed graphical analysis of the noise emissions of L-category vehicles under real-world driving conditions. The results shown are based on the driving patterns defined in Table 2-2 for vehicles with manual transmissions (MT) and in Table 2-3 for vehicles with continuously variable transmissions (CVT). The analysis distinguishes between these two transmission types, as this differentiation is also relevant in the legal regulations for Type Approval (TA).

For the assessment of acoustic emissions, the A-weighted sound pressure level in dB(A) was selected as the key analysis parameter. This metric serves as the primary reference in all current TA procedures and thus represents the main criterion for evaluating regulatory compliance. For the comparative analysis in this appendix, the focus was placed on A-weighted sound pressure level as it is the primary reference in all current TA procedures and the main criterion for evaluating regulatory compliance. While this single metric allows for a targeted comparison of overall noise levels, a more in-depth evaluation of other noise characteristics, such as spectral content and temporal variations, is provided in other sections of the report (e.g., Section 3.2.3 and Appendix E: Sound characteristics of critical driving conditions measured on test tracks) to build a comprehensive understanding.

To visualize the measurement results, violin plots are used. These plots effectively illustrate both the central tendency and the distribution of measured values within individual vehicle classes. The width of the violin represents a normalized depiction of the data distribution and reaches its maximum at the peak of the distribution. The absolute width has no direct meaning; rather, it indicates the relative density of measurement values. The shape of the violin provides an intuitive understanding of whether the sound pressure levels of a given vehicle category are clustered around a specific value or dispersed across a wider range. Since the width is scaled, it does not reflect the absolute number of data points but rather the relative distribution of the values.

For each analyzed driving pattern, two individual measurements were generally conducted per vehicle. In the analysis, the maximum of the two measured A-weighted sound pressure levels measured at the roadside microphone position on the PP' line is considered in each case. Each data point shown thus represents a single vehicle and its maximum determined noise emission under the respective driving pattern.

This project has received funding from the European Union's Horizon Europe research and innovation programme under grant agreement No 101056777

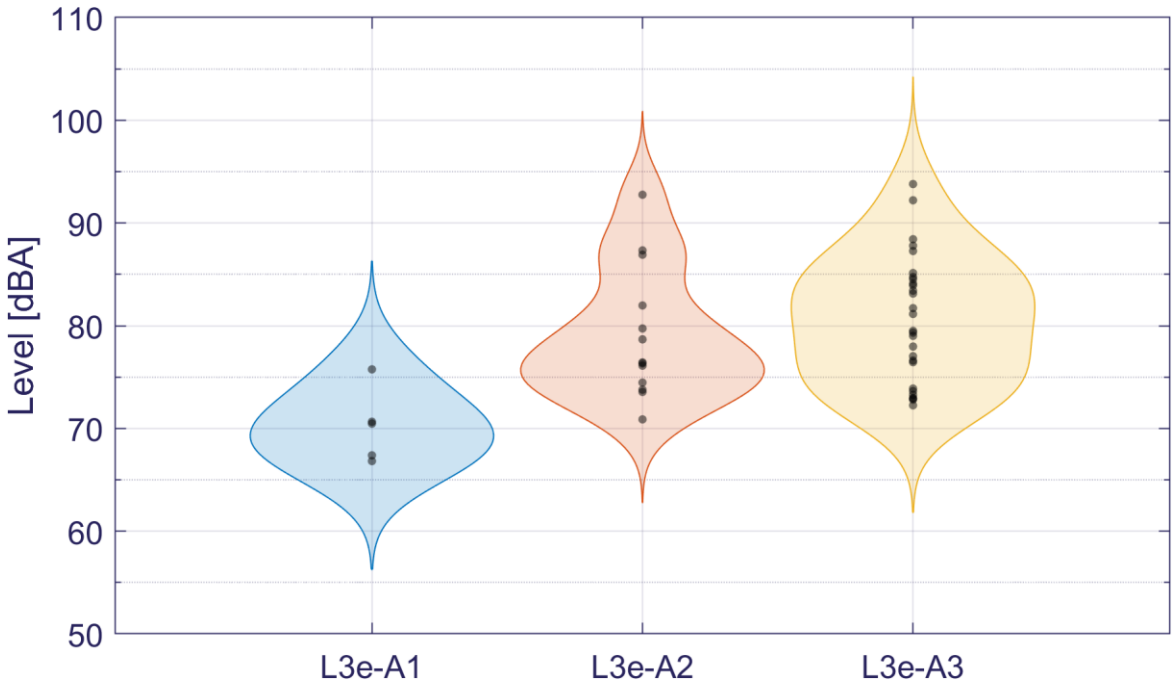

Figure D-1: Sound level vs. subcategory for on-road measurements for driving pattern 4 (moderate acc. from standstill).

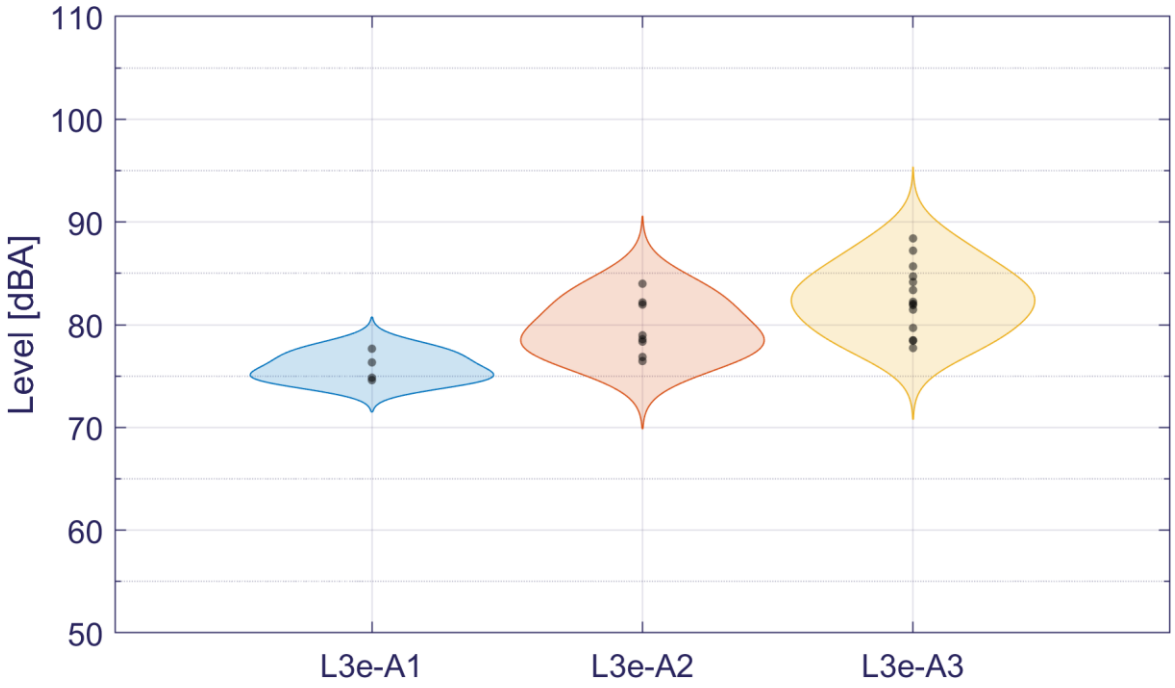

Figure D-2: Sound level vs. subcategory for on-road measurements for driving pattern 5 (Gear shift, first to second, from standstill).

This project has received funding from the European Union's Horizon Europe research and innovation programme under grant agreement No 101056777

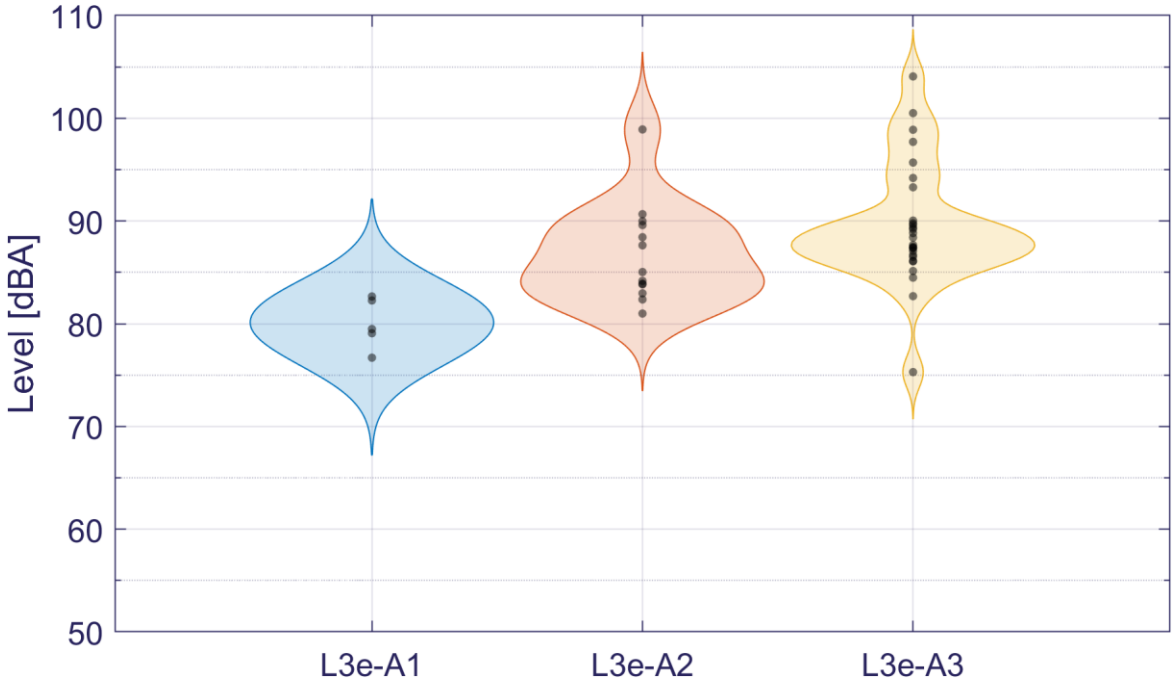

Figure D-3: Sound level vs. subcategory for on-road measurements for driving pattern 6 (Aggressive acc. from const. speed, first gear).

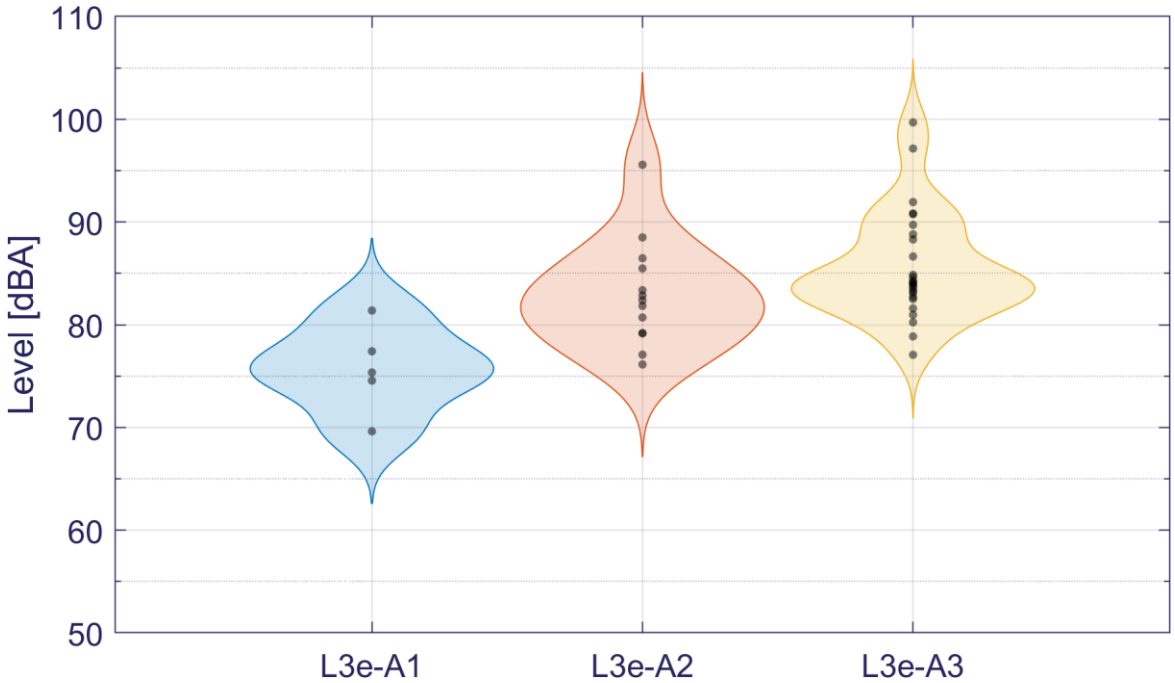

Figure D-4: Sound level vs. subcategory for on-road measurements for driving pattern 7 (Gear shift, first to second, const. speed).

This project has received funding from the European Union's Horizon Europe research and innovation programme under grant agreement No 101056777

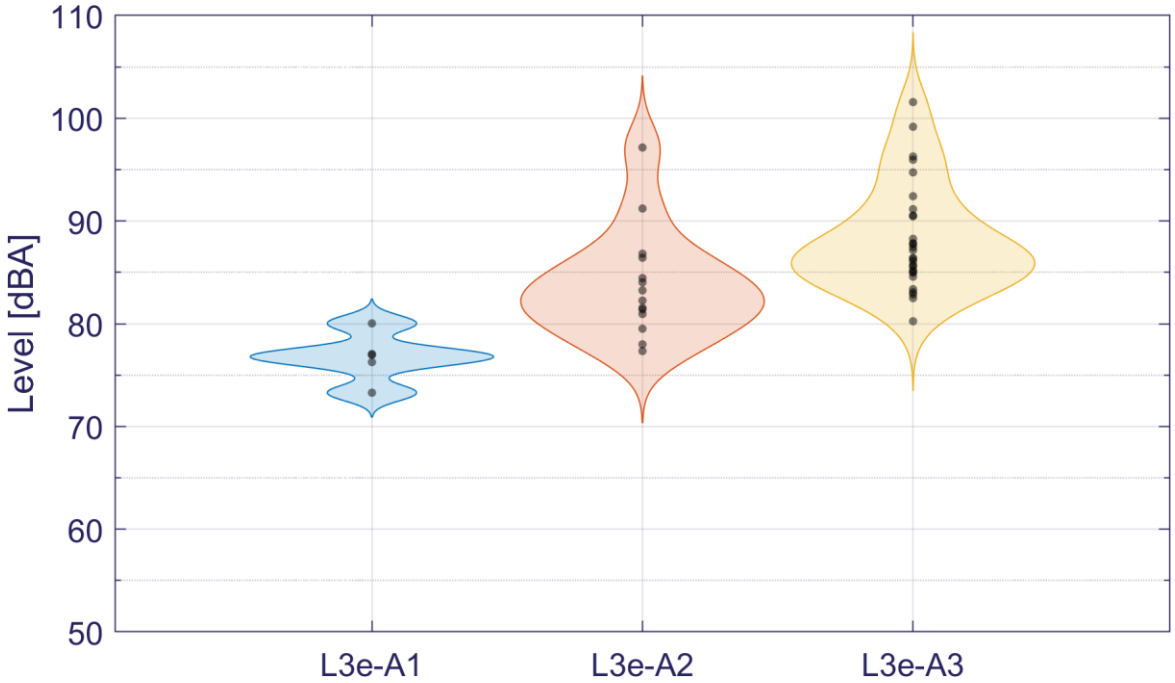

Figure D-5: Sound level vs. subcategory for on-road measurements for driving pattern 8 (Full/ max. throttle acc., gear 2).

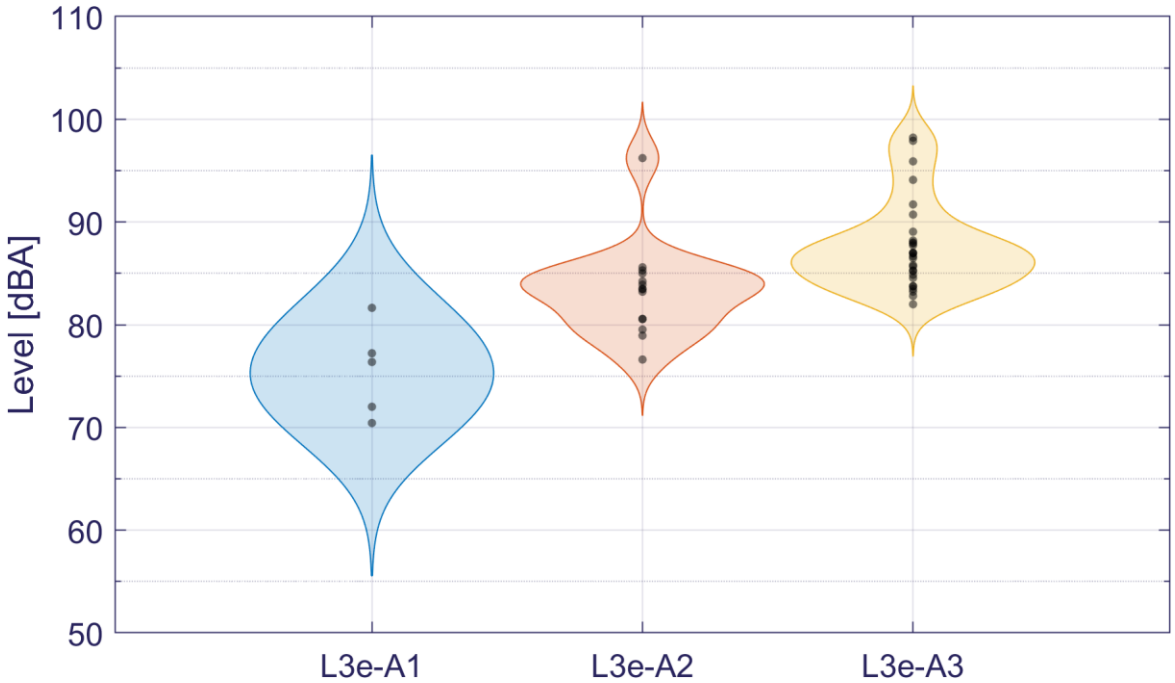

Figure D-6: Sound level vs. subcategory for on-road measurements for driving pattern 8 (Full/ max. throttle acc., gear 3).

This project has received funding from the European Union's Horizon Europe research and innovation programme under grant agreement No 101056777

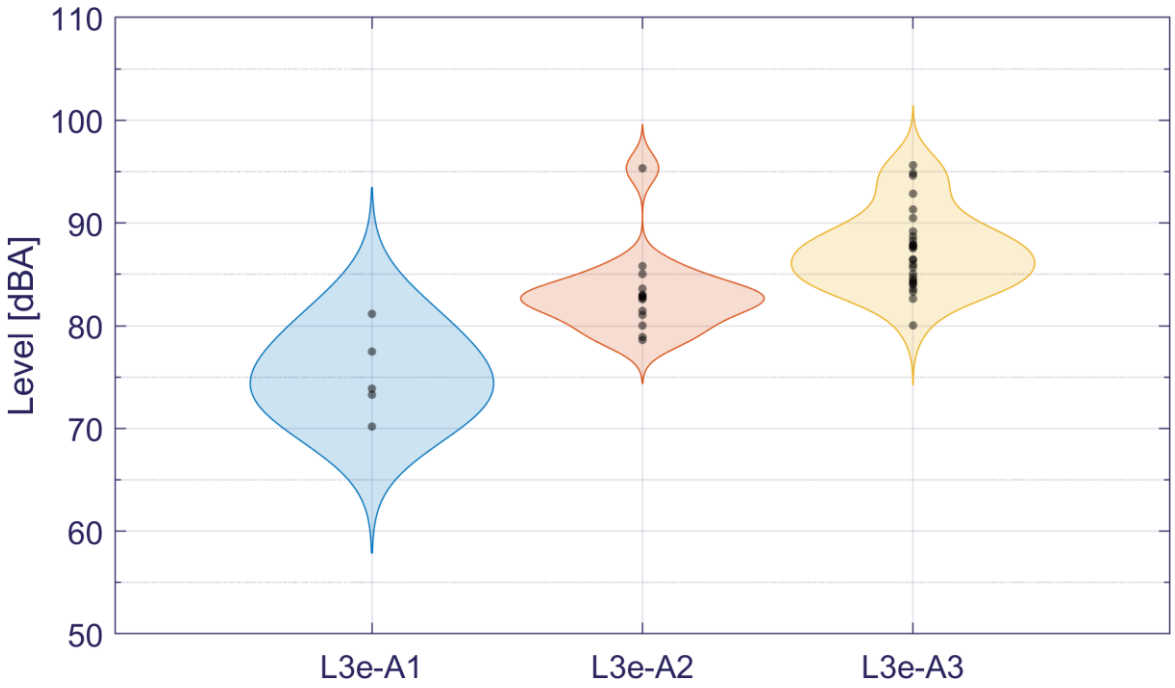

Figure D-7: Sound level vs. subcategory for on-road measurements for driving pattern 8 (Full/ max. throttle acc., gear 4).

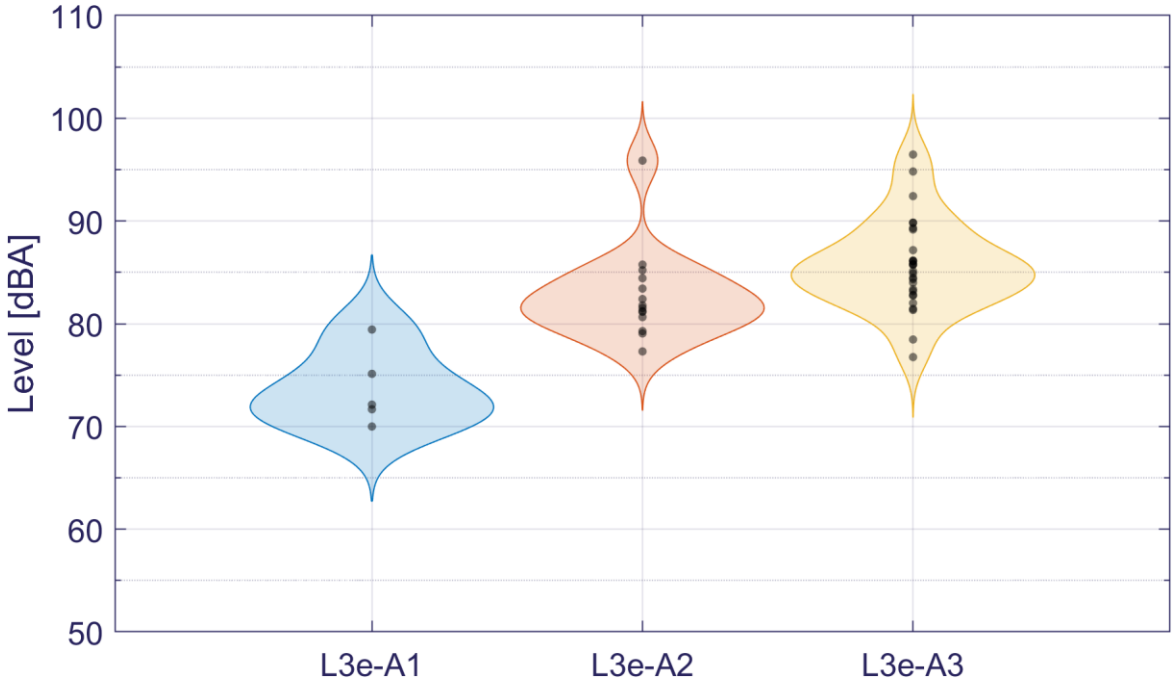

Figure D-8: Sound level vs. subcategory for on-road measurements for driving pattern 9 (Gear shift, from const. Speed, gear 2 to 3).

This project has received funding from the European Union's Horizon Europe research and innovation programme under grant agreement No 101056777

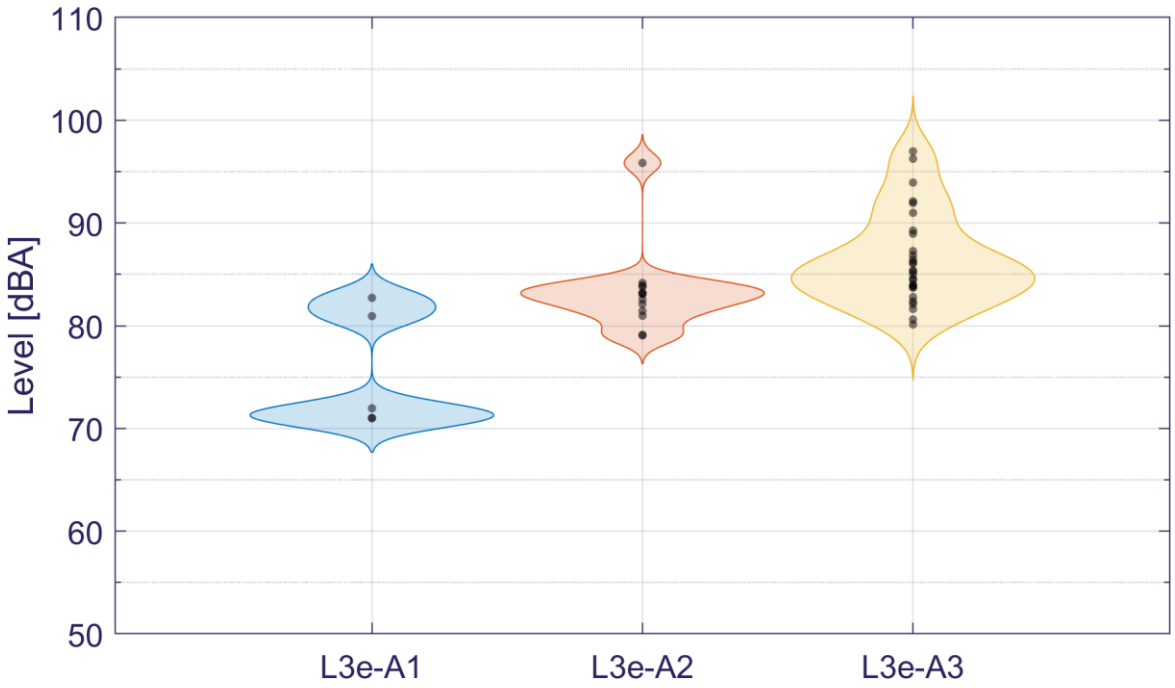

Figure D-9: Sound level vs. subcategory for on-road measurements for driving pattern 9 (Gear shift, from const. Speed, gear 3 to 4).

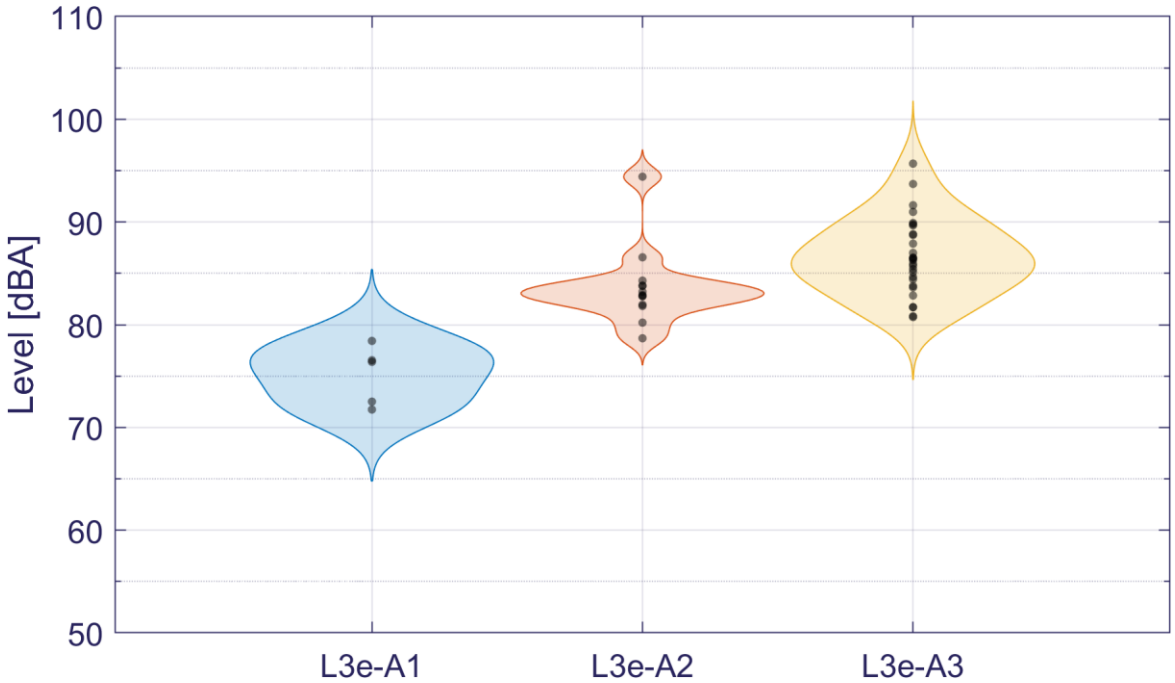

Figure D-10: Sound level vs. subcategory for on-road measurements for driving pattern 9 (Gear shift, from const. Speed, gear 4 to 5).

This project has received funding from the European Union's Horizon Europe research and innovation programme under grant agreement No 101056777

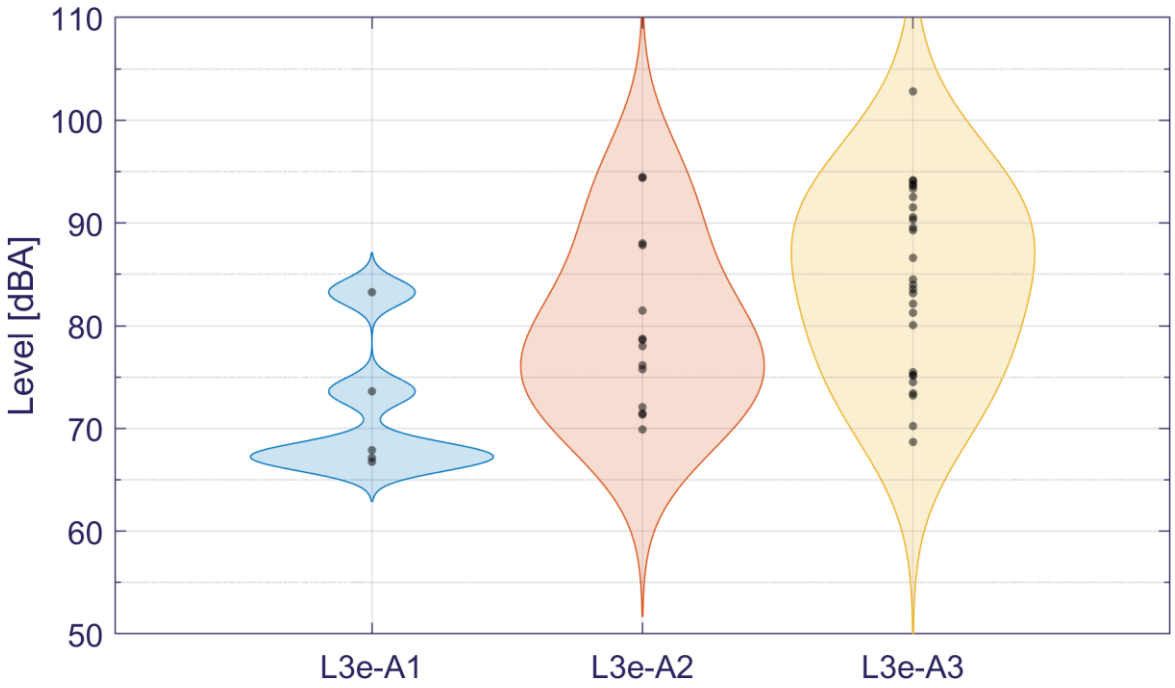

Figure D-11: Sound level vs. subcategory for on-road measurements for driving pattern 10 (Constant speed, high/max. engine speed, gear 1).

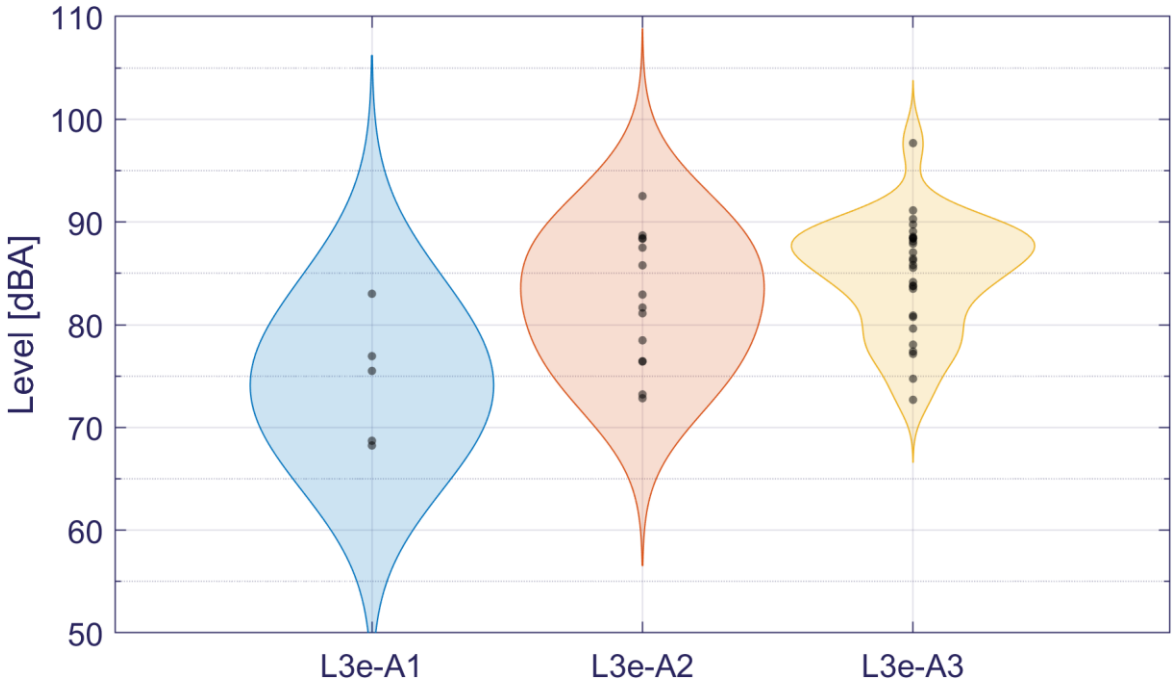

Figure D-12: Sound level vs. subcategory for on-road measurements for driving pattern 10 (Constant speed, high/max. engine speed, gear 2).

This project has received funding from the European Union's Horizon Europe research and innovation programme under grant agreement No 101056777

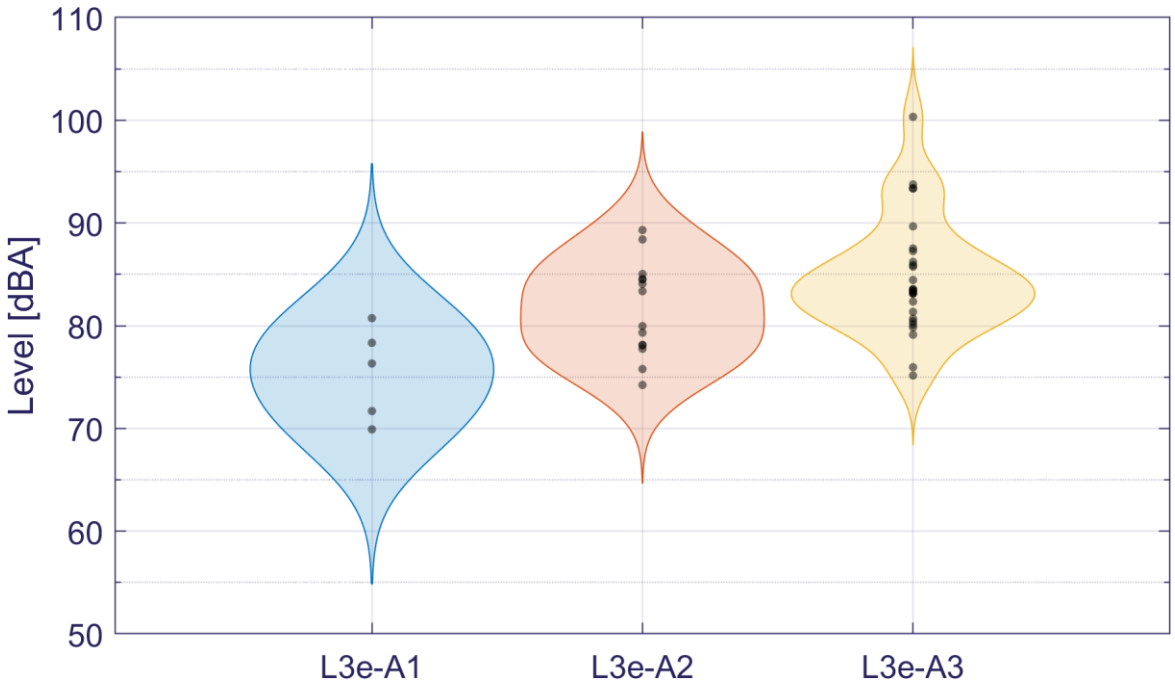

Figure D-13: Sound level vs. subcategory for on-road measurements for driving pattern 10 (Constant speed, high/max. engine speed, gear 3).

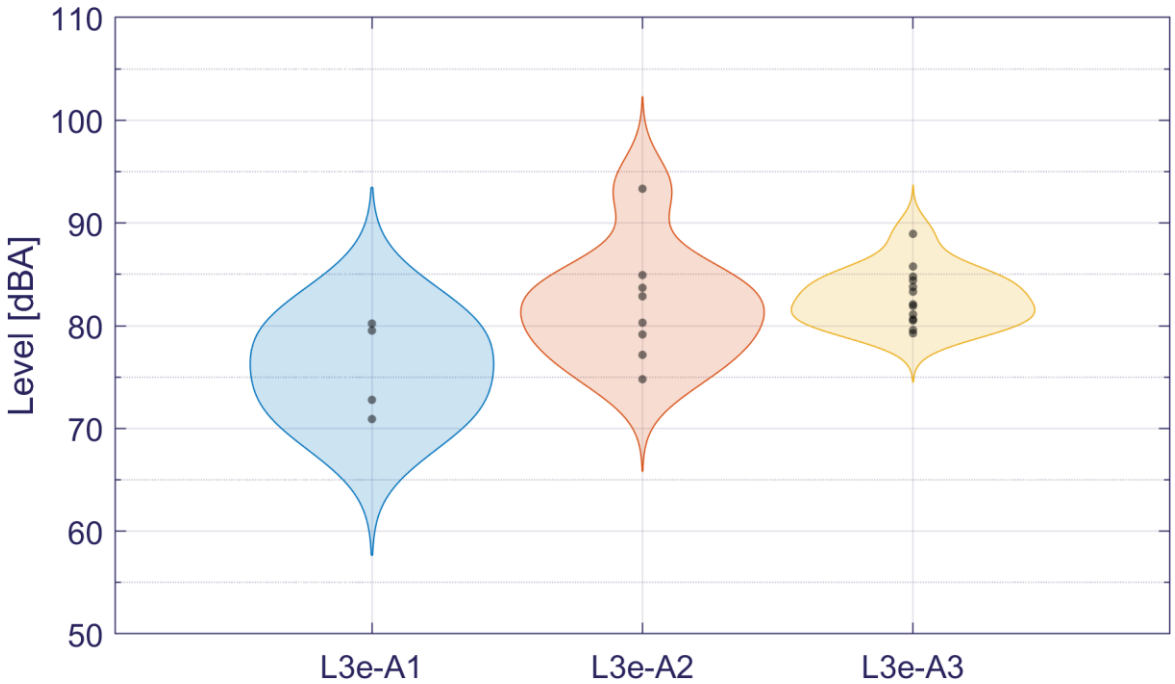

Figure D-14: Sound level vs. subcategory for on-road measurements for driving pattern 10 (Constant speed, high/max. engine speed, gear 4).

This project has received funding from the European Union's Horizon Europe research and innovation programme under grant agreement No 101056777

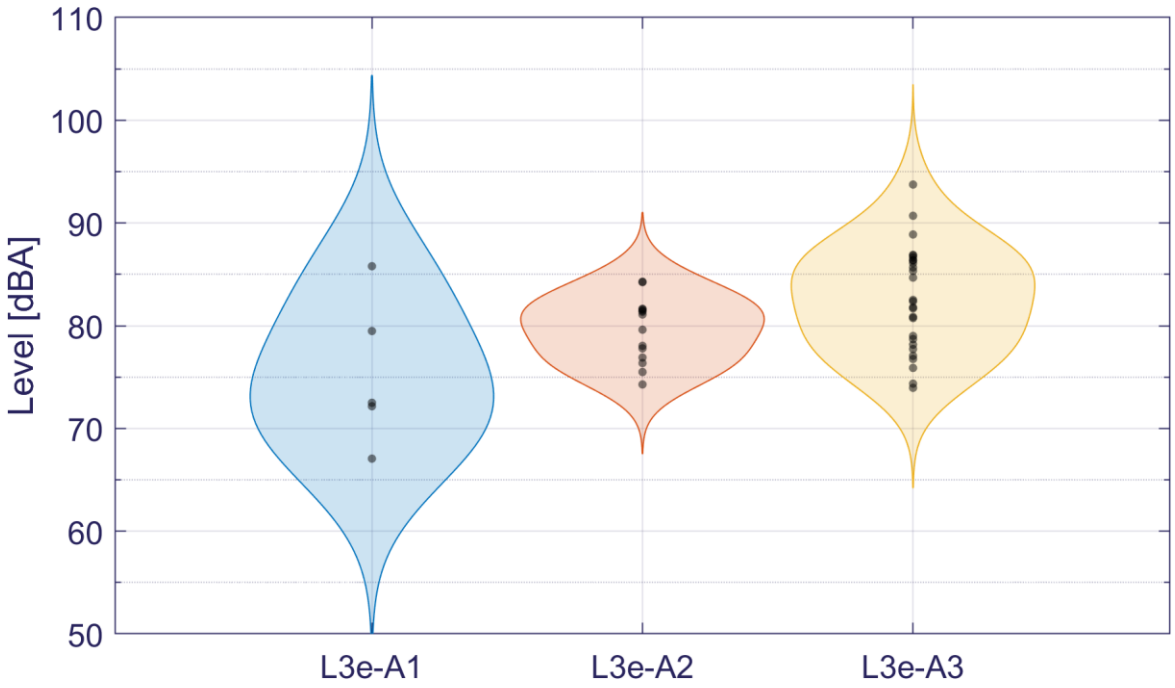

Figure D-15: Sound level vs. subcategory for on-road measurements for driving pattern 11 (Gear shift, from const. Speed, gear 2 to 1).

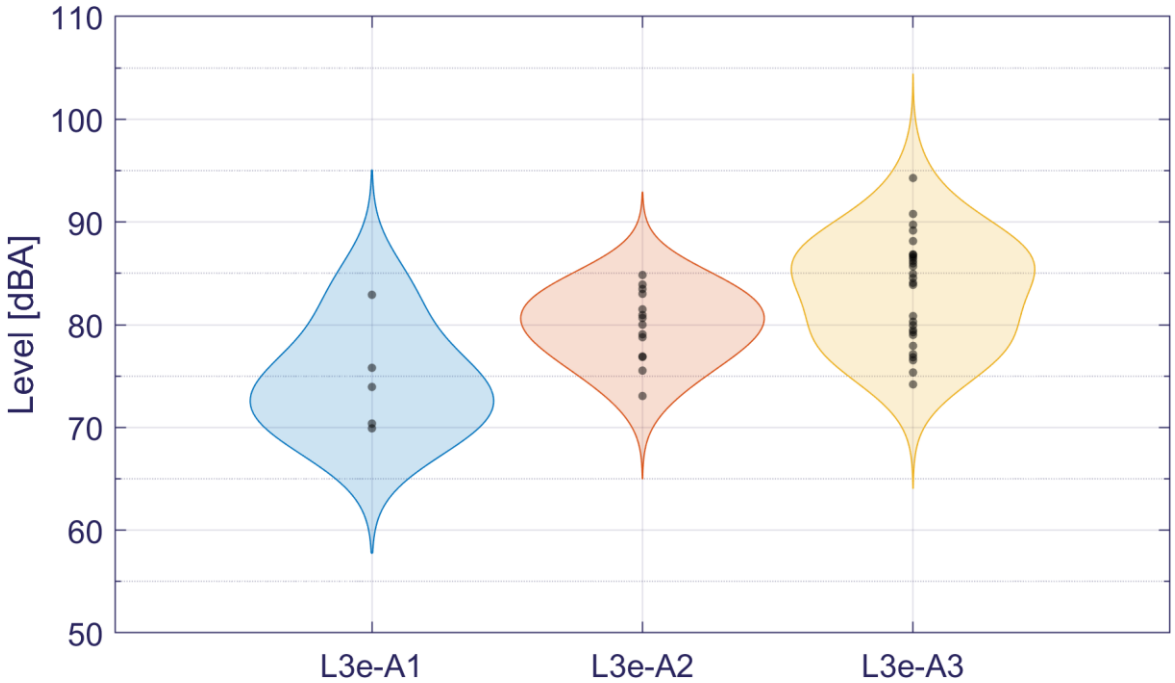

Figure D-16: Sound level vs. subcategory for on-road measurements for driving pattern 11 (Gear shift, from const. Speed, gear 3 to 2).

This project has received funding from the European Union's Horizon Europe research and innovation programme under grant agreement No 101056777

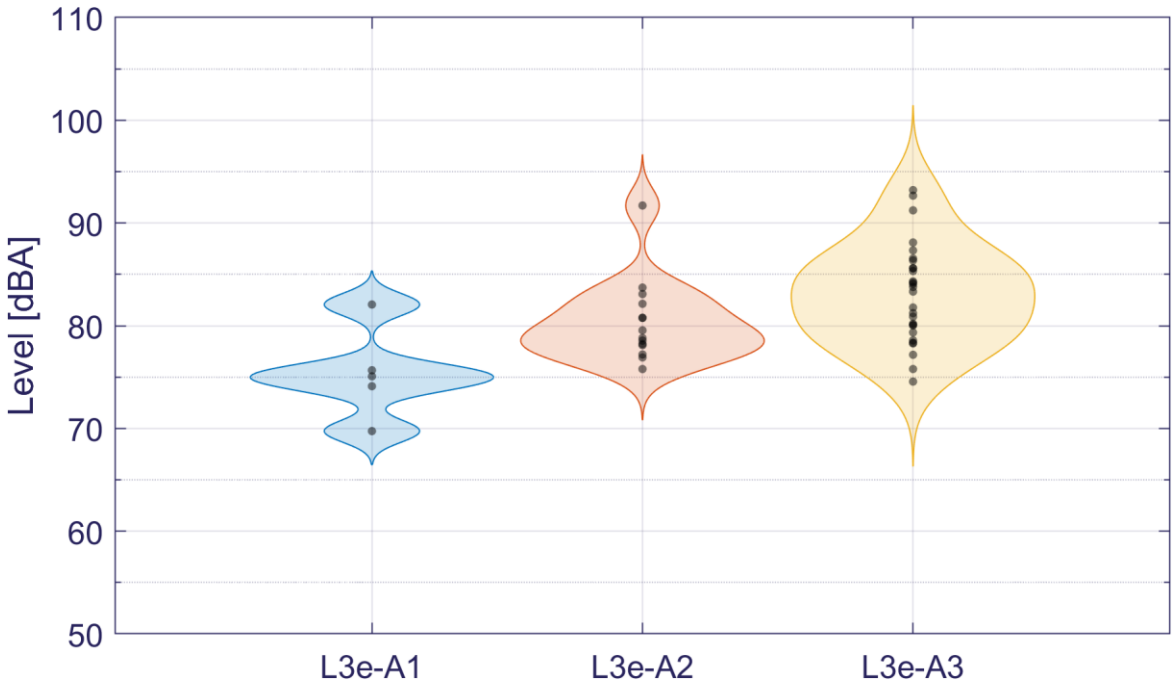

Figure D-17: Sound level vs. subcategory for on-road measurements for driving pattern 11 (Gear shift, from const. Speed, gear 4 to 3).

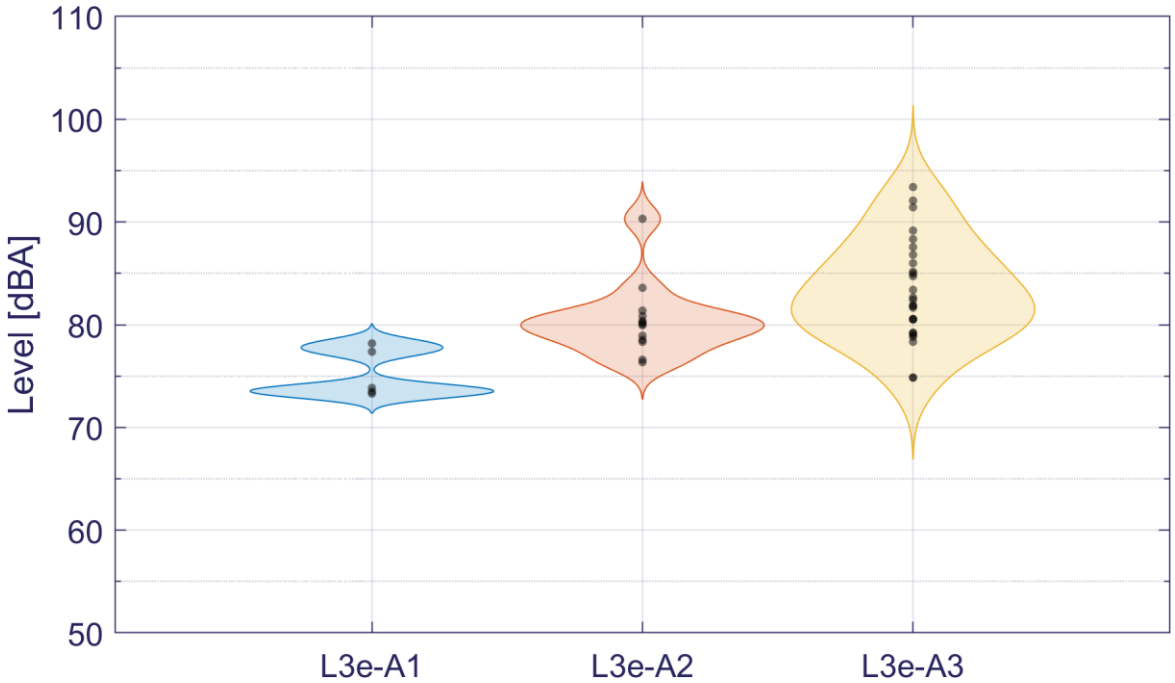

Figure D-18: Sound level vs. subcategory for on-road measurements for driving pattern 11 (Gear shift, from const. Speed, gear 5 to 4).

This project has received funding from the European Union's Horizon Europe research and innovation programme under grant agreement No 101056777

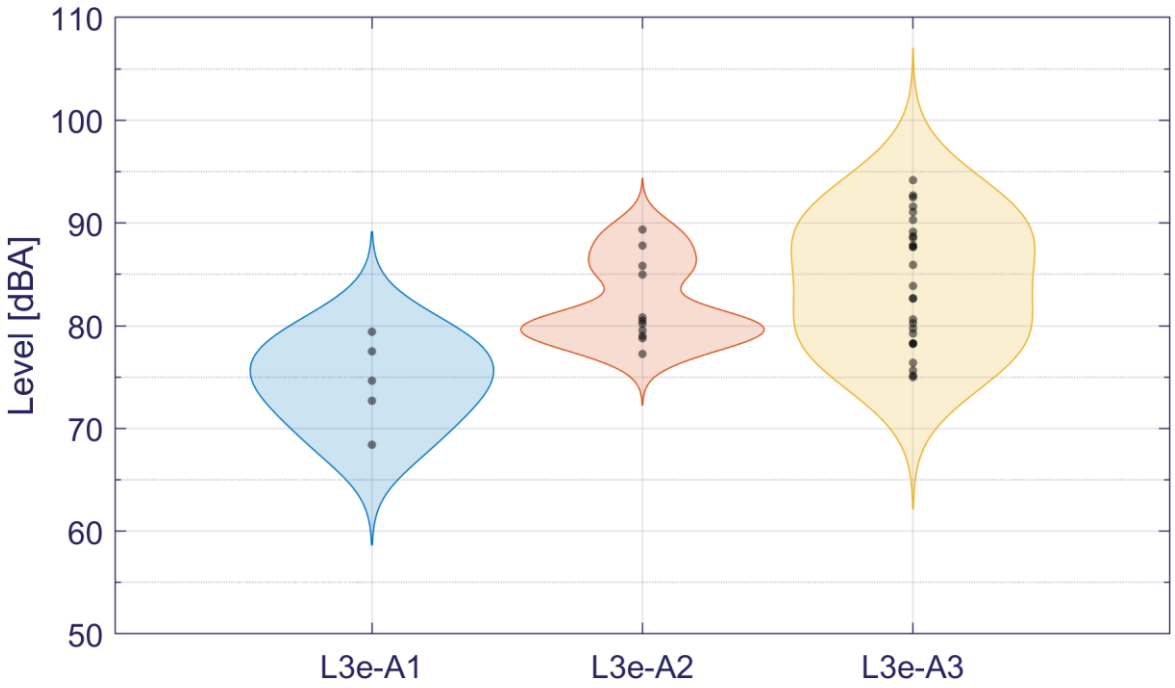

Figure D-19: Sound level vs. subcategory for on-road measurements for driving pattern 13 (Intermittent throttle control, gear 1).

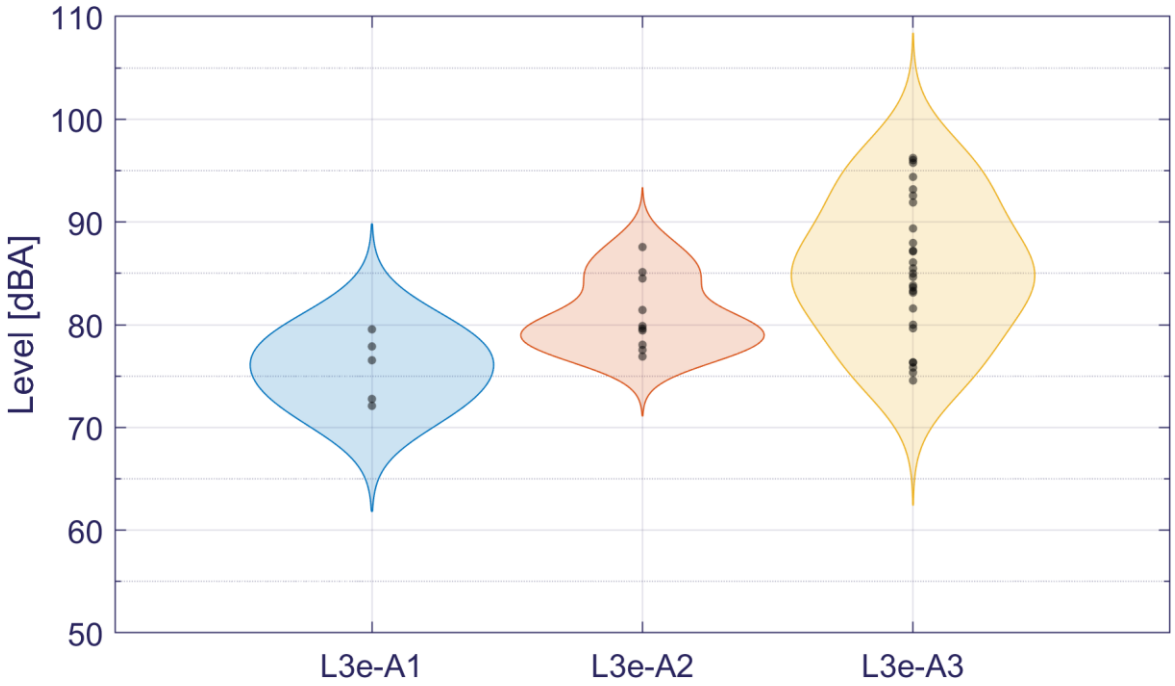

Figure D-20: Sound level vs. subcategory for on-road measurements for driving pattern 13 (Intermittent throttle control, gear 2).

This project has received funding from the European Union's Horizon Europe research and innovation programme under grant agreement No 101056777

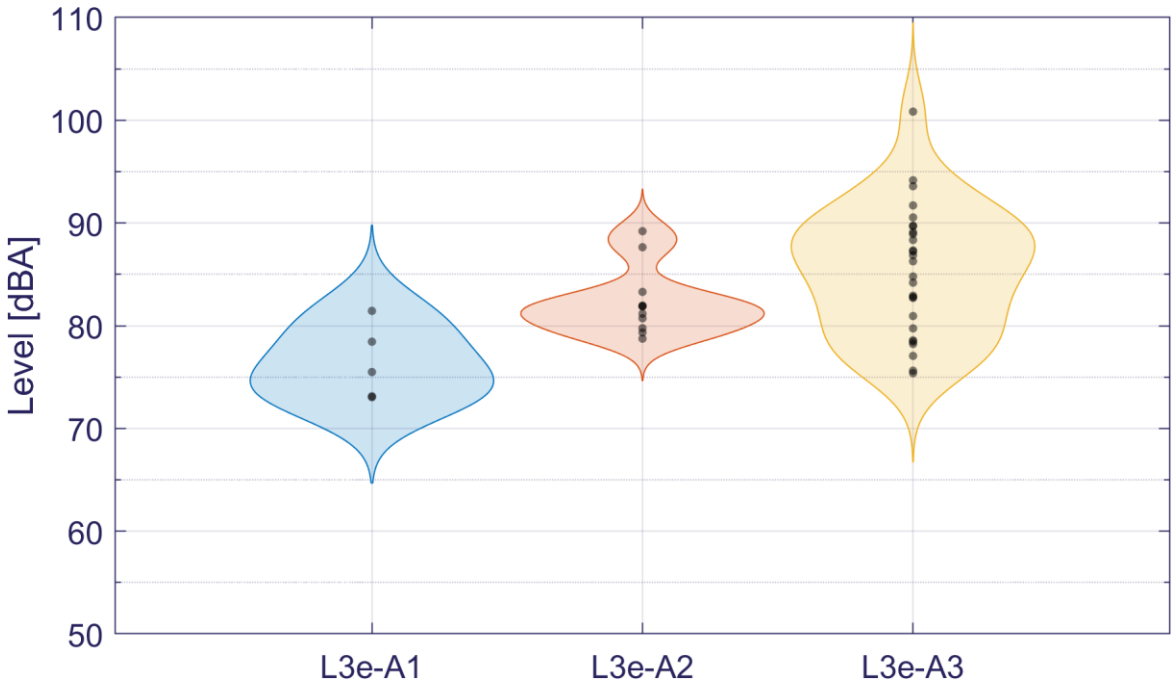

Figure D-21: Sound level vs. subcategory for on-road measurements for driving pattern 13 (Intermittent throttle control, gear 3).

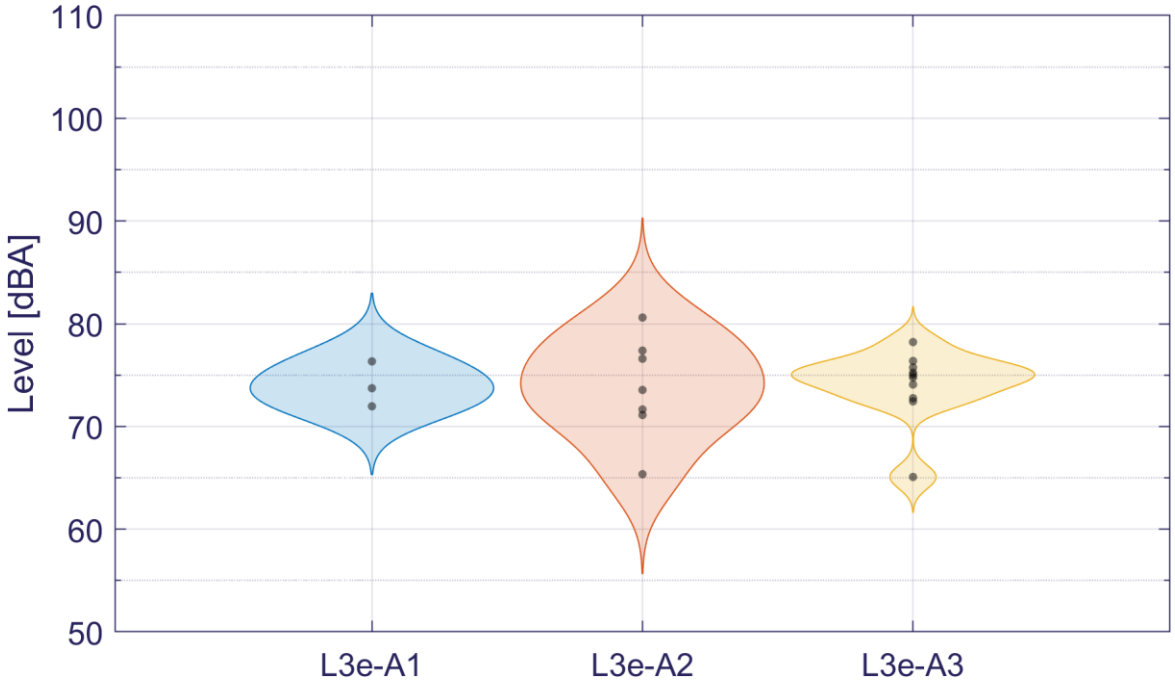

Figure D-22: Sound level vs. subcategory for on-road measurements for driving pattern 14 (Deceleration, gear 1).

This project has received funding from the European Union's Horizon Europe research and innovation programme under grant agreement No 101056777

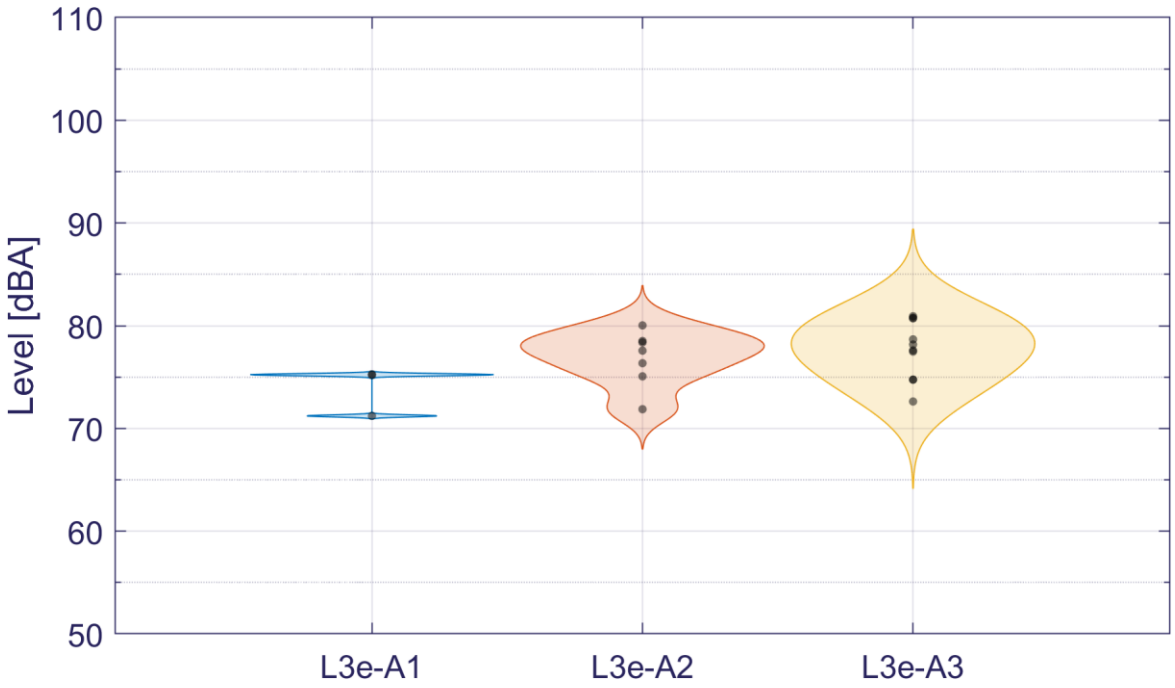

Figure D-23: Sound level vs. subcategory for on-road measurements for driving pattern 14 (Deceleration, gear 2).

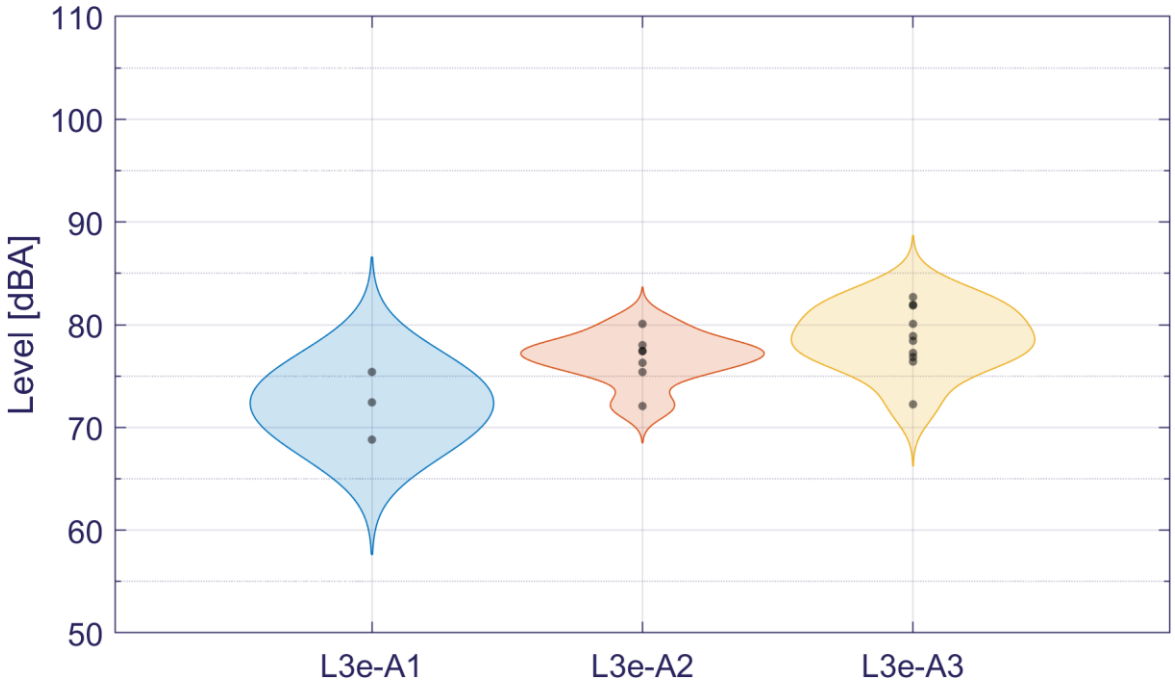

Figure D-24: Sound level vs. subcategory for on-road measurements for driving pattern 14 (Deceleration, gear 3).

This project has received funding from the European Union's Horizon Europe research and innovation programme under grant agreement No 101056777

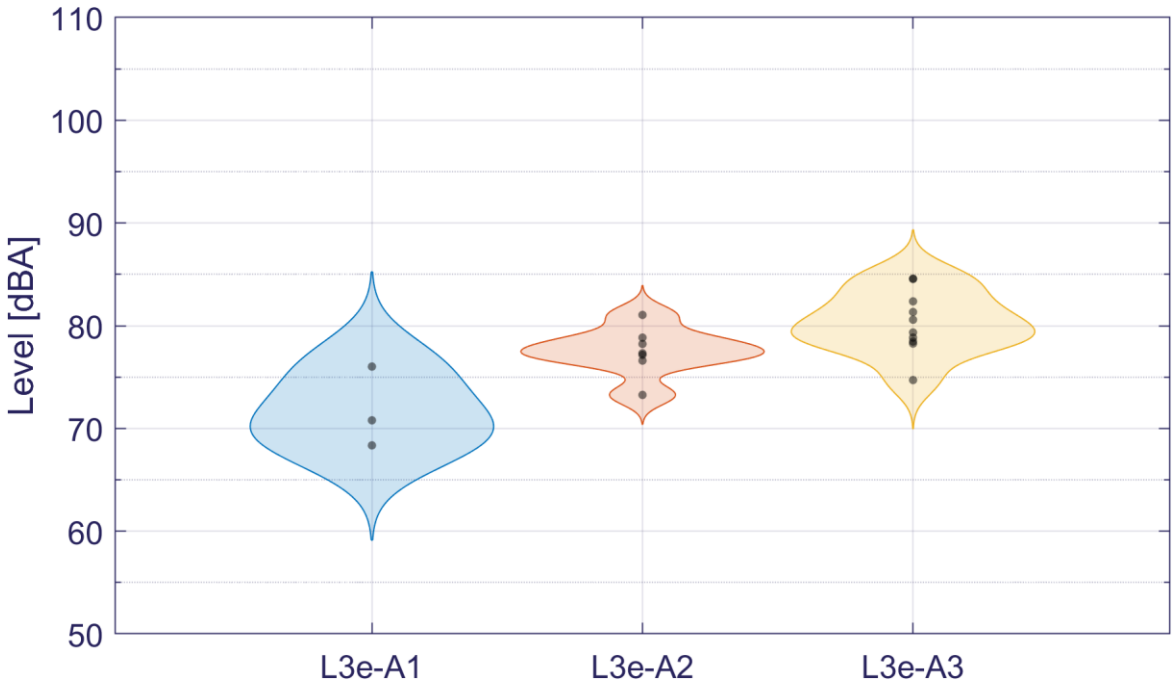

Figure D-25: Sound level vs. subcategory for on-road measurements for driving pattern 14 (Deceleration, gear 4).

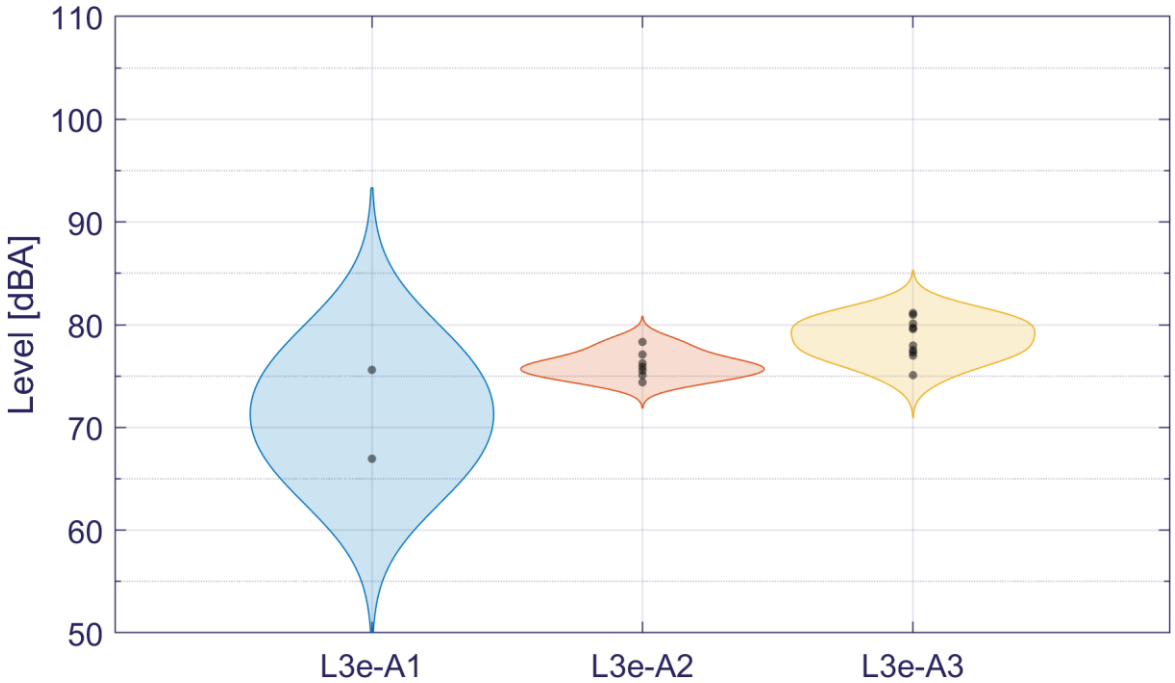

Figure D-26: Sound level vs. subcategory for on-road measurements for driving pattern 14 (Deceleration, gear 5).

This project has received funding from the European Union's Horizon Europe research and innovation programme under grant agreement No 101056777

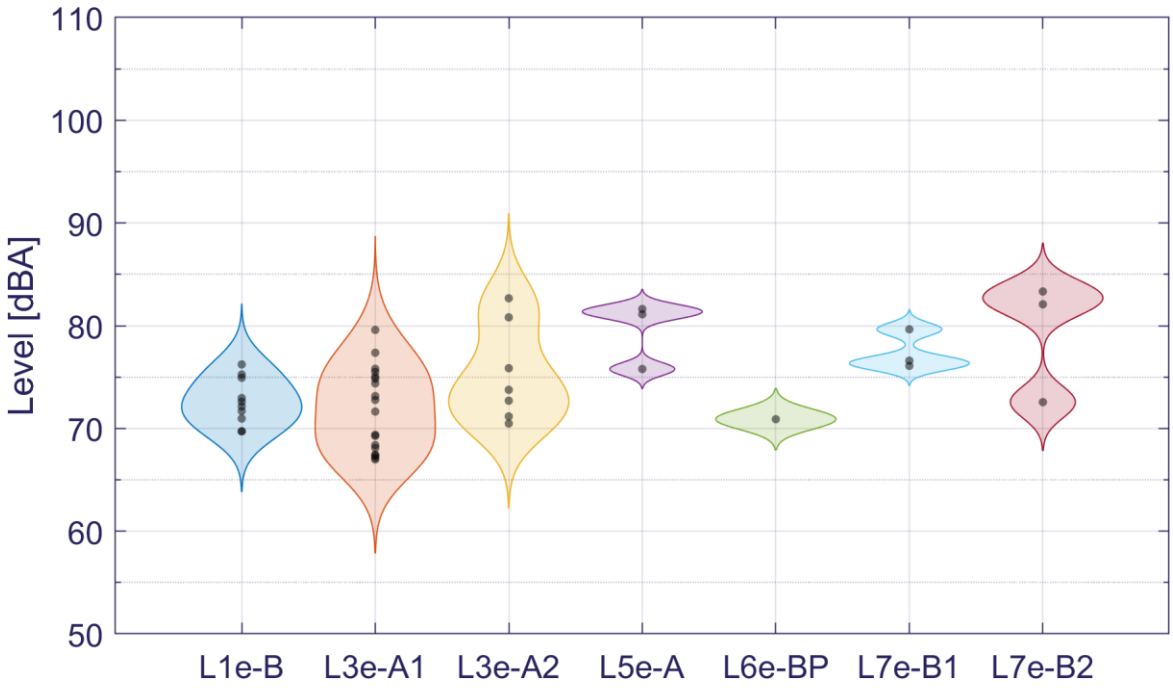

Figure D-27: Sound level vs. subcategory for on-road measurements for driving pattern 4 (moderate acc. from standstill).

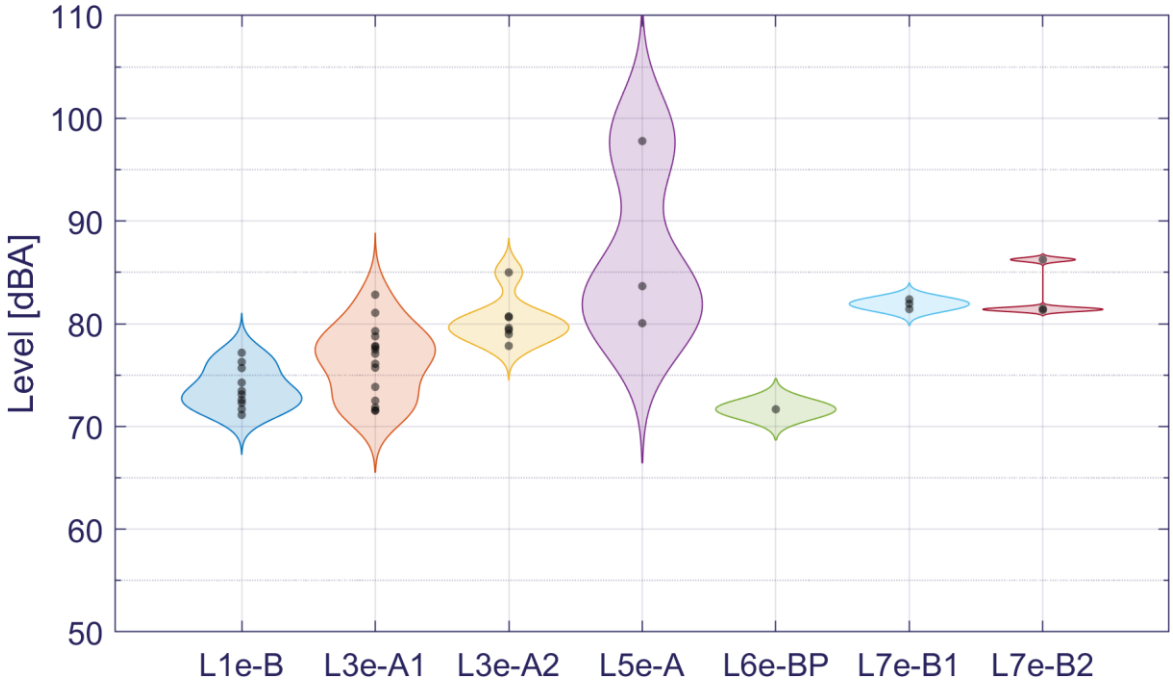

Figure D-28: Sound level vs. subcategory for on-road measurements for driving pattern 5 (Aggressive acc. from const. Speed, below 10 km/h).

This project has received funding from the European Union's Horizon Europe research and innovation programme under grant agreement No 101056777

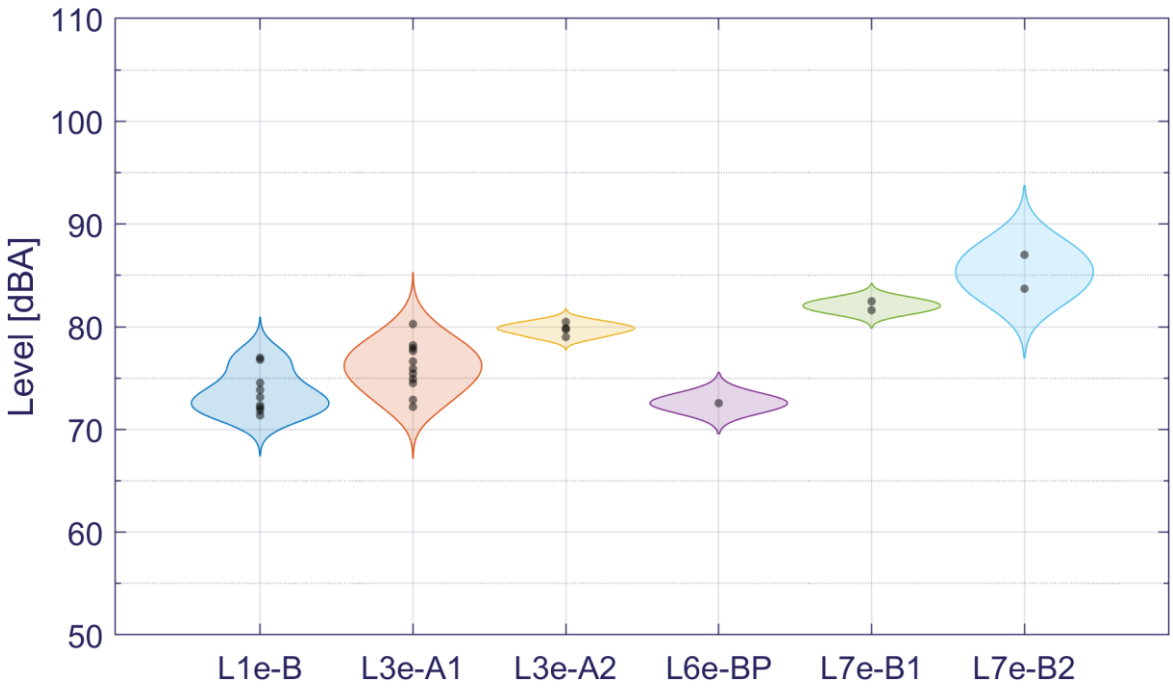

Figure D-29: Sound level vs. subcategory for on-road measurements for driving pattern 6 (Aggressive acc. from const. Speed, 20 km/h).

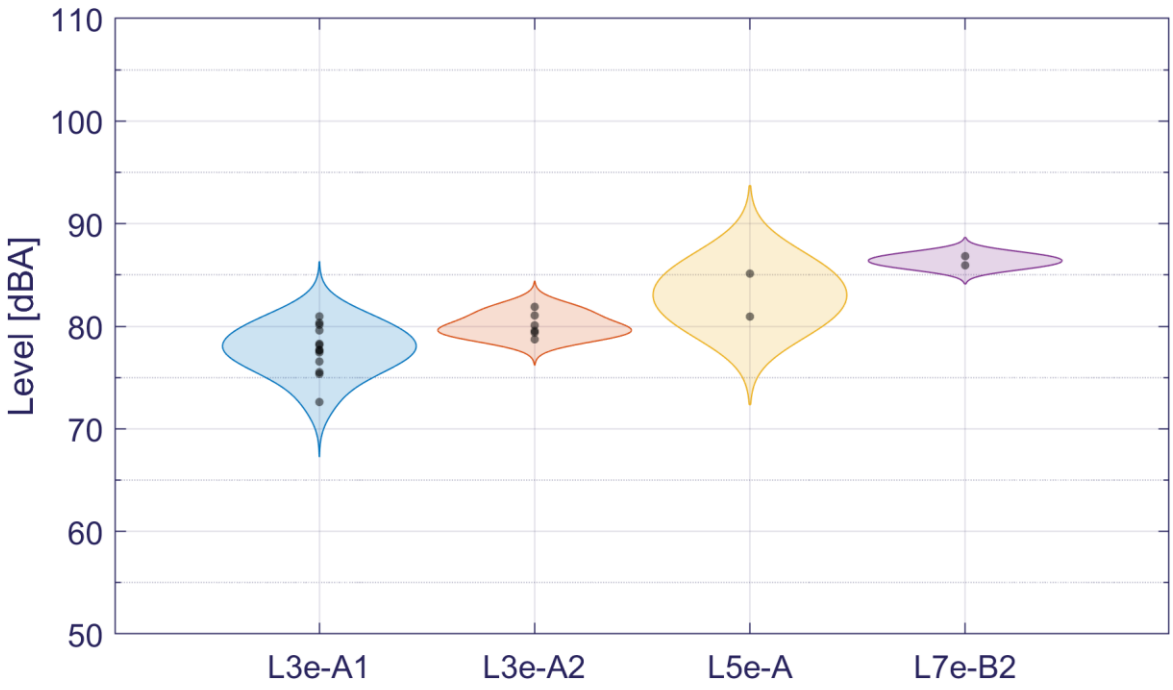

Figure D-30: Sound level vs. subcategory for on-road measurements for driving pattern 7 (Aggressive acc. from const. Speed, 50 km/h).

This project has received funding from the European Union's Horizon Europe research and innovation programme under grant agreement No 101056777

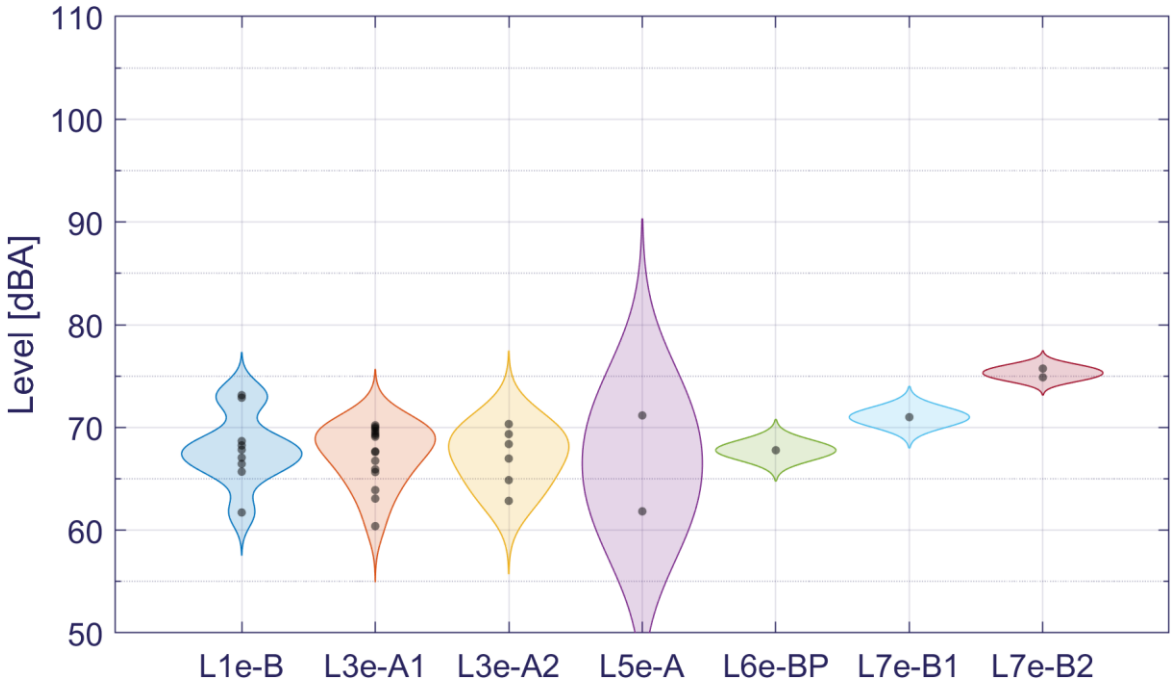

Figure D-31: Sound level vs. subcategory for on-road measurements for driving pattern 8 (Constant speed, high/ engine speed).

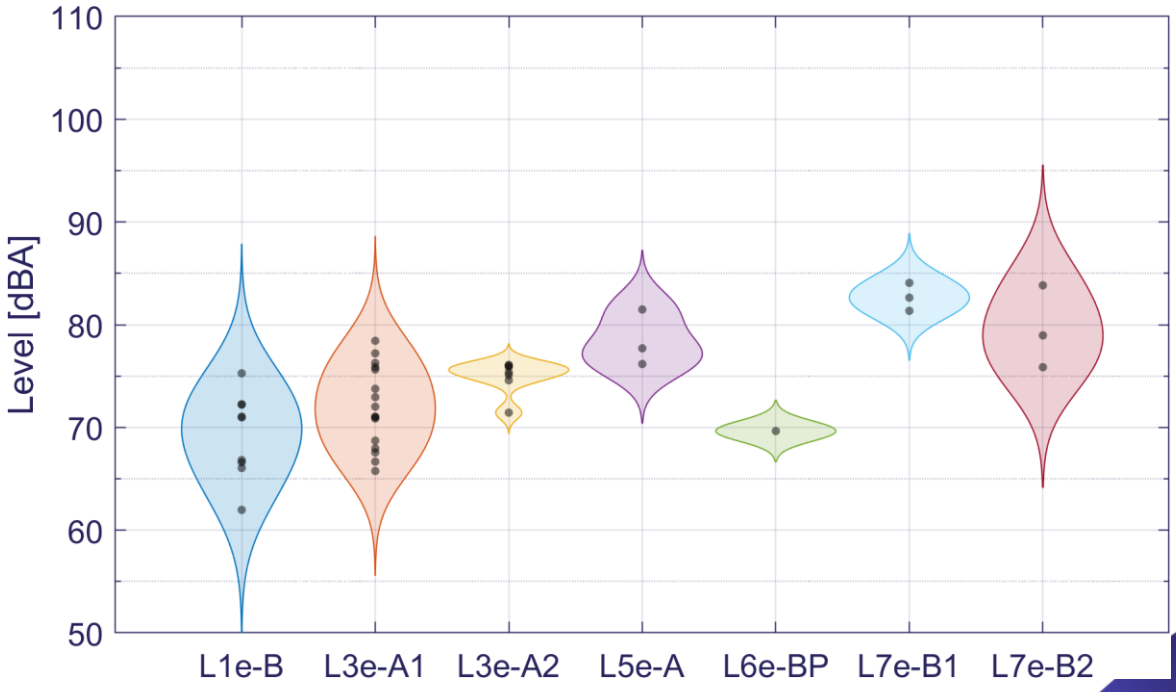

Figure D-32: Sound level vs. subcategory for on-road measurements for driving pattern 9 (Deceleration from 50 km/h).

This project has received funding from the European Union's Horizon Europe research and innovation programme under grant agreement No 101056777

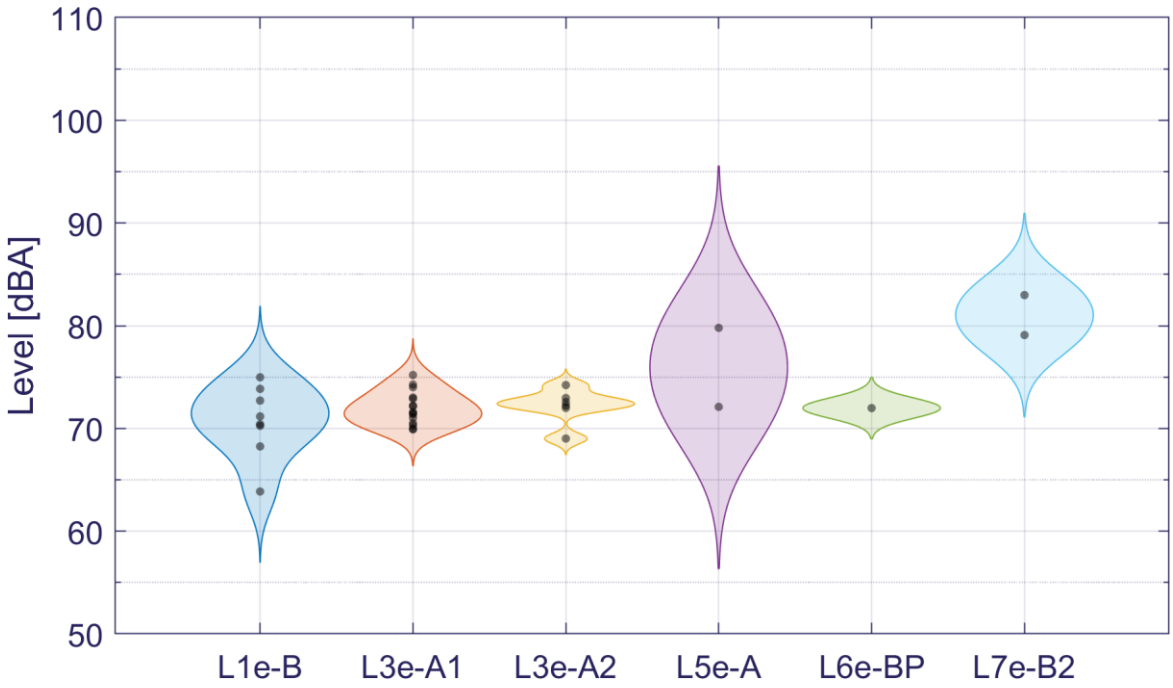

Figure D-33: Sound level vs. subcategory for on-road measurements for driving pattern 11 (Constant speed driving at 50 km/h).

This project has received funding from the European Union's Horizon Europe research and innovation programme under grant agreement No 101056777

Appendix E: Sound characteristics of critical driving conditions measured on test tracks

Some illustrative examples of the sound characteristics of individual driving conditions measured on test tracks are shown in Figure E-1 to Figure E-5 below. 2650 events were analyzed in total for 108 different vehicles.

These show the time signal, third octave spectrum and spectrogram, level history, narrowband spectrum and spectrogram, parametric sound quantities and vehicle type and driving condition.
The sound pressure signal of the microphone with the highest L_{pAFmax} level at 7.5 m is used, which can be either side of the vehicle, and in some cases at cross-sections AA', PP', or BB'.

The parametric sound quantities are derived from the sound levels, spectra and spectrograms and level histories. They each give an indication of specific characteristics such as strongest tones, rise time of sound level, dominant frequency range (low, medium or high) and a sound label indicating the possible engine speed behavior. The quantities are:
L_{pAFmax} , L_{pFmax} , $L_{pAeq,4s}$, $L_{peq,4s}$, SEL

- L_{pAFmax} - $L_{pAeq,4s}$, L_{pFmax} – L_{pFAmax}
- Normalised low, medium and high frequency levels, defined as
- L_{pFmax}(total)-L_{pFmax}(f_{range}), with f_{range} = 20-250 Hz, 250-1000 Hz and 1000-10000 Hz
- Rise time of the sound level history $(dL/dt)_{max}$
- Strongest frequencies fi (typically ignition frequency), spectrum amplitudes $L_p(f_i)$ and peak prominence
- Text labels indicative of sound content, such as '*impact*', '*siren*', '*claxon*', '*engine*', '*repet*', '*fcontlo*', '*fconthi*', '*voice*', determined with specific algorithms, to qualify vehicle and non-vehicle sounds
- Text labels for engine speed related sound content determined with specific algorithms

The labels for engine noise are for example '*rpmburst*' for throttle control and engine start, '*fconthi*' for constant speed or minor acceleration, '*rpmshortacc*' for fast acceleration. The algorithms used here are based on the parametric sound quantities but are not yet fully capable of identifying each driving condition due to the specific dynamics of each event and vehicle.
The examples shown below are all '*rpmburst*' with peaks of short duration.
The narrowband spectrum and spectrogram clearly show the engine harmonics which are directly related to the engine speed. For larger motorcycles a strong low frequency content is often observed including strong tonal peaks.

This project has received funding from the European Union's Horizon Europe research and innovation programme under grant agreement No 101056777

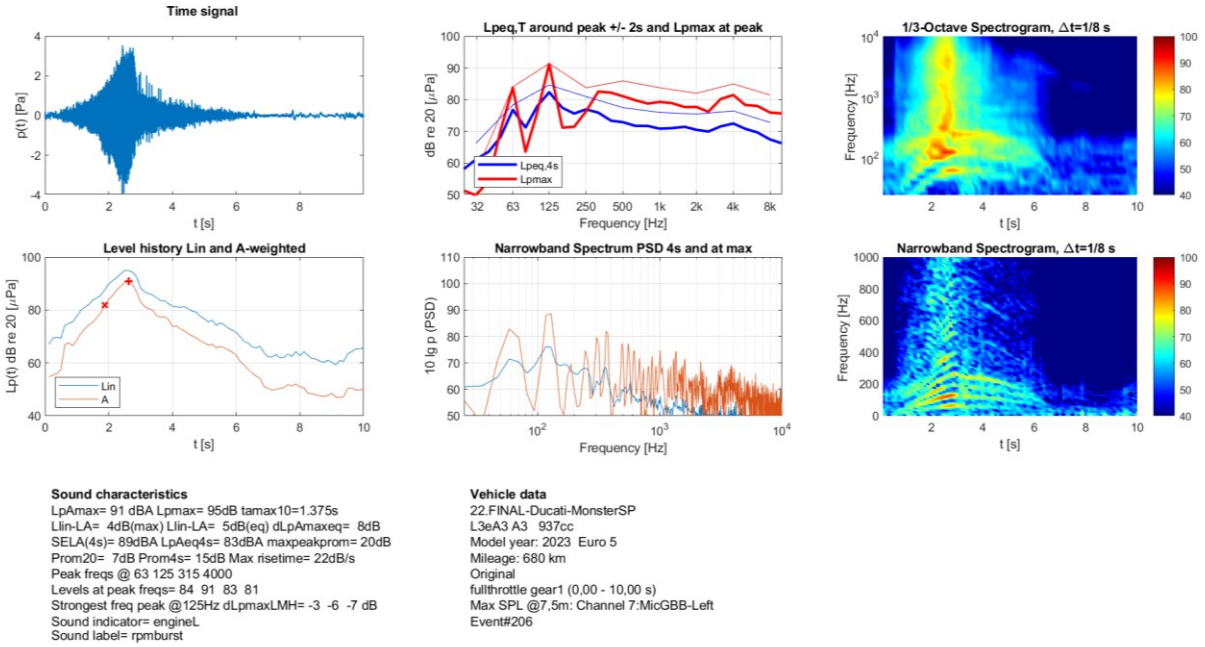

Sound characteristics
LpAmax= 91 dBA Lpmax= 95dB tamax10=1.375s
Llin-LA= 4dB(max) Llin-LA= 5dB(eq) dLpAmaxeq= 8dB
SELA(4s)= 89dBA LpAeq4s= 83dBA maxpeakprom= 20dB
Prom20= 7dB Prom4s= 15dB Max risetime= 22dB/s
Peak freqs @ 63 125 315 4000
Levels at peak freqs= 84 91 83 81
Strongest freq peak @125Hz dLpmaxLMH= -3 -6 -7 dB
Sound indicator= engineL
Sound label= rpmburst

Vehicle data
22.FINAL-Ducati-MonsterSP
L3eA3 A3 937cc
Model year: 2023 Euro 5
Mileage: 680 km
Original
fullthrottle gear1 (0,00 - 10,00 s)
Max SPL @7,5m: Channel 7:MicGBB-Left
Event#206

Figure E-1: Sound characteristics of L3-A3 motorcycle Vehicle 22, full throttle acceleration, gear 1.

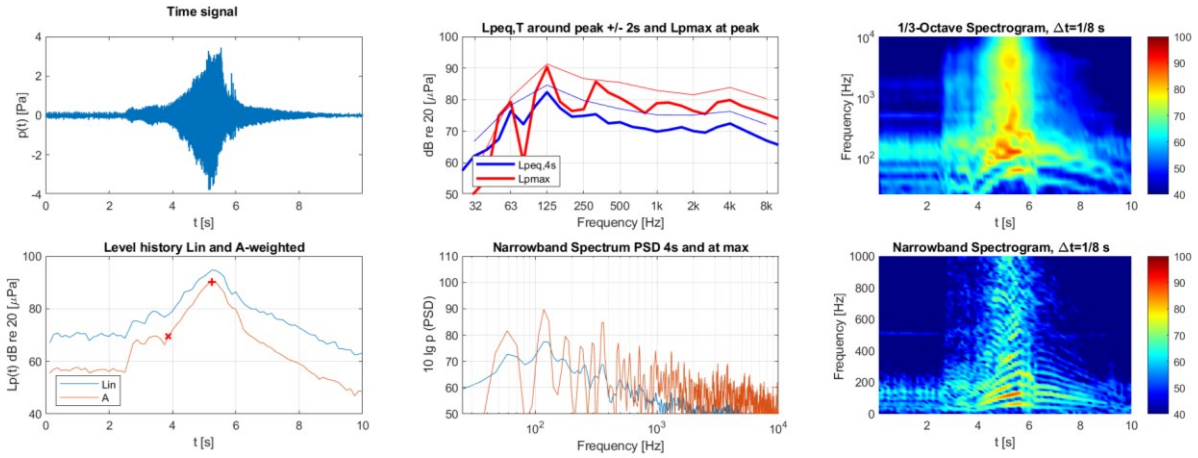

Sound characteristics
LpAmax= 90 dBA Lpmax= 95dB tamax10=1.375s
Llin-LA= 5dB(max) Llin-LA= 5dB(eq) dLpAmaxeq= 7dB
SELA(4s)= 89dBA LpAeq4s= 83dBA maxpeakprom= 16dB
Prom20= 10dB Prom4s= 16dB Max risetime= 26dB/s
Peak freqs @ 63 125 315 1250 4000
Levels at peak freqs= 79 90 86 79 80
Strongest freq peak @125Hz dLpmaxLMH= -3 -5 -8 dB
Sound indicator= engineL
Sound label= rpmburst

Vehicle data
22.FINAL-Ducati-MonsterSP
L3eA3 A3 937cc
Model year: 2023 Euro 5
Mileage: 680 km
Original
heavy acc standstill gear1 (0,00 - 10,00 s)
Max SPL @7,5m: Channel 7:MicGBB-Left
Event#214

Figure E-2: Sound characteristics of L3-A3 motorcycle Vehicle 22, heavy acceleration from standstill, gear1.

This project has received funding from the European Union's Horizon Europe research and innovation programme under grant agreement No 101056777

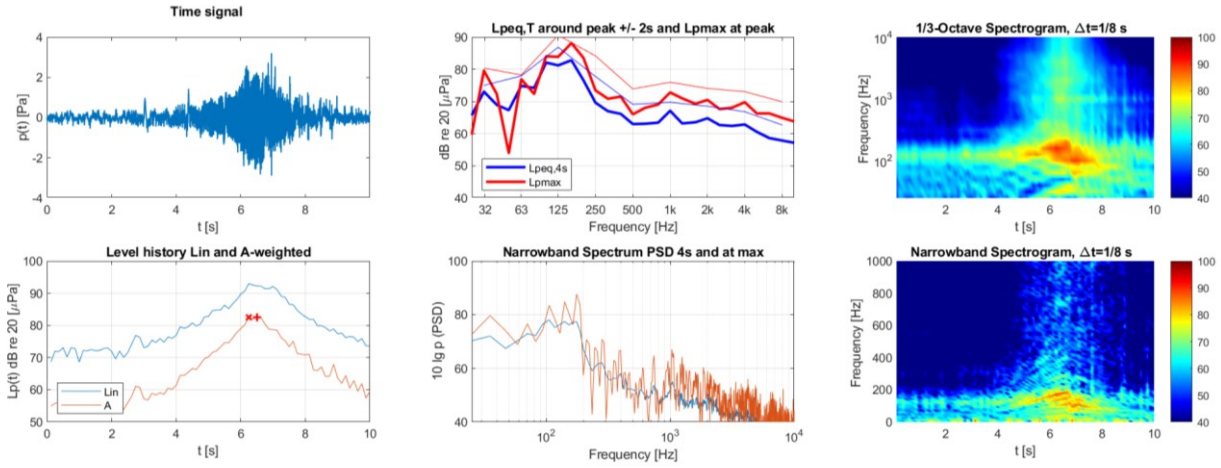

Sound characteristics
LpAmax= 83 dBA Lpmax= 93dB tamax10=2.375s
Llin-LA= 10dB(max) Llin-LA= 11dB(eq) dLpAmaxeq= 6dB
SELA(4s)= 83dBA LpAeq4s= 77dBA maxpeakprom= 24dB
Prom20= 7dB Prom4s= 14dB Max risetime= 18dB/s
Peak freqs @ 32 63 160 1000
Levels at peak freqs= 80 77 88 73
Strongest freq peak @160Hz dLpmaxLMH= -2 -8 -16 dB
Sound indicator= engineL
Sound label= rpmburst

Vehicle data
21.FINAL-Ducati-PanigaleV2
L3eA3 A3 890cc
Model year: 2023 Euro 5
Mileage: 500 km
Original
mod acc standstill gear1 (0,00 - 10,00 s)
Max SPL @7,5m: Channel 6:MicGBB-Right
Event#193

Figure E-3: Sound characteristics of L3-A3 motorcycle Vehicle 22, moderate acceleration from standstill, gear1.

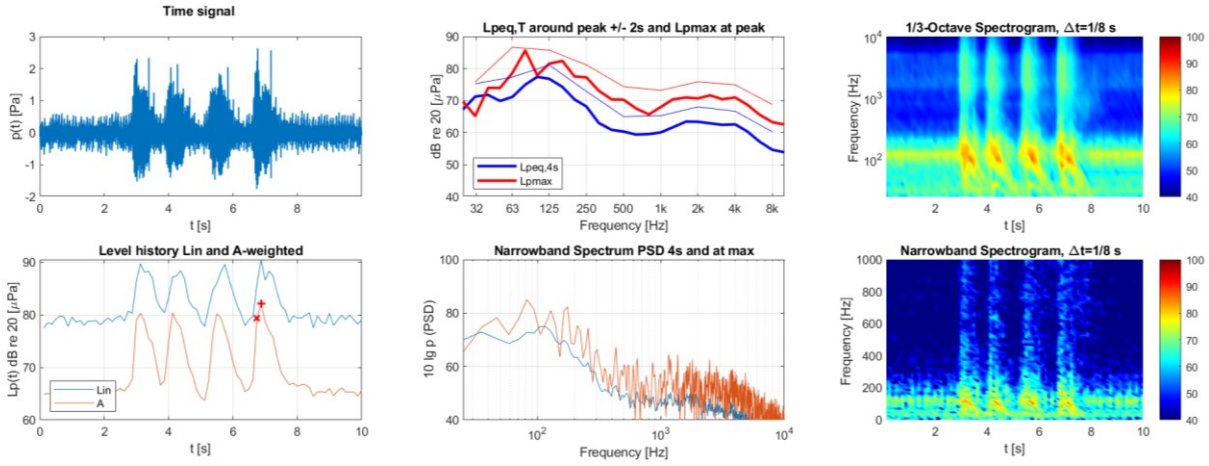

Sound characteristics
LpAmax= 82 dBA Lpmax= 91dB tamax10=2.5s
Llin-LA= 8dB(max) Llin-LA= 10dB(eq) dLpAmaxeq= 8dB
SELA(4s)= 80dBA LpAeq4s= 74dBA maxpeakprom= 20dB
Prom20= 9dB Prom4s= 15dB Max risetime= 93dB/s
Peak freqs @ 80 160 2500
Levels at peak freqs= 86 82 72
Strongest freq peak @ 80Hz dLpmaxLMH= -1 -8 -12 dB
Sound indicator= engineL fcontlo
Sound label= rpmburst

Vehicle data
22.FINAL-Ducati-MonsterSP
L3eA3 A3 937cc
Model year: 2023 Euro 5
Mileage: 680 km
Original
throttle control (0,00 - 10,00 s)
Max SPL @7,5m: Channel 4:MicGPP-Right
Event#222

Figure E-4: Sound characteristics of L3-A3 motorcycle Vehicle 22, throttle_control (rpm revving).

This project has received funding from the European Union's Horizon Europe research and innovation programme under grant agreement No 101056777

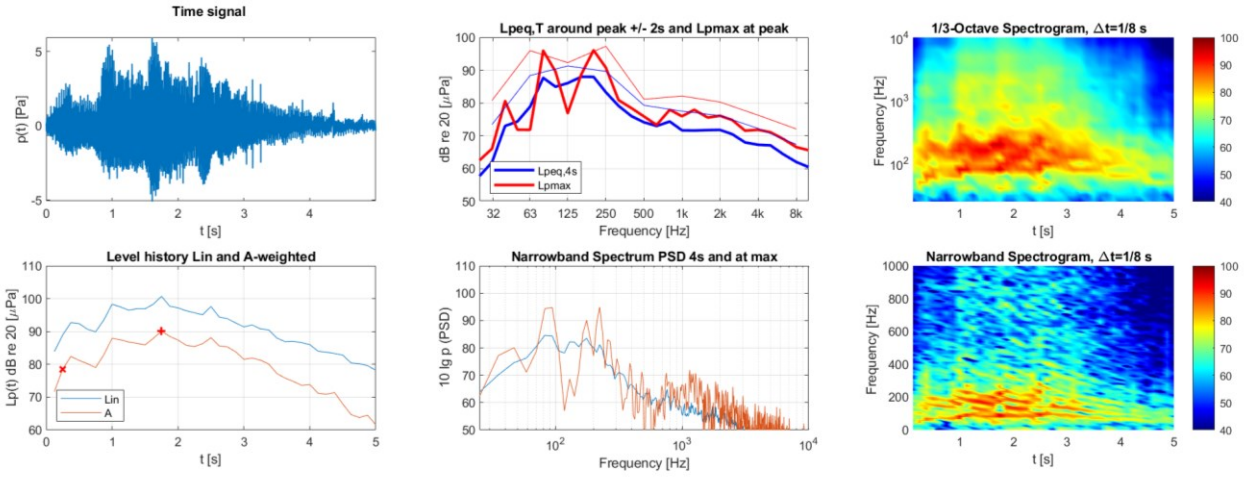

Sound characteristics
LpAmax= 90 dBA Lpmax=101dB tamax10=2.875s
Llin-LA= 11dB(max) Llin-LA= 10dB(eq) dLpAmaxeq= 5dB
SELA(4s)= 91dBA LpAeq4s= 85dBA maxpeakprom= 30dB
Prom20= 5dB Prom4s= 13dB Max risetime= 54dB/s
Peak freqs @ 40 80 200 800
Levels at peak freqs= 81 96 96 78
Strongest freq peak @200Hz dLpmaxLMH= -3 -3 -19 dB
Sound indicator= engineL
Sound label= rpmburst

Vehicle data
27.FINAL-HarleyDavidson-XLH53C
L3eA3 A3 883cc
Model year: 2002 Euro 2
Mileage: 34940 km
Original
intermitt throttle 30 (0,00 - 5,00 s)
Max SPL @7,5m: Channel 4:MicGPP-Right
Event#328

Figure E-5: Sound characteristics of L3-A3 motorcycle Vehicle 27, intermitt_throttle_30, (rpm revving).

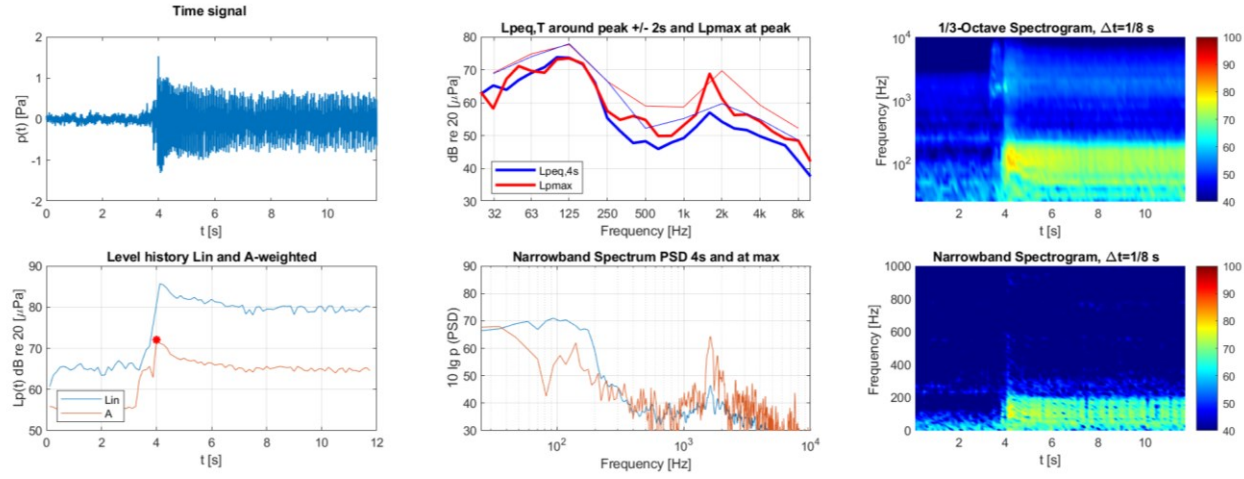

Sound characteristics
LpAmax= 72 dBA Lpmax= 86dB tamax10=8.5s
Llin-LA= 14dB(max) Llin-LA= 14dB(eq) dLpAmaxeq= 6dB
SELA(4s)= 72dBA LpAeq4s= 66dBA maxpeakprom= 15dB
Prom20= 7dB Prom4s= 12dB Max risetime= 74dB/s
Peak freqs @125 1600
Levels at peak freqs= 74 69
Strongest freq peak @125Hz dLpmaxLMH= -6 -18 -16 dB
Sound indicator= engineL fcontlo
Sound label= rpmburst

Vehicle data
BMW F 900 R
L3eA3 A3 900cc
Model year: Unknown Euro 0
Mileage: Unknown
Original
engine start 01 (0,00 - 11,75 s)
Max SPL @7,5m: Channel 2:R3
Event#1101

Figure E-6: Sound characteristics of L3-A3 motorcycle, engine start.

This project has received funding from the European Union's Horizon Europe research and innovation programme under grant agreement No 101056777

Appendix F: Rotranomo RDE Processed data for noise emissions modelling

Time series of cycle under normal driving conditions

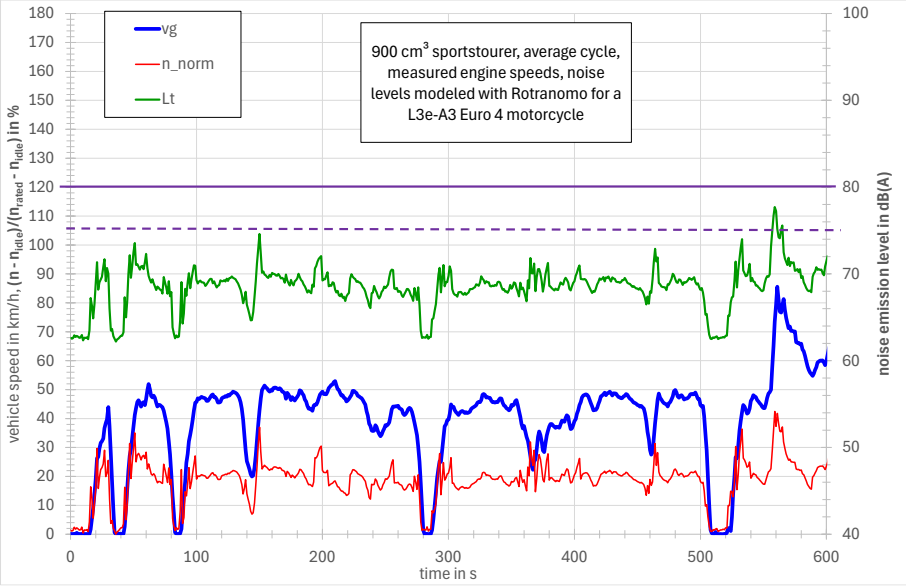

Figure F-1: Time series of the cycle with average driving behavior.

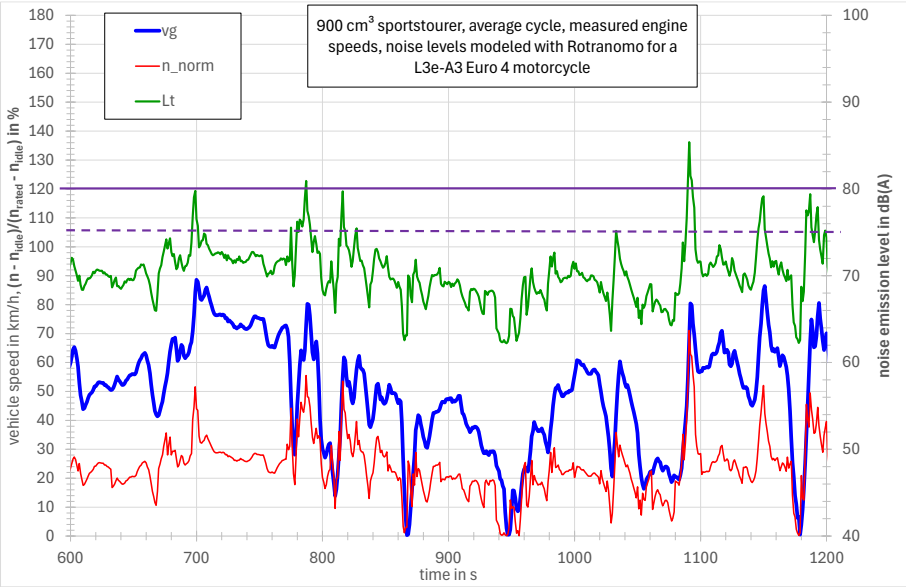

Figure F-2: Time series of the cycle with average driving behavior.

This project has received funding from the European Union's Horizon Europe research and innovation programme under grant agreement No 101056777

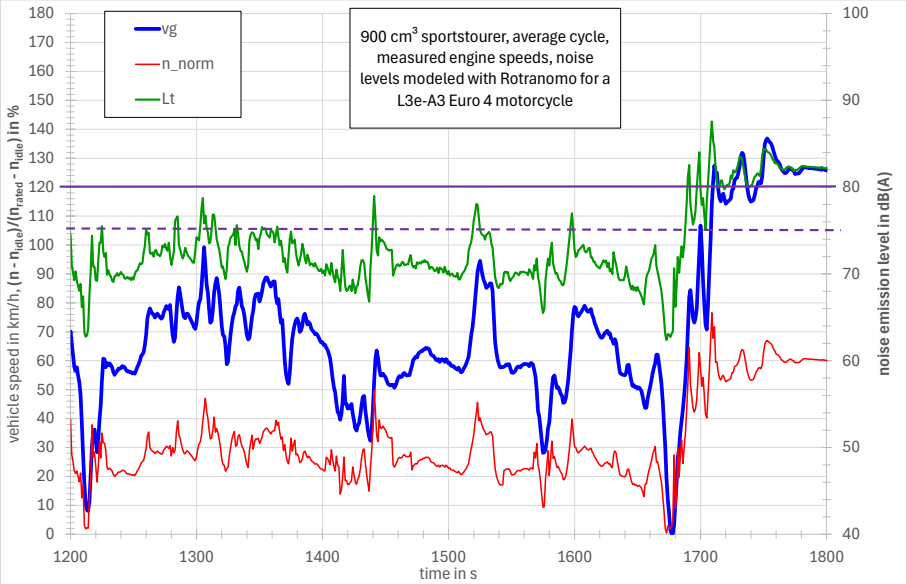

Figure F-3: Time series of the cycle with average driving behavior.

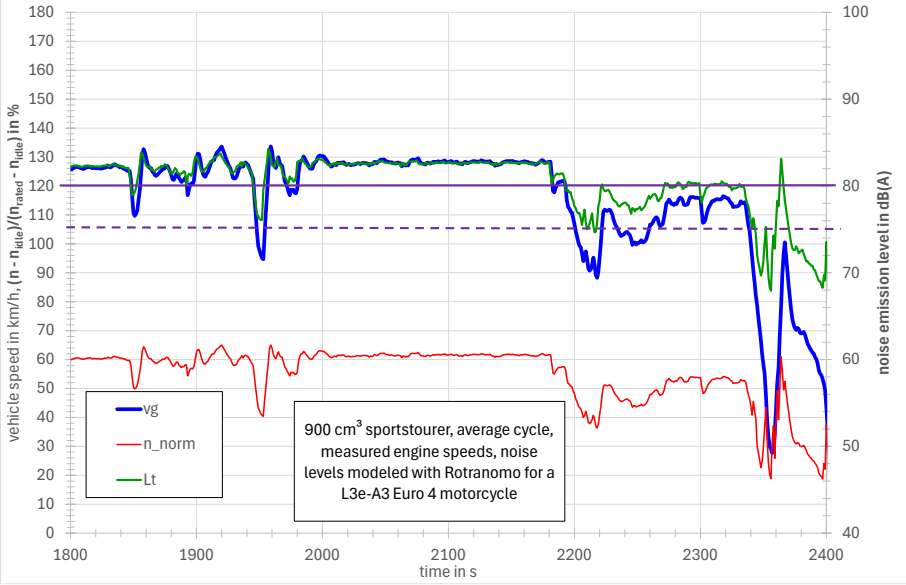

Figure F-4: Time series of the cycle with average driving behavior.

This project has received funding from the European Union's Horizon Europe research and innovation programme under grant agreement No 101056777

Time series of cycle under aggressive driving conditions

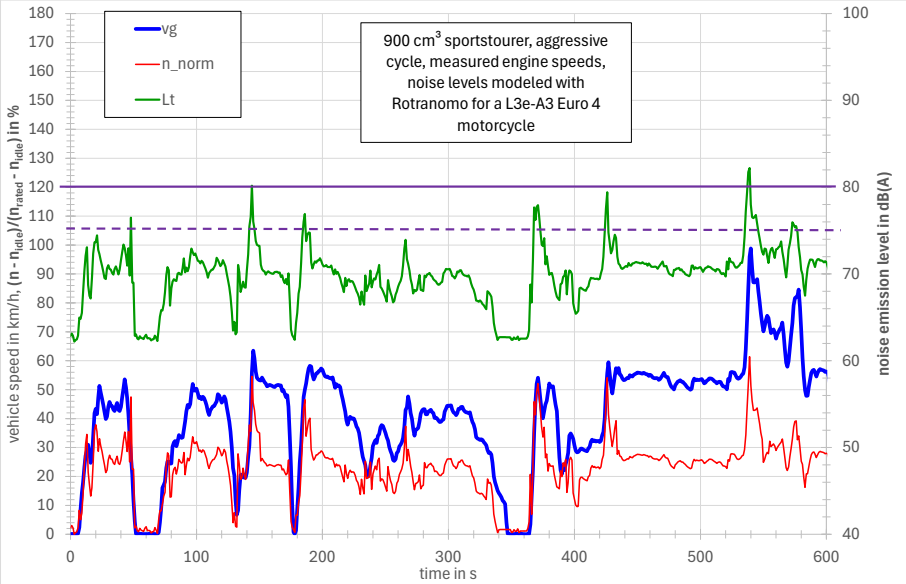

Figure F-5: Time series of the cycle with aggressive driving behavior.

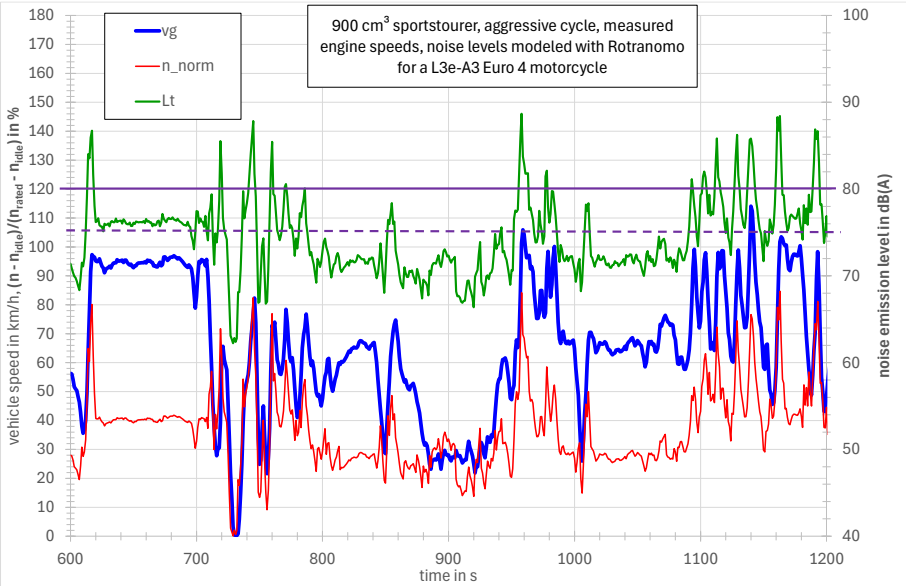

Figure F-6: Time series of the cycle with aggressive driving behavior.

This project has received funding from the European Union's Horizon Europe research and innovation programme under grant agreement No 101056777

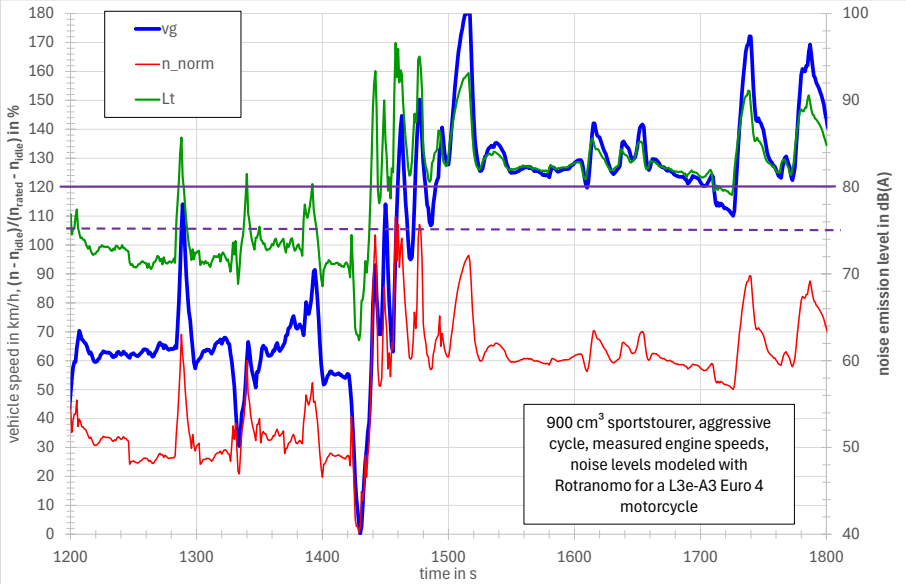

Figure F-7: Time series of the cycle with aggressive driving behavior.

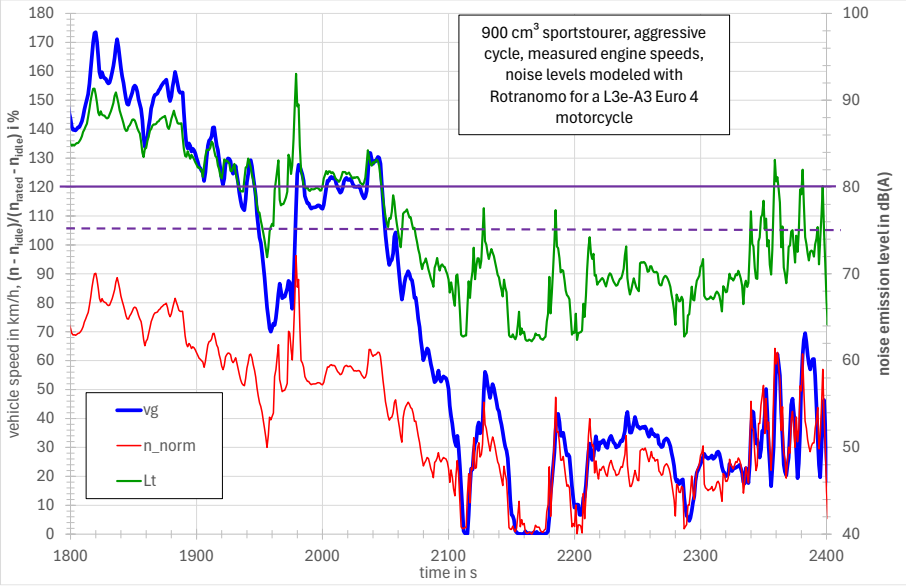

Figure F-8: Time series of the cycle with aggressive driving behavior.

This project has received funding from the European Union's Horizon Europe research and innovation programme under grant agreement No 101056777

Appendix G: Impact of Phases discretization on emissions

0-60-90

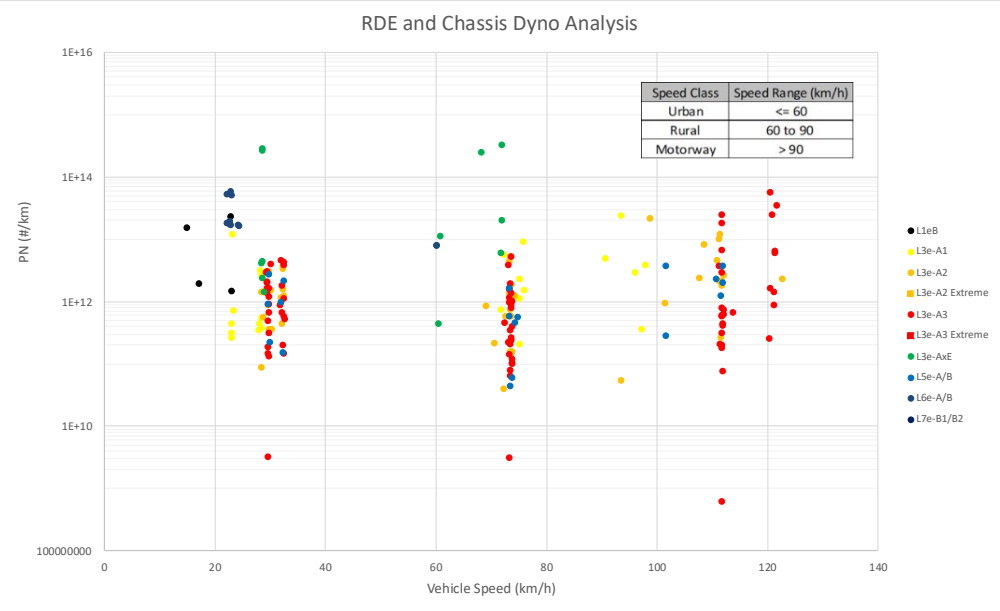

Figure G-1: PN emissions (#/km) against vehicle mean speed (km/h) for urban, rural and motorway. when discretizing phases as 0-60 urban phase, 60-90 rural phase, and >90 for motorway phase.

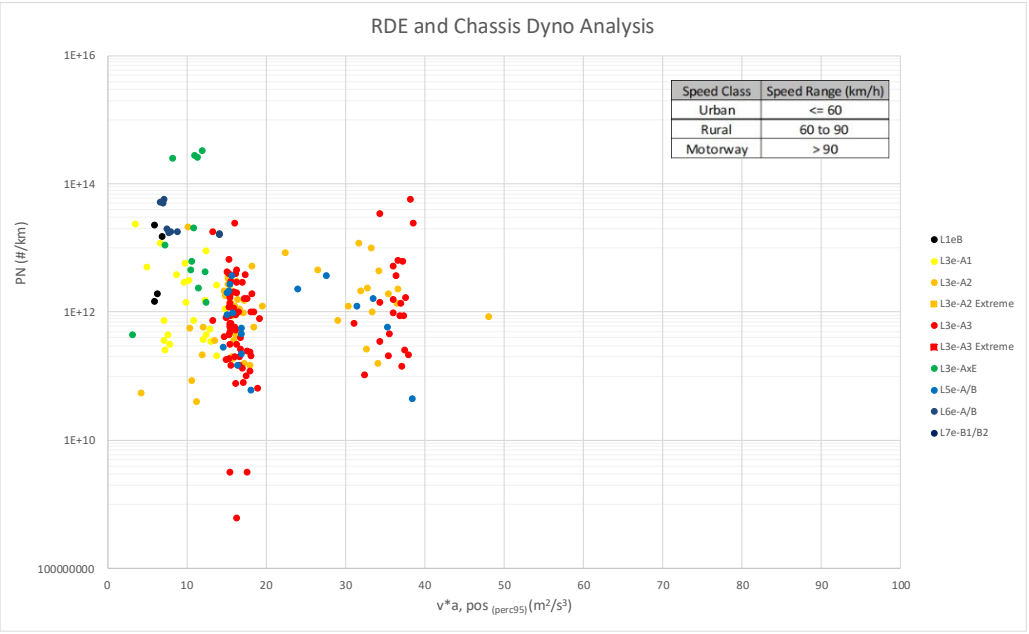

Figure G-2: PN emissions (/km) against v*a,pos perc 95 (m^2/s^3) for urban, rural and motorway. when discretizing phases as 0-60 urban phase, 60-90 rural phase, and >90 for motorway phase.

This project has received funding from the European Union's Horizon Europe research and innovation programme under grant agreement No 101056777

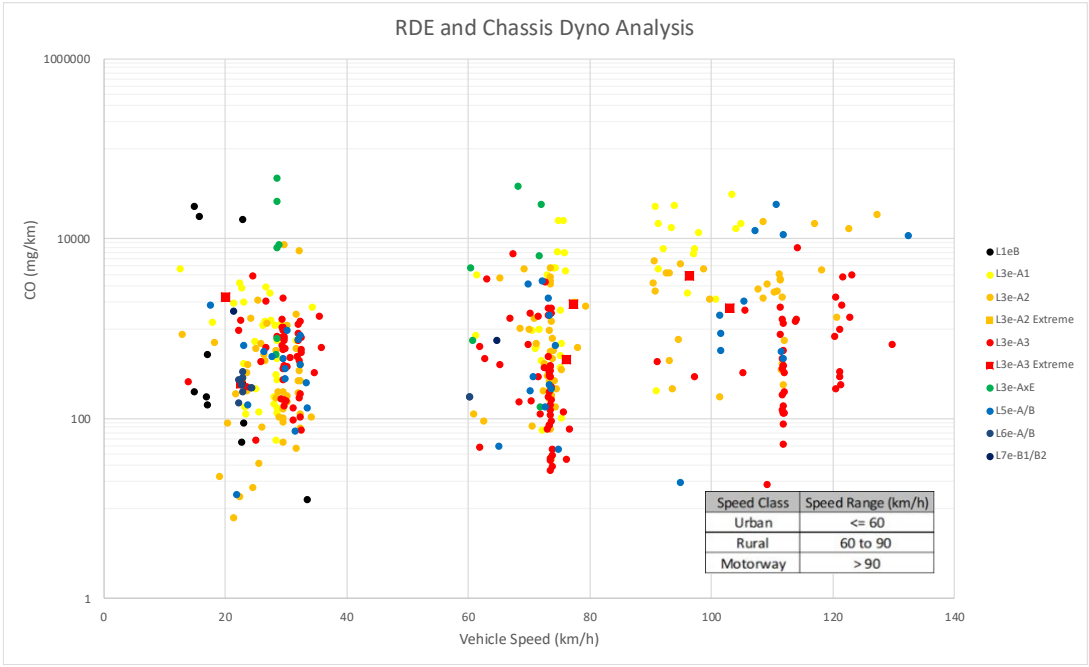

Figure G-3: CO emissions (mg/km) against vehicle mean speed (km/h) for urban, rural and motorway. when discretizing phases as 0-60 urban phase, 60-90 rural phase, and >90 for motorway phase.

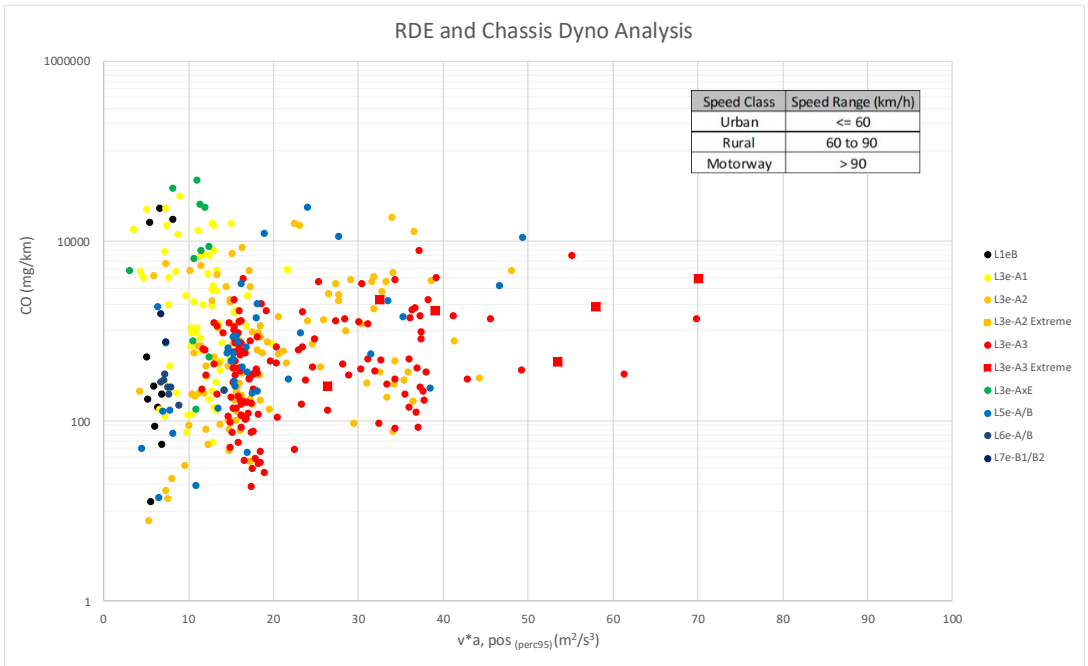

Figure G-4: CO emissions (mg/km) against v*a,pos perc 95 (m^2/s^3) for urban, rural and motorway. when discretizing phases as 0-60 urban phase, 60-90 rural phase, and >90for motorway phase.

This project has received funding from the European Union's Horizon Europe research and innovation programme under grant agreement No 101056777

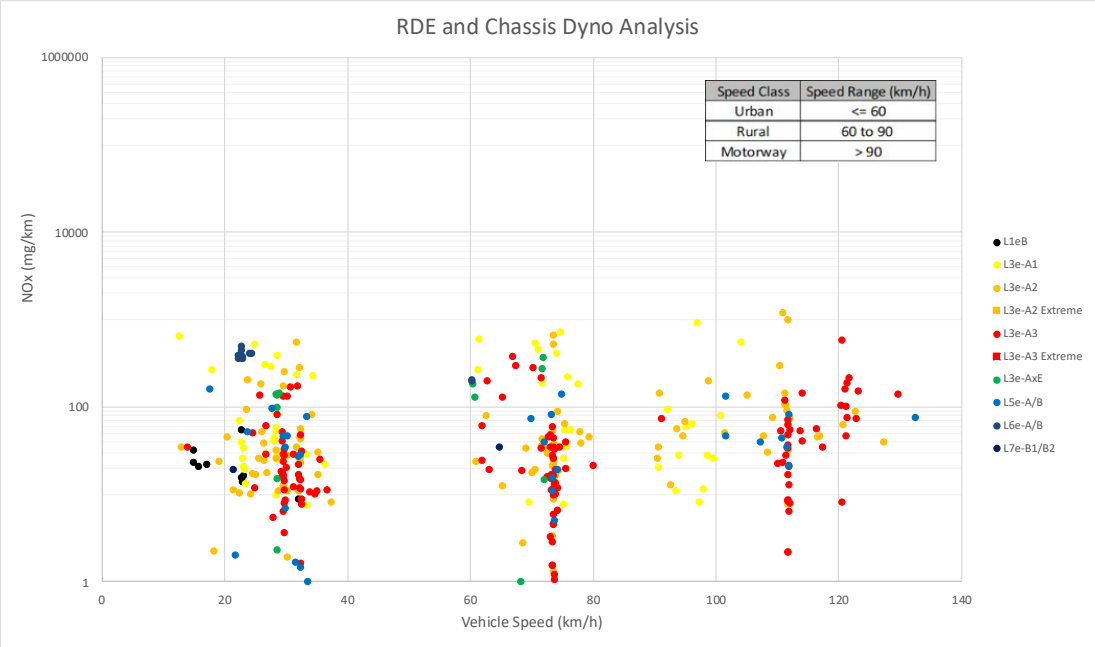

Figure G-5: NOx emissions (mg/km) against vehicle mean speed (km/h) for urban, rural and motorway. when discretizing phases as 0-60 urban phase, 60-90 rural phase, and >90 for motorway phase.

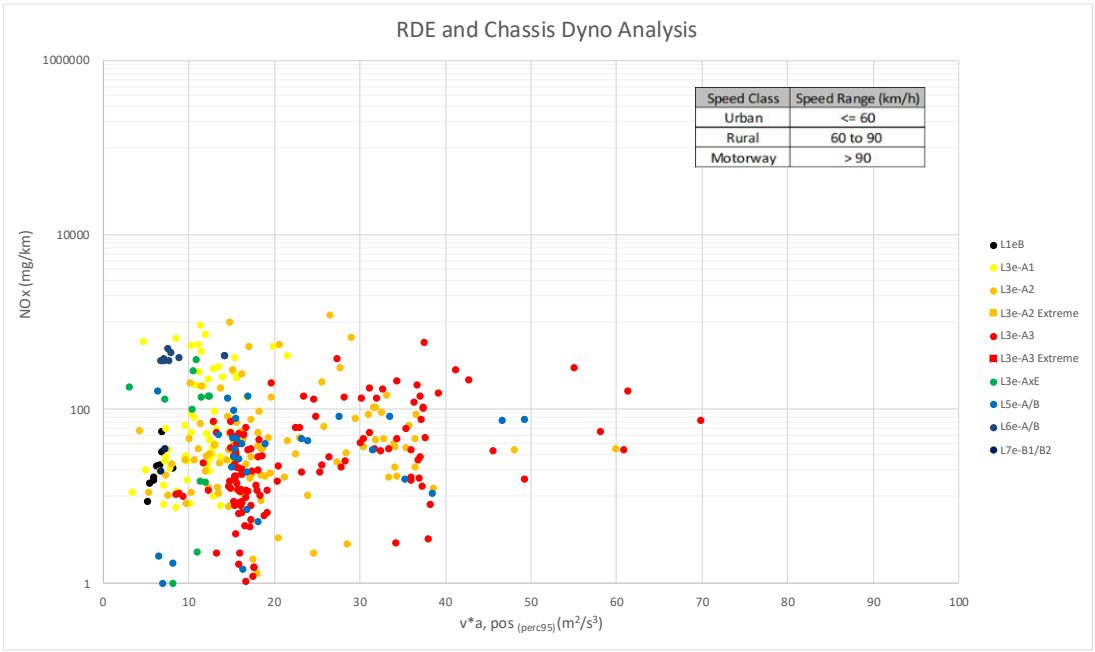

Figure G-6: NOx emissions (mg/km) against v*a,pos perc 95 (m^2/s^3) for urban, rural and motorway. when discretizing phases as 0-60 urban phase, 60-90 rural phase, and >90 for motorway phase.

This project has received funding from the European Union's Horizon Europe research and innovation programme under grant agreement No 101056777

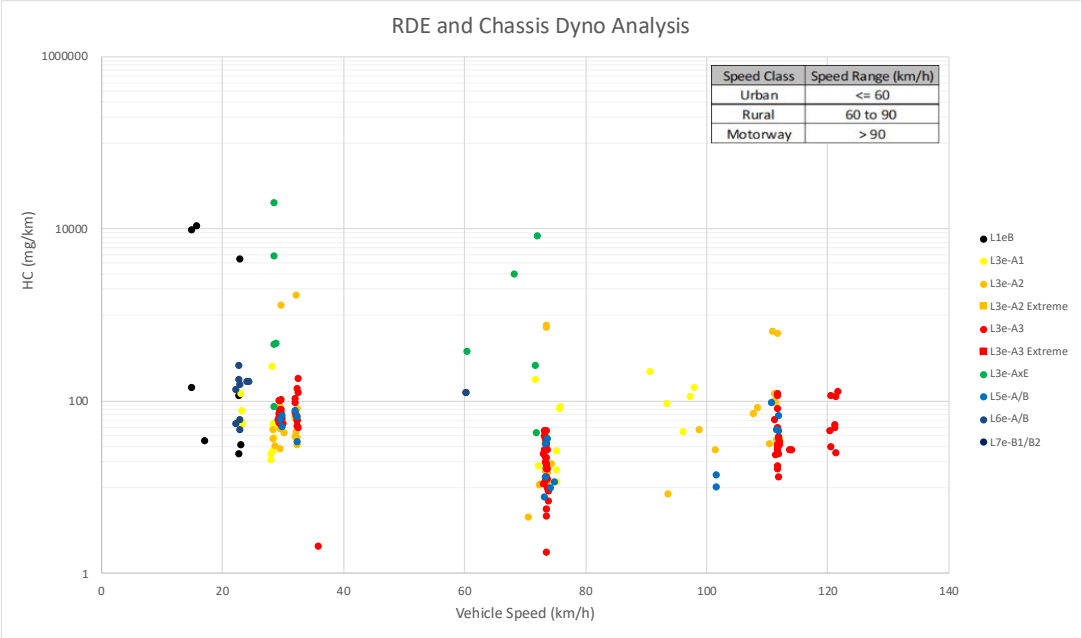

Figure G-7: HC emissions (mg/km) against vehicle mean speed (km/h) for urban, rural and motorway. when discretizing phases as 0-60 urban phase, 60-90 rural phase, and >90 for motorway phase.

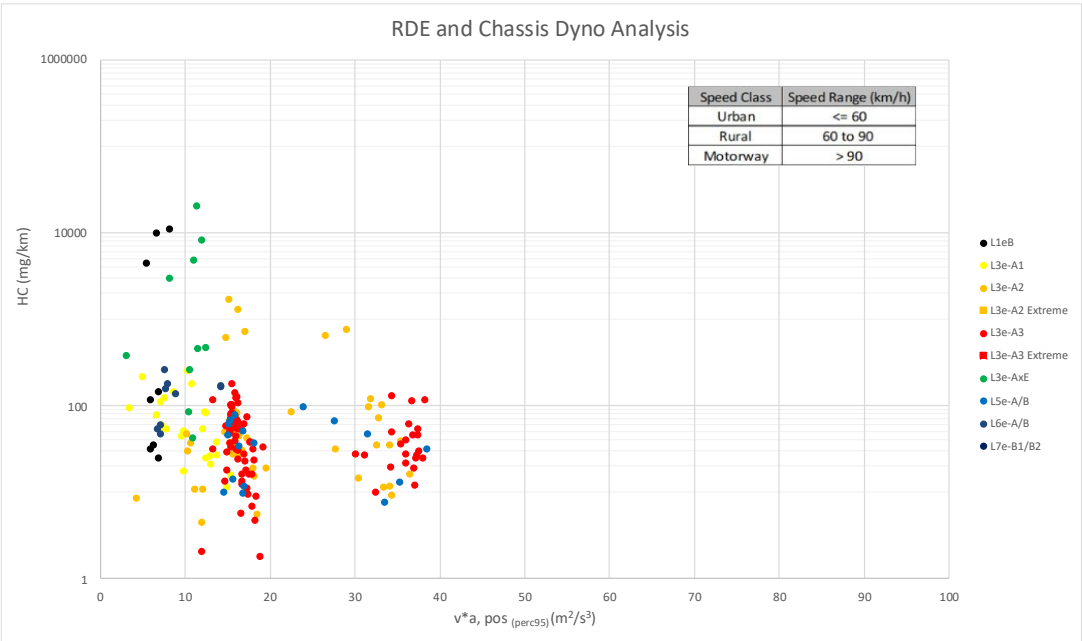

Figure G-8: HC emissions (mg/km) against v*a,pos perc 95 (m^2/s^3) for urban, rural and motorway. when discretizing phases as 0-60 urban phase, 60-90 rural phase, and >90 for motorway phase.

This project has received funding from the European Union's Horizon Europe research and innovation programme under grant agreement No 101056777

0-60-90-120

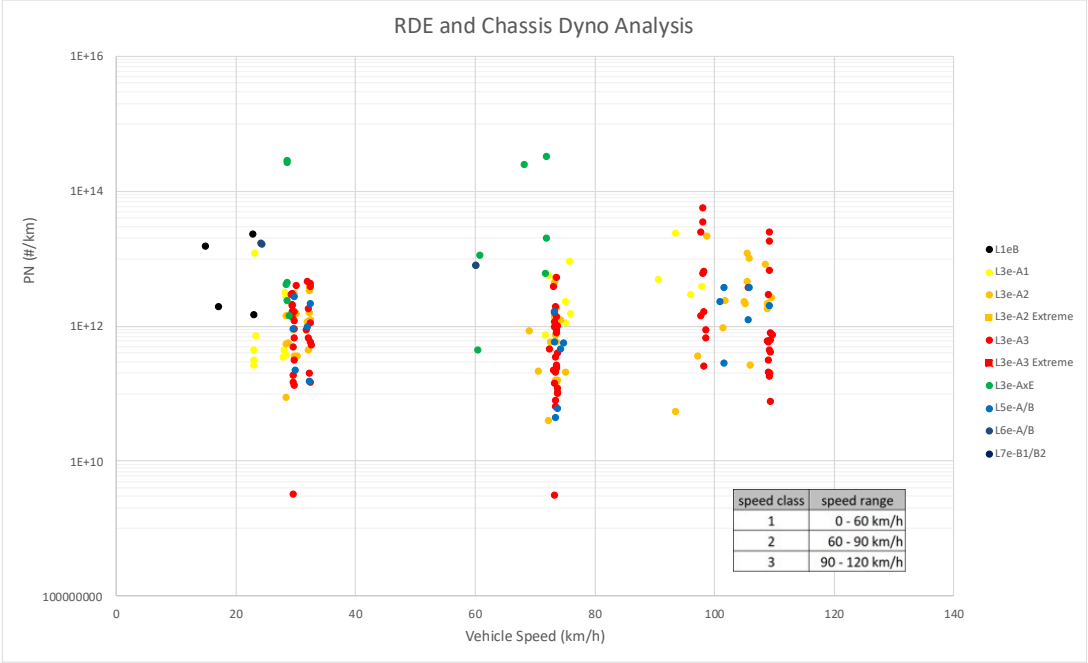

Figure G-9: PN emissions (#/km) against vehicle mean speed (km/h) for urban, rural and motorway. when discretizing phases as 0-60 urban phase, 60-90 rural phase, and 90-120 for motorway phase.

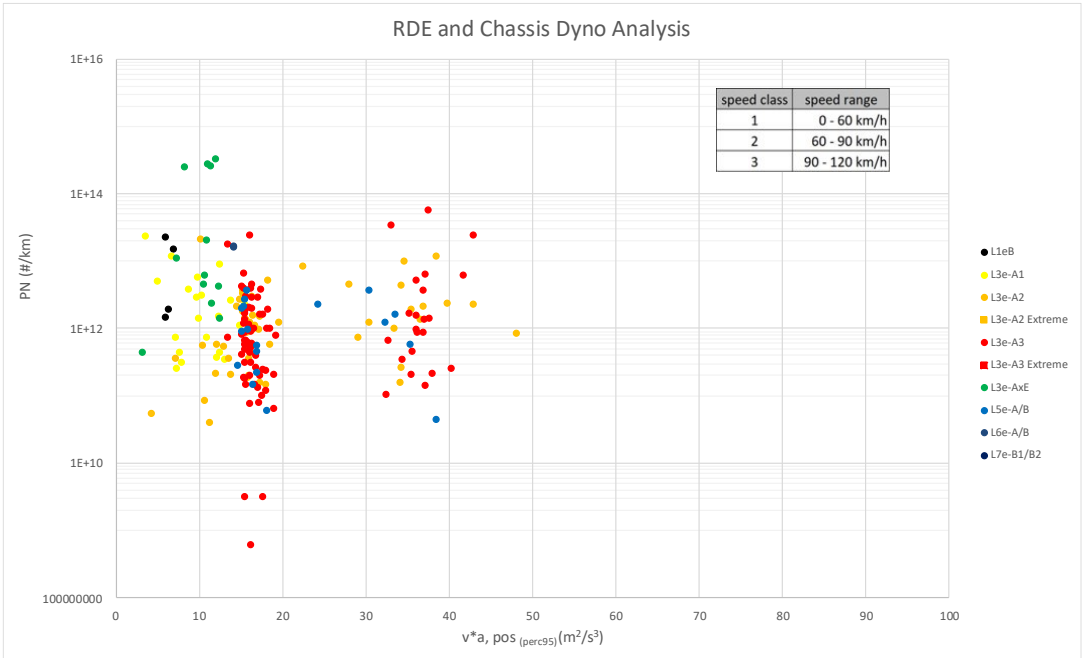

Figure G-10: PN emissions (#/km) against v*a,pos perc 95 (m^2/s^3) for urban, rural and motorway. when discretizing phases as 0-60 urban phase, 60-90 rural phase, and 90-120 for motorway phase.

This project has received funding from the European Union's Horizon Europe research and innovation programme under grant agreement No 101056777

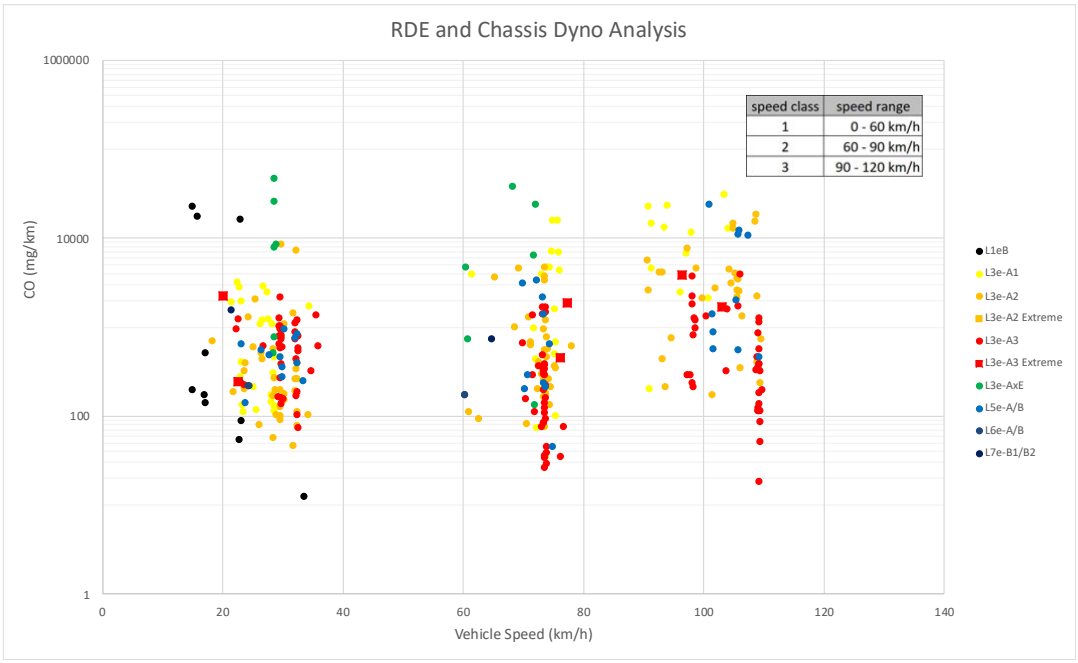

Figure G-11: CO emissions (mg/km) against vehicle mean speed (km/h) for urban, rural and motorway. when discretizing phases as 0-60 urban phase, 60-90 rural phase, and 90-120 for motorway phase.

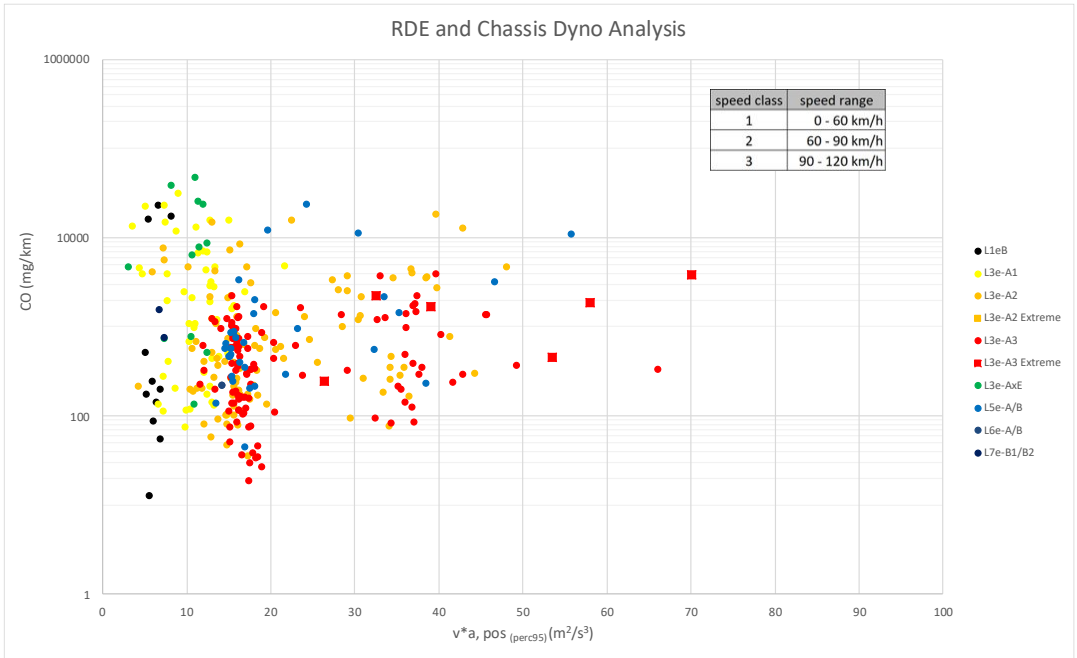

Figure G-12: CO emissions (mg/km) against v*a,pos perc 95 (m^2/s^3) for urban, rural and motorway. when discretizing phases as 0-60 urban phase, 60-90 rural phase, and 90-120 for motorway phase.

This project has received funding from the European Union's Horizon Europe research and innovation programme under grant agreement No 101056777

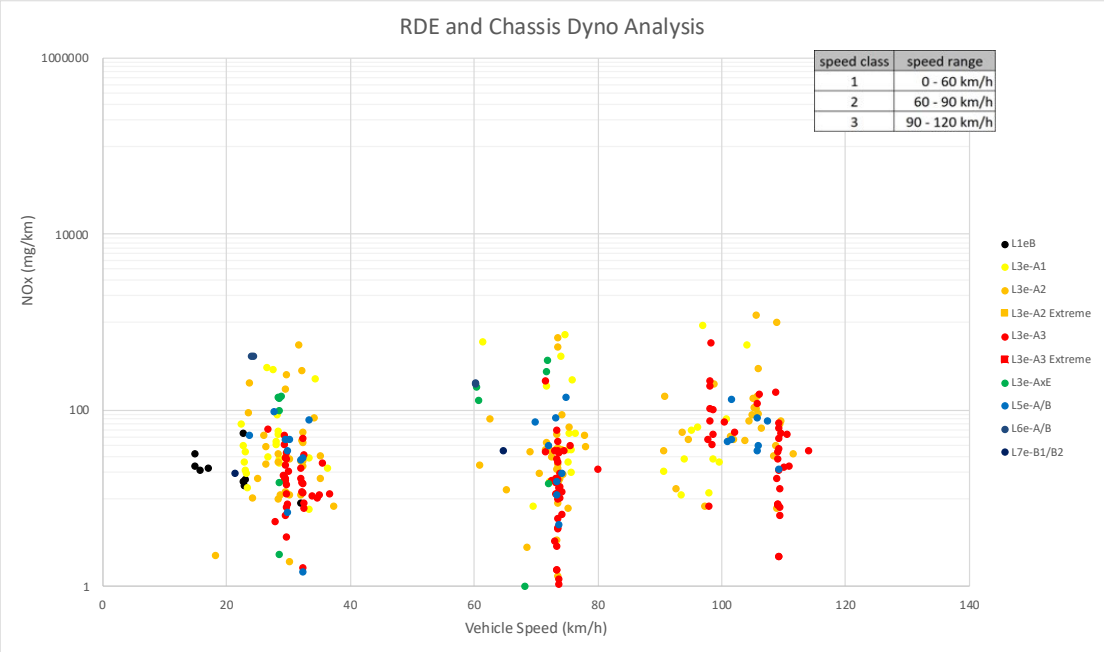

Figure G-13: NOx emissions (mg/km) against vehicle mean speed (km/h) for urban, rural and motorway. when discretizing phases as 0-60 urban phase, 60-90 rural phase, and 90-120 for motorway phase.

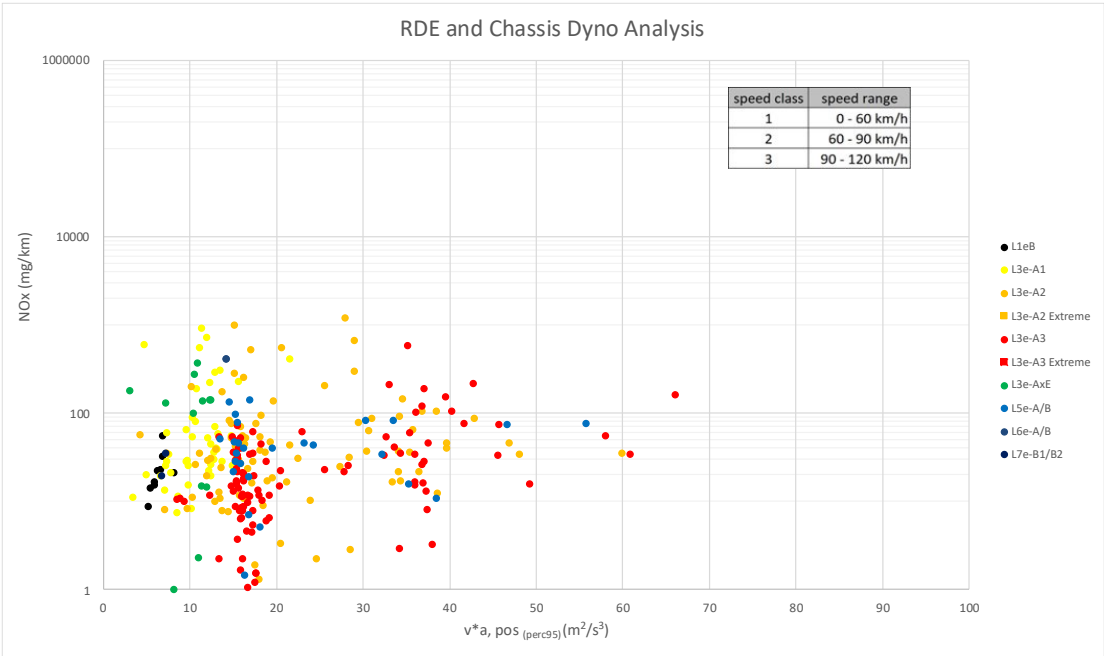

Figure G-14: NOx emissions (mg/km) against v*a,pos perc 95 (m^2/s^3) for urban, rural and motorway. when discretizing phases as 0-60 urban phase, 60-90 rural phase, and 90-120 for motorway phase.

This project has received funding from the European Union's Horizon Europe research and innovation programme under grant agreement No 101056777

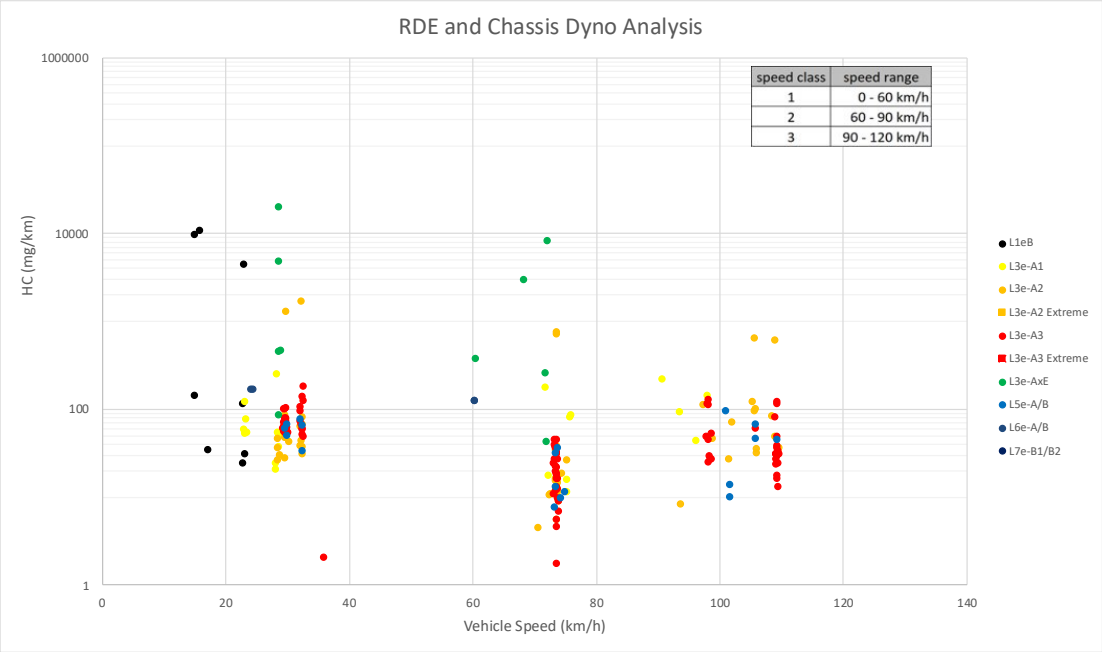

Figure G-15: HC emissions (mg/km) against vehicle mean speed (km/h) for urban, rural and motorway. when discretizing phases as 0-60 urban phase, 60-90 rural phase, and 90-120 for motorway phase.

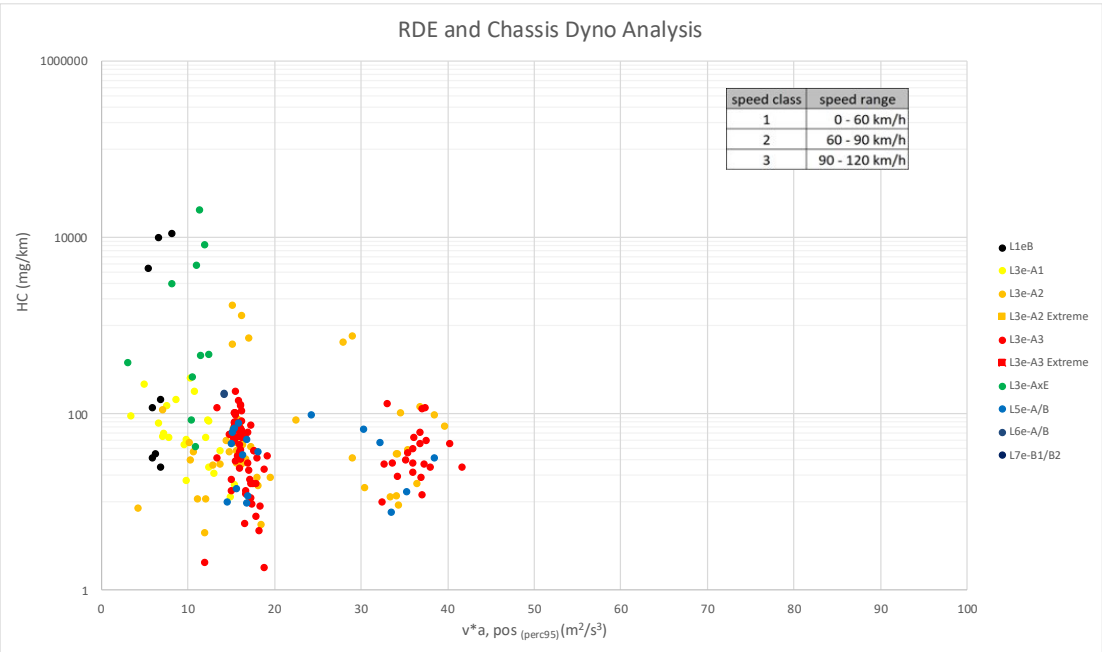

Figure G-16: HC emissions (mg/km) against v*a,pos perc 95 (m^2/s^3) for urban, rural and motorway. when discretizing phases as 0-60 urban phase, 60-90 rural phase, and 90-120 for motorway phase.

This project has received funding from the European Union's Horizon Europe research and innovation programme under grant agreement No 101056777

0-60-100

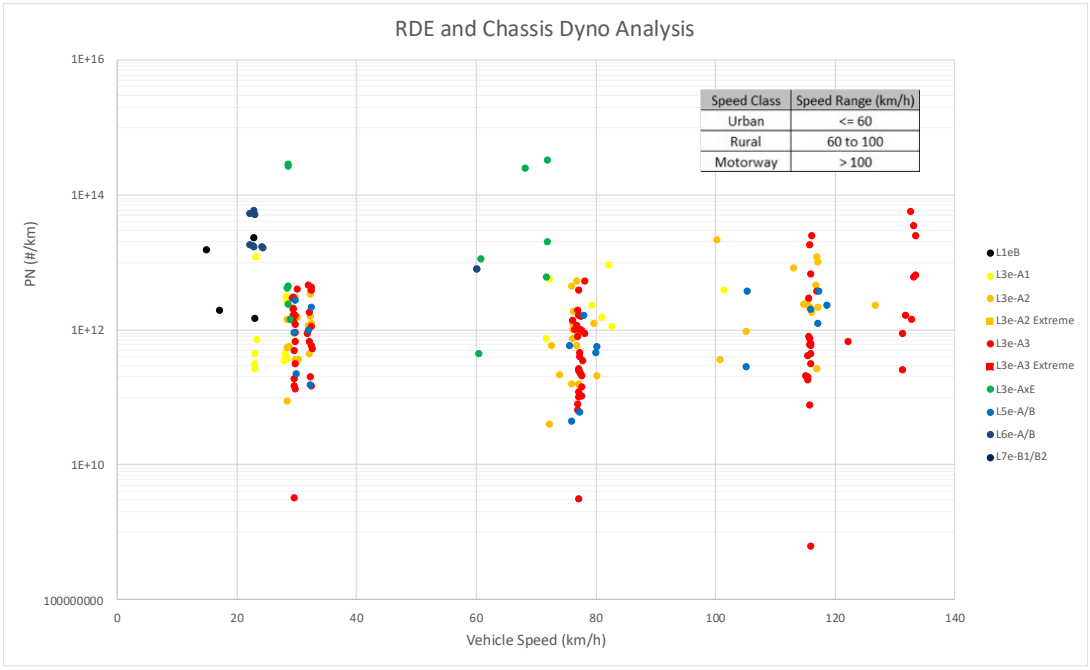

Figure G-17: PN emissions (#/km) against vehicle mean speed (km/h) for urban, rural and motorway. when discretizing phases as 0-60 urban phase, 60-100 rural phase, and >100 for motorway phase.

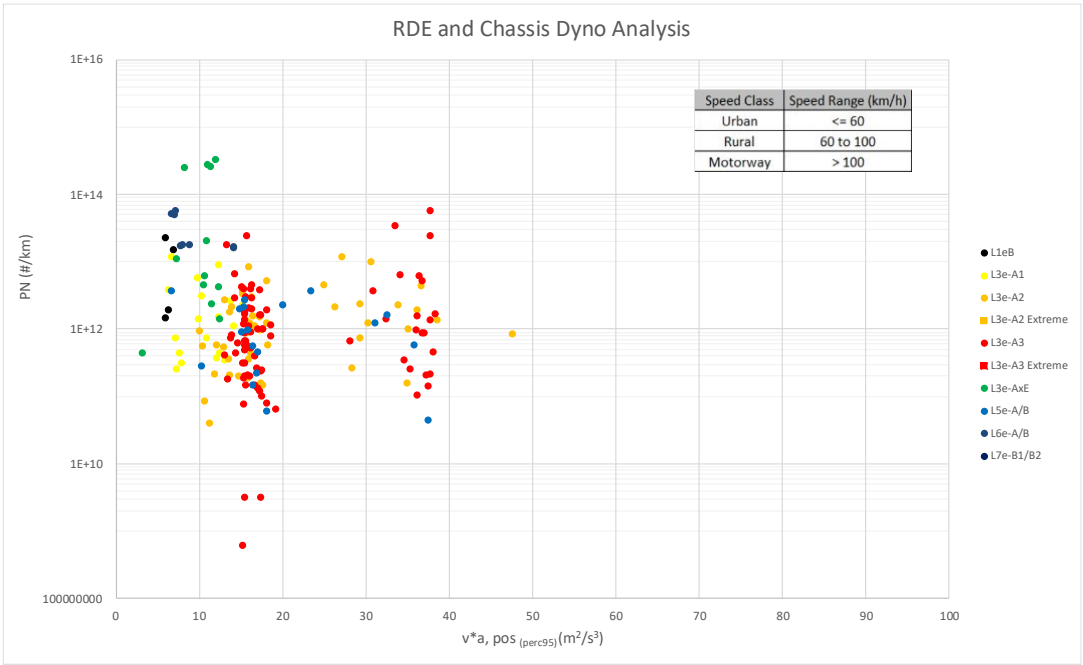

Figure G-18: PN emissions (#/km) against v*a,pos perc 95 (m^2/s^3) for urban, rural and motorway. when discretizing phases as 0-60 urban phase, 60-100 rural phase, and >100 for motorway phase.

This project has received funding from the European Union's Horizon Europe research and innovation programme under grant agreement No 101056777

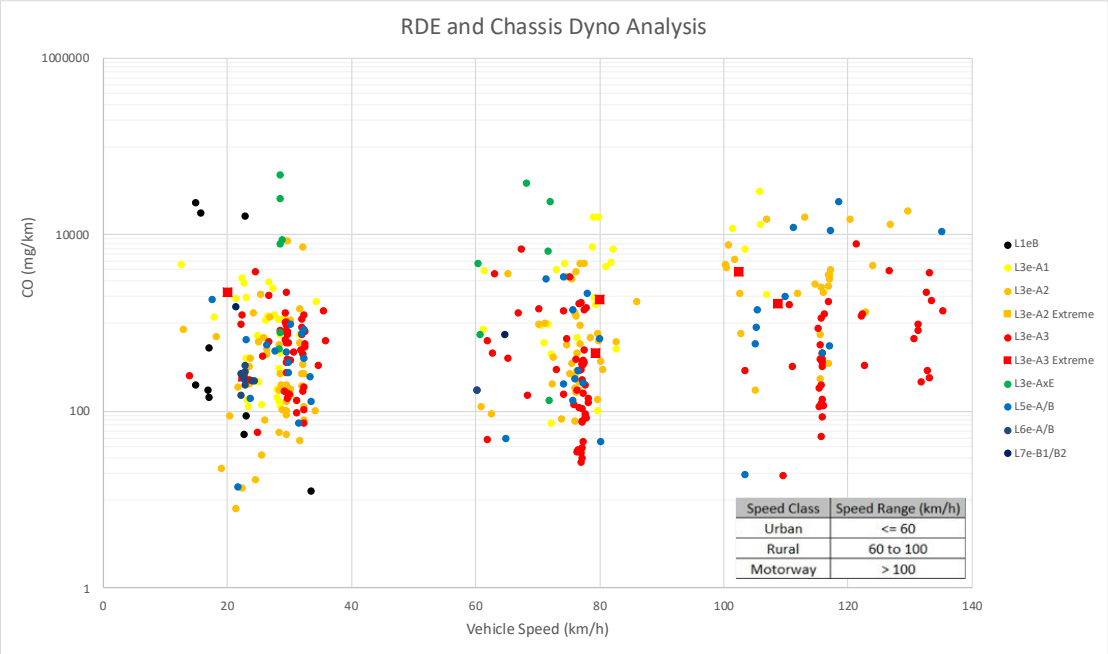

Figure G-19: CO emissions (mg/km) against vehicle mean speed (km/h) for urban, rural and motorway. when discretizing phases as 0-60 urban phase, 60-100 rural phase, and >100 for motorway phase.

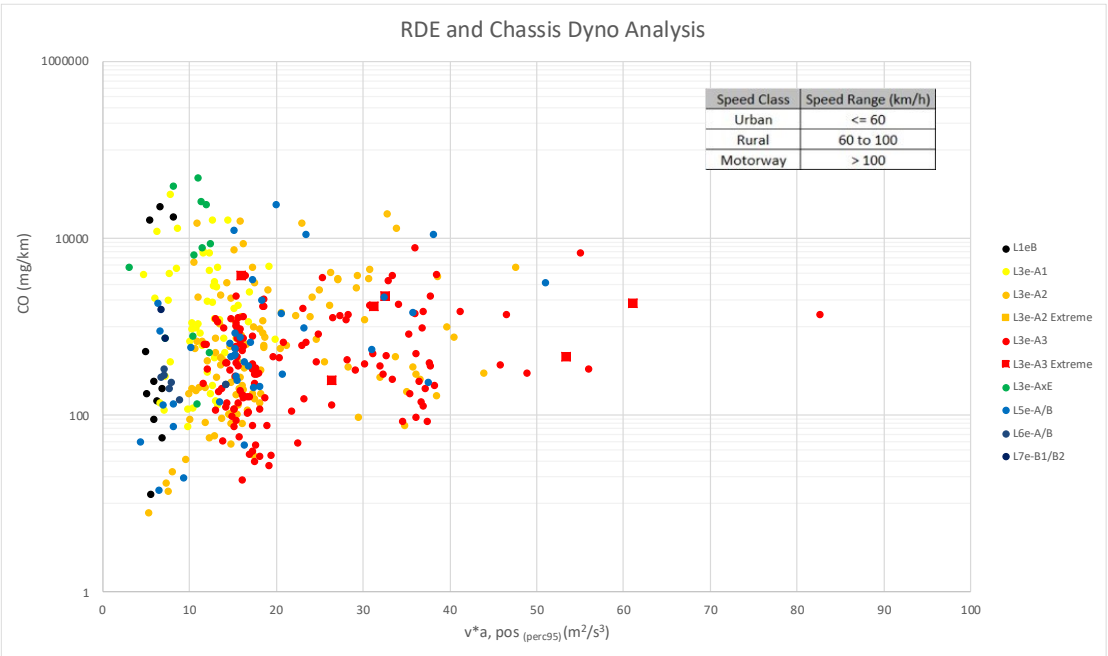

Figure G-20: CO emissions (mg/km) against v*a,pos perc 95 (m^2/s^3) for urban, rural and motorway. when discretizing phases as 0-60 urban phase, 60-100 rural phase, and >100 for motorway phase.

This project has received funding from the European Union's Horizon Europe research and innovation programme under grant agreement No 101056777

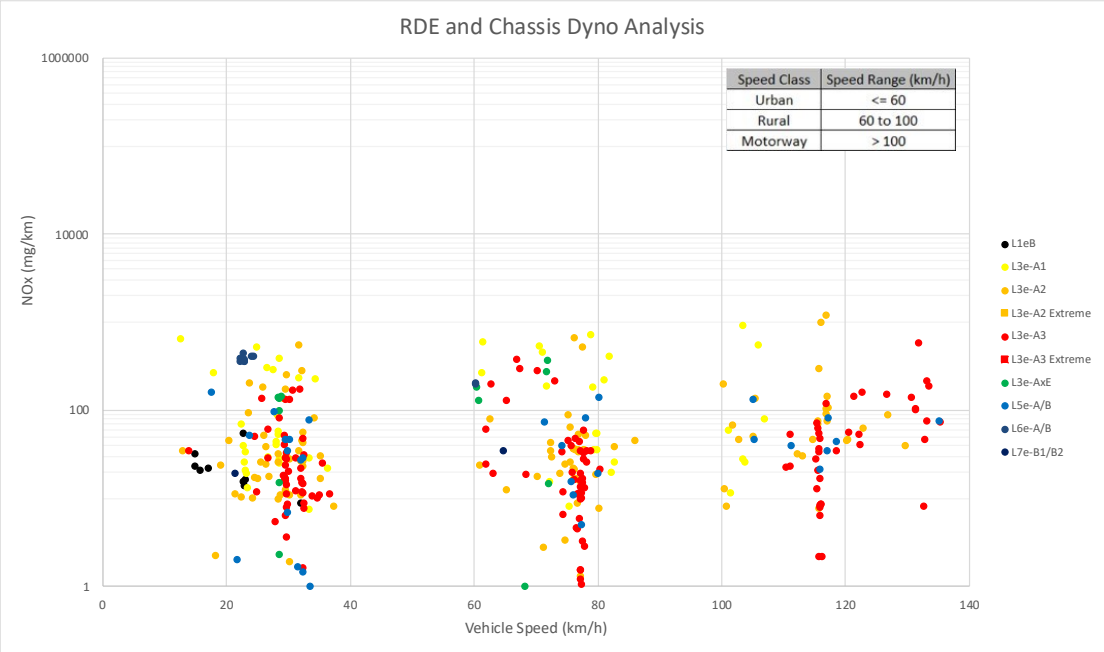

Figure G-21: NOx emissions (mg/km) against vehicle mean speed (km/h) for urban, rural and motorway. when discretizing phases as 0-60 urban phase, 60-100 rural phase, and >100 for motorway phase.

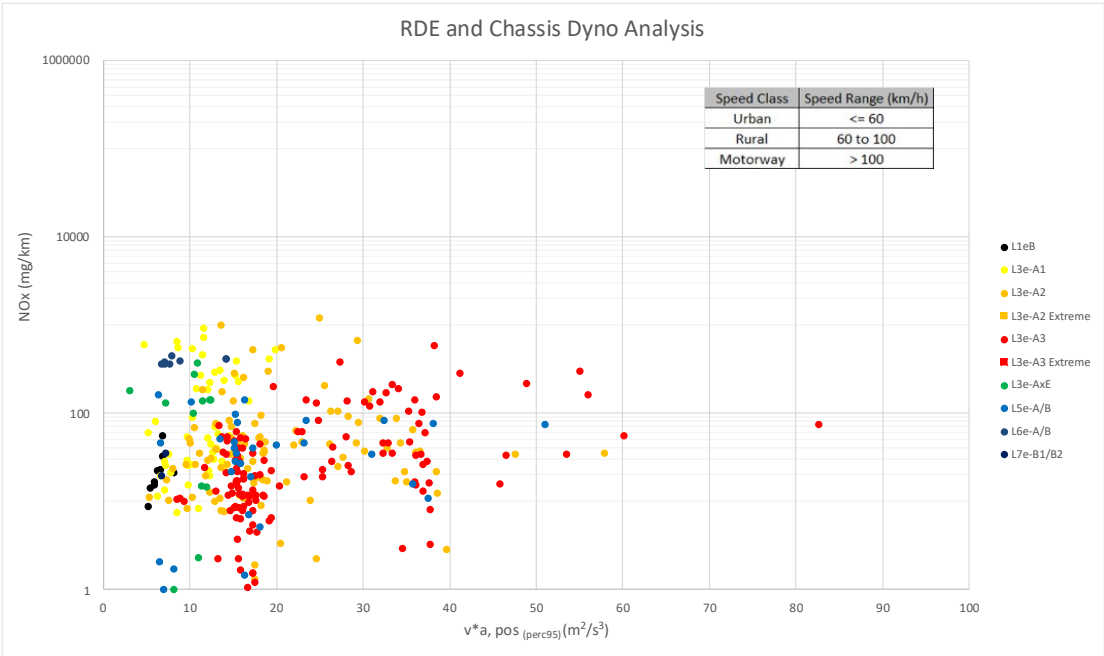

Figure G-22: NOx emissions (mg/km) against v*a,pos perc 95 (m^2/s^3) for urban, rural and motorway. when discretizing phases as 0-60 urban phase, 60-100 rural phase, and >100 for motorway phase.

This project has received funding from the European Union's Horizon Europe research and innovation programme under grant agreement No 101056777

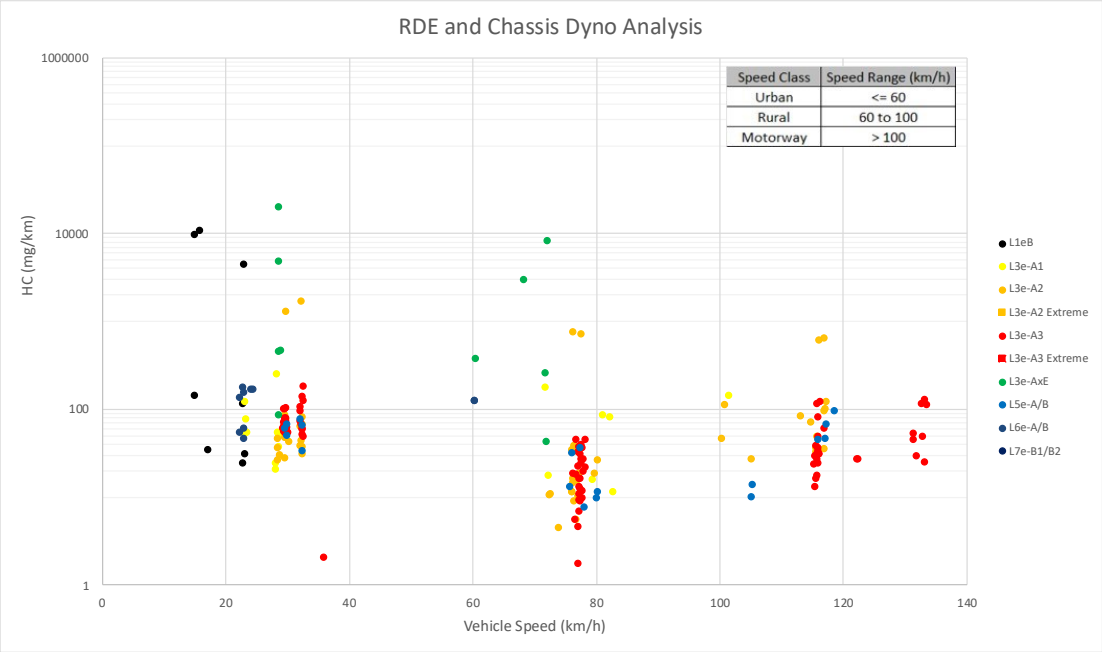

Figure G-23: HC emissions (mg/km) against vehicle mean speed (km/h) for urban, rural and motorway. when discretizing phases as 0-60 urban phase, 60-100 rural phase, and >100 for motorway phase.

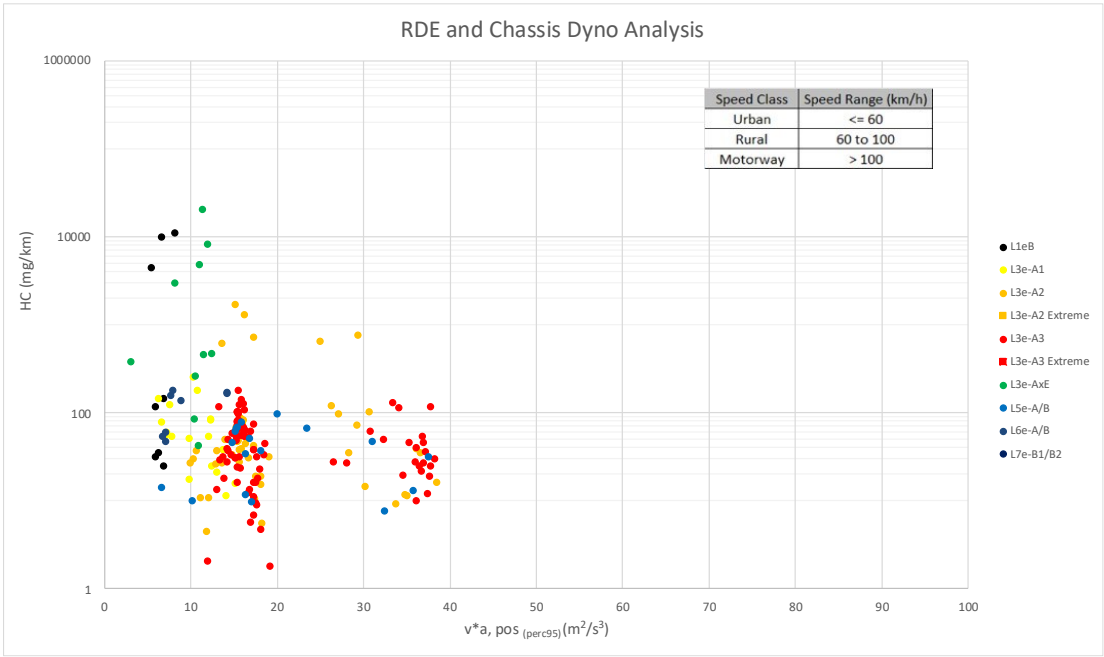

Figure G-24: HC emissions (mg/km) against v*a,pos perc 95 (m^2/s^3) for urban, rural and motorway. when discretizing phases as 0-60 urban phase, 60-100 rural phase, and >100 for motorway phase.

This project has received funding from the European Union's Horizon Europe research and innovation programme under grant agreement No 101056777

0-50-100

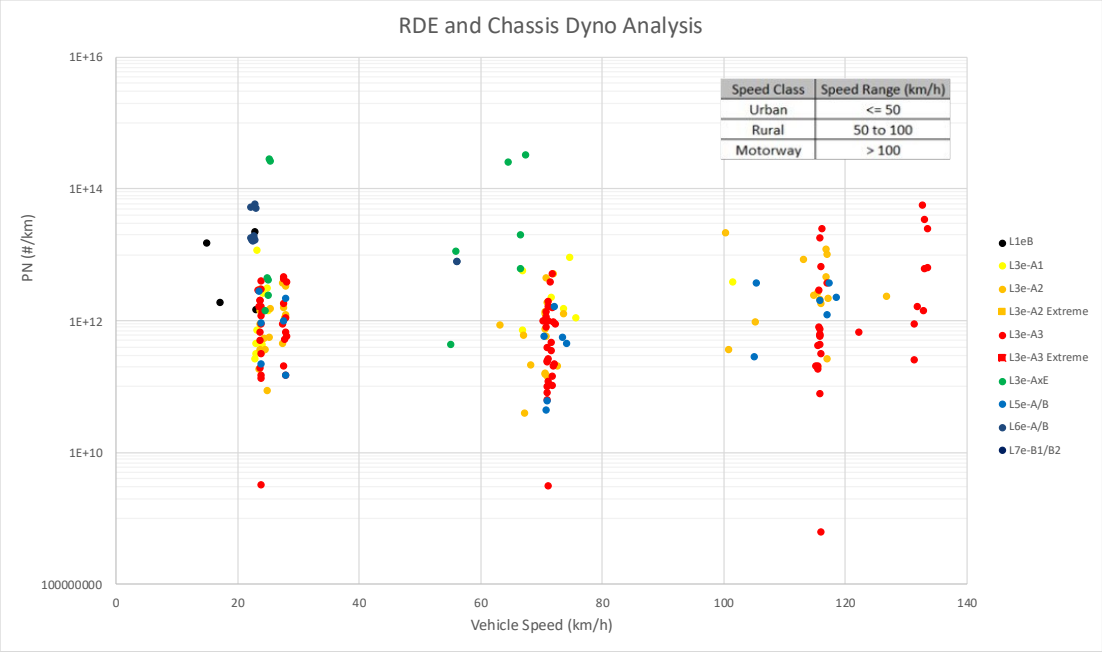

Figure G-25: PN emissions (#/km) against vehicle mean speed (km/h) for urban, rural and motorway. when discretizing phases as 0-50 urban phase, 50-100 rural phase, and >100 for motorway phase.

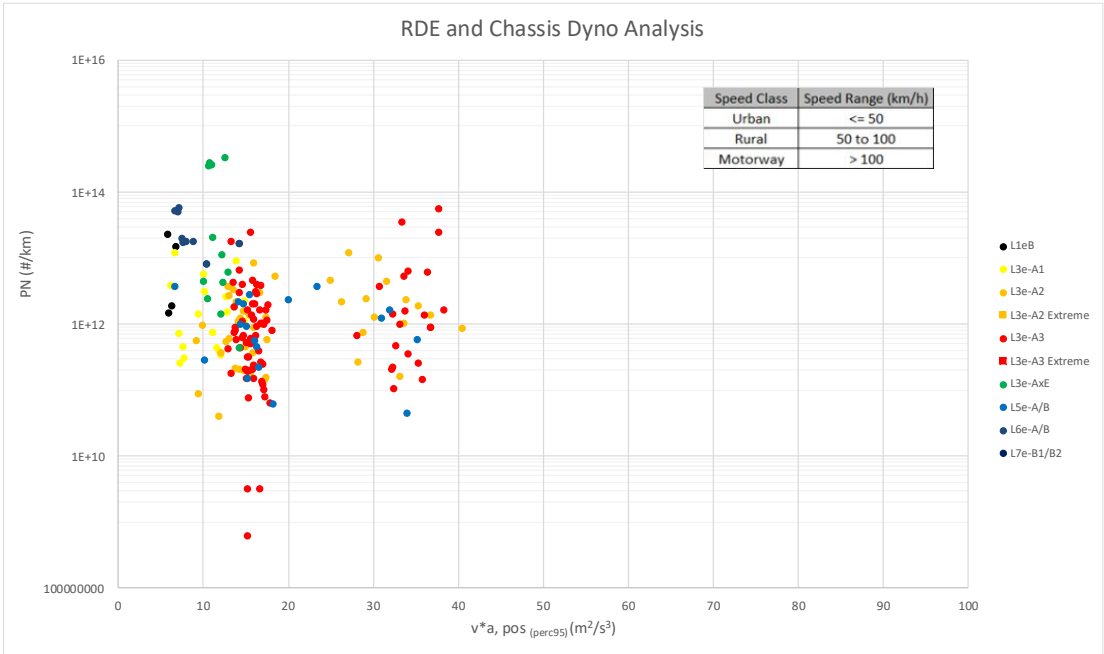

Figure G-26: PN emissions (#/km) against v*a,pos perc 95 (m^2/s^3) for urban, rural and motorway. when discretizing phases as 0-50 urban phase, 50-100 rural phase, and >100 for motorway phase.

This project has received funding from the European Union's Horizon Europe research and innovation programme under grant agreement No 101056777

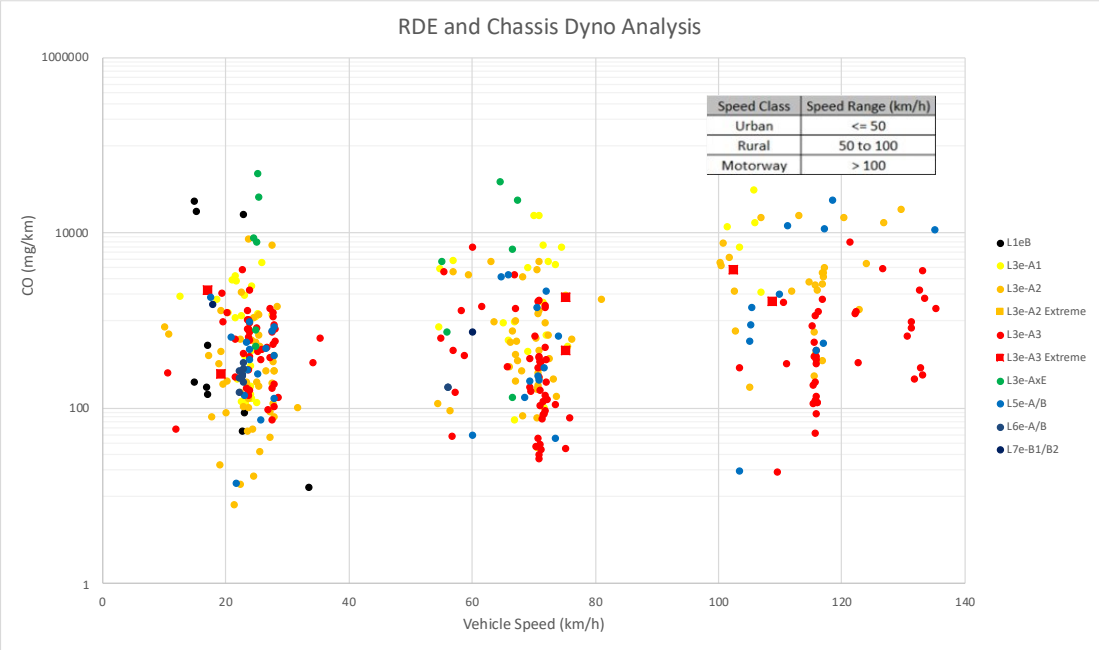

Figure G-27: CO emissions (mg/km) against vehicle mean speed (km/h) for urban, rural and motorway. when discretizing phases as 0-50 urban phase, 50-100 rural phase, and >100 for motorway phase.

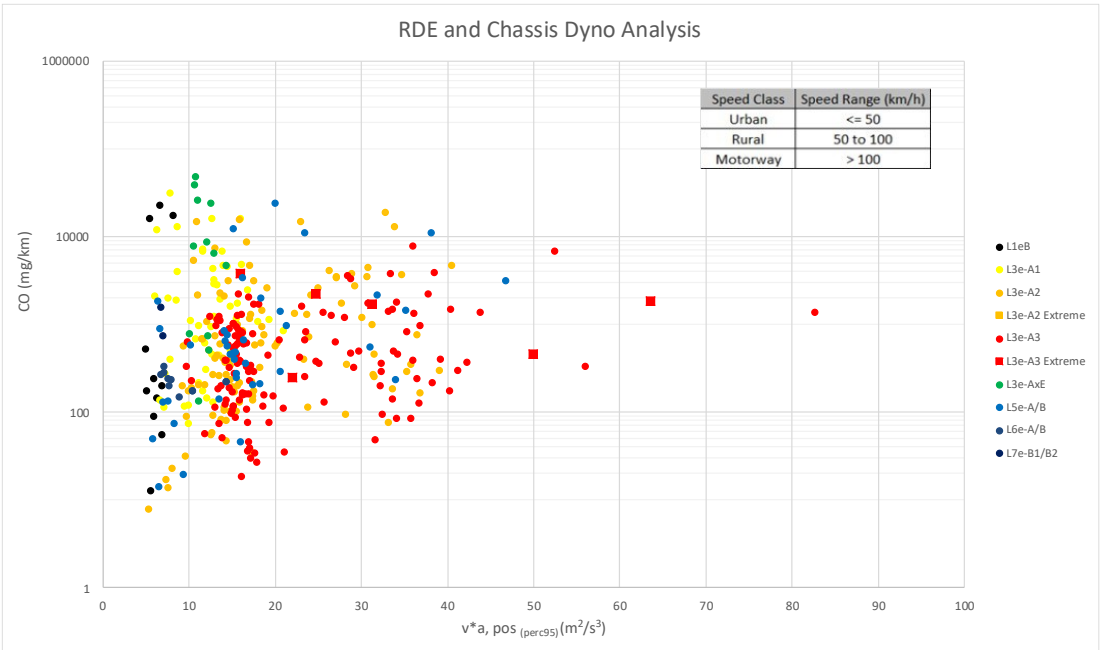

Figure G-28: CO emissions (mg/km) against v*a,pos perc 95 (m^2/s^3) for urban, rural and motorway. when discretizing phases as 0-50 urban phase, 50-100 rural phase, and >100 for motorway phase.

This project has received funding from the European Union's Horizon Europe research and innovation programme under grant agreement No 101056777

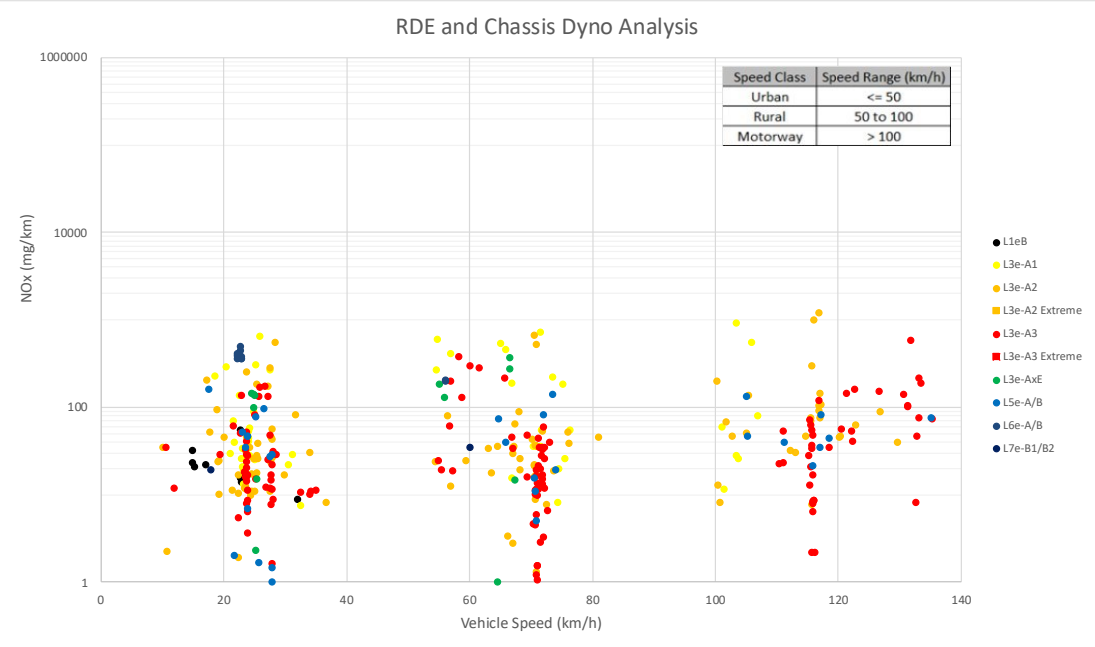

Figure G-29: NOx emissions (mg/km) against vehicle mean speed (km/h) for urban, rural and motorway. when discretizing phases as 0-50 urban phase, 50-100 rural phase, and >100 for motorway phase.

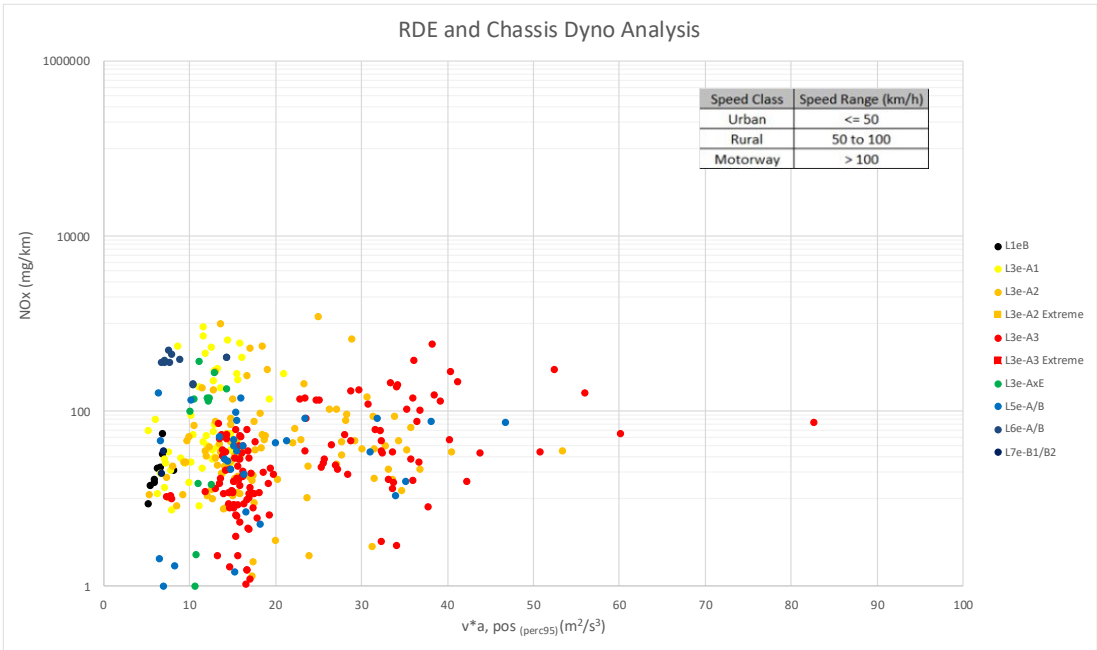

Figure G-30: NOx emissions (mg/km) against v*a,pos perc 95 (m^2/s^3) for urban, rural and motorway when discretizing phases as 0-50 urban phase, 50-100 rural phase, and >100 for motorway phase.

This project has received funding from the European Union's Horizon Europe research and innovation programme under grant agreement No 101056777

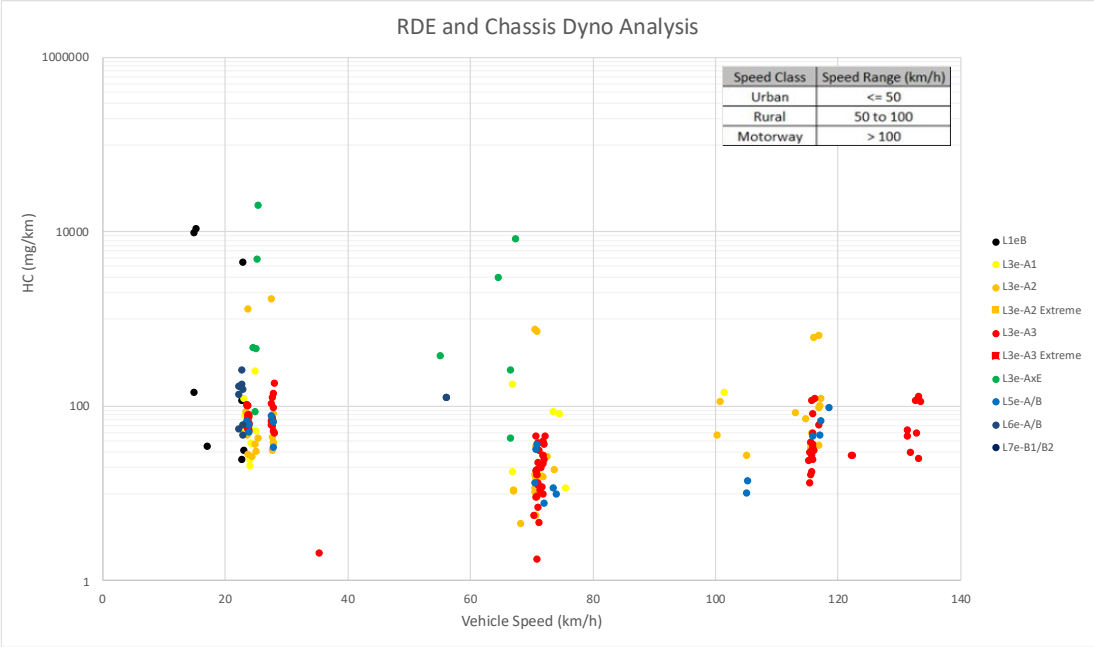

Figure G-31: HC emissions (mg/km) against vehicle mean speed (km/h) for urban, rural and motorway. when discretizing phases as 0-50 urban phase, 50-100 rural phase, and >100 for motorway phase.

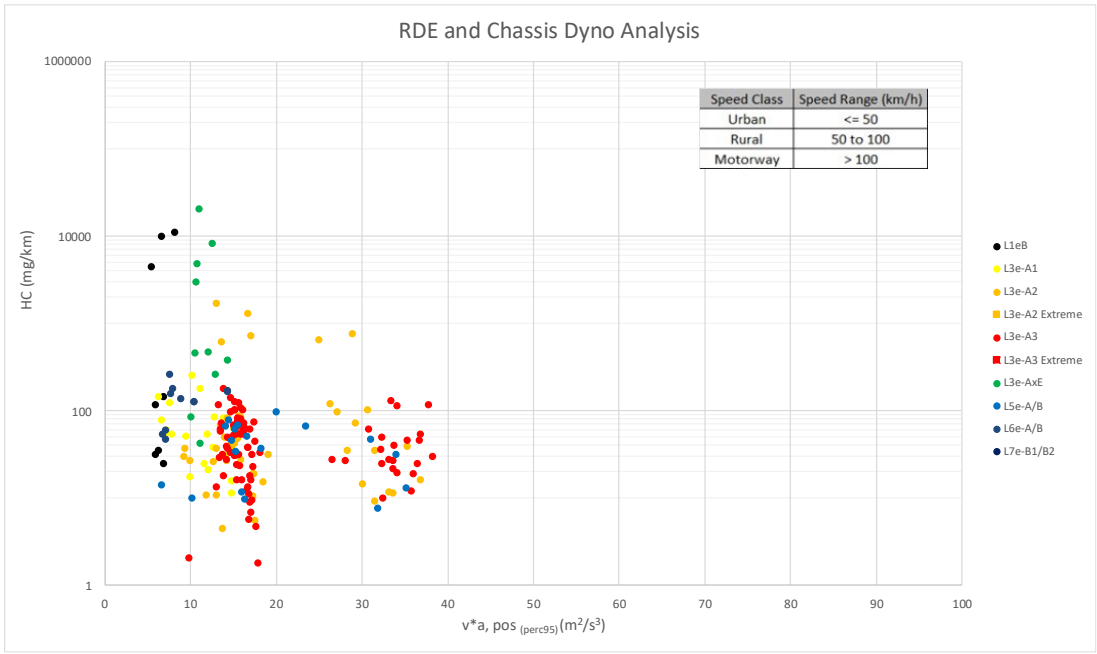

Figure G-32: HC emissions (mg/km) against v*a,pos perc 95 (m^2/s^3) for urban, rural and motorway. when discretizing phases as 0-50 urban phase, 50-100 rural phase, and >100 for motorway phase.

This project has received funding from the European Union's Horizon Europe research and innovation programme under grant agreement No 101056777

Road Type

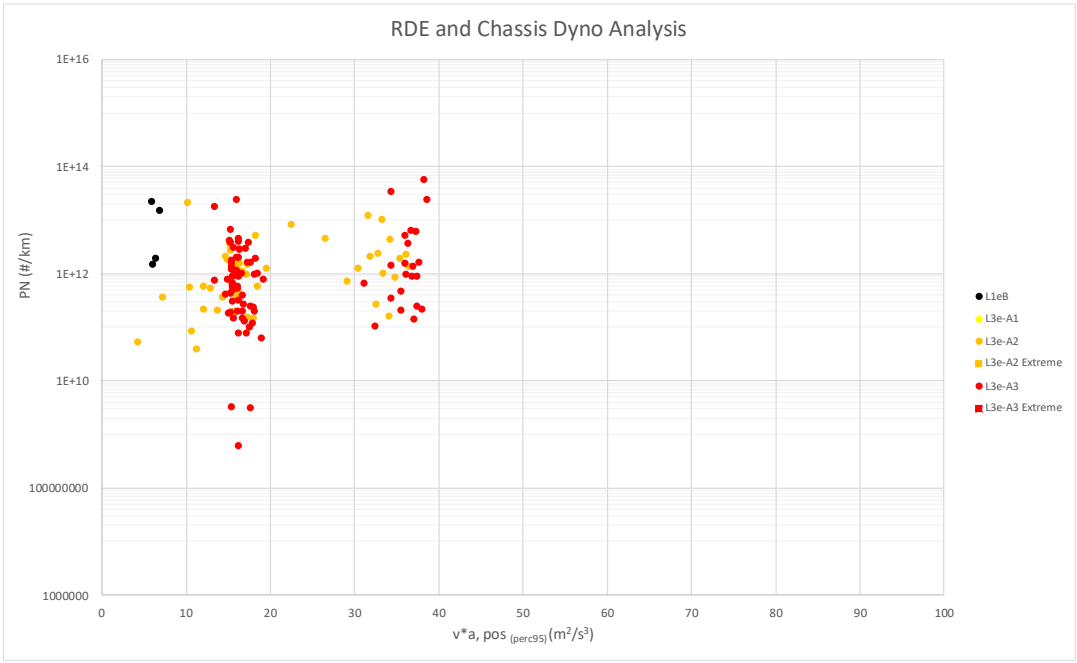

Figure G-33: PN emissions (#/km) against v*a,pos perc 95 (m^2/s^3) for urban, rural and motorway when discretizing phases per road type.

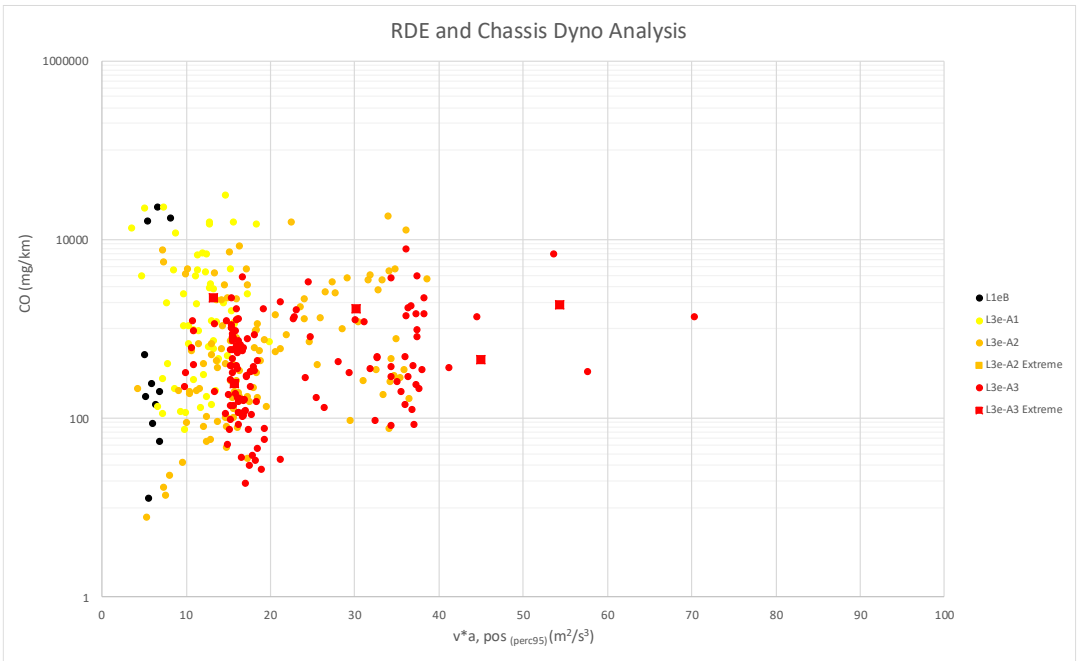

Figure G-34: CO emissions (mg/km) against v*a,pos perc 95 (m^2/s^3) for urban, rural and motorway when discretizing phases per road type.

This project has received funding from the European Union's Horizon Europe research and innovation programme under grant agreement No 101056777

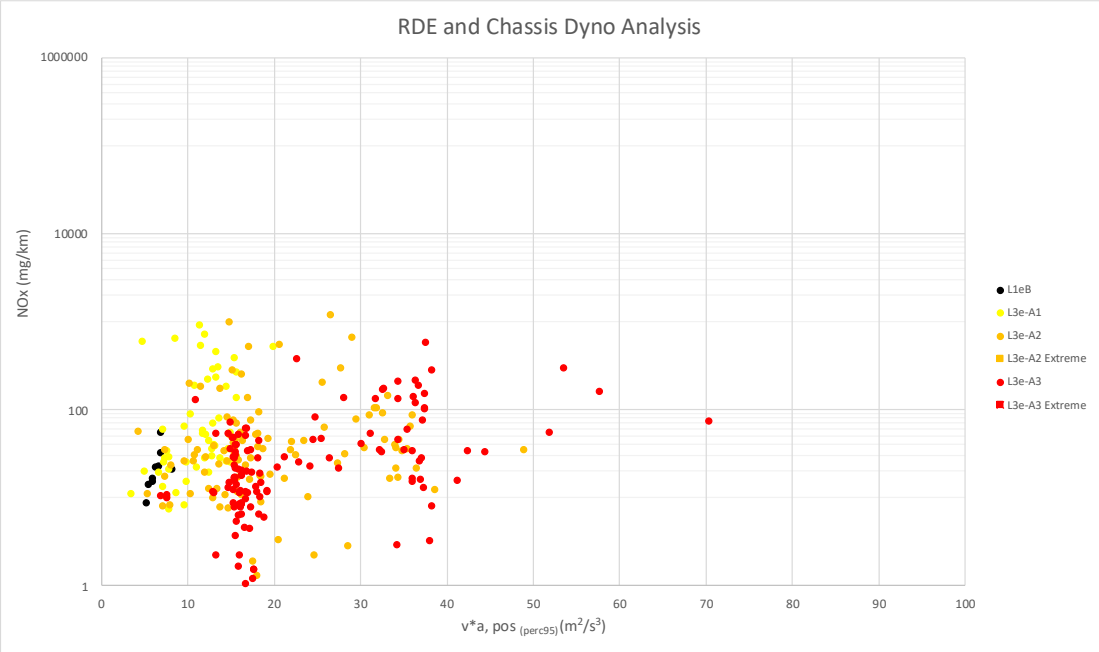

Figure G-35: NOx emissions (mg/km) against v*a,pos perc 95 (m^2/s^3) for urban, rural and motorway when discretizing phases per road type.

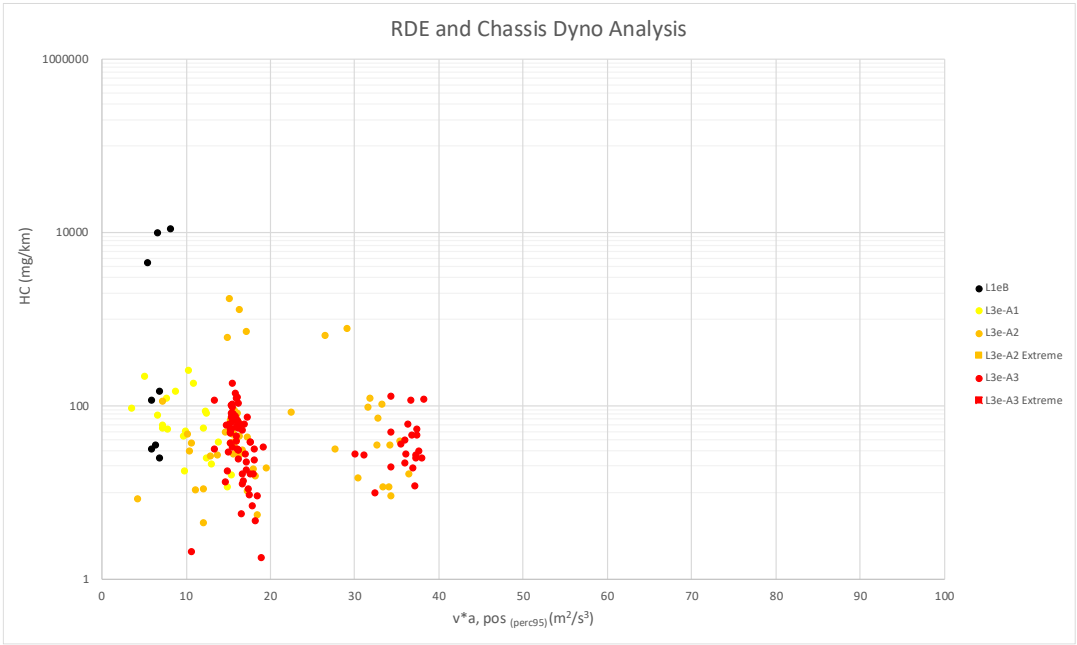

Figure G-36: HC emissions (mg/km) against v*a,pos perc 95 (m^2/s^3) for urban, rural and motorway when discretizing phases per road type.

This project has received funding from the European Union's Horizon Europe research and innovation programme under grant agreement No 101056777

Appendix H: v*apos analysis

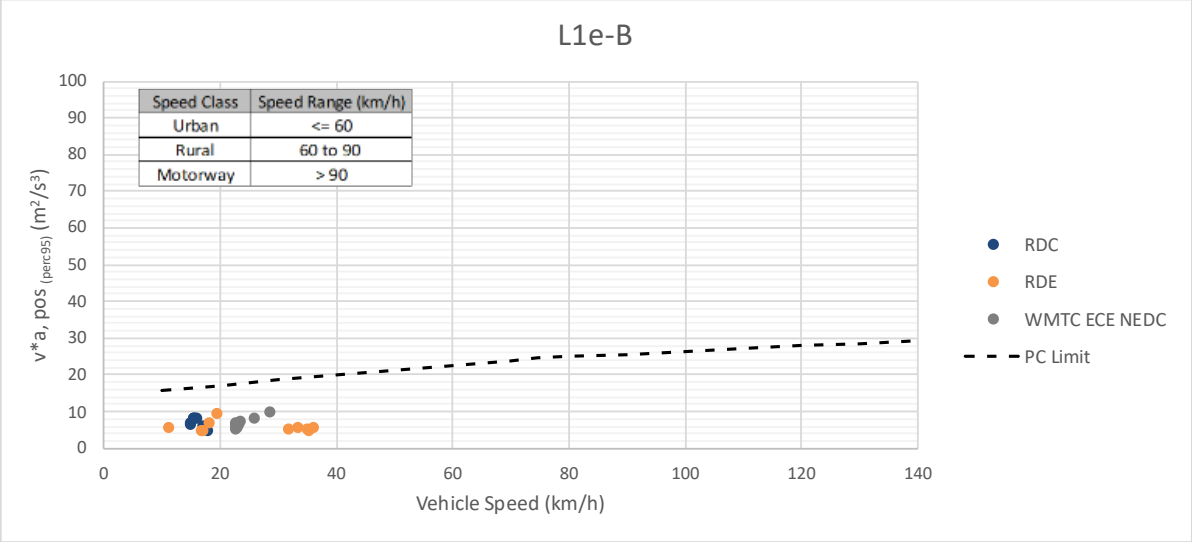

Figure H-1: L1e-B vehicle dynamics v*a pos perc 95 (m^2/s^3) against vehicle mean speed (km/h) for urban, rural and motorway.

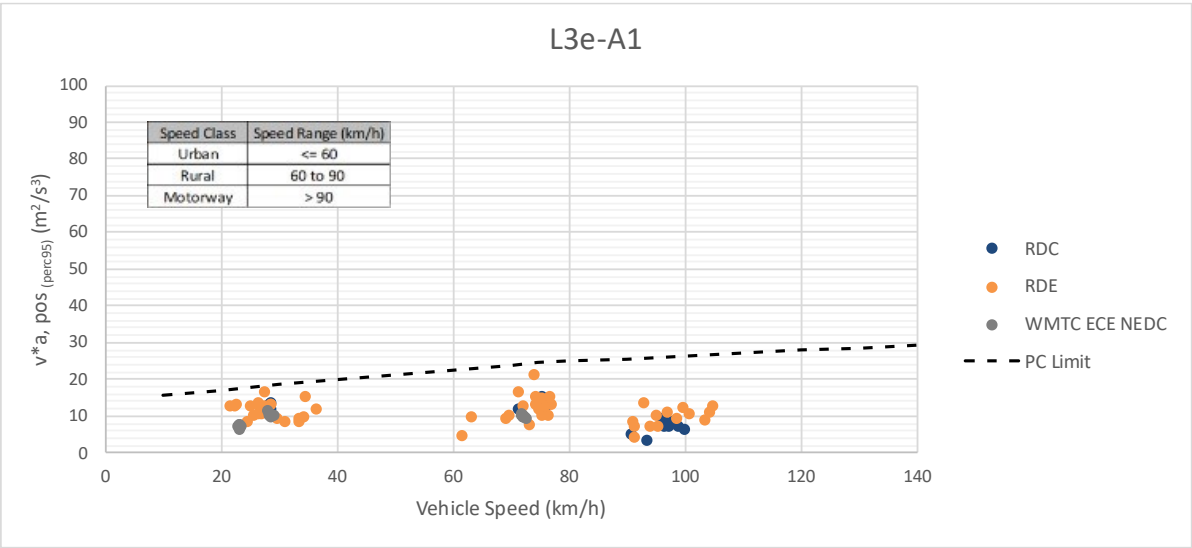

Figure H-2: L3e-A1 vehicle dynamics v*a pos perc 95 (m^2/s^3) against vehicle mean speed (km/h) for urban, rural and motorway.

This project has received funding from the European Union's Horizon Europe research and innovation programme under grant agreement No 101056777

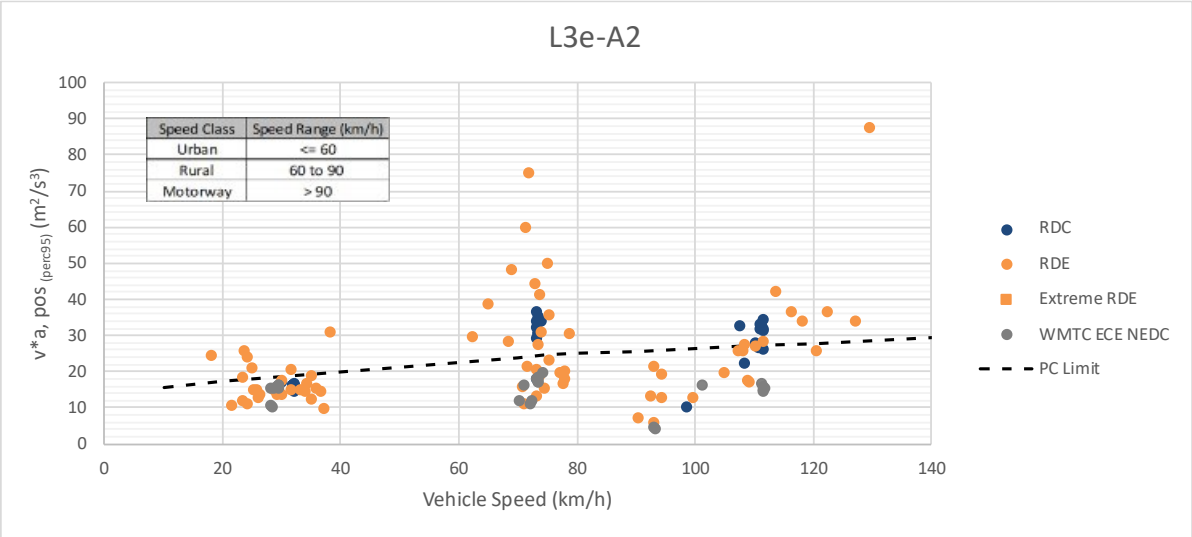

Figure H-3: L3e-A2 vehicle dynamics v*a pos perc 95 (m²/s³) against vehicle mean speed (km/h) for urban, rural and motorway.

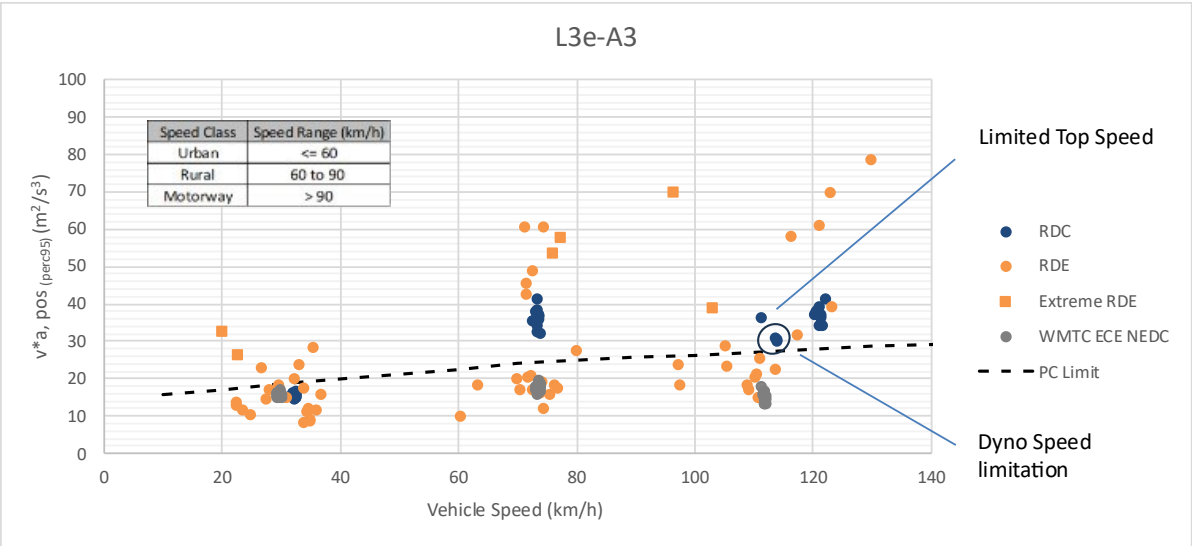

Figure H-4: L3e-A4 vehicle dynamics v*a pos perc 95 (m²/s³) against vehicle mean speed (km/h) for urban, rural and motorway.

This project has received funding from the European Union's Horizon Europe research and innovation programme under grant agreement No 101056777

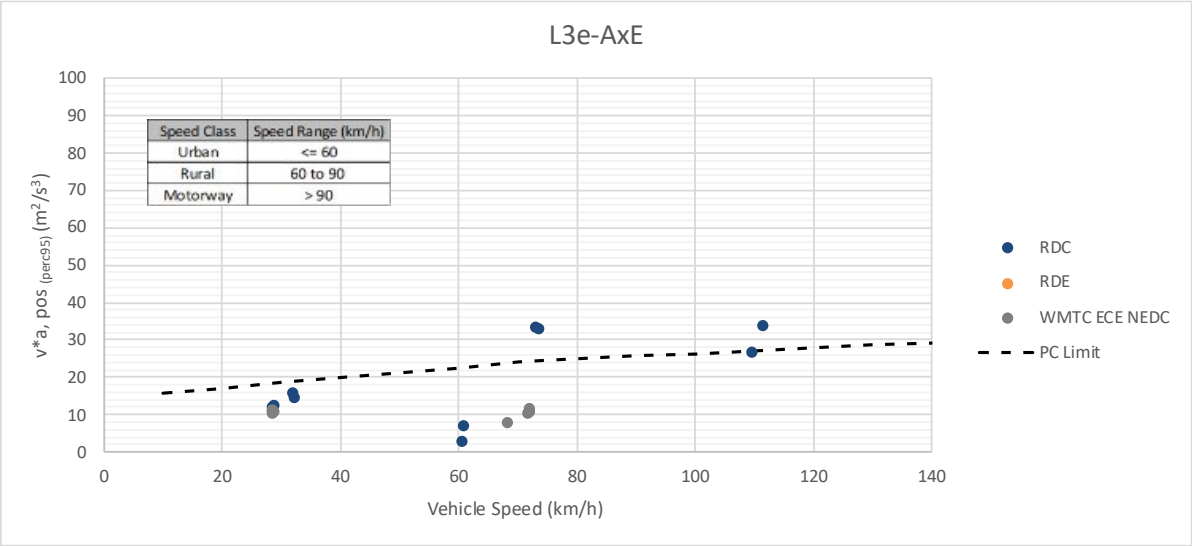

Figure H-5: L3e-AxE vehicle dynamics v*a pos perc 95 (m^2/s^3) against vehicle mean speed (km/h) for urban, rural and motorway.

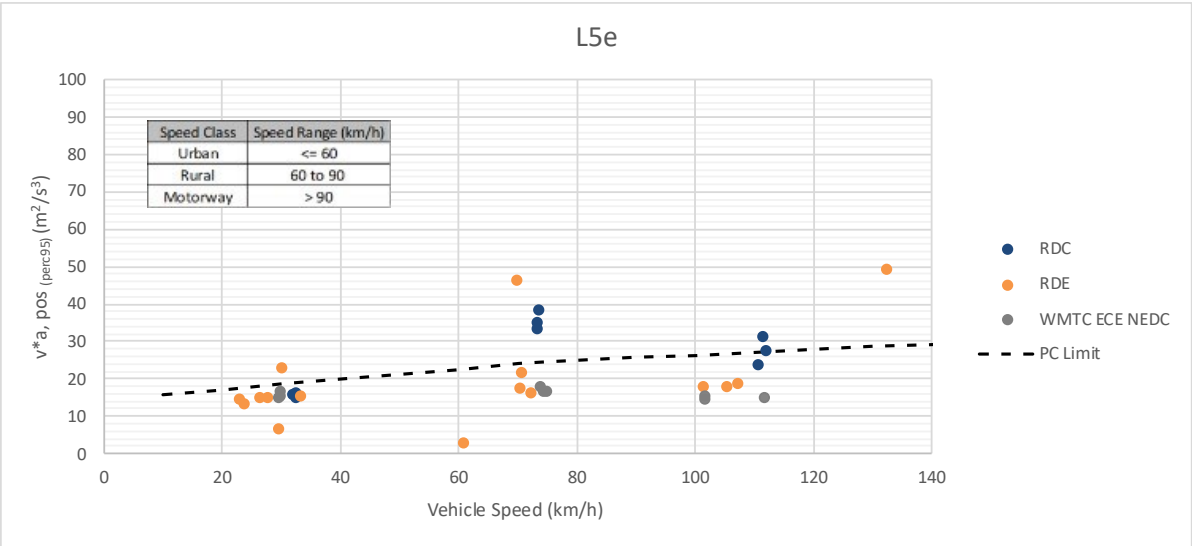

Figure H-6: L5e vehicle dynamics v*a pos perc 95 (m^2/s^3) against vehicle mean speed (km/h) for urban, rural and motorway.

This project has received funding from the European Union's Horizon Europe research and innovation programme under grant agreement No 101056777

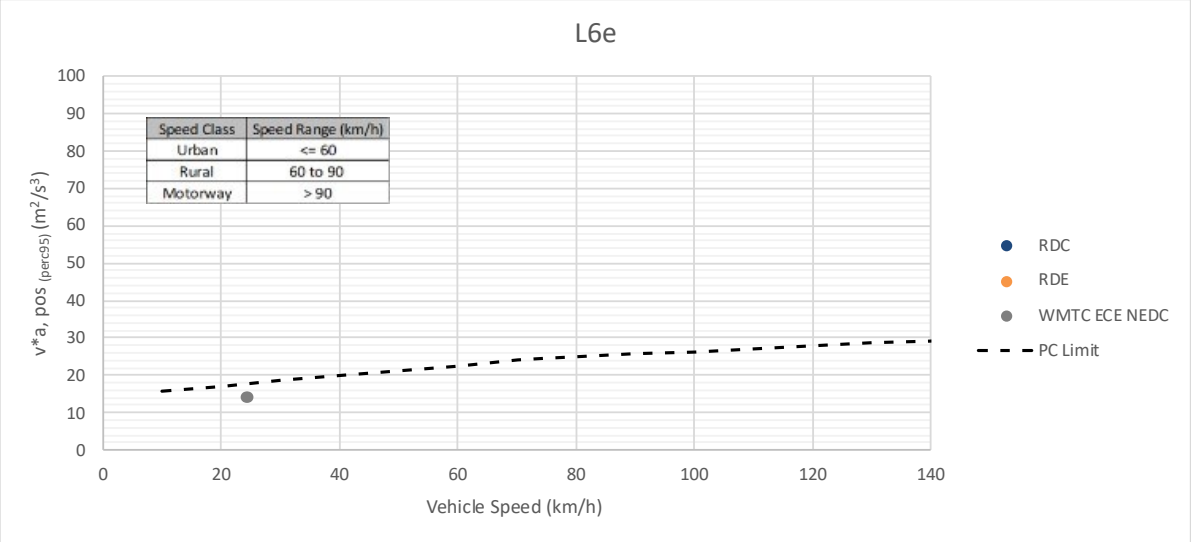

Figure H-7: L6e vehicle dynamics v*a pos perc 95 (m^2/s^3) against vehicle mean speed (km/h) for urban, rural and motorway.

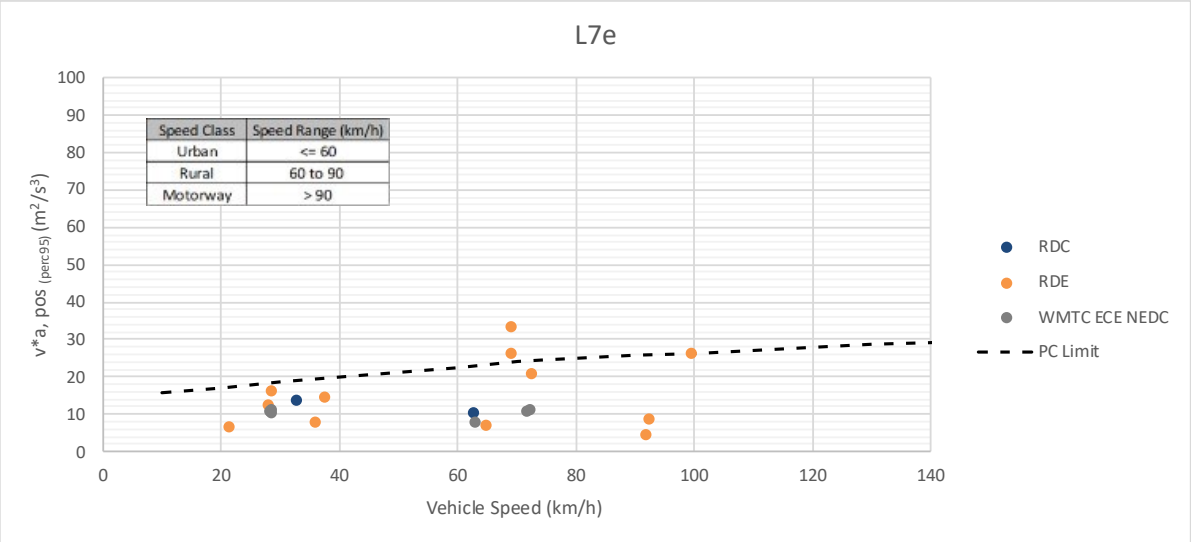

Figure H-8: L7e vehicle dynamics v*a pos perc 95 (m^2/s^3) against vehicle mean speed (km/h) for urban, rural and motorway.

This project has received funding from the European Union's Horizon Europe research and innovation programme under grant agreement No 101056777

Appendix I: Impact of Phases discretization on driving dynamics

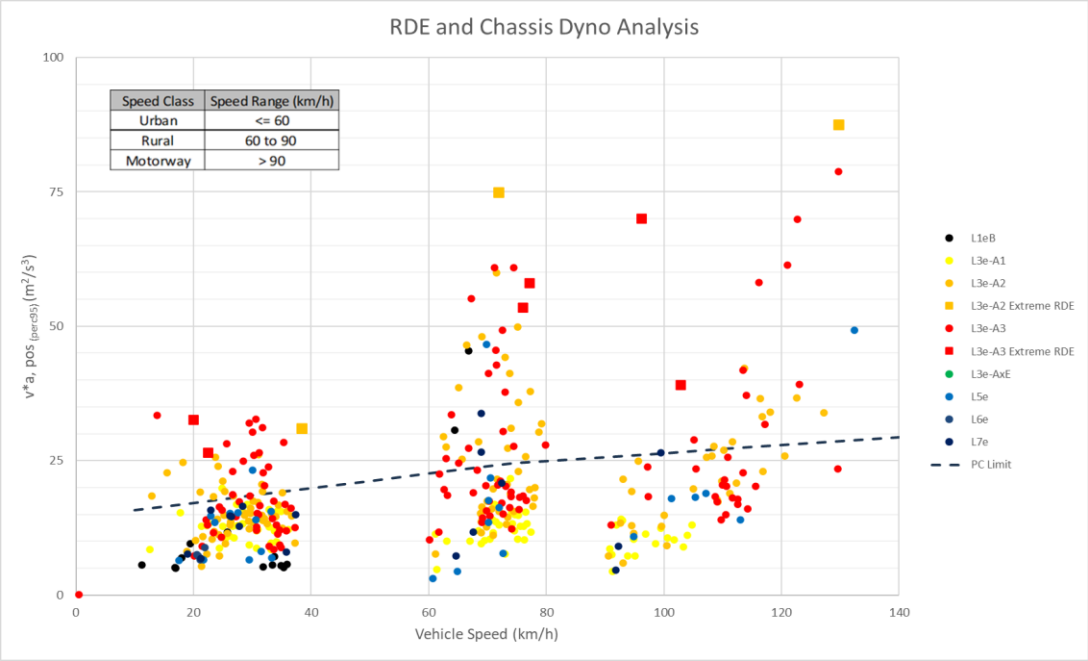

Figure I-1: veI-cle dynamics v*a pos perc 95 (m^2/s^3) against veI-cle mean speed (km/h) for urban, rural and motorway. when discretizing phases as 0-60 urban phase, 60-90 rural phase, and >90 for motorway phase.

This project has received funding from the European Union's Horizon Europe research and innovation programme under grant agreement No 101056777

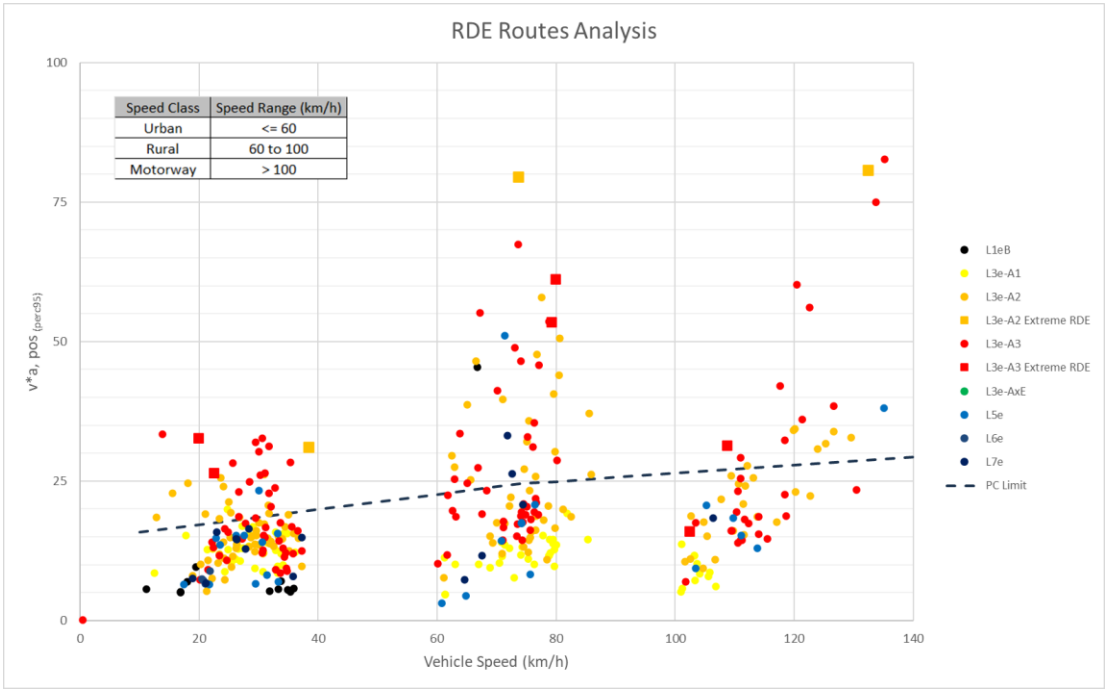

Figure I-2: veI-cle dynamics v*a pos perc 95 (m^2/s^3) against veI-cle mean speed (km/h) for urban, rural and motorway. when discretizing phases as 0-60 urban phase, 60-100 rural phase, and >100 for motorway phase.

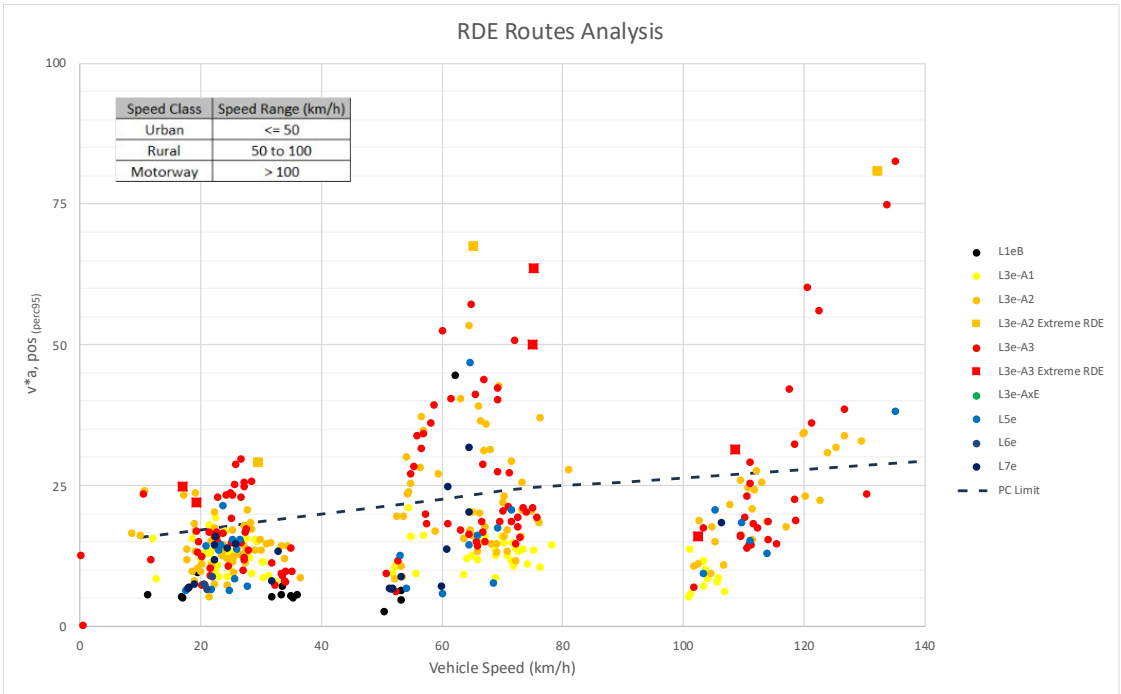

Figure I-3: veI-cle dynamics v*a pos perc 95 (m^2/s^3) against veI-cle mean speed (km/h) for urban, rural and motorway. when discretizing phases as 0-50 urban phase, 50-100 rural phase, and >100 for motorway phase.

This project has received funding from the European Union's Horizon Europe research and innovation programme under grant agreement No 101056777

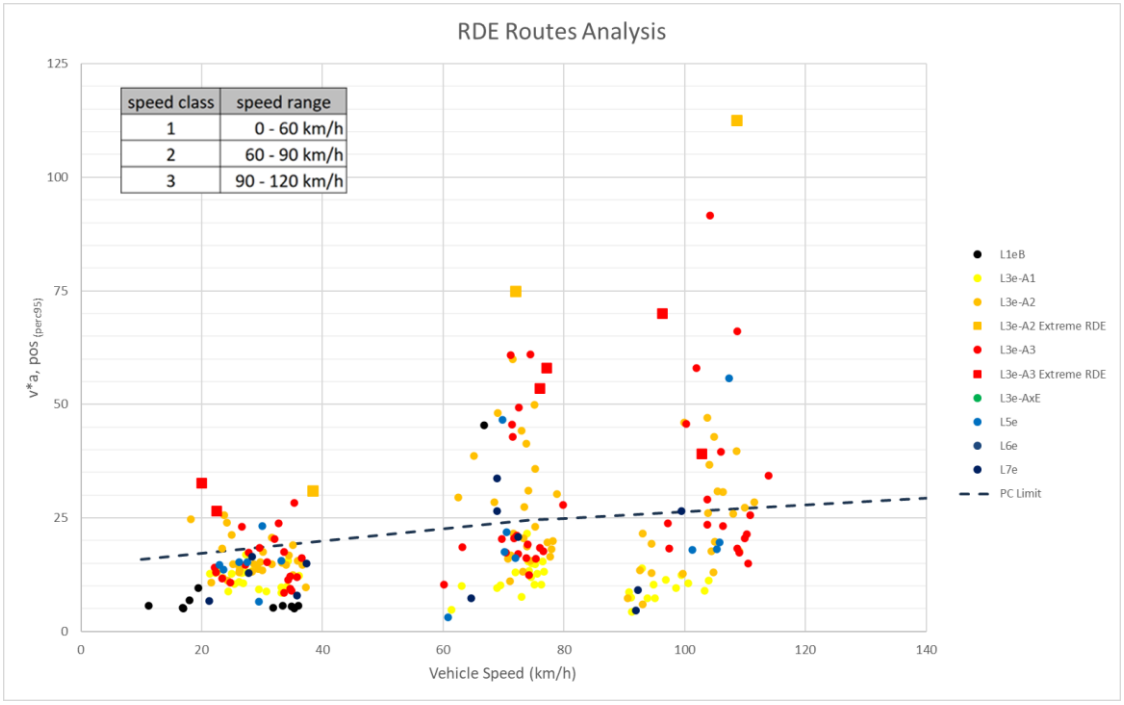

Figure I-4: veI-cle dynamics v*a pos perc 95 (m^2/s^3) against veI-cle mean speed (km/h) for urban, rural and motorway. when discretizing phases as 0-60 urban phase, 60-90 rural phase, and 90-120 for motorway phase.

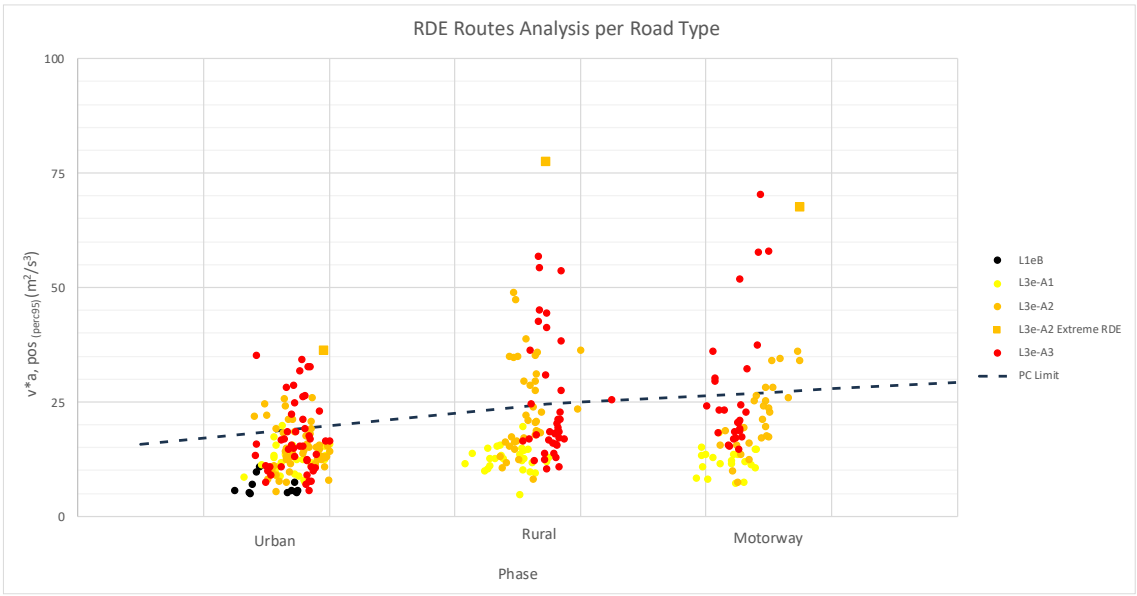

Figure I-5: veI-cle dynamics v*a pos perc 95 (m^2/s^3) against veI-cle mean speed (km/h) for urban, rural and motorway. when discretizing phases per road type.

This project has received funding from the European Union's Horizon Europe research and innovation programme under grant agreement No 101056777

Appendix J: Representative real-world driving cycles from LENS data

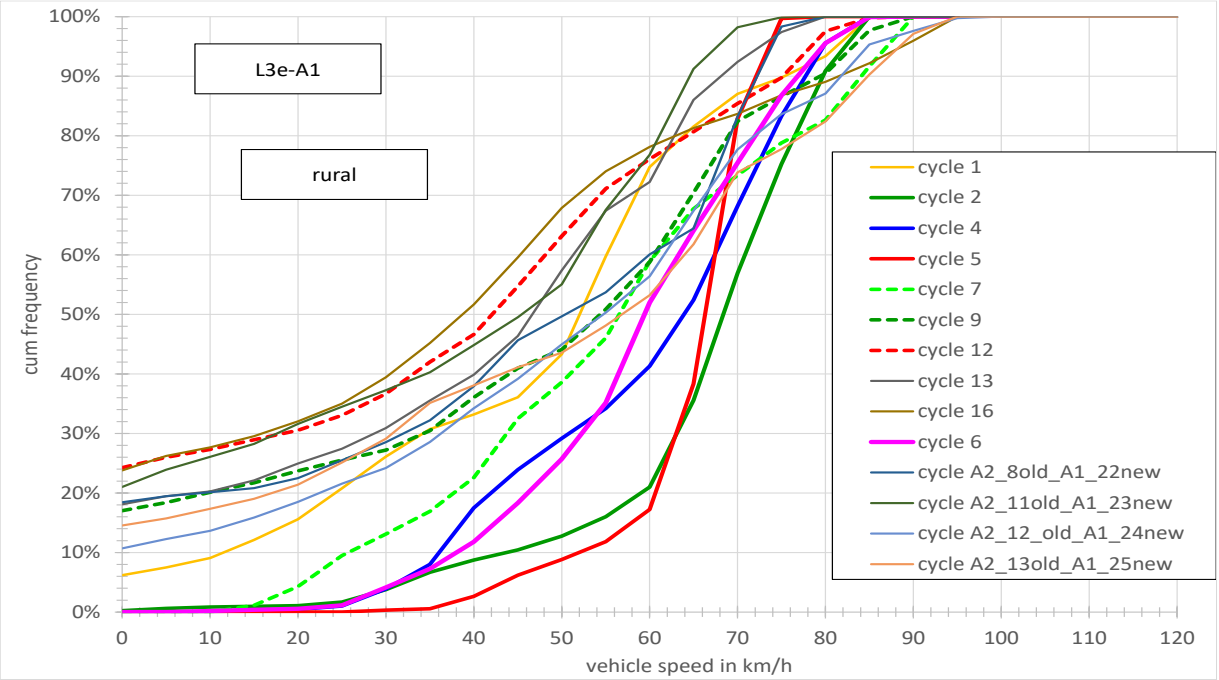

Figure J-1: Vehicle speed distributions vehicles L3e-A1, rural.

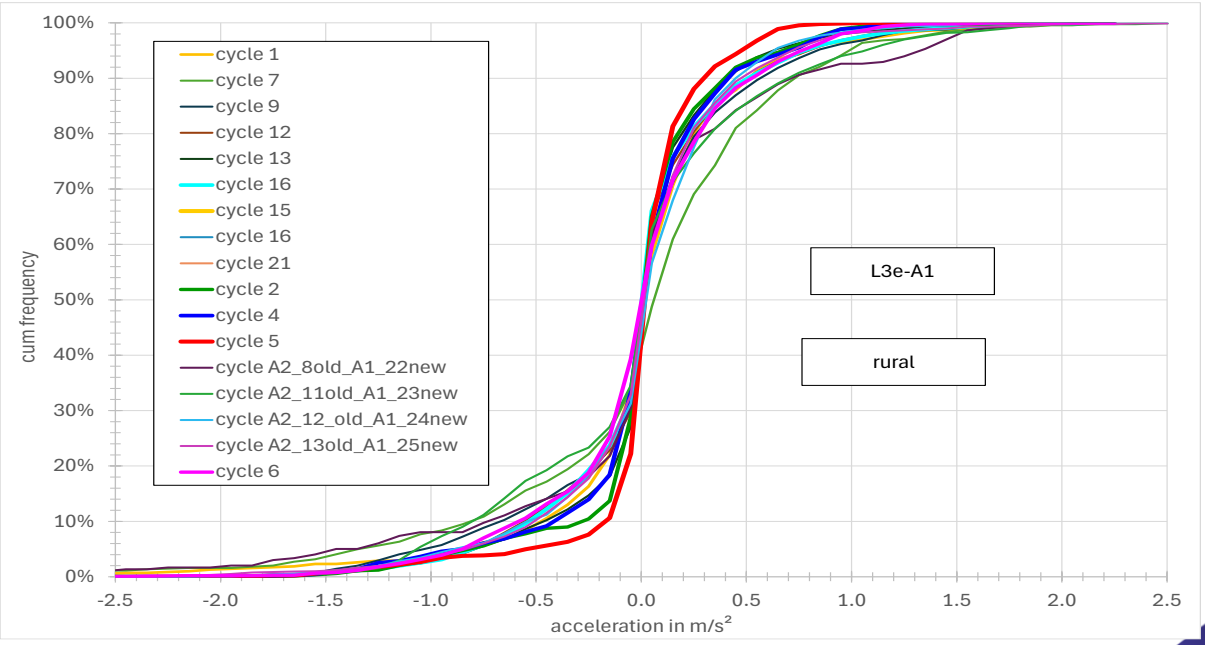

Figure J-2: Acceleration distributions vehicles L3e-A1, rural.

This project has received funding from the European Union's Horizon Europe research and innovation programme under grant agreement No 101056777

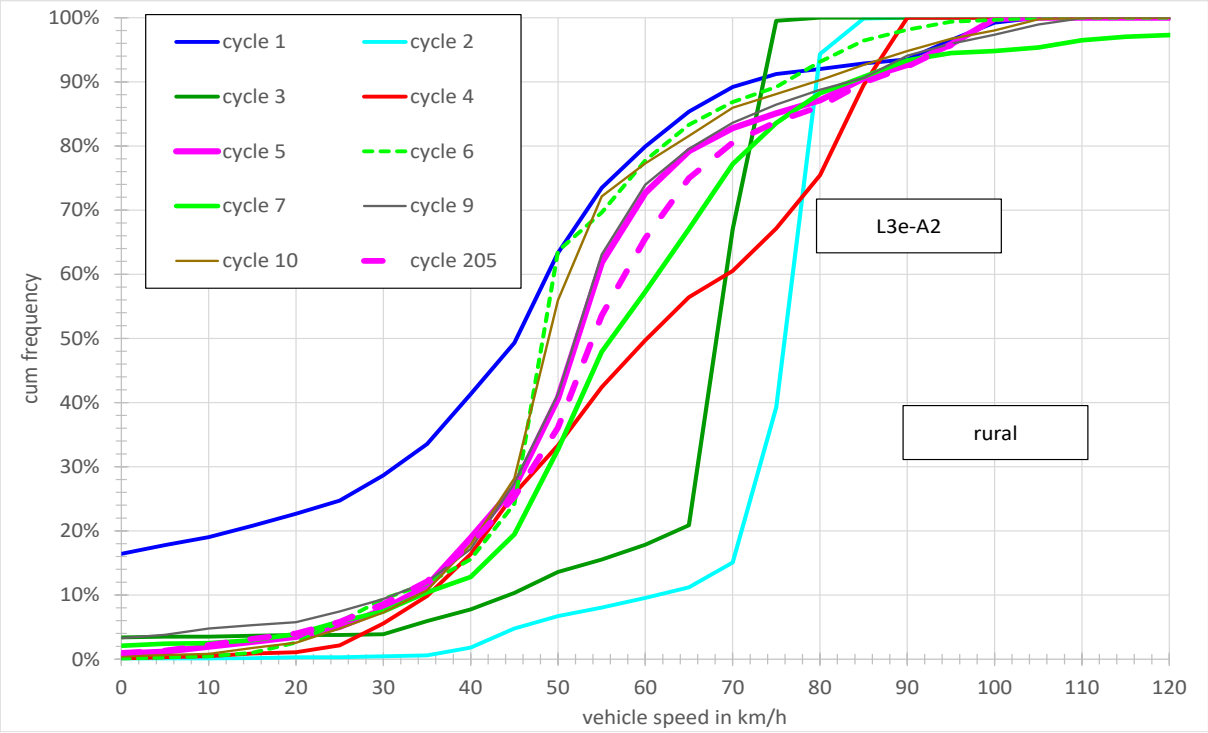

Figure J-3: Vehicle speed distributions vehicles L3e-A2, rural.

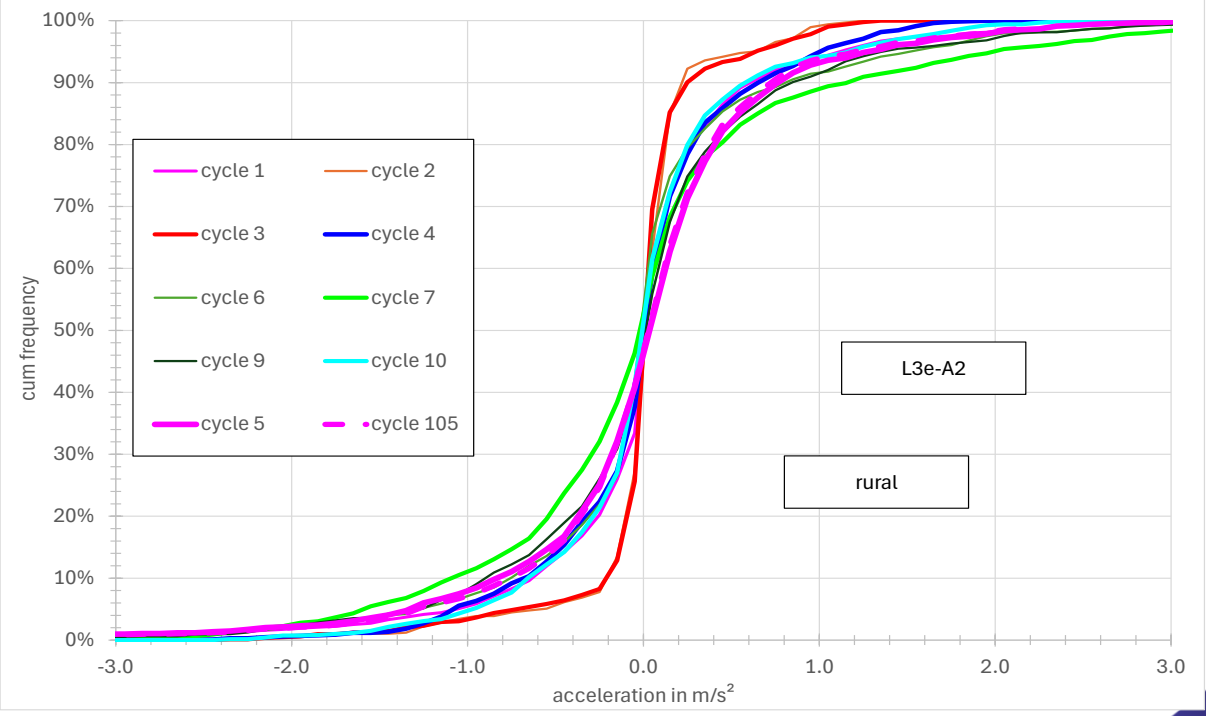

Figure J-4: Acceleration distributions vehicles L3e-A2, rural.

This project has received funding from the European Union's Horizon Europe research and innovation programme under grant agreement No 101056777

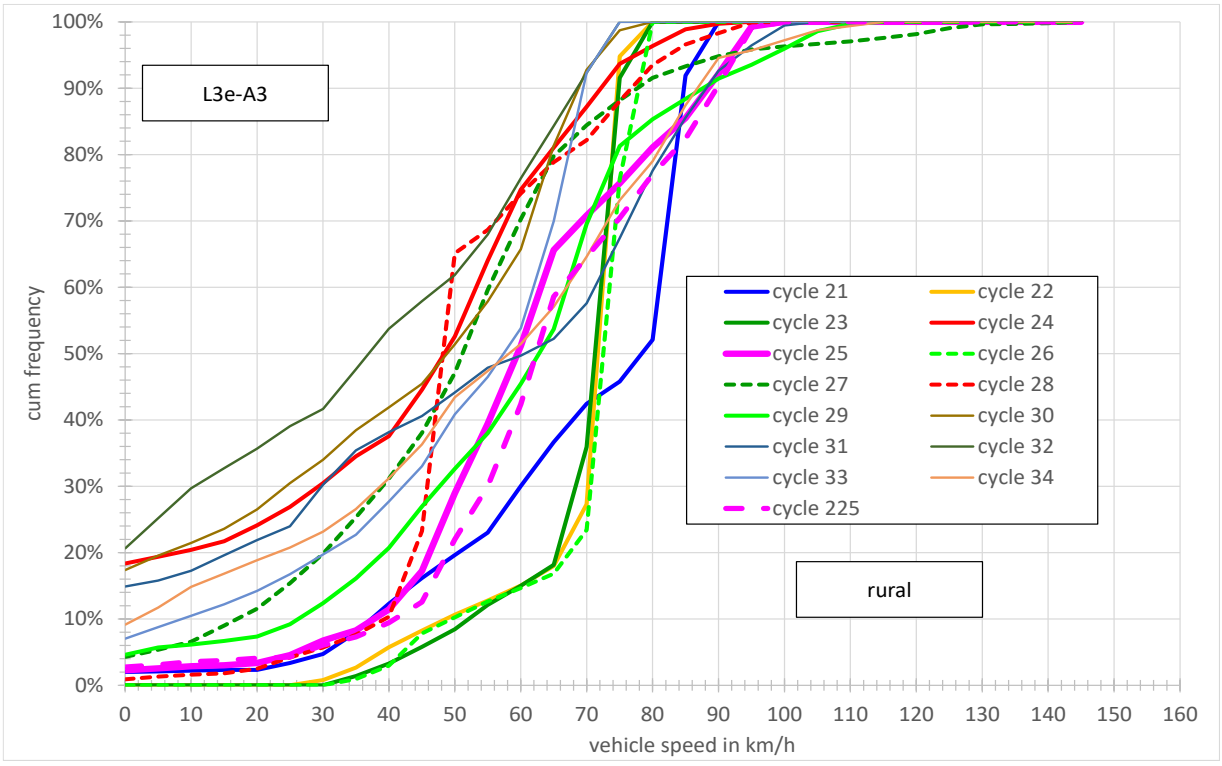

Figure J-5: Vehicle speed distributions vehicles L3e-A3, rural.

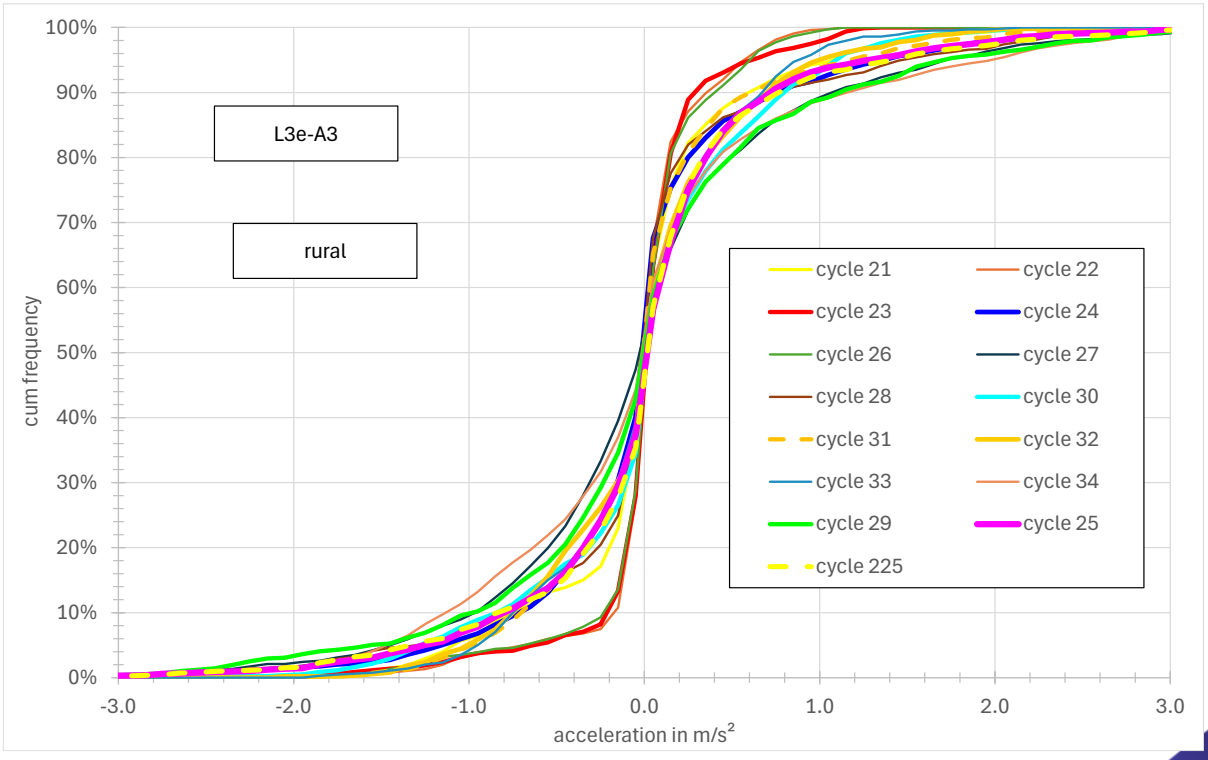

Figure J-6: Acceleration distributions vehicles L3e-A3, rural.

This project has received funding from the European Union's Horizon Europe research and innovation programme under grant agreement No 101056777

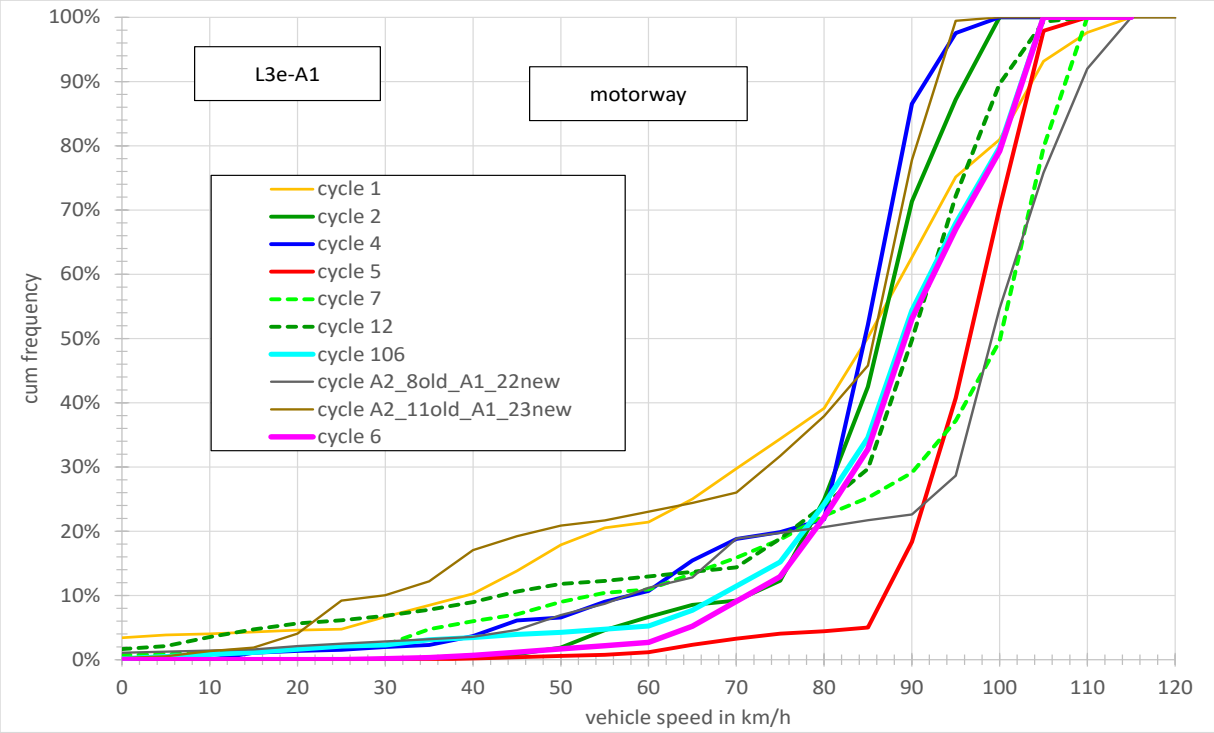

Figure J-7: Vehicle speed distributions vehicles L3e-A1, motorway.

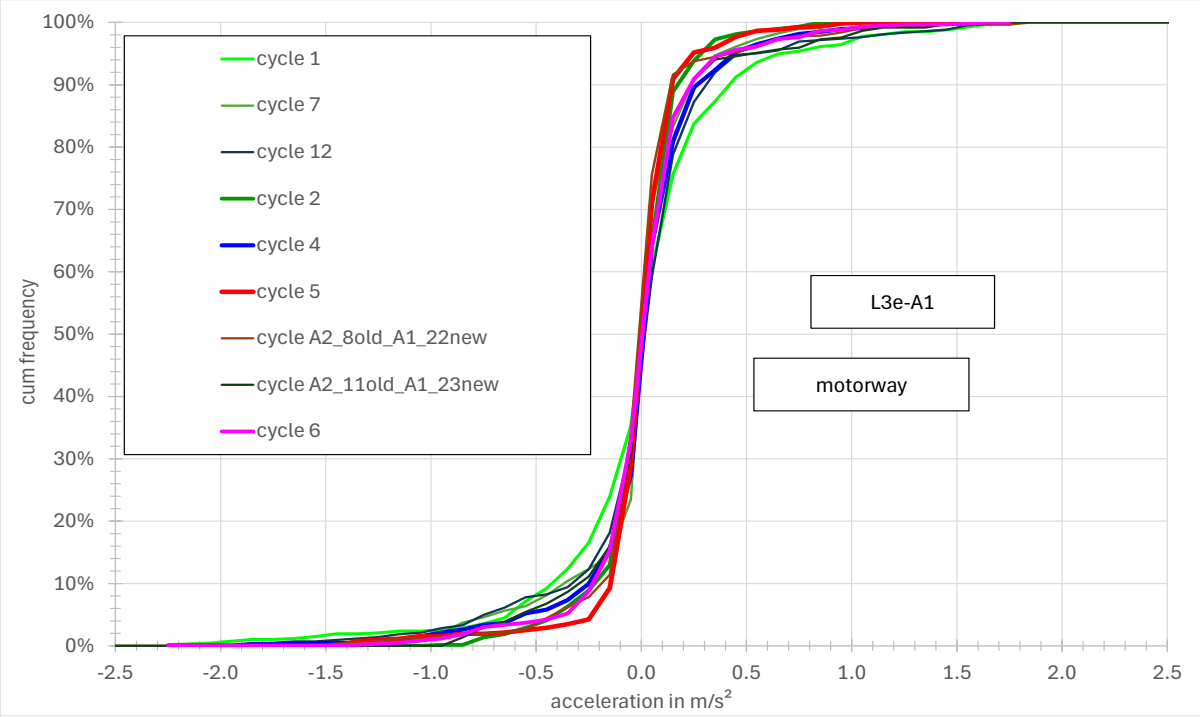

Figure J-8: Acceleration distributions vehicles L3e-A1, motorway.

This project has received funding from the European Union's Horizon Europe research and innovation programme under grant agreement No 101056777

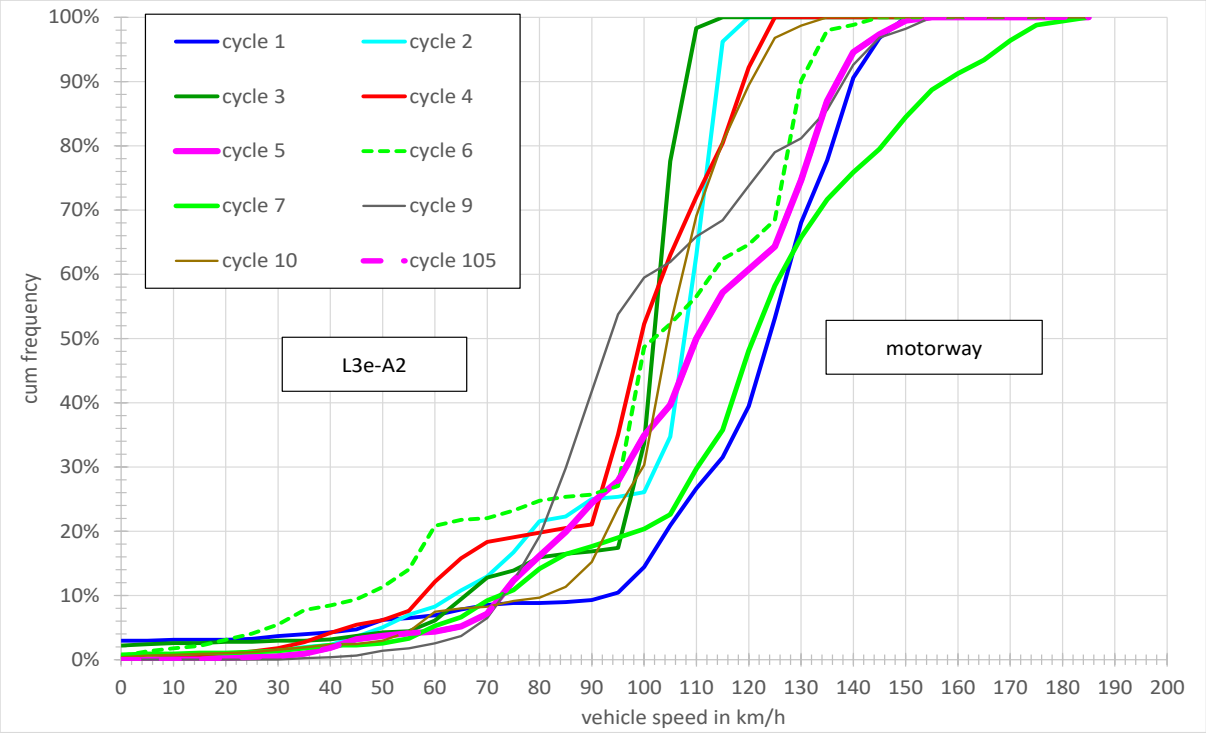

Figure J-9: Vehicle speed distributions vehicles L3e-A2, motorway.

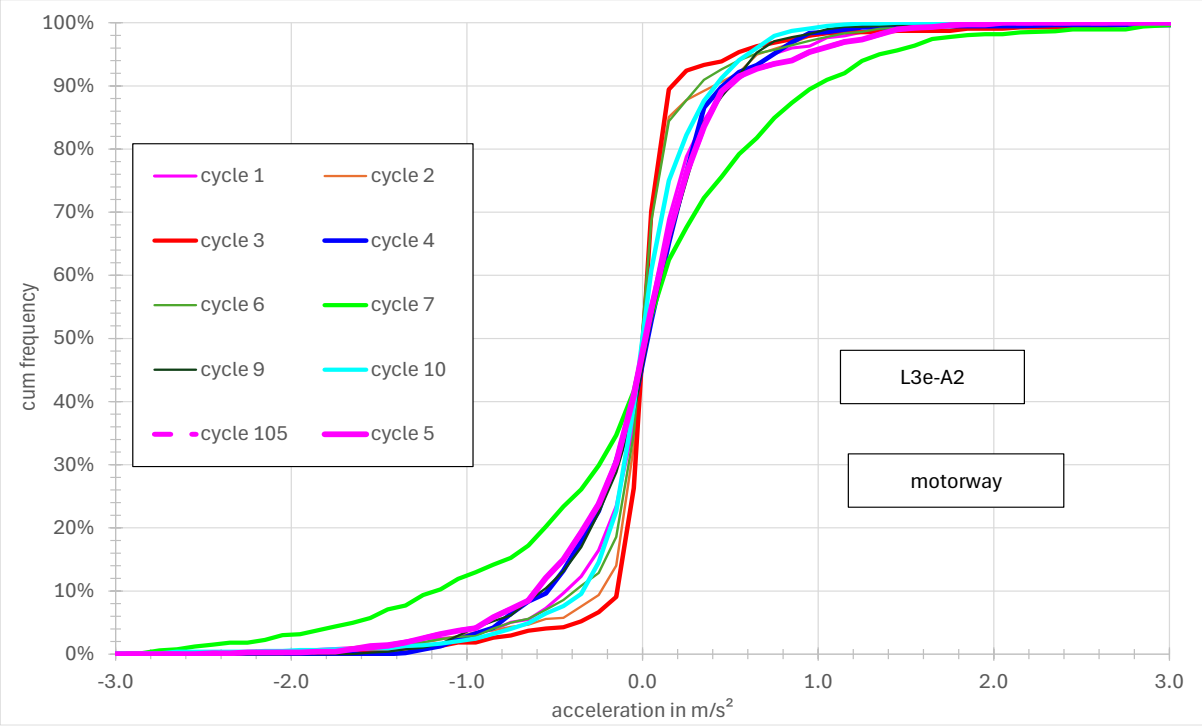

Figure J-10: Acceleration distributions vehicles L3e-A2, motorway.

This project has received funding from the European Union's Horizon Europe research and innovation programme under grant agreement No 101056777

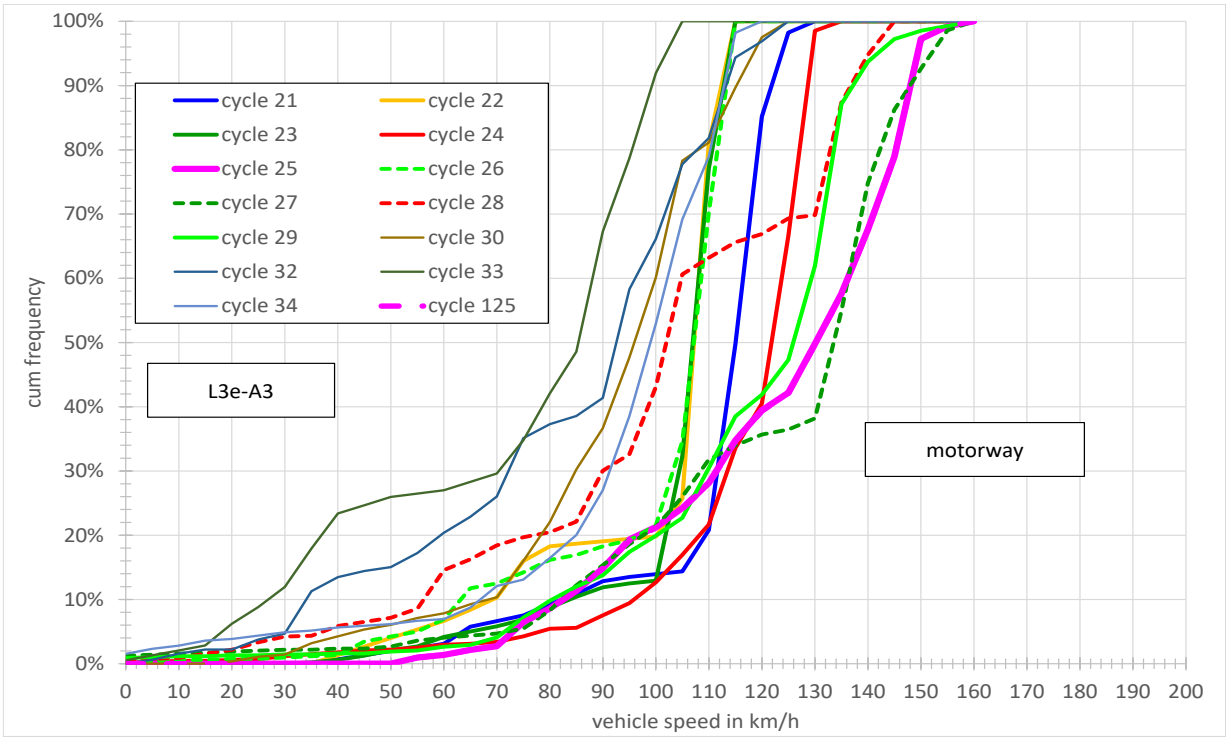

Figure J-11: Vehicle speed distributions vehicles L3e-A3, motorway.

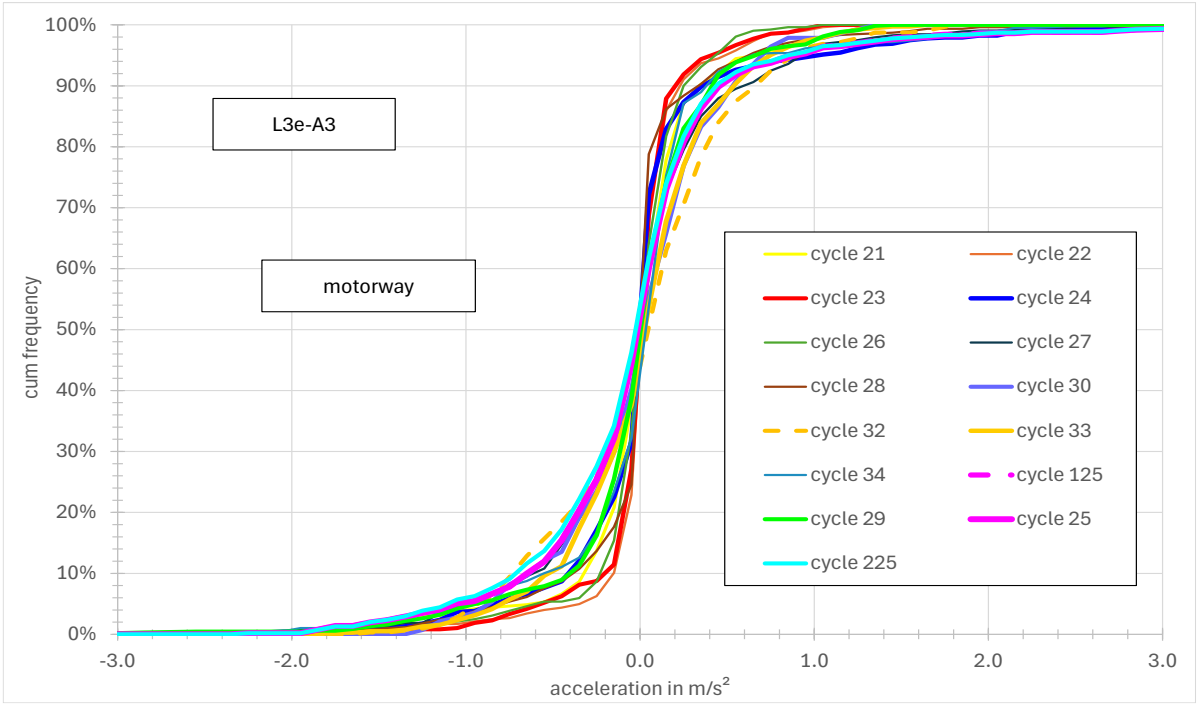

Figure J-12: Acceleration distributions vehicles L3e-A3, motorway.

This project has received funding from the European Union's Horizon Europe research and innovation programme under grant agreement No 101056777

Appendix K: Tailpipe emissions analysis from representatives LV's

Plots of the analysis for a L3e-A2 CVT motorcycle

Table K-1: L3e-A2 CVT motorcycle WMTC Class 2-2 table of occurrence (% over test time).

	WMTC Class 2-2								
	NOx			THC			CO		
	over (% time)	under (% time)	Relative occurrence (%)	over (% time)	under (% time)	Relative occurrence (%)	over (% time)	under (% time)	Relative occurrence (%)
Total EU5 limit	25.3%	74.7%		8.6%	91.4%		8.0%	92.0%	
During cold start (100s)	4.0%	4.4%	47.5%	7.6%	0.8%	90.1%	3.8%	4.7%	44.6%
During accel (>0.1 m/s^2)	16.0%	19.6%	45.0%	0.4%	35.2%	1.0%	1.6%	33.9%	4.6%
During decel (<-0.1 m/s^2)	0.9%	30.7%	2.9%	0.3%	31.4%	0.9%	0.6%	31.0%	2.0%
No accel (-0.1< x <0.1 m/s^2) & >1 km/h	6.3%	15.6%	28.8%	0.5%	21.5%	2.1%	2.4%	19.6%	10.8%
Standstill (-0.1< x <0.1 m/s^2) & <1 km/h	0.0%	10.8%	0.0%	0.0%	10.8%	0.0%	0.0%	10.8%	0.0%
Stable speed RPM>60%	5.3%	6.2%	46.0%	0.0%	11.5%	0.0%	2.4%	9.1%	20.6%

Table K-2: L3e-A2 CVT motorcycle WMTC Class 2-2 table of averages (mg/s).

	WMTC Class 2-2					
	NOx (Total av.)	0.32	THC (Total av.)	0.30	CO (Total av.)	1.56
	Average over (mg/s)	Average under (mg/s)	Average over (mg/s)	Average under (mg/s)	Average over (mg/s)	Average under (mg/s)
Total EU5 limit	1.10	0.06	2.91	0.06	13.46	0.52
During cold start (100s)	0.92	0.12	3.23	0.04	20.16	1.68
During accel (>0.1 m/s^2)	1.27	0.10	0.55	0.08	7.97	0.62
During decel (<-0.1 m/s^2)	0.58	0.04	0.58	0.04	13.61	0.38
No accel (-0.1< x <0.1 m/s^2) & >1 km/h	0.84	0.07	0.53	0.07	5.62	0.55
No accel (-0.1< x <0.1 m/s^2) & <1 km/h	0.00	0.02	0.00	0.03	0.00	0.04
Stable speed RPM>60%	0.93	0.10	0.00	0.10	5.62	0.98

This project has received funding from the European Union's Horizon Europe research and innovation programme under grant agreement No 101056777

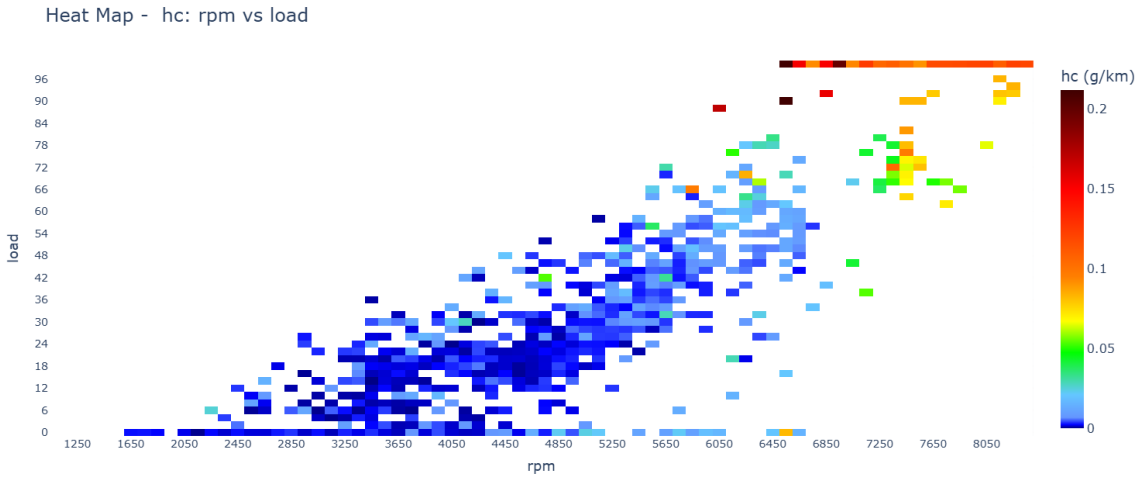

Figure K-1: HC emissions (g/km) against engine speed (rpm) and engine load (%). L3e-A2 300cc Euro 5 CVT.

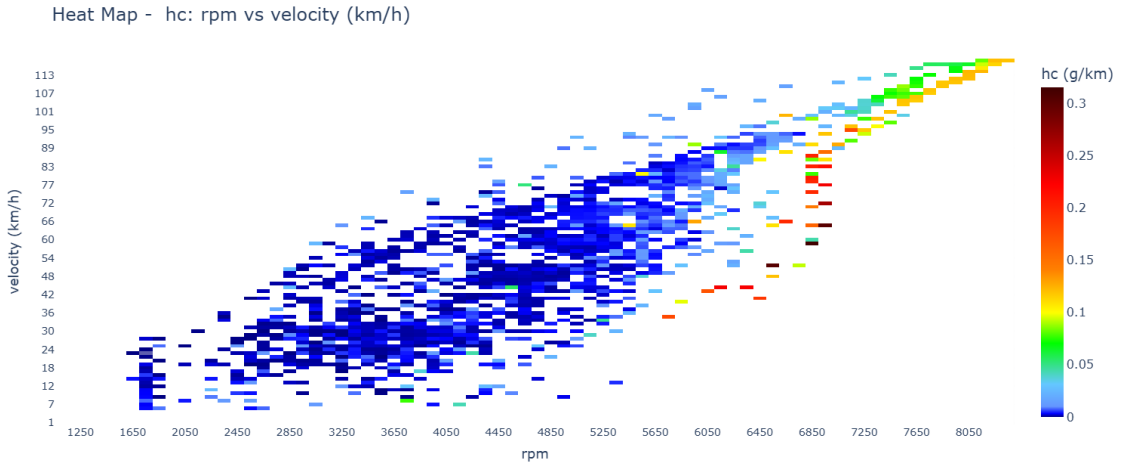

Figure K-2: HC emissions (g/km) against engine speed (rpm) and vehicle speed (km/h). L3e-A2 300cc Euro 5 CVT.

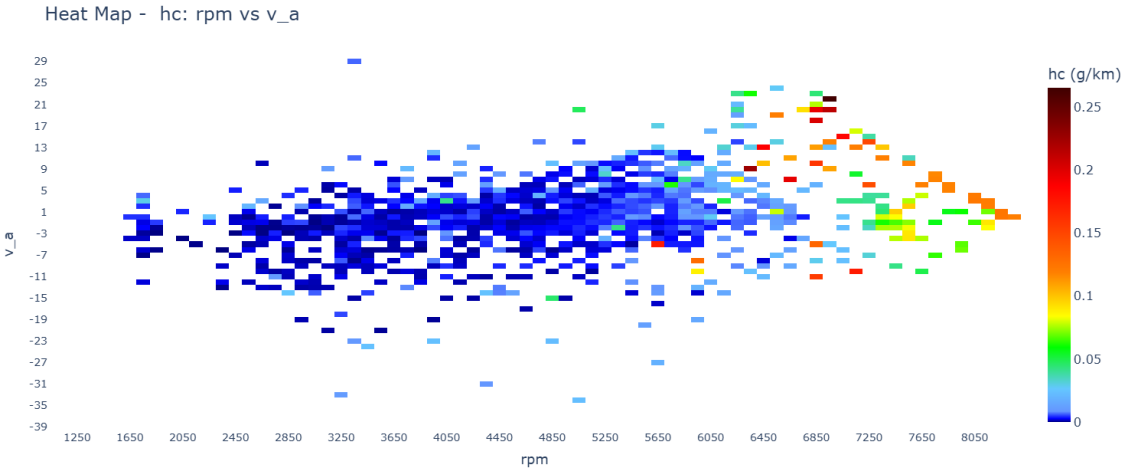

Figure K-3: HC emissions (g/km) against engine speed (rpm) and v*a (m^2/s^3). L3e-A2 300cc Euro 5 CVT.

This project has received funding from the European Union's Horizon Europe research and innovation programme under grant agreement No 101056777

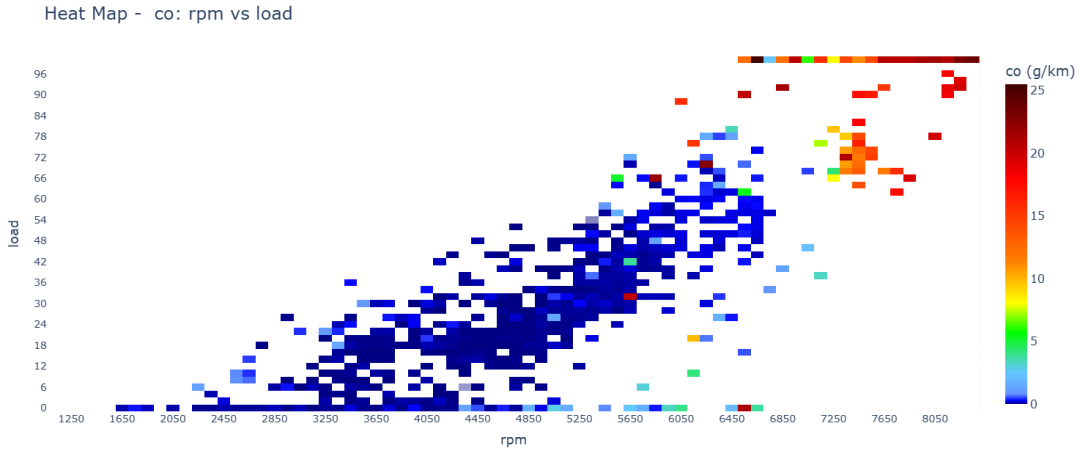

Figure K-4: CO emissions (g/km) against engine speed (rpm) and engine load (%). L3e-A2 300cc Euro 5 CVT.

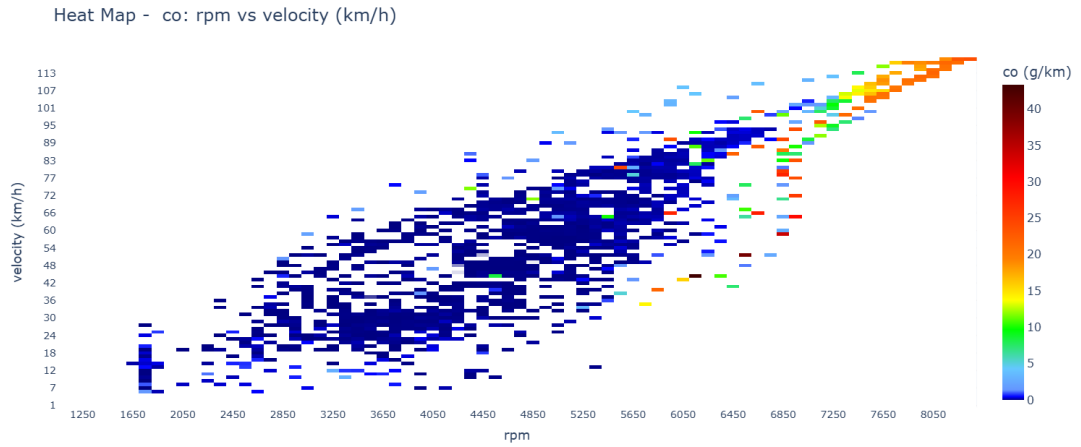

Figure K-5: CO emissions (g/km) against engine speed (rpm) and vehicle speed (km/h). L3e-A2 300cc Euro 5 CVT.

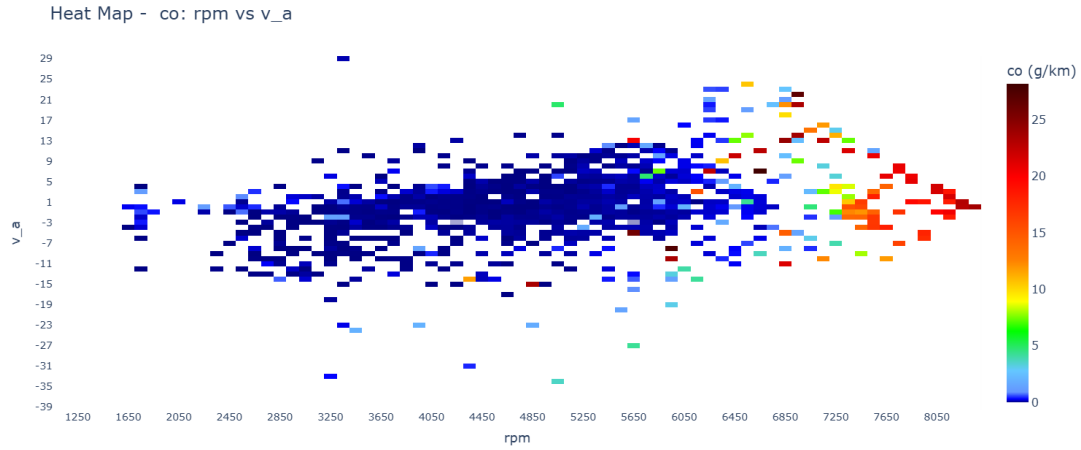

Figure K-6: CO emissions (g/km) against engine speed (rpm) and v*a (m^2/s^3). L3e-A2 300cc Euro 5 CVT.

This project has received funding from the European Union's Horizon Europe research and innovation programme under grant agreement No 101056777

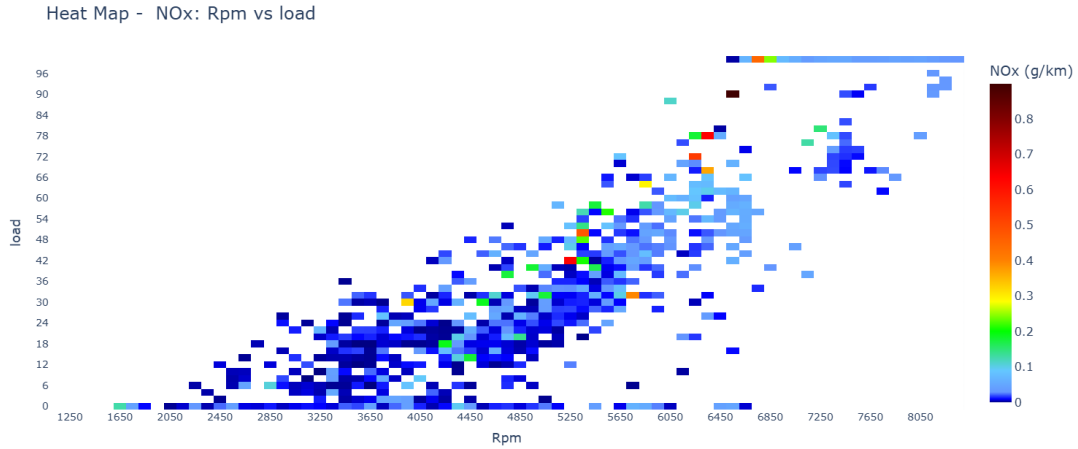

Figure K-7: NOx emissions (g/km) against engine speed (rpm) and engine load (%). L3e-A2 300cc Euro 5 CVT.

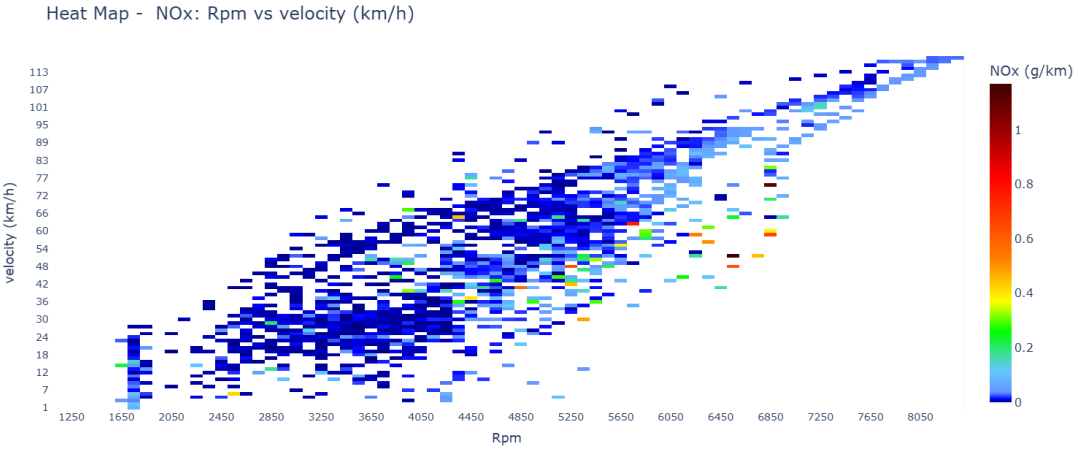

Figure K-8: NOx emissions (g/km) against engine speed (rpm) and vehicle speed (km/h). L3e-A2 300cc Euro 5 CVT.

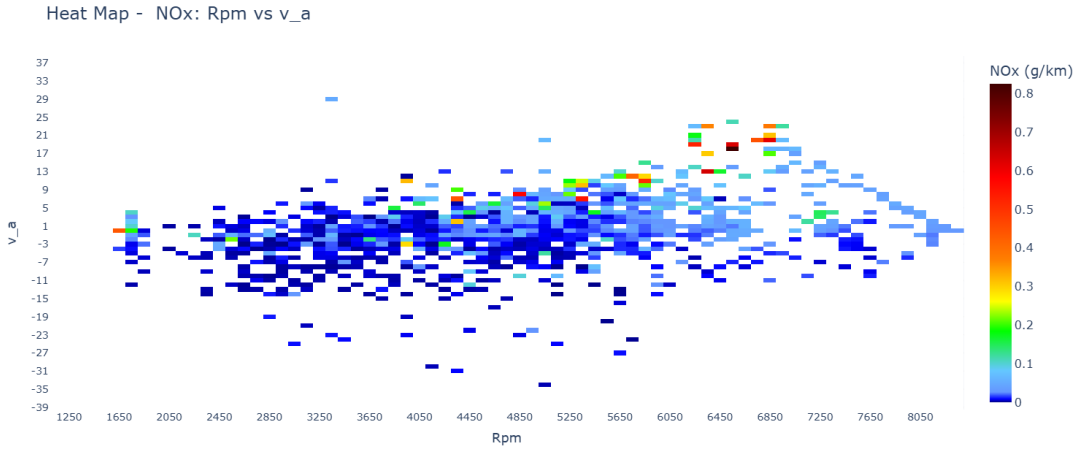

Figure K-9: NOx emissions (g/km) against engine speed (rpm) and v*a (m^2/s^3). L3e-A2 300cc Euro 5 CVT.

This project has received funding from the European Union's Horizon Europe research and innovation programme under grant agreement No 101056777

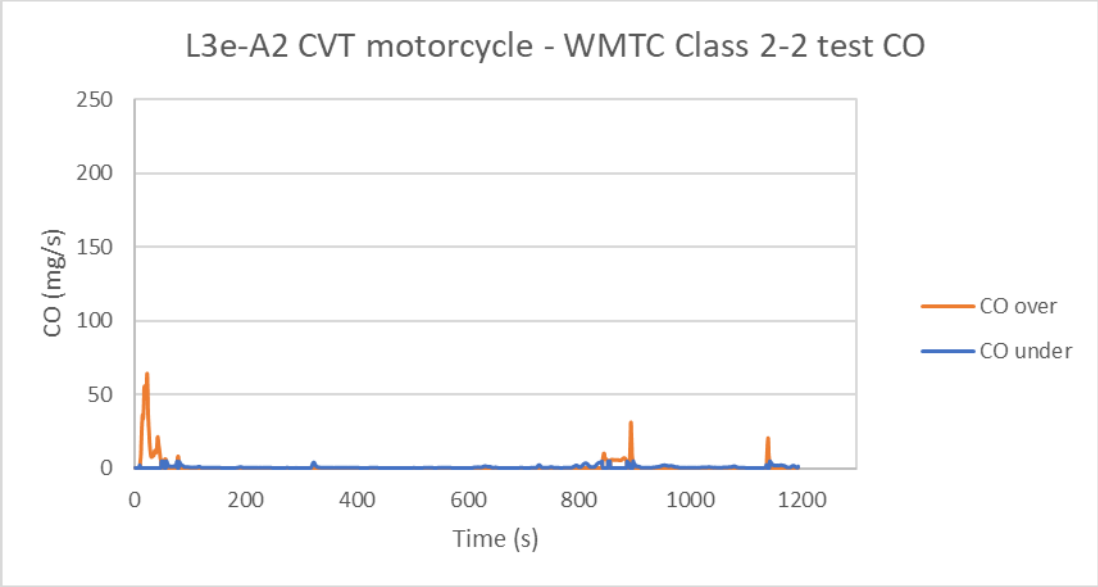

Figure K-10: L3e-A2 CVT motorcycle - CO results in WMTC Class 2-2 test.

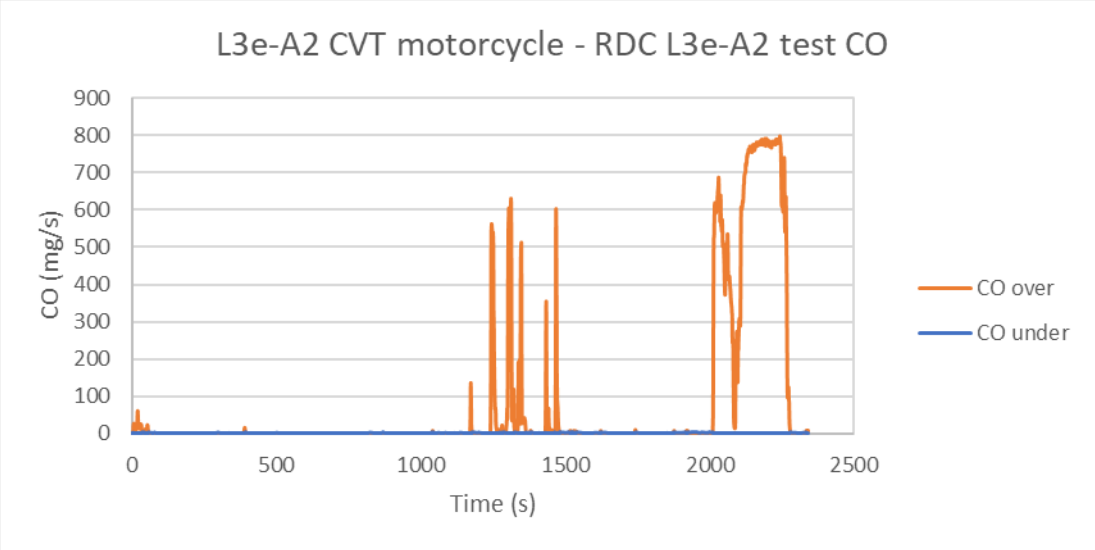

Figure K-11: L3e-A2 CVT motorcycle - CO results in RDC L3e-A2 test.

This project has received funding from the European Union's Horizon Europe research and innovation programme under grant agreement No 101056777

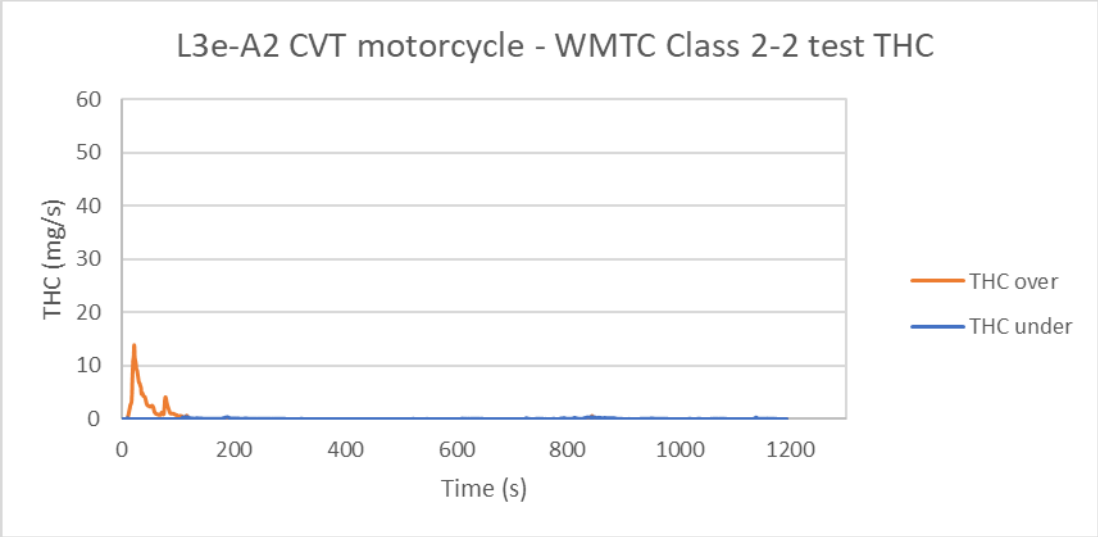

Figure K-12: L3e-A2 CVT motorcycle - THC results in WMTC Class 2-2 test.

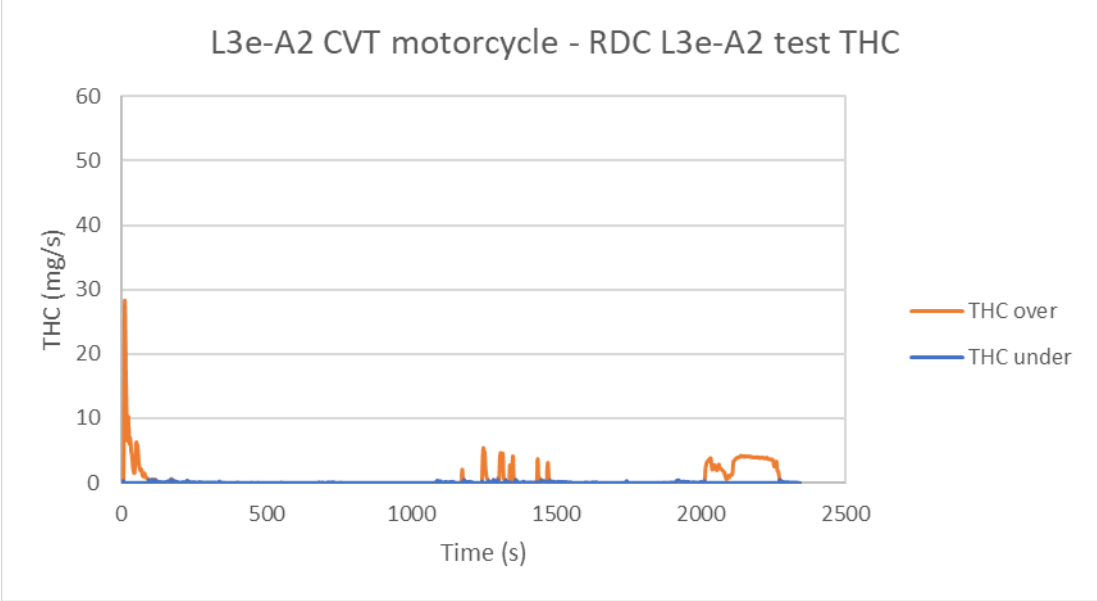

Figure K-13: L3e-A2 CVT motorcycle - THC results in RDC L3e-A2 test.

This project has received funding from the European Union's Horizon Europe research and innovation programme under grant agreement No 101056777

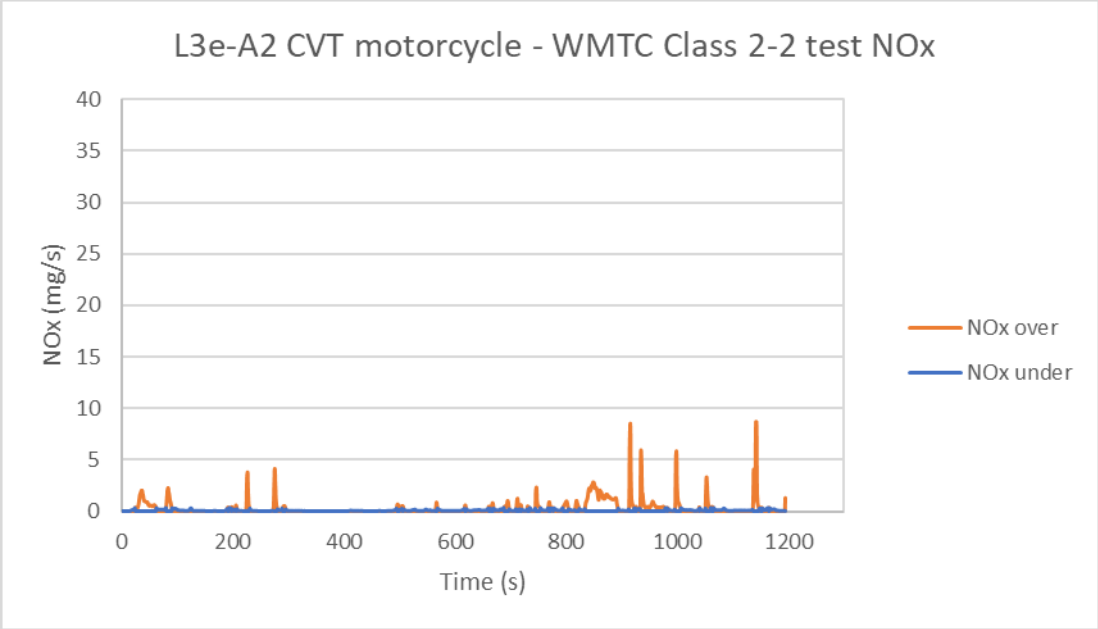

Figure K-14: L3e-A2 CVT motorcycle - NOx results in WMTC Class 2-2 test.

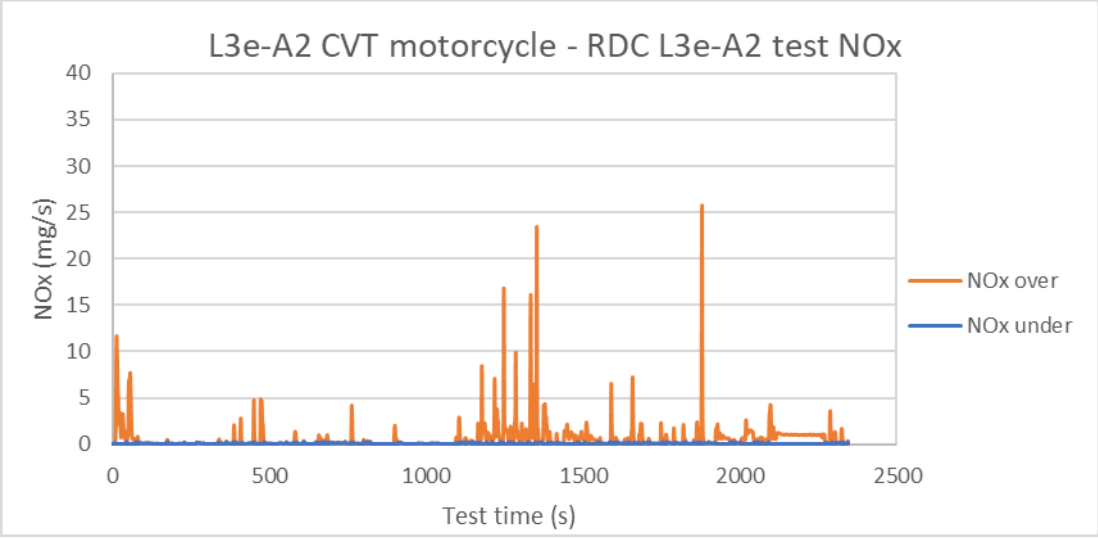

Figure K-15: L3e-A2 CVT motorcycle - NOx results in RDC L3e-A2 test.

This project has received funding from the European Union's Horizon Europe research and innovation programme under grant agreement No 101056777

Plots of the analysis for a L3e-A2 Sport Touring motorcycle

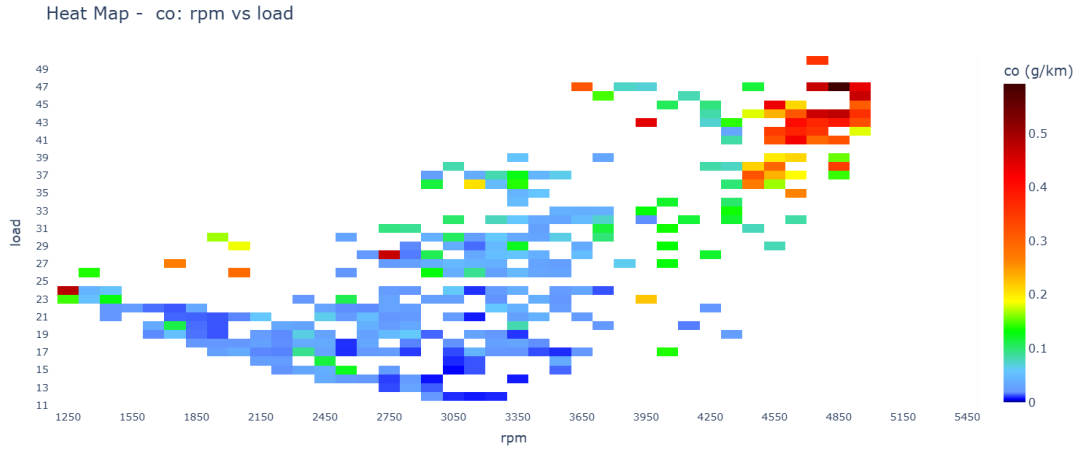

Figure K-16: CO emissions (g/km) against engine speed (rpm) and engine load (%) from L3e-A2 equipped with manual transmission. RDC and RDE tests are represented.

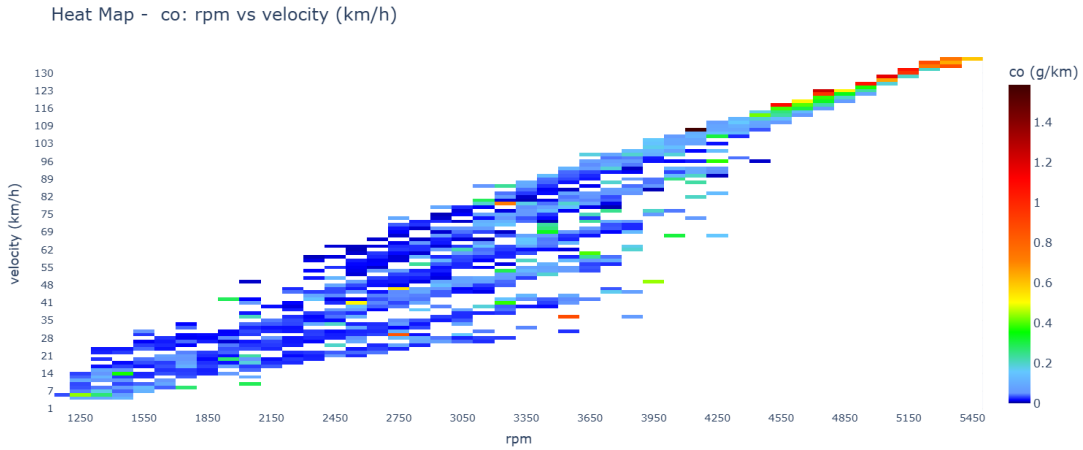

Figure K-17: CO emissions (g/km) against engine speed (rpm) and vehicle speed (km/h) from L3e-A2 equipped with manual transmission. RDC and RDE tests are represented.

This project has received funding from the European Union's Horizon Europe research and innovation programme under grant agreement No 101056777

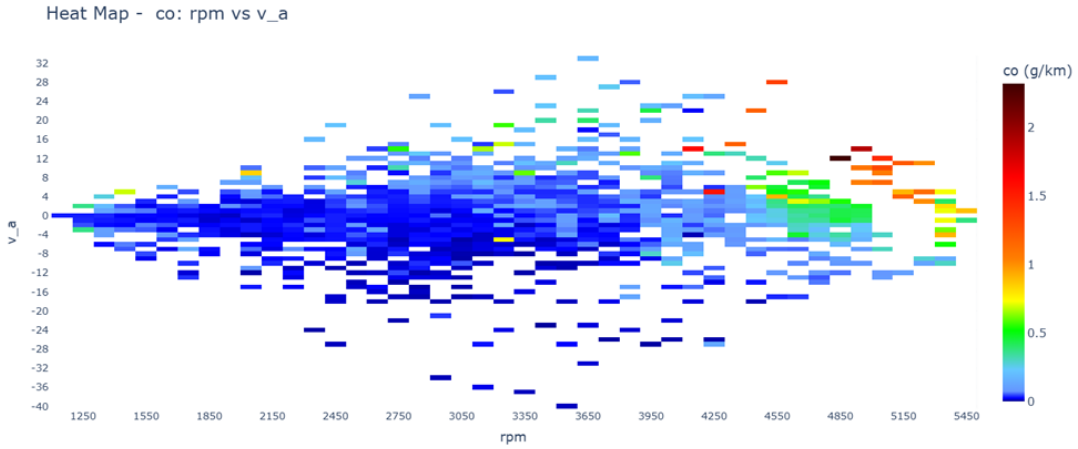

Figure K-18: CO emissions (g/km) against engine speed (rpm) and v*a (m^2/s^3) from L3e-A2 equipped with manual transmission. RDC and RDE tests are represented.

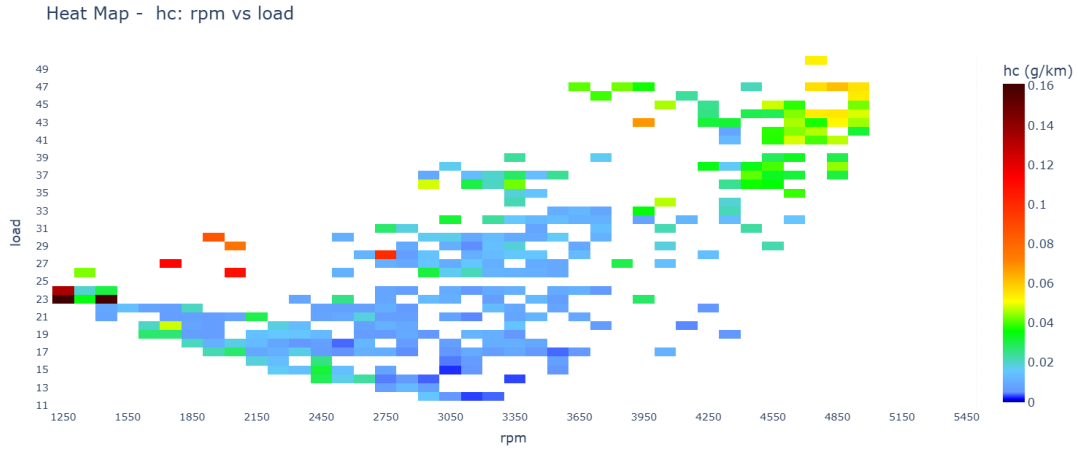

Figure K-19: HC emissions (g/km) against engine speed (rpm) and engine load (%) from L3e-A2 equipped with manual transmission. RDC and RDE tests are represented.

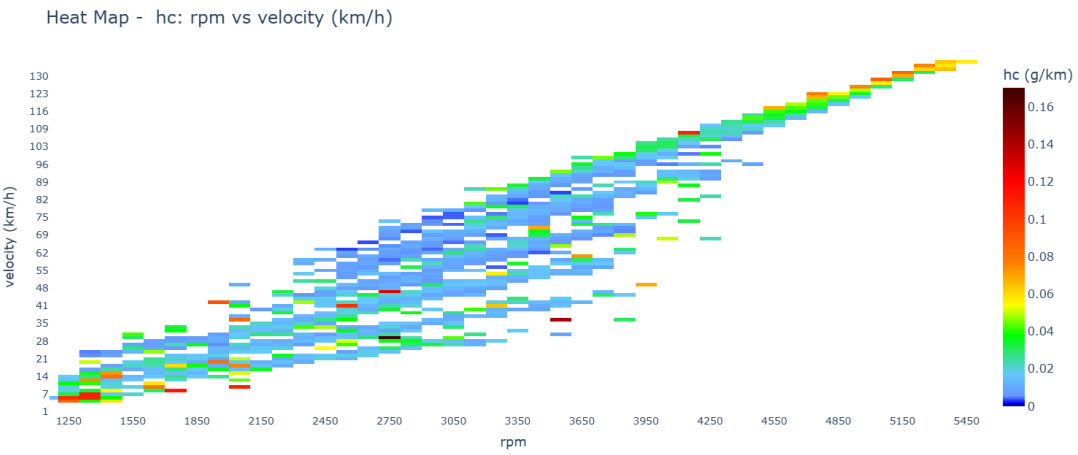

Figure K-20: HC emissions (g/km) against engine speed (rpm) and vehicle speed (km/h) from L3e-A2 equipped with manual transmission. RDC and RDE tests are represented.

This project has received funding from the European Union's Horizon Europe research and innovation programme under grant agreement No 101056777

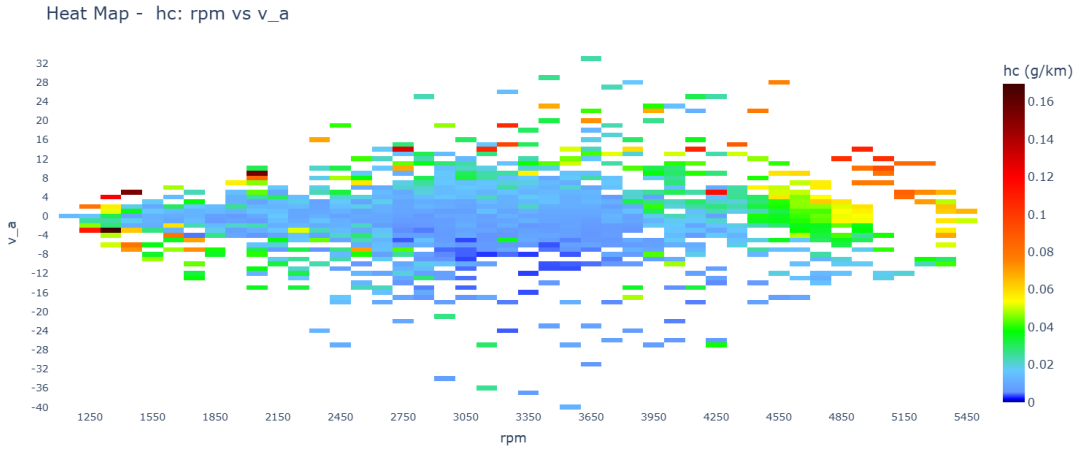

Figure K-21: HC emissions (g/km) against engine speed (rpm) and v*a (m^2/s^3) from L3e-A2 equipped with manual transmission. RDC and RDE tests are represented.

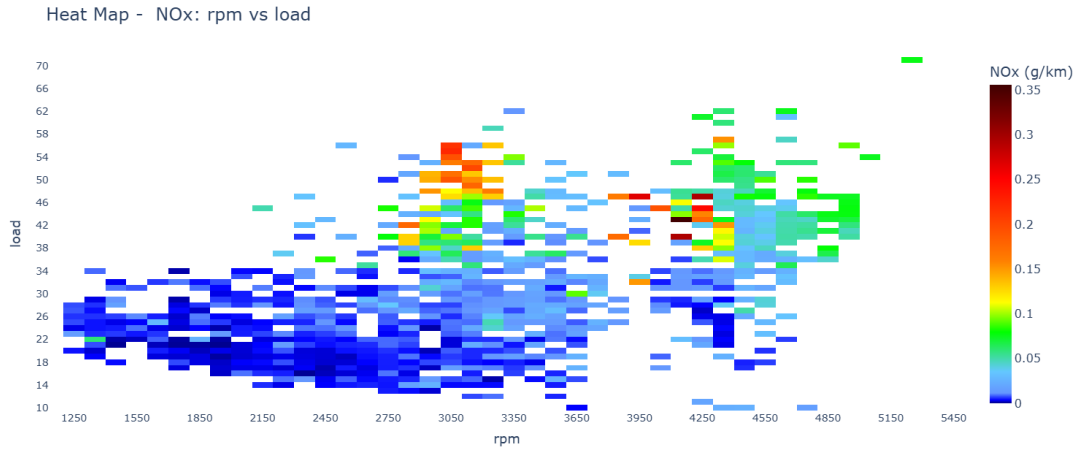

Figure K-22: NOx emissions (g/km) against engine speed (rpm) and engine load (%) from L3e-A2 equipped with manual transmission. RDC and RDE tests are represented.

This project has received funding from the European Union's Horizon Europe research and innovation programme under grant agreement No 101056777

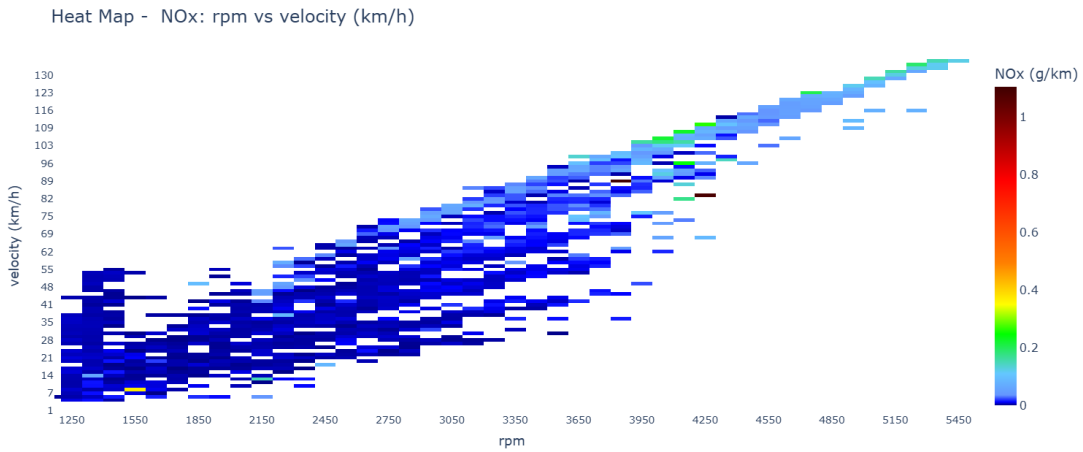

Figure K-23: NOx emissions (g/km) against engine speed (rpm) and vehicle speed (km/h) from L3e-A2 equipped with manual transmission. RDC and RDE tests are represented.

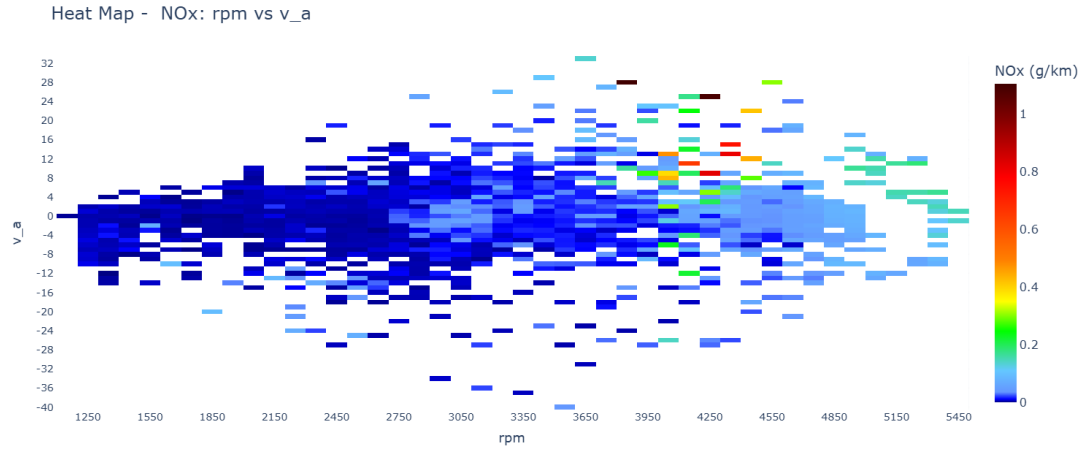

Figure K-24: NOx emissions (g/km) against engine speed (rpm) and v*a (m^2/s^3) from L3e-A2 equipped with manual transmission. RDC and RDE tests are represented.

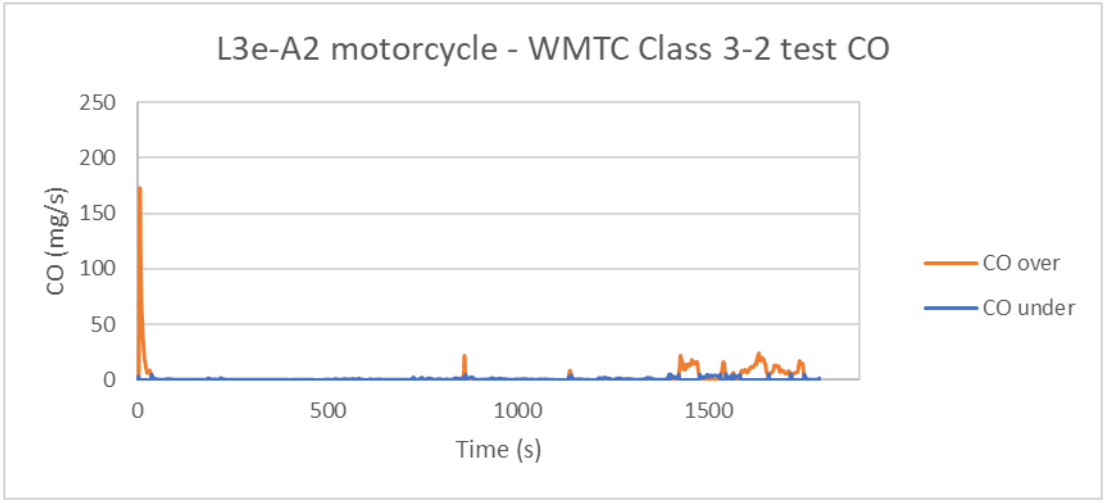

Figure K-25: L3e-A2 Sport Touring motorcycle - CO results in WMTC Class 3-2 test.

This project has received funding from the European Union's Horizon Europe research and innovation programme under grant agreement No 101056777

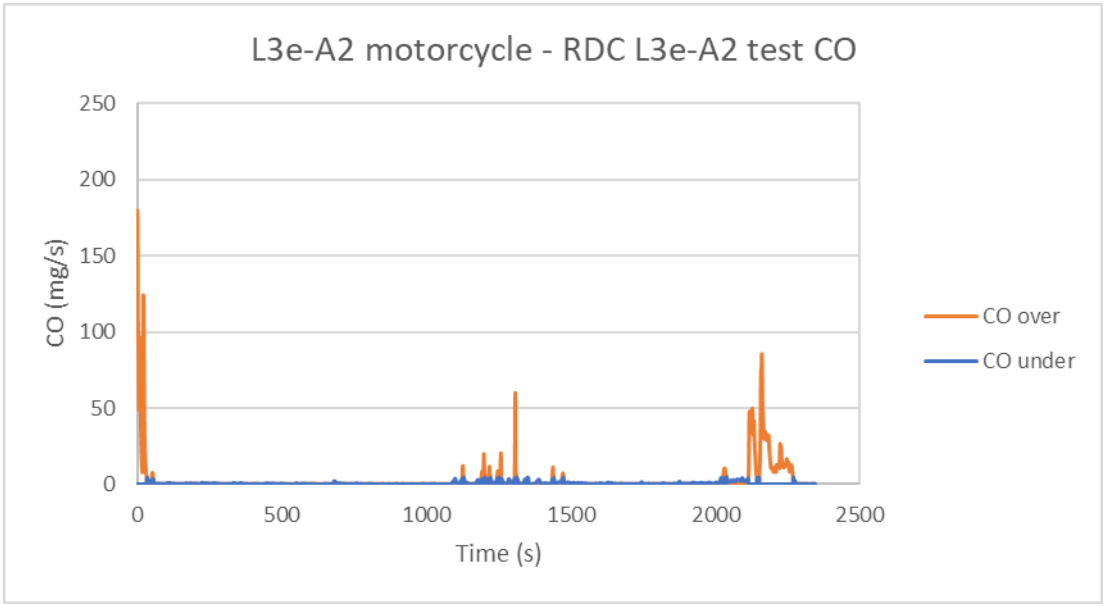

Figure K-26: L3e-A2 Sport Touring motorcycle - CO results in RDC L3e-A2 test.

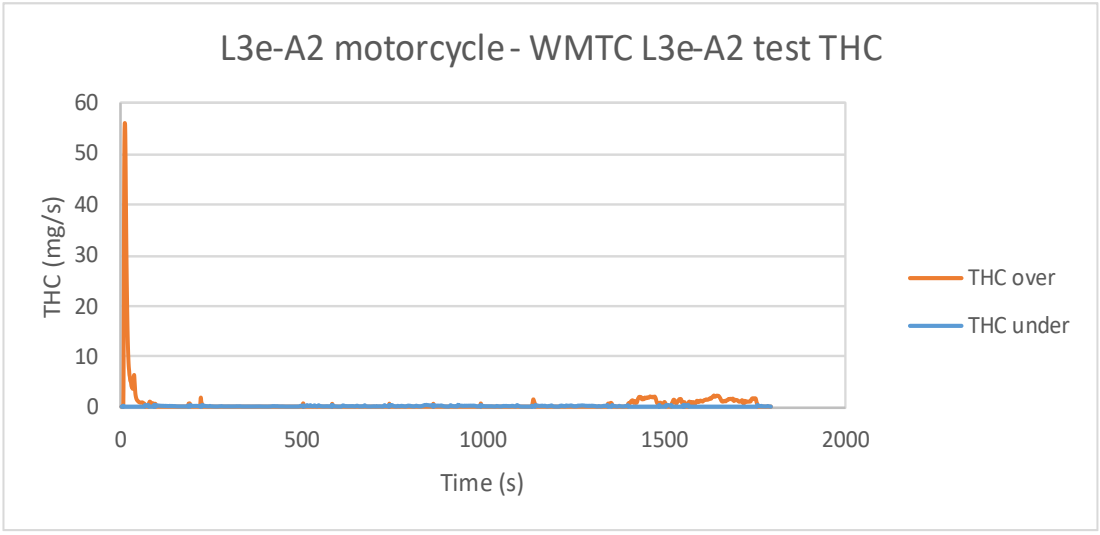

Figure K-27: L3e-A2 Sport Touring motorcycle - THC results in WMTC Class 3-2 test.

This project has received funding from the European Union's Horizon Europe research and innovation programme under grant agreement No 101056777

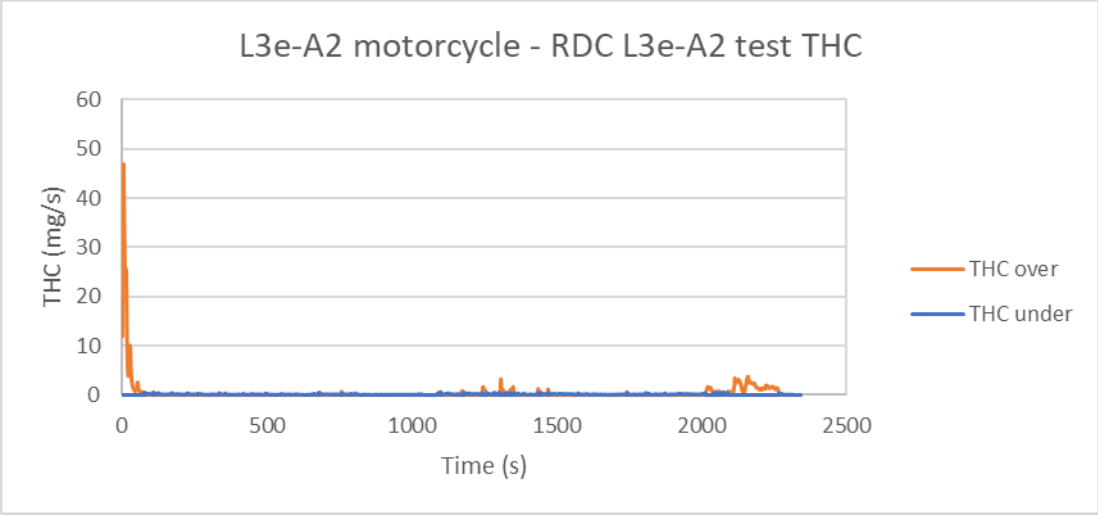

Figure K-28: L3e-A2 Sport Touring motorcycle - THC results in RDC L3e-A2 test.

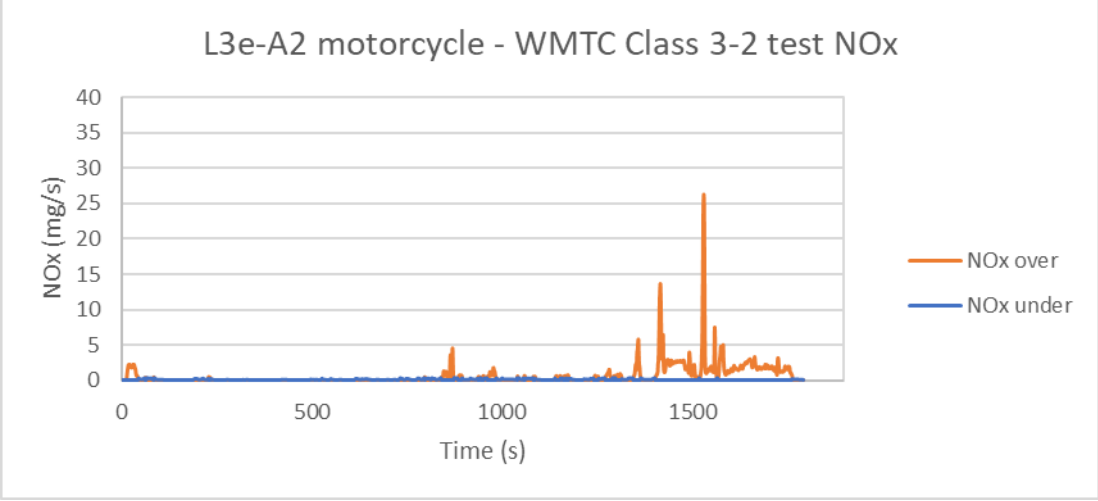

Figure K-29: L3e-A2 Sport Touring motorcycle - NOx results in WMTC Class 3-2 test..

This project has received funding from the European Union's Horizon Europe research and innovation programme under grant agreement No 101056777

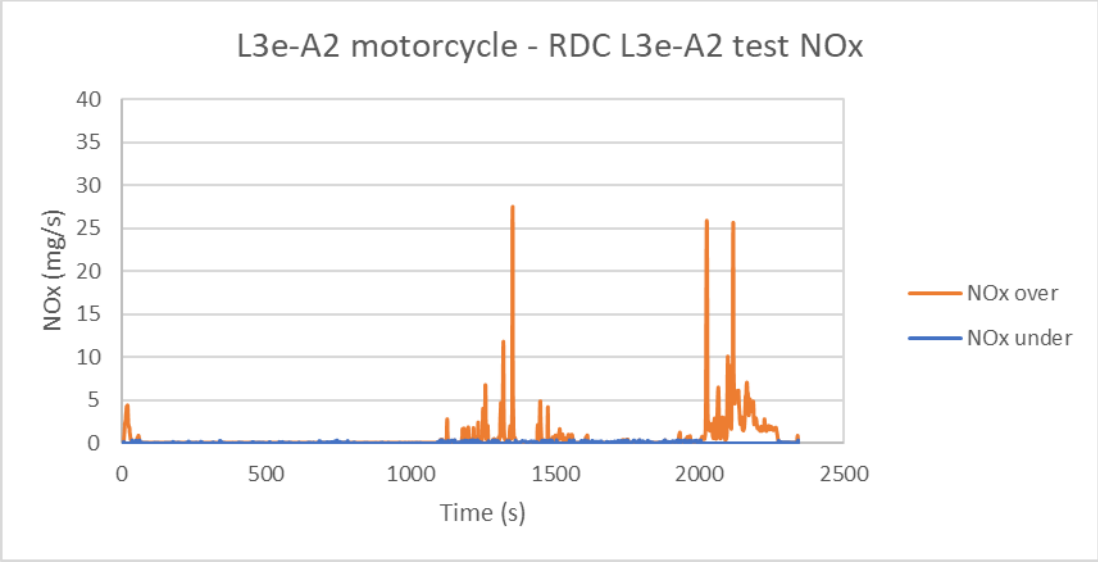

Figure K-30: L3e-A2 Sport Touring motorcycle - NOx results in RDC L3e-A2 test.

Plots of the analysis of a L3e-A3 Sport Touring motorcycle

Table K-3: L3e-A3 Sport Touring motorcycle WMTC Class 3-2 table of occurrence (% over test time).

	WMTC Class 3-2								
	NOx			THC			CO		
	over (% time)	under (% time)	Relative occurrence (%)	over (% time)	under (% time)	Relative occurrence (%)	over (% time)	under (% time)	Relative occurrence (%)
Total over/under threshold	37.0%	63.0%		24.5%	75.5%		13.3%	86.7%	
During cold start (100s)	3.4%	2.2%	60.4%	4.6%	1.0%	82.2%	1.2%	4.4%	21.8%
During accel (>0.1 m/s^2)	11.0%	23.3%	32.1%	7.0%	27.2%	20.5%	3.1%	31.2%	9.0%
During decel (<-0.1 m/s^2)	6.8%	23.3%	22.6%	3.0%	27.1%	9.8%	0.6%	29.5%	2.0%
No accel (-0.1< x <0.1 m/s^2) & >1 km/h	17.8%	10.4%	63.0%	11.0%	17.2%	39.1%	9.1%	19.1%	32.4%
Standstill (-0.1< x <0.1 m/s^2) & <1 km/h	0.1%	7.4%	0.8%	0.0%	7.5%	0.0%	0.0%	7.5%	0.0%
Stable speed RPM>60%	0.0%	0.0%	0.0%	0.0%	0.0%	0.0%	0.0%	0.0%	0.0%

Table K-4: L3e-A3 Sport Touring motorcycle WMTC Class 3-2 table of averages (mg/s).

	WMTC Class 3-2					
	NOx (Total av.)	0.68	THC (Total av.)	0.63	CO (Total av.)	2.15
	Average over (mg/s)	Average under (mg/s)	Average over (mg/s)	Average under (mg/s)	Average over (mg/s)	Average under (mg/s)
Total over/under threshold	1.71	0.07	2.11	0.16	11.98	0.64
During cold start (100s)	1.09	0.12	6.53	0.39	39.50	0.99
During accel (>0.1 m/s^2)	2.43	0.09	1.02	0.18	10.44	0.81
During decel (<-0.1 m/s^2)	1.18	0.06	0.83	0.14	6.54	0.44
No accel (-0.1< x <0.1 m/s^2) & >1 km/h	1.60	0.08	1.19	0.17	8.94	0.80
No accel (-0.1< x <0.1 m/s^2) & <1 km/h	3.00	0.01	0.00	0.05	0.00	0.10

This project has received funding from the European Union's Horizon Europe research and innovation programme under grant agreement No 101056777

Stable speed RPM>60%	0.00	0.00	0.00	0.00	0.00	0.00

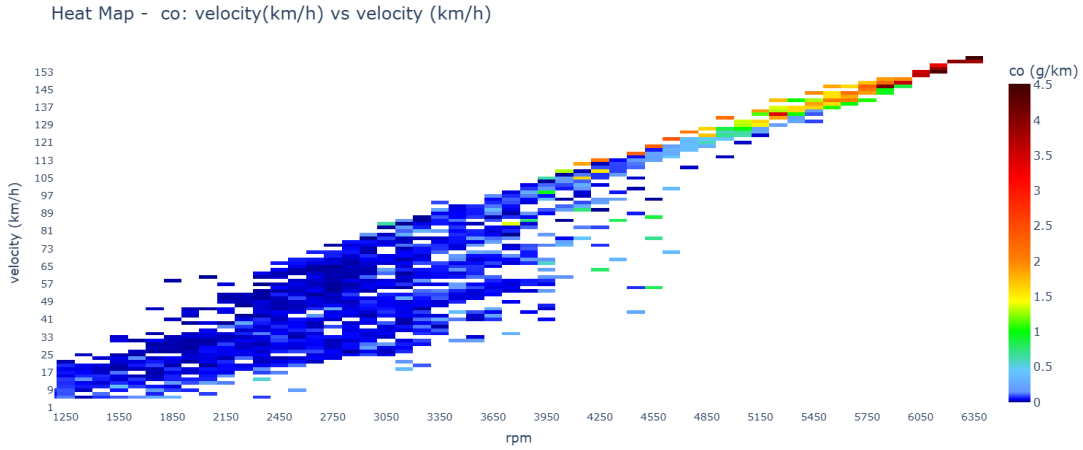

Figure K-31: CO emissions (g/km) against engine speed (rpm) and vehicle speed (km/h) from L3e-A3 equipped with manual transmission. RDC and RDE tests are represented.

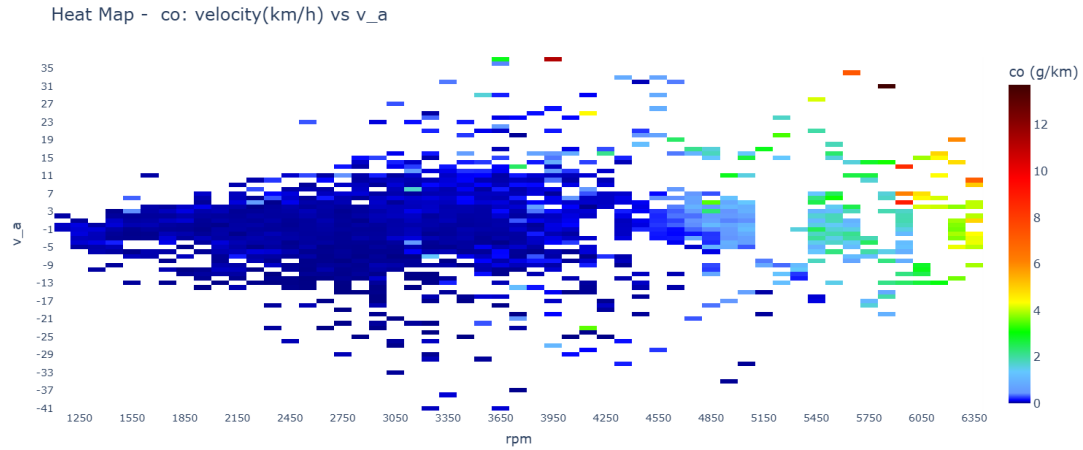

Figure K-32: CO emissions (g/km) against engine speed (rpm) and v*a (m^2/s^3) from L3e-A3 equipped with manual transmission. RDC and RDE tests are represented.

This project has received funding from the European Union's Horizon Europe research and innovation programme under grant agreement No 101056777

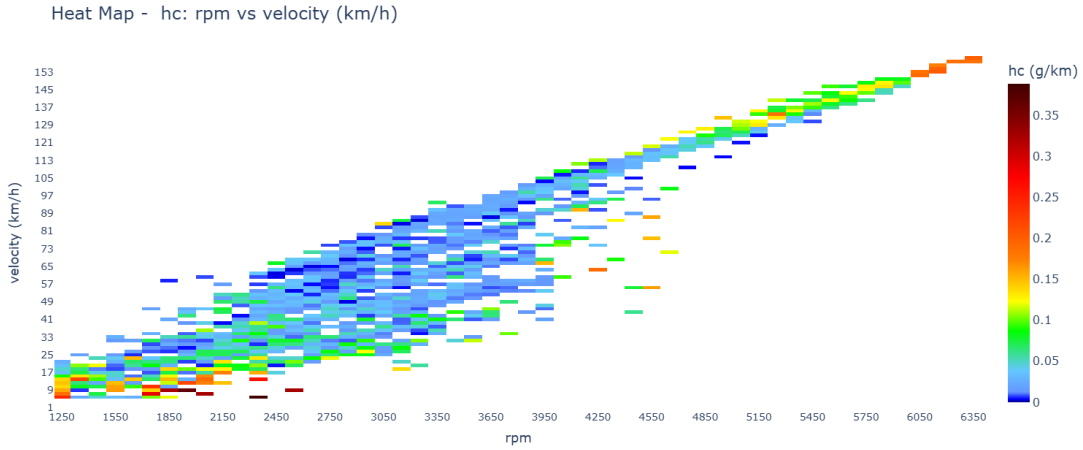

Figure K-33: HC emissions (g/km) against engine speed (rpm) and vehicle speed (km/h) from L3e-A3 equipped with manual transmission. RDC and RDE tests are represented.

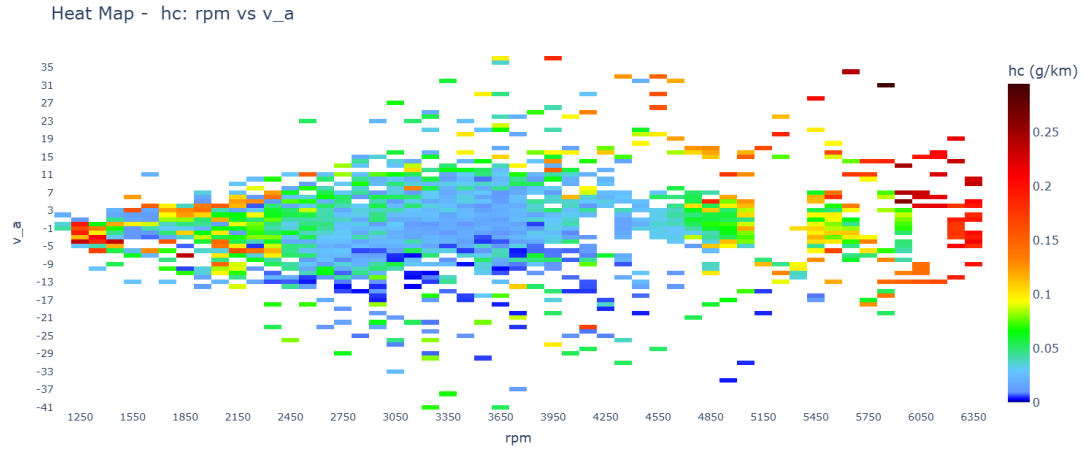

Figure K-34: HC emissions (g/km) against engine speed (rpm) and v*a (m^2/s^3) from L3e-A3 equipped with manual transmission. RDC and RDE tests are represented.

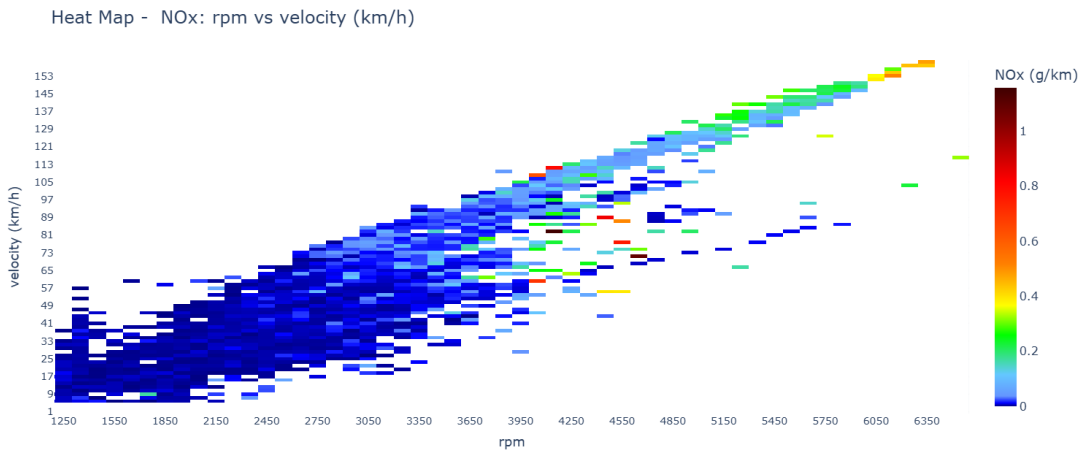

Figure K-35: NOx emissions (g/km) against engine speed (rpm) and vehicle speed (km/h) from L3e-A3 equipped with manual transmission. RDC and RDE tests are represented.

This project has received funding from the European Union's Horizon Europe research and innovation programme under grant agreement No 101056777

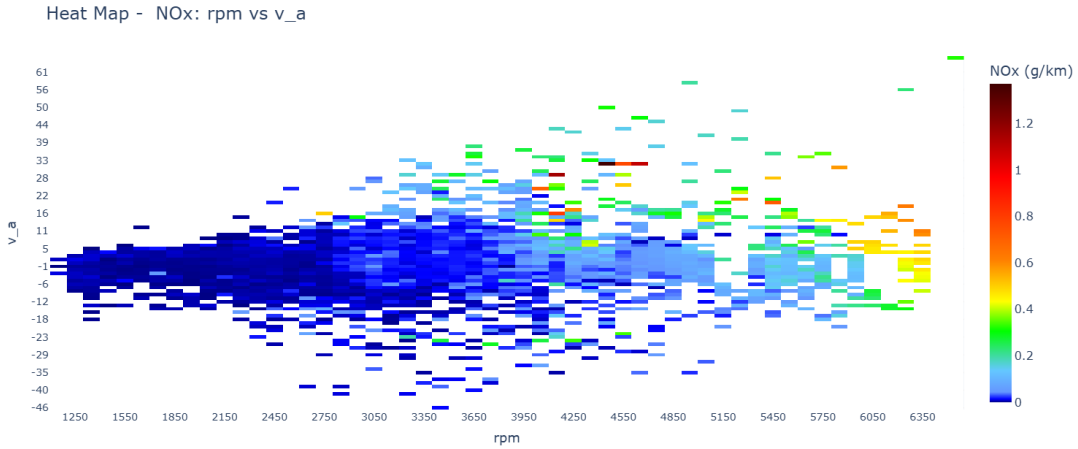

Figure K-36: NOx emissions (g/km) against engine speed (rpm) and v*a (m^2/s^3) from L3e-A3 equipped with manual transmission. RDC and RDE tests are represented.

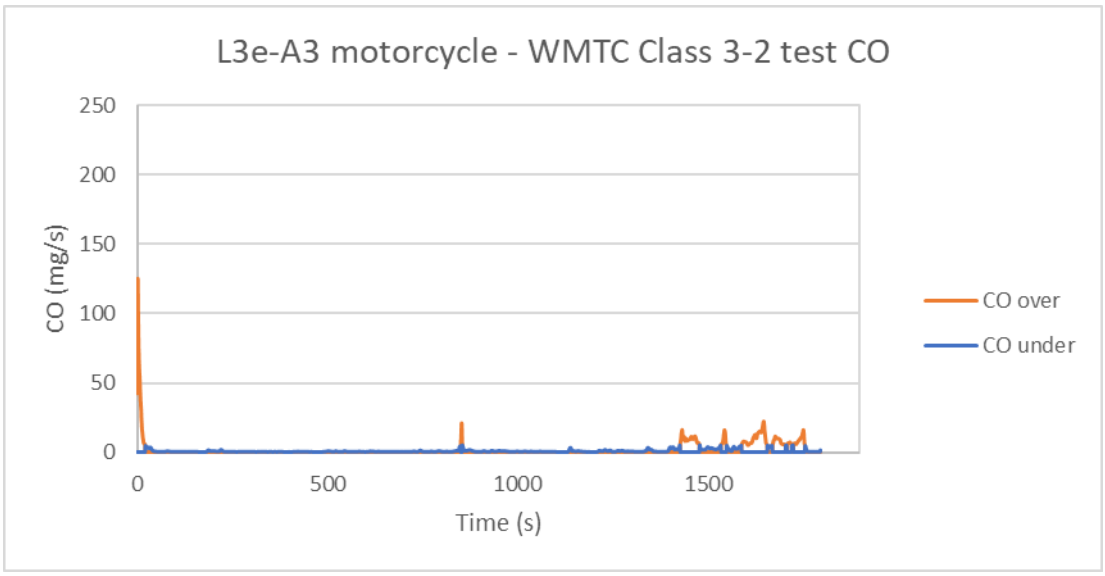

Figure K-37: L3e-A3 Sport Touring motorcycle - CO results in WMTC Class 3-2 test.

This project has received funding from the European Union's Horizon Europe research and innovation programme under grant agreement No 101056777

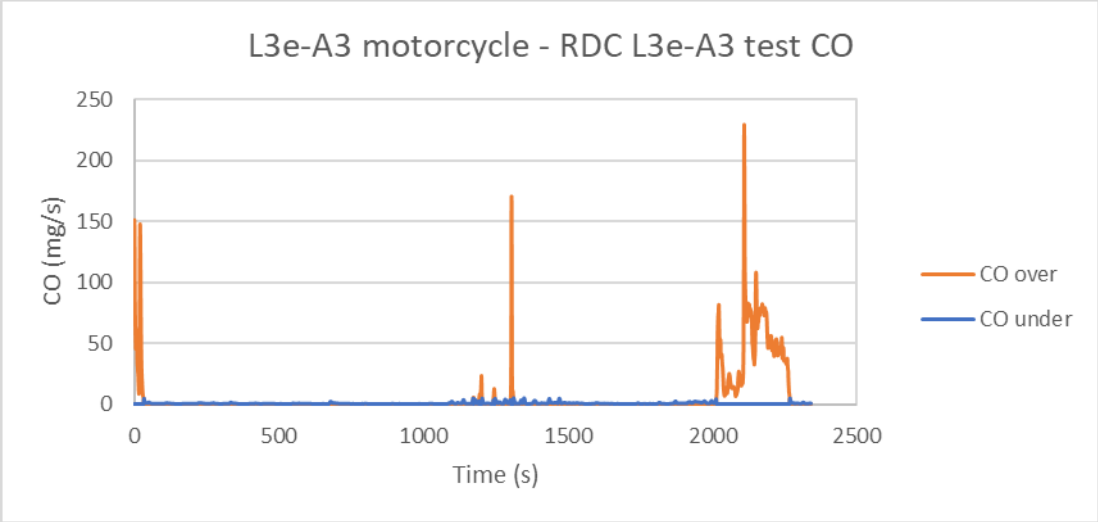

Figure K-38: L3e-A3 Sport Touring motorcycle - CO results in RDC L3e-A3 test.

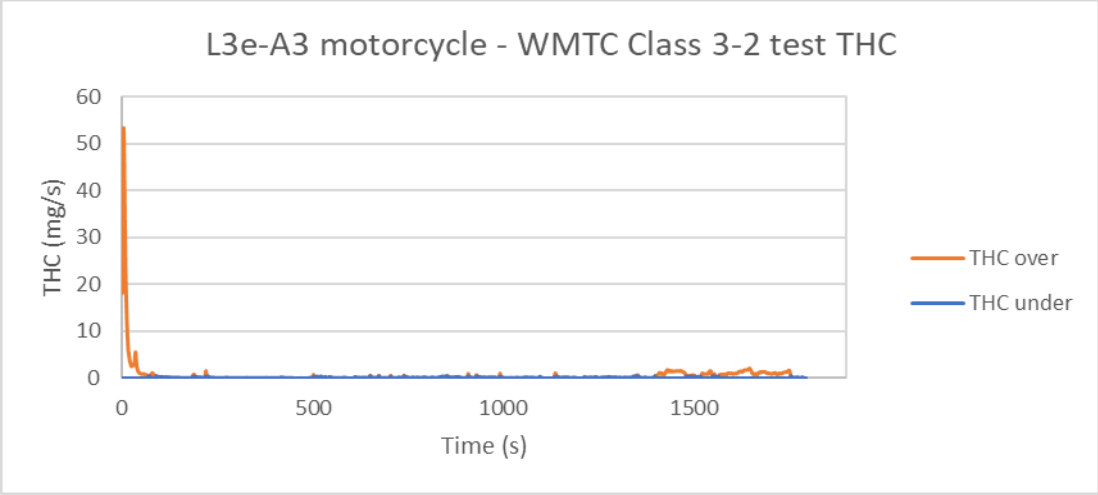

Figure K-39: L3e-A3 Sport Touring motorcycle - THC results in WMTC Class 3-2 test.

This project has received funding from the European Union's Horizon Europe research and innovation programme under grant agreement No 101056777

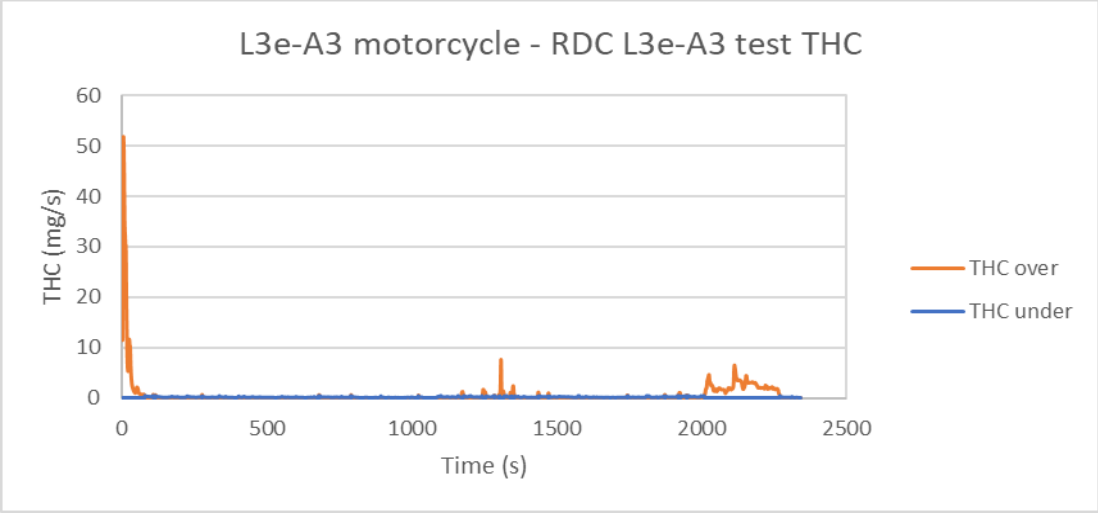

Figure K-40: L3e-A3 Sport Touring motorcycle - THC results in RDC L3e-A3 test.

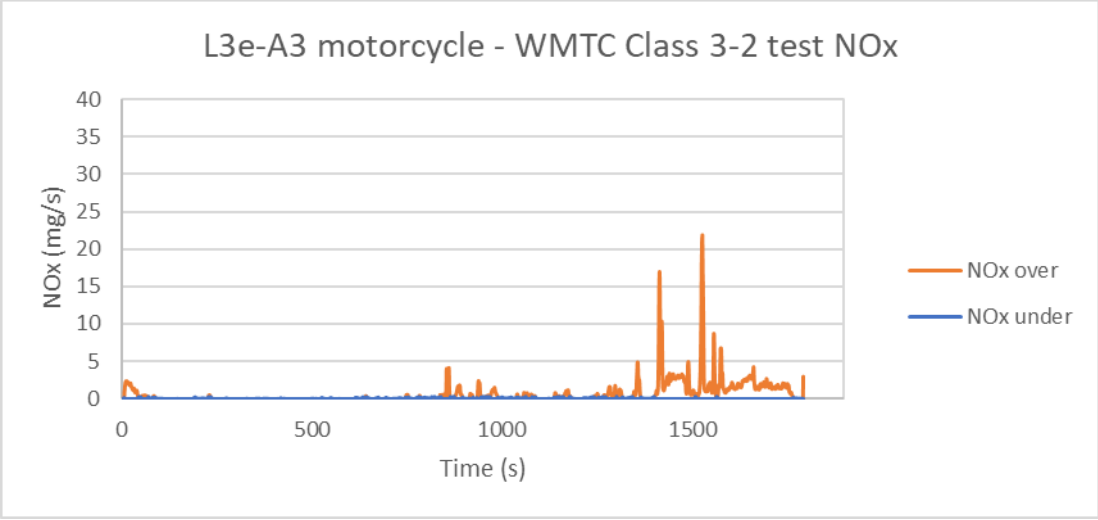

Figure K-41: L3e-A3 Sport Touring motorcycle - NOx results in WMTC Class 3-2 test.

This project has received funding from the European Union's Horizon Europe research and innovation programme under grant agreement No 101056777

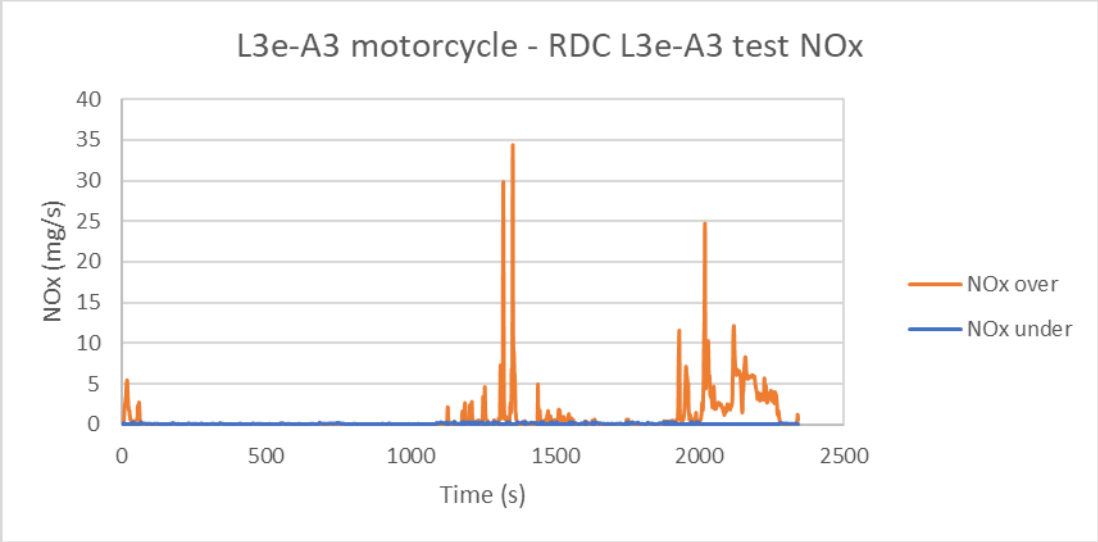

Figure K-42: L3e-A3 Sport Touring motorcycle - NOx results in RDC L3e-A3 test.

This project has received funding from the European Union's Horizon Europe research and innovation programme under grant agreement No 101056777

Appendix L: LENS db high tailpipe emissions analysis

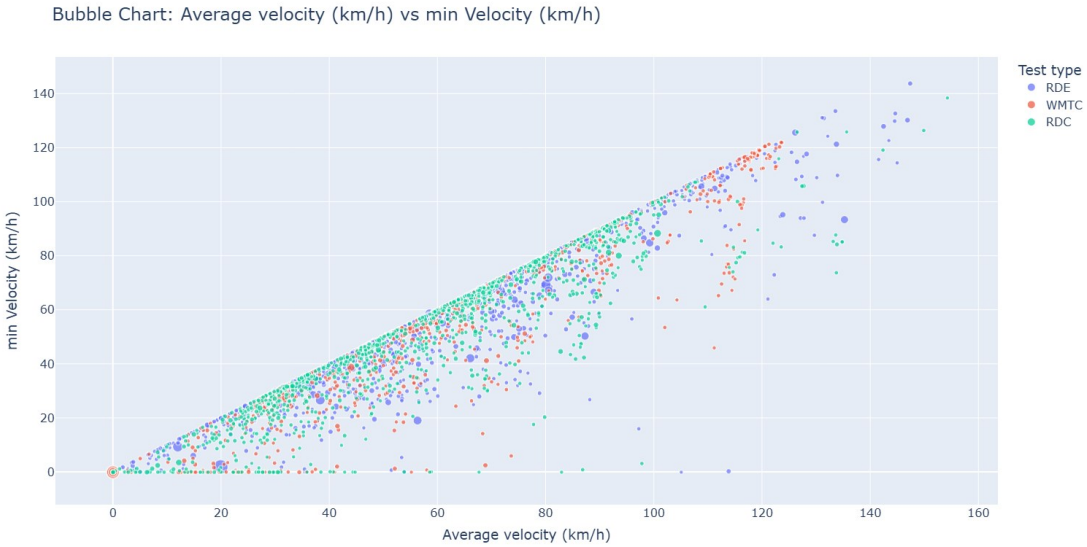

Figure L-1: NOx emission in (mg/s) for the different vehicle speeds and minimum velocities.

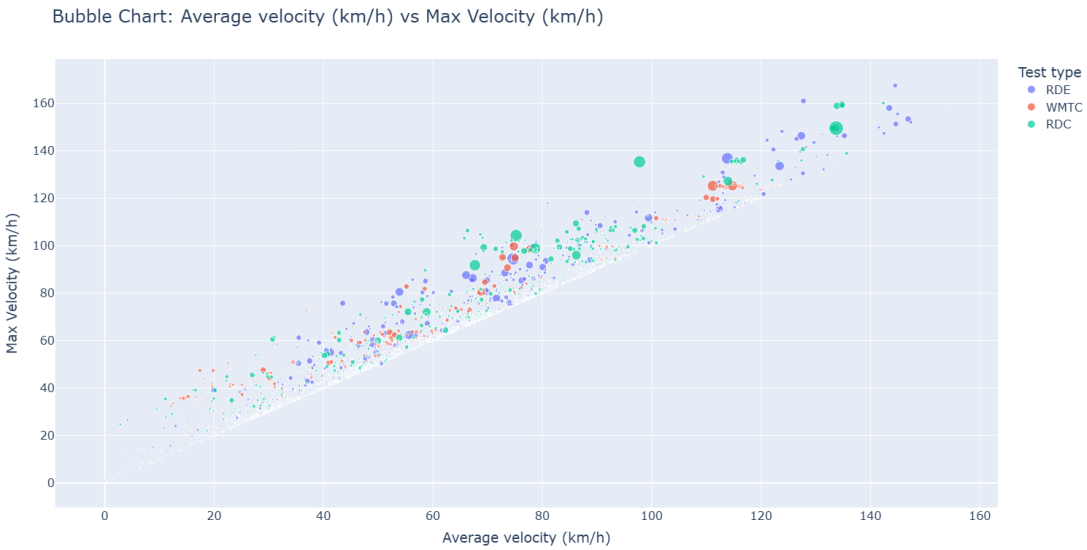

Figure L-2: NOx emission in (mg/s) for the different vehicle speeds and maximum velocities.

This project has received funding from the European Union's Horizon Europe research and innovation programme under grant agreement No 101056777

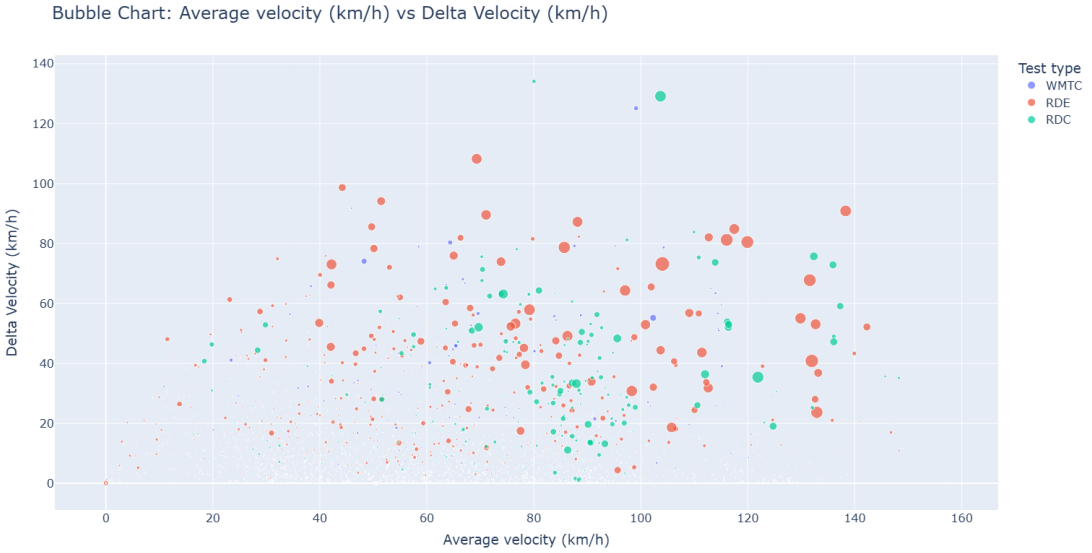

Figure L-3: CO emission in (mg/s) for the different vehicle speeds and delta velocities.

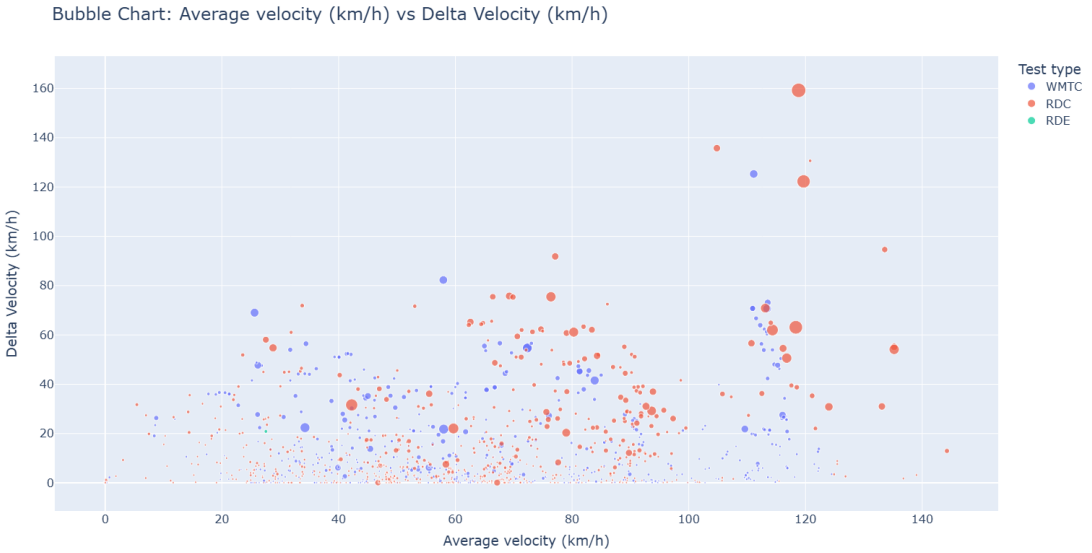

Figure L-4: HC emission in (mg/s) for the different vehicle speeds and delta velocities.

This project has received funding from the European Union's Horizon Europe research and innovation programme under grant agreement No 101056777

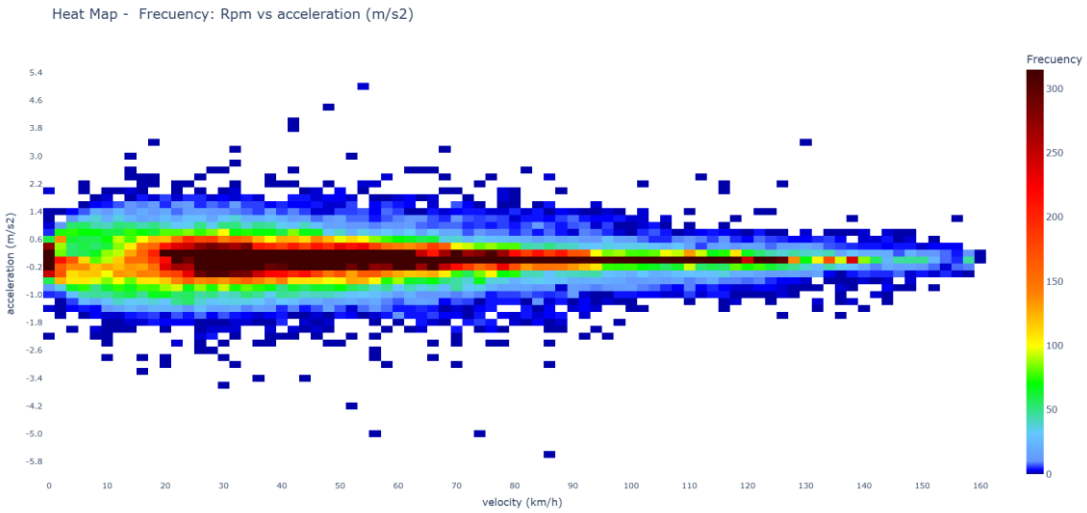

Figure L-5: Occurrence in total number of vehicles' operating points acceleration (m/s²) and vehicle speed (km/h).

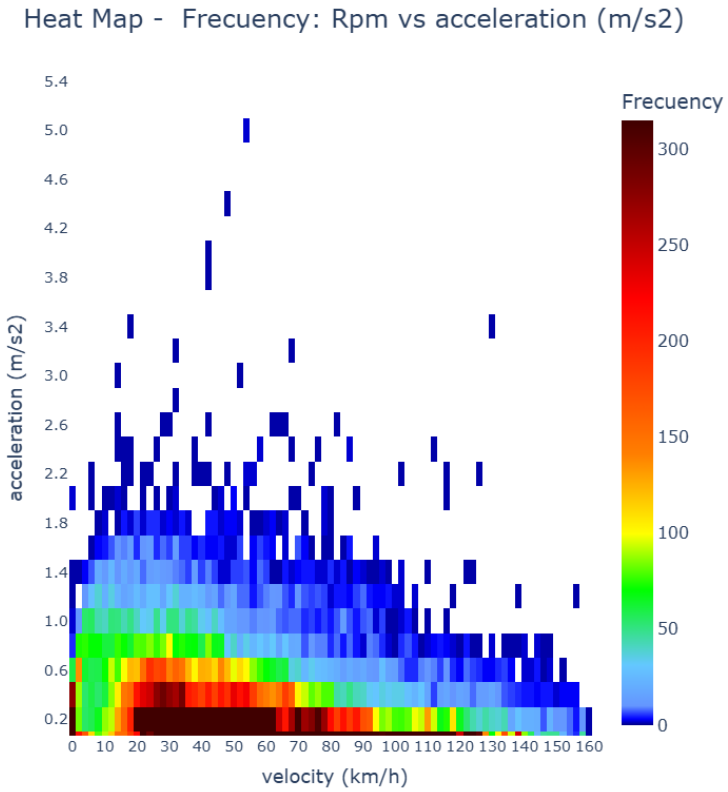

Figure L-6: Occurrence in total number of vehicles' operating points of positive acceleration (m/s²) and vehicle speed (km/h).

This project has received funding from the European Union's Horizon Europe research and innovation programme under grant agreement No 101056777

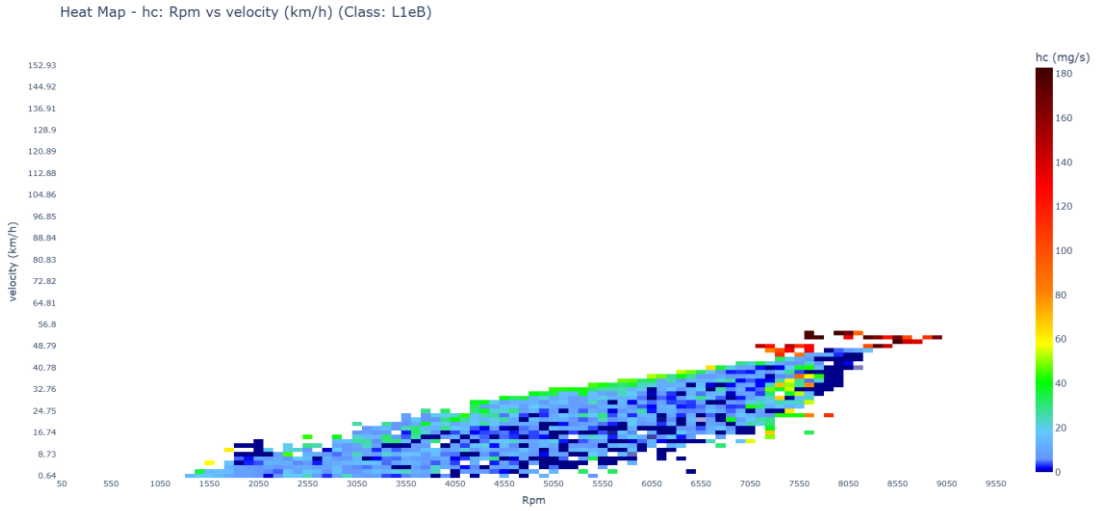

Figure L-7: HC emissions in (mg/s) against engine speed (rpm) and vehicle speed (km/h) for L1e-B sub-category.

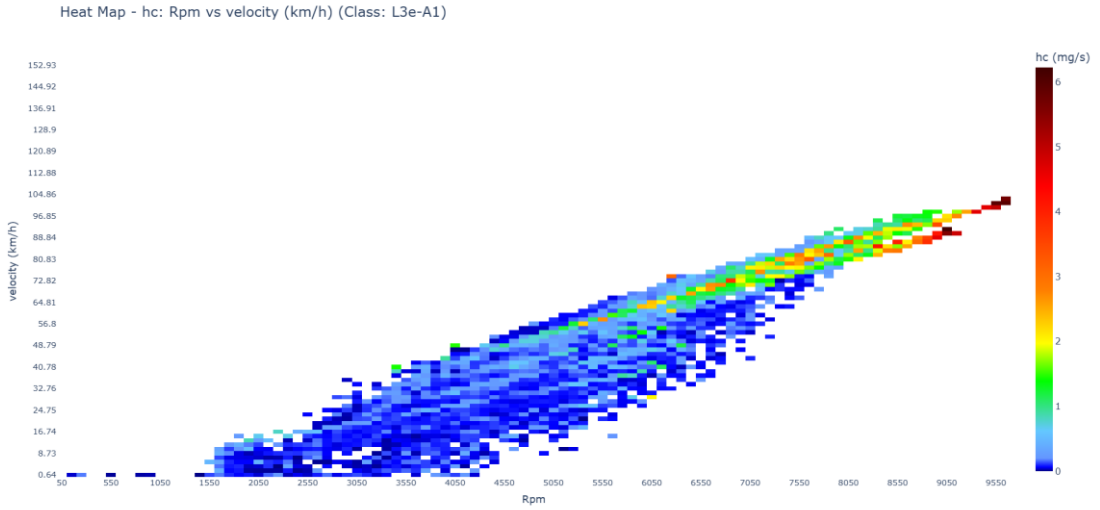

Figure L-8: HC emissions in (mg/s) against engine speed (rpm) and vehicle speed (km/h) for L3e-A1 sub-category.

This project has received funding from the European Union's Horizon Europe research and innovation programme under grant agreement No 101056777

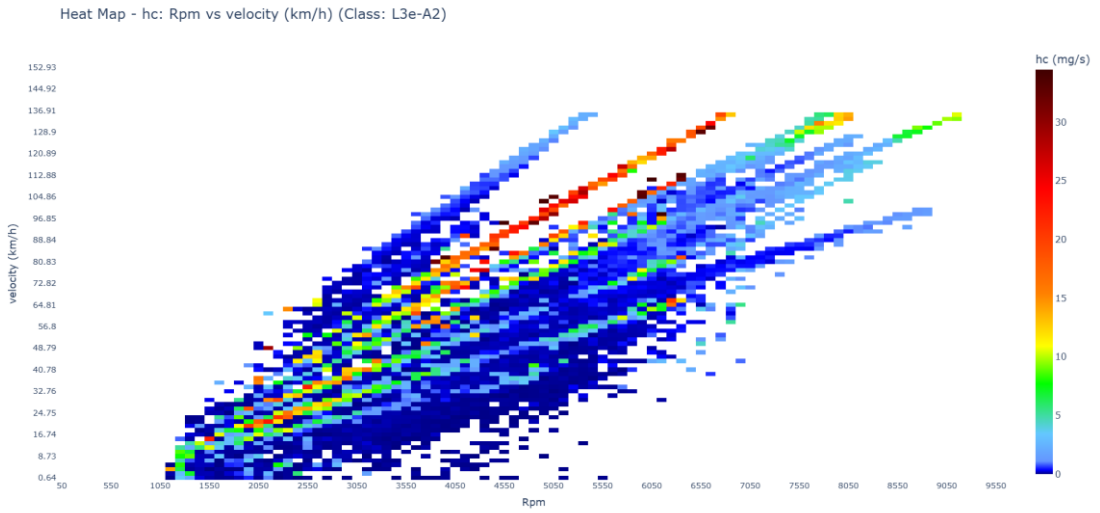

Figure L-9: HC emissions in (mg/s) against engine speed (rpm) and vehicle speed (km/h) for L3e-A2 sub-category.

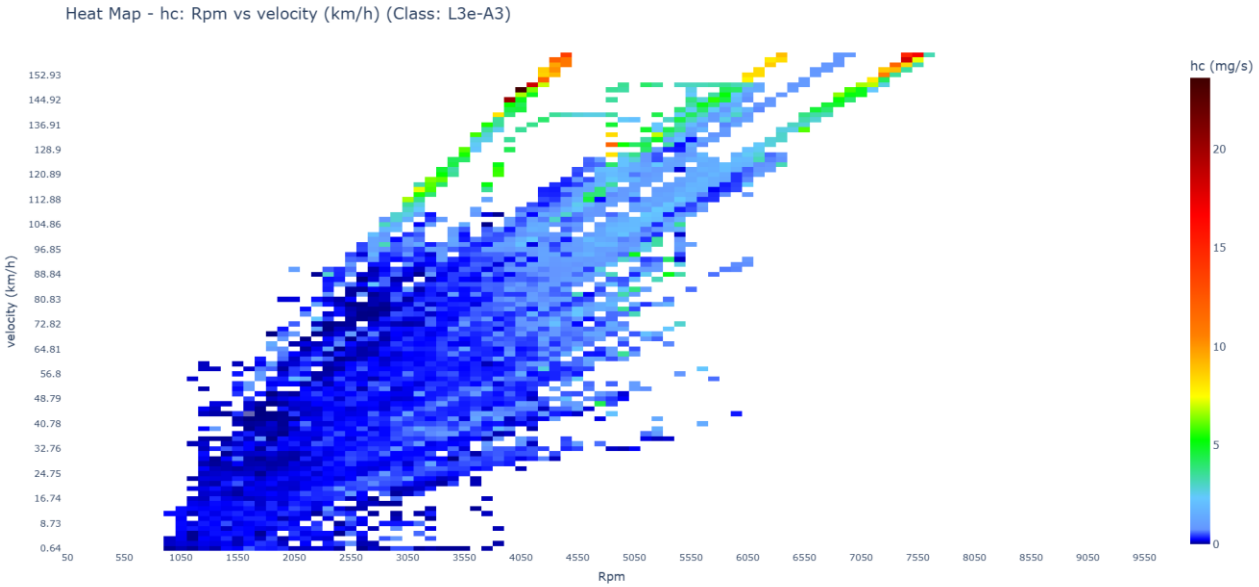

Figure L-10: HC emissions in (mg/s) against engine speed (rpm) and vehicle speed (km/h) for L3e-A3 sub-category.

This project has received funding from the European Union's Horizon Europe research and innovation programme under grant agreement No 101056777

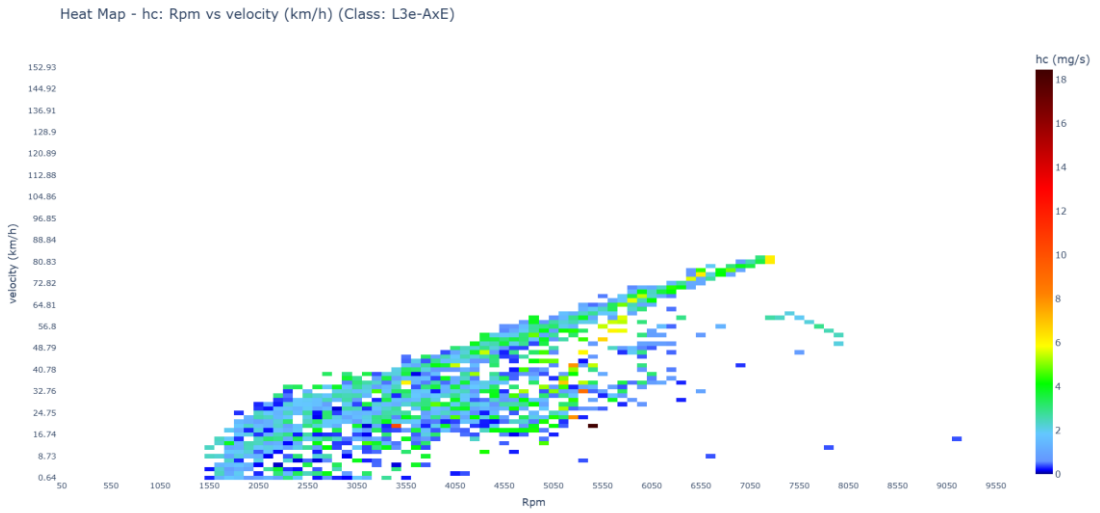

Figure L-11: HC emissions in (mg/s) against engine speed (rpm) and vehicle speed (km/h) for L3e-AxE sub-category.

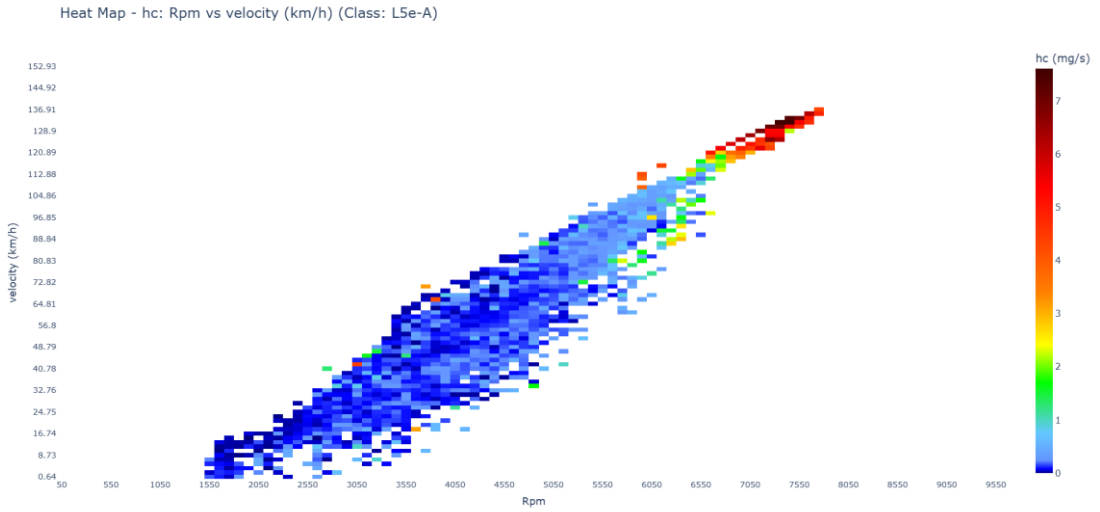

Figure L-12: HC emissions in (mg/s) against engine speed (rpm) and vehicle speed (km/h) for L5e-A sub-category.

This project has received funding from the European Union's Horizon Europe research and innovation programme under grant agreement No 101056777

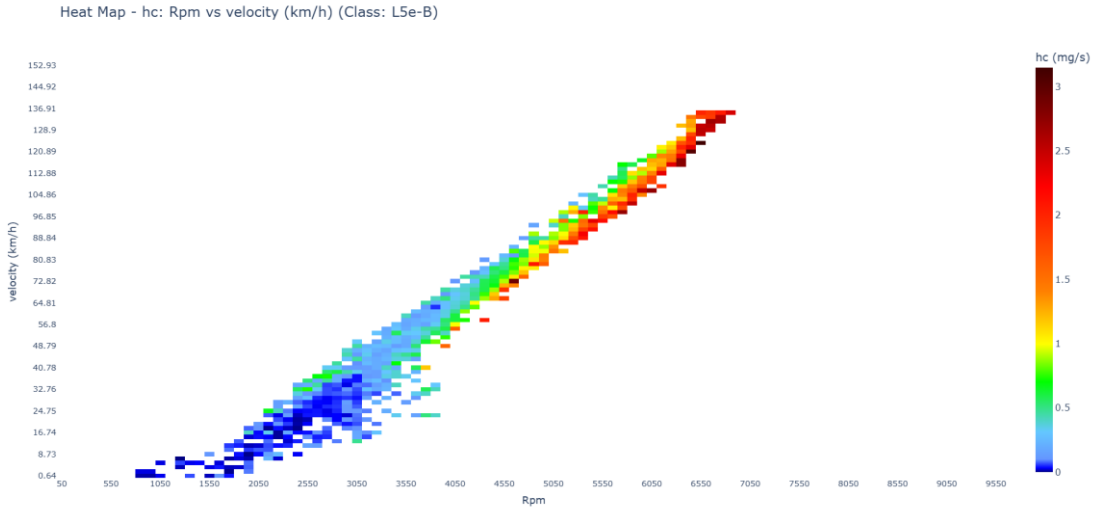

Figure L-13: HC emissions in (mg/s) against engine speed (rpm) and vehicle speed (km/h) for L5e-B sub-category.

This project has received funding from the European Union's Horizon Europe research and innovation programme under grant agreement No 101056777

Appendix M: Metadata from measurements

Table M-1: Metadata for each measurement extracted from the LENS db based on the selection criteria in Section 4.5.1

Measurement ID	Chronological Test NB	Size Class	EU Emission Standard	Test Bench Type	Fuel Type
0	001_RDE-000001	L3e-A2	5	On Road PEMS	petrol
1	005_RDE-000001	L3e-A1	5	On Road PEMS	petrol
2	008_RDE-000002	L3e-A3	5	On Road PEMS	petrol
3	009_RDE-000006	L3e-A3	5	On Road PEMS	petrol
4	014_RDE-000002	L3e-A1	5	On Road PEMS	petrol
5	023_RDE-000001	L3e-A2	5	On Road PEMS	petrol
6	028_RDE-000001	L3e-A3	5	On Road PEMS	petrol
7	031_RDE-000001	L3e-A3	5	On Road PEMS	petrol
8	03_SEMS_BMW_F850GS	L3e-A3	5	On Road PEMS	petrol
9	04_SEMS_Ducati_Multistada_V4S	L3e-A3	5	On Road PEMS	petrol
10	05_SEMS_Ducati_Monster	L3e-A3	5	On Road PEMS	petrol
11	06_SEMS_Piaggio_Vespa_125	L3e-A1	5	On Road PEMS	petrol
12	07_SEMS_Piaggio_Vespa_50	L1eB	5	On Road PEMS	petrol
13	08_SEMS_Piaggio_Fly_50	L1eB	2	On Road PEMS	petrol
14	09A_SEMS_BMW_F900XR_A3	L3e-A3	5	On Road PEMS	petrol
15	10_SEMS&IFPEN_BMW_F900XR_A2	L3e-A2	5	On Road PEMS	petrol
16	11_SEMS_Vespa_300	L3e-A2	5	On Road PEMS	petrol
17	14_SEMS_Honda_PS_125	L3e-A1	3	On Road PEMS	petrol
18	15_SEMS_Honda_Forza_300	L3e-A2	4	On Road PEMS	petrol

This project has received funding from the European Union's Horizon Europe research and innovation programme under grant agreement No 101056777

19	16_SEMS_Honda_Forza_125	L3e-A1	5	On Road PEMS	petrol
20	17_SEMS_SH_125	L3e-A1	5	On Road PEMS	petrol
21	2024.06.13_1	L3e-A3	5	On Road PEMS	petrol
22	202406271	L3e-A1	5	On Road PEMS	petrol
23	202406272	L3e-A1	5	On Road PEMS	petrol
24	202406273	L3e-A1	5	On Road PEMS	petrol
25	202406274	L3e-A1	5	On Road PEMS	petrol
26	202406275	L3e-A1	5	On Road PEMS	petrol
27	202406276	L3e-A1	5	On Road PEMS	petrol
28	20240814	L3e-A1	4	On Road PEMS	petrol
29	202408151	L3e-A1	4	On Road PEMS	petrol
30	202408152	L3e-A1	4	On Road PEMS	petrol
31	2405201	L3e-A1	5	On Road PEMS	petrol
32	2405202	L3e-A1	5	On Road PEMS	petrol
33	2406261	L3e-A3	4	On Road PEMS	petrol
34	2406262	L3e-A3	4	On Road PEMS	petrol
35	2406263	L3e-A3	4	On Road PEMS	petrol
36	2407022	L3e-A2	5	On Road PEMS	petrol
37	2407023	L3e-A2	5	On Road PEMS	petrol
38	2407031	L3e-A2	5	On Road PEMS	petrol
39	2407032	L3e-A2	5	On Road PEMS	petrol
40	2407033	L3e-A2	5	On Road PEMS	petrol

This project has received funding from the European Union's Horizon Europe research and innovation programme under grant agreement No 101056777

41	2407034	L3e-A2	5	On Road PEMS	petrol
42	2407035	L3e-A2	5	On Road PEMS	petrol
43	2407036	L3e-A2	5	On Road PEMS	petrol
44	2407101	L3e-A2	5	On Road PEMS	petrol
45	2407102	L3e-A2	5	On Road PEMS	petrol
46	2407103	L3e-A2	5	On Road PEMS	petrol
47	2407104	L3e-A2	5	On Road PEMS	petrol
48	2407241	L3e-A3	2	On Road PEMS	petrol
49	2407242	L3e-A3	2	On Road PEMS	petrol
53	020_RDE-000001	L3e-A2	5	On Road PEMS	petrol
54	026_RDE-000001	L3e-A3	4	On Road PEMS	petrol
55	029_RDE-000001	L3e-A2	4	On Road PEMS	petrol
56	032_RDE-000001	L3e-A2	5	On Road PEMS	petrol
57	034_RDE-000001	L3e-A2	4	On Road PEMS	petrol
58	035_RDE-000001	L3e-A1	5	On Road PEMS	petrol
59	038_RDE-000001	L3e-A2	5	On Road PEMS	petrol
60	039_RDE-000001	L1eB	3	On Road PEMS	petrol(2Stroke)
61	040_RDE-000001	L1eB	3	On Road PEMS	petrol(2Stroke)
62	041_RDE-000001	L1eB	4	On Road PEMS	petrol(2Stroke)
63	043_RDE	L3e-A1	3	On Road PEMS	petrol
64	12_SEMS_HOR_Yamaha_Aerox_50cc2T	L1eB	2	On Road PEMS	petrol(2Stroke)
65	18_SEMS_V-STORM_1000	L3e-A3	3	On Road PEMS	petrol

This project has received funding from the European Union's Horizon Europe research and innovation programme under grant agreement No 101056777

66	18_SEMS_V-STORM_1000_b	L3e-A3	3	On Road PEMS	petrol
67	19_miniPEMS_HONDAAfricaTwin	L3e-A3	5	On Road PEMS	petrol
68	19_miniPEMS_HONDAAfricaTwin_b	L3e-A3	5	On Road PEMS	petrol
69	2024.02.19_1	L3e-A1	5	On Road PEMS	petrol
70	2024.02.20_1	L3e-A1	5	On Road PEMS	petrol
71	2024.02.23_1	L3e-A2	5	On Road PEMS	petrol
72	2024.03.04_1	L1eB	5	On Road PEMS	petrol
73	2024.04.09_1	L3e-A1	5	On Road PEMS	petrol
74	2024.06.12_1	L3e-A3	5	On Road PEMS	petrol
75	2024.06.26_1	L3e-A3	5	On Road PEMS	petrol
76	2024.07.03_1	L3e-A2	4	On Road PEMS	petrol
77	2024.08.28_1	L3e-A2	5	On Road PEMS	petrol
78	2024.08.30_1	L3e-A1	5	On Road PEMS	petrol
79	2024.09.13_1	L3e-A2	5	On Road PEMS	petrol
80	2024.10.01_1	L3e-A3	5	On Road PEMS	petrol
81	2024.10.07_1	L3e-A3	5	On Road PEMS	petrol
82	202405201	L3e-A1	5	On Road PEMS	petrol
83	202405202	L3e-A1	5	On Road PEMS	petrol
84	20_miniPEMS_Piaggio_ZIP_50cc	L1eB	5	On Road PEMS	petrol
85	21_miniPEMS_Yamaha_Tenere 700_b	L3e-A2	4	On Road PEMS	petrol
86	21_miniPEMS_Yamaha_Tenere_700	L3e-A2	4	On Road PEMS	petrol
87	22_miniPEMS_Piaggio_Vespa_ET4	L1eB	2	On Road PEMS	petrol

This project has received funding from the European Union's Horizon Europe research and innovation programme under grant agreement No 101056777

88	23_miniPEMS_Yamaha_TMAX_530DX	L3e-A2	4	On Road PEMS	petrol
89	240911	L1eB	3	On Road PEMS	petrol
90	2409251	L1eB	3	On Road PEMS	petrol
91	2409252	L1eB	3	On Road PEMS	petrol
92	2409253	L1eB	3	On Road PEMS	petrol

This project has received funding from the European Union's Horizon Europe research and innovation programme under grant agreement No 101056777

Annex 1: Non-regulated pollutant emissions in real-world with mFTIR

On-road measurement equipment was in some cases specifically developed in order to understand the behavior of L-category vehicles when driving on-road. A total of 21 motorcycles were tested on-road using a highly compact FTIR analyzer. The observed emissions patterns are analogous to those observed over several decades of on-road emissions monitoring of light-duty gasoline vehicles. On newer engines equipped with fuel injection, oxygen sensor and three-way catalytic converter, exhaust emissions of HC, CO and NOx are relatively low, provided the catalytic converter is warmed up and the engine is running at stoichiometric air-fuel ratio. On Euro 5 engines, high emissions expressed in all common metrics (emissions per kg fuel, per kW power, per second, per km driven), can be, in general, attributed to one of the following situations:

1. Low temperature of the catalytic converter during a brief period following a cold start
2. Air-fuel ratio imbalance during transients
3. Commanded enrichment during transients
4. Commanded enrichment during sustained high load
5. Decreased catalytic converter efficiency due to short residence time during high exhaust flows (high engine loads)

Emissions assessment

Of emerging gaseous pollutants of interest, greenhouse gases methane (CH4) and nitrous oxide (N2O), reactive nitrogen species nitrogen dioxide (NO2) and ammonia (NH3), and formaldehyde are regulated or proposed to be regulated under major legislations for light vehicles and for engines for heavy duty on-road vehicles. Table A1-1 shows the summary results of on-road tests of 13 Euro 5 motorcycles tested on the road with a portable FTIR analyzer.

- **Methane**: emissions are relatively low, on the order of 10 mg/km (average 14 mg/km, range 1-33 mg/km), corresponding to less than 1 g/km CO2 equivalent. The emissions of N2O, a greenhouse gas typically generated in NOx reduction aftertreatment at intermediate temperatures, were also low, from less than 1 to 5 mg/km, with average value 2 mg/km corresponding to less than 1 g/km CO2 equivalent.
- **Formaldehyde**: emissions are generally low, on the order of 1 mg/km. The emissions of acetaldehyde, another aldehyde of concern, are below the detection limit estimated at 1 ppm or 1 mg/km.
- **NO2**: emissions are generally low, on the order of units of percent of NO and units of mg/km. This is expected, as spark ignition engines do not generally operate with much excess oxygen in the exhaust.
- **Ammonia:** emissions were mostly on the order of tens mg/km, with both average and median value of 36 mg/km. Ammonia is believed to originate entirely from the three-way catalyst and is mostly

This project has received funding from the European Union's Horizon Europe research and innovation programme under grant agreement No 101056777

correlated with fuel-rich conditions during transients and during commanded enrichment when the catalyst is at its operating temperature.

It is expected that efforts aimed at reducing the usage of commanded enrichment and at improving the air-fuel ratio control during transients, both believed to be necessary to reduce on-road emissions CO and NO to levels corresponding to the Euro 5 limit (applicable to laboratory test conditions), will also reduce the emissions of ammonia. While some insights can be obtained through additional data mining and analysis, the fact that ammonia emissions from light-duty petrol vehicles are regulated suggest that this might remain an open question for L-category vehicles, and on-road monitoring should be at least considered.

Table A1-1: Summary results of on-road tests of 13 Euro 5 motorcycles tested on the road with a portable FTIR analyzer.

Distance			*CO2*	*CO*	*CH4*	*HCHO*	*CH3CHO*	*N2O*	*NH3*	*NO*	*NO2*	*NOx*	*Fuel*	*Fuel*
	km		*g/km*	*mg/km*	*mg/km*	*mg/km*	*mg/km*	*mg/km*	*mg/km*	*mg/km*	*mg/km*	*mg/km*	*g/km*	*l/100 km*
Euro 5	48.2	L3e-A1	62	3748	23	1.0		5	102	442	21	463	22	2.9
Euro 5	50.0	L3e-A1	41	5133	14	0.5		1	49	31	0	31	16	2.1
Euro 5	60.6	L5e-A1	114	2558	7	0.4		1	40	67	1	67	37	5.0
Euro 5	56.4	L3e-A1	74	1429	23	7	0.00	4	7	303	14	317	24	3.2
Euro 5	61.9	L3e-A2	58	8625	20	2.4		3	68	36	1	36	23	3.0
Euro 5	58.4	L3e-A2	87	612	8	0.9		1	20	31	1	32	28	3.7
Euro 5	42.1	L3e-A2	108	617	13	1.5		3	8	123	1	124	35	4.6
Euro 5	56.5	L3e-A2	85	3209	17	0.6	0.01	1	33	36	0	36	29	3.8
Euro 5	65.6	L3e-A2	61	3300	11	0.8	0.01	1	49	12	0	12	21	2.8
Euro 5	47.0	L3e-A2	122	144	12	0.4	0.01	3	36	4	0	5	39	5.2
Euro 5	61.4	L3e-A3	122	3897	33	0.8	0.02	3	47	60	0	60	41	5
Euro 5	57.8	L3e-A3	137	446	6	1.3	0.01	2	8	68	10	78	44	5.8
Euro 5	60.8	L5e	130	159	1	0.4	0.01	1	8	5	3	8	41	5.5
	56	Average	92	2606	14	1.4	0.01	2	36	94	4	98	31	4.1
	58	Median	87	2558	13	0.8	0.01	2	36	36	1	36	29	3.8
	42	Min	41	144	1.2	0.4	0.00	0.6	7	4	0.1	5	16	2.1
	66	Max	137	8625	33	7.0	0.02	5	102	442	21	463	44	5.8
	average	L3e-A1	73	3217	17	2	0	3	49	211	9	219	25	3.3
	average	L3e-A2	87	2751	13	1	0	2	36	40	1	41	29	3.9

This project has received funding from the European Union's Horizon Europe research and innovation programme under grant agreement No 101056777

Funded by the European Union. Views and opinions expressed are however those of the author(s) only and do not necessarily reflect those of the European Commission or CINEA. Neither the European Commission nor CINEA can be held responsible for them.